Thesis

on

# Hybrid Optimization Technique to Solve Unit Commitment of Electric Power System

Submitted in fulfillment of the requirements

of

**DOCTOR OF PHILOSOPHY**

*Submitted by*


**HIMANSHU ANAND**

(Registration No. 951504004)


*Under the supervision of*


**Dr. Nitin Narang**
*Associate Professor*
Department of Electrical &
Instrumentation Engineering
Thapar Institute of Engineering &
Technology, Patiala

**Dr. J. S. Dhillon**
*Professor*
Department of Electrical &
Instrumentation Engineering
Sant Longowal Institute of Engineering
& Technology, Longowal


THAPAR INSTITUTE
OF ENGINEERING & TECHNOLOGY
(Deemed to be University)


Department of Electrical & Instrumentation Engineering
Thapar Institute of Engineering & Technology
Patiala-147004 (Punjab), India


June, 2021

*Dedicated to*

*My Respected Father*

***Shri Vijay Kumar Anand***

*and*

*Respected Mother*

***Smt. Ravi Anand***

# CERTIFICATE

Certified that the thesis entitled, "**Hybrid Optimization Technique to Solve Unit Commitment of Electric Power System**", which is being submitted by Himanshu Anand in fulfillment of the requirements for the award of the degree of **Doctor of Philosophy**, to the Department of Electrical and Instrumentation Engineering, Thapar Institute of Engineering & Technology, Patiala, is a bonafide records of the candidate's own work carried out by him under our supervision and guidance.

The matter presented in this Thesis has not been submitted for the award of any other degree of this or any other University.

Himanshu Anand

**Mr. Himanshu Anand**
Regd. No. 951504004

This is to certify that the above statement made by the candidate is correct to the best of our knowledge.

N Narang

**Dr. Nitin Narang**
*Associate Professor*
Department of Electrical &
Instrumentation Engineering
Thapar Institute of Engineering &
Technology, Patiala

JSDhillon
19.06.2021

**Dr. J. S. Dhillon**
*Professor*
Department of Electrical &
Instrumentation Engineering
Sant Longowal Institute of Engineering
& Technology, Longowal

# ACKNOWLEDGMENT

First of all, I thank the Almighty, for giving me the grace and health to complete my research work. I would like to express my deepest gratitude to my guides and mentors Dr. Nitin Narang, and Dr. J.S. Dhillon for giving me an opportunity to complete my thesis under their able supervision. They have always been a pillar of support and constant source of inspiration. This thesis would never have been possible without their kind support and valuable guidance.

I feel highly obliged to Dr. Teena Narang wife of Dr. Nitin Narang for her being so kind, co-operative and generous during the whole period of research work.

I sincerely thank my all colleagues especially, Dr. Nirbhowjap Singh, Mrs. Manbir Kaur, Mr. Nagendra Singh, Mr. Vinit Kumar, Mr. Rituraj Singh and Mr. Anurag Verma for encouraging and supporting me throughout. I would like to thank my Ph.D. doctoral committee members Dr. S.K. Jain, Dr. Saurabh Bhardwaj and Dr. M.K. Sharma for their time and valuable suggestion during my research period.

I am also extremely grateful and thankful to my father Shri Vijay Kumar Anand, mother Smt. Ravi Anand, sisters Dr. Aditi and Dr. Shikha for their infinite patience, love and unending support.

Mr. Himanshu Anand
Regd. No. 951504004
Thapar Institute of Engineering &
Technology, Patiala

# TABLE OF CONTENTS

# TABLE OF CONTENTS (Continued)

# TABLE OF CONTENTS (Continued)

# TABLE OF CONTENTS (Continued)

# LIST OF TABLES

# LIST OF TABLES (Continued)

# LIST OF TABLES (Continued)

# LIST OF TABLES (Continued)

# LIST OF FIGURES

# LIST OF FIGURES (Continued)

# LIST OF FIGURES (Continued)

# LIST OF FIGURES (Continued)

# LIST OF FIGURES (Continued)

# NOMENCLATURE

The main symbols and notations used in this thesis are listed below. Sometimes a symbol may have alternate meaning, but in such a case, the context is sufficient to avoid confusion.

| **Indices** | **Description** |
|---|---|
| $i$ | Index for the total number of generating units |
| $j$ | Index for the cogeneration unit |
| $k$ | Index for a number of iteration |
| $m$ | Index for heat unit |
| $s$ | Index for the number of particles |
| $t$ | Index for hour |

| **Input data** | **Description** |
|---|---|
| $a_i, b_i, c_i, d_i, e_i$ | Cost coefficients of $i^{th}$ thermal unit |
| $\alpha_i, \beta_i, \delta_i, \chi_j, \chi_j^c$ | The cost coefficient of $j^{th}$ CHP units |
| $cb, ce$ | The CHP operated in backpressure and extraction mode |
| $C_{SL1}, C_{SL2}, C_1, C_{SM1}, C_{SM2}$ | The acceleration coefficient |
| $CS_i, HS_i$ | The cold and hot start-up cost of $i^{th}$ unit ($/h) |
| $\underline{F_n}, \overline{F_n}$ | Lower and upper value of $n^{th}$ objective functions |
| $\underline{H_j^{cb}}, \overline{H_j^{cb}}$ | The heat minimum and maximum limit of $j^{th}$ CHP unit (MWth) |
| $\underline{H_j^{ce}}, \overline{H_j^{ce}}$ | The heat minimum and maximum limit of $j^{th}$ CHP unit (MWth) |
| $\underline{H_m^h}, \overline{H_m^h}$ | The heat minimum and maximum limit of $m^{th}$ heat unit (MWth) |
| $HD_t$ | The forecasted heat load at $t^{th}$ hour |
| $IT^{max}$ | Maximum number of iteration for BSA-CSO method |
| $k^{max}$ | The maximum number of CSO iteration |
| $\underline{\lambda_j^{cbe}}, \overline{\lambda_j^{cbe}}$ | The fuel minimum and maximum limit of $j^{th}$ CHP units (MW) |
| $\underline{\lambda_m^h}, \overline{\lambda_m^h}$ | The fuel minimum and maximum limit of $m^{th}$ heat unit (MW) |
| $\lambda_t$ | Heat price at $t^{th}$ hour ($/MW$^{th}$) |
| $N$ | The total number of units |
| $NL$ | List of unit based on PL |
| $N_g$ | The number of thermal units |
| $N_c$ | The number of CHP units |
| $N_h$ | The number of heat units |

# NOMENCLATURE (Continued)

| | |
|---|---|
| $N_b$ | The number of battery units |
| $N_p$ | Number of particles |
| $N_s$ | Number of societies |
| $N_m$ | Number of societies member |
| $\eta_b$ | The battery efficiency |
| $\eta_i, \kappa_i, \varphi_i, \rho_i, \theta_i$ | Emission coefficients of $i^{th}$ thermal unit |
| $\overline{P_{ti}^{R}}, \underline{P_{ti}^{R}}$ | Upper and lower power for ramp up/down limit of $i^{th}$ thermal unit at $t^{th}$ hour (MW/h) |
| $\underline{P_i^{th}}, \overline{P_i^{th}}$ | The power minimum and maximum limit of $i^{th}$ thermal units (MW) |
| $\underline{P_j^{cb}}, \overline{P_j^{cb}}$ | The power minimum and maximum limit of $j^{th}$ CHP units (MW) |
| $\underline{P_j^{ce}}, \overline{P_j^{ce}}$ | The power minimum and maximum limit of $j^{th}$ CHP units (MW) |
| $PD_t$ | The forecasted power load at $t^{th}$ hour |
| $PR$ | The rated power generation from  PV (MW) |
| $PU_c$ | The per unit cost of PV power ($/KWh) |
| $\overline{P^b}$ | The maximum power limit of the battery (MW) |
| $\psi_1$ | Penalty factor |
| $\psi_h^q$ | The fuel consumption per generated heat of $h^{th}$ heat unit |
| $\psi_j^q, \psi_j^p$ | The fuel consumption per generated heat and power of $j^{th}$ CHP unit |
| $Q_s, Q_f$ | The initial and final state of charge (Ah) |
| $\underline{Q}, \overline{Q}$ | The lower and upper state of charge of battery (Ah) |
| $ran()$ | The uniformly distributed random number |
| $\underline{R_j^{ce}}, \overline{R_j^{ce}}$ | The power to heat ratio of $j^{th}$ CHP unit |
| $SR_t$ | The incident solar radiation at $t^{th}$ hour (W/m$^2$) |
| $SP_t$ | The power reserve at $t^{th}$ hour |
| $SH_t$ | The heat reserve at $t^{th}$ hour |
| $\sigma_i$ | Energy price at $t^{th}$ interval ($/MWh) |
| $T$ | The total hour (h) |
| $T_i^{cold}$ | The time taken by of $i^{th}$ unit to reach its cooling point (h) |
| $T_i^{dw}, T_i^{up}$ | The minimum down and up time of $i^{th}$ unit (h) |

# NOMENCLATURE (Continued)

| | |
|---|---|
| $T_r, T_t^c$ | The reference and PV cell temperature ($^0$C) |
| $T_{ti}^{off}, T_{ti}^{on}$ | The OFF and ON time of $i^{th}$ unit at $t^{th}$ hour |
| $UR_i^{th}, DR_i^{th}$ | The up and down ramp limit of $i^{th}$ thermal unit (MW/h) |
| $UR_j^{cb}, DR_j^{cb}$ | The up and down ramp limit of $j^{th}$ CHP unit (MW/h) |
| $UR_i^p, DR_i^p$ | Ramp up and down limit of $i^{th}$ thermal unit (MW/h) |
| $UR_j^f, DR_j^f$ | Ramp up and down limit of $j^{th}$ CHP unit (MW/h) |
| $V_t^b$ | The battery voltage at $t^{th}$ hour (V) |
| $w^{max}, w^{min}$ | The maximum and minimum inertia weight |

| **Decision variable** | **Description** |
|---|---|
| $C_{1i}^k, C_{2i}^k, C_i^k$ | The binary number at $k^{th}$ base point of $i^{th}$ unit |
| $CP_{ti}$ | Constrained power at $t^{th}$ time of $i^{th}$ unit (MW) |
| $\gamma_i^k$ | The CL velocity of $i^{th}$ dimension at $k^{th}$ iteration |
| $H_{tm}^h$ | The generated heat from $m^{th}$ heat unit at $t^{th}$ hour (MWth) |
| $H_{tj}^c$ | The generated heat from $j^{th}$ CHP unit at $t^{th}$ hour |
| $I_{ti}$ | The status of $i^{th}$ unit at $t^{th}$ hour |
| $\mu_{si}^k$ | The $s^{th}$ SL velocity and position of $i^{th}$ dimension at $k^{th}$ iteration |
| $\mu_{sr}^k,\ \mu'^k_{sr}$ | The position of $s^{th}$ dimension of $r^{th}$ particle at $k^{th}$ iteration |
| $\mu_{sr}^{best},\ \mu'^{best}_{sr}$ | The personal best position of $s^{th}$ dimension of $r^{th}$ particle |
| $\mu_r^{Gbest},\ \mu'^{Gbest}_r$ | The global best position of $r^{th}$ particle |
| $\upsilon_{sr}^k$ | The velocity of $s^{th}$ dimension of $r^{th}$ particle at $k^{th}$ iteration |
| $P_t^{pv}$ | The generated power from the PV panel at $t^{th}$ hour (MW) |
| $P_t^b$ | The generated power from the battery at $t^{th}$ hour (MW) |
| $P_t^u$ | The utility power at $t^{th}$ hour (a positive value states, power flow from PV-ESS to utility and a negative value states, as power flow from utility to PV-ESS) (MW) |
| $P_t^c$ | The generated power from $j^{th}$ CHP unit at $t^{th}$ hour |
| $P_{ti}^{th}$ | The generated power from $i^{th}$ thermal units at $t^{th}$ hour (MW) |
| $P_t^s$ | The spillage power at $t^{th}$ hour (MW) |

# NOMENCLATURE (Continued)

| | |
|---|---|
| $v_{smi}^{k}$ | The velocity of $i^{th}$ dimension for $m^{th}$ SM of $s^{th}$ society at $k^{th}$ iteration |
| $\varphi_{si}^{best}$ | The $s^{th}$ SL best position of $i^{th}$ dimension |
| $\varphi_{si}^{k}$ | The $s^{th}$ SL position of $i^{th}$ dimension at $k^{th}$ iteration |
| $Q_t$ | The battery state of charge at $t^{th}$ hour (Ah) |
| $\sigma_{i}^{best}$ | The best CL position of $i^{th}$ dimension |
| $\sigma_{i}^{k}$ | The CL position of $i^{th}$ dimension at $k^{th}$ iteration |
| $\theta_{smi}^{best}$ | The best position for $m^{th}$ SM of $s^{th}$ society $i^{th}$ dimension |
| $\theta_{smi}^{k}$ | The position of $i^{th}$ dimension for $m^{th}$ SM of $s^{th}$ society at $k^{th}$ iteration |

| **Function** | **Description** |
|---|---|
| $C_g(P_{ti}^{th})$ | The fuel cost of $i^{th}$ thermal unit at $t^{th}$ hour ($/h) |
| $C_c(P_{tj}^{c}, H_{tj}^{c})$ | The fuel cost of $j^{th}$ CHP unit at $t^{th}$ hour ($/h) |
| $C_h(H_{tm}^{h})$ | The fuel cost of $m^{th}$ heat unit at $t^{th}$ hour ($/h) |
| $C_{pv,t}$ | The fuel cost of the solar unit at $t^{th}$ hour ($/h) |
| $C_{b,t}$ | The fuel cost of battery unit at $t^{th}$ hour ($/h) |
| $D_S$ | Euclidean distance |
| $E_{g,i}$ | Emission of $i^{th}$ thermal unit (Kg/h) |
| $E_t^1, E_t^2$ | Error for power and heat demand in MO economic scheduling |
| $E_t^{1'}, E_t^{2'}$ | Error for power and heat demand in MO-PB scheduling |
| $E_t^4, E_t^3$ | Error for fuel and ramp fuel limit |
| $ER, ER'$ | Total error for MO economic and profit based scheduling |
| $F_1, F_2, F_3$ | The objective function for economic, emission and profit model |
| $\lambda$ | The fuel consumption (MWh) |
| $\lambda_{tj}^{cb,e}$ | The fuel consumption of $j^{th}$ CHP unit at $t^{th}$ hour (MWh) |
| $\lambda_{tm}^{h}$ | The fuel consumption of $m^{th}$ heat unit at $t^{th}$ hour (MWh) |
| $\mu_d$ | Final membership value of MO economic and profit based problem |
| $\mu(F_1), \mu(F_2), \mu(F_3)$ | Membership value of operating cost, emission and profit |
| $PF$ | Profit ($) |
| $TC$, $TE$ | The total cost ($) and total emission (Kg) |

# GLOSSARY OF ACRONYMS

| Acronym | Description |
|---|---|
| ACO | Ant colony optimization |
| AFCBPSO | Advanced fuzzy controlled binary particle swarm optimization |
| AGA | Annealing genetic algorithm |
| AHLN | Annealing hopfield Lagrange neural network |
| BCGA | Binary coded genetic algorithm |
| BFSA | Binary fish swarm algorithm |
| BFWA | Binary fireworks algorithm |
| BPSO | Binary particle swarm optimization |
| BPSO-PSO | Binary particle swarm optimization and particle swarm optimization technique |
| BSA | Binary successive approximation |
| BSO | Backtracking search optimization |
| CHP | Combined heat and power |
| CHPED | Combined heat and power economic dispatch |
| CHPS | Combined heat and power system |
| CHPUC | Combined heat and power unit commitment |
| COA | Crisscross optimization algorithm |
| CPM | Cardinal priority method |
| CRGA | Continuous relaxation and genetic algorithm |
| CSO | Civilized swarm optimization |
| DE | Differential evolution |
| DM-CHP | Dual-mode combined heat and power |
| DP | Dynamic programming |
| EA | Evolutionary algorithm |
| ELD | Economic load dispatch |
| EP | Evolutionary programming |
| ES | Evolutionary search |
| ESA | Enhanced simulated annealing |
| ESS | Energy storage system |
| ESU | Energy storage unit |
| FA | Firefly algorithm |
| FOR | Feasible operating region |
| GA | Genetic algorithm |
| GENCOs | Generating companies |
| GS | Gravitational search |
| HASP | Hybrid ant system/priority list |
| HHS-RS | Hybrid harmony search and random search |
| HPSO | Hybrid particle swarm optimization |
| HPSO-SQP | Hybrid particle swarm optimization and sequential quadratic programming |
| HS | Harmony search |
| IBPSO | Improved binary particle swarm optimization |
| ICA | Imperialist competitive algorithm |
| ICGA | Integer coded genetic algorithm |
| ICHPS | Integrated combined heat and power system |

# GLOSSARY OF ACRONYMS (Continued)

| Acronym | Description |
|---|---|
| ICHPUC | Integrated combined heat and power unit commitment |
| ILR | Improved Lagrangian relaxation |
| IPPD | Improved pre-prepared power demand |
| IPPDTM | Improved pre-prepared power demand table and Muller’s |
| IPSO | Improved particle swarm optimization |
| LCA-BPSO | Local convergence averse binary particle swarm optimization |
| LR | Lagrangian relaxation |
| LRGA | Lagrangian relaxation and genetic algorithm |
| LRPSO | Lagrangian relaxation and particle swarm optimization |
| LS-GA | Lagrangian search and genetic algorithm |
| MFO | Moth flame optimization |
| MILP | Mixed-integer linear programming |
| MINLP | Mixed-integer nonlinear programming |
| MO | Multiobjective |
| MO-CHPUC | Multiobjective CHPUC |
| MOOP | Multiobjective optimization problem |
| MO-PBCHPUC | Multiobjective profit based combined heat and power unit commitment |
| MO-UC | Multiobjective unit commitment |
| MPSO | Binary particle swarm optimization with bit change mutation |
| NACO | Nodal ant colony optimization |
| NLP | Nonlinear programming |
| NP | Nondeterministic polynomial |
| PABC | Parallel artificial bee colony |
| PBCHPUC | Profit based combined heat and power unit commitment |
| PBUC | Profit based unit commitment |
| PL | Priority list |
| PNACO | Parallel nodal ant colony optimization |
| PPSO | Parallel particle swarm optimization |
| PSO | Particle swarm optimization |
| PV | Photovoltaic |
| PV-CHP | Photovoltaic and combined heat and power |
| RES | Renewable energy resources |
| RP | Random perturbation |
| RP-PBUC | Ramp rate constrained profit based unit commitment |
| RP-THUC | Ramp rate constrained thermal unit commitment |
| SA | Simulated annealing |
| SCA | Society civilization algorithm |
| SCUC | Security constrained unit commitment |
| SGA | Standard genetic algorithm |
| SGA | Standard genetic algorithm |
| SM | Seeded memetic |
| SMO | Spider monkey optimization |
| SOC | States of charge |
| ST | Steam turbine |
| TC | Total operating cost |

# GLOSSARY OF ACRONYMS (Continued)

| **Acronym** | **Description** |
|---|---|
| THUC | Thermal unit commitment |
| TS | Tabu search |
| TSGA | Two-stage genetic based technique |
| TS-IRP | Tabu search improved random perturbation |
| TS-RP | Tabu search-random perturbation |
| UC | Unit commitment |
| UCC-GA | Genetic algorithm based on unit characteristics |
| WS | Weighted sum |

# ABSTRACT

Electricity plays a significant role in community life and the development of various sectors of the economy. The standard of living and growth of any country depends on the per capita electric energy consumption. In the past decades, electricity demand has been increased gradually, due to industrialization, modern transportations demand, domestic appliances, etc. Therefore, the dependency of electricity generation from coal and petroleum-based power plant has been increased in the electric systems. The electric power systems consist of generation, transmission, and distribution systems. In the electric power systems, the large number of thermal power plants is connected to different load centers through the transmission network. Hence, the study of the generation system having multiple types of generating units is a challenging task for utility planners. The thermal units take some time to start-up/shut-down the generation. Moreover, the power generation from thermal units depends on the ramp-up/ramp-down rate of generators. Because of this, utility companies need an optimum *unit commitment* (UC) decision in advance when to turn ON or OFF the generating units. The main objective of the UC problem is to minimize the total system production cost of thermal units with the satisfaction of power system constraints. The UC problem is subjected to various constraints such as the generation capacities, ramp rate limit, minimum up/down time, and reserve requirement. The day-ahead UC is a mixed-integer nondeterministic, polynomial, and highly dimensional hard problem of electric power systems. In electric power systems, the optimum UC schedule of generating units has played an important role in the saving of fuel cost. In the current scenario, the structure of the power system is transforming from the conventional centralized system to the deregulated environment. In the deregulation environment, the *generation companies* (GENCOs) act as a service provider, and the main motive of GENCOs is to achieve the maximum profit. Hence, the focus of researchers has been transformed from the UC problem to *profit based unit commitment* (PBUC) problem.

The demand of steam, hot water, and heated households has increased drastically in various countries. The power sector is modernized due to an increase in power and heat demand in the modern world. In order to fulfill the needs of industries and public demand, the *combined heat and power* (CHP) units have been installed by the western

world and developing countries. The cogeneration unit has higher energy conversion efficiency, short ramp limits, and start-up/down periods as compared to thermal units. The CHP unit has additional flexibility, such as heat storage facilities and the variable ratio of heat to power output. Based on the variable heat to power output ratio, two modes of CHP unit, *i.e.*, extraction and backpressure have been defined. In extraction mode, the *dual mode combined heat and power* (DM-CHP) unit provides the flexible power generation, whereas, in the backpressure mode, it has high heat generation capacity. In the current scenario, still, fossil fuels are predominant for power and heat generation. The generation from fossil fuels has two major drawbacks: the eventual depletion of fossil fuels and the release of pollutants emission. In order to overcome these drawbacks, the focus of the power industry is toward the participation of *renewable energy sources* (RESs). In the power system operation, to unlock the full potential of CHP with RESs, significant attention has been given to solve the UC problem of a cogeneration system. The *combined heat and power unit commitment* (CHPUC) problem is a more challenging and complicated task as compared to the *thermal unit commitment* (THUC) problem, both in a conventional and deregulated environment, due to interdependency of heat and power units during the operation of the cogeneration system. Due to growing environmental concerns, the CHPUC and *profit based CHPUC* (PBCHPUC) problem have considered the pollutants emission as an important objective and hence, single objective UC problem has been extended as a *multiobjective* (MO) optimization problem.

The UC is a nonlinear, mixed-integer, and highly constrained optimization problem. The various conventional methods such as *Lagrange relaxation* (LR), *dynamic programming* (DP), and *mixed-integer linear programming* (MILP) techniques have been successfully applied to solve the THUC problem. In conventional search techniques, the search quality depends on the initial point of search, and it also requires certain presumptions. However, such techniques do not require any derivative information and can be applied to solve discontinuous, non-linear, and multimodal optimization problems. Further, these search techniques require high computational time for large-size, multimodal optimization problems due to their local search capabilities. In order to overcome the limitations of conventional search techniques, researchers have proposed global optimization techniques.

The power system researchers have extensively applied various global search techniques to solve the UC problems. The global search techniques have excellent exploration capability; however, the convergence rate of these techniques is very slow as it approaches the optimal best solution. For the large-scale UC problem, the number of fitness function evaluations required by global search techniques increases drastically, hence faces a high computational burden. In order to achieve a global optimal solution with a minimal computational burden, there is a need of hybrid optimization techniques to solve the UC problem. The hybrid optimization techniques search the optimum solution based on their knowledge regarding the behavior of the function and experience and do not follow a set of the predefined path. The proper balance is maintained between exploration and exploitation in hybrid optimization techniques. The hybrid optimization technique is able to solve the nondeterministic polynomial hard constraint optimization problem. The researchers have explored hybrid search techniques to solve the *multiobjective unit commitment* (MO-UC) problems. In MO optimization problems, the objective functions are conflicting in nature, and there is no single solution exists for simultaneous optimization of objective functions. Hence, the number of Pareto optimal solutions are present in the MO problems. The solution of one objective function cannot be improved without degrading other objective functions is called a non-dominated solution. Therefore, the MO optimization technique has been applied to find the most satisfying the non-dominated solutions in the presence of trade-offs between two or more conflicting objectives.

The intent of the thesis is to cover the problem formulation of *unit commitment* (UC) for the thermal units only as well as for the cogeneration system with due consideration of *dual mode combined heat and power* (DM-CHP) units. Further, the solar photovoltaic and energy storage units are also considered in the *combined heat and power unit commitment* (CHPUC) problem formulation. In addition to that, the UC problem is solved to minimize operating cost under regulated environment as well as to maximize the profit of GENCOs under a deregulated environment. In the current scenario, utility planners not only optimize operating cost and GENCOs profit objective, however, they are also bound to minimize the pollutants emission. Due to conflicting objectives, the unit commitment problem has been framed as a multiobjective optimization problem. Further, the significant contribution of research work relates to the solution methodology for the unit commitment optimization problem. The nature-inspired *binary particle swarm optimization* (BPSO) and *particle swarm optimization* (PSO) (BPSO-PSO) technique has applied to deal with binary and real variables of the UC problem, respectively. In order to achieve a global optimal solution with the least computational burden, the hybrid optimization technique is also proposed. The hybrid optimization technique is based on the integration of conventional and global search techniques that has the advantages of both search techniques. The *civilized swarm optimization* (CSO) is undertaken as a hybrid optimization technique. The CSO technique is based on PSO with a *society civilized algorithm* (SCA). The combination of PSO and SCA algorithm maintains the proper balance between exploration and exploitation capability of the algorithm. The *binary successive approximation* (BSA) technique is applied to deal with binary variables of the UC problem. The BSA technique has less number of function evaluations. In this work, the optimization technique integrates BSA and CSO techniques to achieve a global optimal solution with the least computational burden. The proposed optimization technique is applied to solve various types of unit commitment problems and results are compared with other state-of-art optimization techniques. For the multiobjective optimization problem, the fuzzy membership function is used to club different objectives, and the cardinal priority ranking method is used to select the best non-dominated solution. The effect of extraction and backpressure mode of CHP unit has been analyzed in terms of cost, pollutant emission, and system flexibility. The effect of solar photovoltaic and energy storage units on the commitment status of CHP, thermal, and heat units have been examined. The brief discussion regarding each chapter of the thesis is presented in the following sub-sections.

The significant contributions of several researchers related to the UC problems and its various aspects have been briefly reviewed in Chapter-1. The theoretical and computational backgrounds of various local, and global optimization techniques are studied, which are employed in the present study to determine the solution of the optimization UC problem.

In Chapter-2, the *thermal UC* (THUC) problem has been solved by the proposed *binary successive approximation and civilized swarm optimization* (BSA-CSO) technique. In the proposed technique, the BSA technique is used to deal with the binary variables, and the CSO technique searches the generation schedule of the committed units. In order to satisfy the various operational constraints of the UC problem, the heuristic method is applied. Two small size test systems have been undertaken and results reveal that the proposed ‘BSA-CSO’ technique is superior as compared to other state-of-art techniques. To check the statistical performance of the BSA-CSO technique, Wilcoxon signed-rank test is applied, and the performance of the proposed technique found satisfactory.

In Chapter-3, the *profit based UC* (PBUC) problem is formulated for the restructured power system. In this system, the aim of *generation companies* (GENCOs) is to maximize profit by generating and distributing electricity. The BSA-CSO optimization technique has been applied on the profit based THUC problem, and the performance is compared with the BPSO-PSO optimization technique. The three test systems have been undertaken, and obtained results have been compared with other published results and are found satisfactory. It has been found that the BSA-CSO optimization technique has attained a global optimum solution with the satisfaction of operational constraints for three PBUC test systems. Further, the quality of the solution is very less sensitive to the parametric variation of the hybrid optimization technique.

In Chapter-4, the THUC problem formulation is extended to the dual mode CHPUC problem. The dual mode CHPUC model consists of backpressure and extraction mode of CHP units. The backpressure and extraction mode of the CHP unit has variable heat to power output ratio and diverse feasible operating region. The *multiobjective CHPUC* (MO-CHPUC) and *multiobjective profit based CHPUC* (MO-PBCHPUC) problem are addressed, in which operating cost and GENCO's profit are optimized along with pollutants, respectively. The BSA-CSO technique is applied to search the optimal results, and the BPSO-PSO technique has also been implemented. In the multiobjective framework, a fuzzy membership approach unifies the different objectives. The cardinal priority ranking method decides the best-satisfied non dominated solution among Pareto optimal solutions. The three test systems have been undertaken to examine the impact of dual mode CHP unit on an optimum unit commitment schedule. It has been examined from results that the backpressure and extraction mode of dual mode CHP unit has a significant impact on operating cost, GENCOs profit, and pollutants emission of the combined system.

In Chapter-5, the dual mode CHPUC model is integrated with solar photovoltaic and energy storage units. The proposed BSA-CSO technique has been implemented to solve the integrated CHPUC problem. Three integrated CHPUC test system have been considered. The study reveals that the energy storage and DM-CHP units have a significant impact on fuel cost.

In this thesis, the validity and effectiveness of the proposed BSA-CSO method have been extensively verified and numerically tested by analyzing small, medium, and large THUC and PBUC problems. The performance of the proposed optimization technique is compared with the reported results in the literature. Further, the CHPUC, PBCHPUC, MO-CHPUC, and integrated CHPUC problems have also been solved with the consideration of the DM-CHP unit. Finally, the main conclusions and contributions of the thesis are presented and suggestions for the future of research in this field are indicated.

# CHAPTER – 1

# INTRODUCTION

## 1.1 INTRODUCTION

In the modern world scenario, electricity demand has been increased globally due to industrialization, agriculture, commercialization, electric cars, high-speed bullet trains, and domestic appliances. Therefore, to meet the electricity demands, the generation plant with higher capacity is required. Though the electricity generation at large extent is a very challenging task of power system operation and it can be possible with proper planning of the generation plants. In electric power systems, the planning and operation of the generating plants have an important role in electricity generation. The economical operation of large generating plants requires generation scheduling. One of the prime activities in the scheduling of generating units is the turning ON and OFF of units. The commitment of generating units provides a significant saving in operating costs. The turning ON/OFF of units and power schedule of committed units in an economical manner with respect to time is known as *unit commitment* (UC). The UC is one of the main problems of electric power systems. The aim of the UC problem is to minimize the total operating cost by the ON/OFF status of generating units for power generation **(Wood *et al.*, 2013)**. The UC problem is subjected to many physical constraints such as the generation capacities, minimum up/down time, energy demand, spinning reserve requirement, and ramp-up/ramp-down rate of generators **(Ongsakul and Vo, 2013)**. The UC is a challenging task that saves millions of dollars annually in terms of fuel cost. Moreover, amongst the various type of generating plants **(Wood *et al.*, 2013)**, a thermal based power plant plays a major role in electricity generation. Thus, the scheduling of the thermal units or *thermal unit commitment* (THUC) is the main concern of the researchers. The main motive of the THUC problem is to reduce the operating cost of electricity generation from thermal units. Now, in the deregulation environment, the restructuring of power systems has been carried out in which the major challenges are the planning, operation, and control of *generation companies* (GENCO's). In the deregulated electricity market, GENCOs are trying to maximize the profit by generating and selling electricity **(Ongsakul and Vo, 2013**). In conventional electric power systems, the main aim of the

UC problem is to minimize the cost, whereas, in the deregulated electricity market, the main aim of *profit based unit commitment* (PBUC) problem is to maximize profit. The profit and operating cost of power systems also dependent on the heat requirement in industrial purpose, drying, space, and water heating, and cooking in the building sectors.

The demand of steam, hot water, and heated households has risen drastically in various countries **(Jensen, 2010)**. In order to fulfill the public heat demand, the *combined heat and power* (CHP) and heat plants are installed. The CHP is one of the well-established, reliable, and affordable technologies for the generation of heat and power **(Kerr, 2010)**. According to the G8 summit and International Energy Agency report, the electricity generation from the CHP unit has reduces the emission level and escalates the finical benefit of the electric power utility **(Kerr, 2008)**. In addition, the generation flexibility of the CHP units are increased by heat storage facilities. Further, the cogeneration units have been upgraded by replacing the single-shaft turbine with multi-shaft turbines, which is known as *dual-mode CHP* (DM-CHP) **(Breeze, 2019)**. The DM-CHP unit can operate in extraction and backpressure mode. These operating modes have different characteristics, such as the flexible power generation provided by extraction mode and high heat generated capability during backpressure mode. In modern power systems, the utilization of CHP units has been increased drastically. In order to utilize the CHP units effectively, the *combined heat and power unit commitment* (CHPUC) is an emerging area for power system researchers. The CHPUC problem is a complicated task as compared to the THUC problem. In the deregulated environment, the CHPUC problem has been changed to a *profit based CHPUC* (PBCHPUC) problem.

The heat and power generation from the thermal, DM-CHP, and heat units produces a significant amount of harmful pollutant emission that affects entire living beings. Hence, it is necessary to minimize the harmful emission emitted during the heat and power generation from the generating units **(Kothari and Dhillon, 2011)**. Environmental pollution leads to an increase of the emission problem in electric power systems. Hence, the reduction of environment pollution is an additional challenging task for the researchers in the UC problem. Researchers have given attention to *multiobjective combined heat and power unit commitment* (MO-CHPUC) problem, in which emission and cost are minimized, simultaneously. Though the fossil fuel based generating units have economic and environmental problems, therefore the main aim in the electric power system is to find a suitable alternative. The most effective way to reduce emissions and fossil fuels usage is to increase the participation of renewable energy sources (RESs) with energy storage facility. From the last two decades, the power generation from RESs are accelerated to meet global electricity demand growth. In Germany, the power generation from RESs exceeded the power generation from coal-fired units. Therefore, the inclusion of RESs and *energy storage unit* (ESU) with CHPUC problem is one of the most challenging optimization problems in the electric power system **(Sadeghian and Ardehali, 2016)**.

As aforementioned, due to the consideration of RESs and *energy storage unit* (ESU) with thermal units, the dimensions of the generating units are increasing. Therefore, the mathematical representation of the UC problem is complex, which includes discontinuous, non-differential, and high dimensional functions. Moreover, the UC problem involves binary and continuous decision variables, hence the UC is a mixed-integer optimization problem **(Wang and Shahidehpour, 1993)**. Researchers have conducted extensive studies on effective optimization techniques to find the optimum UC decisions for power system operations. In the past decades, researchers have employed classical optimization methods such as *Lagrange relaxation* (LR) **(Guan *et al.,* 1992)**, *dynamic programming* (DP) **(Fan *et al.,* 2002)**, *nonlinear programming* (NLP) **(Kim and Edgar, 2014)**, *mixed-integer linear programming* (MILP) **(Zhai *et al.,* 2009)**, and *priority list* (PL) **(Kothari and Ahmad, 1995)** to solve the UC problem. These methods are usually dependent on starting point or require certain presumptions, hence there is a possibility to stuck solution in local optima **(Rao, 1996)**. Global search algorithms emerge as effective optimization tools for the UC problem **(Guan *et al.,* 1992; Wang and Shahidehpour, 1993)**. The global search techniques such as *evolutionary programming* (EP) **(Jeong *et al.,* 2009)**, *genetic algorithm* (GA) **(Ma *et al.,* 1995)**, *particle swarm optimization* (PSO) **(Zhao *et al.,* 2006)**, and *differential evolution* (DE) **(Uyar *et al.,* 2011)** have been explored by researchers.

The global search techniques result in lower accuracy and increase the computational burden for high dimensional optimization problems **(Khan *et al.,* 2019)**. Therefore, to improve the accuracy of the optimization technique with the minimal computational burden, hybrid optimization techniques are developed by the researchers **(Peska *et al.,* 2019)**. The hybrid optimization algorithm is based on the integration of two or more techniques that operate collectively and maintain the proper balance between diversification and intensification **(Selvakumar and Thanushkodi, 2009)**. However, these optimization techniques are used to solve the single objective problems. Hence, for multiobjective problems, multiobjective optimization techniques are introduced.

In the *multiobjective* (MO) problem, no single solution exists that simultaneously optimizes each objective of the MO problem. Due to multiple Pareto optimal solutions in the MO problems, the complexity of the MO problem is more as compared to the conventional single-objective optimization problems. In order to solve the MO optimization problem, various classical numerical methods have been applied. The classical numerical methods are stuck into local optimum solutions for large scale MO optimization problems. Researchers have also suggested various MO evolutionary algorithms to solve the MO problems **(Qu *et al.*, 2018)**. These algorithms are not capable to the find best compromise solution of the MO problems. The ultimate goal of the MO optimization technique is to achieve the conflicting goals of the MO problems. A fuzzy based MO optimization techniques have been applied by researchers **(Agrawal *et al.*, 2008)**. The fuzzy based method has the capability to search the best compromise solution of the MO problems. A fuzzy based MO optimization techniques showed its robustness and reliability while dealing with the MO problems **(Hota *et al.*, 2010)**.

## 1.2 UNIT COMMITMENT PROBLEMS

The electric power system consists of the number of generating units which are integrated to different load centers through the transmission network. The generating units such as thermal, cogeneration, heat, and RES units have played an important role in the power sector. In order to utilize the thermal, heat, CHP and RES units more economically, the UC of generating units is used in electric power systems. The objective of the UC problems is to determine both power generation and heat production from units by minimizing the fuel cost and emission. Further, deregulation in the electric power systems is increasing worldwide day by day, hence the major changes are carried out in the planning, and operation of the vertically integrated electric power systems. In the deregulated environment, the minimization of operating costs in the UC problem has been renovated into the maximization of profit in the PBUC problem. A brief overview of the different UC models is presented in the following sub-sections.

### 1.2.1 Thermal Unit Commitment

Globally, the power generation sector is rapidly growing due to an increase in demand of industrial, agriculture, and commercial sectors. In order to meet demand, the large number of thermal power units are connected to different load centers through the transmission network in the electric power system. A coordinated action plan is necessary for utility planners to execute programs for the proper generation scheduling to meet demand at each sub-interval. The UC collectively performs the 'ON/OFF' of generating units and schedules the committed units to search the optimum generation schedule in an economical manner **(Guan *et al.*, 1992)**. The main objective of the THUC problem is to minimize the production cost with the satisfaction of load demand, spinning reserve requirement, and inequality constraints. The inequality constraints include minimum on and off time limits, power capacity, ramp up/down, and prohibited operating zone of generating unit and fuel constraints **(Cohen and Wan, 1987)**. The stochastic nature of the load and unavailability of the generator decline the system reliability, and it is handled with consideration of spinning reserve. The THUC problem bounded by all equality and inequality constraints is a real-world *nondeterministic polynomial* (NP) hard constraint optimization problem.

Over the last decade, researchers have extensively applied classical and global search optimization techniques to solve the THUC problem. Aoki *et al.* **(1987)** have applied the LR technique to find the optimum solution of the large-scale UC problem considering fuel constrained and pumped-storage hydro units. They have also applied the subgradient 'variable metric method' to update Lagrange multipliers to reduce the computational time. Cohen and Wan **(1987)** have investigated the fuel constrained THUC problem by the implementation of Lagrangian decomposition and successive approximation techniques. Guan *et al.* **(1992)** have solved the THUC problem by a mathematical tool based on the LR technique. Dieu and Ongsakul **(2006)** have applied the enhanced augmented Lagrangian Hopfield algorithm to search the optimum UC schedule of generating units. Tseng *et al.* **(2000)** have introduced LR and unified de-commitment method for the THUC problem. The hybrid approach based on variable neighborhood search and LR technique has been applied to find the UC schedule **(Wang *et al.*, 2011)**. A brief survey on the different classical optimization techniques for the THUC has also been presented by Sen and Kothari **(1998)**. Most of the classical methods have limitations to provide the optimum solution for non-differential, discontinuous, and high dimensional problems **(Sen and Kothari, 1998)**.

In order to solve non-differential and discontinuous problems, researchers have solved the UC problem by making decisions sequentially at different points of time. Kothari and Ahmad **(1995)** have presented a hybrid expert system (PL method) and the DP technique to solve the THUC problem. The THUC problem has been solved by the implementation of the LR technique with a constructive DP technique **(Fan *et al.*, 2002)**. The DP technique has ability to deal with non-convex, discontinuous, and non-differentiable functions. However, the DP technique suffers from a major drawback, known as the "curse of dimensionality". To overcome this limitation of DP, several techniques have been proposed, *i.e.*, benders decomposition **(Niknam *et al.*, 2009)**, constraint oriented neighborhoods method **(Viana *et al.*, 2008)**, branch and bound technique **(Lauer *et al.*, 1982)**, MILP techniques **(Zhai *et al.*, 2009)**, PL **(Senjyu *et al.*, 2003)**, *mixed integer programming* (MIP) **(Yang *et al.*, 2015)**. Tan and Shaaban **(2016)** have solved the THUC problem by projected disjunctive MILP reformulation. Yang *et al.* **(2017)** have proposed a Multi-cuts outer approximation method that decomposes the UC problem into a MILP master problem, which reduces the time consumption. Miyamoto *et al.* **(2016)** have applied Walrasian auction to solve distributed THUC problem. Cardenas *et al.* **(2016)** have solved the UC problem using a polyhedral-based approach. However, these techniques stuck at local optima for high dimensional problems and increase the computational time.

Researchers have proposed an alternative approach, which is efficient and flexible than classical methods are global search optimization techniques. Jeong *et al.* **(2009)** have applied a quantum-inspired EP based approach for the THUC problem. Duo *et al.* **(1999)** have implemented an approach, which combines LR principle and EP for short-term THUC problem. The main drawback of EP is a slower convergence rate and high computational burden for multimodal functions and high dimensional problem. Hence, another method in the optimization research field has been explored by researchers. The GA is well suited for finding the global optimum solution of the THUC problem **(Ma *et al.*, 1995; Kazarlis *et al.*, 1996; Swarup and Yamashiro, 2003; Dudek, 2004; Abookazemi *et al.*, 2011; Lazo *et al.*, 2011)**. In order to solve mixed-integer THUC problem, Sheble *et al.* **(1994)** have introduced the hybridization of a GA and different PL methods to provide the optimum solution for the THUC problem. An algorithm based on the integration of the GA and tabu search technique has been implemented to the THUC problem **(Mantawy *et al.*, 1999)**. However, these techniques are not always effective to deal with larger-scale real-world NP-hard THUC problem **(Guan *et al.*, 1992; Sumim and Ongsakul, 2003)**.

The PSO and some of its variants have been applied to solve the THUC problem **(Zhao *et al.*, 2006; Kuo *et al.*, 2011; Wang and Singh, 2009)**. Researchers have applied different versions of PSO, such as quantum PSO **(Jeong *et al.*, 2010)**, elite PSO **(Chen,**

**2012)**, improved BPSO **(Yuan *et al.*, 2009)** algorithms to solve the THUC optimization problem. In swarm based techniques, the computational burden increases with an increase in population size. In order to reduce the computational burden, Amiri *et al.* **(2013)** have applied the PL method and PSO algorithm to find the optimum solution of the THUC problem. Yuan *et al.* **(2009)** have explored the improved *binary PSO* (BPSO) method to search the optimum generation schedule for the THUC problem, in which the BPSO technique has been integrated with the lambda-iteration method. Yu and Zhang **(2014)** have developed a hybridization of LR and PSO to solve the UC problem. The performance of the synergy of PSO with other techniques is better than conventional PSO techniques. However, one of the major problem is the selection of parameters in the PSO-PL, PSO-LR, and BPSO techniques. Uyar *et al.* **(2011)** have investigated the DE algorithm for the UC problem. Datta *et al.* **(2012)** have solved the UC problem by the implementation of binary-real-coded DE algoritm. Yuan *et al.* **(2009)** have investigated enhanced discrete DE with the Lambda-iteration method to deal with the THUC problem. Liao **(2006)** has implemented an immune algorithm with the annealing immune method to solve the THUC problem. Victoire *et al.* **(2006)** have developed a hybrid technique based on the integration of Tabu search, PSO, and sequential quadratic programming method to find the UC and generation schedule of thermal units.

Currently, the field of optimization is evolving very fast, and researchers are trying to get the optimum solution in a quick time. Researchers have implemented global search optimization techniques, such as ant colony system **(Simon *et al.*, 2006)**, memory-bounded ant colony system **(Saber and Alshareef, 2008)** and binary real coded firefly **(Chandrasekaran and Simon, 2012)**, the binary coded artificial bee colony **(Chandrasekaran *et al.*, 2012)** to solve the UC problem. Other widely known nature inspired optimization techniques such as quasi-oppositional teaching-learning **(Roy and Sarkar, 2014)**, binary gravitational search **(Yuan *et al.*, 2014)**, *imperialist competitive algorithm* (ICA) **(Saber *et al.*, 2016)** and binary coded modified *moth flame optimization* (MFO) **(Reddy *et al.*, 2018)** have been applied to solve the UC problem.

Recently researchers have worked on real-world models of THUC such as dynamic ramping model **(Posada *et al.*, 2017)**, risk-limiting UC **(Peng *et al.*, 2017)**, structural model for self-commitment **(Camelo *et al.*, 2018)**, security-constrained UC (SCUC) **(Alvarez *et al.*, 2018)**, and stochastic UC **(Mantawy, 2004; Haberg, 2019; Zhu *et al.*, 2019)** problems. Bruninx and Delarue **(2017)** have proposed the THUC model including endogenous probabilistic reserve sizing and allocation. Researchers have solved the *ramp-rate constrained THUC* (RP-THUC) problem by various optimization techniques. The RP-THUC problem has been solved by augmented Lagrange Hopfield network based LR and improved PL technique **(Dieu and Ongsakul, 2008)**. Dieu and Ongsakul **(2011)** have solved the RP-THUC problem by *Annealing Hopfield Lagrange neural network* (AHLN). In another attempt, Dieu and Ongsakul **(2006)** have presented an enhanced merit order based AHLN to solve the RP-THUC problem. Researchers have applied artificial intelligence technique with DP **(Wang and Shahidehpour, 1993)**, DE **(Patra *et al.*, 2008)**, modified binary artificial bee colony **(Singhal *et al.*, 2015)** technique to deal with ramp-rate constrained UC problem. The review of literature of the past several years has contributed to the global optimum solution, convergence rate, and computational aspects of optimization techniques for the THUC problem. Zheng *et al.* **(2015)** have discussed future research in the field of the UC problem. In recent years, the focus of research has been transformed from traditional UC problem to CHPUC, PBUC, and integrated UC problems.

### 1.2.2 Profit Based Unit Commitment

Traditionally, a power market has focused on the THUC problem. In 1996, the federal energy regulatory commission is formed to encourage the competitiveness between regional electricity markets to increase the efficiency of the generation, transmission, and distribution of power, with lower offer prices and higher quality, increased reliability and security **(Kumar *et al.*, 2016)**. Hence, the system is transforming from traditional to the deregulated environment. In the restructured electricity market, the aim is to maximize the profit of GENCOs by producing and selling the electricity with the satisfaction of constraints **(Ongsakul and Vo, 2013; Yamin *et al.*, 2007; Jain and Jain, 2009)**. In the deregulated power system, the UC problem is a vital optimization problem **(Yamin *et al.*, 2007)**.

From the last few decades, various optimization techniques have been implemented to search the most profitable solution for the PBUC problem. Kumar *et al.* **(2018)** have analyzed the impact of electricity generation in the power system market. A hybridization of LR and EP techniques has been applied to solve the PBUC problem by considering the reserve uncertainty **(Yamin *et al.*, 2007)**. The researchers have also investigated global and hybrid optimization approaches to find the optimum solution of the PBUC problem. Raglend *et al.* **(2010)** have solved the PBUC problem by the implementation of various

PSO techniques such as chaotic PSO and dispersed PSO. Columbus *et al.* **(2012)** have solved the PBUC problem using nodal ant colony and *parallel artificial bee colony* (PABC) optimization technique **(Columbus and Simon, 2012)**. Sharma *et al.* **(2013)** have implemented an intelligent multi-agent algorithm to find the UC schedule of the PBUC problem. The *binary fireworks algorithm* (BFWA) **(Reddy *et al.*, 2016)**, the binary grey wolf **(Reddy *et al.*, 2019),** and binary fish swarm optimization **(Singhal *et al.*, 2015[1])** techniques have been implemented to solve the PBUC problem. The improved pre-prepared demand table and memory management algorithm **(Syed and Gopalakrishnan, 2016)**, improved teaching-learning based algorithm **(Krishna and Rao, 2016)**, and improved bacterial foraging algorithm **(Selvakumar *et al.*, 2016)** have been applied to find UC schedule of PBUC problem. Columbus *et al.* **(2013)** have introduced the PABC technique to solve the RP-PBUC problem. Dimitroulas and Georgilakis **(2011)** have applied a memetic algorithm for the PBUC problem with consideration of ramp rate constraint. The RP-PBUC problem has been solved by the BFWA technique **(Reddy *et al.*, 2016)**. The global optimization techniques are sensitive to parameter settings and may converge to the local optima solution. In order to overcome these problems, the ICA with an EA technique has been applied to solve the PBUC **(Ghadi *et al.*, 2016)** and the RP-PBUC problem **(Ghadi *et al.*, 2016[2])**. Sudhakar *et al.* **(2017)** have solved the PBUC problem by the LR-DE method.

### 1.2.3 Cogeneration Based Unit Commitment

In the modern world, the power industry has been modernized to fulfill customer power and heat demands. The few industries require steam and power for their process, *i.e.*, pulp and paper mills, aluminum plants, refineries, and chemical plants **(Jensen, 2010)**. In order to fulfill the public heat demand, the heat and power generation from CHP units has been increased in electric power systems **(Kerr, 2010)**. The CHP unit enhances the energy supply efficiency and utilizes the waste heat for energy generation **(Jensen, 2010)**. Furthermore, the process of heat and power generation from the CHP unit has less impact on the environment **(Kerr, 2010)**. The cogeneration has been recognized as a proven, efficient, reliable, and cost-effective energy option. Another important feature of CHP is its flexible operation and short ramp-up/-down, start-up/-down periods **(Kerr, 2008)**. The G8 summit also acknowledged the impact of cogeneration by suggesting “adapting instruments and measures to significantly increase the share of CHP in the generation of electricity" **(Mitra *et al.*, 2013)**. The potential of CHP developments has been observed throughout the world and reported by the International Energy Agency.

The cogeneration units are up-gradated by different steam turbine CHP units **(Kerr, 2010)**. The hybridization of extraction and backpressure steam turbine is known as DM-CHP **(Breeze, 2019)**. The researchers have worked on the cogeneration model that consists of the multiple-steam turbine **(Yang and Zhai, 2018)**. The operating mode of the DM-CHP unit provides flexible heat generation when the penetration level of heat demand is high or low **(Veerapenand and Beerepoot, 2011)**. The CHP unit in extraction mode operation provides flexible power, which helps to overcome the unpredictability of renewable resources and load demand **(Brand *et al.*, 2004; Veerapenand and Beerepoot, 2011; Zhang *et al.*, 2018)**. Wang *et al.* **(2015)** have investigated the DM-CHP unit based on the thermodynamic cycle and obtained the generation schedule by the MIP algorithm. Liu *et al.* **(2009)** have applied the MIP algorithm to obtain the optimum generation schedule of the CHP unit. It has been verified by researchers that combined heat and power system provides higher generation flexibility to larger electrical fluctuation **(Chen *et al.*, 2015; Wang *et al.*, 2015)**. The utility planners of various countries are trying to upgrade their strategies to provide the available heat and power at an affordable level under the legal framework **(Rong and Peter, 2018)**.

The optimum generation schedule, UC, integrated operation with other generating units, different operating modes, efficiency, and generation flexibility are some of the emerging areas of cogeneration units. The focus of the research work is to solve the fundamental problem such as UC of CHP, heat, and power generating units. Due to the interdependencies of heat and power in CHP, the CHPUC problem is a more complicated task as compared to the THUC problem. The author has covered a literature survey on a few of the important aspects of CHP related to the cogeneration unit. The efforts have been made by system operators to search the optimum UC schedule of the cogeneration system **(Wang *et al.*, 2017)**. From the last decade, researchers have applied various optimization techniques to solve the CHPUC problem. Kim and Edgar **(Kim and Edgar, 2014)** have applied a *mixed-integer nonlinear programming* (MINLP) approach to solve the UC problem of CHP units. They have considered various practical constraints, *i.e.*, minimum/maximum power output, steam flow restrictions, minimum up/down times, start-up and shut-down procedures, and fuel limits. The CHPUC problem has been solved by the implementation of various variants of the DP algorithm **(Rong *et al.*, 2008)**. Rong *et al.* **(2009)** have applied an improved unit de-commitment algorithm to solve the

CHPUC problem. Rong *et al.* **(2009)** have solved the CHPUC problem by the employment of dynamic regrouping based on a sequential DP algorithm. In another attempt, a dynamic regrouping-based DP algorithm **(Rong and Peter, 2018)** has been applied to solve the transmission-constrained multi-site CHPUC problem. Ommen *et al.* **(2014)** have applied linear, mixed-integer, and non-linear programming methods to obtain a generation schedule of heat and power. The UC and generation schedule of CHP-thermal-heat unit has been obtained by two-stage *stochastic MILP* (SMILP) **(Kia *et al.*, 2017[2])**. The heuristic-deterministic based algorithm has been applied to solve the emission constrained CHPUC problem **(Nazari and Ardehali, 2017)**. An efficient algorithm has been applied to solve the SC-CHPUC problem **(Rong and Lahdelma, 2017)**. The SC-UC problem incorporating the district heat network has been solved by the implementation of the LR-MILP algorithm **(Li *et al.*, 2016)**. Hermans *et al.* **(2018)** have investigated the UC model comprises of fast start-up capabilities CHP having multiple operating modes and finds that significant reduction of fuel cost and improvement of generation flexibility. It has been verified by Wogrin *et al.* **(2016)** that the operational flexibility of the generation has increased by consideration of DM-CHP units. Chen and Wang **(2017)** have applied a modified MIP algorithm to optimize the CHP unit based SCUC problem. In the past years, researchers have also worked on the *profit based CHPUC* (PBCHPUC) problem. The Benders decomposition method has been applied to solve the PBCHPUC problem **(Sadeghian and Ardehali, 2016)**. Aghaei *et al.* **(2016)** have applied information-gap decision theory for dealing with uncertainty in the pool price operation of the CHPUC problem. An affinely adjustable robust optimization technique has been applied to obtain the optimum UC schedule of heat and power units for energy trading **(Zugno *et al.*, 2016)**. As per the best of author knowledge, no literature is available on DM-CHPUC and DM-PBCHPUC problem.

### 1.2.4 Unit Commitment of Integrated System

In modern power systems, power generation from RES, such as wind and solar units has been accelerated. The higher penetration of energy generation from RES is a challenging task for the system operator **(Gaing, 2003)**. The economical and technical challenges faced by the system operator in the presence of large-scale PV systems has been presented by Nghitevelekwa and Bansal **(2018)**. The researchers have studied the THUC models with consideration of RES. The UC schedule with RES integration has been investigated by Abujarad *et al.* **(2017)**. Govardhan *et al.* **(2014)** have solved the UC problem incorporation of distributed energy resources. Ummels *et al.* **(2007)** have analyzed the impacts of wind power on the THUC problem. Kumar *et al.* **(2018)** have applied mixed integer nonlinear programming to optimize the RES system. Murty and Kumar **(2019)** have applied the hybrid technique based on the gravitational search algorithm and general algebraic modelling system to solve the integrated RES system. Zhou *et al.* **(2016)** have formulated a UC model that coordinates hydro, wind, and thermal power generation and Benders decomposition technique has been applied to find the optimum generation schedule. A review of operating spinning reserves under the high generation of RES has been presented by Ortega and Watts **(2017)**. They have concluded that generation flexibility has been increased by the *electric storage system* (ESS) **(Kneiske and Braun, 2017)**. Researchers have also analyzed the impact of ESS on the UC models. Yang *et al.* **(2017)** have implemented a hybrid meta-heuristic method to solve the hybrid UC framework that considers RES, ESU, and demand-side management. Saber *et al.* **(2009)** have solved the UC problem in the presence of RES and ESU by the implementation of the PSO technique.

The CHP unit and RES are considered a leading technology in combined heat and power system **(Veerapenand and Beerepoot, 2011)**. Therefore, the system operators of various countries have upgraded their strategies to provide the available generation under permissible framework **(Kasaeiana *et al.*, 2018)**. Koltsaklisa *et al.* **(2017)** have investigated the integrated UC model of Greek interconnected electric systems and applied MILP to search the optimum generation schedule. They have concluded that the system needs generating units having a higher ramping ability in the presence of higher RES penetration. Kneiske *et al.* **(2018)** have developed the combined control algorithm based on a cloud-based application to optimize the PV-CHP system of Germany and concluded that the storage unit has been required to improve system generation flexibility. The optimal schedule of the integrated system comprises of CHP, and ESU unit has been obtained by non-dominated sorting GA-II **(Shang *et al.*, 2017)**. The system generation flexibility has been improved by unlocking the full potential of CHP in the combined PV and heat-power systems **(Kopiske *et al.*, 2017; Wang *et al.*, 2015)**.

### 1.2.5 Multiobjective Unit Commitment

The major worldwide concern is to minimize environmental pollution. Society's demands adequate and secure electricity at the cheapest possible price with less impact on the environment. The significant amount of harmful pollutants produces from the thermal, CHP, and heat units that affect entire living beings. Hence, it is necessary to minimize the harmful emission emits from the generating units. The economic/profit and emission objectives are conflicting objective functions **(Shukla and Singh, 2016[1])**, hence the UC problem has turned to the MO-UC optimization problem. The MO-THUC problem is more challenging as compared to the THUC problem **(Shukla and Singh, 2016[1])**. Several MO optimization techniques have been applied to solve the MO-THUC problem. Shukla *et al.* **(2016)[1]** have applied the weighted sum method to solve the MO-THUC problem and employed an efficient hybrid algorithm to find the optimum generation schedule. In another attempt, Shukla and Singh **(2016)[2]** have employed fuzzy based decision making and search space-based crazy PSO technique to solve the MO-THUC problem. In order to find the best compromise solution of the MO-THUC problem, Wang *et al.* **(2016)** have applied multiobjective particle swarm optimization algorithm and fuzzy set theory. In the combined heat and power system, Nazari and Ardehali **(2017)** have solved the MO-PBCHPUC problem using the weighted sum method with PL method. As per the best of author knowledge, few researchers have worked on the MO-THUC and MO-CHPUC problems.

## 1.3 OPTIMIZATION TECHNIQUES

Nowadays, the optimized decision of planning, operation, and design problems is an important task of real-world problem. From past decades, researchers are constantly working on various optimization techniques to solve optimization problems. In 1950s, the DP method has developed by Richard Bellman. The DP has been implemented in various field of optimization such as aerospace engineering, power system, economics, *etc*. As the complexity and dimension of optimization problems increases, DP fail to converge, and the computational burden is increased. In 1986, Glover has introduced the Tabu search algorithm based on local search **(Glover, 1989)**. In the Tabu search algorithm, the search space is explored by a sequence of moves for all feasible solutions that increase computational burden **(Gandomi *et al.*, 2013)**. The modular nonlinear optimization technique has been applied to solve the optimization problem **(Mbamalu *et al.*, 1995)**.

The conventional method depends on the initial point, and objective function derivative information is required. Researchers have implemented the local search method to solve various optimization problems. The local search method is easy to implement and understand. The hill-climbing is a local search technique that starts with randomly selected initial point and finds the optimum solution by an incremental change to the point. The optimal solution obtained from the hill-climbing method has been stuck into local minima for complex optimization problems **(Gonzalez and Perez, 2001)**. The multi-agent approach has been implemented to solve nonlinear optimization problems with randomly selected initial point **(Rahman *et al.*, 2015)**. In the local search method, the computational burden is high in complex optimization problems **(Saber and Alshareef, 2008)**. Moreover, in the case of highly nonlinear optimization problems local search method may prematurely converge to an unsatisfactory solution. In order to reduce computational burden and avoid local optima, Dhillon *et al.* **(2009)** have proposed the *binary successive approximation* (BSA) technique. Researchers have implemented the BSA to solve optimization problems such as economic load dispatch **(Dhillon *et al.*, 2009)**, multiobjective economic and emission dispatch **(Dhillon *et al.*, 2009)**, design of IIR filter **(Kaur *et al.*, 2015)**. In the BSA technique, the optimum solution has been achieved with less number of function evaluations **(Dhillon *et al.*, 2009)**. The proper selection of the local search method is an effective tool to solve complex optimization problems.

In order to deal with complex optimization problems, global optimization techniques have been developed by researchers **(Khan *et al.*, 2019)**. The optimization technique aim is to achieve a global best solution within a certain limited time cycle. According to ‘no free lunch theorem’, no optimization technique can suppress all other techniques for every problem (**Deb, 2004**; **Rao, 1996**). Form past decades, global search optimization techniques have been used for solving optimization problems. The global search techniques are inspired by nature and evolution, *i.e.,* swarm intelligence, bio-inspired algorithms, physics, and social culture inspired algorithms.

In 1859, Darwinian evolution has been proposed, which is inherently a robust search and optimization tool. Evolutionary algorithms use the “survival of the fittest” principle **(Rao, 1996)**. In evolutionary-based techniques, the population is randomly initialized, and no derivative is required. In order to search for the optimal solution, the *evolutionary strategies* (ES) and *evolutionary programming* (EP) have been explored by the researchers **(Rao, 1996)**. The basic differences between these techniques representation are the reproduction and mutation operators and the selection methods. These methods have drawn much attention in the research community in conjunction with parallel and distributed computations. EP is a useful method of optimization when other techniques such as gradient descent are not possible. One disadvantage of EP in solving some of the multimodal optimization problems is its slow convergence to a good near-optimum.

The biology-inspired algorithms such as GA **(Grefensttete, 1986)**, DE **(Elaziz *et al.* 2019)**, HS **(Li *et al.*, 2019)**, artificial neural network **(Mahmud *et al.*, 2017)** have been developed by researchers to solve optimization problems. In 1960, John Holland introduced GA, which is based on the concept of Darwin's theory of evolution. The GA is based on bio-inspired operators such as mutation, crossover, and selection. The DE is another promising optimization technique explored by researchers. It is also a class of evolution strategy optimizers. The DE has few advantages as compared to other techniques, *i.e.*, only a few parameters to be set, and able to solve high-dimensional complex optimization problems efficiently **(Elaziz *et al.* 2019)**. In 2013, Civicioglu **(2013[1])** has been proposed a *backtracking search optimization* (BSO) algorithm. The *crisscross optimization algorithm* (COA) has been proposed by Meng *et al.* **(2014)**, which is inspired by the Confucian doctrine of gold mean and the crossover operation in GA **(Meng *et al.*, 2016)**.

The culture-inspired algorithms are one of the branches of evolutionary algorithms. The optimization technique that incorporates the social and cultural evolution theory has been known as social culture-inspired algorithms. The social culture algorithms are an extension of the conventional genetic algorithm which has knowledge component in addition to the population. In 1989, a local heuristic search based Memetic Algorithm has been proposed by Moscato, in which the mutation process backed up by a large amount of professional knowledge **(Du and Li, 2020)**. In 2003, Ray and Liew have proposed society and civilized algorithm, which used intra and intersociety interactions within a society and the civilization model. The *society civilization algorithm* (SCA) has high exploitation capability as compared to exploration search capability. The society and civilized algorithm have applied to optimize the welded beam design, speed reducer design, spring design, three-bar truss design, economic load dispatch problem **(Selvakumar and Thanushkodi, 2009)**.

The swarm based algorithms are inspired by the social nature and collective behavior of populations. The swarm individuals cooperate to search for food, necessary for their survival, and also keep safe from other agents **(Gandomi and Kashani, 2018)**. The swarm based optimization techniques such as PSO, firefly algorithm **(Naidu *et al.*, 2014)**, bat algorithm **(Setiadi *et al.*, 2019)**, artificial bee colony **(Chen *et al.*, 2019)**, bacterial foraging based optimization **(Nanda *et al.*, 2009; Tripathy *et al.*, 2007)**, teaching-learning based optimization **(Roy and Sarkar, 2014)**, ant colony optimization **(Vaisakh and Srinivas, 2011)** have been explored by researchers.

In 1995, Kennedy and Eberhart have proposed a bird flocking optimization technique called the "PSO" technique **(Kennedy and Eberhart, 1997; Eberhart and Shi, 1998)**. The PSO has been widely used in various fields to solve different kinds of optimization problems. Many variants of the PSO algorithm have been proposed to maintain or strengthen the diversity, so as to escape from local optima or premature convergence. The literature review on global search optimization techniques *i.e.,* basic PSO and BPSO has been presented by Mahor *et al.* **(2009)**. The PSO technique has an advantage in terms of computational speed. In recent years, some of the promising swarm based optimization techniques have been proposed such as coral reef optimization algorithm **(Yan *et al.*, 2019)**, bacteria foraging optimization **(Tripathy and Mishra, 2007)**, cuckoo search optimization algorithm **(Gandomi *et al.*, 2013; Chitara *et al.*, 2018)**, pigeon inspired optimization **(Jiang *et al.*, 2019)**, ant lion optimizer **(Mirjalili, 2015[1])**, grey wolf optimizer **(Mirjalilia *et al.*, 2016; Sanjay *et al.*, 2017; Mirjalilia *et al.*, 2016)**, artificial cooperative search **(Civicioglu, 2013[2])**. Bansal *et al.* **(2014)** have developed a *spider monkey optimization* (SMO) algorithm, based on fission-fusion social systems. Sharma *et al.* **(2016)** have introduced an improved version of SMO called the "ageist SMO" algorithm based upon the difference in age and other dynamic abilities of spider monkeys. Mirjalili **(2015[2])** has proposed a nature-inspired paradigm called the "MFO" algorithm. The MFO algorithm is based on a navigation method of moths **(Mirjalili, 2015[2]; Jangir *et al.*, 2016)**. In 2016, Mirjalili and Lewis **(2016)** have proposed whale optimization algorithm. The whale optimization algorithm is mostly used to solve optimization problems. Heidari *et al.* **(2019)** have proposed a nature-inspired optimization paradigm called as Harris hawks optimizer.

The physics laws are applied for physical behavior and properties. The optimization techniques inspired by physics laws have been the branch of evolutionary algorithms. The physics inspired algorithms **(Fatma *et al.*, 2019; Javidy *et al.*, 2015; Tamura and Yasuda, 2011)** such as artificial electric field, intelligent water drops, magnetic optimization, gravitational search, central force optimization, Ion's motion, spiral dynamic algorithm, galaxy-based search have been implemented to solve various optimization problems.

Researchers have worked on hybrid optimization techniques. In hybrid techniques, two or more optimization techniques are operated collectively to find the optimum solution of optimization problems. The optimization techniques have common searching features, *i.e.,* diversification and intensification **(Mirjalili, 2015[1])**. The advantage of a hybrid optimization technique is to maintain the proper balance between diversification and intensification. In the past few years, the *civilized swarm optimization* (CSO) algorithm has been received much attention. The civilized swarm technique is the integration of PSO and society civilized algorithms. The PSO has exploration capability, whereas in SCA has exploitation capability. The CSO algorithm has been successfully applied to solve CHPED problem **(Meng *et al.,* 2015)**, and optimal distributed generation allocation with Monte Carlo simulation **(Peng *et al.,* 2015)**. The hybrid optimization technique is able to converge at global optimum and avoid the local optima effectively. The quantum swarm evolutionary algorithm has been proposed in **(Xiao *et al.,* 2009)** which is the hybridization of the quantum algorithm and PSO. The hybrid technique based on quantum-inspired and bacterial swarm optimization technique has been developed to solve optimization problems **(Dey *et al.,* 2019)**. A review of the hybridization of swarm intelligence techniques has been presented by Peska *et al.* **(2019)**. Rahman and Saleh **(2018)** have presented a summary of significant hybrid bio-inspired computational intelligence techniques utilized for optimization problems.

## 1.4 MULTIOBJECTIVE OPTIMIZATION

In electric power systems, the main focus of researchers is to minimize the cost, maximize the profit, minimize environmental pollution, etc. The MO optimization problems are difficult to solve due to the conflicting nature of objective functions. There is a set of solutions for MO problems. Researchers have applied various MO optimization techniques to solve MO problems **(Qu *et al.,* 2018)**. In 1951, Koopmans introduced the concept of Pareto solution set, which is used to determine the optimal solutions and form the Pareto frontier for MO optimization problems **(Rao, 1996)**. The MO problems are converted into single objective problems by using weighted sum method, ε-Constraint, and interactive method, and then optimization technique is applied to solve problems. Researchers have explored interactive, new dominance, Pareto-dominated, and trade-off methods to find the optimal solution of MO optimization problems. The optimization of the MO problem based on decision making strategies has been discussed by Kumar **(2010)**. In 1994, a non-dominating sorting GA technique has applied to find the Pareto front of the MO optimization problems **(Qu *et al.,* 2018)**. In recent times, the global search optimization techniques based on Pareto-dominated methods have been used to solve the MO optimization problem. Heris *et al.* **(2018)** have presented a comprehensive review of heuristic optimization algorithms for MO problems. Zhang *et al.* **(2019)** have implemented dynamic artificial bee multi-colony algorithm for multiobjective optimization problems. Moreover, the fuzzy membership function has used to select the optimal trade-off solution from the Pareto set **(Hota *et al.,* 2010)**. Kumar and Bauer **(2007)** have solved the MO optimization of permanent magnet brushless DC motors using GA. Patwal and Narang **(2018)** have solved the MO pumped storage hydrothermal system by the fuzzy set theory with cardinal priority ranking method (CPM). The CPM is applied to find the best compromised non-dominated solution of the MO optimization problem having multiple conflicting objectives.

## 1.5 SCOPE OF WORK

The electric power systems involve various types of generating units *i.e.*, thermal, heat, CHP, and renewable energy sources, which are connected to different load centers through the transmission network. The cogeneration units are an important part of the industry and utility to satisfy the electricity and heat demand. The large proportions of generating units, high interconnections, and high nonlinearities in the characteristic of generating units have increased system complexity. The utility planner faces a great challenge to satisfy consumer power and heat demand during the entire scheduling interval at a reasonable cost. The challenge is to supply electricity at a reasonable cost, which converts government policy into a deregulation environment.

Over the years, the researchers have got major breakthroughs to solve various problems of the power system. However, technology advancement in the field of the CHP unit and more exposure to green energy creates new challenges to achieve desired solutions of the power system. Further, the decentralization of the power system network has changed the priorities of utility planners. Hence, there is a need to relook the power system policies and strategies under a diverse environment. The optimum thermal UC schedule may save millions of dollars per year in production cost. The main focus of this research work is on the UC problem. The UC problem becomes more complex when the dynamic power limit based ramp constraint is also considered. The UC of the thermal, CHP, heat and RES units, which is part of the integrated generation system, makes the problem really complicated. Since, UC is a complex optimization problem, and it is further challenging due to various other constraints imposed by the CHP, and RES unit. In addition to this, restrictions imposed due to clean air act amendments, the utility planner is bound to generate the required power and heat with minimum pollutant emission. The UC is an important optimization task in planning the operations of electric power systems. In the UC problem, the number of combinations of binary variables (0 and 1) grows exponentially as being a large-scale problem. Therefore, the UC problem is one of the most difficult optimization problems of power systems. Several researchers have tried to solve the UC problem at various levels by applying optimization techniques. Over the years, a lot of research has been conducted on developing efficient UC algorithms. According to 'No Free Lunch', no optimization technique has been accepted as best. The ultimate aim of any optimization technique is to achieve a global best solution within a certain limited time cycle. Hence, there is a need to develop optimization technique which is able to deal with mixed-integer, high dimensional, and highly constrained real-world UC optimization problem.

## 1.6 OBJECTIVES OF THE RESEARCH

The main aim of the thesis is to solve the different UC models such as THUC, PBUC, CHPUC, and PBCHPUC by proposing a new optimization technique. The main objective of the research work is to consider system operating cost, GENCOs profit, and emission of pollutants as objective functions. The objectives of the research work were as follows:

1) To propose a hybrid optimization technique for solving unit commitment problem.

2) To solve profit based unit commitment problem.

3) To solve unit commitment problem for cogeneration (combined heat and power unit).

4) To solve unit commitment problem of power system consisting different types of generating units.

## 1.7 OUTLINE OF THE THESIS

This thesis employ new *binary successive approximation and civilized swarm optimization* (BSA-CSO) technique to solve various UC models involving various generating units such as thermal only, heat only, dual mode CHP, photovoltaic, and energy storage units in the context of the regulated and deregulated environment of power system structure. The Chapter-wise overview of thesis is represented in Figure 1.1.

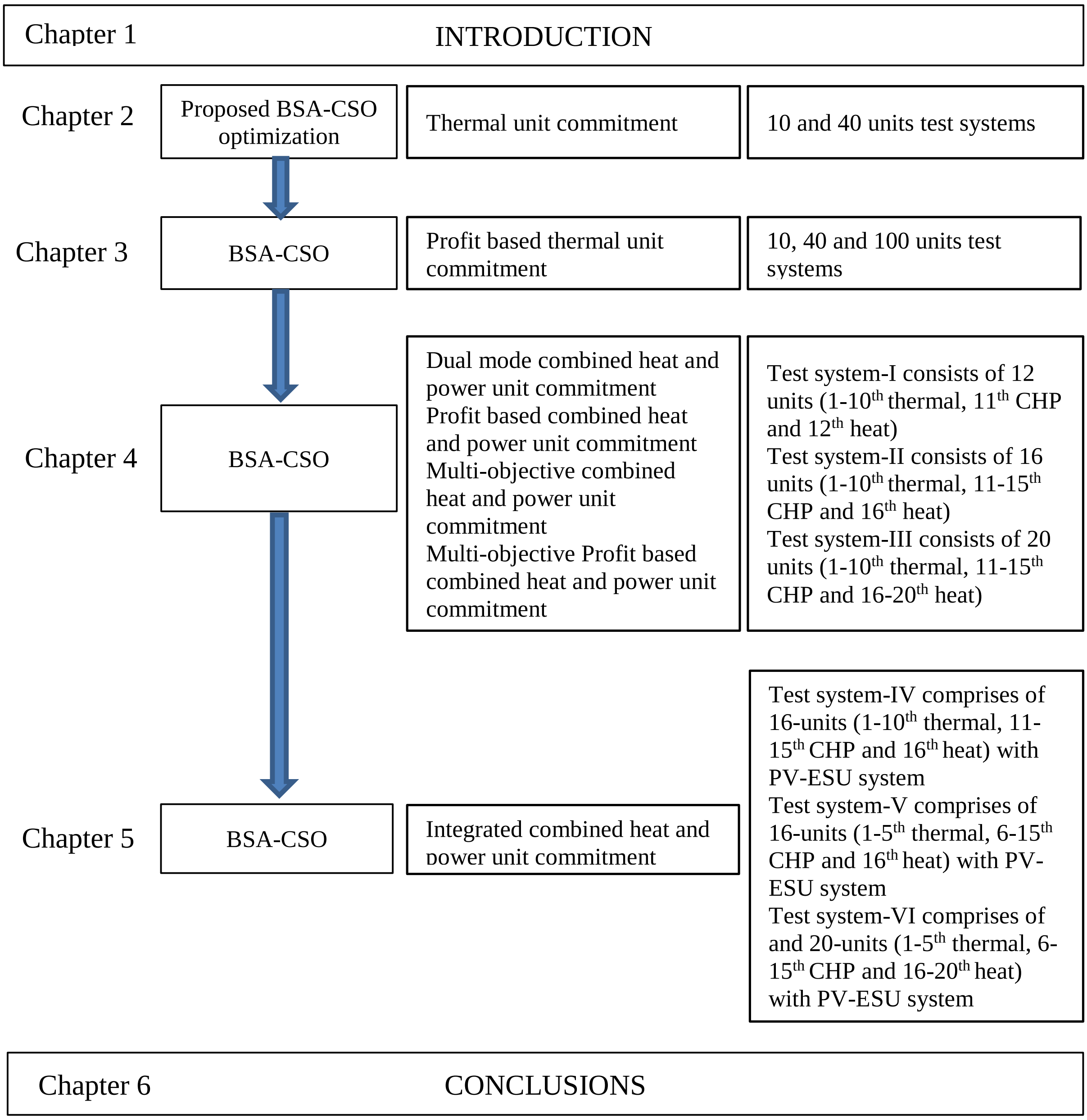


**Figure 1.1:** Chapter-wise overview of thesis

Chapter 2 presents BSA-CSO optimization techniques. The proposed BSA-CSO optimization technique has been implemented for the thermal UC problem, considering unit commitment constraints like minimum up/down time, and reserve requirements and generation constraints such as generation limit, ramp rate limit and power balance. The thermal UC problem is a mixed-integer optimization problem. In the proposed optimization technique, the BSA and CSO techniques deal with binary and continuous decision variables, respectively, of the thermal UC problem. The proposed BSA-CSO optimization technique has an advantage of less computational burden and fast search property. A heuristic method handles minimum up/down time and spinning reserve constraints. The exterior penalty method takes care of generation constraints. The effectiveness of the proposed optimization technique is demonstrated on small and medium size test systems of thermal UC problem. The results obtained from the proposed optimization technique is compared with reported results. The performance of the hybrid optimization technique has been checked by the implementation of a non-parametric Wilcoxon signed-rank test.

The ensuing, Chapter 3, addresses the profit based UC problem in a deregulated environment. In the profit based UC problem, the spinning reserve and power balance are taken as soft constraints. The proposed BSA-CSO technique is implemented to solve the profit based UC problem. To verify the effectiveness of the proposed optimization technique, three test systems (*i.e.*, 10, 40 and 100 units) of the profit based UC problem have been undertaken. The proposed BSA-CSO technique provides improved results with less number of function evaluations as compared to other existing techniques.

The succeeding, Chapter 4, illustrates the *combined heat and power unit commitment* (CHPUC) problem being a cogeneration system, which is an extended version of thermal UC problem. The CHPUC problem consists of thermal, dual mode CHP, and heat generating units. The dual mode CHP unit operates in backpressure and extraction mode. Further, the multiobjective CHPUC problem is addressed for the regulated and restructure power sector. In the multiobjective CHPUC problem, the main objectives such as operating cost and gaseous pollutants emission are taken up together, whereas in the multiobjective profit based CHPUC problem, the profit of GENCOs is maximized and gaseous pollutants emission objective is minimized, simultaneously. The proposed BSA-CSO optimization technique is implemented to search optimum power and heat generation schedule for dual mode CHPUC problem. The fuzzy based decision making strategy is applied to decide solution among the Pareto optimum solutions. The heuristics are applied to handle the minimum up/down time, heat, and power spinning reserve constraints whereby generation constraints are taken care by an exterior penalty method. The three test systems of cogeneration based UC problem have been undertaken to verify the effectiveness of the proposed optimization technique. The results of backpressure and extraction mode for multiobjective CHPUC problem have been compared in term of UC schedule. Further, the impact of dual mode CHP unit on the operating cost, GENCOs profit, and environmental emissions have been evaluated for three test systems.

The intent of Chapter 5 is to expound the CHPUC problem incorporating photovoltaic and battery. The BSA-CSO optimization technique is implemented to search the optimum commitment schedule and generation schedule of committed units at minimum operating cost for the integrated CHPUC problem. The impact of dual mode CHP, photovoltaic, and energy storage units is demonstrated on three integrated solar and CHPUC systems. The results show the importance of photovoltaic and energy storage units in terms of UC schedule and operating cost.

Finally, Chapter 6 summarizes the conclusions and contributions of research work in the present thesis. The contribution in the proposed hybrid optimization technique is presented for solving the various UC problems. The contribution of multiobjective optimization solution procedure technique is also presented for the multiobjective CHPUC and profit based CHPUC problems. The dual mode CHPUC problem shows the importance of operating mode of dual mode CHP units. The future scope of research work in this field is also documented.

# CHAPTER – 2

# THERMAL UNIT COMMITMENT SCHEDULE

## 2.1 INTRODUCTION

The advancement in industrial, agricultural, residential, and commercial sectors have led to an increase in the electricity demand globally exponentially. In order to meet this increasing electricity demand, the generating units have also increased rapidly in the electric power system. A general electric power system comprises of a large number of thermal units and several other types of generating units. The scheduling of generation units is one of the key tasks in the operation of a power system to meet the electricity demand. Therefore, it is necessary to involve the commitment of units for effective scheduling of generating units. The *unit commitment* (UC) is one of the major problems of power system operation. The UC problem in the electric power system is used to decide hourly generating units ON/OFF schedule to fulfill electricity demand for a 24/168 hours scheduling interval **(Dhaliwal and Dhillon, 2018)**. The UC problem reduces the operating cost of generating units with the satisfaction of unit commitment and generation scheduling constraints. Therefore, the UC problem is a mixed-integer problem. The unit commitment constraints include the minimum up/down time, and spinning reserve requirement **(Ongsakul and Vo, 2013)**. The generation scheduling constraint includes the generation and ramp-up/ramp-down limits **(Ongsakul and Vo, 2013)**. The complexity of the *thermal UC* (THUC) problem increases with consideration of the start-up/shut-down ramp-rate constraint **(Sheble and Maifeld, 1994)**. The THUC problem is a real-world *nondeterministic polynomial* (NP) hard constraint optimization problem.

In the past decades, the optimization techniques have been implemented by researchers to solve the THUC problem. Researchers have explored various classical techniques to solve the THUC problem. The *Lagrangian relaxation* (LR) method has been employed to find the optimum solution for the UC problem **(Cheng *et al.*, 2000[1])**. Due to the non-convexities and complexity nature of the THUC problem, the solution may not converge to the optimum point. The gradient based LR method has been used to accelerate the convergence, whereas the solution obtained by the gradient based LR method may be struck at the local minima **(Ongsakul and Petcharaks, 2004)**.

Researchers have also employed *dynamic programming* (DP) **(Kazarlis *et al.*, 1996)** and *mixed-integer linear programming* (MILP) **(Wang and Singh, 2009)** approach to solving the THUC problem. In large scale THUC problem, the computational burden increases in classical search methods. These classical search methods are based on the selection of initial point and follow a single path search that results in non-optimal solutions and a huge loss of revenue **(Cheng *et al.*, 2000[1]; Senjyu, 2003)**.

Over the last decade, researchers have proposed an alternative approach called stochastic optimization techniques, which are efficient and flexible than the classical search techniques. These search techniques are based on certain biological, molecular, neurological, and nature inspired phenomena. Among these, nature inspired optimization techniques includes *genetic algorithm* (GA) **(Ma *et al.*, 1995; Kazarlis *et al.*, 1996; Marifeld and Sheble, 1996; Abookazemi *et al.*, 2011; Lazo and Cartes, 2011)**, *evolutionary programming* (EP) **(Duo *et al.*, 1999; Juste *et al.*, 1999)**, quantum-inspired EP **(Jeong *et al.*, 2009)**, *differential evolution* (DE) **(Uyar *et al.*, 2011)**, *particle swarm optimization* (PSO) **(Zhao *et al.*, 2006)**, *binary PSO* (BPSO) **(Yuan *et al.*, 2009)** and *simulated annealing* (SA) **(Simopoulos *et al.*, 2006)** have been implemented to solve the THUC problem. The PSO and BPSO show incomparable advantages in searching speed and precision when compared with the other nature inspired optimization techniques **(Zhao *et al.*, 2006)**. Inspite of numerous pros of PSO, it has some flaws such as convergence behavior, and it depends upon the choice of its parameters **(Ting *et al.*, 2006)**. Further, implementation of PSO to large scale THUC problem suffers from premature convergence problem **(Zhao *et al.*, 2006)**. In order to improve the performance of PSO, researchers have developed dispersed PSO and chaotic PSO techniques **(Raglend *et al.*, 2010)**. Currently, the field of optimization is evolving rapidly, and researchers are still trying to get the optimum solution in a quick time. In this attempt, researches have solved the UC problem by applying recently proposed global optimization techniques, *i.e.*, *ant colony system* (ACS) **(Simon *et al.*, 2006)**, nodal ant colony **(Saber and Alshareef, 2008)**, binary/real coded artificial bee colony **(Chandrasekaran *et al.*, 2012)**, quasi-oppositional teaching learning **(Roy and Sarkar, 2014)**, and binary gravitational search **(Yuan *et al.*, 2014)**. However, global search optimization techniques are parameter sensitive, which results in the solutions to converge at sub-optimal solutions for large scale UC problems. The search capability of global search techniques is enhanced by the hybridization of global search techniques with local search techniques **(Victoire and Jeyakumar, 2006)**. Victoire and Jeyakumar **(2005; 2006)** have presented an idea for the hybridization of global search and classical search techniques that may be suitable for optimization problems.

Researchers have also explored hybrid optimization techniques for solving the THUC problem. Chusanapiputt *et al.* **(2008)** have solved the THUC problem by a hybrid technique based on the global search technique (ant system) and classical optimization (priority list method). The hybrid optimization techniques such as LR-EP **(Duo *et al.*, 1999)** and LR-GA **(Cheng *et al.*, 2000[1])** also have been employed to find the optimum solution of the THUC problem. Yuan *et al.* **(2009)** have proposed enhanced discrete DE with Lambda-iteration method to obtain the UC schedule of thermal units. Victoire *et al.* **(2006)** have developed a hybrid technique based on the integration of Tabu search, PSO, and sequential quadratic programming method to solve the THUC problem. Other hybrid optimization techniques have also developed by researchers to solve complex optimization problems. The PSO technique is integrated with classical techniques LR **(Yu and Zhang, 2014)**, Tabu search **(Victoire and Jeyakumar, 2006)**.

One of the main challenges for researchers is to deal with the high dimensionality of the THUC problem while applying global search techniques. For a 24-hour scheduling interval containing N generating units, forms ($24^{2N}$) possible unit status of the problem. As the population size increases, the number of fitness evaluations increases drastically, that increases the computational burden and CPU time. In order to achieve a global optimal solution with the least computational burden for the THUC problem, there is a need for optimization technique based on conventional and hybrid search techniques. The *binary successive approximation* (BSA) is one of the potential conventional search algorithm and is based on the evolutionary search technique. It initiates a search with random base-point, and a hypercube is formed around the base point. Each base point further selects two corners of the hypercube to perform the comparison. The search moves toward the corner having a lower value of the objective function and turn into a new base point. This method continues until the search explores all the possibilities and finally reaches the last branch of the BSA tree. This strategy reduces the computational burden while searching for the optimal solution. The BSA has been successfully applied to solve various optimization problems and able to achieve quality solutions with fast convergence **(Dhillon *et al.*, 2009)**. Among the hybrid optimization techniques, the *civilized swarm optimization* (CSO) has proven its credential, due to integration of PSO and *society civilization algorithm* (SCA) in a meaningful manner. The CSO is capable to maintain a balance between exploration and exploitation capability. The CSO has been successfully applied to solve combined heat and power economic dispatch **(Narang *et al.*, 2017)**, ELD **(Selvakumar and Thanushkodi, 2009),** and multi-objective short-term hydrothermal scheduling problems **(Selvakumar, 2013)**.

The intent of the research work is to propose an optimization technique. The main goal is to obtain the optimum commitment and generation schedule of thermal generating units at minimum operating cost. The main contributions of this Chapter are:

- To propose optimization technique based on the integration of BSA and CSO.
- The main objective of an integrated BSA-CSO based technique is to obtain the optimum commitment and the generation schedule of units. The conventional BSA technique is used iteratively to update the thermal unit status and to search the optimal generation schedule, the hybrid optimization technique 'CSO' is explored.

This Chapter summarizes the THUC and *ramp-rate constrained THUC* (RP-THUC) model of electric power systems, which is solved by optimization techniques. The proposed optimization technique is applied to solve the nondeterministic polynomial hard constraint optimization problem. The BPSO and PSO technique is discussed in Appendix A.1 and A.2, respectively. The effectiveness of the proposed optimization technique has been tested on two standard test systems of THUC. The graphical overview of Chapter 2 is represented in Figure 2.1.

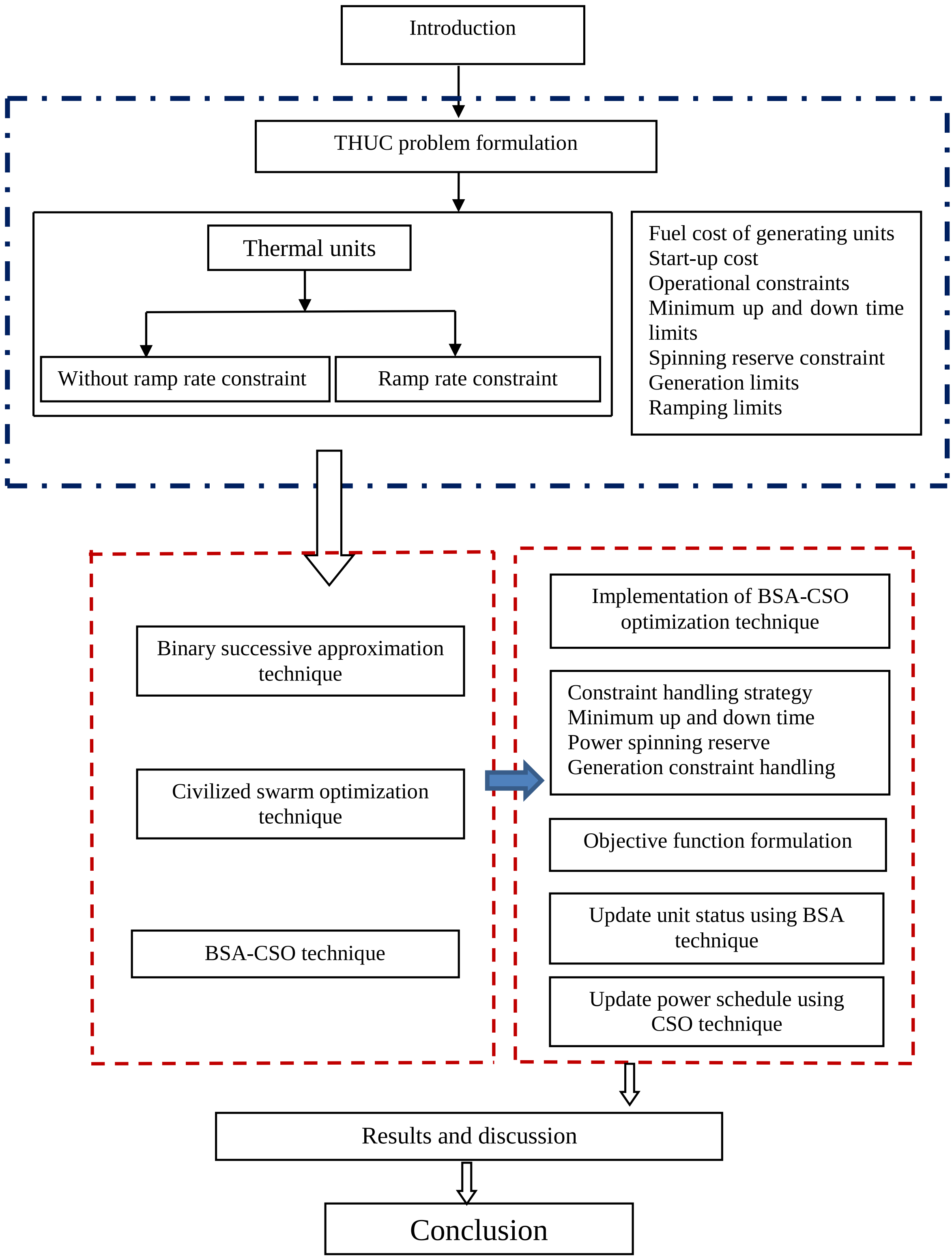


**Figure 2.1:** Graphical overview of Chapter 2

## 2.2 STATEMENT OF THERMAL UNIT COMMITMENT PROBLEM

The THUC is a mixed integer problem, since the commitment of generating unit is controlled by binary decision variables and power generation is continuous in nature. The unit requires a particular pressure and temperature to turn ON. In order to achieve the minimum cost of generation, there is a requirement of turn ON or OFF the generating unit and schedule the power generation from the committed unit in an economic manner with satisfaction of various constraints. The main objective of THUC problem is to minimize the operating cost of power generation from UC schedule with satisfaction of constraints. The THUC constraints include unit commitment constraints (spinning reserve requirement, minimum up and down time, start-up and shut-down ramp-rate limits) and generation constraints (power balance, generation, and ramping limits). It is represented as an array (I/P) of unit status and power generation variables of the dimension (2×T×Ng) and it is given as:

$$I/P = \begin{bmatrix} I_{11} & I_{12} & \cdots & \cdots & I_{1Ng} \\ I_{21} & I_{22} & \cdots & \cdots & I_{2Ng} \\ I_{31} & I_{32} & \vdots & \vdots & I_{3Ng} \\ . & . & . & . & . \\ I_{T1} & I_{T2} & \cdots & \cdots & I_{TNg} \end{bmatrix} \vdots \begin{bmatrix} P^{th}_{11} & P^{th}_{12} & \cdots & \cdots & P^{th}_{1Ng} \\ P^{th}_{21} & P^{th}_{22} & \cdots & \cdots & P^{th}_{2Ng} \\ P^{th}_{31} & P^{th}_{32} & \vdots & \vdots & P^{th}_{3Ng} \\ . & . & . & . & . \\ P^{th}_{T1} & P^{th}_{T2} & \cdots & \cdots & P^{th}_{TNg} \end{bmatrix} \quad (2.1)$$

The total operating cost consists of fuel and start-up cost of a thermal unit and it is given as:

$$\text{TC} = \sum_{t=1}^{T} \sum_{i=1}^{Ng} \left[ F(P^{th}_{ti}) + ST_{ti}\left(1 - I_{(t-1)i}\right) \right] I_{ti} + SD_{ti}\left(1 - I_{ti}\right) I_{(t-1)i} \quad (2.2)$$

where $F(P^{th}_{ti})$ is the fuel cost of $i^{th}$ generating unit at $t^{th}$ sub-interval ($/h); $ST_{ti}$ and $SD_{ti}$ is the starting and shut-down cost of $i^{th}$ generating unit at $t^{th}$ sub-interval ($/h); $I_{ti}$ is the unit ON/OFF status of $i^{th}$ generating unit at $t^{th}$ sub-interval; $P^{th}_{ti}$ is the power generation of $i^{th}$ generating unit at $t^{th}$ sub-interval (MW); *TC* is the total operating cost ($); *T* is total time interval; and *Ng* is the total number of generating units.

The fuel cost of the thermal unit consists of quadratic function and valve-point loading effect. The valve-point loading effect introduces the non-convexity in the cost function and the fuel cost function is expressed as **(Ongsakul and Vo, 2013)**:

$$F(P_{ti}^{th}) = a_i + b_i P_{ti}^{th} + c_i (P_{ti}^{th})^2 + \left| d_i sin(e_i(\underline{P}_i^{th} - P_{ti}^{th})) \right| \qquad i \in [1, Ng], t \in [1, T] \tag{2.3}$$

where $a_i, b_i, c_i, d_i, e_i$ are the cost coefficients of $i^{th}$ generating units; and $\underline{P}_i^{th}$ is the minimum power generation of $i^{th}$ generating unit (MW).

The start-up cost of thermal units is based on the operating state of generating unit *i.e.*, hot start-up or cold start-up and is expressed as:

$$ST_{ti} = \begin{cases} HS_i & T_i^{dw} \le T_{ti}^{off} \le T_i^{dw} + T_i^{cold} \\ CS_i & T_{ti}^{off} > T_i^{dw} + T_i^{cold} \end{cases} \qquad i \in [1, Ng], t \in [1, T] \tag{2.4}$$

where $HS_i$ and $CS_i$ are the hot and cold start-up cost of $i^{th}$ generating units (\$/h), respectively; $T_i^{dw}$ is the minimum down time of $i^{th}$ generating unit (h); $T_{ti}^{off}$ is the off time of $i^{th}$ generating unit at $t^{th}$ sub-interval (h); and $T_i^{cold}$ is the time taken by $i^{th}$ generating unit to reach its cooling point (h).

### 2.2.1 Commitment and Generation Constraints

The THUC constraints include unit commitment constraints and generation constraints. The details regarding the constraints are given in the following sub-sections:

*Minimum up and down time constraint:* Thermal unit requires a minimum time to commit or de-commit the unit and is described as **(Ongsakul and Vo, 2013)**:

$$I_{ti} = \begin{cases} 1 & ; T_{(t-1)i}^{on} < T_i^{up} \\ 0 & ; T_{(t-1)i}^{off} < T_i^{dw} \\ 1 \text{ or } 0 & ; otherwise \end{cases} \qquad i \in [1, Ng], t \in [1, T] \tag{2.5}$$

The on and off time of generating unit is evaluated using Equation 16 and 18, respectively.

$$T_{ti}^{on} = (T_{(t-1)i}^{on} + 1) I_{ti} \tag{2.6}$$

$$T_{ti}^{off} = (T_{(t-1)i}^{off} + 1)(1 - I_{ti}) \tag{2.7}$$

where $I_{ti}$ is $i^{th}$ generating unit ON/OFF status at $t^{th}$ sub-interval; $T_i^{up}$ and $T_i^{dw}$ are the minimum ON and OFF time of $i^{th}$ generating unit (h), respectively; and $T_{ti}^{on}$ and $T_{ti}^{off}$ are the ON and OFF time of $i^{th}$ generating unit at $t^{th}$ sub-interval from its start-up and shut-down time (h), respectively.

*Spinning reserve constraint:* The maximum available power should be more than power demand along with spinning power reserve and is given as **(Ongsakul and Vo, 2013)**:

$$\sum_{i=1}^{Ng} \overline{P_i^{th}} I_{ti} \geq PD_t + SP_t \qquad t \in [1,T] \qquad (2.8)$$

where $I_{ti}$ is $i^{th}$ generating unit ON/OFF status at $t^{th}$ sub-interval; $\overline{P_i^{th}}$ is the maximum power generation of $i^{th}$ generating unit (MW); and $PD_t$ and $SP_t$ are the power demand and spinning reserve requirement at $t^{th}$ sub-interval, respectively (MW).

*Start-up and shut-down ramp constraints:* The start-up and shut-down of the unit require $T_i^{dh}$ and $T_i^{uh}$ time to reach its generation limit and it is shown in Figure 2.2.

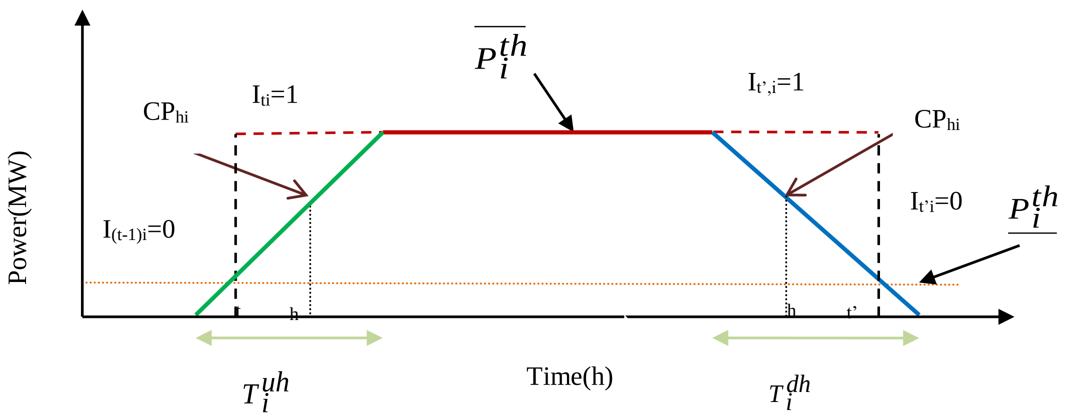


**Figure 2.2**: Unit start-up and shut-down ramp constraint

The maximum power generation restricts due to start-up and shut-down constraint **(Kumar *et al.*, 2016)**. During the start-up process of unit, the generated power is known as constrained power. The power generation is reached its maximum power after start-up time as illustrated in Figure 2.2. The constrained power is computed for start-up process as:

$$CP_{hi} = Min(\overline{P_i^{th}}, UR_i^{th}(h-n))$$

$$h \in [t, t + T_i^{uh}] \, , n = [t] \, , i \in [1, Ng] \, , t \in [1,T] \qquad (2.9)$$

where $CP_{hi}$ is the constrained power of $i^{th}$ generating unit at $h^{th}$ hour (MW); $UR_i^{th}$ is the ramp-up rate of $i^{th}$ generating unit (MW/h), $\overline{P_i^{th}}$ is the maximum power of $i^{th}$ generating unit (MW); and $T_i^{uh}$ is the start-up time of $i^{th}$ generating unit (h).

In the shut-down process, the unit will operate at constrained power, which is less than the maximum power and takes $T_i^{dh}$ hours to reach the zero power generation as illustrated in Figure 2.2. The constrained power is computed for shut-down process as:

$$CP_{hi} = \overline{P_i^{th}} - DR_i^{th} \times (h-n)$$

$$h \in [t' - T_i^{dh}, t'] \text{ , } n = [t' - T_i^{dh}] \text{ , } i \in [1, Ng] \text{ , } t' \in [1,T] \qquad (2.10)$$

where $CP_{hi}$ is the constrained power of $i^{th}$ generating unit at $h^{th}$ sub-interval (MW); $DR_i^{th}$ is the ramp-down rate of $i^{th}$ generating unit (MW/h); $\overline{P_i^{th}}$ is the maximum power of $i^{th}$ generating unit (MW); and $T_i^{dh}$ is the shut-down time of $i^{th}$ generating unit (h).

*Power demand constraint:* The generated power from the committed generators should be greater than or equal to the forecast load demand ($PD_t$) and is represented as **(Ongsakul and Vo, 2013)**:

$$\sum_{i=1}^{Ng} P_{ti}^{th} I_{ti} = PD_t \qquad t \in [1,T] \qquad (2.11)$$

where $P_{ti}^{th}$ is the power generation of $i^{th}$ generating unit at $t^{th}$ sub-interval (MW); and $PD_t$ is the power demand at $t^{th}$ sub-interval (MW).

*Power inequality constraint:* Each committed thermal unit is able to generate power within generation limit, which is expressed as **(Ongsakul and Vo, 2013)**:

$$\underline{P_i^{th}} \le P_{ti}^{th} \le \overline{P_i^{th}} \qquad i \in [1, Ng] \text{ , } t \in [1,T] \qquad (2.12)$$

where $\overline{P_i^{th}}$ and $\underline{P_i^{th}}$ is the maximum and minimum power of $i^{th}$ generating unit, respectively (MW).

*Generation ramp limit:* The generated power must satisfy ramp-up and ramp-down limits which is given as **(Ongsakul and Vo, 2013)**:

$$P_{ti}^{th} - P_{(t-1)i}^{th} \le UR_i^{th} \qquad i \in [1, Ng] \text{ , } t \in [1,T] \qquad (2.13)$$

$$P^{th}_{(t-1)i} - P^{th}_{ti} \leq DR^{th}_{i} \qquad i \in [1, Ng]\ , t \in [1,T] \qquad (2.14)$$

where $UR^{th}_{i}$ and $DR^{th}_{i}$ is the ramp-up and ramp-down rate of $i^{th}$ generating unit, respectively (MW/h).

Consolidated Unit commitment formulation is written as:

Objection function is given as:

$$Min \quad TC = \sum_{t=1}^{T} \sum_{i=1}^{Ng} \left[ F(P^{th}_{ti}) + ST_{ti}\left(1 - I_{(t-1)i}\right) \right] I_{ti} + SD_{ti}\left(1 - I_{ti}\right) I_{(t-1)i}$$

$$F(P^{th}_{ti}) = a_i + b_i P^{th}_{ti} + c_i (P^{th}_{ti})^2 + \left| d_i \sin(e_i(\underline{P^{th}_{i}} - P^{th}_{ti})) \right|$$

$$ST_{ti} = \begin{cases} HS_i & T^{dw}_{i} \leq T^{off}_{ti} \leq T^{dw}_{i} + T^{cold}_{i} \\ CS_i & T^{off}_{ti} > T^{dw}_{i} + T^{cold}_{i} \end{cases}$$

$$Subjected \quad to \quad \begin{cases} I_{ti} = \begin{cases} 1 & ; T^{on}_{(t-1)i} \leq T^{up}_{i} \\ 0 & ; T^{off}_{(t-1)i} \leq T^{dw}_{i} \\ 1 \text{ or } 0 & ; otherwise \end{cases} \\ T^{on}_{ti} = (T^{on}_{(t-1)i} + 1) I_{ti} \\ T^{off}_{ti} = (T^{off}_{(t-1)i} + 1)(1 - I_{ti}) \\ \sum_{i=1}^{Ng} \overline{P^{th}_{i}} I_{ti} \geq PD_t + SP_t \\ \sum_{i=1}^{Ng} P^{th}_{ti} I_{ti} = PD_t \\ \underline{P^{th}_{i}} \leq P^{th}_{ti} \leq \overline{P^{th}_{i}} \\ P^{th}_{ti} - P^{th}_{(t-1)i} \leq UR^{th}_{i} \\ P^{th}_{(t-1)i} - P^{th}_{ti} \leq DR^{th}_{i} \\ CP_{hi} = Min(\overline{P^{th}_{i}}, UR^{th}_{i}(h-n)) \\ CP_{hi} = \overline{P^{th}_{i}} - DR^{th}_{i} \times (h-n) \end{cases}$$

## 2.3 BINARY SUCCESSIVE APPROXIMATION TECHNIQUE

The BSA method is based on the *evolutionary search* (ES) technique. In the ES method, the hypercube is formed around the base point. For the N dimension problem, $2^N$ possible combinations represent all corners of the hypercube as shown in Figure 2.3. Each corner of the hypercube represents one possible solution. The base point is updated by comparing with all possible solutions. In spite of the good searching ability of ES, it requires high computational time, since a *number of function evaluations* ($N_{FE}$) for N dimension problem is $2^N$. In the BSA method, the base point is updated by comparing two corners of the hypercube which reduces the computation burden and the $N_{FE}$ **(Dhillon *et al.*, 2009)**. The $N_{FE}$ for the BSA and ES technique is given in Table 2.1.

**Table 2.1:** Comparison of the number of function evaluation for a different technique

| **Number of decision variables (*N*)** | **ES strategy ($2^N$)** | **BSA strategy (*2N-1*)** |
|---|---|---|
| 10 | 1024 | 19 |
| 12 | 4096 | 23 |
| 14 | 1638 | 27 |
| 20 | 1048576 | 39 |

In this technique, search procedure starts by randomly initialize the base point $C_i^k$ and each base point generates two new combinations of binary number or nodes ( $C_{1i}^k, C_{2i}^k$ ) and is given as follows:

$$C_{1i}^k = \begin{cases} 1; & for \quad [i+1] \\ C_j^k; & for \quad j = [1,2.....i,i+2,....N] \end{cases}$$
$$C_{2i}^k = \begin{cases} 0; & for \quad [i] \\ C_{1j}^k; & for \quad j = [1,2.....i\text{-}1,i+1,....N] \end{cases} \tag{2.15}$$

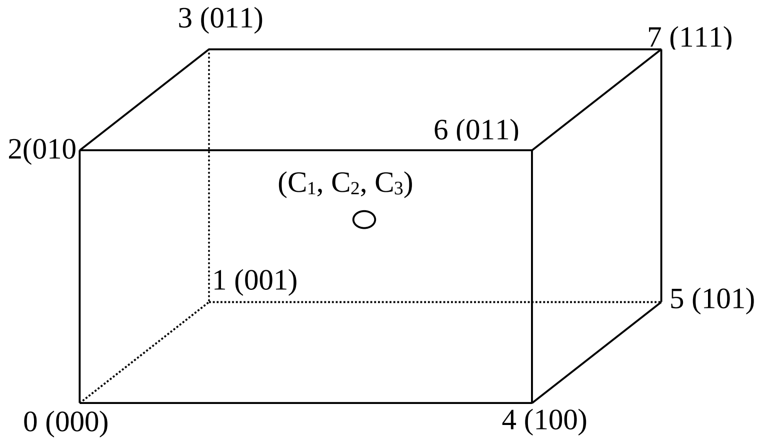


**Figure 2.3:** Three-dimensional hypercube representing corners in decimal

where $C_i^k$ is the base point of the tree for $k^{th}$ base point of $i^{th}$ dimension; $C_{1i}^k$ and $C_{2i}^k$ are the two new nodes created from $k^{th}$ base point of $i^{th}$ dimension.

The new base point is decided according to a minimum value of objective function obtained from $C_{1i}^k$ and $C_{2i}^k$. In Figure 2.4, the base point for the formulation of the tree for 4 variables is randomly initialized as '8' and represented as binary number '1000'. The selected base point has generated two points '12(1100)' and '4(0100)' of the tree. Based on objective function evaluation, the best point among (12, 4) these is selected as a base point for the next step. The solution moves toward the better performing node of a tree. To avoid local optima and to increase the performance of the technique, the next base point is selected from the minimum objective value of two new points and search is performed in the direction of the new base point. The search is performed in the direction of the base point marked with green color. This procedure is repeated until the last branch of the tree reached at 13 as illustrated in Figure 2.4. Hence, the search path passes through base point 8, 12, 14, and 13. The base point for the next iteration is dependent on the minimum objective value from these base points. For the next iteration, the objective function is evaluated for these base points and the same procedure is repeated.

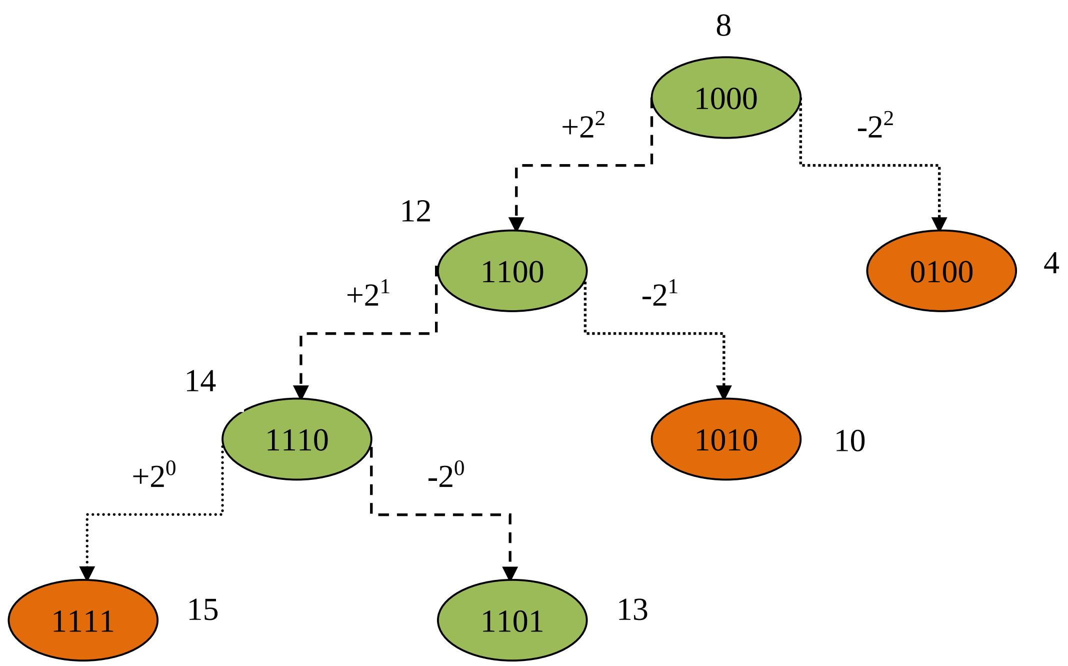


**Figure 2.4:** BSA for 4 bits code

## 2.4 CIVILIZED SWARM OPTIMIZATION TECHNIQUE

The CSO technique is the hybrid optimization technique based on the integration of SCA and PSO (**Ray and Liew, 2003)**. The PSO has good exploration capability and SCA technique is emerging to improve the exploitation capability of the algorithm. The balance between local-global search ability of the CSO provides global or a near global solution with the low computational burden. In CSO technique, the swarm is divided into a number of societies ($N_s$) and it is shown in Figure 2.5. The particles are sorted in descending order according to objective function evaluation and designation hierarchy is set as *civilization leader* (CL), *society leader* (SL), and *society member* (SM). The civilization leader is the best performing particle of the swarm and the next few best performing particles act as a society leader. Every society having one society leader and remaining particles of swarm act as society members.

The society member is assigned to a particular society based on the minimum Euclidean distance between society member and society leaders and is given as:

$$D_S = \sum_{i=1}^{N} \left( SM_{ji}^{k} - SL_{si}^{k} \right)^2 \qquad s \in [1, N_S],\ j \in [1, N_m],\ i \in [1, N] \qquad (2.16)$$

where $D_S$ is the Euclidean distance between society member and society leaders of $s^{th}$ society; $SM_{ji}^{k}$ is the $i^{th}$ dimension of $j^{th}$ society member at $k^{th}$ iteration; $SL_{si}^{k}$ is the $i^{th}$ dimension of $s^{th}$ society at $k^{th}$ iteration; $N_S$ is the number of society; $N_m$ is the number of society member; and $N$ is the number of dimensions.

The graphical representation of CSO particles and their up gradation process is illustrated in Figure 2.5.

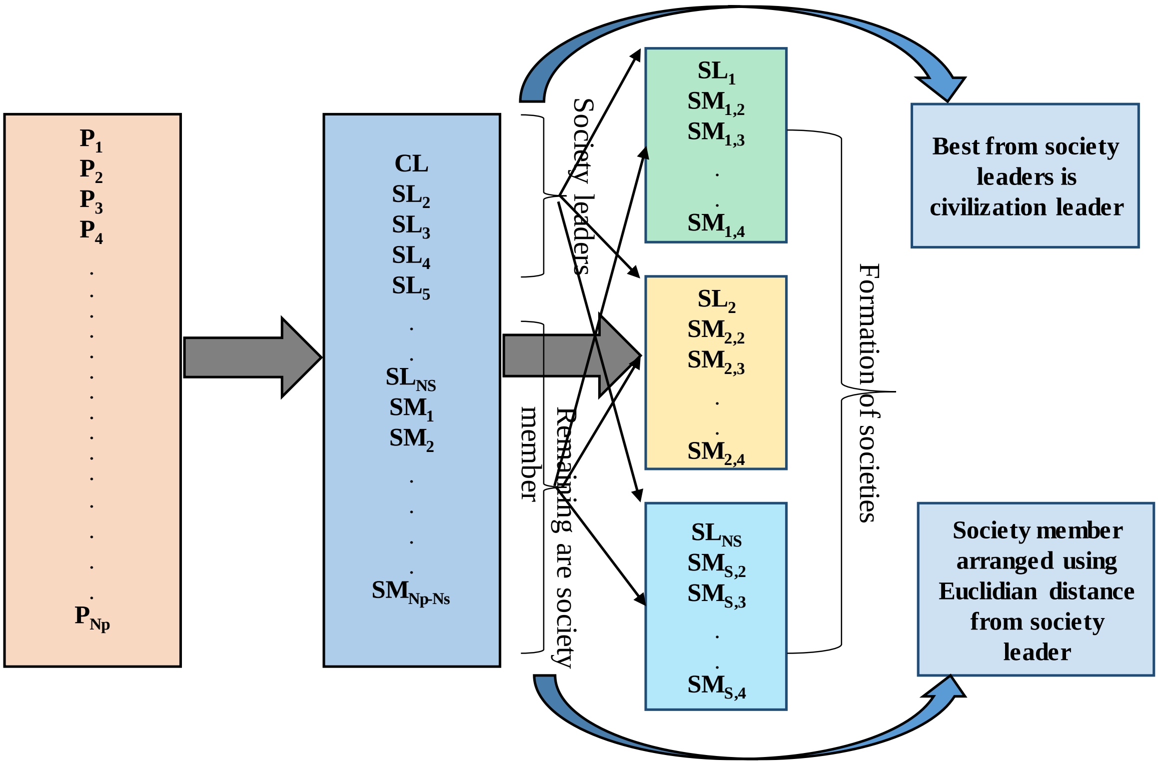


**Figure 2.5:** Formulation of society in CSO algorithm

*Velocity and position upgradation:* The search is performed by inter-society and intra-society interactions among the swarm particles. The intra-society interactions occur between society members and society leader. The society members follow its society leader and use their own experience to update their velocity and position and given as:

$$VM_{smi}^{k+1} = wVM_{smi}^{k} + C_{SM1}ran()(SM_{smi}^{best} - SM_{smi}^{k}) + C_{SM2}ran()(SL_{si} - SM_{smi}^{k}) \tag{2.17}$$

$$SM_{smi}^{k+1} = VM_{smi}^{k+1} + SM_{smi}^{k} \quad s \in [1, N_s], m \in [1, N_m], i \in [1, N], k \in [1, k^{max}] \tag{2.18}$$

where $VM_{smi}^{k}$, $SM_{smi}^{k}$ are the $i^{th}$ dimension velocity and position for $m^{th}$ society member of $s^{th}$ society at $k^{th}$ iteration, respectively; $SM_{smi}^{best}$ is the $i^{th}$ dimension best position for $m^{th}$ society member of $s^{th}$ society; ran() is the uniformly distributed random number; $C_{SM1}$ and $C_{SM2}$ are the acceleration coefficient; $N_s$ and $N_m$ are the numbers of societies and member of societies, respectively; $k^{max}$ is the maximum number of CSO iteration; and $w$ is the inertia weight.

During inter-society interactions, each society leader interacts with civilization leader to share its information. The society leader follows the civilization leader and utilizes own experience for exploring the new promising area.

$$VL_{si}^{k+1} = wVL_{si}^{k} + C_{SL1}ran()(SL_{si}^{best} - SL_{si}^{k}) + C_{SL2}ran()(CL_{i}^{k} - SL_{si}^{k}) \quad (2.19)$$

$$SL_{si}^{k+1} = VL_{si}^{k+1} + SL_{si}^{k} \qquad s \in [1, N_S], i \in [1, N], k \in [1, k^{max}] \quad (2.20)$$

where $SL_{si}^{best}$ is the $i^{th}$ dimension best position for $s^{th}$ society leader; $VL_{si}^{k}, SL_{si}^{k}$ are the $i^{th}$ dimension velocity and position of $s^{th}$ society leader at $k^{th}$ iteration, respectively; $CL_{i}^{k}$ is the $i^{th}$ dimension position of a civilized leader at $k^{th}$ iteration; $C_{SL1}$ and $C_{SL2}$ are the acceleration coefficient.

The civilization leader updates its position by considering own best position as:

$$VC_{i}^{k+1} = wVC_{i}^{k} + C_{L}ran()(CL_{i}^{best} - CL_{i}^{k}) \quad (2.21)$$

$$CL_{i}^{k+1} = VC_{i}^{k+1} + CL_{i}^{k} \qquad i \in [1, N], k \in [1, k^{max}] \quad (2.22)$$

The personal best of particles are updated as:

$$P_{ji}^{best} = \begin{cases} P_{ji}^{k} + V_{ji}^{k+1}; & If\ obj^{k+1} < obj^{k} \\ P_{ji}^{best}; & otherwise \end{cases} \qquad j \in [1, Np], i \in [1, N], k \in [1, k^{max}] \quad (2.23)$$

where $VC_{i}^{k}$ is the $i^{th}$ dimension velocity of a civilized leader at $k^{th}$ iteration; $CL_{i}^{best}$ is the $i^{th}$ dimension best position of civilized leader; $CL_{i}^{k}$ is the $i^{th}$ dimension position of a civilized leader at $k^{th}$ iteration; $C_L$ is the acceleration coefficient; $P_{ji}^{best}$ is the $i^{th}$ dimension personal best position of $j^{th}$ particle; $P_{ji}^{k}$ is the $i^{th}$ dimension position of $j^{th}$ particle at $k^{th}$ iteration; and $obj^{k}$ is the objective function value of $j^{th}$ particle at $k^{th}$ iteration.

New swarm is created as a null matrix for the next iteration *i.e.,* []→Swarm, and civilization leader is directly included in the new swarm matrix. The updating the position of the particle by the CSO method is illustrated in Figure 2.6.

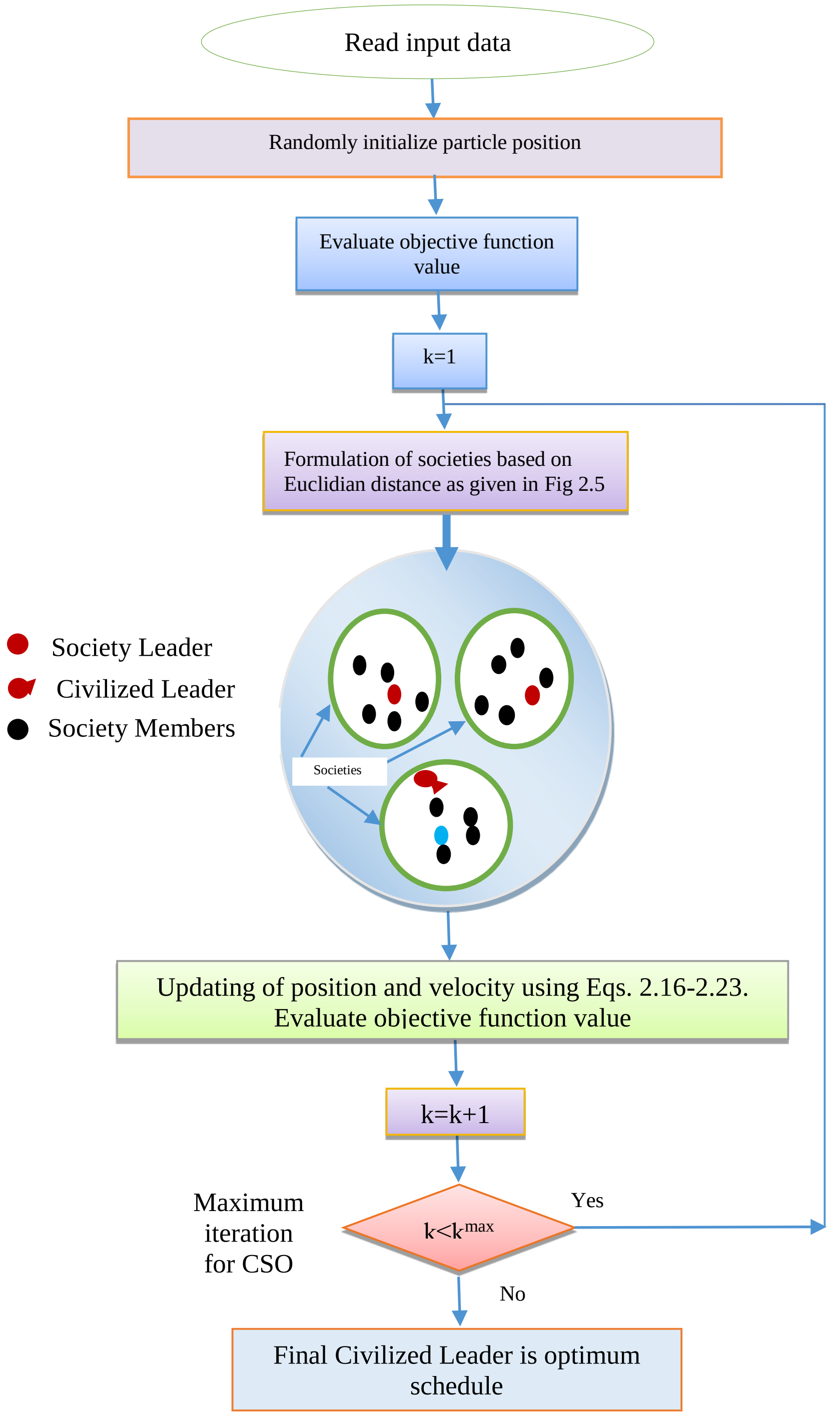


**Figure 2.6:** Civilized swarm optimization technique

## 2.5 BINARY SUCCESSIVE APPROXIMATION AND CIVILIZED SWARM OPTIMIZATION TECHNIQUE

The BSA-CSO technique is hybridization of BSA and CSO technique. The elaborated steps of BSA-CSO technique is given as follows:

Step 1: Input the BSA and CSO technique parameter *i.e.*, number of particles, number of societies, number of leaders, maximum CSO and BSA-CSO iteration *etc*.

Step 2: Randomly initialize the binary and continuous position of all particles which is given as:

$$U_i = \begin{cases} 1; & \text{If } ran() \geq 0.5 \\ 0; & \text{otherwise} \end{cases} \qquad i \in [1, Np] \qquad (2.24)$$

$$X_i = \underline{X}_i + ran()(\overline{X}_i - \underline{X}_i) \qquad i \in [1, Np] \qquad (2.25)$$

Step 4: For the BSA method, the initial base point is the randomly chosen binary position from any particles. Two new points are formed on basis of BSA tree using Eq. (2.15) and the fitness function is evaluated for these points. The new base point is decided by fitness function and this procedure continues until the end of the tree as represented in Figures. 2.4.

Step 5: In order to search optimum position of binary variable search by BSA, CSO technique has been explored. The position of particles of the swarm is randomly initialized. The fitness function is evaluated for each particle position. The particles of a swarm are sorted based on fitness function evaluation and swarm divided into societies. The societies are represented as circles and each society is having one society leader and society members as shown in Figure 2.6. The best performing society leader is designated as civilization leader. The detailed procedure regarding up gradation of position and velocity has been discussed in section 2.4. The CSO algorithms continue until the maximum iteration ($k^{max}$) is met.

Step 6: The updated binary position along with optimum continuous position of particle is assigned for the next iteration of the BSA algorithm for the base point. The same procedure is followed as discussed in step 4 and 5 till the termination criteria are met.

## 2.6 IMPLEMENTATION OF HYBRID OPTIMIZATION TECHNIQUE FOR THERMAL UNIT COMMITMENT PROBLEM

The THUC is a nonlinear, non-convex and mixed variable optimization problem, hence the need for efficient optimization technique arises to search optimal solution without much computational burden. The BSA-CSO technique is implemented to solve the THUC problem. The binary (unit status) and continuous (power generation) decision variables are updated by the implementation of BSA technique and CSO technique, respectively. The elaborated steps of implementation to solve the THUC by applying the proposed approach are given as follows:

Step 1: **Input:** Define system data, *i.e.*, number of generating units, cost coefficients, generation capacities, minimum up and down time, load demand, *etc*.

Step 2: **Initialization:** The unit status is represented by T x Ng binary unit commitment matrix (I) as:

$$I = \begin{bmatrix} I_{11} & I_{12} & \cdots & \cdots & I_{1Ng} \\ I_{21} & I_{22} & \cdots & \cdots & I_{2Ng} \\ I_{31} & I_{32} & \vdots & \vdots & I_{3Ng} \\ \vdots & \vdots & \vdots & \vdots & \vdots \\ I_{T1} & I_{T2} & \cdots & \cdots & I_{TNg} \end{bmatrix} \tag{2.27}$$

The initial status (ON/OFF) of generating units is randomly generated as:

$$I_{ti} = \begin{cases} 1; & If\ ran() \geq 0.5 \\ 0; & otherwise \end{cases} \qquad i \in [1,Ng]\ ,\ t \in [1,T] \tag{2.28}$$

The power generation is represented by continuous variable generation schedule matrix (P) as:

$$P = \begin{bmatrix} P_{11}^{th} & \cdots & \cdots & P_{1Ng}^{th} \\ P_{21}^{th} & \cdots & \cdots & P_{2Ng}^{th} \\ P_{31}^{th} & \vdots & \vdots & P_{3Ng}^{th} \\ . \quad . & . & . & . \\ P_{T1}^{th} & \cdots & \cdots & P_{TNg}^{th} \end{bmatrix} \tag{2.29}$$

The initial power ( $P_{ti}^{th}$ ) is randomly generated for thermal units and is expressed as:

$$P_{ti}^{th} = \underline{P_{ti}^{th}} + ran()(\overline{P_{ti}^{th}} - \underline{P_{ti}^{th}}) \qquad i \in [1,Ng]\ ,\ t \in [1,T] \tag{2.30}$$

Step 3: **Objective function formulation:** The objective of THUC problem is to minimize the operating cost while satisfaction of unit commitment and power generation constraints. The detail discussion regarding constraint handling and objective function formulation is given as follows:

(i) **Minimum up and down time constraint:** The pseudo code to satisfy minimum up and down time constraint is given in Figure 2.7.

(ii) **Power spinning reserve requirement:** Reserve requirement of power must be satisfied for the THUC problem. The stochastic nature of the load and unavailability of the generator reduces the system reliability, hence there is requirement to commit another generating unit to meet spinning reserve along with demand. If the power spinning reserve requirement is not met, then turn on additional unit based on the *priority list* (PL) **(Senjyu *et al.*, 2003)** and it is illustrated in Figure 2.8.

Read input T, Ng, PL, PD$_t$, $\underline{P}_i^{th}, \overline{P}_i^{th}, T_i^{up}, T_i^{dw}$ and $T_i^{in}$ .

For t=1: T
    For i= 1: Ng
        If ( $I_{ti} = 0$ ) Then
            $T_{ti}^{on} = 0$ , $T_{ti}^{off} = T_{(t-1)i}^{off} + 1$
        End if
    If ( $I_{ti} = 1$ ) Then
            $T_{ti}^{on} = T_{(t-1)i}^{on} + 1$ ,   $T_{ti}^{on} = 0$
        End if
  End for
End for
For t=1: T
    For i= 1: Ng
        If ( $I_{ti} = 0$ & $I_{(t-1)i} = 1$ & { $T_{(t-1)i}^{on} < T_i^{up}$ }) Then
            $I_{ti} = 1$
        End if
        If ( $I_{ti} = 0$ & $I_{(t-1)i} = 1$ & { $(t-1-T_i^{dw} \le T)$ } & { $T_{j,i}^{off} < -T_i^{dw}, j \in t-1-T_i^{dw}$ })
            $I_{ti} = 1$
        End if
        If ( $I_{ti} = 0$ & $I_{(t-1)i} = 1$ & {( $t-1-T_i^{dw} > T$ )} & { $\sum_{m=t}^{T} I_{mi} > 0$ })
            $I_{ti} = 1$
        End if
        Update $T_{ti}^{on}, T_{ti}^{off}$
    End for
End for

**Figure 2.7**: Pseudo code for minimum up and down time constraint handling

(iii) **Unit de-commitment:** The satisfaction of minimum up and down time constraints may lead to excessive spinning reserve. Hence, there is a need to de-commit some of the units based on the PL **(Senjyu *et al.*, 2003)** to satisfy spinning reserve constraint given by Eq. (2.8). The procedure of de-commitment of unit is given in Figure 2.9.

```
//////……………….........................Power Spinning Reserve......................................................//////
//Read input data.
//Output power spinning reserve satisfied
For t=1:T
        Compute spinning reserve using Eq. (2.8).
        SPR_t = Σ_{i=1}^{Ng} \overline{P_i^{th}} × I_ti − PD_t − SP_t
         For i=1:Ng
        If ( I_ti = 0 ) then
            Count=Count+1
            NL_Count=i
        End if
        End for
    Sort ascending NL_count based on PL.
    Compute spinning reserve using SPp_t.
        For k=1:Count
            If (SPR_t< 0) then
                I_ti=1,  i=NL_k
            End if
    Compute spinning reserve using SPR_t
End for
```

**Figure 2.8:** Power reserve requirement strategy

```
Read input T, Ng, PL, PD_t, \underline{P_i^{th}}, \overline{P_i^{th}} , I_ti and T_i^{in} .
For t=1: T
        SPR_t = Σ_{i=1}^{Ng} \overline{P_i^{th}} × I_ti − PD_t − SP_t
        Count=0
        For i=1: Ng
                If ( I_ti = 1 )
                Count=count+1
                NL(count)= i
                End if
        End for
        Sort NL based on PL.
        For k=1: Count
                If ( SPR_t > min( \overline{P_1^{th}}, \overline{P_2^{th}},... \overline{P_{Ng}^{th}} ))
                    I_tk = 0 based on time constraints handling  I_tk ∈ NL_k
                End if
    End for
End for
```

**Figure 2.9:** Pseudo code for de-commitment process

(iv) **Ramp rate constraint:** The unit maximum power limit is sacrificed during the start-up and shut-down process as given by Eq. (2.9), and (2.10), respectively. During the start-up process, the constrained power **(Kumar *et al.*, 2016)** has leaned forward to reach at maximum power as illustrated in Figure 2.2 and given by Eq. (2.9). In the shut-down process, the unit will operate at constrained power, which is below than the maximum power and represented by Eq. (2.10). The procedure of heuristic adjustment to satisfy ramp-rate constraint is given in Figure 2.10.

(v) **Generation ramp limit:** The ramp up and down constraint must be satisfied throughout the procedure in the THUC problem which is given as:

$$P_{ti}^{Rmax} = \min(\overline{P_i^{th}}, P_{(t-1)i}^{th} + UR_i^{th}) \text{ as } i^{th} \text{ unit ramp up.} \quad i \in [1,Ng],\ t \in [1,T] \tag{2.31}$$

$$P_{ti}^{Rmin} = \max(\underline{P_i^{th}}, P_{(t-1)i}^{th} - DR_i^{th}) \text{ as } i^{th} \text{ unit ramp down.} \quad i \in [1,Ng],\ t \in [1,T] \tag{2.32}$$

where $P_{ti}^{Rmax}$ and $P_{ti}^{Rmin}$ is the ramping maximum and minimum power limit of $i^{th}$ unit at $t^{th}$ sub-interval, respectively (MW).

```
Read input T, Ng, P_i^th(min), P_i^th(max), T_i^up, T_i^dw, UR_i^th and DR_i^th.
CP_ti = P_i^th(max)
For t=1: T
        For i=1: Ng
                If ( I_ti = I_(t+1)i = 0 & I_ti = 1, I_(t+1)i = 1 )
                        CP_ti = CP_ti
                End if
        If ( I_ti = 1, I_(t+1)i = 0 )
                        CP_hi = Min(P_i^th(max), UR_i^th × (h−n)), h∈[t, t+T_i^uh], n=[t]
                End if
        If ( I_ti = 0, I_(t+1)i = 1 )
                        CP_hi = P_i^th(max) − DR_i^th × (h−n)  , h∈[t−T_i^dh, t], n = [t − T_i^dh]
                End if
        End for
End for
```

**Figure 2.10**: Pseudo code for ramp-rate constraint handling

(vi) **Power demand constraint:** In order to satisfy, the power demand constraint, exterior penalty approach is applied. Hence, the objective function is formulated as:

$$obj = TC + \psi_1 \sum_{t=1}^{T} E_t \qquad i \in [1, Ng] \qquad (2.33)$$

where
$$E_t = \begin{Bmatrix} \left(\sum_{i=1}^{Ng} P_{ti}^{th} I_{ti} - PD_t\right)^2 ; & \sum_{i=1}^{Ng} I_{ti} P_{ti}^{th} \neq PD_t \\ 0; & Otherwise \end{Bmatrix} \qquad t \in [1, T] \qquad (2.34)$$

with $TC$ is the total cost (\$); $E_t$ is the error for power demand at $t^{th}$ sub-interval; $\psi_1$ is the penalty factor; $T$ is total time interval; and $Ng$ is the total number of generating units.

Step 4: **Update unit status by BSA:** The base point entries 1/0 represents ON/OFF unit status, respectively. For the first iteration, the unit status is randomly generated for all sub-intervals. For the BSA method, the initial base point is the randomly chosen sub-interval unit status. The base point must satisfy the minimum up and down time and spinning reserve constraint during the de-commitment process. The power assigned to the committed units in the BSA method is based on the PL and it is shown in Figure 2.11. The power generation should meet the power demand constraint (Eq. 2.11), and ramp rate constraints (Eq. 2.31 and 2.32). The objective function (obj) is evaluated using Eq. (2.33). Two new points are formed based on BSA tree using Eq. (2.15) and the objective function is evaluated for both points by following the same procedure. The new base point is decided based on objective function evaluation and this procedure continues until the end of the tree as represented in Figures. 2.4 and 2.11. In the next cycle, again, one randomly selected sub-interval unit status is chosen as a base point. In this process, every time the search starts with a new point that helps to avoid the local optimal solution. This procedure is continued until all sub-intervals have been undertaken.

**Step 5: Optimum power schedule by CSO:** In order to search optimum power schedule for selected unit status obtained by BSA, CSO technique has been explored. The graphical representation of swarm for the power generation from the committed units are shown in Figure 2.12. The power obtained from the base point during BSA search is assigned to one particle of CSO, whereas remaining particles of the swarm are randomly initialized.

Read input T, Ng, PL, $PD_t$, $\underline{P_i^{th}}, \overline{P_i^{th}}$ .

ON unit set at $P_{ti}^{th} = \overline{P_i^{th}}$

For t=1: T

$ER_t = \sum_{i=1}^{Ng} P_{ti}^{th} I_{ti} - PD_t$

Sort NL based on PL as shown in Figure 2.8.

For k=1: Count

If ( $\sum_{i=1}^{Ng} P_{ti}^{th} I_{ti} < PD_t$ ) // $ER_t$ is negative

$P_{tk}^{th} I_{tk} = (P_{tk}^{th} - ER_t) I_{tk} \quad I_{tk} \in NL_k$

Check the maximum limit ( $\overline{P_i^{th}}$ )

Evaluate the $ER_t$

Else if ( $\sum_{i=1}^{Ng} P_{ti}^{th} I_{ti} > PD_t$ ) // $ER_t$ is positive

$P_{tk}^{th} I_{tk} = (P_{tk}^{th} - ER_t) I_{tk} \quad I_{tk} \in NL_k$

Check the minimum limit ( $\underline{P_i^{th}}$ )

Evaluate the $ER_t$

End if

End for

End for

**Figure 2.11:** Pseudo code for power assign in BSA method

For each particle, the objective function is evaluated as given in Eq. (2.33). The particles of a swarm are sorted based on objective function evaluation and swarm divided into societies. The societies are represented as circles and each society is having one society leader and society members as shown in Figure 2.12. The best performing society leader is designated as civilization leader. The detailed procedure regarding up gradation of position and velocity has been discussed in section 2.4. The CSO algorithms continue until the maximum iteration ($k^{max}$) is met.

**Step 6: Overall up gradation process:** The updated unit status along with optimum power generation schedule is assigned for the next iteration of the BSA algorithm for the base point. The two new base point is generated according to BSA algorithm and power is assigned on the basis of PL. The same procedure is followed as discussed in step 4 and 5 till the termination criteria are met.

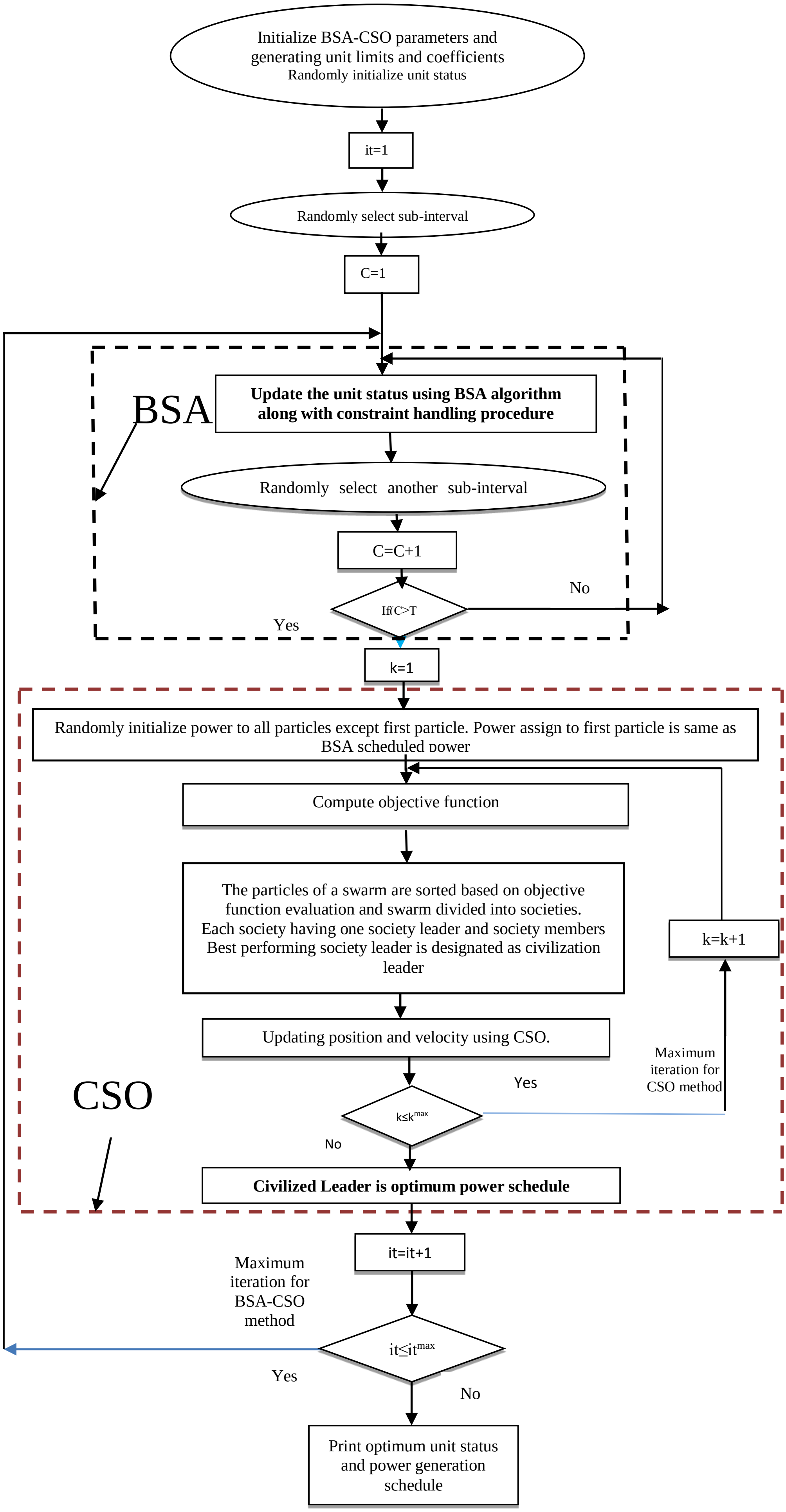


**Figure 2.12:** Implementation of BSO-CSO technique.

## 2.7 THERMAL UNIT COMMITMENT TEST SYSTEMS AND RESULTS

The THUC test systems-I and II having non-linear and non-convex characteristics of generating units have been undertaken to authenticate the effectiveness of the novel BSA-CSO technique. These test system consists of 10 and 40 thermal units. The input data of THUC systems has been referred from Ref. **(Reddy *et al.*, 2018)** and it is given Appendix-B.1. The generation schedule has been obtained during 24-hour period at one-hour sub-interval. In this proposed work, the implementation of BPSO-PSO and BSA-CSO algorithms in solving THUC has been carried out in FORTRAN 90 environment on a personal computer (1.66 GHz, Pentium-IV, with 2 GB RAM). Moreover, the four different cases of THUC systems have been considered which is given as:

Case-I: The THUC problem without consideration of unit ramp-rate constraint and valve-point loading effect.

Case-II: The THUC problem with consideration of the valve point loading effect of generating unit.

Case-III: The THUC problem with unit ramp-rate constraint.

Case-IV: The THUC problem with consideration of the valve point loading effect and unit ramp-rate constraint

### 2.7.1 Parameter Tuning

The choice of optimal parameters in the BSA-CSO and BPSO-PSO optimization technique has been determined after several trials executed on THUC test systems. In the BPSO-PSO technique, the parameters are swarm size ($N_p$=40), minimum inertia weight ($W_{min}$=0.4), maximum inertia weight ($W_{max}$=0.9), acceleration coefficients ($C_1$=2, $C_2$=2), and iteration ($it^{max}$=50). The parameters of BSA-CSO algorithm are swarm size ($N_p$=20), society ($N_s$=4), inertia weight ($W_{max}$=0.9, $W_{min}$=0.4), acceleration coefficients ($C_L$=2, $C_{SL1}$=0.5, $C_{SL2}$ = .5, $C_{SM1}$=0.25, $C_{SM2}$=0.75) and iteration ($it^{max}$=10, $k^{max}$=50).

### 2.7.2 Thermal Unit Commitment Test System-I

In this sub-section, results obtained from the BPSO-PSO and BSA-CSO optimization techniques in all four cases of THUC test system-I have been discussed. In case-I, the minimum, average, and worst cost obtained from optimization techniques have been tabulated in Table 2.2. The results of BSA-CSO technique has been compared with various optimization techniques and presented in Table 2.2. The proposed BSA-CSO technique is able to achieve a lower cost as compared to other techniques reported in the literature. The CPU time consumed during the proposed technique in case-I is 65.3 sec, which is more compare to other techniques, but it has been also depends on processor. In BSA-CSO technique, the commitment status and power generation schedule in case-I/II has been given in Table 2.3.

The cost obtained from BSA-CSO technique for case-II is '\$582577.1', which is '\$18588' more as compared to case-I due to consideration of valve point effect. In case-III, inclusion of ramp-rate constraint in THUC problem has increases the cost by '\$7653.7' as compare to case-I. Due to valve-point loading and ramp-rate constraint, the cost '\$592259.2' has obtained in case-IV more as compare to case-III.

In case-III/IV for BSA-CSO technique, the effect of start-up and shut-down with ramp-rate constraint on units 3$^{rd}$ and 4$^{th}$ has given in Table 2.4. The units 3$^{rd}$ and 4$^{th}$ have been turned ON at 6$^{th}$ and 5$^{th}$ sub-interval, respectively. These units require certain time interval to generate maximum power. While the power generation during shut-down process of unit 5$^{th}$ at 24$^{th}$ sub-interval is reaches to constrained power in case-III and case-IV. The convergence curve of BSA-CSO for best, average and worst cost is shown in Figure 2.13.

**Table 2.2:** Comparison of cost and CPU time for THUC test system-I, case-I

| Technique | Average cost (\$) (10^3) | Worst cost (\$)(10^3) | Best cost (\$) (10^3) | CPU (sec) |
|---|---|---|---|---|
| **Genetic-based method (Sheble *et al.*, 1996)** | 623.441 | - | NA | - |
| **Genetic-based method (Sheble *et al.*, 1996)** | 623.441 | - | NA | - |
| **Integer coded genetic algorithm (ICGA) (Damousis *et al.*, 2004)** | 566.404 | - | NA | - |
| **Lagrangian search genetic algorithm (LSGA) (Kazarlis *et al.*, 1996)** | - | - | 609.023 | - |
| **Improved binary particle swarm optimization (IBPSO) (Yuan *et al.*, 2009)** | - | - | 599.782 | 14.48 |
| **New genetic algorithm (Ganguly *et al.*, 200+4)** | - | - | 591.715 | 677 |
| **PSO (Victoire and Jeyakumar, 2004)** | - | - | 581.450 | - |
| **Binary particle swarm optimization with bit change mutation (MPSO) (Lee *et al.*, 2007)** | - | - | 574.905 | 15.73 |
| **HPSO (Gaing, 2003)** | - | - | 574.153 | - |
| **LCA-PSO (Wang *et al.*, 2011)** | - | - | 570.006 | 18.34 |
| **Two-stage genetic based technique (TSGA) (Eldin *et al.*, 2008)** | - | - | 568.315 | - |
| **Hybrid PSO-SQP (Victoire and** | - | - | 568.032 | - |

| | | | | |
|---|---|---|---|---|
| **Jeyakumar, 2004)** | | | | |
| **BCGA (Damousis *et al.*, 2004)** | - | - | 567.367 | - |

**Table 2.2:** Comparison of cost and CPU time for THUC test system-I, case-I (Continued)

| Technique | Average cost ($) (10^3) | Worst cost ($)(10^3) | Best cost ($) (10^3) | CPU (sec) |
|---|---|---|---|---|
| **SM (Simopoulos *et al.*, 2006)** | 566.787 | 567.022 | 566.686 | - |
| **LR (Simopoulos *et al.*, 2006)** | 566.493 | 566.817 | 566.107 | - |
| **GA (Simopoulos *et al.*, 2006)** | 567.329 | 571.336 | 565.866 | - |
| **Genetic algorithm (GA) (Kazarlis *et al.*, 1996)** | - | 570.032 | 565.852 | 221 |
| **Enhanced simulated annealing (ESA) (Simopoulos *et al.*, 2006)** | 565.988 | 566.260 | 565.828 | 3.35 |
| **Lagrangian relaxation (LR) (Kazarlis *et al.*, 1996)** | - | - | 565.825 | - |
| **Dynamic programming (DP) (Kazarlis *et al.*, 1996)** | - | - | 565.825 | - |
| **Improved lagrangian relaxation (ILR) (Sriyanyong and Song, 2005)** | - | - | 565.823 | - |
| **LRPSO (Sriyanyong and Song, 2005)** | - | - | 565.275 | - |
| **Lagrangian relaxation and genetic algorithm (LRGA) (Cheng *et al.*, 2000)** | 564.800 | - | 564.800 | 518 |
| **Evolutionary programming (EP) (Juste *et al.*, 1999)** | 565.352 | - | 564.551 | 5.61 |
| **EP (Simopoulos *et al.*, 2006)** | 565.352 | 566.231 | 564.551 | 100 |
| **Particle swarm optimization (PSO) (Zhao *et al.*, 2006)** | 565.103 | 565.783 | 564.212 | - |
| **Ant colony search algorithm (ACSA) (Sumim and Ongsakul, 2003)** | - | - | 564.049 | - |
| **Hybrid ant system/Priority list (HASP) (Chusanapiputt *et al.*, 2008)** | 564.324 | 564.490 | 564.029 | - |
| **B. SMP (Khanmohammadi *et al.*, 2010)** | 564.121 | 564.401 | 567.017 | - |
| **Annealing genetic algorithm (AGA) (Cheng *et al.*, 2000[2])** | - | - | 564.005 | - |
| **Binary differential evolution (Jeong *et al.*, 2009)** | 563.997 | 563.997 | 563.997 | - |
| **Harmony search (HS) (Najafi *et al.*, 2012)** | - | - | 564.367 | - |
| **BPSO-PSO** | 566.745 | 566.139 | 565.149 | 110 |
| **Proposed method** | **564.129** | **564.289** | **563.989** | **65.3** |

The total operating cost obtained from BPSO-PSO and BSA-CSO technique in case-I, II, III, and IV have been given in Table 2.5. The optimum operating cost '$565149.30' obtained from the BPSO-PSO technique in case-I, which has been found '$1160.2' more as compare to BSA-CSO technique. In case-II, the cost attained from BPSO-PSO technique is '$591751.3', which is more by 1.57% as compare to BSA-CSO technique. The cost achieved from BPSO-PSO technique for case-III and case-IV are 2.89% and 4.2% more as compare to BSA-CSO technique. The time consumed by CPU in BPSO-PSO optimization is more in all cases of THUC problem as compare to BSA-CSO technique.

**Table 2.3:** Hourly power dispatch obtained by BSA-CSO for THUC test system-I, case-I and case-II

| Sub-intervals (h) | Power demand (MW) | Units status | Power Generation (MW) | | | | | | | | | | Required spinning reserve (MW) | Spinning reserve (MW) | Total power Generation (MW) |
|---|---|---|---|---|---|---|---|---|---|---|---|---|---|---|---|
| | | | P1 | P2 | P3 | P4 | P5 | P6 | P7 | P8 | P9 | P10 | | | |
| **1** | 700 | 1100000000 | 455 | 245 | 0 | 0 | 0 | 0 | 0 | 0 | 0 | 0 | 70 | 210 | 700 |
| **2** | 750 | 1100000000 | 455 | 295 | 0 | 0 | 0 | 0 | 0 | 0 | 0 | 0 | 75 | 160 | 750 |
| **3** | 850 | 1100100000 | 455 | 370 | 0 | 0 | 25 | 0 | 0 | 0 | 0 | 0 | 85 | 222 | 850 |
| **4** | 950 | 1100100000 | 455 | 455 | 0 | 0 | 40 | 0 | 0 | 0 | 0 | 0 | 95 | 122 | 950 |
| **5** | 1000 | 1101100000 | 455 | 390 | 0 | 130 | 25 | 0 | 0 | 0 | 0 | 0 | 100 | 202 | 1000 |
| **6** | 1100 | 1111100000 | 455 | 360 | 130 | 130 | 25 | 0 | 0 | 0 | 0 | 0 | 110 | 232 | 1100 |
| **7** | 1150 | 1111100000 | 455 | 410 | 130 | 130 | 25 | 0 | 0 | 0 | 0 | 0 | 115 | 182 | 1150 |
| **8** | 1200 | 1111100000 | 455 | 455 | 130 | 130 | 30 | 0 | 0 | 0 | 0 | 0 | 120 | 132 | 1200 |
| **9** | 1300 | 1111111000 | 455 | 455 | 130 | 130 | 85 | 20 | 25 | 0 | 0 | 0 | 130 | 197 | 1300 |
| **10** | 1400 | 1111111100 | 455 | 455 | 130 | 130 | 162 | 33 | 25 | 10 | 0 | 0 | 140 | 152 | 1400 |
| **11** | 1450 | 1111111110 | 455 | 455 | 130 | 130 | 162 | 73 | 25 | 10 | 10 | 0 | 145 | 157 | 1450 |
| **12** | 1500 | 1111111111 | 455 | 455 | 130 | 130 | 162 | 80 | 25 | 43 | 10 | 10 | 150 | 162 | 1500 |
| **13** | 1400 | 1111111100 | 455 | 455 | 130 | 130 | 162 | 33 | 25 | 10 | 0 | 0 | 140 | 152 | 1400 |
| **14** | 1300 | 1111111000 | 455 | 455 | 130 | 130 | 85 | 20 | 25 | 0 | 0 | 0 | 130 | 197 | 1300 |
| **15** | 1200 | 1111100000 | 455 | 455 | 130 | 130 | 30 | 0 | 0 | 0 | 0 | 0 | 120 | 132 | 1200 |
| **16** | 1050 | 1111100000 | 455 | 310 | 130 | 130 | 25 | 0 | 0 | 0 | 0 | 0 | 105 | 282 | 1050 |
| **17** | 1000 | 1111100000 | 455 | 260 | 130 | 130 | 25 | 0 | 0 | 0 | 0 | 0 | 100 | 332 | 1000 |
| **18** | 1100 | 1111100000 | 455 | 360 | 130 | 130 | 25 | 0 | 0 | 0 | 0 | 0 | 110 | 232 | 1100 |
| **19** | 1200 | 1111100000 | 455 | 455 | 130 | 130 | 30 | 0 | 0 | 0 | 0 | 0 | 120 | 132 | 1200 |
| **20** | 1400 | 1111111100 | 455 | 455 | 130 | 130 | 162 | 33 | 25 | 10 | 0 | 0 | 140 | 152 | 1400 |
| **21** | 1300 | 1111111000 | 455 | 455 | 130 | 130 | 85 | 20 | 25 | 0 | 0 | 0 | 130 | 197 | 1300 |
| **22** | 1100 | 1100111000 | 455 | 455 | 0 | 0 | 145 | 20 | 25 | 0 | 0 | 0 | 110 | 137 | 1100 |
| **23** | 900 | 1100100000 | 455 | 415 | 0 | 0 | 30 | 0 | 0 | 0 | 0 | 0 | 90 | 172 | 900 |
| **24** | 800 | 1100000000 | 455 | 345 | 0 | 0 | 0 | 0 | 0 | 0 | 0 | 0 | 80 | 110 | 800 |
| | | **Maximum limit of unit** | 455 | 455 | 130 | 130 | 162 | 80 | 85 | 55 | 55 | 55 | | | |

**Table 2.4:** Hourly power dispatch obtained by BSA-CSO for THUC test system-I, case-III and case-IV

| Sub-intervals (h) | Power demand (MW) | Units status | Power Generation (MW) | | | | | | | | | | Required spinning reserve (MW) | Spinning reserve (MW) | Total power Generation (MW) |
|---|---|---|---|---|---|---|---|---|---|---|---|---|---|---|---|
| | | | P1 | P2 | P3 | P4 | P5 | P6 | P7 | P8 | P9 | P10 | | | |
| **1** | 700 | 1100000000 | 455 | 245 | 0 | 0 | 0 | 0 | 0 | 0 | 0 | 0 | 70 | 210 | 700 |
| **2** | 750 | 1100000000 | 455 | 295 | 0 | 0 | 0 | 0 | 0 | 0 | 0 | 0 | 75 | 160 | 750 |
| **3** | 850 | 1100100000 | 455 | 370 | 0 | 0 | 25 | 0 | 0 | 0 | 0 | 0 | 85 | 222 | 850 |
| **4** | 950 | 1100100000 | 455 | 455 | 0 | 0 | 40 | 0 | 0 | 0 | 0 | 0 | 95 | 122 | 950 |
| **5** | 1000 | 1101100000 | 455 | 420 | 0 | 100 | 25 | 0 | 0 | 0 | 0 | 0 | 100 | 202 | 1000 |
| **6** | 1100 | 1111100000 | 455 | 385 | 105 | 130 | 25 | 0 | 0 | 0 | 0 | 0 | 110 | 232 | 1100 |
| **7** | 1150 | 1111100000 | 455 | 410 | 130 | 130 | 25 | 0 | 0 | 0 | 0 | 0 | 115 | 182 | 1150 |
| **8** | 1200 | 1111110000 | 435 | 455 | 130 | 130 | 30 | 20 | 0 | 0 | 0 | 0 | 120 | 212 | 1200 |
| **9** | 1300 | 1111111100 | 445 | 455 | 130 | 130 | 85 | 20 | 25 | 10 | 0 | 0 | 130 | 252 | 1300 |
| **10** | 1400 | 1111111111 | 435 | 455 | 130 | 130 | 162 | 33 | 25 | 10 | 10 | 10 | 140 | 262 | 1400 |
| **11** | 1450 | 1111111111 | 445 | 455 | 130 | 130 | 162 | 73 | 25 | 10 | 10 | 10 | 145 | 212 | 1450 |
| **12** | 1500 | 1111111111 | 455 | 455 | 130 | 130 | 162 | 80 | 25 | 43 | 10 | 10 | 150 | 162 | 1500 |
| **13** | 1400 | 1111111100 | 455 | 455 | 130 | 130 | 162 | 33 | 25 | 10 | 0 | 0 | 140 | 152 | 1400 |
| **14** | 1300 | 1111111000 | 455 | 455 | 130 | 130 | 85 | 20 | 25 | 0 | 0 | 0 | 130 | 197 | 1300 |
| **15** | 1200 | 1111100000 | 455 | 455 | 130 | 130 | 30 | 0 | 0 | 0 | 0 | 0 | 120 | 132 | 1200 |
| **16** | 1050 | 1111100000 | 455 | 310 | 130 | 130 | 25 | 0 | 0 | 0 | 0 | 0 | 105 | 282 | 1050 |
| **17** | 1000 | 1111100000 | 455 | 260 | 130 | 130 | 25 | 0 | 0 | 0 | 0 | 0 | 100 | 332 | 1000 |
| **18** | 1100 | 1111101100 | 420 | 360 | 130 | 130 | 25 | 0 | 25 | 10 | 0 | 0 | 110 | 372 | 1100 |
| **19** | 1200 | 1111111100 | 400 | 455 | 130 | 130 | 30 | 20 | 25 | 10 | 0 | 0 | 120 | 352 | 1200 |
| **20** | 1400 | 1111111100 | 455 | 455 | 130 | 130 | 162 | 33 | 25 | 10 | 0 | 0 | 140 | 152 | 1400 |
| **21** | 1300 | 1111111000 | 455 | 455 | 130 | 130 | 85 | 20 | 25 | 0 | 0 | 0 | 130 | 197 | 1300 |
| **22** | 1100 | 1100111000 | 455 | 455 | 0 | 0 | 145 | 20 | 25 | 0 | 0 | 0 | 110 | 137 | 1100 |
| **23** | 900 | 1100100000 | 455 | 410 | 0 | 0 | 35 | 0 | 0 | 0 | 0 | 0 | 90 | 172 | 900 |
| **24** | 800 | 1100100000 | 430 | 345 | 0 | 0 | 25 | 0 | 0 | 0 | 0 | 0 | 80 | 210 | 800 |
| **Maximum limit of unit** | | | 455 | 455 | 130 | 130 | 162 | 80 | 85 | 55 | 55 | 55 | | | |

**Table 2.5:** Cost of all cases for THUC test system-I

| Technique | Case-I ($) | Case-II ($) | Case-III ($) | Case-IV ($) |
|---|---|---|---|---|
| **BPSO-PSO** | 565149.3 | 591751.3 | 588183.7 | 617192.8 |
| **BSA-CSO** | 563989.1 | 582577.1 | 571642.8 | 592259.2 |

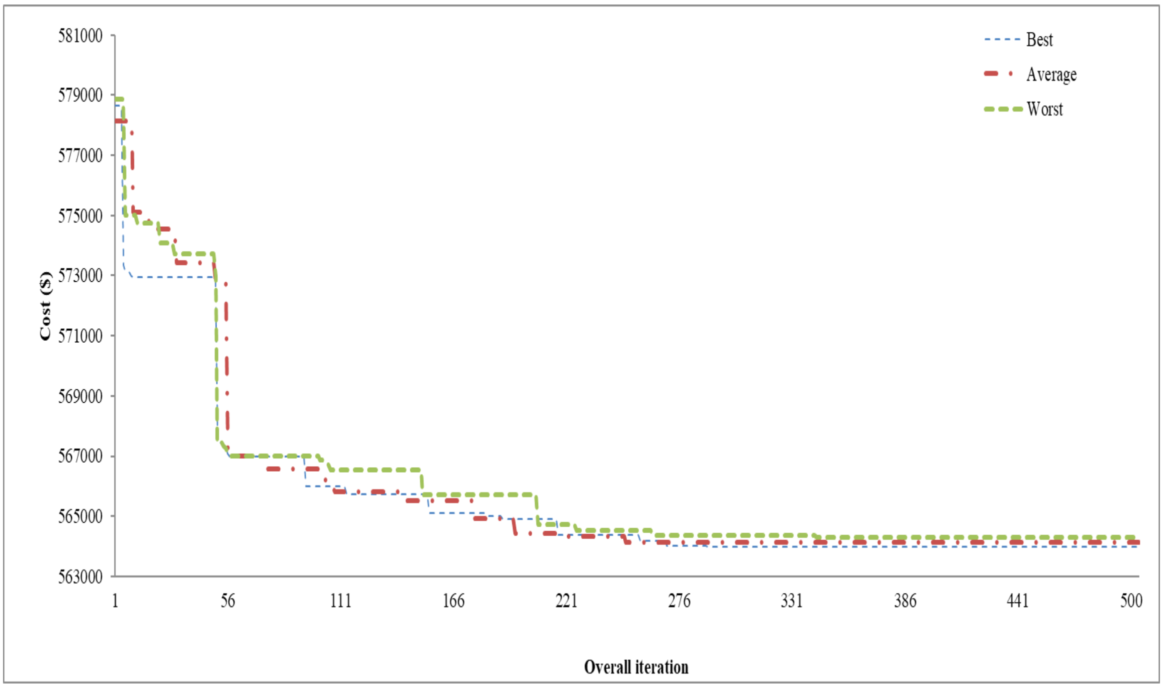


**Figure 2.13:** Convergence curve of BSA-CSO for THUC test system-I, case-I

### 2.7.3 Thermal Unit Commitment Test System-II

In test system-II for case-I, the minimum, average, and worst cost obtained from the BSA-CSO and BPSO-PSO techniques have been given in Table 2.6. The best cost obtained from BSA-CSO proposed technique is $2248510 whereas, in other techniques it has more. The unit commitment schedule of 40 thermal units obtained from BSA-CSO optimization technique has been presented in Table 2.7. It has been observed that the generation schedule obtained from BSA-CSO technique satisfy UC constraints.

The operating cost '$2338497' obtained from BSA-CSO technique for case-II is more in comparison to cost '$2248510' of case-I due to the valve point loading effect. Similarly, the cost of case-III has been increase by '$65654' in comparison to case-I due to inclusion of ramp-rate constraint. On the other hand, in case-IV the cost has been increased by '$150930' due to ramp-rate constraint and valve-point loading effect.

**Table 2.6:** Comparison of cost and CPU time for THUC test system-II, case-I

| Technique | Average Cost ($) (10^4) | Worst Cost ($) (10^4) | Best Cost ($)(10^4) | CPU (sec) |
|---|---|---|---|---|
| **Hybrid CRGA (Tokoro *et al.*, 2008)** | 224.379 | - | - | 265 |
| **Lagrangian relaxation and genetic algorithm (LRGA) (Cheng *et al.*, 2000[1])** | 224.217 | - | - | 2165 |
| **Integer coded genetic algorithm (ICGA) (Damousis *et al.*, 2004)** | 225.412 | - | - | 316.86 |
| **Improved binary particle swarm optimization (IBPSO) (Yuan *et al.*, 2009)** | - | - | 240.172 | 317.29 |
| **Binary particle swarm optimization with bit change mutation (MPSO) (Lee *et al.*, 2007)** | - | - | 232.343 | 274.67 |
| **Local convergence averse BPSO (LCA-BPSO) (Chandrasekaran *et al.*, 2012)** | - | - | 227.739 | - |
| **Advanced fuzzy controlled binary PSO (AFCBPSO) (Chakraborty *et al.*, 2012)** | - | - | 226.604 | - |
| **LR (Sriyanyong and Song, 2005)** | - | - | 225.850 | 199.55 |
| **Enhanced simulated annealing (ESA) (Simopoulos *et al.*, 2006)** | 225.697 | 225.889 | 225.586 | - |
| **GA (Simopoulos *et al.*, 2006)** | 226.258 | 226.928 | 225.290 | 2697 |
| **GA (Kazarlis *et al.*, 1996)** | - | 225.970 | 225.191 | - |
| **LR (Simopoulos *et al.*, 2006)** | 225.022 | 225.022 | 225.022 | 88.28 |
| **Enhanced simulated annealing (ESA) (Simopoulos *et al.*, 2006)** | 225.212 | 225.453 | 225.006 | - |
| **PSO (Zhao *et al.*, 2006)** | - | 225.714 | 225.001 | 614 |
| **Intelligent mutation based genetic algorithm (UCC-GA) (Senjyu *et al.*, 2002)** | - | 225.682 | 224.971 | 2697 |
| **GA (Kazarlis *et al.*, 1996)** | - | 225.682 | 224.971 | - |
| **SM (Simopoulos *et al.*, 2006)** | 224.958 | 224.958 | 224.958 | 1176 |
| **EP (Monteiro *et al.*, 2009)** | 225.261 | - | 224.909 | - |
| **EP (Simopoulos *et al.*, 2006)** | 225.261 | 225.608 | 224.909 | 467 |
| **Harmony search (HS) (Najafi *et al.*, 2012)** | 225.096 | - | - | 78 |
| **BPSO-PSO** | 225.567 | 225.622 | 225.538 | 720 |
| **Proposed method** | **224.875** | **224.882** | **224.851** | **503** |

**Table 2.7:** Hourly status of units obtained by BSA-CSO for THUC test system-II, case-I

| Sub-intervals (h) | Unit status |
|---|---|
| **1** | 11111111000000000000000000000000000000000 |
| **2** | 11111111000000000000000000000000000000000 |
| **3** | 11111111000001000000000000000000000000000 |
| **4** | 11111111000001001110000000000000000000000 |
| **5** | 11111111000001001111000000000000000000000 |
| **6** | 11111111111111001111000000000000000000000 |
| **7** | 11111111111111001111000000000000000000000 |
| **8** | 11111111111111111111000000100000000000000 |
| **9** | 11111111111111111111111011101000000000000 |
| **10** | 11111111111111111111111111111111100000000 |

| | |
|---|---|
| **11** | 1111111111111111111111111111111111110000 |
| **12** | 1111111111111111111111111111111111111111 |
| **13** | 1111111111111111111111110111111100000000 |
| **14** | 1111111111111111111111010001000000000000 |
| **15** | 1111111111111111111100000000000000000000 |
| **16** | 1111111111111111111100000000000000000000 |
| **17** | 1111111111111111111100000000000000000000 |
| **18** | 1111111111111111111100000000000000000000 |
| **19** | 1111111111111111111100000110000000000000 |
| **20** | 1111111111111111111111111111111100001000 |
| **21** | 1111111111111100111111111111000000000000 |
| **22** | 1111111100100000111011110011000000000000 |
| **23** | 1111111100000000101000000000000000000000 |
| **24** | 1111111100000000000000000000000000000000 |

The results obtained from BPSO-PSO and BSA-CSO technique in cases of THUC problem has been given in Table 2.8. From this table it is clear that the cost obtained from the BPSO-PSO technique in case-I is $6874 more as compare to BSA-CSO technique. It has been also found that the CPU time consumed during BSA-CSO optimization is less compare to BPSO-PSO in case-I. Similarly, similar results have been obtained in all other cases also. Therefore, the results obtained from BSA-CSO technique is better as compare to BPSO-PSO technique for THUC problem.

**Table 2.8:** Cost of all cases for THUC test system-II

| Technique | Case-I ($) | Case-II ($) | Case-III ($) | Case-IV ($) |
|---|---|---|---|---|
| **BPSO-PSO** | 2255384 | 2354829 | 2373972 | 2478348 |
| **BSA-CSO** | 2248510 | 2338497 | 2314162 | 2399440 |

### 2.7.4 Statistical Analysis

To check the performance of the BSA-CSO, nonparametric Wilcoxon signed rank test is applied on case-I of test system-I. The Wilcoxon signed rank test helps to identify the significant difference between a single sample and median of the sample. The test is performed at a level of significance α=0.01. It is evident from Table 2.9 that test statistic $W>W_{crt}$ (203>120), the null hypothesis cannot be rejected (p>0.01). Hence, there is no significant difference between the sample and median of data.

**Table 2.9:** Wilcoxon signed rank test for THUC test system-I, case-I

| | **Values** |
|---|---|
| **Parameters** | **Test system-I** |
| **Test statistic (W)** | 203 |
| **p-value** | 0.27093 |
| **Critical value of test statistic ($W_{crt}$)** | 120 |

In the BSA-CSO technique, the best cost, average cost, worst cost and standard deviation obtained for case-I of test systems have been given in Table 2.10.

**Table 2.10:** Statistical results obtained from BSA-CSO technique for THUC test systems, case-I

| | **Test system-I** | **Test system-II** |
|---|---|---|
| **Best cost ($)** | 563989 | 2248510 |
| **Average cost ($)** | 564129 | 2248751.68 |
| **Worst cost ($)** | 564289 | 2248827.5 |
| **Standard deviation** | 0.00576 | 0.1415024 |

## 2.8 CONCLUSIONS

In this work, the proposed BSA-CSO technique has verified on 10, and 40 unit THUC systems with various constraints. A hybrid technique is proposed which is the integration of the BSA and CSO techniques. The BSA method has applied to find optimal unit status with minimum computational burden whereas the optimal generation schedule of committed units has obtained by CSO technique. The CSO technique is a combination of PSO and SCA algorithm that helps to maintain the proper balance between diversification and intensification of the algorithm. In test system-I, cost obtained from BSA-CSO technique in case-I, II, III and IV are 0.21%, 1.57%, 2.89% and 4.21%, respectively less as compare to the BPSO-PSO technique. In test system-II, the results obtained from BSA-CSO technique in case-I, II, III and IV are 0.30%, 0.69%, 2.58% and 3.18%, respectively less as compare to BPSO-PSO technique. The solution obtained from BSA-CSO algorithm has given realistic results when ramp-rate constraints is included in the THUC problem. It has been observed that total operating cost of RP-THUC problem has increases as compared to THUC problem. The cost achieved by the BSA-CSO technique has lower as compared to other techniques developed for single processor systems; the performance of the multiprocessor system is superior and underlines the future scope.

# CHAPTER – 3

# PROFIT BASED THERMAL UNIT COMMITMENT SCHEDULE

## 3.1 INTRODUCTION

The conventional power system is focused on the *unit commitment* (UC) problem **(Wood *et al.*, 2013; Ongsakul and Vo, 2013)**. In the conventional electric power systems, the cost minimization is considered as an objective of the UC problem. The UC problem consists of binary and continuous decision variables; hence UC problem is a mixed-integer optimization problem. In the recent trend, the power systems structure has been transformed from the conventional system into a deregulated environment. The restructuration of the electric system has renovated the vertically integrated power system. Therefore, significant changes have been carried out in the traditional operational system of the power sector. In the deregulated environment, the *generation companies* (GENCOs) act as a service provider. The traditional generation scheduling policies have been changed for GENCOs to sustain in the deregulated power sector. The main aim of the *profit based UC* (PBUC) problem is to maximize the profit of GENCOs **(Ongsakul and Vo, 2013)**. In the PBUC problem, forecast demand and reserve requirement are considered as soft constraints.

Various optimization approaches have been applied to search the optimum solution of the PBUC problem. The Lagrangian multiplier adjustment approach **(Kazarlis *et al.*, 1996)**, *mixed-integer linear programming* (MILP) **(Zhai *et al.*, 2009)** are implemented to solve the PBUC problem. In order to improve the solution quality, the Lagrange multipliers are updated with a gradient based *Lagrangian Relaxation* (LR) approach **(Cheng *et al.*, 2000)**. In the MILP method, the computation burden is high for large range PBUC problem.

In order to overcome limitations of conventional search technique, researchers have explored global search optimization techniques such as *genetic algorithm* (GA) **(Kazarlis *et al.*, 1996; Sheble *et al.*, 1996; Marifeld and Sheble, 1996)**, *evolutionary programming* (EP) **(Juste *et al.*, 1999)**, *particle swarm optimization* (PSO) **(Raglend *et al.*, 2010; Christopher and Sishaj, 2011)**. The binary and continuous version of the PSO technique has been employed by researchers to solve the UC optimization problem **(Lee *et al.*, 2007; Zhao *et al.*, 2006)**. Researchers have implemented global search optimization techniques such as *nodal ant colony optimization* (NACO) **(Columbus *et al.*, 2012)**, *binary fish swarm algorithm* (BFSA) **(Singhal *et al.*, 2015)**, *ant colony optimization* (ACO) **(Vaisakh and Srinivas, 2011)**, *binary fireworks algorithm* (BWFA) **(Reddy *et al.*, 2016)**, *parallel artificial bee colony* (PABC) **(Columbus and Simon, 2012)**, *imperialist competitive algorithm* (ICA) **(Ghadi *et al.*, 2016)** and *gravitational search* (GS) **(Roy, 2013)** to solve the PBUC problem.

For large scale PBUC problem, the solution obtained from global search optimization techniques is prone to fall into local optima. The global search optimization techniques are parameter sensitive towards the selection of parameters. In addition to the aforementioned global search optimization techniques, researchers have explored hybrid optimization techniques to solve the PBUC problem. In past years, various optimization techniques based on the integration of two or more optimization techniques are studied. The hybrid techniques such as LR-GA **(Sheble *et al.*, 1996; Cheng *et al.*, 2000)**, LR and differential evolution **(Sudhakar *et al.*, 2017)**, LR-PSO **(Sriyanyong and Song, 2005)**, LR-ACO **(Saber and Alshareef, 2008)**, ICA and evolutionary algorithm **(Ghadi *et al.*, 2016)** have implemented to solve PBUC problem. The hybrid techniques provide more profitable solutions to the PBUC problem as compared to the global search optimization technique.

The intent of this Chapter is to solve the PBUC problem by implementing the proposed optimization technique. The proposed optimization technique is based on the integration of *civilized swarm optimization* (CSO) and *binary successive approximation* (BSA) algorithm, which boosts the exploration and exploitation capability of the technique. The *binary PSO and PSO* (BPSO-PSO) and *BSA and CSO* (BSA-CSO) optimization techniques are implemented to find the optimum UC status and generation schedule of thermal generating units. The heuristics method has been implemented for commitment and de-commitment constraint handling scheme to satisfy the PBUC constraints. In order to satisfy the practical generation dispatch constraints such as generation limits, ramp-rate limits, and power demand of the PBUC problem, the penalty function approach has been applied, and it is discussed in step 3 of section 2.5 of Chapter 2. In order to authenticate the applicability of the BSA-CSO technique, three PBUC test systems have been undertaken, which are of small, medium, and large size with due consideration of various practical constraints. Further, the statistical test has been performed to investigate the quality of the obtained solutions.

## 3.2 STATEMENT OF PROFIT BASED UNIT COMMITMENT PROBLEM

With the opening of the power industry to competition, the power system structure is changing. According to these changes, power system operation, planning, and control need modifications. In the past, utilities had to produce power to satisfy their customers with objective to minimize costs and all demand/reserve were met. However, it is not necessary in a restructured system. Under new structure, generation companies (GENCOs) schedule their generators with objective to maximize their own profit without regard for system social benefit whereas the main aim of THUC problem is to minimize the overall cost. Power and reserve prices become important factors in decision process. The PBUC is a mixed integer problem. The generation schedule is controlled by binary (unit status (I)) and continuous (power (P)) decision variables. In order to achieve the maximum profit of GENCOs, there is a requirement of a turn ON or OFF the thermal unit and schedule the power generation from the committed unit. The PBUC constraints include unit commitment and generation constraints such as spinning reserve requirement, minimum up and down time, start-up and shut-down ramp-rate limits, power demand, generation, and ramp up/down limits.

The objective of the PBUC problem is to maximize the GENCOs profit by scheduling the power from the UC schedule, which is based on energy price, revenue, fuel cost and start-up cost and is represented as **(Columbus and Simon, 2012)**:

Maximum $PF = RV - TC$ (3.1)

The revenue is generated by selling the generated power at appropriate energy price and is given in Eq. 3.2 **(Columbus and Simon, 2012)**. The total operating cost ($TC$) is given in Eq. 3.3. The fuel cost ($F(P_{ti}^{th})$) comprises of valve-point loading effect and quadratic function and start-up cost which is discussed in Eq. 3.4 and 3.5.

$$RV = \sum_{t=1}^{T} \sum_{i=1}^{Ng} \sigma t\, P_{ti}^{th} I ti \quad (3.2)$$

$$TC = \sum_{t=1}^{T} \sum_{i=1}^{Ng} \left[ F(P_{ti}^{th}) + ST_{ti} \left( 1 - I(t-1)i \right) \right] I ti + SD_{ti} \left( 1 - I_{ti} \right) I(t-1)i \quad (3.3)$$

$$F(P_{ti}^{th}) = a_i + b_i P_{ti}^{th} + c_i (P_{ti}^{th})^2 + \left| d_i sin(e_i(\underline{P_i^{th}} - P_{ti}^{th})) \right|$$
$$i \in [1, Ng] \ , t \in [1,T] \qquad (3.4)$$

$$STti = \begin{cases} HSi & T_i^{dw} \le T_{ti}^{off} \le T_i^{dw} + T_i^{cold} \\ CSi & T_{ti}^{off} > T_i^{dw} + T_i^{cold} \end{cases} \qquad i \in [1, Ng] \ , t \in [1,T] \qquad (3.5)$$

where *PF* is the profit obtained by selling the generated power from thermal units ($); *RV* is the revenue generated ($); *TC* is the total operating cost ($); $\sigma_t$ is the energy price at $t^{th}$ sub-interval ($/MWh); $I_{ti}$ is the unit ON/OFF status of $i^{th}$ generating unit at $t^{th}$ sub-interval; $P_{ti}^{th}$ is the power generation of $i^{th}$ generating unit at $t^{th}$ sub-interval (MW); *T* is total time interval; and *Ng* is the total number of generating units.

The complete PBUC formulation is given below:

$$Max \quad PF = \sum_{t=1}^{T} \sum_{i=1}^{Ng} \left[ \sigma t P_{ti}^{th} Iti - \left( F(P_{ti}^{th}) + ST_{ti} \left(1 - I_{(t-1)i}\right) Iti \right) \right] \qquad (3.6)$$

Subjected to technical constraints which are specified in the following sub-sections:

$$I_{ti} = \begin{cases} 1 & ; T_{(t-1)i}^{on} < T_i^{up} \\ 0 & ; T_{(t-1)i}^{off} < T_i^{dw} \\ 1 \text{ or } 0 & ; otherwise \end{cases} \qquad (3.7)$$

$$\sum_{i=1}^{N} \overline{P_i^{th}} I_{ti} \le PD_t + SP_t \qquad (3.8)$$

$$\sum_{i=1}^{Ng} P_{ti}^{th} I_{ti} \le PD_t \qquad (3.9)$$

$$\underline{P_i^{th}} \le P_{ti}^{th} \le \overline{P_i^{th}} \qquad (3.10)$$

$$P_{ti}^{th} - P_{(t\text{-}1)i}^{th} \le UR_i^{th} \qquad (3.11)$$

$$P_{(t\text{-}1)i}^{th} - P_{ti}^{th} \le DR_i^{th} \qquad (3.12)$$

$$CP_{hi} = Min(\overline{P_i^{th}}, UR_i^{th}(h-n)) \qquad (3.13)$$

$$CP_{hi} = \overline{P_i^{th}} - DR_i^{th} \times (h-n) \qquad (3.14)$$

The minimum up and down time (Eq. 3.7), power (Eq. 3.10), generation ramp (Eqs. 3.11-3.12) and start-up/shut-down generation (Eqs. 3.13-3.14) limits are same as discussed in section 2.2 of Chapter 2. In PBUC problem, the maximum available power from committed thermal units should not be more than power demand along with spinning power reserve at $t^{th}$ sub-interval and is given in Eq. 3.8 **(Columbus and Simon, 2012)** whereas in THUC problem, the maximum available power from committed thermal units should be more than power demand along with spinning power reserve. In the deregulated power market, generated power from the committed generators should be less than or equal to the forecast load demand ( $PD_t$ ) and is represented in Eq. 3.9 **(Columbus and Simon, 2012)** whereas in THUC problem, generated power from the committed generators should be equal to the forecast load demand. Fig. 3.1 represents the flowchart of profit based unit commitment formulation, the objective function of PBUC problem is based on power price, revenue and cost whereas in THUC, the objective function consist of cost function only.

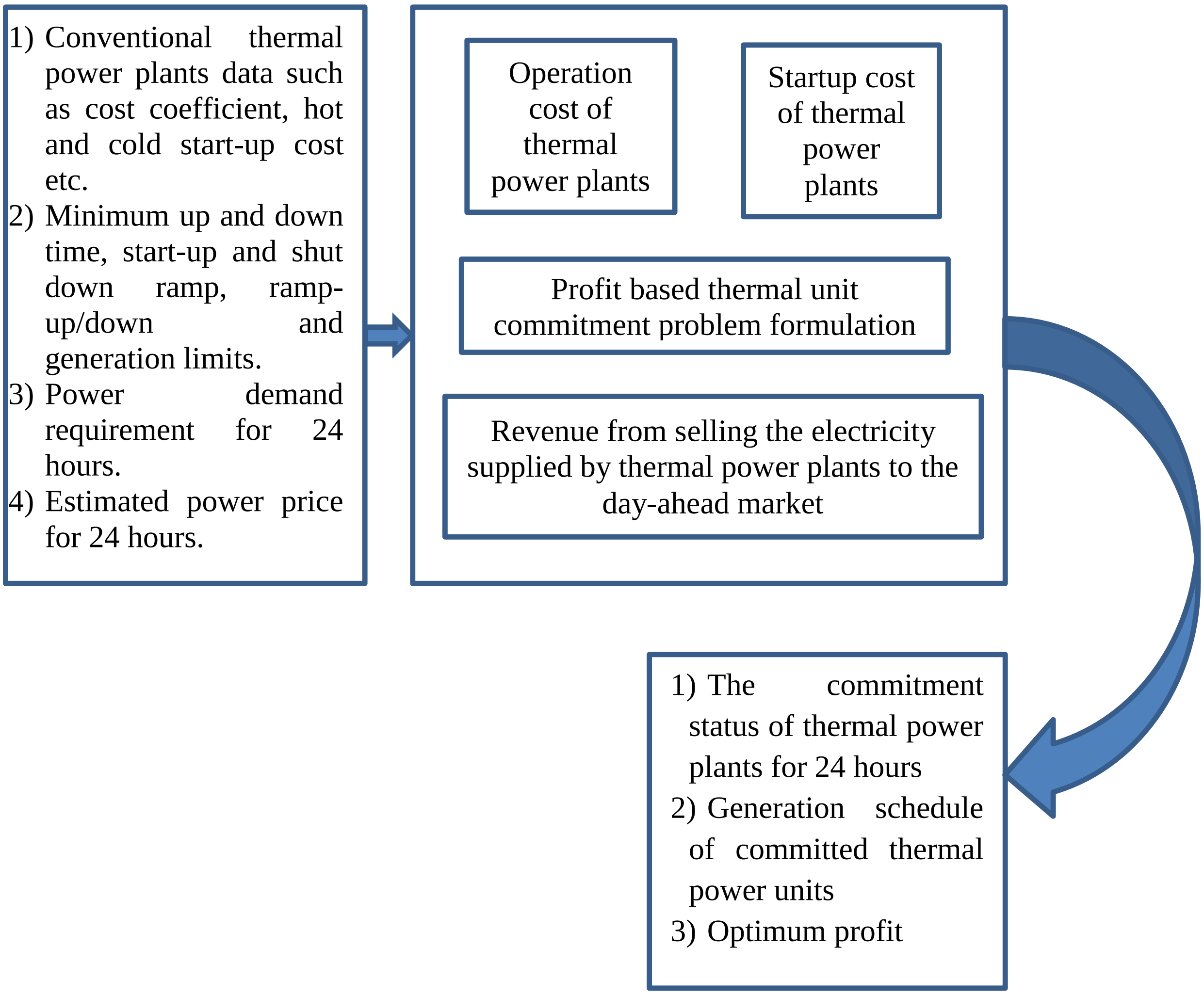


**Figure 3.1:** The flow chart of PBUC problem formulation

where $P_{ti}^{th}$ is the power generation of $i^{th}$ thermal unit at $t^{th}$ sub-interval (MW); and $PD_t$ is the power demand at $t^{th}$ sub-interval (MW). where $I_{ti}$ is $i^{th}$ generating unit ON/OFF status at $t^{th}$ sub-interval; $\overline{P_i^{th}}$ is the maximum power generation of $i^{th}$ thermal generating unit (MW); $PD_t$ and $SP_t$ are the power demand and spinning reserve requirement at $t^{th}$ sub-interval, respectively (MW).

## 3.3 IMPLEMENTATION OF BINARY SUCCESSIVE APPROXIMATION AND CIVILIZED SWARM OPTIMIZATION TECHNIQUE FOR PROFIT BASED UNIT COMMITMENT PROBLEM

The BSA-CSO technique is proposed to solve the PBUC problem. The detail discussion regarding the BSA-CSO technique is presented in sections 2.3, 2.4 and 2.5 of Chapter 2. In the solution procedure, the unit status is updated by BSA and it should satisfy the minimum up and down time and reserve constraints. The CSO technique is applied to search the optimum power generation schedule from the committed thermal unit. The elaborated steps of implementation of BSA-CSO approach to solving the PBUC problem are given as:

Step 1: **Input:** Read the input data of the system such as power demand, electricity price, cost coefficient of thermal units, optimization technique parameters.

Step 2: **Initialization:** The unit status and power generation are randomly initialized within the bounds.

Step 3: **Objective function formulation:** The objective of the PBUC problem is to maximize the profit while satisfaction of various UC and generation constraints. The detail discussion regarding constraint handling and objective function formulation is given as follows:

(i) **Minimum up and down time constraint:** The committed thermal unit should satisfy minimum up and down time constraints. The pseudo code to satisfy minimum up and down time constraint is presented in Figure 2.7 of Chapter 2.

(ii) **Unit de-commitment:** The satisfaction of time constraints may lead to excessive spinning reserve, which inclines the system towards the lower profit. Hence, there is a need to de-commit some of the units. The de-commitment process is done based on the priority list **(Senjyu *et al.*, 2003)**. The procedure of heuristic adjustment of de-commitment is given in Figure 3.2.

```
Read input T, Ng, PL, PD_t, P_i^th (min), P_i^th (max), T_i^up, T_i^dw and T_i^in.
For t=1: T
        SPR_t = Σ_{i=1}^{Ng} P̄_i^th I_ti − PD_t − SP_t
        Count=0
        For i=1: Ng
                If (I_ti = 1)
                Count=count+1
                NL(count)= i
                End if
        End for
        Sort NL based on PL.
        For k=1: Count
                If ( SPR_t > 0 )
                        I_tk = 0 based on time constraints handling I_tk ∈ NL_k
                End if
    End for
End for
```

**Figure 3.2:** Pseudo code for de-commitment process

(iii) **Ramp rate constraint:** The procedure of heuristic adjustment to satisfy ramp-rate constraint is illustrated in Figure 2.10 of Chapter 2.

(iv) **Generation ramp limit:** The ramp up and down constraint must be satisfied throughout the procedure in the PBUC problem which is specified in step 3 of section 2.6 of Chapter 2.

(v) **Power demand constraint:** In order to satisfy, the power demand constraint is given by Eq. (3.9), the exterior penalty approach is applied.

Hence, the objective function is formulated as:

$$obj = PF - \psi_1 \times \sum_{t=1}^{T} E_t \tag{3.15}$$

where
$$E_t = \begin{cases} \left( \sum_{i=1}^{Ng} I_{ti} \times P_{ti}^{th} - PD_t \right)^2 ; & \sum_{i=1}^{Ng} I_{ti} P_{ti}^{th} > PD_t \\ 0; & Otherwise \end{cases} \qquad t \in [1,T] \tag{3.16}$$

where *PF* is the profit ($); $E_t$ is the error for power demand at $t^{th}$ sub-interval; $\psi_1$ is the penalty factor; *T* is total time interval; and *Ng* is the total number of generating units

The constraint handling procedure of PBUC problem with BSA-CSO technique is different from THUC problem due to soft constraints such as power spinning reserve and power demand constraints and it is shown in Figure 3.3. Therefore, decommitment process and exterior penalty method is modified accordingly.

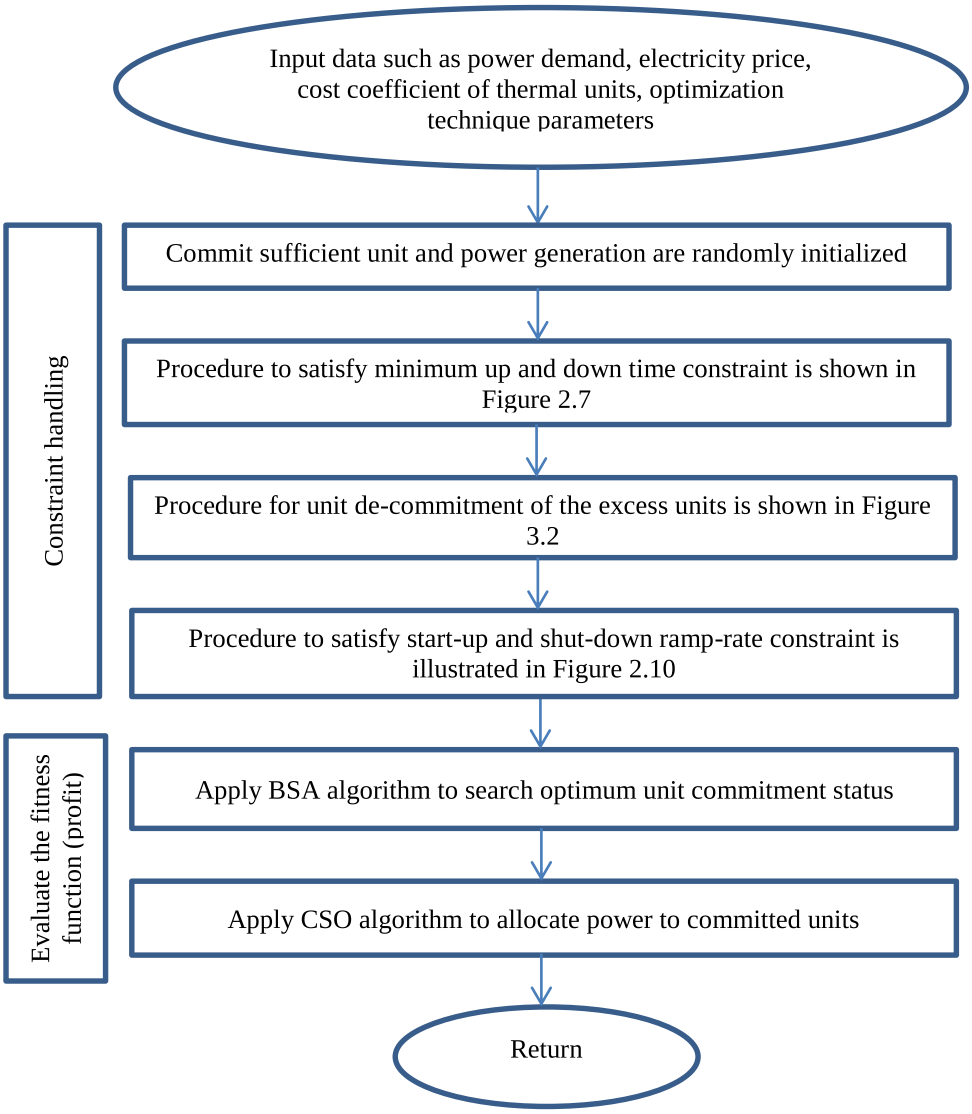


**Figure 3.3:** Constraint handling procedure of PBUC problem with BSA-CSO technique

Step 4: The unit status of generating units is updated using the BSA technique. The power generated from committed units is updated by the CSO technique and the objective function is evaluated using Eq. 3.15. The detail regarding the updating of decision variables *i.e.,* unit and power using the BSA-CSO technique is discussed in section 2.6 of Chapter 2.

Step 5: The overall upgradation procedure is repeated till the termination criteria is met.

## 3.4 PROFIT BASED UNIT COMMITMENT TEST SYSTEMS AND RESULTS

In order to validate the effectiveness of the proposed technique, three PBUC test systems having non-convex and non-linear characteristics are undertaken. The test system-I, II and III are having 10, 40, and 100 units, respectively, and 24-sub-interval scheduling period with one sub-interval. The input data of these test systems in the deregulated environment are taken from reference **(Sudhakar *et al.*, 2017)** and it is given in Appendix-B.2. The implementation of the proposed BSA-CSO algorithm for solving PBUC is coded in FORTRAN 90 environment on a personal computer (1.66 GHz, Pentium-IV, with 2 GB RAM). For the simulation study, four different cases have been undertaken. The PBUC problem without consideration of ramp-rate constraint and valve-point loading effect is considered as case-I. The case-II incorporates the valve point loading effect of generating unit, whereas the case-III incorporates ramp-rate constraint only. The case-IV of PBUC problem includes the valve point loading effect and unit ramp-rate constraints.

### 3.4.1 Parameter Tuning

The successful implementation of the proposed algorithms requires the optimum parameter selection of the BSA-CSO algorithm. The algorithm parameters are selected after many trails performed on these test systems. The set values of the BSA-CSO algorithm parameters, *i.e.*, swarm size, society, inertia weight and acceleration coefficients for obtaining optimal solutions for test system-I are given in Table 3.1.

**Table 3.1:** Optimal parameters of the proposed algorithm

| **Parameter** | **BSA-CSO** |
|---|---|
| $\mathbf{N_p}$ | 20 |
| $\mathbf{N_s}$ | 4 |
| **Inertia weight** | $W_{max}$=0.9, $W_{min}$=0.4 |
| **Acceleration coefficients** | $C_L$=2, $C_{SL1}$=0.5, $C_{SL2}$=0.5, $C_{SM1}$=0.25, $C_{SM2}$=0.75 |
| **Iteration** | $it^{max}$=10 |

In order to set the maximum iteration for the CSO algorithm, initially, it has been taken as 100 iterations. It has been observed after a number of trials, that there is no significant improvement after around 50 iterations. Hence, the maximum iteration is set to 50.

### 3.4.2 Profit Based Unit Commitment Test System-I

The BPSO-PSO and BSA-CSO techniques have been applied on 30 individual trails for four cases. The obtained results have been compared with the state of the art techniques for case-I. The maximum, average, and worst profit obtained by the BPSO-PSO and BPSO-PSO techniques have been tabulated in Table 3.2, for case-I. For the BSA-CSO technique, the commitment status and power generation at each sub-interval for case-I has been given in Table 3.3. The results have been compared with BPSO-PSO, *TS-random perturbation* (RP) (TS-RP) **(Victoire and Jeyakumar, 2005)**, *TS improved RP* (TS-IRP) **(Victoire and Jeyakumar, 2005)**, Muller method **(Chandram *et al.*, 2008)**, ACO **(Vaisakh and Srinivas, 2011)**, *improved pre-prepared power demand* (IPPD) **(Chandram *et al.*, 2009)**, NACO **(Columbus *et al.*, 2012)**, *variable neighbourhood Tabu search parallel enhanced PSO* (VTS-PEPSO) **(Mori and Okawa, 2009)**, PABC **(Columbus and Simon, 2012)**, *parallel NACO* (PNACO) **(Columbus and Simon, 2013)**, BFWA **(Reddy *et al.*, 2016)**, and ICA **(Ghadi *et al.*, 2016)**. It is evident from Table 3.2 that the proposed technique is able to achieve higher profit as compared to other techniques. As per the author knowledge, other cases have not been reported in the literature.

Further, to compare the computational performance of the proposed technique, the *number of function evaluations* ($N_{FE}$) has been given in Table 3.2. It is evident from Table 3.2 that $N_{FE}$ required by the proposed technique is least as compared to other optimization algorithms. The CPU time of the proposed technique for case-I is 57.8 sec, which is more as compared to VTS-PEPSO **(Mori and Okawa, 2009)** and ICA **(Ghadi *et al.*, 2016)**, however, it is processor dependent. In order to compare the results of PBUC with THUC problem, the unit status, power generation and available spinning reserve during each hour represents in Table 3.4. It has been observed that the total power generation and available spinning reserve from committed units in PBUC is less or equal to total power generation in THUC problem.

**Table 3.2:** Comparison for profit, $N_{FE}$ and CPU time for PBUC test system-I, case-I

| Technique | Average Profit ($)($\times 10^3$) | Best Profit ($) ($\times 10^3$) | Worst Profit ($) ($\times 10^3$) | Standard Deviation ($\times 10^{-4}$) | $N_{FE}$($\times 10^4$) | CPU (sec) ($\times 10^2$) |
|---|---|---|---|---|---|---|
| **TS-RP** (**Victoire and Jeyakumar, 2005**) | - | 101.08 | - | - | - | - |
| **TS-IRP** (**Victoire and Jeyakumar, 2005**) | - | 103.26 | - | - | - | - |
| **Muller method** (**Chandram *et al.*, 2008**) | - | 103.29 | - | - | - | - |
| **ACO** (**Vaisakh and Srinivas, 2011**) | - | 103.89 | - | - | - | 129.60 |
| **Improved pre-prepared power demand** (**Chandram *et al.*, 2009**) | - | 105.54 | - | - | - | - |
| **NACO** (**Columbus *et al.*, 2012**) | - | 105.87 | - | - | 144 | 3.37 |
| **VTS-PEPSO** (**Mori and Okawa, 2009**) | - | 105.87 | - | - | - | 0.39 |
| **PABC** (**Columbus and Simon, 2012**) | - | 105.87 | - | - | 144 | 1.35 |
| **PNACO** (**Columbus and Simon, 2013**) | - | 105.94 | - | - | 480 | 2.23 |
| **BFWA** (**Reddy *et al.*, 2016**) | 106.20 | 106.85 | 105.90 | 9.00 | - | 0.58 |
| **ICA** (**Ghadi *et al.*, 2016**) | - | 107.68 | - | - | 600 | 0.20 |
| **BPSO-PSO** | 89.927 | 90.060 | 89.876 | 10.00 | 400 | 105 |
| **Proposed method** | **107.63** | **107.70** | **107.60** | **7.00** | **2.85** | **0.57** |

**Table 3.3:** Hourly power dispatch obtained from BSA-CSO for PBUC test system-I, case-I and case-II

| **Sub-intervals (h)** | **Power demand (MW)** | **Price ($/MWh)** | **Units status** | **Generated power (MW)** | | | | | | | | | | **Spinning reserve (MW)** | **Total power Generation (MW)** | **Case-I** | **Case-II** |
|---|---|---|---|---|---|---|---|---|---|---|---|---|---|---|---|---|---|
| | | | | **P1** | **P2** | **P3** | **P4** | **P5** | **P6** | **P7** | **P8** | **P9** | **P10** | | | **Profit ($/h)** | **Profit ($/h)** |
| **1** | 700 | 22.15 | 1100000000 | 455 | 245 | 0 | 0 | 0 | 0 | 0 | 0 | 0 | 0 | 210 | 700 | 1821.87 | 1629.37 |
| **2** | 750 | 22 | 1100000000 | 455 | 295 | 0 | 0 | 0 | 0 | 0 | 0 | 0 | 0 | 160 | 750 | 1945.5 | 1393.55 |
| **3** | 850 | 23.1 | 1100000000 | 455 | 395 | 0 | 0 | 0 | 0 | 0 | 0 | 0 | 0 | 60 | 850 | 3333.11 | 2964.363 |
| **4** | 950 | 22.65 | 1100000000 | 455 | 455 | 0 | 0 | 0 | 0 | 0 | 0 | 0 | 0 | 0 | 910 | 3258.199 | 2630.672 |
| **5** | 1000 | 23.25 | 1101000000 | 455 | 415 | 0 | 130 | 0 | 0 | 0 | 0 | 0 | 0 | 40 | 1000 | 3177.607 | 2402.79 |
| **6** | 1100 | 22.95 | 1101000000 | 455 | 455 | 0 | 130 | 0 | 0 | 0 | 0 | 0 | 0 | 0 | 1040 | 3654.041 | 2887.7 |
| **7** | 1150 | 22.5 | 1101000000 | 455 | 455 | 0 | 130 | 0 | 0 | 0 | 0 | 0 | 0 | 0 | 1040 | 3186.04 | 2419.7 |
| **8** | 1200 | 22.15 | 1101000000 | 455 | 455 | 0 | 130 | 0 | 0 | 0 | 0 | 0 | 0 | 0 | 1040 | 2822.04 | 2055.7 |
| **9** | 1300 | 22.8 | 1111000000 | 455 | 455 | 130 | 130 | 0 | 0 | 0 | 0 | 0 | 0 | 0 | 1170 | 2470.24 | 1684.2 |
| **10** | 1400 | **29.35** | **1111110000** | **455** | **455** | **130** | **130** | **162** | **68** | **0** | **0** | **0** | **0** | **12** | **1400** | **10181.79** | **8965.77** |
| **11** | 1450 | **30.15** | **1111110000** | **455** | **455** | **130** | **130** | **162** | **80** | **0** | **0** | **0** | **0** | **0** | **1412** | **13523.8** | **12457.97** |
| **12** | 1500 | **31.65** | **1111110000** | **455** | **455** | **130** | **130** | **162** | **80** | **0** | **0** | **0** | **0** | **0** | **1412** | **15641.82** | **14575.97** |
| **13** | **1400** | **24.6** | **1111100000** | **455** | **455** | **130** | **130** | **162** | **0** | **0** | **0** | **0** | **0** | **0** | **1332** | **5915.58** | **4929.91** |
| **14** | **1300** | **24.5** | **1111100000** | **455** | **455** | **130** | **130** | **130** | **0** | **0** | **0** | **0** | **0** | **32** | **1300** | **5665.97** | **4788.73** |
| **15** | 1200 | 22.5 | 1101100000 | 455 | 455 | 0 | 130 | 160 | 0 | 0 | 0 | 0 | 0 | 2 | 1200 | 3082.15 | 2093.1 |
| **16** | 1050 | 22.3 | 1101000000 | 455 | 455 | 0 | 130 | 0 | 0 | 0 | 0 | 0 | 0 | 0 | 1040 | 2978.041 | 2211.7 |
| **17** | 1000 | 22.25 | 1101000000 | 455 | 415 | 0 | 130 | 0 | 0 | 0 | 0 | 0 | 0 | 40 | 1000 | 2737.5 | 1962.8 |
| **18** | 1100 | 22.05 | 1101000000 | 455 | 455 | 0 | 130 | 0 | 0 | 0 | 0 | 0 | 0 | 0 | 1040 | 2718.4 | 1951.71 |
| **19** | 1200 | 22.2 | 1101000000 | 455 | 455 | 0 | 130 | 0 | 0 | 0 | 0 | 0 | 0 | 0 | 1040 | 2874.4 | 2107.7 |
| **20** | 1400 | 22.65 | 1101000000 | 455 | 455 | 0 | 130 | 0 | 0 | 0 | 0 | 0 | 0 | 0 | 1040 | 3342.04 | 2575.7 |
| **21** | 1300 | 23.1 | 1101000000 | 455 | 455 | 0 | 130 | 0 | 0 | 0 | 0 | 0 | 0 | 0 | 1040 | 3810.5 | 3043.7 |
| **22** | 1100 | 22.95 | 1101000000 | 455 | 455 | 0 | 130 | 0 | 0 | 0 | 0 | 0 | 0 | 0 | 1040 | 3654.04 | 2887.7 |
| **23** | 900 | 22.75 | 1100000000 | 455 | 445 | 0 | 0 | 0 | 0 | 0 | 0 | 0 | 0 | 10 | 900 | 3297.09 | 2711.3 |
| **24** | 800 | 22.55 | 1100000000 | 455 | 345 | 0 | 0 | 0 | 0 | 0 | 0 | 0 | 0 | 110 | 800 | 2612.58 | 2181.8 |
| **Maximum limit of unit** | | | | 455 | 455 | 130 | 130 | 162 | 80 | 85 | 55 | 55 | 55 | | **Total** | 107707 | 89513.75 |

**Table 3.4:** Comparison of status, power generation and spinning reserve for THUC and PBUC test system-I, case-I

| | **Unit status** | | **Power generation (MW)** | | **Available spinning reserve (MW)** | |
|---|---|---|---|---|---|---|
| **Sub-intervals (h)** | **THUC** | **PBUC** | **THUC** | **PBUC** | **THUC** | **PBUC** |
| **1** | 1100000000 | 1100000000 | 700 | 700 | 210 | 210 |
| **2** | 1100000000 | 1100000000 | 750 | 750 | 160 | 160 |
| **3** | 1100100000 | 1100000000 | 850 | 850 | 222 | **60** |
| **4** | 1100100000 | 1100**0**00000 | 950 | 910 | 122 | **0** |
| **5** | 1101100000 | 11**0**1**0**00000 | 1000 | 1000 | 202 | **40** |
| **6** | 1111100000 | 11**01**0**0**00000 | 1100 | **1040** | 232 | **0** |
| **7** | 1111100000 | 11**01**0**0**00000 | 1150 | **1040** | 182 | **0** |
| **8** | 1111100000 | 11**01**0**0**00000 | 1200 | **1040** | 132 | **0** |
| **9** | 1111111000 | 1111**000**000 | 1300 | **1170** | 197 | **0** |
| **10** | 1111111100 | 111111**00**00 | 1400 | 1400 | 152 | **12** |
| **11** | 1111111110 | 111111**000**0 | 1450 | **1412** | 157 | **0** |
| **12** | 1111111111 | 111111**0000** | 1500 | **1412** | 162 | **0** |
| **13** | 1111111100 | 11111**000**00 | 1400 | **1332** | 152 | **0** |
| **14** | 1111111000 | 11111**00**000 | 1300 | 1300 | 197 | **32** |
| **15** | 1111100000 | 11**0**1100000 | 1200 | 1200 | 132 | **2** |
| **16** | 1111100000 | 11**01**0**0**00000 | 1050 | **1040** | 282 | **0** |
| **17** | 1111100000 | 11**01**0**0**00000 | 1000 | 1000 | 332 | **40** |
| **18** | 1111100000 | 11**01**0**0**00000 | 1100 | **1040** | 232 | **0** |
| **19** | 1111100000 | 11**01**0**0**00000 | 1200 | **1040** | 132 | **0** |
| **20** | 1111111100 | 11**010000**00 | 1400 | **1040** | 152 | **0** |
| **21** | 1111111000 | 11**01000**000 | 1300 | **1040** | 197 | **0** |
| **22** | 1100111000 | 1101**000**000 | 1100 | **1040** | 137 | **0** |
| **23** | 1100100000 | 1100**0**00000 | 900 | 900 | 172 | **10** |
| **24** | 1100000000 | 1100000000 | 800 | 800 | 110 | 110 |

The profit attained by BPSO-PSO and BSA-CSO technique for case-I, case-II, case-III and case-IV have been given in Table 3.5. The profit attained by the BPSO-PSO technique for case-I is $90060.66 which is '$17646.34' lower as compared to the profit obtained by the BSA-CSO technique. For case-II, the profit achieved by the BPSO-PSO technique is '$67333.94', which is lower by 24.77% as compared to the BSA-CSO technique. The profit attained from the BSA-CSO technique for case-II is '$89513.75', which is '$18193' less as compared to case-I, due to consideration of valve-point loading effect of the thermal unit. The unit commitment schedule of thermal generating units is similar for case-I and case-II. The obtained profit from the BPSO-PSO technique, case-III and case-VI are 16.74% and 24.36% less as compared to the BSA-CSO technique, respectively. Hence, a huge increase in profit for GENCOs is possible by the BSA-CSO algorithm for large scale electric power systems. Case-III considers the ramp-rate constraint of thermal units during ON/OFF operations. The impact of ramp-rate constraint, drop off the profit by '$1204' which is 1.11% of the profit obtained during case-I in the BSA-CSO technique. The profit obtained by the BSA-CSO technique in case-IV is '$89513', which is less due to the consideration of valve-point loading effect and ramp-rate constraint. It has been observed from Table 3.5 that $N_{FE}$ and CPU time obtained for the BPSO-PSO technique for all cases is high as compared to the BSA-CSO technique. The obtained $N_{FE}$ for case-IV is the same as of case-III.

The commitment status and power generation for case III/IV at each sub-interval has been given in Table 3.6. It has been observed that the effect of start-up and shut-down ramp-rate constraint at 5$^{th}$ unit. The 5$^{th}$ unit is ON at 10$^{th}$ sub-interval and it requires a certain time to produce its maximum power. At 15$^{th}$ sub-interval, the power generation of 5$^{th}$ unit is limited to its constrained power due to ramping constraint during the shut-down process. Further, the unit status, total power generation and spinning reserve for case-III in THUC and PBUC is given in Table 3.7.

**Table 3.5:** Profit obtained from optimization techniques for all cases, PBUC test system-I

| | **BPSO-PSO technique** | | | **BSA-CSO technique** | | |
|---|---|---|---|---|---|---|
| | **Profit ($)** | **$N_{FE}$(×10$^4$)** | **CPU time (×10$^2$)** | **Profit ($)** | **$N_{FE}$(×10$^4$)** | **CPU time (×10$^2$)** |
| **Case-I** | 90060.66 | 400 | 105 | 107707 | 2.85 | 0.57 |
| **Case-II** | 67333.94 | 400 | 105 | 89513.75 | 2.85 | 0.57 |
| **Case-III** | 88672.16 | 480 | 123 | 106503 | 3.42 | 0.68 |
| **Case-IV** | 67702.13 | 480 | 123 | 89513 | 3.42 | 0.68 |

**Table 3.6:** Hourly power dispatch obtained from BSA-CSO for PBUC test system-I, case-III and case-IV

| **Sub-intervals (h)** | **Power demand (MW)** | **Price ($/MWh)** | **Units status** | **Generated power (MW)** | | | | | | | | | | **Spinning reserve (MW)** | **Total power Generation (MW)** | **Case-III** | **Case-IV** |
|---|---|---|---|---|---|---|---|---|---|---|---|---|---|---|---|---|---|
| | | | | **P1** | **P2** | **P3** | **P4** | **P5** | **P6** | **P7** | **P8** | **P9** | **P10** | | | **Profit ($/h)** | **Profit ($/h)** |
| **1** | 700 | 22.15 | 1100000000 | 455 | 245 | 0 | 0 | 0 | 0 | 0 | 0 | 0 | 0 | 210 | 700 | 1821.87 | 1629.37 |
| **2** | 750 | 22 | 1100000000 | 455 | 295 | 0 | 0 | 0 | 0 | 0 | 0 | 0 | 0 | 160 | 750 | 1945.5 | 1393.55 |
| **3** | 850 | 23.1 | 1100000000 | 455 | 395 | 0 | 0 | 0 | 0 | 0 | 0 | 0 | 0 | 60 | 850 | 3333.11 | 2964.363 |
| **4** | 950 | 22.65 | 1100000000 | 455 | 455 | 0 | 0 | 0 | 0 | 0 | 0 | 0 | 0 | 0 | 910 | 3258.199 | 2630.672 |
| **5** | 1000 | 23.25 | 1101000000 | 455 | 445 | 0 | 100 | 0 | 0 | 0 | 0 | 0 | 0 | 40 | 1000 | 3154.06 | 2402.79 |
| **6** | 1100 | 22.95 | 1101000000 | 455 | 455 | 0 | 130 | 0 | 0 | 0 | 0 | 0 | 0 | 0 | 1040 | 3654.041 | 2887.7 |
| **7** | 1150 | 22.5 | 1101000000 | 455 | 455 | 0 | 130 | 0 | 0 | 0 | 0 | 0 | 0 | 0 | 1040 | 3186.04 | 2419.7 |
| **8** | 1200 | 22.15 | 1101000000 | 455 | 455 | 0 | 130 | 0 | 0 | 0 | 0 | 0 | 0 | 0 | 1040 | 2822.04 | 2055.7 |
| **9** | 1300 | 22.8 | 1111000000 | 455 | 455 | 105 | 130 | 0 | 0 | 0 | 0 | 0 | 0 | 25 | 1145 | 2326.9 | 1339.82 |
| 10 | 1400 | 29.35 | 1111110000 | 455 | 455 | 130 | 130 | 105 | 40 | 0 | 0 | 0 | 0 | 97 | 1315 | 9515.318 | 8210.23 |
| 11 | 1450 | 30.15 | 1111110000 | 455 | 455 | 130 | 130 | 162 | 80 | 0 | 0 | 0 | 0 | 0 | 1412 | 13523.8 | 12457.97 |
| 12 | 1500 | 31.65 | 1111110000 | 455 | 455 | 130 | 130 | 162 | 80 | 0 | 0 | 0 | 0 | 0 | 1412 | 15641.82 | 14575.97 |
| **13** | 1400 | 24.6 | 1111100000 | 455 | 455 | 130 | 130 | 162 | 0 | 0 | 0 | 0 | 0 | 0 | 1332 | 5915.58 | 4929.91 |
| **14** | 1300 | 24.5 | 1111100000 | 455 | 455 | 130 | 130 | 102 | 0 | 0 | 0 | 0 | 0 | 60 | 1272 | 5557.43 | 4494.03 |
| **15** | 1200 | 22.5 | 1101100000 | 455 | 455 | 0 | 130 | 42 | 0 | 0 | 0 | 0 | 0 | 120 | 1082 | 2846.62 | 1834.53 |
| **16** | 1050 | 22.3 | 1101000000 | 455 | 455 | 0 | 130 | 0 | 0 | 0 | 0 | 0 | 0 | 0 | 1040 | 2978.04 | 2211.7 |
| **17** | 1000 | 22.25 | 1101000000 | 455 | 415 | 0 | 130 | 0 | 0 | 0 | 0 | 0 | 0 | 40 | 1000 | 2714.5 | 1962.8 |
| **18** | 1100 | 22.05 | 1101000000 | 455 | 455 | 0 | 130 | 0 | 0 | 0 | 0 | 0 | 0 | 0 | 1040 | 2718.4 | 1951.71 |
| **19** | 1200 | 22.2 | 1101000000 | 455 | 455 | 0 | 130 | 0 | 0 | 0 | 0 | 0 | 0 | 0 | 1040 | 2874.4 | 2107.7 |
| **20** | 1400 | 22.65 | 1101000000 | 455 | 455 | 0 | 130 | 0 | 0 | 0 | 0 | 0 | 0 | 0 | 1040 | 3342.04 | 2575.7 |
| **21** | 1300 | 23.1 | 1101000000 | 455 | 455 | 0 | 130 | 0 | 0 | 0 | 0 | 0 | 0 | 0 | 1040 | 3810.5 | 3043.7 |
| **22** | 1100 | 22.95 | 1101000000 | 455 | 455 | 0 | 130 | 0 | 0 | 0 | 0 | 0 | 0 | 0 | 1040 | 3654.04 | 2887.7 |
| **23** | 900 | 22.75 | 1100000000 | 455 | 445 | 0 | 0 | 0 | 0 | 0 | 0 | 0 | 0 | 10 | 900 | 3297.09 | 2711.3 |
| **24** | 800 | 22.55 | 1100000000 | 455 | 345 | 0 | 0 | 0 | 0 | 0 | 0 | 0 | 0 | 110 | 800 | 2612.58 | 2181.8 |
| **Maximum limit of unit** | | | | 455 | 455 | 130 | 130 | 162 | 80 | 85 | 55 | 55 | 55 | | **Total** | 106503.5 | 87860.66 |

**Table 3.7:** Comparison of status, power generation and spinning reserve for THUC and PBUC test system-I, case-III

| | **Unit status** | | **Power generation (MW)** | | **Available spinning reserve (MW)** | |
|---|---|---|---|---|---|---|
| **Sub-intervals (h)** | **THUC** | **PBUC** | **THUC** | **THUC** | **PBUC** | **THUC** |
| **1** | 1100000000 | 1100000000 | 700 | 700 | 210 | 210 |
| **2** | 1100000000 | 1100000000 | 750 | 750 | 160 | 160 |
| **3** | 1100100000 | 1100**0**00000 | 850 | 850 | 222 | **60** |
| **4** | 1100100000 | 1100**0**00000 | 950 | **910** | 122 | **0** |
| **5** | 1101100000 | 1101**0**00000 | 1000 | 1000 | 202 | **40** |
| **6** | 1111100000 | 1101000000 | 1100 | **1040** | 232 | **0** |
| **7** | 1111100000 | 1101000000 | 1150 | **1040** | 182 | **0** |
| **8** | 1111110000 | 1101000000 | 1200 | **1040** | 212 | **0** |
| **9** | 1111111100 | 1111000000 | 1300 | **1145** | 252 | **25** |
| **10** | 1111111111 | 1111110000 | 1400 | **1315** | 262 | **97** |
| **11** | 1111111111 | 1111110000 | 1450 | **1412** | 212 | **0** |
| **12** | 1111111111 | 1111110000 | 1500 | **1412** | 162 | **0** |
| **13** | 1111111100 | 1111100000 | 1400 | **1332** | 152 | **0** |
| **14** | 1111111000 | 1111100000 | 1300 | **1272** | 197 | **60** |
| **15** | 1111100000 | 1101100000 | 1200 | **1082** | 132 | **120** |
| **16** | 1111100000 | 1101000000 | 1050 | **1040** | 282 | **0** |
| **17** | 1111100000 | 1101000000 | 1000 | 1000 | 332 | **40** |
| **18** | 1111101100 | 1101000000 | 1100 | **1040** | 372 | **0** |
| **19** | 1111111100 | 1101000000 | 1200 | **1040** | 352 | **0** |
| **20** | 1111111100 | 1101000000 | 1400 | **1040** | 152 | **0** |
| **21** | 1111111000 | 1101000000 | 1300 | **1040** | 197 | **0** |
| **22** | 1100111000 | 1101000000 | 1100 | **1040** | 137 | **0** |
| **23** | 1100100000 | 1100000000 | 900 | 900 | 172 | **10** |
| **24** | 1100100000 | 1100000000 | 800 | 800 | 210 | 110 |

### 3.4.3 Profit Based Unit Commitment Test System-II

The test system-II consists of 40-thermal units. For test system-II, the obtained results from the BSA-CSO technique in case-I have been compared with the ICA technique **(Ghadi *et al.*, 2016)**. The profit of GENCOs obtained by the proposed technique is '\$430407', while the profit reported for ICA is '\$443595'. The unit schedule obtained from the BSA-CSO technique satisfies all the constraints, however, the results reported for ICA **(Ghadi *et al.*, 2016)**, does not satisfy spinning reserve constraint at 17$^{th}$ sub-interval of the scheduling period. The actual demand during the 17$^{th}$ sub-interval is 4000 MW and results are reported in Ref. **(Ghadi *et al.*, 2016)**, indicates generation is 4179.775 MW. Therefore, the reported results cannot be compared with the BSA-CSO technique. Table 3.8 presents the commitment status of 40 units.

**Table 3.8:** Hourly commitment status of units obtained from BSA-CSO for PBUC test system-II, case-I

| Sub-intervals (h) | Power demand (MW) | Price ($/MWh) | Unit status | Spinning reserve (MW) | Total power Generation (MW) | Profit ($/h) |
|---|---|---|---|---|---|---|
| **1** | 2800 | 22.15 | 111111110000000000000000000000000000 | 0 | 2800 | 7268 |
| **2** | 3000 | 22 | 111111110000000000000000000000000000 | 0 | 3000 | 7771.49 |
| **3** | 3400 | 23.1 | 111111110000000000000000000000000000 | 0 | 3400 | 13330.5 |
| **4** | 3800 | 22.65 | 111111110000000000000000000000000000 | 160 | 3640 | 13032.9 |
| **5** | 4000 | 23.25 | 111111110000110000000000000000000000 | 100 | 3900 | 15378.8 |
| **6** | 4400 | 22.95 | 111111110100111100000000000000000000 | 110 | 4290 | 14707.8 |
| **7** | 4600 | 22.5 | 111111111101111100000000000000000000 | 50 | 4550 | 12843.9 |
| **8** | 4800 | 22.15 | 111111111101111100000000000000000000 | 250 | 4550 | 11251 |
| **9** | 5200 | 22.8 | 111111111111111111010000000000000000 | 34 | 5166 | 14124 |
| **10** | **5600** | **29.35** | **111111111111111111110000000000000000** | **272** | **5328** | **48970.2** |
| **11** | **5800** | **30.15** | **111111111111111111110000000000000000** | **472** | **5328** | **53232.8** |
| **12** | **6000** | **31.65** | **111111111111111111110000000000000000** | **672** | **5328** | **61224.8** |
| **13** | **5600** | **24.6** | **111111111111111111110000000000000000** | **272** | **5328** | **23662.39** |
| **14** | **5200** | **24.5** | **111111111110111111110000000000000000** | **2** | **5198** | **22836.38** |
| **15** | 4800 | 22.5 | 111111111110111100100000000000000000 | 88 | 4712 | 12742.96 |
| **16** | 4200 | 22.3 | 111111111110111100000000000000000000 | 0 | 4200 | 11933.8 |
| **17** | 4000 | 22.25 | 111111110000111000000000000000000000 | 0 | 4000 | 11530.9 |
| **18** | 4400 | 22.05 | 111111110000111000000000000000000000 | 370 | 4030 | 10866.34 |
| **19** | 4800 | 22.2 | 111111110000111000000000000000000000 | 770 | 4030 | 11470.82 |
| **20** | 5600 | 22.65 | 111111110000111000000000000000000000 | 1570 | 4030 | 13284.4 |
| **21** | 5200 | 23.1 | 111111110000111000000000000000000000 | 1170 | 4030 | 15097.84 |
| **22** | 4400 | 22.95 | 111111110000111000000000000000000000 | 370 | 4030 | 14493.33 |
| **23** | 3600 | 22.75 | 111111110000000000000000000000000000 | 0 | 3600 | 13188 |
| **24** | 3200 | 22.55 | 111111010000000000000000000000000000 | 15 | 3185 | 11297 |

The profit attained by the BPSO-PSO and BSA-CSO technique for case-I, case-II, case-III and case-IV are given in Table 3.9. In the BSA-CSO technique, the profit of GENCOs in case-II has been decreased by '$70894' as compared to the case-I, due to the incorporation of a valve point loading effect. Owing to the effect of the ramp-rate constraint of thermal units during ON/OFF operations, the profit of case-III has been also decreased to '$8466.6' as compared to case-I. The consideration of both ramp-rate and valve-point loading effect in case-IV reduces the profit by '$80368' as compared to case-I. The obtained profit from BPSO-PSO for all cases is less as compared to the BSA-CSO algorithm. It has been evident from Table 3.9 that the required $N_{FE}$ is more for case-II, case-III and case-IV as compared to case-I.

**Table 3.9:** Profit obtained from optimization techniques for all cases, PBUC test system-II

| | **BPSO-PSO technique** | | | **BSA-CSO technique** | | |
|---|---|---|---|---|---|---|
| | **Profit ($)** | **$N_{FE}$ ($\times 10^4$)** | **CPU time ($\times 10^2$)** | **Profit ($)** | **$N_{FE}$ ($\times 10^4$)** | **CPU time ($\times 10^2$)** |
| **Case-I** | 321779.4 | 640 | 221 | 430407 | 17.68 | 7.37 |
| **Case-II** | 311427.8 | 664 | 243 | 359513 | 19.45 | 8.13 |
| **Case-III** | 216571.9 | 696 | 261 | 421940.4 | 26.53 | 9.45 |
| **Case-IV** | 203750.4 | 712 | 283 | 350039 | 28.30 | 9.88 |

### 3.4.4 Profit Based Unit Commitment Test System-III

In case-I, the maximum, average, and worst profit obtained by the proposed technique is compared with the profit reported for BPSO-PSO, TS-RP **(Ghadi *et al.*, 2016)**, TS-IRP **(Ghadi *et al.*, 2016)**, Muller method **(Ghadi *et al.*, 2016)**, ACO **(Ghadi *et al.*, 2016)**, PSO **(Ghadi *et al.*, 2016)**, *Parallel PSO* (PPSO) **(Christopher and Sishaj, 2011)**, IPPD **(Ghadi *et al.*, 2016)**, NACO **(Columbus and Simon, 2013)**, PABC **(Columbus and Simon, 2012)**, PNACO **(Columbus and Simon, 2013)**, BFWA **(Reddy *et al.*, 2016)** and ICA **(Ghadi *et al.*, 2016)** techniques and are tabulated in Table 3.10. It is evident from Table 3.10 that the BSA-CSO technique is able to achieve more profit as compared to other techniques.

Further, to compare the computational performance of the BSA-CSO technique, the $N_{FE}$ is given in Table 3.10. It is evident from Table 3.10 that $N_{FE}$ required by the BSA-CSO technique is least as compared to other state of the art algorithms. The fair comparison of CPU time required by various optimization techniques are possible if these are executed on the same platform, however, CPU time has been given in Table 3.10. The commitment status obtained from the BSA-CSO technique at each sub-interval for case-I has been given in Table 3.11.

**Table 3.10:** Comparison for profit, $N_{FE}$ and CPU time for PBUC test system-III, case-I

| Technique | Average Profit ($) ($\times 10^4$) | Best Profit($) ($\times 10^4$) | Worst Profit ($) ($\times 10^4$) | Standard Deviation ($\times 10^{-3}$) | $N_{FE}$ ($\times 10^4$) | CPU (sec) ($\times 10^2$) |
|---|---|---|---|---|---|---|
| **TS-RP** (**Ghadi *et al.*, 2016**) | - | 101.75 | - | - | - | - |
| **TS-IRP** (**Ghadi *et al.*, 2016**) | - | 103.65 | - | - | - | - |
| **Muller Method** (**Ghadi *et al.*, 2016**) | - | 103.93 | - | - | - | - |
| **ACO** (**Ghadi *et al.*, 2016**) | - | 105.29 | - | - | - | - |
| **PSO** (**Ghadi *et al.*, 2016**) | - | 104.79 | - | - | - | - |
| **PPSO** (**Christopher and Sishaj, 2011**) | - | 104.80 | - | - | - | - |
| **IPPD** (**Ghadi *et al.*, 2016**) | - | 105.82 | - | - | - | - |
| **NACO** (**Columbus and Simon, 2013**) | - | 105.53 | - | - | 144 | 12.63 |
| **PABC** (**Columbus and Simon, 2012**) | - | 105.66 | - | - | 144 | 12.16 |
| **PNACO** (**Columbus and Simon, 2013**) | - | 106.03 | - | - | 480 | 7.62 |
| **BFWA** (**Reddy *et al.*, 2016**) | 105.51 | 106.14 | 105.27 | 2.80 | - | 11.24 |
| **ICA** (**Ghadi *et al.*, 2016**) | - | 107.69 | - | - | 1600 | - |
| **BPSO-PSO** | 72.665 | 72.670 | 72.661 | 3.20 | 800 | 20.23 |
| **Proposed method** | **107.68** | **108.12** | **107.31** | **2.40** | **73.88** | **12.80** |

**Table 3.11:** Hourly commitment status of units obtained from BSA-CSO for PBUC test system-III, case-I

| **Sub-intervals (h)** | **Power demand (MW)** | **Price ($/MWh)** | **Unit status** | **Spinning reserve (MW)** | **Total power Generation (MW)** | **Profit ($/h)** |
|---|---|---|---|---|---|---|
| **1** | 7000 | 22.15 | 1111111111111111111100000000000000000000000000000000000000000000000000000000000000000000000000000000 | 0 | 7000 | 18159.8 |
| **2** | 7500 | 22 | 1111111111111111111100000000000000000000000000000000000000000000000000000000000000000000000000000000 | 0 | 7500 | 19363.47 |
| **3** | 8500 | 23.1 | 1111111111111111111100000000000000000000000000000000000000000000000000000000000000000000000000000000 | 0 | 8500 | 33299.64 |
| **4** | 9500 | 22.65 | 1111111111111111111100000000000000000000000000000000000000000000000000000000000000000000000000000000 | 400 | 9100 | 32582.14 |
| **5** | 10000 | 23.25 | 1111111111111111111100000000001111111000000000000000000000000000000000000000000000000000000000000000 | 0 | 10000 | 39117.5 |
| **6** | 11000 | 22.95 | 1111111111111111111100000000001111111111000000000000000000000000000000000000000000000000000000000000 | 600 | 10400 | 36532.42 |
| **7** | 11500 | 22.5 | 1111111111111111111100000000001111111111000000000000000000000000000000000000000000000000000000000000 | 1100 | 10400 | 31860.4 |
| **8** | 12000 | 22.15 | 1111111111111111111100000000001111111111000000000000000000000000000000000000000000000000000000000000 | 1600 | 10400 | 28224.93 |
| **9** | 13000 | 22.8 | 1111111111111111111100000000001111111111000000000000000000000000000000000000000000000000000000000000 | 2600 | 10400 | 34980.91 |
| **10** | **14000** | **29.35** | **1111111111111111111111111111111111111111111111111111110111110000000000000000000000000000000000000000** | **0** | **14000** | **123633.5** |
| **11** | **14500** | **30.15** | **1111111111111111111111111111111111111111111111111111111111110000000000000000000000000000000000000000** | **380** | **14120** | **135238.8** |
| **12** | **15000** | **31.65** | **1111111111111111111111111111111111111111111111111111111111110000000000000000000000000000000000000000** | **880** | **14120** | **156418.8** |
| **13** | **14000** | **24.6** | **1111111111111111111111111111111111111111111111111110001000000000000000000000000000000000000000000000** | **356** | **13644** | **58699.1** |
| **14** | **13000** | **24.5** | **1111111111111111111111111111111111111111111111111100000000000000000000000000000000000000000000000000** | **0** | **13000** | **56542.68** |
| 15 | 12000 | 22.5 | 1111111111111111111100000001001111111111111111111100000000000000000000000000000000000000000000000000 | 0 | 12000 | 30583.08 |
| **16** | 10500 | 22.3 | 1111111111111111111100000000001111111111000000000000000000000000000000000000000000000000000000000000 | 100 | 10400 | 30142.5 |
| **17** | 10000 | 22.25 | 1111111111111111111100000000001111111111000000000000000000000000000000000000000000000000000000000000 | 0 | 10000 | 27282.32 |
| **18** | 11000 | 22.05 | 1111111111111111111100000000001111111111000000000000000000000000000000000000000000000000000000000000 | 600 | 10400 | 27180.46 |
| **19** | 12000 | 22.2 | 1111111111111111111100000000001111111111000000000000000000000000000000000000000000000000000000000000 | 1600 | 10400 | 28740.47 |
| **20** | 14000 | 22.65 | 1111111111111111111100000000001111111111000000000000000000000000000000000000000000000000000000000000 | 3600 | 10400 | 33420.46 |
| **21** | 13000 | 23.1 | 1111111111111111111100000000001111111111000000000000000000000000000000000000000000000000000000000000 | 2600 | 10400 | 38100.48 |
| **22** | 11000 | 22.95 | 1111111111111111111100000000000011111111000000000000000000000000000000000000000000000000000000000000 | 860 | 10140 | 36294.79 |
| **23** | 9000 | 22.75 | 1111111111111111111100000000000000000000000000000000000000000000000000000000000000000000000000000000 | 0 | 9000 | 32969.82 |
| **24** | 8000 | 22.55 | 1111111111111111010100000000000000000000000000000000000000000000000000000000000000000000000000000000 | 0 | 8000 | 27965 |

The profit attained by BPSO-PSO and BSA-CSO techniques for all cases are presented in Table 3.12. The profit attained from the BSA-CSO technique for case-II is '\$896329.9', which is '\$185030.1' less as compared to case-I, due to consideration of valve-point loading effect of the thermal unit. The case-III considers the ramp-rate constraint of thermal units during ON/OFF operations. In the BSA-CSO technique, the impacts of ramp-rate constraint drop off the profit by '\$30439' which is 2.814% of the profit during case-I. The profit obtained from the BSA-CSO technique in case-IV is '\$866007', which is less due to consideration of valve-point loading effect and ramp-rate constraint. The maximum profit obtained from the BPSO-PSO technique in all four cases are less when compared with the BSA-CSO technique. It has also evident that $N_{FE}$ required for the BSA-CSO technique is less for all cases as compare to the BPSO-PSO technique.

**Table 3.12:** Profit obtained from optimization techniques for all cases, PBUC test system-III

| | **BPSO-PSO technique** | | | **BSA-CSO technique** | | |
|---|---|---|---|---|---|---|
| | **Profit (\$)** | **$N_{FE}$ (×10$^4$)** | **CPU time (×10$^2$)** | **Profit (\$)** | **$N_{FE}$ (×10$^4$)** | **CPU time (×10$^2$)** |
| **Case-I** | 726703.5 | 800 | 20.23 | 1081360 | 73.88 | 12.80 |
| **Case-II** | 459129 | 880 | 20.23 | 896329.9 | 77.57 | 12.80 |
| **Case-III** | 682243 | 960 | 21.51 | 1050761 | 88.65 | 14.45 |
| **Case-IV** | 410099 | 1040 | 21.72 | 866007 | 92.35 | 14.67 |

### 3.4.5 Statistical Analysis

In order to investigate the effect of parameter variation on the BSA-CSO technique, the set parameters are perturbed by $\pm 5\%$. As illustrated in Figure 3.4, the percentage decrease in profit in case-I of test system-I lies in range of $4\times10^{-04}$ to $1.2\times10^{-04}$. Hence, it is concluded that effect of parameter variation does not affect profit significantly. In this work, to check the performance of the BSA-CSO, the nonparametric Wilcoxon-signed rank test is applied on case-I of test system-I. The Wilcoxon signed rank test helps to identify significant difference between a single sample and a median of the sample **(Wild, 1997)**. The test is performed at a level of significance $\alpha$=0.01. It is evident from Table 3.13 that test statistic $W>W_{crt}$ (86.5>42), the null hypothesis cannot be rejected ($p>0.01$). Hence, there is no significant difference between the sample and the median of data.

**Table 3.13:** Wilcoxon-signed rank test for PBUC test system-I, case-I

| **Parameters** | **Values** |
|---|---|
| **Test statistic (W)** | 86.5 |
| **p-value** | 0.3125 |
| **Critical value of test statistic ($W_{crt}$)** | 42 |

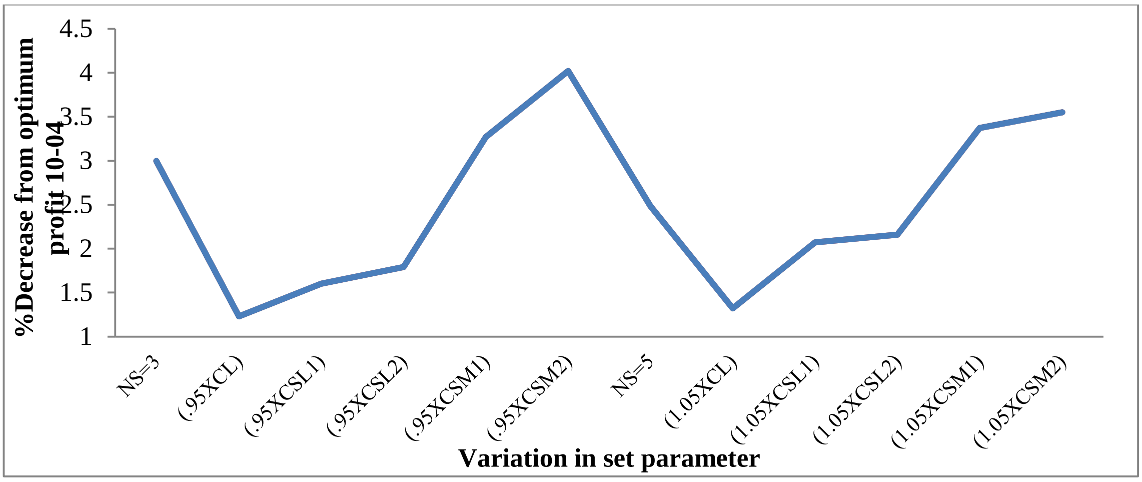


**Figure 3.4:** Percentage decrease in profit w.r.t variation in set parameter for test system-I, case-I

The statistical results best profit, average profit, worst profit and standard deviation obtained from the BSA-CSO technique in case-I of three test systems have been given in Table 3.14.

**Table 3.14:** Statistical results obtained from BSA-CSO technique for PBUC test systems, case-I

| | Test system-I | Test system-II | Test system-III |
|---|---|---|---|
| **Best profit ($)** | 107708 | 430407 | 1081360 |
| **Average profit ($)** | 107639 | 426872 | 1076898 |
| **Worst profit ($)** | 107604 | 407457 | 1073187 |
| **Standard deviation** | 0.0007 | 0.158892 | 0.0024 |

## 3.5 CONCLUSIONS

In this Chapter, three test systems have undertaken consist of thermal units. The proposed BSA-CSO technique has applied to maximize the profit obtained by GENCOs. The optimization techniques have tested on 10, 40, and 100 unit systems with various operational constraints, *i.e.*, load balance, unit ramp-rate, minimum up and down time. It has been concluded that the results achieved from the BSA-CSO algorithm are better than the other algorithms. In case-I, the obtained profit from BSA-CSO for test systems-I, II and III are 19.59%, 19.71% and 20.64% more as compared to the BPSO-PSO technique. The results obtained from the BSA-CSO technique in case-II, III and IV for all three test systems are far better as compare to the BPSO-PSO technique. The proposed technique is able to achieve a higher profit with less number of functions of evaluation as compared to other techniques. The global optimum solution achieved from the BSA-CSO algorithm provides a realistic result when the ramp-rate constraints are incorporated. Incorporation of ramp-rate constraint has reduced the total profit in the PBUC problem. It has also concluded that the inclusion of ramp rate constants in the PBUC has changed the UC schedule.

# CHAPTER – 4

# COGENERATION BASED UNIT COMMITMENT SCHEDULE

## 4.1 INTRODUCTION

In the modern world, electricity and heat demand is increased due to the revolution in industrialization and urbanization. In order to satisfy high heat and electricity demand, fossil fuel consumption in the thermal power and heat plant has been increased extensively. The rising concern about the depletion of fossil fuel has motivated the researchers to find an alternative generating unit which has higher efficiency as compared to conventional thermal and heat units. The heat and power generation from the thermal and heat units produces a significant amount of harmful pollutants that affect entire living beings. The policymakers and governments are concerned about fossil fuel consumption and global warming. In the Paris agreement, the various countries have set their target for a significant reduction of greenhouse gas emissions **(Jensen, 2010)**. Therefore, it is necessary to minimize harmful emissions. An adopting of higher efficient *combined heat and power* (CHP) units results in the reduction of the pollutants emission. The cogeneration is capable of the simultaneous production of heat and electricity with an energy efficiency of 85% **(Thorin *et al.*, 2005)**. In the cogeneration unit, the waste heat is utilized during the power and heat generation process. In conventional thermal plants, the amount of energy is lost as heat during the power generation. Hence, a significant amount of fuel saving can be attained by the CHP unit as compared to conventional thermal and heat units. The available CHP units in the system have few other important features, *i.e.*, flexible operation, short start-up/shut-down time, reliable, safer operating conditions and short ramp-up/down rate **(Salgado and Pedrero, 2008)**.

Policymakers have authenticated the benefits and high performance of cogeneration units. The German Government set the policies in the area of expansion of CHP units to supply 25% of the electrical demand by CHP units **(Kneiske and Braun, 2017)**. In the European Union, a new framework of policy has been used by the CHP Directive to increase the share of CHP units to meet the electrical and thermal demand **(Harwell, 2010)**. The declaration for expansion of CHP units has been done in the G8 summit

**(Mitra *et al.*, 2013)**. The different types of CHP units, such as extraction steam turbine, backpressure steam turbine, and a condensing steam turbine has been used in the combined heat and power system. The emerging technology and developments in the cogeneration unit have been reported by the International Energy Agency **(Kerr, 2008)**. In order to increase the efficiency and flexibility of CHP unit, researchers have been focused on hybrid strategies of CHP unit such as integration of cogeneration plant with the solar collector, and heat storage unit **(Li *et al.*, 2017; Martinez *et al.*, 2017; Wang *et al.*, 2017; Kneiske and Braun, 2017; Kasaeian *et al.*, 2018)**. The implementation of these upgradations needs additional investment and infrastructure. Researchers have modified the CHP unit by replacing the single-shaft turbine with multi-shaft turbines. The CHP unit based on multiple shaft turbine is known as *dual-mode CHP* (DM-CHP) **(Zugno *et al.*, 2016)**. The DM-CHP unit is a combination of extraction and backpressure steam turbines **(Breeze, 2019)**. The extraction and backpressure mode of the DM-CHP unit has flexible power generation and high heat generation capacity, respectively **(Wogrin *et al.*, 2016)**. The energy generation from the DM-CHP unit can be evaluated by the ratio of the heat and power generation. The utility planners of various countries have upgraded their strategies to provide the available heat and power at an affordable level under the legal framework **(Chen and Wang, 2017)**. It is important for combined heat and power systems to unlock the full potential of DM-CHP. The scheduling of conventional power, heat, and DM-CHP units is a challenging task as compared to conventional combined heat and power system. Efforts of researchers are underway in numerous emerging fields of electric power systems such as *unit commitment* (UC) modelling by considering power, heat, and CHP units.

In the UC problem, the DM-CHP unit increases the complexity of the *combined heat and power unit commitment* (CHPUC) problem. The main objective of CHPUC problem is to minimize the overall operating cost with satisfaction of UC and generation scheduling constraints such as minimum up and down time, heat and power spinning reserve, heat and power balance, generation limits, fuel limits and ramp-up/down constraints, *etc*. **(Rong and Peter, 2018; Kia *et al.*, 2017[1])**.

In the deregulation environment, the generation scheduling policies have been modified for generating companies (GENCOs) **(Reddy *et al.*, 2019)**. The focus of researchers has been transformed from CHPUC problem to *profit based CHPUC* (PBCHPUC) problem **(Mitra *et al.*, 2013; Ongsakul and Vo, 2013)**. In the PBCHPUC problem, the demand and reserve constraints are treated as soft constraints. The CHPUC and PBCHPUC problem are more challenging in the presence of environmental concerns **(Shukla and Singh, 2016[1])**. The cost and emission objective functions are conflicting in nature, hence the CHPUC problem is converted into *multiobjective CHPUC* (MO-CHPUC) optimization problem. The objective of the MO-CHPUC problem is to minimize the total production cost and emission simultaneously. In the deregulated environment, the aim of *multiobjective profit based CHPUC* (MO-PBCHPUC) problem is to maximize the profit and minimize the emission. The MO-CHPUC and MO-PBCHPUC problems are a nonlinear, mixed-integer, and highly constrained optimization problem. The various optimization techniques have been applied to solve the CHPUC problem.

The CHPUC problem has been solved by implementation of various variants of the *dynamic programming* (DP) algorithm **(Rong *et al.*, 2008)**, an improved unit de-commitment algorithm **(Rong *et al.*, 2009)**, dynamic regrouping based on a sequential DP algorithm **(Rong *et al.*, 2009)**. Kim and Edgar **(2014)** have employed a *mixed-integer nonlinear programming* (MINLP) approach to search optimum CHPUC solution. Kia *et al.* **(2017[2])** have obtained the generation schedule of combined heat and power system having CHP, power, and heat unit by the implementation of two-stage *stochastic MILP* (SMILP). Information-Gap decision theory has been employed to obtain a schedule of the cogeneration system **(Aghaei *et al.*, 2016)**. The Benders decomposition method has been applied to obtain the optimal scheduling of the CHP system to achieve maximum profit and minimum emission **(Sadeghian and Ardehali, 2016)**.

In previous work, the conventional techniques have been applied to solve the CHPUC problem. Most of the conventional techniques have been successfully applied at a certain level of satisfaction and having few limitations **(Heris *et al.*, 2018)**. These techniques cannot be applied to solve discontinuous, non-differential, and high dimensional optimization problems without any approximation. The global search techniques such as *binary particle swarm optimization* (BPSO) **(Yuan *et al.*, 2009)**, PSO **(Zhao *et al.*, 2006)**, *ant colony optimization* (ACO) **(Vaisakh and Srinivas, 2011)**, *genetic algorithm* (GA) **(Kazarlis *et al.*, 1996)** have been applied to solve the thermal UC and profit based UC problems and it is discussed in Chapter 2 and 3. The global optimization techniques are computationally expensive, whereas, local search techniques are used to find optimum solutions in affordable times **(Alonso *et al.*, 2018)**.

In the *multiobjective* (MO) optimization problem, there are a set of solutions for the MO problem. In order to solve the multiobjective problem, the direct method has been used to transfer the MO problem into a single objective problem by using the weighted sum method, boundary intersection method, ε-Constraint **(Qu *et al.*, 2018)**. After that optimization techniques are applied to solve single objective problem. The MO-CHPUC problem has been solved by the implementation of a deterministic and heuristic optimization algorithm **(Sedighizadeh *et al.*, 2018)**. A two-stage MO thermal UC problem has been solved by the implementation of fuzzy set theories **(Wang *et al.*, 2016)**. The fuzzy membership function with the *cardinal priority method* (CPM) has been used to select the optimal trade-off solution from the Pareto set **(Patwal and Narang, 2018)**. As per the best of author knowledge, the researchers has not explored the DM-CHP for multiobjective CHPUC and PBCHPUC problems.

In light of these observations, the main contributions of this research work are given as:

- In a maiden attempt, the MO-PBCHPUC and MO-CHPUC problem have been formulated by considering DM-CHP, thermal, and heat units.
- The optimum commitment and generation schedule of units is obtained by the implementation of the BSA-CSO technique. The fuzzy membership method with CPM is implemented to find the best-satisfied non dominated solution among Pareto optimal solutions of the multiobjective problem.
- The impact of extraction and backpressure mode of combined heat and power unit has been compared in terms of total operating cost, GENCOs profit, emission and generation flexibility.
- To validate the effectiveness of the optimization technique, three cogeneration based unit commitment test systems have been undertaken, which are of small, and medium size.

## 4.2 MATHEMATICAL MODELLING OF GENERATING UNITS

The detail discussion regarding generating units, *i.e.*, combined heat and power, thermal and heat units are given in this section. The operating constraints such as generation limits, fuel limits, ramping limits, the mutual dependency of heat and power limits are discussed for generating units.

### 4.2.1 Combined Heat and Power Units

The heat and power generation in the CHP unit depends on the size of the turbine and the pressure of the extracted steam. There are commonly used turbines such as backpressure steam turbine, an extraction steam turbine, a simple cycle gas turbine and combined-cycle gas turbine for CHP plants. The DM-CHP unit is the combination of multiple turbines such as backpressure steam turbine and extraction steam turbine **(Liu *et al.*, 2009)**. It has many advantages, *i.e.*, higher efficiency, more flexible operation, lower capital investment and lower environmental impact **(Jensen, 2010)**. Moreover, the DM-CHP unit has a quick start-up capability that provides more benefits to the utility. The DM-CHP unit operates in backpressure and extraction mode, which is having a different operating characteristic. The heat and power output from the CHP unit is coupled and restricted within the feasible operating region (FOR) and it is shown in Figures 4.1 (a) and 4.1 (b) for extraction and backpressure mode, respectively. The detail description regarding backpressure and extraction modes are given in the following sub-sections **(Zugno *et al.*, 2016)**:

#### 4.2.1.1 Backpressure mode

In this mode of operation, the turbine does not utilize all the energy from the steam that resulted in output steam with a high temperature which is enough to heat the district heating by heat exchange process **(Zugno *et al.*, 2016)**. Hence, the energy generated from the CHP unit depends on a fixed ratio of power and heat and is given as:

$$P_{tj}^{b} = R_{j}^{b} H_{tj}^{b} \qquad j \in [1, Nc], t \in [1, T] \qquad (4.1)$$

$$\underline{P}_{j}^{b} = R_{j}^{b} \underline{H}_{j}^{b} \qquad j \in [1, Nc], t \in [1, T] \qquad (4.2)$$

$$\overline{P}_{j}^{b} = R_{j}^{b} \overline{H}_{j}^{b} \qquad j \in [1, Nc], t \in [1, T] \qquad (4.3)$$

where $\underline{P}_{j}^{b}$ and $\overline{P}_{j}^{b}$ are the lower and upper power limit of $j^{th}$ CHP units (MW) in backpressure mode, respectively; $\underline{H}_{j}^{b}$ and $\overline{H}_{j}^{b}$ are the lower and upper heat limit of $j^{th}$ CHP unit (MWth) in backpressure mode, respectively and $R_{j}^{b}$ is the power to heat ratio of $j^{th}$ CHP unit in backpressure mode (MW/MWth).

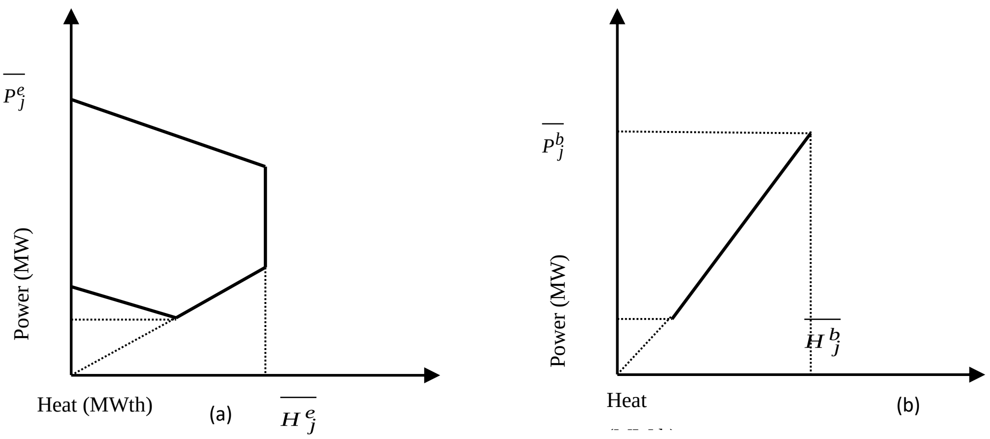


**Figure 4.1:** The operating mode of CHP unit (a) Extraction and (b) Backpressure.

*Generation constraints:* The lower and upper limits of power generation are evaluated using Eq. (4.2) and (4.3), respectively. The power and heat generation must be within a certain limit and are given in Eq. (4.4) and (4.5), respectively. The upper and lower limits of the fuel consumption are given in Eq. (4.6). The ramp up and down limit of fuel consumption is expressed in Eq. (4.7).

$$\underline{P_j^b} \le P_{tj}^b(H_{tj}^b) \le \overline{P_j^b} \qquad j \in [1,Nc], t \in [1,T] \qquad (4.4)$$

$$\underline{H_j^b} \le H_{t,j}^b \le \overline{H_j^b} \qquad j \in [1,Nc], t \in [1,T] \qquad (4.5)$$

$$\underline{\lambda_j^b} \le \lambda_{t,j}^b \le \overline{\lambda_j^b} \qquad j \in [1,Nc], t \in [1,T] \qquad (4.6)$$

$$DR_j^f \le \lambda_{tj}^b - \lambda_{(t-1)j}^b \le UR_j^f \qquad j \in [1,Nc], t \in [1,T] \qquad (4.7)$$

where $\underline{\lambda_j^b}$ and $\overline{\lambda_j^b}$ are the lower and upper fuel input limit of $j^{th}$ CHP units (MWh), respectively; $UR_j^f$ and $DR_j^f$ are the ramp up and down limit of $j^{th}$ CHP unit (MW/h), respectively, and $\lambda_{tj}^b$ is the fuel consumption requirement for the heat and power generation from the $j^{th}$ CHP unit at $t^{th}$ sub-interval (MWh).

*Generation cost:* The generation cost of the CHP unit is a function of fuel consumption for energy generation and is given as:

$$C_{ctj}^b = \chi_j^b \lambda_{tj}^b \qquad j \in [1,Nc], t \in [1,T] \qquad (4.8)$$

where $C^{b}_{ctj}$ is the fuel cost of $j^{th}$ CHP units at $t^{th}$ sub-interval in backpressure mode ($/h); $P^{b}_{tj}$ and $H^{b}_{tj}$ are the power and heat output from the $j^{th}$ CHP units at $t^{th}$ sub-interval in backpressure mode, respectively; $\chi^{b}_{j}$ is the cost coefficient of $j^{th}$ CHP unit ($/MWh); $Nc$ is the number of CHP units; and $T$ is the total time interval.

*Fuel consumption:* The fuel consumption is a linear function of the heat and power generation from the CHP unit and is expressed as:

$$\lambda^{b}_{j}(P^{b}_{tj},H^{b}_{tj})=\psi^{qb}_{j}H^{b}_{tj}+\psi^{pb}_{j}P^{b}_{tj} \qquad j\in[1,Nc],t\in[1,T] \qquad (4.9)$$

where $\psi^{qb}_{j}$ and $\psi^{pb}_{j}$ are the fuel coefficient for power and heat generation from the $j^{th}$ cogeneration plant, respectively (h).

#### 4.2.1.2 Extraction mode

In this mode, electricity is produced when a high pressure steam is sent from the boiler to the turbine. The steam can either be sent to heat up district heating water or to a condenser in which after cooling, the steam is sent to the boiler again. In this process, the ratio between heat and power is relaxed **(Zugno *et al.*, 2016)** and it is expressed as:

$$P^{e}_{tj}\geq R^{e}_{j}H^{e}_{tj} \qquad j\in[1,Nc],t\in[1,T] \qquad (4.10)$$

where $P^{e}_{tj}$ and $H^{e}_{tj}$ are the power and heat output from the $j^{th}$ CHP units at $t^{th}$ sub-interval during the extraction mode, respectively; $R^{e}_{j}$ is the power to heat ratio in extraction mode (MW/MWth).

*Generation cost:* The fuel cost of the CHP unit operating in extraction mode is given as:

$$C^{e}_{ctj}=C^{e}_{ctj}(P^{e}_{tj},H^{e}_{tj})=\chi^{e}_{j}\lambda^{e}_{tj}(P^{e}_{tj},H^{e}_{tj}) \qquad j\in[1,Nc],t\in[1,T] \qquad (4.11)$$

where $C^{e}_{c}$ is the fuel cost of CHP units ($/h), $\lambda^{e}_{tj}$ is the fuel consumption required for the heat and power generation from the $j^{th}$ CHP unit (MWh) and $\chi^{e}_{j}$ is the cost coefficient of $j^{th}$ CHP unit ($/MWh).

*Fuel consumption:* The fuel consumption of the CHP unit is expressed as:

$$\lambda^{e}(P^{e}_{tj},H^{e}_{tj})=\psi^{qe}_{j}H^{e}_{tj}+\psi^{pe}_{j}P^{e}_{tj} \qquad j\in[1,Nc],t\in[1,T] \qquad (4.12)$$

where $\psi_j^{qe}$ and $\psi_j^{be}$ are the fuel coefficient for power and heat generation from the $j^{th}$ cogeneration plant, respectively (h).

*Generation constraints:* The upper and lower power limits are evaluated from Eq. (4.4) and (4.5), respectively. The heat, power and fuel consumption limits are given as:

$$\underline{H_j^e} \le H_{tj}^e \le \overline{H_j^e} \qquad j \in [1,Nc], t \in [1,T] \qquad (4.13)$$

$$\underline{P_j^e} \le P_{tj}^e(H_{tj}^e) \le \overline{P_j^e} \qquad j \in [1,Nc], t \in [1,T] \qquad (4.14)$$

$$\underline{\lambda_j^e} \le \lambda_{tj}^e \le \overline{\lambda_j^e} \qquad j \in [1,Nc], t \in [1,T] \qquad (4.15)$$

where $\underline{P_j^e}$ and $\overline{P_j^e}$ are the lower and upper power limit of $j^{th}$ CHP units (MW) in extraction mode, respectively; $\underline{H_j^e}$ and $\overline{H_j^e}$ are the lower and upper heat limit of $j^{th}$ CHP unit (MWth) in extraction mode, respectively; $\underline{\lambda_j^e}$ and $\overline{\lambda_j^e}$ are the lower and upper fuel input limit of $j^{th}$ CHP units (MWh) in extraction mode, respectively and $\lambda_{tj}^e$ is fuel consumption of $j^{th}$ CHP unit at $t^{th}$ sub-interval (MWh).

### 4.2.2 Thermal Units

The fuel cost of the thermal unit comprises a quadratic equation and sinusoidal function and it is expressed as Eq. (2.2) in section 2.2 of Chapter 2. The generation and ramp up/down limits of the thermal unit are discussed in section 2.2.1 of Chapter 2.

### 4.2.3 Heat Units

The heat generated from the heat unit is used to supply the district and industry heat requirements **(Zugno *et al.*, 2016)**. The generation cost, fuel consumption and its constraints are given here as:

*Fuel consumption:* The fuel consumption of the heat unit is a linear function of the heat output and it is expressed as:

$$\lambda_{tm}^h(H_{tm}^h) = \psi_m^q H_{tm}^h \qquad m \in [1,Nh], t \in [1,T] \qquad (4.16)$$

where $\lambda_{tm}^{h}$ is the fuel consumption required for the heat generated from the $m^{th}$ heat unit (MWh); and $\psi_{m}^{q}$ is the fuel per electricity and heat generation from the $m^{th}$ heat plant (h).

*Generation cost:* The fuel cost of the heat unit depends on fuel consumption, and it is given as:

$$C_h = C_h(H_{tm}^{h} I_{tm}) = \chi_m^h \lambda^h (H_{tm}^{h}) \qquad m \in [1,Nh],\ t \in [1,T] \qquad (4.17)$$

where $C_h$ is the fuel cost of heat units (\$/h); $H_{tm}^{h}$ is the heat output from the $m^{th}$ heat unit at $t^{th}$ sub-interval (MWth); $\chi_m^h$ is the cost coefficient of $m^{th}$ heat unit (\$/MWh); $Nh$ is the number of heat units; and $T$ is the total time interval.

*Generation constraints:* The lower and upper limit of heat generation is given in Eq. (4.18). The fuel limit of heat only unit must be within a certain limit is expressed as Eq. (4.19).

$$\underline{H_m^h} \le H_{tm}^{h} \le \overline{H_m^h} \qquad m \in [1,Nh],\ t \in [1,T] \qquad (4.18)$$

$$\underline{\lambda_m^h} \le \lambda_{tm}^{h} \le \overline{\lambda_m^h} \qquad m \in [1,Nh],\ t \in [1,T] \qquad (4.19)$$

where $\underline{H_m^h}$ and $\overline{H_m^h}$ are the lower and upper heat limit of $m^{th}$ heat unit (MWth), respectively; $\underline{\lambda_m^h}$ and $\overline{\lambda_m^h}$ are the lower and upper fuel limit of $m^{th}$ heat units (MWh), respectively.

## 4.3 MULTIOBJECTIVE COMBINED HEAT AND POWER UNIT COMMITMENT PROBLEM

Combined heat and power system is the coordination of thermal, DM-CHP and heat generating units. The heat demand is met by the heat generated from the DM-CHP and heat units. The power requirement is fulfilled by the power generation from thermal and CHP units. The commitment and generation scheduling of units in the MO-CHPUC problem consists of binary (unit status ON/OFF) and continues (power, heat) decision variables. Hence, the MO-CHPUC is a mixed-integer problem and the decision variable (X) matrix is given as:

$$X = \begin{bmatrix} I_{11} & \cdots & I_{1Ng} & I_{11} & \cdots & I_{1Nc} & I_{11} & \cdots & I_{1Nh} & P_{11}^{th} & \cdots & P_{1Ng}^{th} & P_{11}^{c} & \cdots & P_{1Nc}^{c} & H_{11}^{c} & \cdots & H_{1Nc}^{c} & H_{11}^{h} & \cdots & H_{1Nh}^{h} \\ \vdots & \vdots & \vdots & \vdots & \vdots & \vdots & \vdots & \vdots & \vdots & \vdots & \vdots & \vdots & \vdots & \vdots & \vdots & \vdots & \vdots & \vdots & \vdots & \vdots & \vdots \\ I_{T1} & \cdots & I_{TNg} & I_{T1} & \cdots & I_{TNc} & I_{T1} & \cdots & I_{TNh} & P_{T1}^{th} & \cdots & P_{TNg}^{th} & P_{T1}^{c} & \cdots & P_{TNc}^{c} & H_{T1}^{c} & \cdots & H_{TNc}^{c} & H_{T1}^{h} & \cdots & H_{TNh}^{h} \end{bmatrix}$$

(4.20)

The details regarding the objective function formulation of the MO-CHPUC problem along with UC and generation constraints are given in the following sub-sections.

### 4.3.1 Objective Functions

The main aim of the MO-CHPUC problem is to minimize the total cost and pollutant emission level of generating units, simultaneously with the satisfaction of various constraints. It can be represented as:

Minimize (TC, TE) (4.21)

where *TC* is the total operating cost ($); and *TE* is the total emission emits from generating units (Kg).

The operating cost of the generation schedule includes the fuel cost of thermal, heat and CHP units, and the start-up cost of units. The total operating cost is expressed as:

$$TC = \sum_{t=1}^{T} \left[ \sum_{i=1}^{Ng} C_g(P_{ti}^{th}) I_{ti} + \sum_{j=1}^{Nc} C_c(P_{tj}^{c}, H_{tj}^{c}) I_{tj} + \sum_{m=1}^{Nh} C_h(H_{tm}^{h}) I_{tm} + \sum_{n=1}^{N} ST_{tn} \right] \quad (4.22)$$

where *TC* is the total cost for energy generation ($); $ST_{tn}$ is the start-up cost required for $n^{th}$ units at $t^{th}$ sub-interval ($); $P_{ti}^{th}$ is the power generation from $i^{th}$ units at $t^{th}$ sub-interval (MW); $H_{tm}^{h}$ is the heat generation from $m^{th}$ units at $t^{th}$ sub-interval (MWth); $C_g$, $C_c$ and $C_h$ are the fuel cost of thermal, CHP and heat units ($/h), respectively; $I_{ti}$ is the $i^{th}$ unit ON/OFF status at $t^{th}$ sub-interval; *N* is the total number of units; $Ng$ is the total number of thermal units; $Nc$ is the total number of CHP units; $Nh$ is the total number of heat units; and *T* is the total time interval.

The pollutant emission (*TE*) from thermal generating units is given as:

$$TE = \sum_{t=1}^{T} \left[ \sum_{i=1}^{Ng} E_{gi} I_{ti} \right] \quad (4.23)$$

The pollutant emission ($E_g$) emits from the thermal unit is given as **(Shukla and Singh, 2016[1])**:

$$E_{gi}=\kappa_i+\varphi_i P_{ti}^{th}+\rho_i\left(P_{ti}^{th}\right)^2+\theta_i exp\left(\eta_i P_{ti}^{th}\right) \qquad t\in[1,T],\ i\in[1,Ng] \tag{4.24}$$

where *TE* is the total emission (Kg); $E_{gi}$ is the emission emit from $i^{th}$ thermal unit at $t^{th}$ sub-interval (Kg); and $\kappa_i,\varphi_i,\rho_i,\theta_i$ and $\eta_i$ are the emission coefficient of $i^{th}$ thermal unit.

In order to deal with the MO-CHPUC problem, the fuzzy membership function ( $\mu$ ) is computed for each objective function. The evaluation of fuzzy $\mu(F_n)$ is based on the minimum ($\underline{F_n}$) and maximum ($\overline{F_n}$) limit of each objective function. The monotonic decreasing $\mu(F_n)$ (n=1, 2) for both objectives is computed as **(Patwal and Narang, 2018)**:

$$\mu(F_n)=\begin{cases}1 & F_n<\underline{F_n}\\ \dfrac{\overline{F_n}-F_n}{\overline{F_n}-\underline{F_n}} & \underline{F_n}\le F_n\le\overline{F_n}\\ 0 & F_n>\overline{F_n}\end{cases} \qquad n\in[1,Nf] \tag{4.25}$$

In order to search the best non-dominated solution, the CPM is maximized along with the satisfaction of all the constraints. The mathematical representation is given as **(Patwal and Narang, 2018)**:

$$\mu_d=\{max(min(\mu(F_1),\mu(F_2))\} \tag{4.26}$$

where $F_1,F_2$ are the cost and emission objective function, respectively; $\mu(F_1),\mu(F_2)$ are the membership value of operating cost and emission, respectively; $\mu_d$ is the final membership value of MO-CHPUC problem; $\underline{F_n}$ and $\overline{F_n}$ are the lower and upper value of objective functions, respectively.

### 4.3.2 Constraints

The MO-CHPUC constraints bounded by unit commitment constraints such as minimum up and down time constraint and spinning reserve constraint. The minimum up and down time constraint is represented by Eq. (2.5) of Chapter 2. The generation scheduling constraint comprises power and heat balance equality constraint, and other cogeneration, power only and heat only unit constraints. The generation limits for thermal and DM-

CHP unit and fuel consumption limits for individual heat units are discussed in section 4.2. The unit commitment and generation constraints are given as:

*Power and heat spinning reserve:* It is required to maintain the system reliability due to uncertainty in the load demand and unavailability of the units. The total feasible maximum generation capacity of committed units should be able to satisfy the demand along with spinning reserve at each sub-interval and it is represented as:

$$\sum_{i=1}^{Ng} \overline{P_i^{th}} I_{ti} + \sum_{j=1}^{Nc} P_{tj}^{b,e}(H_{tj}^{b,e}) I_{tj} \geq PD_t + SG_t \qquad t \in [1,T] \qquad (4.27)$$

$$\sum_{j=1}^{Nc} H_{tj}^{b,e}(P_{tj}^{b,e}) I_{tj} + \sum_{m=1}^{Nh} \overline{H_m^h} I_{tm} \geq HD_t + SH_t \qquad t \in [1,T] \qquad (4.28)$$

where $I_{ti}$ is the $i^{th}$ unit ON/OFF status at $t^{th}$ sub-interval; $\overline{P_i^{th}}$ is the upper power limit of $i^{th}$ thermal unit (MW); $P_{tj}^{b,e}$ is the power generation from $j^{th}$ CHP unit for backpressure and extraction mode at $t^{th}$ sub-interval (MW); $PD_t$ and $SG_t$ are the power demand and spinning reserve requirement at $t^{th}$ sub-interval, respectively (MW); $\overline{H_m^h}$ is the upper heat limit of $m^{th}$ heat unit (MWth); $H_{tj}^{b,e}$ is the heat generation from $j^{th}$ CHP unit for backpressure and extraction mode at $t^{th}$ sub-interval (MWth); and $HD_t$ and $SH_t$ are the heat demand and spinning reserve requirement at $t^{th}$ sub-interval, respectively (MWth).

*Power and heat balance:* The total power and heat generation should be equal to the load demand at $t^{th}$ sub-interval and is expressed as:

$$\sum_{i=1}^{Ng} P_{ti}^{th} I_{ti} + \sum_{j=1}^{Nc} P_{tj}^{b,e}(H_{tj}^{b,e}) I_{tj} = PD_t \qquad t \in [1,T] \qquad (4.29)$$

$$\sum_{j=1}^{Nc} H_{tj}^{b,e}(P_{tj}^{b,e}) I_{tj} + \sum_{m=1}^{Nh} H_{tm}^{h} I_{tm} = HD_t \qquad t \in [1,T] \qquad (4.30)$$

## 4.4 MULTIOBJECTIVE PROFIT BASED COMBINED HEAT AND POWER UNIT COMMITMENT PROBLEM

In this section, the objective function formulation of MO-PBCHPUC problem along with constraints is expressed in the following sub-sections:

### 4.4.1 Objective Functions

The aim of the MO-PBCHPUC problem is to maximize the total profit and minimize the pollutant emission, simultaneously with the satisfaction of various constraints. The objective function is formulated as:

Maximize (PF), Minimize (TE) (4.31)

where *PF* is the total profit ($); and *TE* is the emission emits from generating units (Kg).

In the deregulated markets, the main aim of the single objective is to maximize the GENCOs profit by scheduling the power and heat from the generating units. The profit of the GENCOs is the margin between the revenue and total operating cost. The profit of GENCOs is computed as **(Reddy *et al.*, 2016)**:

$$PF = RV - TC \tag{4.32}$$

where *RV* is the revenue generated ($); and *TC* is the total operating cost ($).

A market-clearing price is the price of a good or service at which quantity supplied is equal to quantity demanded, also called the equilibrium price. The theory claims that markets tend to move toward this price. The revenue generated by selling the generated power and heat is expressed as:

$$RV = \sum_{t=1}^{T}\left[\sum_{i=1}^{Ng} \sigma_t P_{ti}^{th} I_{ti} + \sum_{j=1}^{Nc} \sigma_t P_{tj}^{c} I_{tj} + \sum_{j=1}^{Nc} \lambda_t H_{tj}^{c} I_{tj} + \sum_{m=1}^{Nh} \lambda_t H_{tm}^{h} I_{tm}\right] \tag{4.33}$$

where $\sigma_t$ is the power price ($/MWh); $\lambda_t$ is the heat price ($/MWthh); $P_{ti}^{th}$ is the power output from $i^{th}$ thermal unit at $t^{th}$ sub-interval (MW); $H_{tm}^{h}$ is the heat output from $m^{th}$ heat unit at $t^{th}$ sub-interval (MWth); $P_{tj}^{c}, H_{tj}^{c}$ are power and heat generation from $j^{th}$ CHP unit at $t^{th}$ sub-interval; $I_{ti}$ is the $i^{th}$ unit ON/OFF status at $t^{th}$ sub-interval; $Ng$ is the total number of thermal units; $Nc$ is the total number of CHP units; $Nh$ is the total number of heat units; *N* is the total number of units; and *T* is the total time interval.

In the MO-PBCHPUC problem, the maximum value of profit and the minimum value of pollutant emission forms conflicting objectives. In order to form the objective function, the economic model procedure has been used as discussed in sub-section 4.3.1. For profit objective function, the monotonic increasing $\mu(F_n)$ is used and is computed as:

$$\mu(F_n)=\begin{cases} 0 & F_n<\underline{F_n} \\ \dfrac{F_n-\underline{F_n}}{\overline{F_n}-\underline{F_n}} & \underline{F_n}\le F_n\le\overline{F_n} \\ 1 & F_n>\overline{F_n} \end{cases} \qquad n\in[1,Nf] \qquad (4.34)$$

The monotonic decreasing $\mu(F_n)$ function for emission is evaluated as given by Eq. (4.25). the mathematical representation of the CPM for MO-PBCHPUC problem is given as:

$$\mu_d=\{max(min(\mu(F_3),\mu(F_2))\} \qquad (4.35)$$

where $F_2, F_3$ are the objective function of emission and profit, respectively; $\mu(F_2),\mu(F_3)$ are the membership value of emission and profit, respectively; $\mu_d$ is the final membership value of MO profit based problem; $\underline{F_n}$ and $\overline{F_n}$ are the lower and upper value of objective functions, respectively.

### 4.4.2 Constraints

The ramp rate, generation and fuel limits are imposed on generating units and it is given in section 4.2. Minimum up and down time constraint is given in sub-section 2.2.1 of Chapter 2. The details regarding other constraints of MO-PBCHPUC problem are given as:

*Power spinning reserve constraint:* For profit model, maximum available power should be less than or equal to the forecast power demand along with power reserve and is given as:

$$\sum_{i=1}^{Ng}\overline{P_i^{th}}I_{ti}+\sum_{j=1}^{Nc}P_{tj}^{be}(H_{tj}^{be})I_{tj}\le PD_t+SG_t \qquad t\in[1,T] \qquad (4.36)$$

where $I_{ti}$ is the $i^{th}$ unit ON/OFF status at $t^{th}$ sub-interval; $\overline{P_i^{th}}$ is the upper power limit of $i^{th}$ unit (MW); $P_{tj}^{be}$ is the power generation from $j^{th}$ CHP unit for backpressure and extraction mode at $t^{th}$ sub-interval (MW); $PD_t$ and $SG_t$ are the power demand and spinning reserve requirement at $t^{th}$ sub-interval (MW), respectively.

*Heat spinning reserve constraint:* The maximum available heat from backpressure ( $\overline{H_j^b}$ ) or extraction ( $\overline{H_j^e}$ ) mode of CHP and heat unit should be less than or equal to heat demand along with heat reserve is given as:

$$\sum_{j=1}^{Nc} \overline{H_j^{b,e}} I_{tj} + \sum_{m=1}^{Nh} \overline{H_m^h} I_{tm} \leq HD_t + SH_t \qquad t \in [1,T] \qquad (4.37)$$

where $I_{ti}$ is the $i^{th}$ unit ON/OFF status at $t^{th}$ sub-interval; $\overline{H_m^h}$ is the upper heat limit of $m^{th}$ heat unit (MWth); $\overline{H_j^{b,e}}$ is the heat generation from $j^{th}$ CHP unit for backpressure and extraction mode at $t^{th}$ sub-interval (MWth); $HD_t$ and $SH_t$ are the heat demand and spinning reserve requirement at $t^{th}$ sub-interval (MWth), respectively.

*Power demand constraint:* For the deregulated environment, total power generation from the committed units should be less than or equal to the forecast load demand and is expressed as:

$$\sum_{i=1}^{Ng} P_{ti}^{th} I_{ti} + \sum_{j=1}^{Nc} P_{tj}^{b,e}(H_{tj}^{be}) I_{ti} \leq PD_t \qquad t \in [1,T] \qquad (4.38)$$

*Heat demand constraint:* In a deregulated environment, the heat generation from the committed units at $t^{th}$ sub-interval should be less than or equal to the forecast heat demand and is followed as:

$$\sum_{j=1}^{Nc} H_{tj}^{b,e} \times I_{tj} + \sum_{m=1}^{Nh} H_{tm}^{h} \times I_{tm} \leq HD_t \qquad t \in [1,T] \qquad (4.39)$$

## 4.5 SOLUTION METHODOLOGY

The BSA-CSO optimization technique developed for the thermal UC problem has been used to solve the CHPUC problem and it is discussed in sections 2.3 and 2.4 of Chapter 2. The BSA-CSO technique is applied to deal with the binary and continuous variables of the MO-CHPUC problem. In order to deal with the MO problem, the fuzzy membership function is evaluated for each objective function. The heuristic technique is applied to handle the UC constraints of the MO-CHPUC and MO-PBCHUC problems. In order to handle generation constraints, the exterior penalty method is applied. The implementation has been discussed in the following sub-sections.

### 4.5.1 Constraint Handling Procedure

The CHPUC and PBCHPUC includes spinning reserve requirement, minimum up and down time, ramp-rate limits, power and heat balance requirement, fuel limit, and generation limit. The constraint handling of unit commitment and generation constraints are given as follows:

#### 4.5.1.1 Unit commitment constraints handling

The commitment strategy has been required to maintain the heat and power spinning reserve with the satisfaction of the minimum up and down time of generating units. The steps of commitment strategy are mentioned below as:

**Minimum up and down time constraint:** The pseudo code to handle the minimum up and down time constraint of generating units is illustrated in Figure 4.2.

/////……………………………..**Minimum Up and Down Time**………………..………………../////

// Read input data and status of generating units and Output status of units satisfying the time limits.

**For** t=1:T

**For** i=1:Ng

1: **If** ($I_{ti}=1$) **then**

$$T_{ti}^{on}=T_{(t-1)i}^{on}+1, T_{ti}^{off}=0$$

**Else**

$$T_{ti}^{on}=0, T_{ti}^{off}=T_{(t-1)i}^{off}+1$$

**End if**

**2:** $T_i^{up}=T_{ie}^{up}, T_i^{dw}=T_{ie}^{dw}$ for extraction mode; $T_i^{up}=T_{ib}^{up}, T_i^{dw}=T_{ib}^{dw}$ for backpressure mode

**3:** **If** ( $I_{ti}=0, I_{(t-1)i}=1 \& T_{(t-1)i}^{on}<T_i^{up}$ ) **then**

$I_{t,i}=1$

**End if**

**If** ( $I_{ti}=0, I_{(t-1)i}=1 \ \& t-1-T_i^{dw} \le T \ \& T_{r,i}^{off}<-T_i^{dw}$ ) **then**

$I_{ti}=1$

**End if**

**If** ( $I_{ti}=0, I_{(t-1)i}=1 \ \& t-1-T_i^{dw}>T \ \& \sum_{l=t}^{T} I_{li}>0$ ) **then**

$I_{ti}=1$

**End if**

**4:** Update $T_{ti}^{on}, T_{ti}^{off}$ .

**End For**

**End For**

**Figure 4.2**: Pseudo code of minimum up and down time constraint handling strategy

**Power and heat spinning reserve requirement**: The evaluation of the heat and power spinning reserve is based on its maximum generation limits. The heat and power spinning reserve requirement is satisfied by the heuristic method based on the *priority list* (PL) **(Senjyu, 2003)**. The strategy is illustrated in Figures 4.3 and 4.4. The power generation from committed CHP unit is restricted due to mutual dependency on heat generation and it has been considered to satisfy power spinning reserve constraint in Figure 4.4.

**Unit de-commitment:** The satisfaction of minimum up and down time constraints may lead to excessive spinning reserve, which leaned the system towards the lower profit and raise the operating cost. Hence, there is a need to de-commit some of the units based on the PL **(Senjyu, 2003)**. The strategy to de-commit the additional heat and CHP units is given in Figure 4.5 and 4.6. The process of de-commitment the additional thermal units based on the PL with the satisfaction of unit commitment constraints is same as de-commitment of heat and CHP units.

### 4.5.1.2 Generation constraints handling

During the search process, if the decision variables violate their feasible limits, then these are set to their corresponding limits. The ramp rate constraint of the thermal unit has been taken care by using Eq. 2.26 and 2.27 of Chapter 2. In order to satisfy the generation equality constraint, the mismatch between generation and demand, ($\Delta PD_t$, $\Delta HD_t$) at each sub-interval is computed and the exterior penalty approach is applied. In order to satisfy, the upper and lower limits on the fuel consumption of heat and CHP unit in a regulated and deregulated environment, an error ($E_t^{fl}$) is computed between actual used fuel and its respective limit and is given as:

$$E_t^{fl} = \begin{cases} \sum_{j=1}^{N_c+N_h} \left(\lambda(P_{tj}^{c} H_{tj}^{c,h}) - \overline{\lambda_j^{c,h}}\right)^2 & ; \lambda(P_{tj}^{c}, H_{tj}^{c,h}) > \overline{\lambda_j^{c,h}} \\ \sum_{j=1}^{N_c+N_h} \left(\lambda\lambda P_{tj}^{c} H_{tj}^{c,h}) - \underline{\lambda_j^{c,h}}\right)^2 & ; \lambda(P_{tj}^{c} H_{tj}^{c,h}) < \underline{\lambda_j^{c,h}} \end{cases} \quad t \in [1,T] \qquad (4.40)$$

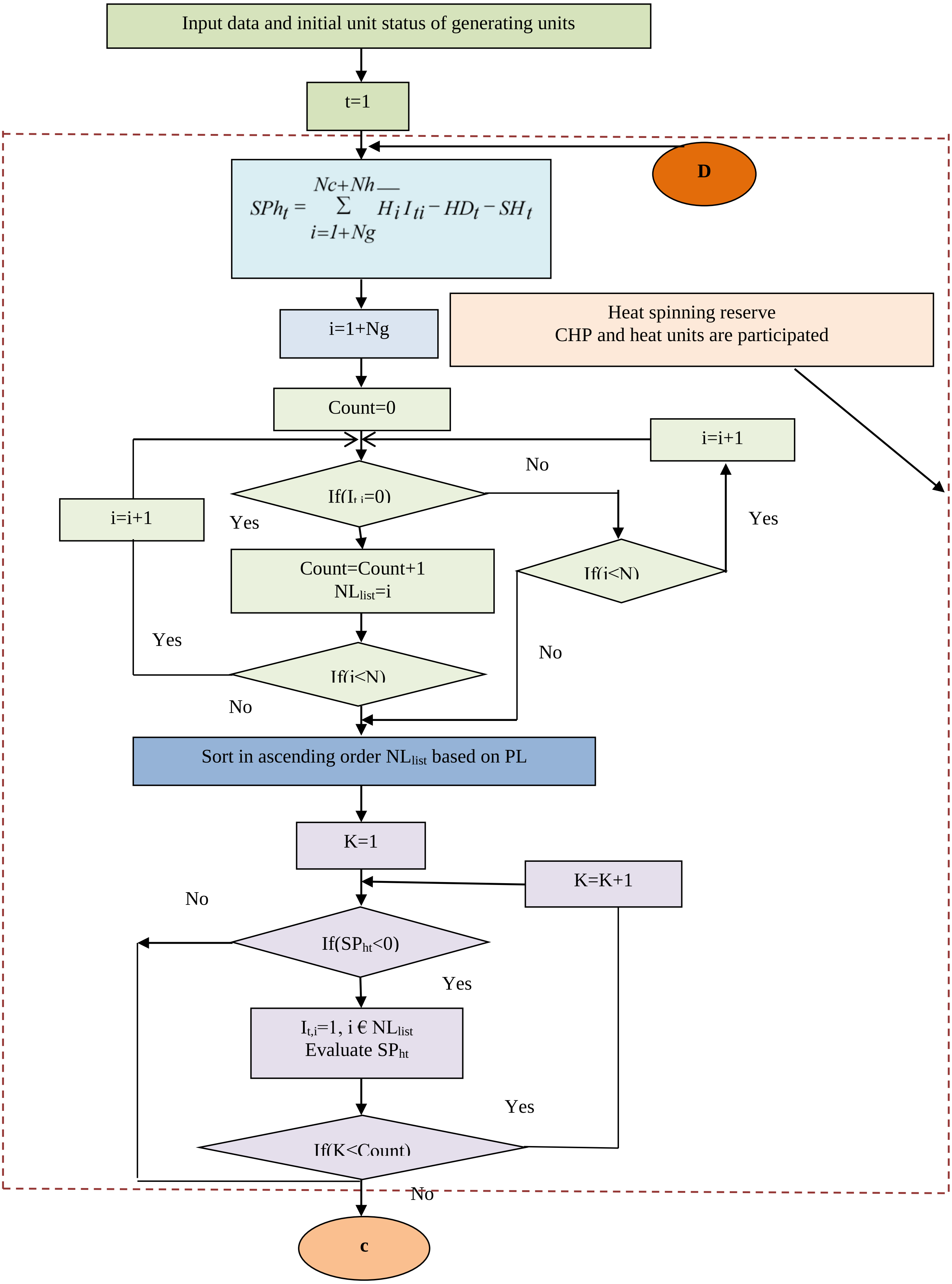


**Figure 4.3:** Heat reserve requirement strategy

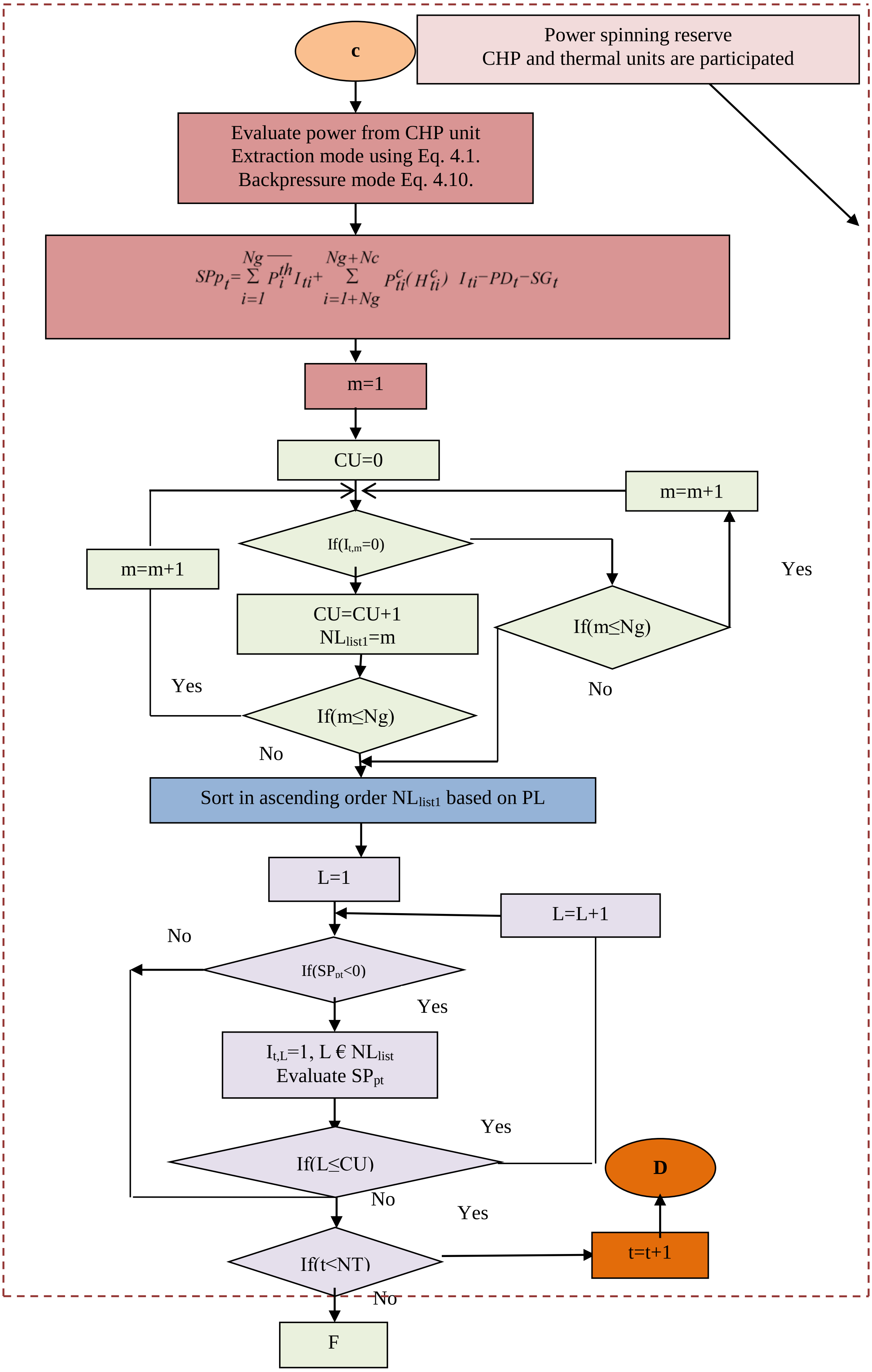


**Figure 4.4:** Power reserve requirement strategy

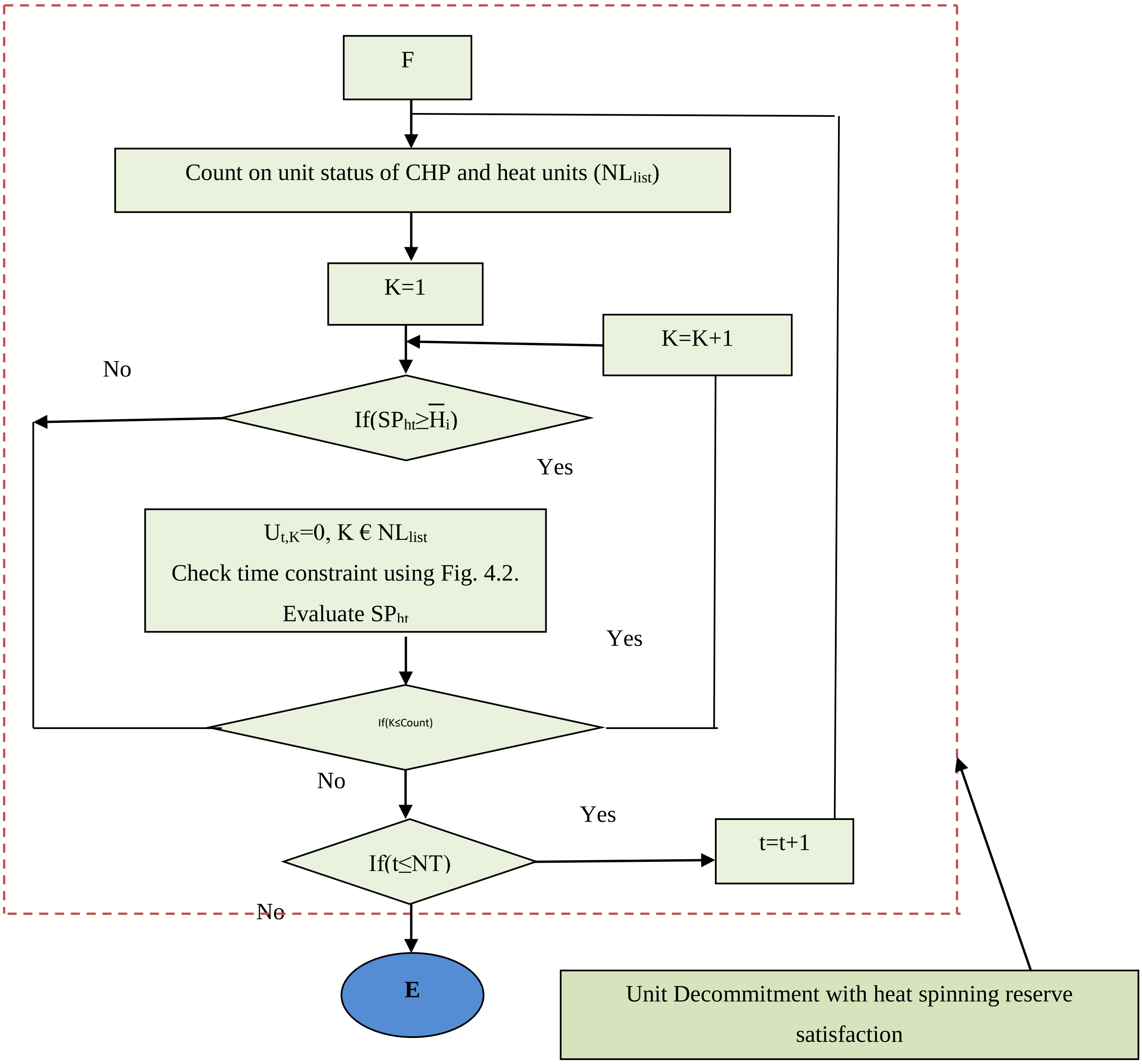


**Figure 4.5:** Heat spinning reserve with de-commitment process

Ramp-rate limit on the CHP fuel consumption is satisfied by computing an error ( $E_t^{fr}$ ) as:

$$E_t^{fr} = \begin{cases} \sum_{j=1}^{N_c} \left( DR_j^f - \lambda_{tj}^b + \lambda_{(t-1)j}^b \right)^2 & ; DR_j^f \le \lambda_{tj}^b - \lambda_{(t-1)j}^b \\ \sum_{j=1}^{N_c} \left( \lambda_{tj}^b - \lambda_{(t-1)j}^b - UR_j^f \right)^2 & ; \lambda_{tj}^b - \lambda_{(t-1)j}^b \le UR_j^f \end{cases} \qquad t \in [1,T] \qquad (4.41)$$

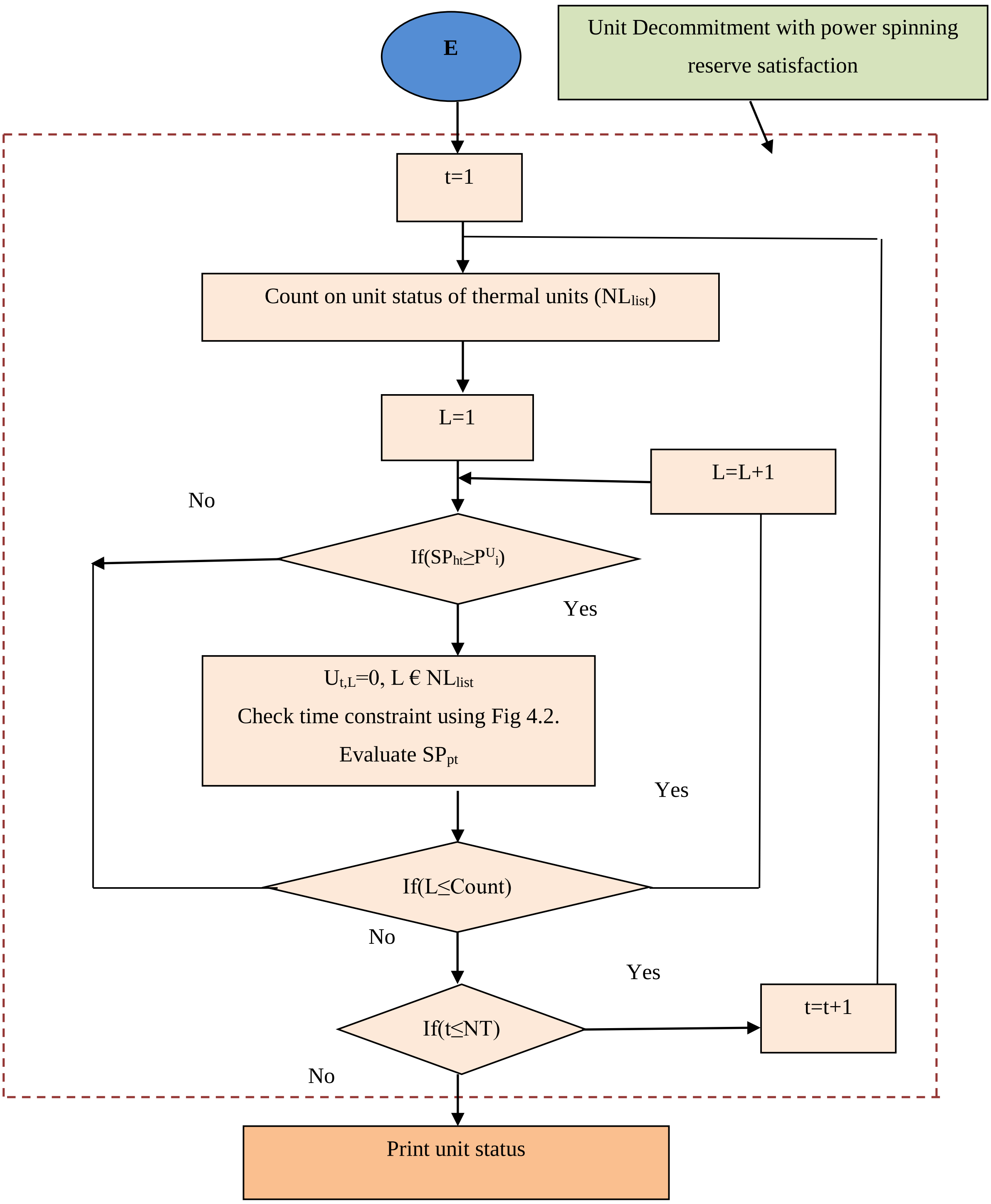


**Figure 4.6:** Power spinning reserve with de-commitment process

In economic and profit based UC problem, the mismatch between generation and demand is satisfied by computing an error ( $E_t^1$,$E_t^2$ ) as:

$$E_t^1 = \begin{cases} \left( PD_t - \sum_{i=1}^{Ng} P_{ti}^{th} - \sum_{j=1}^{Nc} P_{tj}^{b,e}(H_{tj}^{b,e}) \right)^2 ; \sum_{i=1}^{Ng} P_{ti}^{th} + \sum_{j=1}^{Nc} P_{tj}^{b,e}(H_{tj}^{b,e}) \neq PD_t \text{ for CHPUC} \\ \left( PD_t - \sum_{i=1}^{Ng} P_{ti}^{th} - \sum_{j=1}^{Nc} P_{tj}^{b,e}(H_{tj}^{b,e}) \right)^2 ; \sum_{i=1}^{Ng} P_{ti}^{th} + \sum_{j=1}^{Nc} P_{tj}^{b,e}(H_{tj}^{b,e}) > PD_t \text{ for PBCHPUC} \end{cases}$$

$$t \in [1,T] \qquad (4.42)$$

$$E_t^2 = \begin{cases} \left( HD_t - \sum_{j=1}^{N_c} H_{tj}^{b,e} - \sum_{m=1}^{N_h} H_{tm}^{h} \right)^2 ; \sum_{j=1}^{N_c} H_{tj}^{b,e} + \sum_{m=1}^{N_h} H_{tm}^{h} \neq HD_t \text{ for CHPUC} \\ \left( HD_t - \sum_{j=1}^{N_c} H_{tj}^{b,e} - \sum_{m=1}^{N_h} H_{tm}^{h} \right)^2 ; \sum_{j=1}^{N_c} H_{tj}^{b,e} + \sum_{m=1}^{N_h} H_{tm}^{h} > HD_t \text{ for PBCHPUC} \end{cases}$$

$$t \in [1,T] \qquad (4.43)$$

where $E_t^{fl}$ and $E_t^{fr}$ are the error for fuel limit and ramping fuel limit, respectively; $E_t^1$ and $E_t^2$ are the error corresponding to the mismatch between generation and demand for power and heat demand, respectively.

**Scalar objective functions:** In this Chapter, three scalar objective functions have been minimized and maximized *i.e.*, operating cost, pollutant emission, profit of GENCOs. The details regarding these objectives have already been discussed in section 4.3 and 4.4. In order to satisfy all constraints, exterior penalty method is applied and for this, errors have already been computed due to mismatch between actual values and expected values and are given by Eqs. (4.40-4.43). These objective functions are given as:

- *Cost objective function:*

$$F_1 = \sum_{t=1}^{T} \left( \sum_{i=1}^{Ng} Cg_{ti} + \sum_{j=1}^{Nc} Cc_{tj}^{b,e} + \sum_{m=1}^{Nh} Ch_{tm} + \sum_{r=1}^{N} ST_{tr} \right) + \varphi E \qquad (4.44)$$

and

$$E = \sum_{t=1}^{T} [ E_t^1 + E_t^2 + E_t^{fr} + E_t^{fl} ] \qquad (4.45)$$

- *Pollutant emission objective function:*

$$F_2 = \sum_{t=1}^{T}\left(\sum_{i=1}^{Ng} Eg_{ti}\right) + \varphi E \tag{4.46}$$

- *Profit objective function:*

$$F_3 = \sum_{t=1}^{T}\left(\begin{array}{l} \sum_{i=1}^{Ng+Nc} \sigma_t P_{ti}^{th,c} I_{ti} + \sum_{i=1+Ng}^{N} \lambda_t H_{ti}^{c,h} I_{ti} \\ -\sum_{i=1}^{Ng} Cg_{ti} - \sum_{j=1}^{Nc} Cc_{tj}^{b,e} - \sum_{m=1}^{Nh} Ch_{tm} - ST_t - \varphi E \end{array}\right) \tag{4.47}$$

where $F_1, F_2, F_3$ are the objective function of cost, emission and profit for scalar CHPUC problem, respectively; $E$ represents the total error; and $\varphi$ is the penalty factor.

**Multiobjective functions:** In this work, two multi-objective problems have been solved. The objective of the MO-CHPUC problem is to minimize operating cost ($F_1$) and pollutant emission ($F_2$), simultaneously. The objective of the MO-PBCHPUC problem is to maximize the profit of GENCO ($F_3$) and minimize the pollutant emission ($F_2$), simultaneously. In order to search the best non-dominated solution of MO-CHPUC, the CPM is maximized along with the satisfaction of all the constraints. The mathematical formulation of objectives is given as:

- For MO-CHPUC problem, the overall objective function is represented as **(Patwal and Narang, 2018)**:

$$\mu_d = \{max(min(\ \mu(F_1), \mu(F_2), \mu(\varphi E)))\} \tag{4.48}$$

where

The membership function of error is given as:

$$\mu(\varphi E) = \begin{cases} 1 & \varphi E > 0 \\ 0 & Otherwise \end{cases} \tag{4.49}$$

where $\mu(F_1), \mu(F_2), \mu(\varphi E)$ are the membership value of operating cost, emission and error, respectively; $\mu_d$ is the CPM ranking.

- In MO-PBCHPUC problem, the mathematical representation of objective function with the satisfaction of all the constraints is given as:

$$\mu_d = \{max(min(\mu(F_3), \mu(\varphi E), \mu(F_2)))\} \tag{4.50}$$

where $\mu(F_3), \mu(F_2)$ are the membership value of profit and emission.

### 4.5.2 Implementation of Binary Successive Approximation and Civilized Swarm Optimization Technique for Cogeneration Based Unit Commitment Problem

In this section, the implementation of the optimization technique 'BSA-CSO' is discussed to solve mixed-integer CHPUC problem. In the BSA-CSO technique, the BSA technique is used to search the binary variable and the CSO technique is used to search the continuous variable of the CHPUC problem. The steps for implementation of BSA-CSO technique to solve the mixed-integer CHPUC problem are given as follows:

**Step 1:** Read input data, *i.e.*, N, T, $T_i^{up}, T_i^{dw}$, cost coefficients, power and heat generation capacities, demand, *etc*.

**Step 2:** The decision variables (X) matrix of the CHPUC problem is represented in Eq. 40. The initial commitment status of generating unit is randomly generated as:

$$I_{tr} = \begin{cases} 1; & If\ ran() \geq 0.5 \\ 0; & otherwise \end{cases} \qquad r \in [1,N],\, t \in [1,T] \qquad (4.51)$$

The initial power ($P_{ti}^{th}$) and heat ($H_{tm}^{h}$) are randomly generated for thermal and heat units and is expressed as:

$$P_{ti}^{th} = \underline{P_{ti}^{th}} + ran()(\overline{P_{ti}^{th}} - \underline{P_{ti}^{th}}) \qquad i \in [1,Ng],\, t \in [1,T] \qquad (4.52)$$

$$H_{tm}^{h} = \underline{H_{m}^{h}} + ran()(\overline{H_{m}^{h}} - \underline{H_{m}^{h}}) \qquad m \in [1,Nh],\, t \in [1,T] \qquad (4.53)$$

For the CHP unit, the initial heat ($H_{tj}^{b,e}$) is generated randomly using Eq. (4.54).

$$H_{tj}^{b,e} = \underline{H_{j}^{b,e}} + ran()(\overline{H_{j}^{b,e}} - \underline{H_{j}^{b,e}}) \qquad j \in [1,Nc],\, t \in [1,T] \qquad (4.54)$$

The power generation for backpressure mode of the CHP unit is evaluated using Eq. (4.1). The power generation during extraction mode is expressed as:

$$P_{tj}^{e} = R_j^e H_j^e + ran()(\overline{P_j^e} - R_j^e H_j^e) \qquad j \in [1,Nc],\, t \in [1,T] \qquad (4.55)$$

**Step 3: Update unit status by BSA:** The node entries 1/0 of BSA tree represents ON/OFF unit status, respectively. In the BSA algorithm, the initial base node is randomly chosen sub-interval unit status and each node should satisfy the unit commitment constraints. The power and heat have been assigned to the initial base point by a PL method for the first iteration of the overall process. Two new nodes are formed from the base node using Eq. (2.13) and the power and heat have been assigned according to the

PL method. The pseudo code of the PL method to assign power and heat is illustrated in Figure 4.7. The next base node is selected based on objective function evaluation of scalar CHPUC and PBCHPUC problem (Eq. 4.44 and 4.47) and this procedure are repeated until the last branch of the tree is reached and it is shown in Figure 2.12.

In the MO problem, the objective function is evaluated using Eq. 4.48 and 4.50. For the next cycle, again one randomly selected sub-interval unit status is chosen as the base node. By following this procedure, the local optimal solution is avoided as the search starts with different starting points. This procedure repeats until all sub-intervals have been undertaken.

**Step 4: Optimum schedule by civilized swarm optimization technique:** The CSO technique is applied to find optimum power/heat schedule from the selected unit status obtained from the BSA approach. The power and heat generation from the final base point of the BSA method is assigned to one particle of CSO while remaining particles of the swarm are randomly initialized and it is illustrated in Figure 2.12. The updating of power and heat in backpressure and extraction mode is discussed in step 2. The particles of the swarm are sorted based on objective function evaluation and swarm has been divided into societies. The particles of the swarm are updated using CSO algorithms and it continues until the maximum iteration ($k^{max}$) is met.

```
Read input T, N, PL, PD_t, HD_t, P_i(min), P_i(max), H_i(min), H_i(max) .
For t=1: T
ON unit set at H_ti = H_i(min) , i ∈ [Ng+1, N]

ER_t = Σ_{i=1+Ng}^{N} H_ti I_ti − HD_t

Sort NL based on PL and evaluate Count using Figure 4.5.
For k=1: Count
        If ( Σ_{i=1+Ng}^{N} H_ti I_ti < HD_t )          // ER_t is negative
H_tk I_tk = (H_tk − ER_t) I_tk  I_t,k ∀ NL_k
Check the maximum limit ( H_i(max) )
Get λ_tk using Eqs. 4.9, 4.12,4.17  and check the limit λ_j^{b,e}(min) ≤ λ_tj^{b,e} ≤ λ_j^{b,e}(max)
Change H_tk and evaluate P_tk for feasible value of fuel limit. Check λ_j^{b,e}(min) and λ_j^{b,e}(max)
```

**Figure 4.7:** Pseudo code for power/heat assign using priority list method.

**Step 5: Overall up gradation Process:** The updated unit status along with the optimum power/heat generation schedule is assigned as an initial base point for the next iteration. The same procedure is followed until the termination criterion of the overall process ($it^{max}$) is met and it is given in Chapter 2.

Evaluate the $ER_t$

Else if ( $\sum_{i=1+Ng}^{N} H_{ti} I_{ti} > HD_t$ ) // $ER_t$ is positive

$H_{tk} I_{tk} = (H_{tk} - ER_t) I_{tk} \quad I_{tk} \forall NL_k$

Check the minimum limit ( $\underline{H_i}$ )

Get $F_{t,k}$ using Eqs. (4.9, 4.12, 4.17) and check the limit $\underline{\lambda_j^{b,e}} \le \lambda_{tj}^{b,e} \le \overline{\lambda_j^{b,e}}$ . Change $H_{tk}$ and evaluate $P_{tk}$ for feasible value of fuel limit. Check $\underline{\lambda_j^{b,e}}$ and $\overline{\lambda_j^{b,e}}$

Evaluate the $ER_t$

End if

End for

For CHP get $P_{t,i}$ using Eq.(4.1,4.10) while ON thermal unit set at $P_{ti} = \underline{P_i}$

$ER_t = \sum_{i=1}^{N-Nh} P_{ti} I_{ti} - PD_t$

Sort NL based on PL and Count only for thermal unit.

For k=1: Count

If ( $\sum_{i=1}^{N-Nh} P_{ti} I_{ti} < PD_t$ ) // $ER_t$ is negative

$P_{tk} I_{tk} = (P_{tk} - ER_t) I_{tk} \quad I_{tk} \in NL_k$

Check the maximum limit ( $\overline{P_i}$ )

Evaluate the $ER_t$

Else if ( $\sum_{i=1}^{N-Nh} P_{ti} I_{ti} > PD_t$ ) // $ER_t$ is positive

$P_{tk} I_{tk} = (P_{tk} - ER_t) I_{tk} \quad I_{tk} \forall NL_k$

Check the minimum limit ( $\underline{P_i}$ )

Evaluate the $ER_t$

End if

End for

End for

**Figure 4.7:** Pseudo code for power/heat assign using priority list method. (Continued)

## 4.6 COGENERATION BASED UNIT COMMITMENT TEST SYSTEMS

In order to validate the effectiveness of the BSA-CSO technique, three test systems of the CHPUC problem are undertaken. The test systems consist of conventional thermal, DM-CHP and heat units to supply power and heat loads. The total scheduling period is 24-hour with a one-hour sub-interval. The test system-I, II, and III consists of 12 units (1-10$^{th}$ thermal, 11$^{th}$ CHP and 12$^{th}$ heat), 16 units (1-10$^{th}$ thermal, 11-15$^{th}$ CHP and 16$^{th}$ heat) and 20 units (1-10$^{th}$ thermal, 11-15$^{th}$ CHP and 16-20$^{th}$ heat), respectively. The maximum limit of P1, P2, P3, P4, P5, P6, P7, P8, P9, P10 is 455, 455, 130, 130, 12, 80, 85, 55, 55, 55 (MW), respectively whereas P11 maximum limit for extraction and backpressure mode is 263 and 140 (MW), respectively. Other CHP units are ruplicated of CHP unit used in Test system-I. All the test systems, the CHP and heat unit characteristics are given in Appendix B.3. The real provincial data of DM-CHP and heat units, which are located at Denmark have been taken from Ref. **(Zugno *et al.*, 2016)**. The thermal unit characteristics for these test systems are taken from reference **(Panwar *et al.*, 2018)** and it is given in Appendix B.1.

## 4.7 RESULT AND DISCUSSIONS

The BPSO-PSO and BSA-CSO technique have been applied for solving the CHPUC problem, the coding is done in a FORTRAN 90 environment on a personal computer (1.66 GHz, Pentium-IV, with 2 GB RAM). The extraction and backpressure mode of the CHP units have been undertaken for the CHPUC problem. The thirty trails of BPSO-PSO and BSA-CSO technique has been performed for solving the CHPUC problem to get the optimal solution. The cogeneration based unit commitment test systems have been solved by optimization techniques for scalar and multi-objective cogeneration based unit commitment problems which is discussed as:

### 4.7.1 Scalar Objective Combined Heat and Power Unit Commitment Problem

#### 4.7.1.1 Test system-I

The cost obtained from BSA-CSO and BPSO-PSO techniques during dual mode CHPUC problem is given in Table 4.1. The cost obtained by the BSA-CSO technique for backpressure and extraction mode is $518972 and $498786.6, respectively. It has been observed from Table 4.1 that the cost obtained by the implementation of the BPSO-PSO technique in backpressure and extraction mode is higher by '$1963.4' and '$3182.2' as compared to BSA-CSO technique, respectively. It has been evident that the cost attained from the BSA-CSO technique in backpressure and extraction mode is better as compared to the BPSO-PSO technique. The operating cost for extraction mode is reduced by $2874.4 as compared to backpressure mode for the BSA-CSO technique which further confirms the importance of the DM-CHP unit.

**Table 4.1:** Cost obtained for CHPUC problem, test system-I

| Technique | Backpressure mode cost ($) | Extraction mode cost ($) |
|---|---|---|
| **BPSO-PSO** | 520935.4 | 501968.8 |
| **BSA-CSO** | 518972.0 | 498786.6 |

The unit commitment status obtained from the BSA-CSO technique is given in Table 4.2. It has been observed from Table 4.2, during lightly power and heat loaded sub-intervals ($1^{st}$, 23-$24^{th}$), the optimum schedule of committed units is sufficient to meet demand and reserve constraints. During the peak heat demand sub-intervals ($2^{nd}$-$9^{th}$, $11^{th}$, 15-$22^{th}$), additional heat unit is turned on for extraction mode to satisfy heat demand and reserve constraints whereas, in backpressure mode, it is satisfied by the CHP unit only. For remaining lightly heat loaded sub-intervals, the CHP unit is sufficient to meet heat constraints for both modes.

During the upsurge of the power demand at $7^{th}$ sub-interval, the additional $3^{rd}$ thermal unit has been required in backpressure mode to meet the power demand constraint. However, there is no such requirement in extraction mode at $7^{th}$ sub-interval. Similarly, additional thermal units ($4^{th}$, $5^{th}$) have been required at 9-$10^{th}$ sub-intervals for backpressure mode. In order to satisfy the power demand constraint at 8-$22^{th}$ sub-intervals, the lower power capacity thermal unit $9^{th}$ is turned on in extraction mode. However, the higher power capability 4-$5^{th}$ thermal unit is turned on in backpressure mode to meet the power demand constraint. This is due to variable heat and power ratio in extraction mode whereas it is constant in backpressure mode. The escalation of heat/power demand and the mutual dependency of power/heat generation from the CHP unit are resulted in turn-on 5-$6^{th}$ thermal unit at $20^{th}$ sub-interval for extraction mode to satisfy the demand constraint. Due to the curtailment of power demand at $14^{th}$ sub-interval, $5^{th}$ thermal unit is shut-down and the lower power capability $9^{th}$ thermal unit is turned on in extraction mode, whereas in backpressure mode, $5^{th}$ thermal unit has remained in on state. For 15-$19^{th}$ sub-intervals, committed thermal and CHP units are sufficient to meet power demand constraints. The curtailment of power demand at $22^{th}$

sub-interval has resulted in the shut-down of the thermal unit for extraction mode while 4th thermal unit is shut-down for backpressure mode. The power and heat generation schedule obtained from the BSA-CSO technique in extraction and backpressure mode are given in Tables 4.3 and 4.4, respectively. It has been observed that the power and heat generation satisfy the spinning reserve and demand constraints.

**Table 4.2:** Hourly status of units in backpressure/extraction mode by BSA-CSO, CHPUC test system-I

| **Units** | | | **Thermal Units** | | | | | |
|---|---|---|---|---|---|---|---|---|
| **Sub-intervals (h)** | **PD (MW)** | **HD (MWth)** | **1** | **2** | **3** | **4** | **5** | **6** |
| **1** | 700 | 250 | 1/1 | 1/1 | 0/0 | 0/0 | 0/0 | 0/0 |
| **2** | 750 | 310 | 1/1 | 1/1 | 0/0 | 0/0 | 0/0 | 0/0 |
| **3** | 850 | 310 | 1/1 | 1/1 | 0/0 | 0/0 | 0/0 | 0/0 |
| **4** | 950 | 320 | 1/1 | 1/1 | 0/0 | 0/0 | 0/0 | 0/0 |
| **5** | 1000 | 350 | 1/1 | 1/1 | 0/0 | 0/0 | 0/0 | 0/0 |
| **6** | 1100 | 350 | 1/1 | 1/1 | 0/0 | 0/0 | 0/0 | 0/0 |
| **7** | 1150 | 330 | 1/1 | 1/1 | 1/0 | 0/0 | 0/0 | 0/0 |
| **8** | 1200 | 320 | 1/1 | 1/1 | 1/0 | 0/0 | 0/0 | 0/0 |
| **9** | 1300 | 330 | 1/1 | 1/1 | 1/0 | 1/0 | 0/1 | 0/0 |
| **10** | 1400 | 300 | 1/1 | 1/1 | 1/1 | 1/0 | 1/1 | 0/0 |
| **11** | 1450 | 310 | 1/1 | 1/1 | 1/1 | 1/0 | 1/1 | 0/0 |
| **12** | 1500 | 300 | 1/1 | 1/1 | 1/1 | 1/0 | 1/1 | 0/0 |
| **13** | 1400 | 300 | 1/1 | 1/1 | 1/1 | 1/0 | 1/1 | 0/0 |
| **14** | 1300 | 290 | 1/1 | 1/1 | 1/1 | 1/0 | 1/1 | 0/0 |
| **15** | 1200 | 340 | 1/1 | 1/1 | 1/0 | 1/0 | 1/1 | 0/0 |
| **16** | 1050 | 350 | 1/1 | 1/1 | 1/0 | 1/0 | 1/1 | 0/0 |
| **17** | 1000 | 340 | 1/1 | 1/1 | 1/0 | 1/0 | 1/1 | 0/0 |
| **18** | 1100 | 330 | 1/1 | 1/1 | 1/0 | 1/0 | 1/1 | 0/0 |
| **19** | 1200 | 340 | 1/1 | 1/1 | 1/0 | 1/0 | 1/1 | 0/0 |
| **20** | 1400 | 350 | 1/1 | 1/1 | 1/1 | 1/0 | 1/1 | 0/1 |
| **21** | 1300 | 320 | 1/1 | 1/1 | 1/1 | 1/0 | 1/1 | 0/1 |
| **22** | 1100 | 310 | 1/1 | 1/1 | 1/1 | 1/0 | 1/0 | 0/1 |
| **23** | 900 | 300 | 1/1 | 1/1 | 0/1 | 0/0 | 0/0 | 0/0 |
| **24** | 800 | 300 | 1/1 | 1/1 | 0/1 | 0/0 | 0/0 | 0/0 |

**Table 4.2:** Hourly status of units in backpressure/extraction mode by BSA-CSO, CHPUC test system-I

| **Units** | | | **Thermal Units** | | | | **CHP Unit** | **Heat Unit** |
|---|---|---|---|---|---|---|---|---|
| **Sub-intervals (h)** | **PD(MW)** | **HD(MWth)** | **7** | **8** | **9** | **10** | **11** | **12** |
| **1** | 700 | 250 | 0/0 | 0/0 | 0/0 | 0/0 | 1/1 | 0/0 |
| **2** | 750 | 310 | 0/0 | 0/0 | 0/0 | 0/0 | 1/1 | 0/1 |
| **3** | 850 | 310 | 0/0 | 0/0 | 0/0 | 0/0 | 1/1 | 0/1 |
| **4** | 950 | 320 | 0/0 | 0/0 | 0/0 | 0/0 | 1/1 | 0/1 |
| **5** | 1000 | 350 | 0/0 | 0/0 | 0/0 | 0/0 | 1/1 | 0/1 |
| **6** | 1100 | 350 | 0/0 | 0/0 | 0/0 | 0/0 | 1/1 | 0/1 |
| **7** | 1150 | 330 | 0/0 | 0/0 | 0/0 | 0/0 | 1/1 | 0/1 |
| **8** | 1200 | 320 | 0/0 | 0/0 | 0/1 | 0/0 | 1/1 | 0/1 |
| **9** | 1300 | 330 | 0/0 | 0/0 | 0/1 | 0/0 | 1/1 | 0/1 |
| **10** | 1400 | 300 | 0/0 | 0/0 | 0/1 | 0/0 | 1/1 | 0/0 |
| **11** | 1450 | 310 | 0/0 | 0/0 | 0/1 | 0/0 | 1/1 | 0/1 |
| **12** | 1500 | 300 | 0/0 | 0/0 | 0/1 | 0/0 | 1/1 | 0/0 |
| **13** | 1400 | 300 | 0/0 | 0/0 | 0/1 | 0/0 | 1/1 | 0/0 |
| **14** | 1300 | 290 | 0/0 | 0/0 | 0/1 | 0/0 | 1/1 | 0/0 |
| **15** | 1200 | 340 | 0/0 | 0/0 | 0/1 | 0/0 | 1/1 | 0/1 |
| **16** | 1050 | 350 | 0/0 | 0/0 | 0/1 | 0/0 | 1/1 | 0/1 |

**Table 4.2:** Hourly status of units in backpressure/extraction mode by BSA-CSO, CHPUC test system-I (Continued)

| Units | | | Thermal Units | | | | CHP Unit | Heat Unit |
|---|---|---|---|---|---|---|---|---|
| **Sub-intervals (h)** | **PD(MW)** | **HD(MWth)** | **7** | **8** | **9** | **10** | **11** | **12** |
| **17** | 1000 | 340 | 0/0 | 0/0 | 0/1 | 0/0 | 1/1 | 0/1 |
| **18** | 1100 | 330 | 0/0 | 0/0 | 0/1 | 0/0 | 1/1 | 0/1 |
| **19** | 1200 | 340 | 0/0 | 0/0 | 0/1 | 0/0 | 1/1 | 0/1 |
| **20** | 1400 | 350 | 0/0 | 0/0 | 0/1 | 0/0 | 1/1 | 0/1 |
| **21** | 1300 | 320 | 0/0 | 0/0 | 0/1 | 0/0 | 1/1 | 0/1 |
| **22** | 1100 | 310 | 0/0 | 0/0 | 0/1 | 0/0 | 1/1 | 0/1 |
| **23** | 900 | 300 | 0/0 | 0/0 | 0/0 | 0/0 | 1/1 | 0/0 |
| **24** | 800 | 300 | 0/0 | 0/0 | 0/0 | 0/0 | 1/1 | 0/0 |

**Table 4.3:** Power and heat generation schedule in backpressure mode in BSA-CSO, CHPUC test system-I

| | Thermal Units (MW) | | | | | | | | | | CHP Unit (MWth) | | Heat Unit |
|---|---|---|---|---|---|---|---|---|---|---|---|---|---|
| **h** | **P1** | **P2** | **P3** | **P4** | **P5** | **P6** | **P7** | **P8** | **P9** | **P10** | **P11** | **H11** | **H12** |
| **1** | 455 | 175 | 0 | 0 | 0 | 0 | 0 | 0 | 0 | 0 | 70 | 250 | 0 |
| **2** | 455 | 208.2 | 0 | 0 | 0 | 0 | 0 | 0 | 0 | 0 | 86.8 | 310 | 0 |
| **3** | 455 | 308.2 | 0 | 0 | 0 | 0 | 0 | 0 | 0 | 0 | 86.8 | 310 | 0 |
| **4** | 455 | 405.4 | 0 | 0 | 0 | 0 | 0 | 0 | 0 | 0 | 89.6 | 320 | 0 |
| **5** | 455 | 437 | 0 | 0 | 0 | 0 | 0 | 0 | 10 | 0 | 98 | 350 | 0 |
| **6** | 455 | 455 | 0 | 0 | 82 | 0 | 0 | 0 | 10 | 0 | 98 | 350 | 0 |
| **7** | 455 | 455 | 0 | 0 | 137.6 | 0 | 0 | 0 | 10 | 0 | 92.4 | 330 | 0 |
| **8** | 455 | 455 | 130 | 0 | 70.4 | 0 | 0 | 0 | 0 | 0 | 89.6 | 320 | 0 |
| **9** | 455 | 455 | 130 | 130 | 37.6 | 0 | 0 | 0 | 0 | 0 | 92.4 | 330 | 0 |
| **10** | 450 | 455 | 130 | 130 | 121 | 20 | 0 | 0 | 10 | 0 | 84 | 300 | 0 |
| **11** | 455 | 455 | 130 | 130 | 162 | 21.2 | 0 | 0 | 10 | 0 | 86.8 | 310 | 0 |
| **12** | 455 | 455 | 130 | 130 | 162 | 64 | 0 | 10 | 10 | 0 | 84 | 300 | 0 |
| **13** | 455 | 455 | 130 | 130 | 116 | 20 | 0 | 0 | 10 | 0 | 84 | 300 | 0 |
| **14** | 455 | 455 | 130 | 130 | 38.8 | 0 | 0 | 0 | 10 | 0 | 81.2 | 290 | 0 |
| **15** | 455 | 455 | 130 | 0 | 54.8 | 0 | 0 | 0 | 10 | 0 | 95.2 | 340 | 0 |
| **16** | 455 | 442 | 20 | 0 | 25 | 0 | 0 | 0 | 10 | 0 | 98 | 350 | 0 |
| **17** | 455 | 394.8 | 20 | 0 | 25 | 0 | 0 | 0 | 10 | 0 | 95.2 | 340 | 0 |
| **18** | 455 | 455 | 62.6 | 0 | 25 | 0 | 0 | 0 | 10 | 0 | 92.4 | 330 | 0 |
| **19** | 455 | 455 | 130 | 0 | 54.8 | 0 | 0 | 0 | 10 | 0 | 95.2 | 340 | 0 |
| **20** | 445 | 455 | 130 | 130 | 112 | 20 | 0 | 0 | 10 | 0 | 98 | 350 | 0 |
| **21** | 455 | 455 | 130 | 130 | 0 | 30.4 | 0 | 0 | 10 | 0 | 89.6 | 320 | 0 |
| **22** | 455 | 455 | 0 | 73.2 | 0 | 20 | 0 | 0 | 10 | 0 | 86.8 | 310 | 0 |
| **23** | 435 | 361 | 0 | 20 | 0 | 0 | 0 | 0 | 0 | 0 | 84 | 300 | 0 |
| **24** | 435 | 261 | 0 | 20 | 0 | 0 | 0 | 0 | 0 | 0 | 84 | 300 | 0 |

**Table 4.4:** Power and heat generation schedule in extraction mode in BSA-CSO, CHPUC test system-I

| | Thermal Units (MW) | | | | | | | | | | CHP Unit (MWth) | | Heat Unit |
|---|---|---|---|---|---|---|---|---|---|---|---|---|---|
| **h** | **P1** | **P2** | **P3** | **P4** | **P5** | **P6** | **P7** | **P8** | **P9** | **P10** | **P11** | **H11** | **H12** |
| **1** | 332.03 | 150 | 0 | 0 | 0 | 0 | 0 | 0 | 0 | 0 | 218.0 | 250 | 0 |
| **2** | 384.92 | 150 | 0 | 0 | 0 | 0 | 0 | 0 | 0 | 0 | 215.1 | 310 | 0 |
| **3** | 415.16 | 171.84 | 0 | 0 | 0 | 0 | 0 | 0 | 0 | 0 | 263 | 310 | 0 |
| **4** | 406.37 | 288.79 | 0 | 0 | 0 | 0 | 0 | 0 | 0 | 0 | 254.8 | 320 | 0 |
| **5** | 441.88 | 300.93 | 0 | 0 | 0 | 0 | 0 | 0 | 0 | 0 | 257.2 | 331 | 19 |
| **6** | 410.31 | 391.69 | 0 | 0 | 25 | 0 | 0 | 0 | 10 | 0 | 263 | 331 | 19 |
| **7** | 422.71 | 429.29 | 0 | 0 | 25 | 0 | 0 | 0 | 10 | 0 | 263 | 330 | 0 |
| **8** | 433.32 | 455 | 23.68 | 0 | 25 | 0 | 0 | 0 | 0 | 0 | 263 | 320 | 0 |
| **9** | 455 | 455 | 92 | 0 | 25 | 0 | 0 | 0 | 10 | 0 | 263 | 330 | 0 |

**Table 4.4:** Power and heat generation schedule in extraction mode in BSA-CSO, CHPUC test system-I

| | Thermal Units (MW) | | | | | | | | | | CHP Unit (MWth) | | Heat Unit |
|---|---|---|---|---|---|---|---|---|---|---|---|---|---|
| **h** | **P1** | **P2** | **P3** | **P4** | **P5** | **P6** | **P7** | **P8** | **P9** | **P10** | **P11** | **H11** | **H12** |
| **10** | 455 | 455 | 130 | 113.68 | 25 | 0 | 0 | 0 | 10 | 0 | 211.32 | 300 | 0 |
| **11** | 455 | 455 | 130 | 112 | 25 | 0 | 0 | 0 | 10 | 0 | 263 | 310 | 0 |
| **12** | 455 | 455 | 130 | 130 | 37 | 20 | 0 | 0 | 10 | 0 | 263 | 300 | 0 |
| **13** | 455 | 455 | 0 | 130 | 67 | 20 | 0 | 0 | 10 | 0 | 263 | 300 | 0 |
| **14** | 455 | 455 | 0 | 72 | 25 | 20 | 0 | 0 | 10 | 0 | 263 | 290 | 0 |
| **15** | 455 | 447 | 0 | 0 | 25 | 0 | 0 | 0 | 10 | 0 | 263 | 331 | 9 |
| **16** | 455 | 297 | 0 | 0 | 25 | 0 | 0 | 0 | 10 | 0 | 263 | 331 | 19 |
| **17** | 455 | 247 | 0 | 0 | 25 | 0 | 0 | 0 | 10 | 0 | 263 | 331 | 9 |
| **18** | 455 | 347 | 0 | 0 | 25 | 0 | 0 | 0 | 10 | 0 | 263 | 330 | 0 |
| **19** | 455 | 455 | 0 | 0 | 49.6 | 0 | 0 | 0 | 10 | 0 | 230.4 | 331 | 9 |
| **20** | 445 | 455 | 130 | 72 | 25 | 0 | 0 | 0 | 10 | 0 | 263 | 331 | 19 |
| **21** | 455 | 455 | 97 | 20 | 0 | 0 | 0 | 0 | 10 | 0 | 263 | 320 | 0 |
| **22** | 455 | 332 | 20 | 20 | 0 | 0 | 0 | 0 | 10 | 0 | 263 | 310 | 0 |
| **23** | 404.2 | 192.8 | 20 | 20 | 0 | 0 | 0 | 0 | 0 | 0 | 263 | 300 | 0 |
| **24** | 455 | 0 | 104.6 | 20 | 0 | 0 | 0 | 0 | 0 | 0 | 220.39 | 300 | 0 |

**Heat and power flexibility analysis of extraction and backpressure mode:** In order to encounter uncertainties associated with power demand and generation, it is desirable to evaluate the system generation flexibility. A system's generation flexibility is computed by considering the upper and lower generation limit, ramp up and down rate, and production levels of each generating unit **(Lannoye *et al.*, 2012)**. Due to the ramp rate, the operating range of upper and lower generation limits may further restrict. In CHP units, due to the interdependency of power and heat, FOR and power to heat ratio are also considered to compute the generation flexibility. The upward and downward generation flexibility is associated with the upper and lower generation limit, respectively. The upward generation flexibility is the difference between the restricted upper generation limit and actual generation, and similarly, downward generation flexibility is the difference between restricted lower generation limit and actual generation **(Lannoye *et al.*, 2012)**.

**System generation flexibility:** In order to investigate the impact of backpressure and extraction mode of the CHP unit on generation schedule, the system generation flexibility is computed **(Lannoye *et al.*, 2012; Espana and Arango, 2019)**. The system generation flexibility is the cumulative effect of individual generating unit generation flexibility in each sub-interval and is given as:

$$Flex_{t,system,+/-} = \sum_{i=1}^{N} Flex_{t,i+/-} \quad t \,\forall T \tag{4.56}$$

where $Flex_{t,system,+/-}$ is the upward and downward system generation flexibility at $t^{th}$ sub-interval, respectively; $Flex_{t,i,+/-}$ is the upward and downward flexibility of $i^{th}$ unit at $t^{th}$ sub-interval, respectively; and N is the total number of units. The upward and downward system power flexibility are shown in Figures 4.8 and 4.9, respectively. It is evident that during the backpressure mode of CHP units, the downward power flexibility of the system is more as compared to operation in extraction mode whereas in extraction mode, upward power flexibility is more. It is observed from Figures 4.10 and 4.11 that the upward and downward heat flexibility during the backpressure mode of CHP units is more as compared to extraction mode.

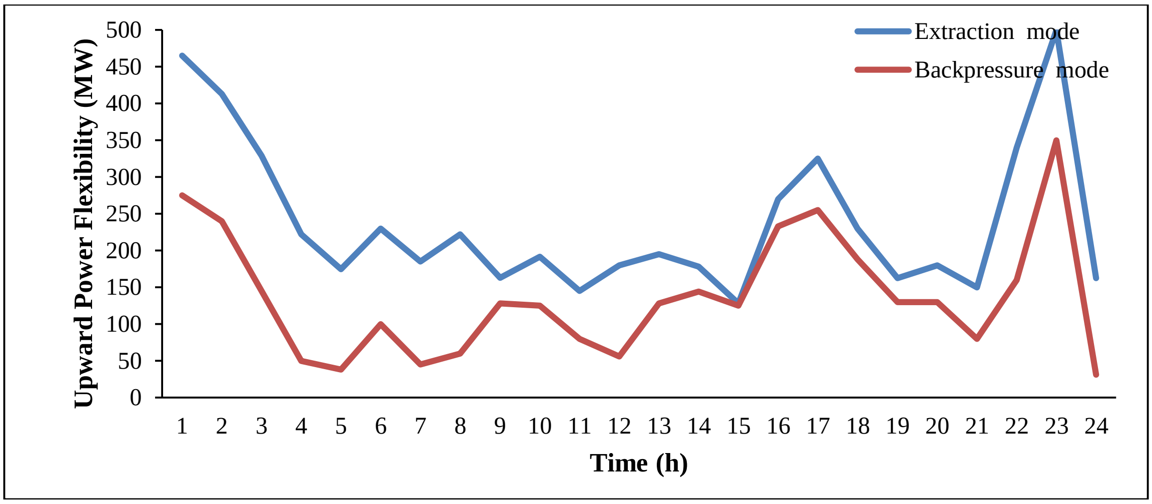


**Figure 4.8:** Upward system flexibility of power in extraction/backpressure mode by BSA-CSO, CHPUC test system-I

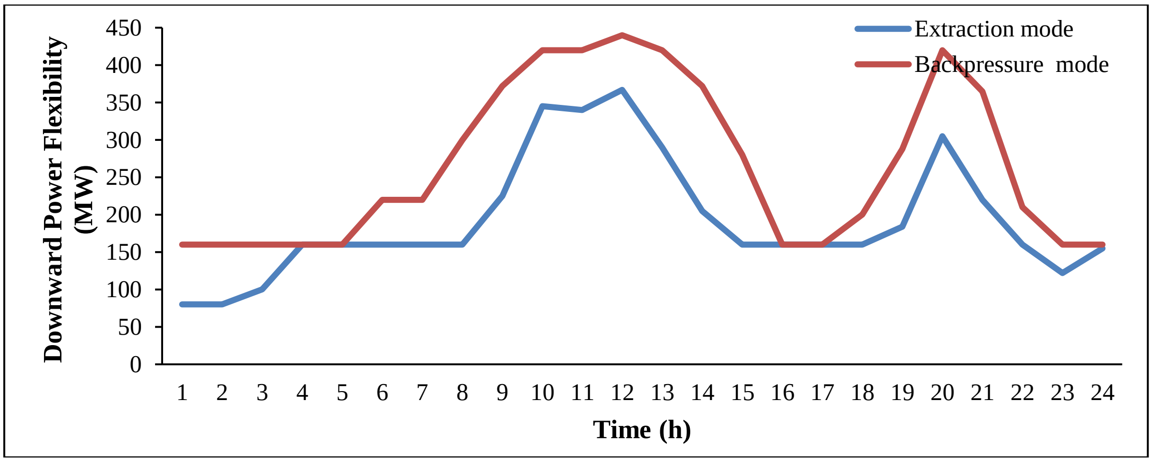


**Figure 4.9:** Downward system flexibility of power in extraction/backpressure mode by BSA-CSO, CHPUC test system-I

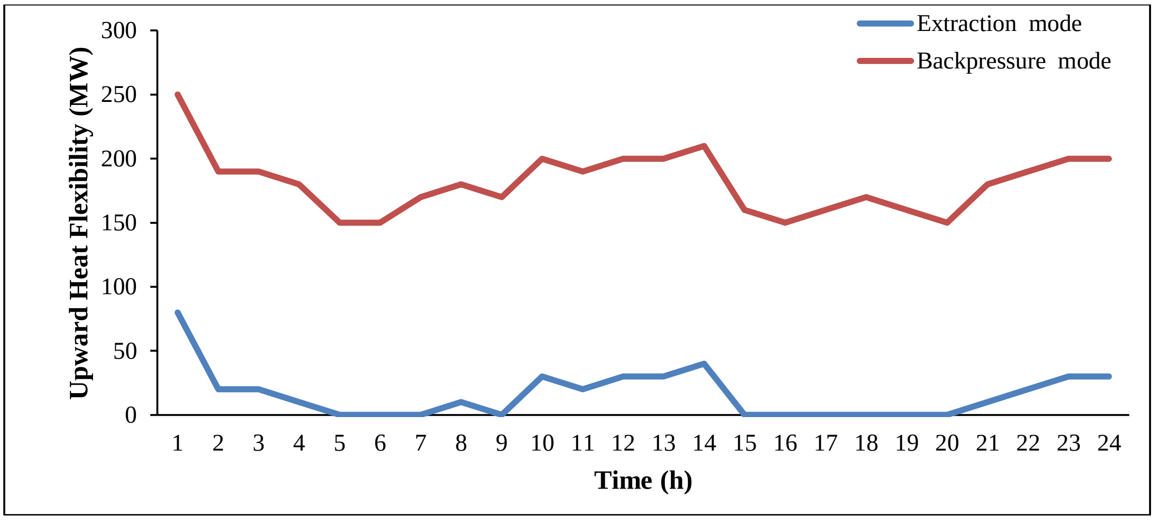


**Figure 4.10:** Upward system flexibility of heat in extraction/backpressure mode by BSA-CSO, CHPUC test system-I

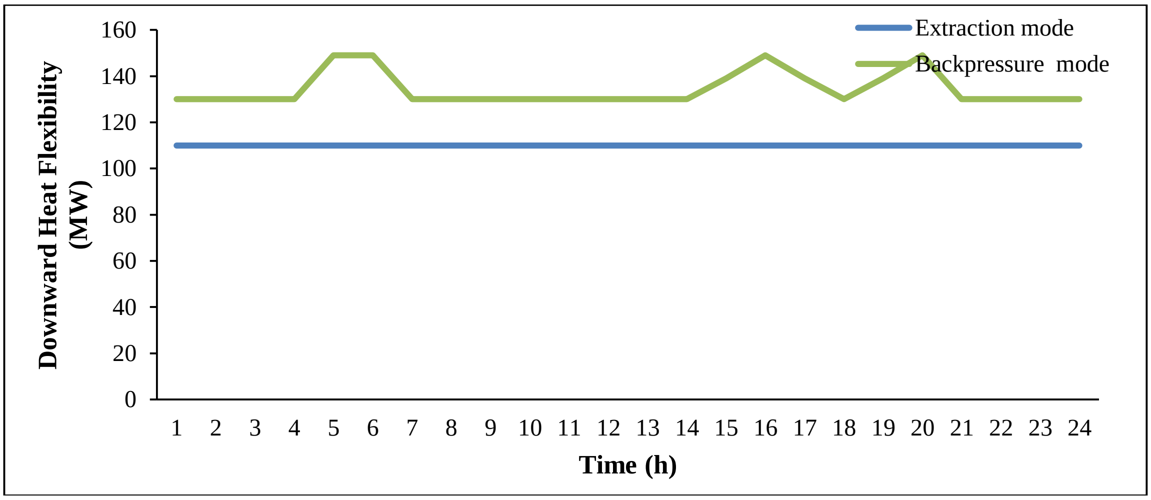


**Figure 4.11:** Downward system flexibility of heat in extraction/backpressure mode by BSA-CSO, CHPUC test system-I

### 4.7.1.2 Test system-II

The CHPUC test system-II consists of 16-units. The cost obtained from BPSO-PSO and BSA-CSO techniques for dual mode CHPUC problem have been given in Table 4.5. The cost obtained by BSA-CSO in the backpressure and extraction mode of the CHPUC problem is $448683.0 and $284267.5, respectively. It has been observed from Table 4.5 that the cost obtained by the BPSO-PSO technique in the backpressure and extraction mode of the CHPUC problem is more as compare to the BSA-CSO technique, respectively.

**Table 4.5:** Cost obtained for CHPUC problem; test system-II

| Technique | Backpressure mode cost ($) | Extraction mode cost ($) |
|---|---|---|
| **BPSO-PSO** | 540323.0 | 377921.7 |
| **BSA-CSO** | 448683.0 | 284267.5 |

The UC schedule of thermal, CHP and heat units are obtained by the BSA-CSO technique and it is shown in Table 4.6. It has been observed from Table 4.6, that during low power and heat demand sub-interval ($1^{st}$), the status of all units is the same in backpressure and extraction mode except for $2^{nd}$ thermal unit, $11$-$12^{th}$ CHP unit. The $11$-$12^{th}$ CHP unit is ON for extraction mode, while in backpressure mode, it remains in OFF position because of other CHP units are able to produce sufficient heat. The $2^{nd}$ thermal unit is ON to produce sufficient power in backpressure mode while in extraction mode, it remains in OFF position because of other thermal and CHP units able to produce sufficient power. During the rise of power and heat demand at $2^{nd}$ sub-interval, the additional $5^{th}$ thermal unit is turned on only for backpressure mode, because in extraction mode, the CHP unit is able to produce more power to fulfill the demand. In the $3^{rd}$ sub-interval, no additional units are required in extraction mode, while in backpressure mode, 2, 5 and 9 surplus thermal units are ON, respectively to satisfy the high power demand. The upsurge of power and heat demand at $4^{th}$ and $5^{th}$ sub-interval, requires $2$-$5^{th}$ surplus thermal units in backpressure mode, while available thermal and CHP units in extraction mode are sufficient to meet power demand. Similarly, the commitment of units has been observed at $6^{th}$, $7^{th}$ and $8^{rd}$ sub-intervals during the escalation of power demand.

**Table 4.6:** Hourly status of units in backpressure/extraction mode by BSA-CSO, CHPUC test system-II

| | | | **Thermal Units** | | | | | | | | | |
|---|---|---|---|---|---|---|---|---|---|---|---|---|
| **h** | **PD (MW)** | **HD (MWth)** | **1** | **2** | **3** | **4** | **5** | **6** | **7** | **8** | **9** | **10** |
| **1** | 882 | 625 | 1/1 | 1/0 | 0/0 | 0/0 | 0/0 | 0/0 | 0/0 | 0/0 | 0/0 | 0/0 |
| **2** | 945 | 775 | 1/1 | 1/0 | 0/0 | 0/0 | 1/0 | 0/0 | 0/0 | 0/0 | 0/0 | 0/0 |
| **3** | 1071 | 775 | 1/1 | 1/0 | 0/0 | 0/0 | 1/0 | 0/0 | 0/0 | 0/0 | 1/0 | 0/0 |
| **4** | 1197 | 800 | 1/1 | 1/0 | 1/0 | 1/0 | 1/0 | 0/0 | 0/0 | 0/0 | 0/0 | 0/0 |
| **5** | 1260 | 875 | 1/1 | 1/0 | 1/0 | 1/0 | 1/0 | 0/0 | 0/0 | 0/0 | 0/0 | 0/0 |
| **6** | 1386 | 875 | 1/1 | 1/0 | 1/0 | 1/0 | 1/1 | 1/0 | 0/0 | 0/0 | 1/0 | 0/0 |
| **7** | 1449 | 825 | 1/1 | 1/0 | 1/0 | 1/0 | 1/1 | 1/0 | 1/0 | 0/0 | 1/0 | 0/0 |
| **8** | 1512 | 800 | 1/1 | 1/0 | 1/0 | 1/0 | 1/1 | 1/0 | 1/0 | 1/0 | 1/0 | 0/0 |
| **9** | 1310 | 1237 | 1/1 | 1/0 | 1/0 | 1/0 | 1/1 | 1/0 | 1/0 | 0/0 | 1/0 | 0/0 |
| **10** | 1411 | 900 | 1/1 | 1/0 | 1/0 | 1/0 | 1/1 | 1/0 | 1/0 | 0/0 | 1/0 | 0/0 |
| **11** | 1461 | 1007 | 1/1 | 1/0 | 1/0 | 1/0 | 1/1 | 1/0 | 1/0 | 0/0 | 1/0 | 0/0 |
| **12** | 1512 | 900 | 1/1 | 1/0 | 1/0 | 1/0 | 1/1 | 1/0 | 1/0 | 1/0 | 1/0 | 0/0 |
| **13** | 1411 | 900 | 1/1 | 1/0 | 1/0 | 1/0 | 1/1 | 1/0 | 1/0 | 0/0 | 1/0 | 0/0 |
| **14** | 1638 | 725 | 1/1 | 1/1 | 1/0 | 1/0 | 1/1 | 1/0 | 1/0 | 1/0 | 1/0 | 1/0 |
| **15** | 1512 | 850 | 1/1 | 1/1 | 1/0 | 1/0 | 1/1 | 1/0 | 1/0 | 1/0 | 1/0 | 0/0 |
| **16** | 1323 | 875 | 1/1 | 1/1 | 1/0 | 1/0 | 1/1 | 1/0 | 0/0 | 0/0 | 1/0 | 0/0 |
| **17** | 1260 | 850 | 1/1 | 1/1 | 1/0 | 1/0 | 1/1 | 1/0 | 0/0 | 0/0 | 1/0 | 0/0 |
| **18** | 1386 | 825 | 1/1 | 1/1 | 1/0 | 1/0 | 1/0 | 1/1 | 0/0 | 0/0 | 1/0 | 0/0 |
| **19** | 1512 | 850 | 1/1 | 1/1 | 1/0 | 1/0 | 1/0 | 1/1 | 1/0 | 1/0 | 1/0 | 0/0 |
| **20** | 1411 | 1050 | 1/1 | 1/1 | 1/0 | 1/0 | 1/0 | 1/1 | 1/0 | 0/0 | 1/0 | 0/0 |
| **21** | 1638 | 800 | 1/1 | 1/1 | 1/0 | 1/0 | 1/0 | 1/0 | 1/0 | 1/0 | 1/0 | 1/0 |
| **22** | 1386 | 775 | 1/1 | 1/1 | 1/0 | 1/0 | 1/0 | 1/0 | 1/0 | 0/0 | 0/0 | 0/0 |
| **23** | 1134 | 750 | 1/1 | 1/0 | 1/0 | 0/0 | 1/0 | 0/0 | 0/0 | 0/0 | 1/0 | 0/0 |
| **24** | 1008 | 750 | 1/1 | 1/0 | 0/0 | 0/0 | 1/1 | 0/0 | 0/0 | 0/0 | 0/0 | 0/0 |

**Table 4.6:** Hourly status of units in backpressure/extraction mode by BSA-CSO, CHPUC test system-II (Continued)

| | | | CHP Units | | | | | Heat Units |
|---|---|---|---|---|---|---|---|---|
| **h** | **PD (MW)** | **HD (MWth)** | **11** | **12** | **13** | **14** | **15** | **16** |
| **1** | 882 | 625 | 0/1 | 0/1 | 1/1 | 1/1 | 1/1 | 0/0 |
| **2** | 945 | 775 | 0/1 | 0/1 | 1/1 | 1/1 | 1/1 | 0/0 |
| **3** | 1071 | 775 | 0/1 | 0/1 | 1/1 | 1/1 | 1/1 | 0/0 |
| **4** | 1197 | 800 | 0/1 | 0/1 | 1/1 | 1/1 | 1/1 | 0/0 |
| **5** | 1260 | 875 | 0/1 | 0/1 | 1/1 | 1/1 | 1/1 | 0/0 |
| **6** | 1386 | 875 | 0/1 | 0/1 | 1/1 | 1/1 | 1/1 | 0/0 |
| **7** | 1449 | 825 | 0/1 | 0/1 | 1/1 | 1/1 | 1/1 | 0/0 |
| **8** | 1512 | 800 | 0/1 | 0/1 | 1/1 | 1/1 | 1/1 | 0/0 |
| **9** | 1310 | 1237 | 0/1 | 0/1 | 1/1 | 1/1 | 1/1 | 0/0 |
| **10** | 1411 | 900 | 0/1 | 0/1 | 1/1 | 1/1 | 1/1 | 0/0 |
| **11** | 1461 | 1007 | 0/1 | 0/1 | 1/1 | 1/1 | 1/1 | 0/0 |
| **12** | 1512 | 900 | 0/1 | 0/1 | 1/1 | 1/1 | 1/1 | 0/0 |
| **13** | 1411 | 900 | 0/1 | 0/1 | 1/1 | 1/1 | 1/1 | 0/0 |
| **14** | 1638 | 725 | 0/1 | 0/1 | 1/1 | 1/1 | 1/1 | 0/0 |
| **15** | 1512 | 850 | 0/1 | 0/1 | 1/1 | 1/1 | 1/1 | 0/0 |
| **16** | 1323 | 875 | 0/1 | 0/1 | 1/1 | 1/1 | 1/1 | 0/0 |
| **17** | 1260 | 850 | 0/1 | 0/1 | 1/1 | 1/1 | 1/1 | 0/0 |
| **18** | 1386 | 825 | 0/1 | 0/1 | 1/1 | 1/1 | 1/1 | 0/0 |
| **19** | 1512 | 850 | 0/1 | 0/1 | 1/1 | 1/1 | 1/1 | 0/0 |
| **20** | 1411 | 1050 | 0/1 | 0/1 | 1/1 | 1/1 | 1/1 | 0/0 |
| **21** | 1638 | 800 | 0/1 | 0/1 | 0/1 | 1/1 | 1/1 | 0/0 |
| **22** | 1386 | 775 | 0/1 | 0/1 | 0/1 | 1/1 | 1/1 | 0/0 |
| **23** | 1134 | 750 | 0/1 | 0/1 | 0/1 | 1/1 | 1/1 | 0/0 |
| **24** | 1008 | 750 | 0/0 | 0/1 | 0/1 | 1/1 | 1/0 | 0/0 |

During the upsurge of heat demand at 9$^{th}$ sub-interval, 13-15$^{th}$ CHP units are sufficient to meet heat demand in backpressure mode and the 8$^{th}$ thermal unit is shut down due to a fixed ratio of heat/power while, 11-15$^{th}$ CHP units are required to satisfy the heat demand in extraction mode.

For the duration of peak power demand sub-intervals (10-13$^{th}$), additional thermal units have been required in backpressure mode to meet power demand, while available thermal and CHP units are sufficient in extraction mode. The curtailment of power demand at sub-intervals (15-17$^{th}$) resulted in turnoff some thermal units in backpressure mode. Moreover, heat demand is satisfied by available CHP units in both modes. The curtailment of power/heat demand at 22-24$^{th}$ sub-intervals has resulted in the turn-off of some CHP and thermal units for both modes.

The maximum heat available from committed heat units and heat available from committed CHP unit is used to evaluate heat spinning reserve. In order to compute the power spinning reserve, maximum power generation from thermal units and power generation from CHP units have been considered. The power generation from CHP units are restricted by their FOR constraint. The hourly power/heat demand, total power/heat generation and power/heat spinning reserve in each sub-interval and it is shown in Figures 4.12-4.15.

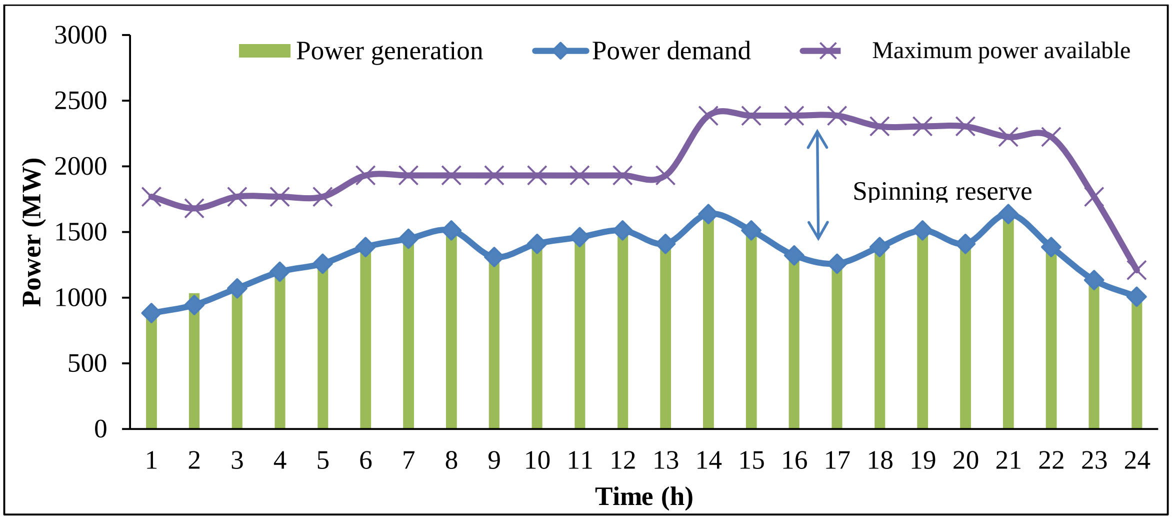


**Figure 4.12:** Power demand and reserve in extraction mode by BSA-CSO, CHPUC test system-II

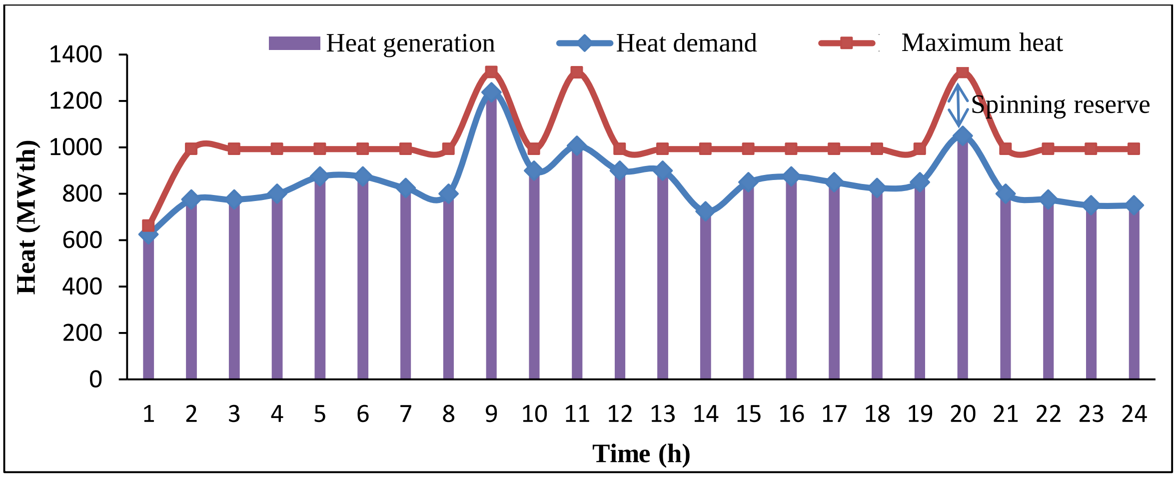


**Figure 4.13:** Heat demand and reserve in extraction mode by BSA-CSO, CHPUC test system-II

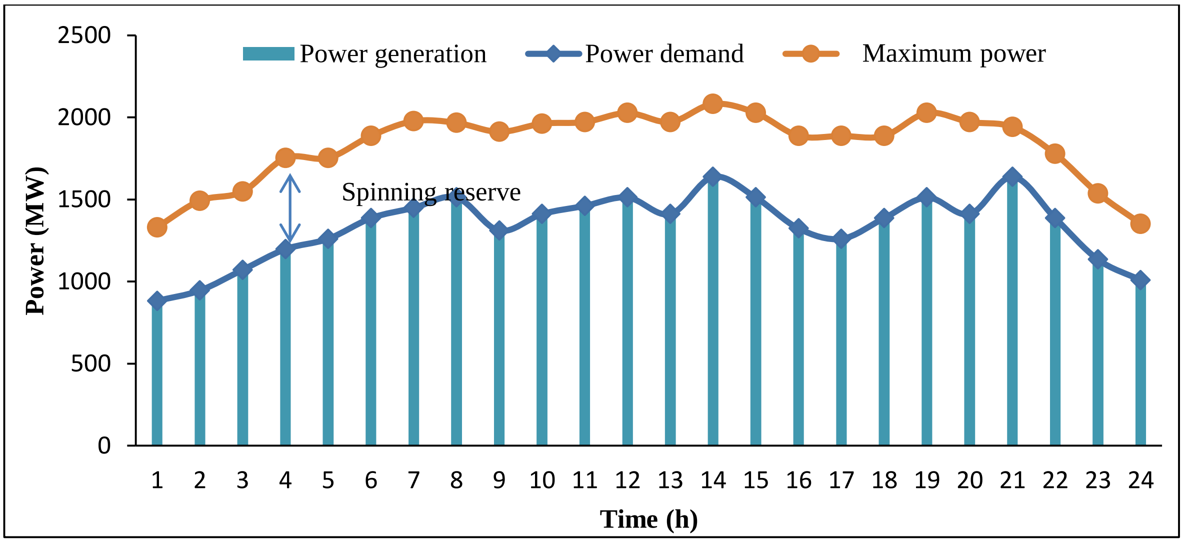


**Figure 4.14:** Power demand and reserve in backpressure mode by BSA-CSO, CHPUC test system-II

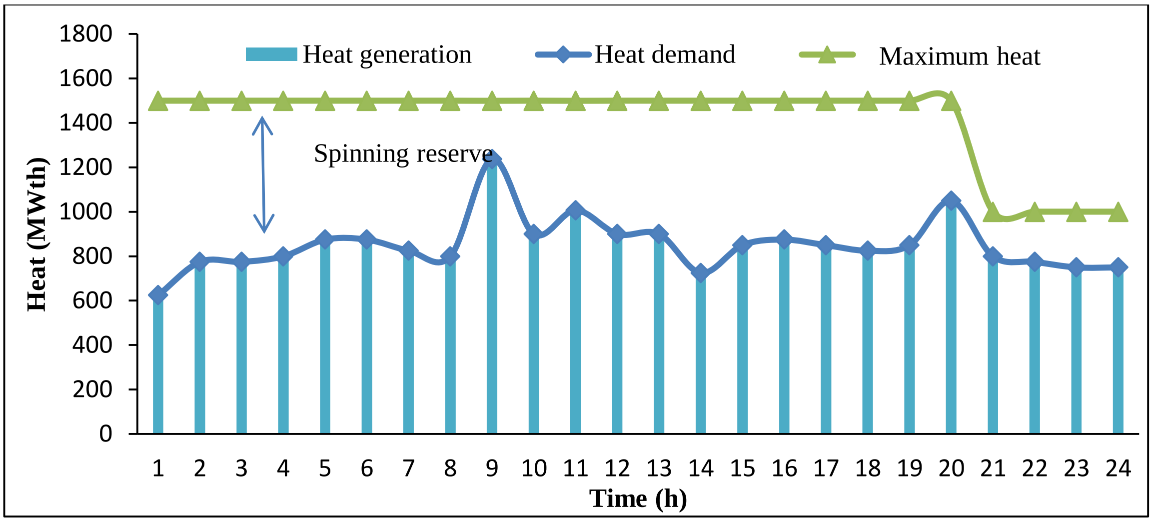


**Figure 4.15:** Heat demand and reserve in backpressure mode by BSA-CSO, CHPUC test system-II

In the BSA-CSO technique, the power generation schedule of committed units in the extraction and backpressure mode is given in Tables 4.7 and 4.8, respectively, and it is evident that power balance equality constraint is satisfied during each sub-interval.

**Table 4.7:** Power generation schedule in extraction mode by BSA-CSO, CHPUC test system-II

| h | Thermal units (MW) | | | | | | | | | | PD |
|---|---|---|---|---|---|---|---|---|---|---|---|
| | P1 | P2 | P3 | P4 | P5 | P6 | P7 | P8 | P9 | P10 | |
| 1 | 181.3 | 0 | 0 | 0 | 0 | 0 | 0 | 0 | 0 | 0 | 882 |
| 2 | 150 | 0 | 0 | 0 | 0 | 0 | 0 | 0 | 0 | 0 | 945 |
| 3 | 218.7 | 0 | 0 | 0 | 0 | 0 | 0 | 0 | 0 | 0 | 1071 |
| 4 | 285.2 | 0 | 0 | 0 | 0 | 0 | 0 | 0 | 0 | 0 | 1197 |
| 5 | 285 | 0 | 0 | 0 | 0 | 0 | 0 | 0 | 0 | 0 | 1260 |
| 6 | 455 | 0 | 0 | 0 | 34.9 | 0 | 0 | 0 | 0 | 0 | 1386 |
| 7 | 455 | 0 | 0 | 0 | 134.9 | 0 | 0 | 0 | 0 | 0 | 1449 |
| 8 | 455 | 0 | 0 | 0 | 101.6 | 0 | 0 | 0 | 0 | 0 | 1512 |
| 9 | 269.8 | 0 | 0 | 0 | 25 | 0 | 0 | 0 | 0 | 0 | 1310 |
| 10 | 455 | 0 | 0 | 0 | 73.5 | 0 | 0 | 0 | 0 | 0 | 1411 |
| 11 | 418.8 | 0 | 0 | 0 | 25 | 0 | 0 | 0 | 0 | 0 | 1461 |
| 12 | 455 | 0 | 0 | 0 | 106 | 0 | 0 | 0 | 0 | 0 | 1512 |
| 13 | 435.6 | 0 | 0 | 0 | 25 | 0 | 0 | 0 | 0 | 0 | 1411 |
| 14 | 232.7 | 418.4 | 0 | 0 | 25 | 0 | 0 | 0 | 0 | 0 | 1638 |
| 15 | 455 | 222.2 | 0 | 0 | 25 | 0 | 0 | 0 | 0 | 0 | 1512 |
| 16 | 271.6 | 150.2 | 0 | 0 | 25 | 0 | 0 | 0 | 0 | 0 | 1323 |
| 17 | 176.5 | 150.2 | 0 | 0 | 25 | 0 | 0 | 0 | 0 | 0 | 1260 |
| 18 | 455 | 213.6 | 0 | 0 | 0 | 20 | 0 | 0 | 0 | 0 | 1386 |
| 19 | 455 | 184.7 | 0 | 0 | 0 | 20 | 0 | 0 | 0 | 0 | 1512 |
| 20 | 384 | 150 | 0 | 0 | 0 | 20 | 0 | 0 | 0 | 0 | 1411 |
| 21 | 455 | 355.7 | 0 | 0 | 0 | 0 | 0 | 0 | 0 | 0 | 1638 |
| 22 | 333.7 | 150 | 0 | 0 | 0 | 0 | 0 | 0 | 0 | 0 | 1386 |
| 23 | 346.2 | 0 | 0 | 0 | 0 | 0 | 0 | 0 | 0 | 0 | 1134 |
| 24 | 390.1 | 0 | 0 | 0 | 25 | 0 | 0 | 0 | 0 | 0 | 1008 |

**Table 4.7:** Power generation schedule in extraction mode by BSA-CSO, CHPUC test system-II (Continued)

| h | CHP units (MW) | | | | | PD | $\sum_{i=1}^{N} P_{ti}$ |
|---|---|---|---|---|---|---|---|
| | P11 | P12 | P13 | P14 | P15 | | |
| 1 | 252.3 | 194.1 | 124.7 | 53.6 | 76 | 882 | 882 |

**Table 4.7:** Power generation schedule in extraction mode by BSA-CSO, CHPUC test system-II (Continued)

| h | CHP units (MW) | | | | | PD | $\sum_{i=1}^{N} P_{ti}$ |
|---|---|---|---|---|---|---|---|
| | P11 | P12 | P13 | P14 | P15 | | |
| 2 | 253 | 75.5 | 243 | 163.3 | 60.2 | 945 | 945 |
| 3 | 263 | 106.2 | 263 | 178.5 | 41.56 | 1071 | 1071 |
| 4 | 244 | 148.5 | 263 | 168.3 | 88 | 1197 | 1197 |
| 5 | 263 | 109.6 | 263 | 206.9 | 132.5 | 1260 | 1260 |
| 6 | 263 | 105.8 | 233.7 | 252 | 41.56 | 1386 | 1386 |
| 7 | 263 | 96.8 | 219.9 | 237.8 | 41.56 | 1449 | 1449 |
| 8 | 263 | 76.3 | 263 | 222.3 | 130.8 | 1512 | 1512 |
| 9 | 231 | 249.8 | 263 | 228.9 | 42.5 | 1310 | 1310 |
| 10 | 263 | 263 | 180.5 | 41.56 | 134.4 | 1411 | 1411 |
| 11 | 263 | 263 | 263 | 126.9 | 101.3 | 1461 | 1461 |
| 12 | 251.2 | 245.7 | 172.6 | 148.5 | 133 | 1512 | 1512 |
| 13 | 226.6 | 262.5 | 242.3 | 92.4 | 126.6 | 1411 | 1411 |
| 14 | 263 | 263 | 175.2 | 147.6 | 113.1 | 1638 | 1638 |
| 15 | 263 | 263 | 163.6 | 78.6 | 41.56 | 1512 | 1512 |
| 16 | 263 | 263 | 165.8 | 60.1 | 124.3 | 1323 | 1323 |
| 17 | 221.6 | 226.3 | 263 | 149.1 | 48.3 | 1260 | 1260 |
| 18 | 246 | 233.1 | 134.9 | 41.56 | 41.56 | 1386 | 1386 |
| 19 | 263 | 263 | 127.2 | 149.2 | 49.9 | 1512 | 1512 |
| 20 | 258.8 | 240.8 | 227.3 | 74.7 | 55.4 | 1411 | 1411 |
| 21 | 263 | 263 | 129.1 | 57.6 | 114.6 | 1638 | 1638 |
| 22 | 263 | 261.6 | 172.8 | 70.7 | 134.2 | 1386 | 1386 |
| 23 | 263 | 263 | 178.7 | 41.56 | 41.56 | 1134 | 1134 |
| 24 | 0 | 263 | 263 | 66.9 | 0 | 1008 | 1008 |

**Table 4.8:** Power generation schedule in backpressure mode by BSA-CSO, CHPUC test system-II

| h | Thermal units (MW) | | | | | | | | | |
|---|---|---|---|---|---|---|---|---|---|---|
| | P1 | P2 | P3 | P4 | P5 | P6 | P7 | P8 | P9 | P10 |
| 1 | 455 | 252 | 0 | 0 | 0 | 0 | 0 | 0 | 0 | 0 |
| 2 | 450 | 253 | 0 | 0 | 25 | 0 | 0 | 0 | 0 | 0 |
| 3 | 455 | 364 | 0 | 0 | 25 | 0 | 0 | 0 | 10 | 0 |
| 4 | 455 | 453 | 20 | 20 | 25 | 0 | 0 | 0 | 0 | 0 |
| 5 | 455 | 455 | 60 | 20 | 25 | 0 | 0 | 0 | 0 | 0 |
| 6 | 455 | 455 | 130 | 46 | 25 | 20 | 0 | 0 | 10 | 0 |
| 7 | 455 | 455 | 130 | 98 | 25 | 20 | 25 | 0 | 10 | 0 |
| 8 | 455 | 455 | 130 | 130 | 53 | 20 | 25 | 10 | 10 | 0 |
| 9 | 445 | 398.5 | 20 | 20 | 25 | 20 | 25 | 0 | 10 | 0 |
| 10 | 445 | 455 | 130 | 49 | 25 | 20 | 25 | 0 | 10 | 0 |
| 11 | 455 | 455 | 130 | 58.9 | 25 | 20 | 25 | 0 | 10 | 0 |
| 12 | 455 | 455 | 130 | 130 | 25 | 20 | 25 | 10 | 10 | 0 |
| 13 | 455 | 455 | 130 | 39 | 25 | 20 | 25 | 0 | 10 | 0 |
| 14 | 455 | 455 | 130 | 130 | 162 | 48 | 25 | 10 | 10 | 10 |
| 15 | 455 | 455 | 130 | 130 | 39 | 20 | 25 | 10 | 10 | 0 |
| 16 | 455 | 455 | 93 | 20 | 25 | 20 | 0 | 0 | 10 | 0 |
| 17 | 455 | 455 | 37 | 20 | 25 | 20 | 0 | 0 | 10 | 0 |
| 18 | 455 | 455 | 130 | 60 | 25 | 20 | 0 | 0 | 10 | 0 |
| 19 | 455 | 455 | 130 | 130 | 39 | 20 | 25 | 10 | 10 | 0 |
| 20 | 445 | 455 | 117 | 20 | 25 | 20 | 25 | 0 | 10 | 0 |
| 21 | 455 | 455 | 130 | 130 | 162 | 27 | 25 | 10 | 10 | 10 |
| 22 | 455 | 455 | 130 | 59 | 25 | 20 | 25 | 0 | 0 | 0 |
| 23 | 455 | 414 | 20 | 0 | 25 | 0 | 0 | 0 | 10 | 0 |
| 24 | 455 | 318 | 0 | 0 | 25 | 0 | 0 | 0 | 0 | 0 |

**Table 4.8:** Power generation schedule in backpressure mode by BSA-CSO, CHPUC test system-II (Continued)

| h | CHP units (MW) | | | | | PD | $\sum_{i=1}^{N} P_{ti}$ |
|---|---|---|---|---|---|---|---|
| | P11 | P12 | P13 | P14 | P15 | | |
| **1** | 0 | 0 | 120.4 | 19.6 | 35 | 882 | 882 |
| **2** | 0 | 0 | 120.4 | 19.6 | 77 | 945 | 945 |
| **3** | 0 | 0 | 120.4 | 19.6 | 77 | 1071 | 1071 |
| **4** | 0 | 0 | 120.4 | 19.6 | 84 | 1197 | 1197 |
| **5** | 0 | 0 | 120.4 | 19.6 | 105 | 1260 | 1260 |
| **6** | 0 | 0 | 120.4 | 19.6 | 105 | 1386 | 1386 |
| **7** | 0 | 0 | 120.4 | 19.6 | 91 | 1449 | 1449 |
| **8** | 0 | 0 | 120.4 | 19.6 | 84 | 1512 | 1512 |
| **9** | 0 | 0 | 140 | 140 | 66.5 | 1310 | 1310 |
| **10** | 0 | 0 | 140 | 92.4 | 19.6 | 1411 | 1411 |
| **11** | 0 | 0 | 140 | 122.5 | 19.6 | 1461 | 1461 |
| **12** | 0 | 0 | 140 | 92.4 | 19.6 | 1512 | 1512 |
| **13** | 0 | 0 | 140 | 92.40 | 19.6 | 1411 | 1411 |
| **14** | 0 | 0 | 140 | 43.4 | 19.6 | 1638 | 1638 |
| **15** | 0 | 0 | 140 | 78.4 | 19.6 | 1512 | 1512 |
| **16** | 0 | 0 | 140 | 85.4 | 19.6 | 1323 | 1323 |
| **17** | 0 | 0 | 140 | 78.4 | 19.6 | 1260 | 1260 |
| **18** | 0 | 0 | 140 | 71.4 | 19.6 | 1386 | 1386 |
| **19** | 0 | 0 | 140 | 78.4 | 19.6 | 1512 | 1512 |
| **20** | 0 | 0 | 140 | 134.4 | 19.6 | 1411 | 1411 |
| **21** | 0 | 0 | 0 | 140 | 84 | 1638 | 1638 |
| **22** | 0 | 0 | 0 | 140 | 77 | 1386 | 1386 |
| **23** | 0 | 0 | 0 | 140 | 70 | 1134 | 1134 |
| **24** | 0 | 0 | 0 | 140 | 70 | 1008 | 1008 |

The heat generation schedule of committed units in the extraction and backpressure mode is given in Tables 4.9 and 4.10, respectively, and it is evident that heat balance equality constraint is satisfied during each sub-interval.

**Table 4.9:** Heat generation schedule in extraction mode by BSA-CSO, CHPUC test system-II

| | CHP units (MWth) | | | | | Heat units (MWth) | | |
|---|---|---|---|---|---|---|---|---|
| h | H11 | H12 | H13 | H14 | H15 | H16 | HD | $\sum_{i=11}^{N} H_{ti}$ |
| **1** | 331 | 294 | 0 | 0 | 0 | 0 | 625 | 625 |
| **2** | 331 | 0 | 331 | 113 | 0 | 0 | 775 | 775 |
| **3** | 331 | 0 | 331 | 113 | 0 | 0 | 775 | 775 |
| **4** | 331 | 0 | 331 | 138 | 0 | 0 | 800 | 800 |
| **5** | 331 | 0 | 331 | 213 | 0 | 0 | 875 | 875 |
| **6** | 331 | 0 | 331 | 213 | 0 | 0 | 875 | 875 |
| **7** | 331 | 0 | 331 | 163 | 0 | 0 | 825 | 825 |
| **8** | 331 | 0 | 331 | 138 | 0 | 0 | 800 | 800 |
| **9** | 331 | 331 | 331 | 244 | 0 | 0 | 1237 | 1237 |
| **10** | 331 | 331 | 238.0 | 0 | 0 | 0 | 900 | 900 |
| **11** | 331 | 331 | 331 | 14 | 0 | 0 | 1007 | 1007 |
| **12** | 331 | 331 | 238.0 | 0 | 0 | 0 | 900 | 900 |
| **13** | 331 | 331 | 238.0 | 0 | 0 | 0 | 900 | 900 |
| **14** | 331 | 331 | 63 | 0 | 0 | 0 | 725 | 725 |
| **15** | 331 | 331 | 188 | 0 | 0 | 0 | 850 | 850 |
| **16** | 331 | 331 | 213 | 0 | 0 | 0 | 875 | 875 |
| **17** | 331 | 331 | 188 | 0 | 0 | 0 | 850 | 850 |

**Table 4.9:** Heat generation schedule in extraction mode by BSA-CSO, CHPUC test system-II (Continued)

| | CHP units (MWth) | | | | | Heat units (MWth) | | |
|---|---|---|---|---|---|---|---|---|
| **h** | **H11** | **H12** | **H13** | **H14** | **H15** | **H16** | **HD** | $\sum_{i=11}^{N} H_{ti}$ |
| **18** | 331 | 331 | 163 | 0 | 0 | 0 | 825 | 825 |
| **19** | 331 | 331 | 188 | 0 | 0 | 0 | 850 | 850 |
| **20** | 331 | 331 | 331 | 57 | 0 | 0 | 1050 | 1050 |
| **21** | 331 | 331 | 138 | 0 | 0 | 0 | 800 | 800 |
| **22** | 331 | 331 | 113 | 0 | 0 | 0 | 775 | 775 |
| **23** | 331 | 331 | 88 | 0 | 0 | 0 | 750 | 750 |
| **24** | 0 | 331 | 331 | 88 | 0 | 0 | 750 | 750 |

**Table 4.10:** Heat generation schedule in backpressure mode by BSA-CSO, CHPUC test system-II

| **h** | CHP units (MWth) | | | | | Heat units (MWth) | **HD** | $\sum_{i=11}^{N} H_{ti}$ |
|---|---|---|---|---|---|---|---|---|
| | **H11** | **H12** | **H13** | **H14** | **H15** | **H16** | | |
| **1** | 0 | 0 | 430 | 70 | 125 | 0 | 625 | 625 |
| **2** | 0 | 0 | 430 | 70 | 275 | 0 | 775 | 775 |
| **3** | 0 | 0 | 430 | 70 | 275 | 0 | 775 | 775 |
| **4** | 0 | 0 | 430 | 70 | 300 | 0 | 800 | 800 |
| **5** | 0 | 0 | 430 | 70 | 375 | 0 | 875 | 875 |
| **6** | 0 | 0 | 430 | 70 | 375 | 0 | 875 | 875 |
| **7** | 0 | 0 | 430 | 70 | 325 | 0 | 825 | 825 |
| **8** | 0 | 0 | 430 | 70 | 300 | 0 | 800 | 800 |
| **9** | 0 | 0 | 500 | 500 | 237 | 0 | 1237 | 1237 |
| **10** | 0 | 0 | 500 | 330 | 70 | 0 | 900 | 900 |
| **11** | 0 | 0 | 500 | 437 | 70 | 0 | 1007 | 1007 |
| **12** | 0 | 0 | 500 | 330 | 70 | 0 | 900 | 900 |
| **13** | 0 | 0 | 500 | 330 | 70 | 0 | 900 | 900 |
| **14** | 0 | 0 | 500 | 155 | 70 | 0 | 725 | 725 |
| **15** | 0 | 0 | 500 | 280 | 70 | 0 | 850 | 850 |
| **16** | 0 | 0 | 500 | 305 | 70 | 0 | 875 | 875 |
| **17** | 0 | 0 | 500 | 280 | 70 | 0 | 850 | 850 |
| **18** | 0 | 0 | 500 | 255 | 70 | 0 | 825 | 825 |
| **19** | 0 | 0 | 500 | 280 | 70 | 0 | 850 | 850 |
| **20** | 0 | 0 | 500 | 480 | 70 | 0 | 1050 | 1050 |
| **21** | 0 | 0 | 0 | 500 | 300 | 0 | 800 | 800 |
| **22** | 0 | 0 | 0 | 500 | 275 | 0 | 775 | 775 |
| **23** | 0 | 0 | 0 | 500 | 250 | 0 | 750 | 750 |
| **24** | 0 | 0 | 0 | 500 | 250 | 0 | 750 | 750 |

**Heat and power flexibility analysis of extraction and backpressure mode:** The flexibility of 4$^{th}$ CHP unit during extraction and backpressure mode are given in Figures 4.16 and 4.17, respectively. In backpressure mode, due to fixed heat and power ratio, power generation during each sub-interval depends on heat generation, while in extraction mode, such imposition does not apply. By considering power to heat fixed/variable ratio during different modes, the power flexibility of the 4$^{th}$ CHP unit during extraction and backpressure mode are given in Figures 4.18 and 4.19, respectively.

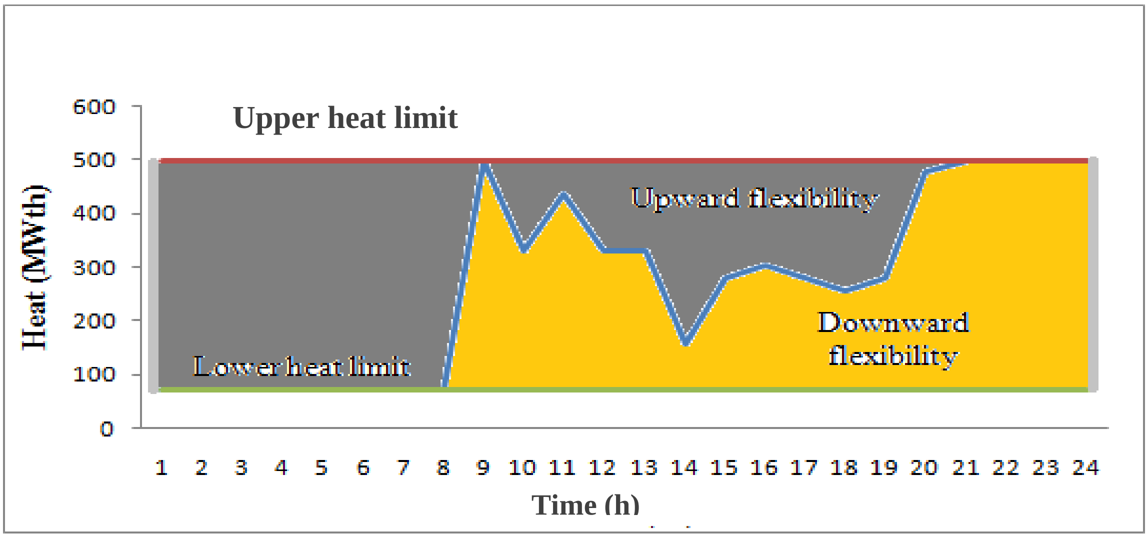


**Figure 4.16:** Heat flexibility of 4th CHP unit in backpressure mode by BSA-CSO, CHPUC test system-II

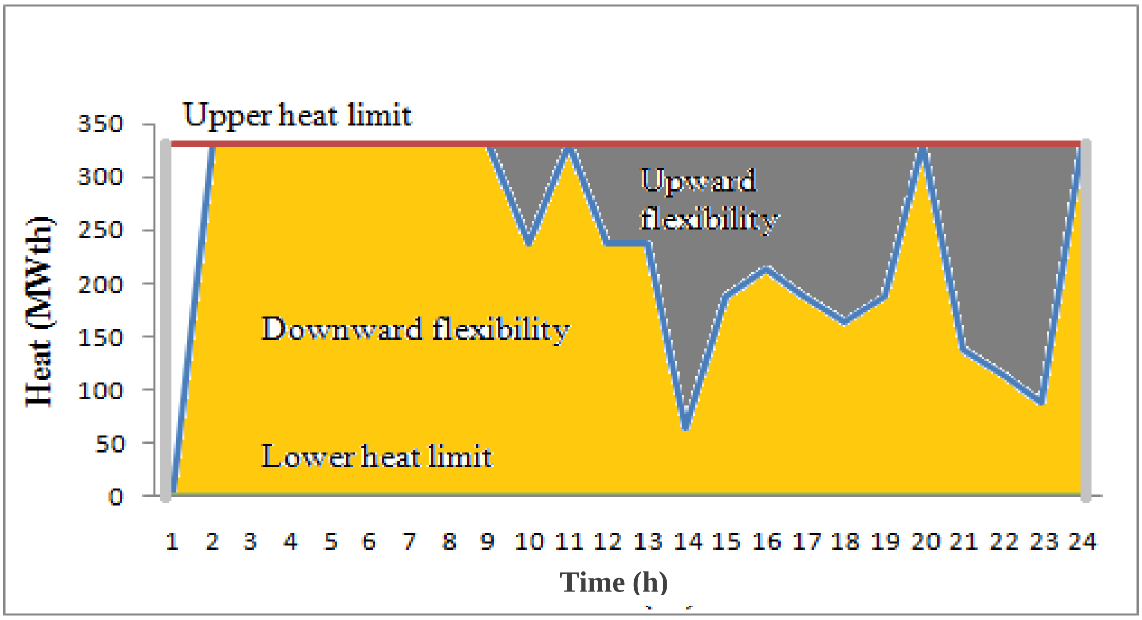


**Figure 4.17:** Heat flexibility of 4th CHP unit in extraction mode by BSA-CSO, CHPUC test system-II

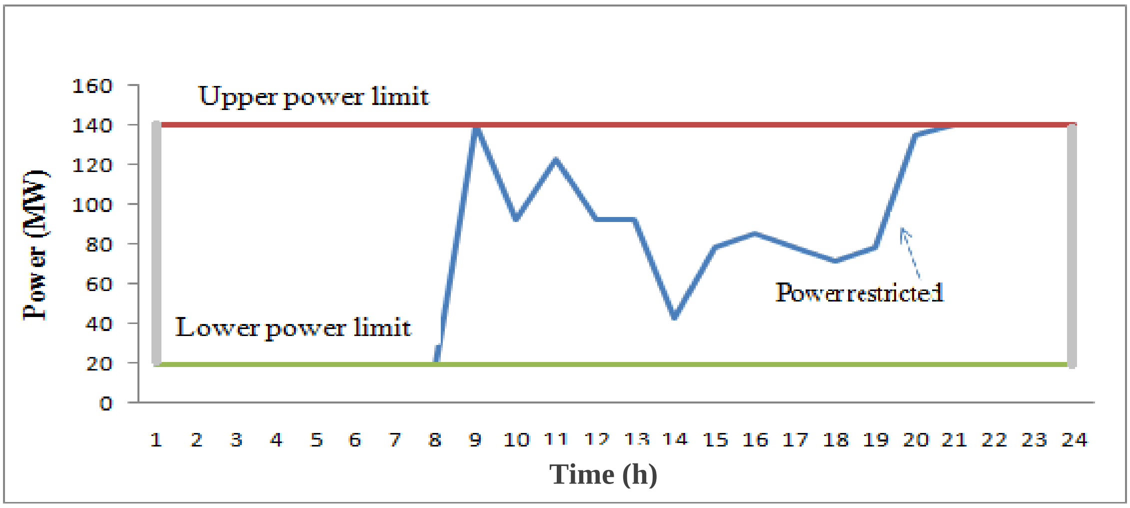


**Figure 4.18:** Power flexibility of 4th CHP unit in backpressure mode by BSA-CSO, CHPUC test system-II

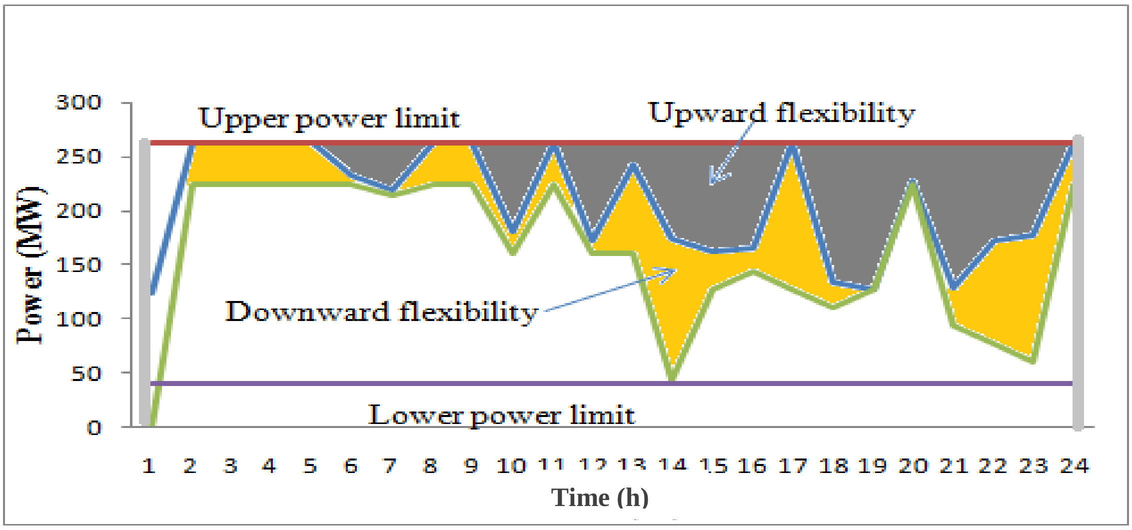


**Figure 4.19:** Power flexibility of 4th CHP unit in extraction mode by BSA-CSO, CHPUC test system-II

The system upward and downward flexibility of power is shown in Figures 4.20 and 4.21, respectively. It is evident from the figures that during the extraction mode of CHP units, the system is more flexible as compared to operation in a backpressure mode at most of the sub-intervals.

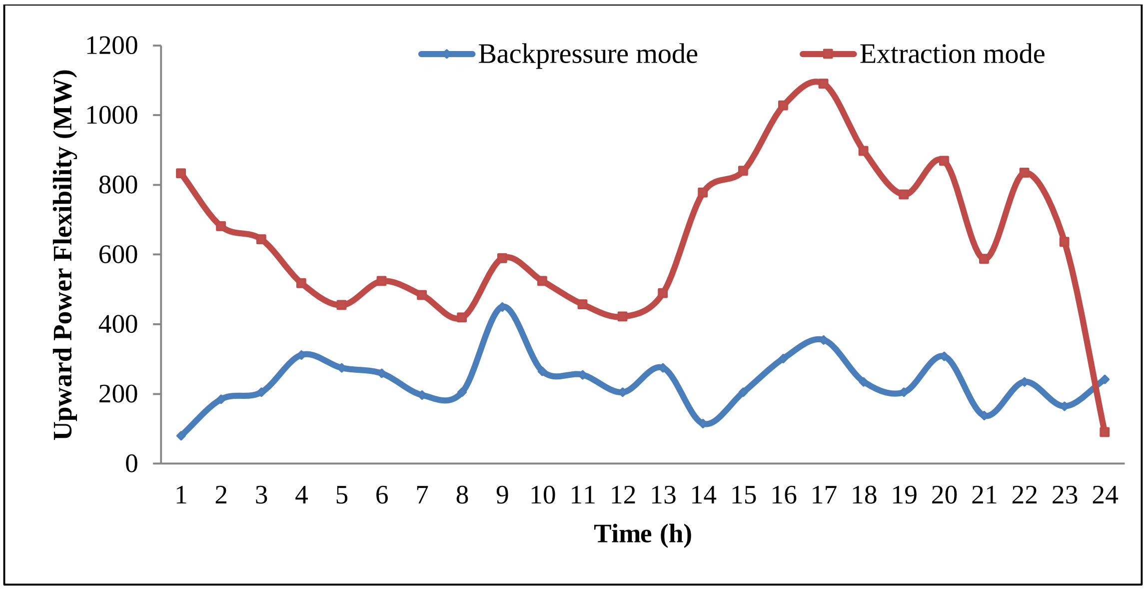


**Figure 4.20:** Upward system flexibility of power in extraction/backpressure mode by BSA-CSO, CHPUC test system-II

The system upward and downward generation flexibility of heat is shown in Figures 4.22 and 4.23, respectively. It is evident from Figure 4.22 that during the backpressure mode of CHP units, upward generation flexibility of the system is more as compared to operation in extraction mode at most of the sub-intervals. While, in backpressure mode, the downward generation flexibility during both the modes is approximately the same.

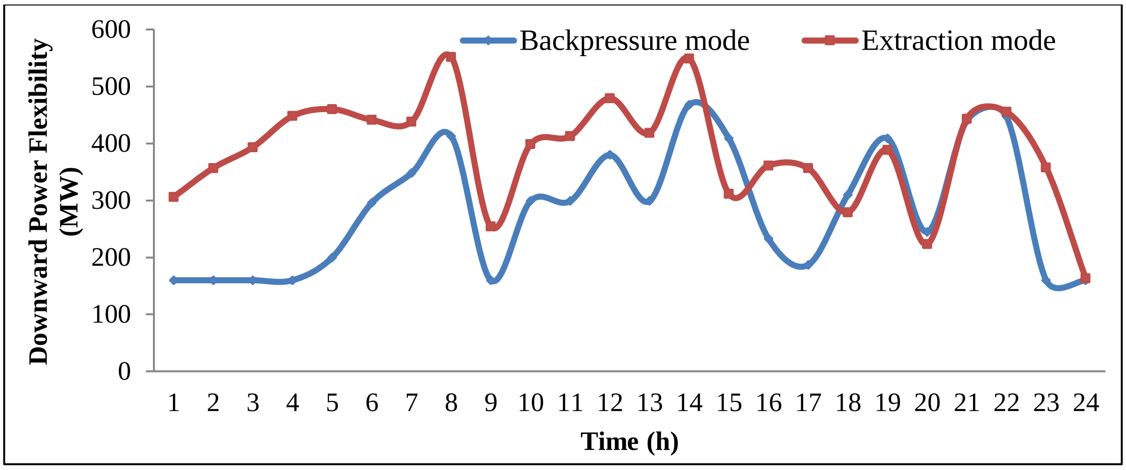


**Figure 4.21:** Downward system flexibility of power in extraction/backpressure mode by BSA-CSO, CHPUC test system-II

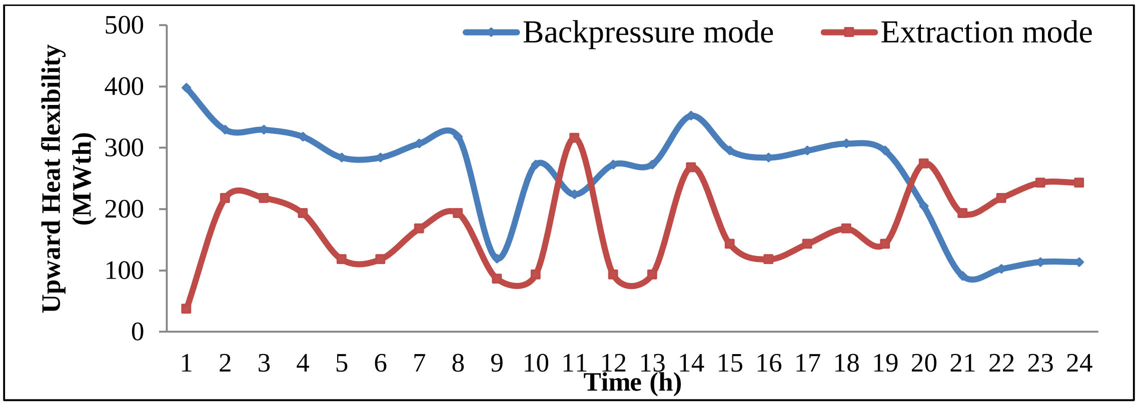


**Figure 4.22:** Upward system flexibility of heat in extraction/backpressure mode by BSA-CSO, CHPUC test system-II

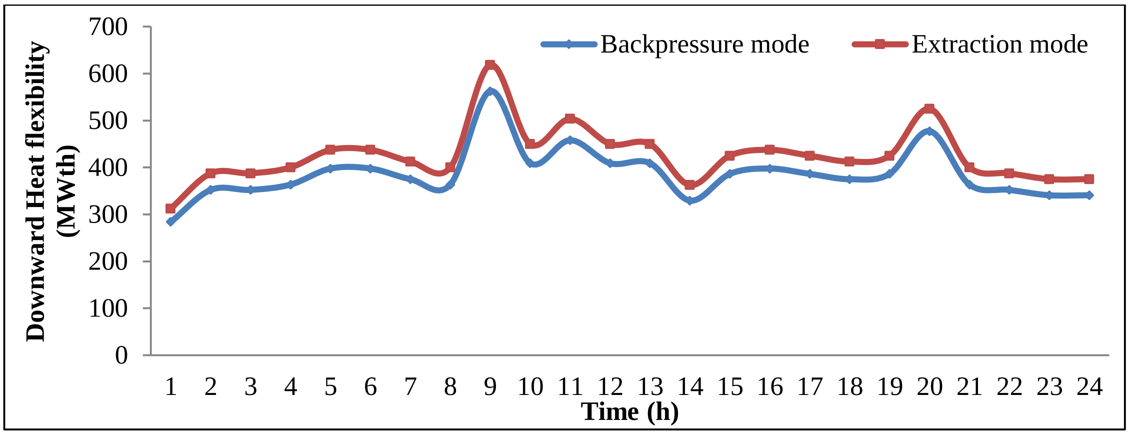


**Figure 4.23:** Downward system flexibility of heat in extraction/backpressure mode by BSA-CSO, CHPUC test system-II

### 4.7.1.3 Test system-III

The CHPUC test system-III consists of 20-units. The obtained operating cost of dual mode CHPUC problem from optimization techniques have been given in Table 4.11. In the BSA-CSO technique, the total operating cost during backpressure and extraction modes are $679416.1 and $560111.4, respectively. It has been observed that there is a huge saving of cost in the extraction mode operation of the CHP unit. It indicates that the operating mode of the CHP unit significantly affects the total operating cost. The obtained cost by the implementation of the BPSO-PSO technique in backpressure and extraction mode is $739894.3 and $667737.1, respectively which is more as compare to the BSA-CSO technique.

**Table 4.11:** Cost obtained for CHPUC problem, test system-III

| Technique | Backpressure mode cost ($) | Extraction mode cost ($) |
|---|---|---|
| **BPSO-PSO** | 739894.3 | 667737.1 |
| **BSA-CSO** | 679416.1 | 560111.4 |

The optimum commitment status of generating units for test system-III by the implementation of the BSA-CSO technique is given in Table 4.12. It is observed from committed status, that during backpressure mode of CHP unit, the commitment of heat units is required only for (4-9$^{th}$ and 15-21$^{th}$) sub-intervals to meet the heat demand, while in extraction mode, the heat units are committed for each sub-interval. In addition to that, few more thermal units are committed in each sub-interval during backpressure mode as compared to an extraction mode of the CHP unit to satisfy the power demand. Hence, it is concluded that the operating mode of the CHP unit has a significant impact on the commitment status of thermal and heat units.

**Table 4.12:** Hourly status of units in backpressure/extraction mode by BSA-CSO, CHPUC test system-III

| | | | **Thermal Units** | | | | | | | | | |
|---|---|---|---|---|---|---|---|---|---|---|---|---|
| **h** | **PD(MW)** | **HD(MWth)** | **1** | **2** | **3** | **4** | **5** | **6** | **7** | **8** | **9** | **10** |
| **1** | 1176 | 1687.5 | 1/1 | 1/1 | 0/0 | 0/0 | 0/0 | 0/0 | 0/0 | 0/0 | 1/1 | 0/0 |
| **2** | 1260 | 2092.5 | 1/1 | 1/1 | 0/0 | 0/0 | 0/0 | 0/0 | 0/0 | 0/0 | 1/1 | 0/0 |
| **3** | 1428 | 2092.5 | 1/1 | 1/1 | 1/0 | 0/0 | 0/0 | 0/0 | 0/0 | 0/0 | 1/0 | 0/0 |
| **4** | 1596 | 2160 | 1/1 | 1/1 | 1/0 | 1/0 | 0/0 | 0/0 | 0/0 | 0/0 | 1/1 | 0/0 |
| **5** | 1680 | 2362.5 | 1/1 | 1/1 | 1/0 | 1/0 | 1/0 | 0/0 | 0/0 | 0/0 | 1/1 | 0/0 |
| **6** | 1848 | 2362.5 | 1/1 | 1/1 | 1/1 | 1/0 | 1/0 | 1/0 | 0/0 | 1/0 | 1/1 | 0/0 |
| **7** | 1932 | 2227.5 | 1/1 | 1/1 | 1/1 | 1/0 | 1/0 | 1/0 | 0/0 | 1/0 | 0/1 | 0/0 |
| **8** | 2016 | 2160 | 1/1 | 1/1 | 1/1 | 1/0 | 1/1 | 1/0 | 0/0 | 1/0 | 1/1 | 1/0 |
| **9** | 1820 | 2227.5 | 1/1 | 1/1 | 1/1 | 1/0 | 1/1 | 1/0 | 0/0 | 0/0 | 1/1 | 0/0 |
| **10** | 1960 | 2025 | 1/1 | 1/1 | 1/1 | 1/1 | 1/1 | 1/0 | 0/0 | 1/0 | 0/1 | 0/0 |
| **11** | 2030 | 2092.5 | 1/1 | 1/1 | 1/1 | 1/1 | 1/1 | 1/0 | 0/0 | 1/0 | 1/1 | 1/0 |
| **12** | 2100 | 2025 | 1/1 | 1/1 | 1/1 | 1/1 | 1/1 | 1/1 | 1/0 | 1/0 | 1/1 | 1/0 |
| **13** | 1960 | 2025 | 1/1 | 1/1 | 1/1 | 1/1 | 1/1 | 1/1 | 1/0 | 1/0 | 0/1 | 0/0 |
| **14** | 1960 | 1957.5 | 1/1 | 1/1 | 1/1 | 1/1 | 1/1 | 1/1 | 1/0 | 1/0 | 0/1 | 0/0 |
| **15** | 2016 | 2295 | 1/1 | 1/1 | 1/1 | 1/1 | 1/0 | 1/0 | 1/0 | 1/0 | 1/1 | 1/0 |
| **16** | 1764 | 2362.5 | 1/1 | 1/1 | 1/1 | 1/1 | 1/0 | 1/0 | 0/0 | 0/0 | 1/1 | 0/0 |
| **17** | 1680 | 2295 | 1/1 | 1/1 | 1/1 | 1/1 | 1/0 | 1/0 | 0/0 | 0/0 | 1/1 | 0/0 |
| **18** | 1848 | 2227.5 | 1/1 | 1/1 | 1/1 | 1/1 | 1/0 | 1/0 | 0/0 | 0/0 | 0/1 | 0/0 |
| **19** | 2016 | 2295 | 1/1 | 1/1 | 1/1 | 1/1 | 1/0 | 1/0 | 1/0 | 1/0 | 1/1 | 1/0 |
| **20** | 1633 | 2362.5 | 1/1 | 1/1 | 1/1 | 1/0 | 0/0 | 0/0 | 1/0 | 0/0 | 1/1 | 0/0 |
| **21** | 1633 | 2160 | 1/1 | 1/1 | 1/1 | 1/0 | 0/1 | 0/0 | 1/0 | 0/0 | 1/1 | 0/0 |
| **22** | 1848 | 2092.5 | 1/1 | 1/1 | 1/1 | 1/0 | 0/1 | 0/0 | 1/0 | 1/0 | 1/1 | 1/0 |
| **23** | 1512 | 2025 | 1/1 | 1/1 | 1/0 | 0/0 | 0/1 | 0/0 | 0/0 | 0/0 | 1/1 | 0/0 |
| **24** | 1344 | 2025 | 1/1 | 1/0 | 0/0 | 0/0 | 0/1 | 0/0 | 0/0 | 0/0 | 1/1 | 0/0 |

**Table 4.12:** Hourly status of units in backpressure/extraction mode by BSA-CSO, CHPUC test system-III (Continued)

| | | | CHP Units | | | | | Heat Units | | | | |
|---|---|---|---|---|---|---|---|---|---|---|---|---|
| **h** | **PD(MW)** | **HD(MWth)** | **11** | **12** | **13** | **14** | **15** | **16** | **17** | **18** | **19** | **20** |
| **1** | 1176 | 1687.5 | 1/0 | 1/1 | 1/1 | 1/1 | 1/0 | 0/0 | 0/1 | 0/0 | 0/0 | 0/0 |
| **2** | 1260 | 2092.5 | 1/0 | 1/1 | 1/1 | 1/1 | 1/1 | 0/0 | 0/1 | 0/0 | 0/0 | 0/0 |
| **3** | 1428 | 2092.5 | 1/0 | 1/1 | 1/1 | 1/1 | 1/1 | 0/0 | 0/1 | 0/0 | 0/0 | 0/0 |
| **4** | 1596 | 2160 | 1/1 | 1/1 | 1/1 | 1/1 | 1/1 | 0/0 | 1/0 | 0/0 | 0/0 | 0/1 |
| **5** | 1680 | 2362.5 | 1/1 | 1/1 | 1/1 | 1/1 | 1/1 | 0/0 | 0/0 | 1/1 | 0/0 | 0/0 |
| **6** | 1848 | 2362.5 | 1/1 | 1/1 | 1/1 | 1/1 | 1/1 | 0/0 | 0/0 | 1/0 | 0/1 | 0/0 |
| **7** | 1932 | 2227.5 | 1/1 | 1/1 | 1/1 | 1/1 | 1/1 | 0/0 | 1/1 | 0/0 | 0/0 | 0/0 |
| **8** | 2016 | 2160 | 1/1 | 1/1 | 1/1 | 1/1 | 1/1 | 1/0 | 0/0 | 0/0 | 0/0 | 0/1 |
| **9** | 1820 | 2227.5 | 1/1 | 1/1 | 1/1 | 1/1 | 1/1 | 1/0 | 0/0 | 0/0 | 0/0 | 0/1 |
| **10** | 1960 | 2025 | 1/0 | 1/1 | 1/1 | 1/1 | 1/1 | 0/0 | 0/1 | 0/0 | 0/0 | 0/0 |
| **11** | 2030 | 2092.5 | 1/0 | 1/1 | 1/1 | 1/1 | 1/1 | 0/0 | 0/1 | 0/0 | 0/0 | 0/0 |
| **12** | 2100 | 2025 | 1/0 | 1/1 | 1/1 | 1/1 | 1/1 | 0/0 | 0/1 | 0/0 | 0/0 | 0/0 |
| **13** | 1960 | 2025 | 1/0 | 1/1 | 1/1 | 1/1 | 1/1 | 0/0 | 0/1 | 0/0 | 0/0 | 0/0 |
| **14** | 1960 | 1957.5 | 1/0 | 1/1 | 1/1 | 1/1 | 1/1 | 0/0 | 0/1 | 0/0 | 0/0 | 0/0 |
| **15** | 2016 | 2295 | 0/1 | 1/1 | 1/1 | 1/1 | 1/1 | 0/0 | 0/1 | 1/0 | 0/0 | 0/0 |
| **16** | 1764 | 2362.5 | 0/1 | 1/1 | 1/1 | 1/1 | 1/1 | 0/0 | 1/1 | 0/0 | 0/0 | 0/0 |
| **17** | 1680 | 2295 | 0/1 | 1/1 | 1/1 | 1/1 | 1/1 | 0/0 | 1/0 | 0/0 | 0/0 | 0/1 |
| **18** | 1848 | 2227.5 | 0/1 | 1/1 | 1/1 | 1/1 | 1/1 | 1/0 | 0/0 | 0/0 | 0/0 | 0/1 |
| **19** | 2016 | 2295 | 0/1 | 1/1 | 1/1 | 1/1 | 1/1 | 0/0 | 1/1 | 0/0 | 0/0 | 0/0 |
| **20** | 1633 | 2362.5 | 0/1 | 1/1 | 1/1 | 1/1 | 1/1 | 0/0 | 1/1 | 0/0 | 0/0 | 0/0 |
| **21** | 1633 | 2160 | 1/1 | 1/1 | 1/1 | 1/1 | 1/1 | 1/0 | 0/0 | 0/0 | 0/0 | 0/1 |
| **22** | 1848 | 2092.5 | 1/0 | 1/1 | 1/1 | 1/1 | 1/1 | 0/0 | 0/1 | 0/0 | 0/0 | 0/0 |
| **23** | 1512 | 2025 | 1/0 | 1/1 | 1/1 | 1/1 | 1/1 | 0/0 | 0/1 | 0/0 | 0/0 | 0/0 |
| **24** | 1344 | 2025 | 1/0 | 1/1 | 1/1 | 1/1 | 1/1 | 0/0 | 0/1 | 0/0 | 0/0 | 0/0 |

The power and heat generation schedule obtained from the BSA-CSO technique in the extraction mode of the CHPUC problem have been given in Tables 4.13 and 4.14, respectively. It has been observed from Tables 4.13 and 4.14 that power and heat generation satisfy the demand constraint in extraction mode. It has been observed from Figures 4.24 and 4.25 that the UC schedule meets the heat and power spinning reserve.

**Table 4.13:** Power generation (MW) schedule in extraction mode by BSA-CSO, CHPUC test system-III

| **h** | Thermal units (MW) | | | | | | | | | |
|---|---|---|---|---|---|---|---|---|---|---|
| | **P1** | **P2** | **P3** | **P4** | **P5** | **P6** | **P7** | **P8** | **P9** | **P10** |
| **1** | 380.48 | 150 | 0 | 0 | 0 | 0 | 0 | 0 | 10 | 0 |
| **2** | 252.64 | 150 | 0 | 0 | 0 | 0 | 0 | 0 | 10 | 0 |
| **3** | 430.64 | 150 | 0 | 0 | 0 | 0 | 0 | 0 | 0 | 0 |
| **4** | 376.80 | 150 | 0 | 0 | 0 | 0 | 0 | 0 | 10 | 0 |
| **5** | 455 | 155.80 | 0 | 0 | 0 | 0 | 0 | 0 | 10 | 0 |
| **6** | 455 | 303.80 | 20 | 0 | 0 | 0 | 0 | 0 | 10 | 0 |
| **7** | 455 | 387.80 | 20 | 0 | 0 | 0 | 0 | 0 | 10 | 0 |
| **8** | 455 | 446.80 | 20 | 0 | 25 | 0 | 0 | 0 | 10 | 0 |
| **9** | 455 | 250.80 | 20 | 0 | 25 | 0 | 0 | 0 | 10 | 0 |
| **10** | 455 | 455 | 130 | 37.64 | 25 | 0 | 0 | 0 | 10 | 0 |
| **11** | 455 | 455 | 130 | 107.64 | 25 | 0 | 0 | 0 | 10 | 0 |
| **12** | 455 | 455 | 130 | 130 | 52.64 | 20 | 0 | 0 | 10 | 0 |
| **13** | 455 | 455 | 127.64 | 20 | 25 | 20 | 0 | 0 | 10 | 0 |
| **14** | 455 | 455 | 127.64 | 20 | 25 | 20 | 0 | 0 | 10 | 0 |
| **15** | 455 | 451.80 | 20 | 20 | 0 | 0 | 0 | 0 | 10 | 0 |
| **16** | 455 | 199.80 | 20 | 20 | 0 | 0 | 0 | 0 | 10 | 0 |

**Table 4.13:** Power generation (MW) schedule in extraction mode by BSA-CSO, CHPUC test system-III (Continued)

| h | Thermal units (MW) | | | | | | | | | |
|---|---|---|---|---|---|---|---|---|---|---|
| | P1 | P2 | P3 | P4 | P5 | P6 | P7 | P8 | P9 | P10 |
| 17 | 420.80 | 150 | 20 | 20 | 0 | 0 | 0 | 0 | 10 | 0 |
| 18 | 455 | 283.80 | 20 | 20 | 0 | 0 | 0 | 0 | 10 | 0 |
| 19 | 455 | 451.80 | 20 | 20 | 0 | 0 | 0 | 0 | 10 | 0 |
| 20 | 394 | 150 | 20 | 0 | 0 | 0 | 0 | 0 | 10 | 0 |
| 21 | 369 | 150 | 20 | 0 | 25 | 0 | 0 | 0 | 10 | 0 |
| 22 | 455 | 455 | 55.64 | 0 | 25 | 0 | 0 | 0 | 10 | 0 |
| 23 | 455 | 174.64 | 0 | 0 | 25 | 0 | 0 | 0 | 10 | 0 |
| 24 | 455 | 0 | 0 | 0 | 31.64 | 0 | 0 | 0 | 10 | 0 |

**Table 4.13:** Power generation (MW) schedule in extraction mode by BSA-CSO, CHPUC test system-III (continued)

| h | CHP units (MW) | | | | | PD | $\sum_{i=1}^{N} P_{ti}$ |
|---|---|---|---|---|---|---|---|
| | P11 | P12 | P13 | P14 | P15 | | |
| 1 | 0 | 211.84 | 211.84 | 211.84 | 0 | 1176 | 1176 |
| 2 | 0 | 211.84 | 211.84 | 211.84 | 211.84 | 1260 | 1260 |
| 3 | 0 | 211.84 | 211.84 | 211.84 | 211.84 | 1428 | 1428 |
| 4 | 211.84 | 211.84 | 211.84 | 211.84 | 211.84 | 1596 | 1596 |
| 5 | 211.84 | 211.84 | 211.84 | 211.84 | 211.84 | 1680 | 1680 |
| 6 | 211.84 | 211.84 | 211.84 | 211.84 | 211.84 | 1848 | 1848 |
| 7 | 211.84 | 211.84 | 211.84 | 211.84 | 211.84 | 1932 | 1932 |
| 8 | 211.84 | 211.84 | 211.84 | 211.84 | 211.84 | 2016 | 2016 |
| 9 | 211.84 | 211.84 | 211.84 | 211.84 | 211.84 | 1820 | 1820 |
| 10 | 0 | 211.84 | 211.84 | 211.84 | 211.84 | 1960 | 1960 |
| 11 | 0 | 211.84 | 211.84 | 211.84 | 211.84 | 2030 | 2030 |
| 12 | 0 | 211.84 | 211.84 | 211.84 | 211.84 | 2100 | 2100 |
| 13 | 0 | 211.84 | 211.84 | 211.84 | 211.84 | 1960 | 1960 |
| 14 | 0 | 211.84 | 211.84 | 211.84 | 211.84 | 1960 | 1960 |
| 15 | 211.84 | 211.84 | 211.84 | 211.84 | 211.84 | 2016 | 2016 |
| 16 | 211.84 | 211.84 | 211.84 | 211.84 | 211.84 | 1764 | 1764 |
| 17 | 211.84 | 211.84 | 211.84 | 211.84 | 211.84 | 1680 | 1680 |
| 18 | 211.84 | 211.84 | 211.84 | 211.84 | 211.84 | 1848 | 1848 |
| 19 | 211.84 | 211.84 | 211.84 | 211.84 | 211.84 | 2016 | 2016 |
| 20 | 211.84 | 211.84 | 211.84 | 211.84 | 211.84 | 1633 | 1633 |
| 21 | 211.84 | 211.84 | 211.84 | 211.84 | 211.84 | 1633 | 1633 |
| 22 | 0 | 211.84 | 211.84 | 211.84 | 211.84 | 1848 | 1848 |
| 23 | 0 | 211.84 | 211.84 | 211.84 | 211.84 | 1512 | 1512 |
| 24 | 0 | 211.84 | 211.84 | 211.84 | 211.84 | 1344 | 1344 |

**Table 4.14:** Heat generation (MWth) schedule in extraction mode by BSA-CSO, CHPUC test system-III

| h | CHP units | | | | | Heat units | | | | | HD | $\sum_{i=11}^{N} H_{ti}$ |
|---|---|---|---|---|---|---|---|---|---|---|---|---|
| | H11 | H12 | H13 | H14 | H15 | H16 | H17 | H18 | H19 | H20 | | |
| 1 | 0 | 331 | 331 | 331 | 0 | 0 | 694.5 | 0 | 0 | 0 | 1687.5 | 1687.5 |
| 2 | 0 | 331 | 331 | 331 | 331 | 0 | 768.5 | 0 | 0 | 0 | 2092.5 | 2092.5 |
| 3 | 0 | 331 | 331 | 331 | 331 | 0 | 768.5 | 0 | 0 | 0 | 2092.5 | 2092.5 |
| 4 | 331 | 331 | 331 | 331 | 331 | 0 | 0 | 0 | 0 | 505 | 2160 | 2160 |
| 5 | 331 | 331 | 331 | 331 | 331 | 0 | 0 | 707.5 | 0 | 0 | 2362.5 | 2362.5 |
| 6 | 331 | 331 | 331 | 331 | 331 | 0 | 0 | 0 | 707.5 | 0 | 2362.5 | 2362.5 |
| 7 | 331 | 331 | 331 | 331 | 331 | 0 | 572.5 | 0 | 0 | 0 | 2227.5 | 2227.5 |
| 8 | 331 | 331 | 331 | 331 | 331 | 0 | 0 | 0 | 0 | 505 | 2160 | 2160 |
| 9 | 331 | 331 | 331 | 331 | 331 | 0 | 0 | 0 | 0 | 572.5 | 2227.5 | 2227.5 |
| 10 | 0 | 331 | 331 | 331 | 331 | 0 | 701 | 0 | 0 | 0 | 2025 | 2025 |

**Table 4.14:** Heat generation (MWth) schedule in extraction mode by BSA-CSO, CHPUC test system-III (Continued)

| h | CHP units | | | | | Heat units | | | | | HD | $\sum_{i=11}^{N} H_{ti}$ |
|---|---|---|---|---|---|---|---|---|---|---|---|---|
| | H11 | H12 | H13 | H14 | H15 | H16 | H17 | H18 | H19 | H20 | | |
| **11** | 0 | 331 | 331 | 331 | 331 | 0 | 768.5 | 0 | 0 | 0 | 2092.5 | 2092.5 |
| **12** | 0 | 331 | 331 | 331 | 331 | 0 | 701 | 0 | 0 | 0 | 2025 | 2025 |
| **13** | 0 | 331 | 331 | 331 | 331 | 0 | 701 | 0 | 0 | 0 | 2025 | 2025 |
| **14** | 0 | 331 | 331 | 331 | 331 | 0 | 633.5 | 0 | 0 | 0 | 1957.5 | 1957.5 |
| **15** | 331 | 331 | 331 | 331 | 331 | 0 | 640 | 0 | 0 | 0 | 2295 | 2295 |
| **16** | 331 | 331 | 331 | 331 | 331 | 0 | 707.5 | 0 | 0 | 0 | 2362.5 | 2362.5 |
| **17** | 331 | 331 | 331 | 331 | 331 | 0 | 0 | 0 | 0 | 640 | 2295 | 2295 |
| **18** | 331 | 331 | 331 | 331 | 331 | 0 | 0 | 0 | 0 | 572.5 | 2227.5 | 2227.5 |
| **19** | 331 | 331 | 331 | 331 | 331 | 0 | 640 | 0 | 0 | 0 | 2295 | 2295 |
| **20** | 331 | 331 | 331 | 331 | 331 | 0 | 707.5 | 0 | 0 | 0 | 2362.5 | 2362.5 |
| **21** | 331 | 331 | 331 | 331 | 331 | 0 | 0 | 0 | 0 | 505 | 2160 | 2160 |
| **22** | 0 | 331 | 331 | 331 | 331 | 0 | 768.5 | 0 | 0 | 0 | 2092.5 | 2092.5 |
| **23** | 0 | 331 | 331 | 331 | 331 | 0 | 701 | 0 | 0 | 0 | 2025 | 2025 |
| **24** | 0 | 331 | 331 | 331 | 331 | 0 | 701 | 0 | 0 | 0 | 2025 | 2025 |

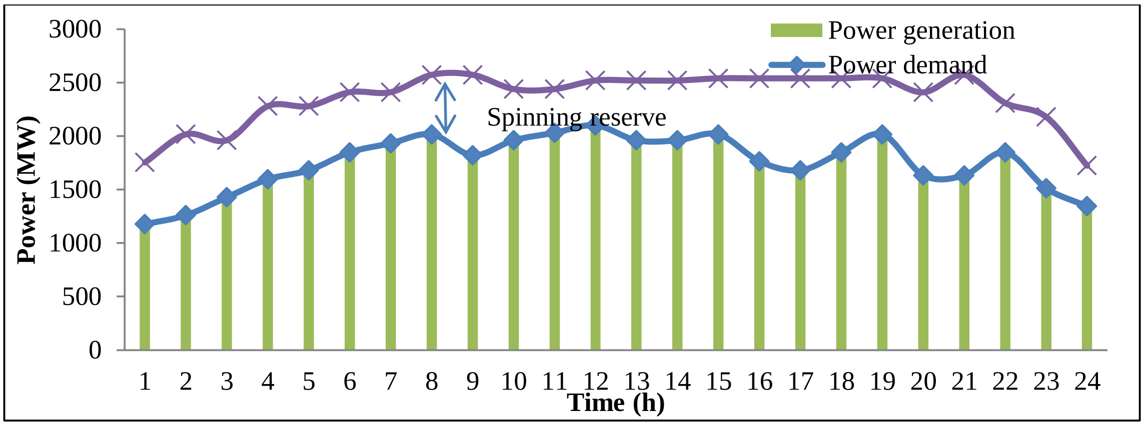


**Figure 4.24:** Power demand and spinning reserve in extraction mode, CHPUC test system-III

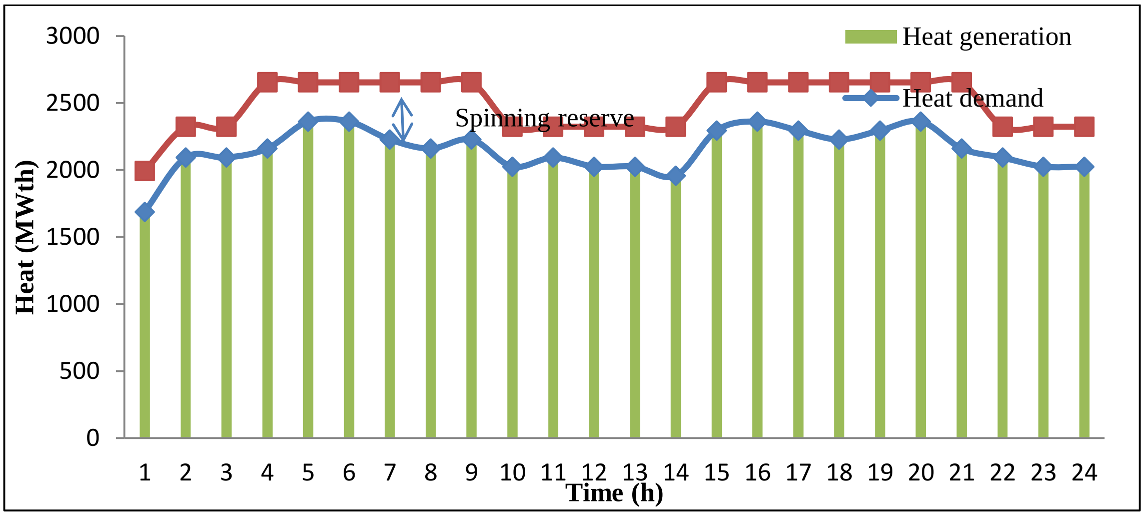


**Figure 4.25:** Heat demand and spinning reserve in extraction mode, CHPUC test system-III

In backpressure mode, the power and heat generation schedule obtained from BSA-CSO technique have been presented in Tables 4.15 and 4.16, respectively. It is evident from Tables 4.15 and 4.16 that power and heat generation satisfy the heat and power demand constraint. The UC schedule meets the heat and power spinning reserve requirement, which has been illustrated in Figures 4.26 and 4.27.

**Table 4.15:** Power generation (MW) schedule in backpressure mode by BSA-CSO, CHPUC test system-III

| h | Thermal units (MW) | | | | | | | | | |
|---|---|---|---|---|---|---|---|---|---|---|
| | P1 | P2 | P3 | P4 | P5 | P6 | P7 | P8 | P9 | P10 |
| 1 | 455 | 238.5 | 0 | 0 | 0 | 0 | 0 | 0 | 10 | 0 |
| 2 | 455 | 209.1 | 0 | 0 | 0 | 0 | 0 | 0 | 10 | 0 |
| 3 | 455 | 357.1 | 20 | 0 | 0 | 0 | 0 | 0 | 10 | 0 |
| 4 | 455 | 455 | 51.2 | 20 | 0 | 0 | 0 | 0 | 10 | 0 |
| 5 | 455 | 455 | 66 | 25 | 25 | 0 | 0 | 0 | 10 | 0 |
| 6 | 455 | 455 | 130 | 66 | 54 | 24 | 0 | 10 | 10 | 0 |
| 7 | 455 | 455 | 130 | 130 | 108.3 | 20 | 0 | 10 | 0 | 0 |
| 8 | 455 | 455 | 130 | 130 | 162 | 49.20 | 0 | 10 | 10 | 10 |
| 9 | 455 | 455 | 130 | 101.3 | 25 | 20 | 0 | 0 | 10 | 0 |
| 10 | 455 | 455 | 130 | 130 | 162 | 51 | 0 | 10 | 0 | 0 |
| 11 | 455 | 455 | 130 | 130 | 162 | 80 | 0 | 12.0 | 10 | 10 |
| 12 | 455 | 455 | 130 | 130 | 162 | 80 | 85 | 16 | 10 | 10 |
| 13 | 455 | 455 | 130 | 130 | 162 | 26 | 25 | 10 | 0 | 0 |
| 14 | 455 | 455 | 130 | 130 | 162 | 44.90 | 25 | 10 | 0 | 0 |
| 15 | 455 | 455 | 130 | 130 | 162 | 69.0 | 25 | 10 | 10 | 10 |
| 16 | 455 | 455 | 130 | 109 | 25 | 20 | 0 | 0 | 10 | 0 |
| 17 | 455 | 455 | 130 | 25 | 25 | 20 | 0 | 0 | 10 | 0 |
| 18 | 455 | 455 | 130 | 130 | 162 | 32 | 0 | 0 | 0 | 0 |
| 19 | 455 | 455 | 130 | 130 | 162 | 69 | 25 | 10 | 10 | 10 |
| 20 | 455 | 455 | 108.3 | 20 | 0 | 0 | 25 | 0 | 10 | 0 |
| 21 | 455 | 455 | 63.5 | 20 | 0 | 0 | 25 | 0 | 10 | 0 |
| 22 | 455 | 455 | 130 | 130 | 0 | 0 | 62.1 | 10 | 10 | 10 |
| 23 | 455 | 455 | 25 | 0 | 0 | 0 | 0 | 0 | 10 | 0 |
| 24 | 455 | 312 | 0 | 0 | 0 | 0 | 0 | 0 | 10 | 0 |

**Table 4.15:** Power generation (MW) schedule in backpressure mode by BSA-CSO, CHPUC test system-III (continued)

| h | CHP units (MW) | | | | | PD | $\sum_{i=1}^{N} P_{ti}$ |
|---|---|---|---|---|---|---|---|
| | P11 | P12 | P13 | P14 | P15 | | |
| 1 | 84 | 112 | 112 | 112 | 52.5 | 1176 | 1176 |
| 2 | 140 | 140 | 140 | 140 | 25.9 | 1260 | 1260 |
| 3 | 140 | 140 | 140 | 140 | 25.9 | 1428 | 1428 |
| 4 | 140 | 140 | 140 | 140 | 44.8 | 1596 | 1596 |
| 5 | 84 | 140 | 140 | 140 | 140 | 1680 | 1680 |
| 6 | 84 | 140 | 140 | 140 | 140 | 1848 | 1848 |
| 7 | 140 | 140 | 140 | 140 | 63.7 | 1932 | 1932 |
| 8 | 140 | 140 | 140 | 140 | 44.8 | 2016 | 2016 |
| 9 | 140 | 140 | 140 | 140 | 63.7 | 1820 | 1820 |
| 10 | 140 | 140 | 140 | 127.4 | 19.6 | 1960 | 1960 |
| 11 | 140 | 140 | 140 | 140 | 25.9 | 2030 | 2030 |
| 12 | 140 | 140 | 140 | 127.4 | 19.6 | 2100 | 2100 |
| 13 | 140 | 140 | 140 | 127.4 | 19.6 | 1960 | 1960 |
| 14 | 140 | 140 | 140 | 108.5 | 19.6 | 1960 | 1960 |
| 15 | 0 | 140 | 140 | 140 | 140 | 2016 | 2016 |
| 16 | 0 | 140 | 140 | 140 | 140 | 1764 | 1764 |
| 17 | 0 | 140 | 140 | 140 | 140 | 1680 | 1680 |
| 18 | 0 | 140 | 140 | 140 | 63.7 | 1847.7 | 1848 |
| 19 | 0 | 140 | 140 | 140 | 140 | 2016 | 2016 |
| 20 | 0 | 140 | 140 | 140 | 140 | 1633.3 | 1633.3 |

**Table 4.15:** Power generation (MW) schedule in backpressure mode by BSA-CSO, CHPUC test system-III (continued)

| h | CHP units (MW) | | | | | PD | $\sum_{i=1}^{N} P_{ti}$ |
|---|---|---|---|---|---|---|---|
| | P11 | P12 | P13 | P14 | P15 | | |
| **21** | 140 | 140 | 140 | 140 | 44.8 | 1633.3 | 1633.3 |
| **22** | 140 | 140 | 140 | 140 | 25.9 | 1848 | 1848 |
| **23** | 140 | 140 | 140 | 127.4 | 19.6 | 1512 | 1512 |
| **24** | 140 | 140 | 140 | 127.4 | 19.6 | 1344 | 1344 |

**Table 4.16:** Heat generation (MWth) schedule in backpressure mode by BSA-CSO, CHPUC test system-III

| h | CHP units (MWth) | | | | | Heat units (MWth) | | | | | HD | $\sum_{i=11}^{N} H_{ti}$ |
|---|---|---|---|---|---|---|---|---|---|---|---|---|
| | H11 | H12 | H13 | H14 | H15 | H16 | H17 | H18 | H19 | H20 | | |
| **1** | 300 | 400 | 400 | 400 | 187.5 | 0 | 0 | 0 | 0 | 0 | 1687.5 | 1687.5 |
| **2** | 500 | 500 | 500 | 500 | 92.5 | 0 | 0 | 0 | 0 | 0 | 2092.5 | 2092.5 |
| **3** | 500 | 500 | 500 | 500 | 92.5 | 0 | 0 | 0 | 0 | 0 | 2092.5 | 2092.5 |
| **4** | 500 | 500 | 500 | 500 | 160 | 0 | 0 | 0 | 0 | 0 | 2160 | 2160 |
| **5** | 300 | 500 | 500 | 500 | 500 | 0 | 0 | 62.5 | 0 | 0 | 2362.5 | 2362.5 |
| **6** | 300 | 500 | 500 | 500 | 500 | 0 | 0 | 62.5 | 0 | 0 | 2362.5 | 2362.5 |
| **7** | 500 | 500 | 500 | 500 | 227.5 | 0 | 0 | 0 | 0 | 0 | 2227.5 | 2227.5 |
| **8** | 500 | 500 | 500 | 500 | 160 | 0 | 0 | 0 | 0 | 0 | 2160 | 2160 |
| **9** | 500 | 500 | 500 | 500 | 227.5 | 0 | 0 | 0 | 0 | 0 | 2227.5 | 2227.5 |
| **10** | 500 | 500 | 500 | 455 | 70 | 0 | 0 | 0 | 0 | 0 | 2025 | 2025 |
| **11** | 500 | 500 | 500 | 500 | 92.5 | 0 | 0 | 0 | 0 | 0 | 2092.5 | 2092.5 |
| **12** | 500 | 500 | 500 | 455 | 70 | 0 | 0 | 0 | 0 | 0 | 2025 | 2025 |
| **13** | 500 | 500 | 500 | 455 | 70 | 0 | 0 | 0 | 0 | 0 | 2025 | 2025 |
| **14** | 500 | 500 | 500 | 387 | 70 | 0 | 0 | 0 | 0 | 0 | 1957.5 | 1957.5 |
| **15** | 0 | 500 | 500 | 500 | 500 | 0 | 0 | 295 | 0 | 0 | 2295 | 2295 |
| **16** | 0 | 500 | 500 | 500 | 500 | 0 | 362 | 0 | 0 | 0 | 2362.5 | 2362.5 |
| **17** | 0 | 500 | 500 | 500 | 500 | 0 | 295 | 0 | 0 | 0 | 2295 | 2295 |
| **18** | 0 | 500 | 500 | 500 | 227.5 | 500 | 0 | 0 | 0 | 0 | 2227.5 | 2227.5 |
| **19** | 0 | 500 | 500 | 500 | 500 | 0 | 295 | 0 | 0 | 0 | 2295 | 2295 |
| **29** | 0 | 500 | 500 | 500 | 500 | 0 | 362 | 0 | 0 | 0 | 2362.5 | 2362.5 |
| **21** | 500 | 500 | 500 | 500 | 160 | 0 | 0 | 0 | 0 | 0 | 2160 | 2160 |
| **22** | 500 | 500 | 500 | 500 | 92.5 | 0 | 0 | 0 | 0 | 0 | 2092.5 | 2092.5 |
| **23** | 500 | 500 | 500 | 455 | 70 | 0 | 0 | 0 | 0 | 0 | 2025 | 2025 |
| **24** | 500 | 500 | 500 | 455 | 70 | 0 | 0 | 0 | 0 | 0 | 2025 | 2025 |

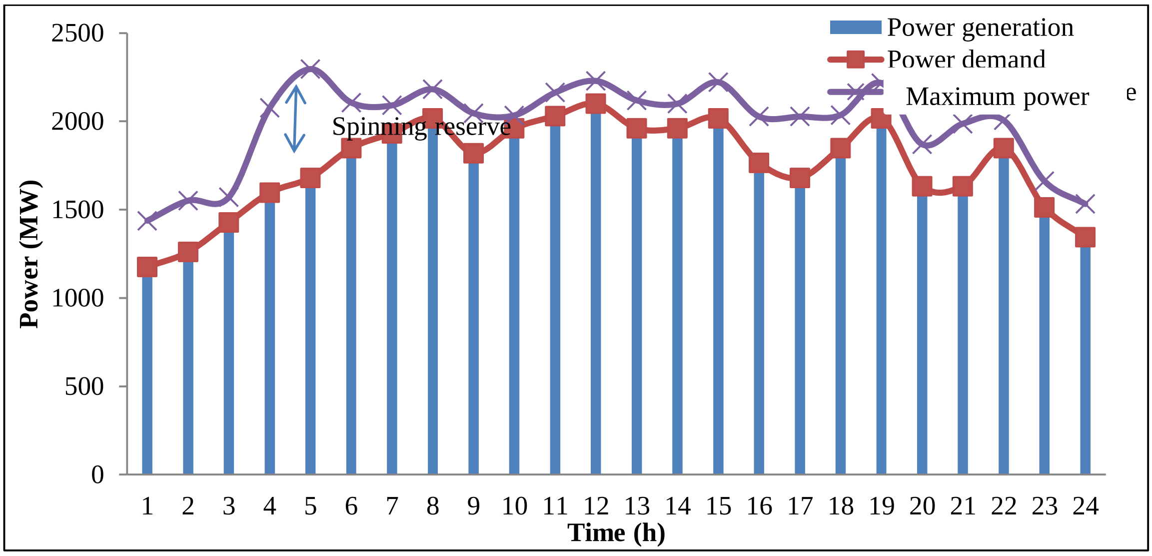


**Figure 4.26:** Power demand and spinning reserve in backpressure mode, CHPUC test system-III

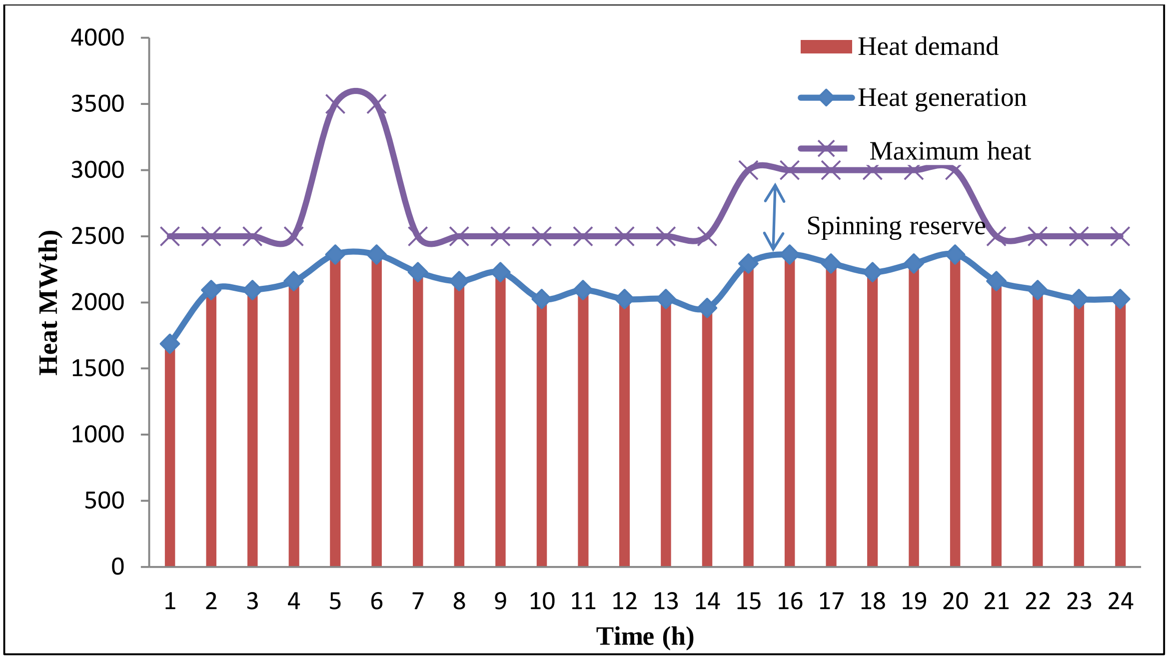


**Figure 4.27:** Heat demand and spinning reserve in backpressure mode, CHPUC test system-III

The system upward and downward flexibility of power is illustrated in Figure 4.28 and 4.29, respectively. It has been observed from the figures that during the extraction mode of CHP units, the upward power generation is more flexible as compared to operation in a backpressure mode at most of the sub-intervals, while downward power generation is more flexible in backpressure mode.

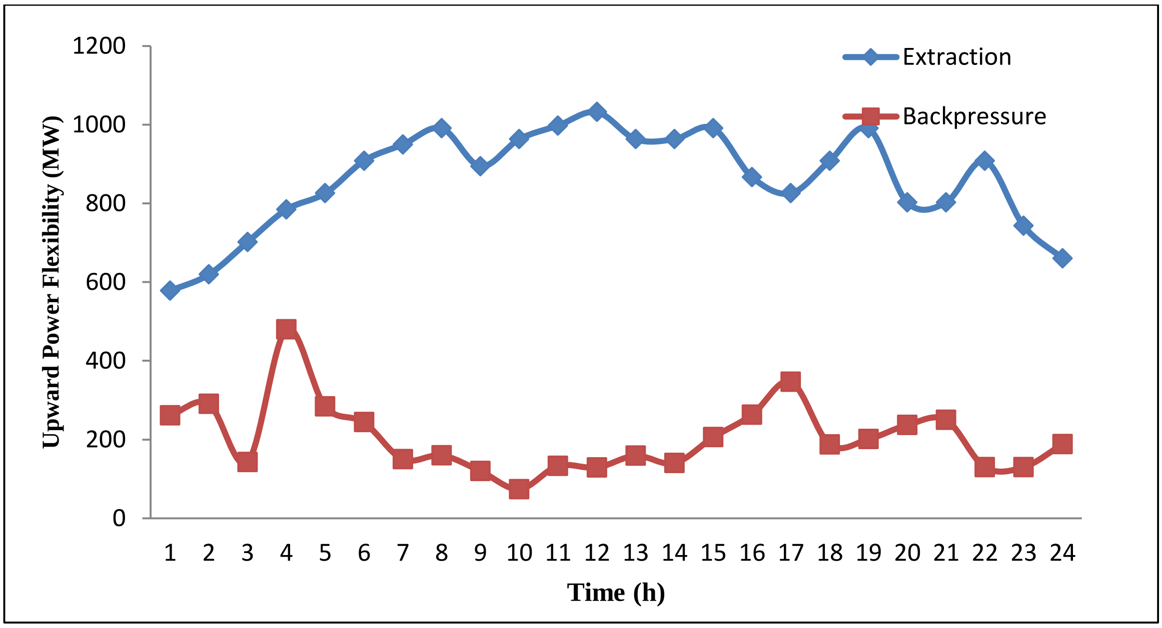


**Figure 4.28:** Upward flexibility of power for extraction/backpressure mode, CHPUC test system III

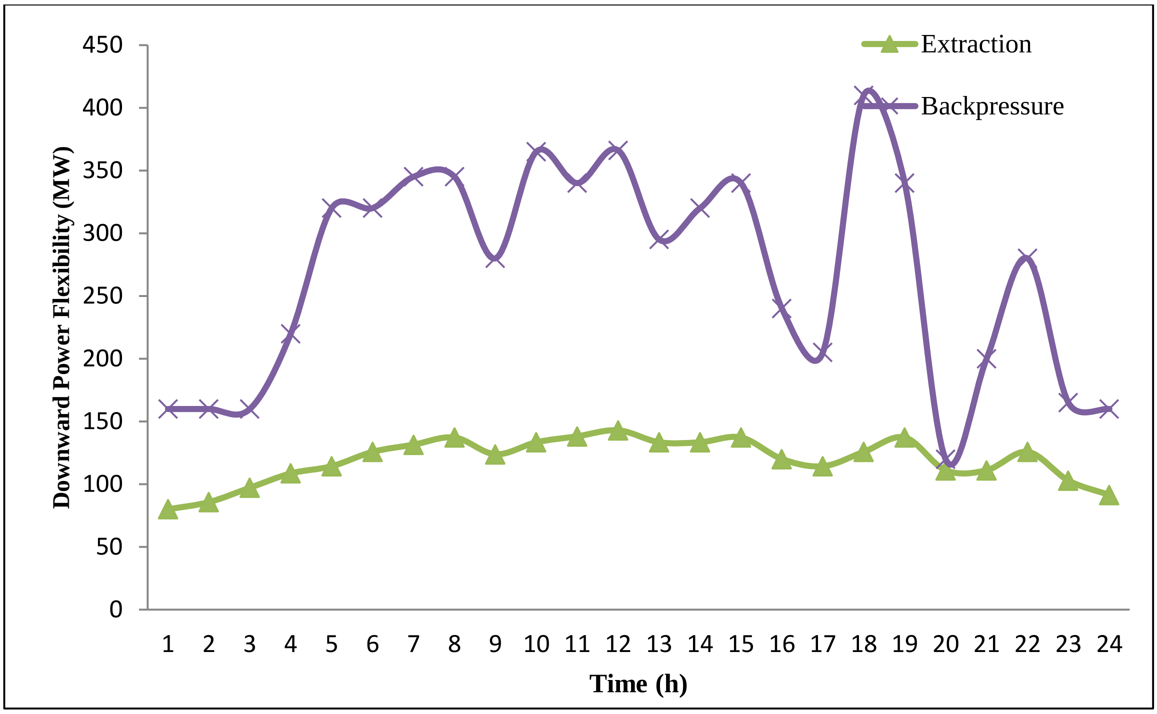


**Figure 4.29:** Downward flexibility of power for extraction/backpressure mode, CHPUC test system-III

The upward and downward heat generation flexibility has been shown in Figures 4.30 and 4.31, respectively. It is evident from Figure 4.30 that during the backpressure mode of CHP units, upward generation flexibility of the system is more as compared to operation in extraction mode at most of the sub-intervals. While, in extraction mode, the downward heat generation flexibility is more as compare to backpressure mode.

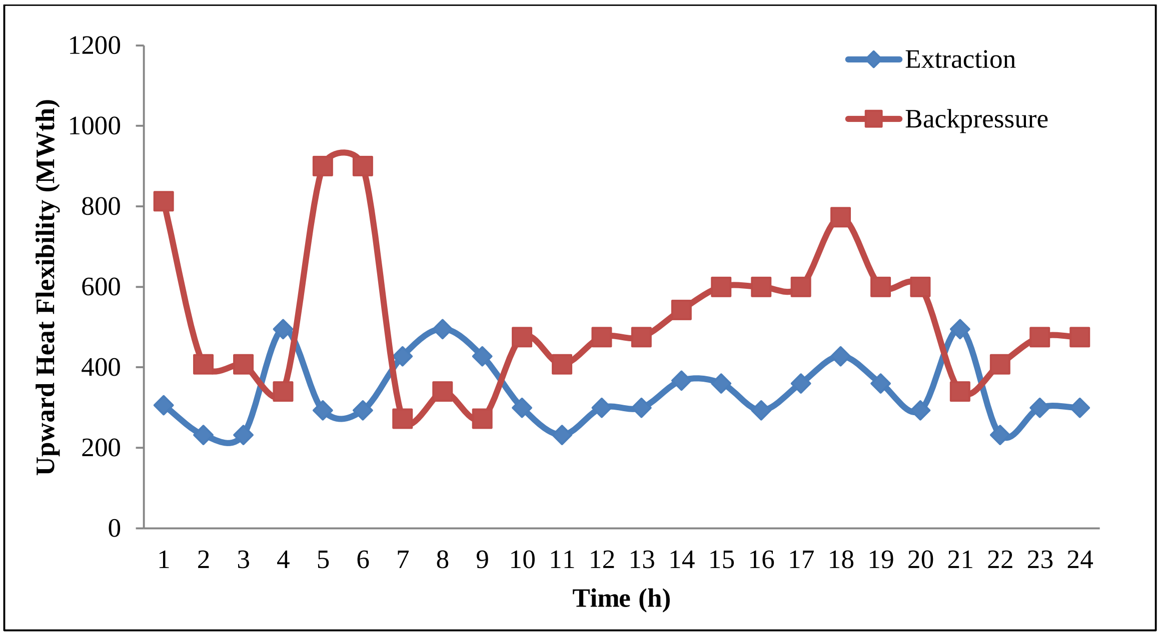


**Figure 4.30:** Upward flexibility of heat for extraction/backpressure mode, CHPUC test system-III

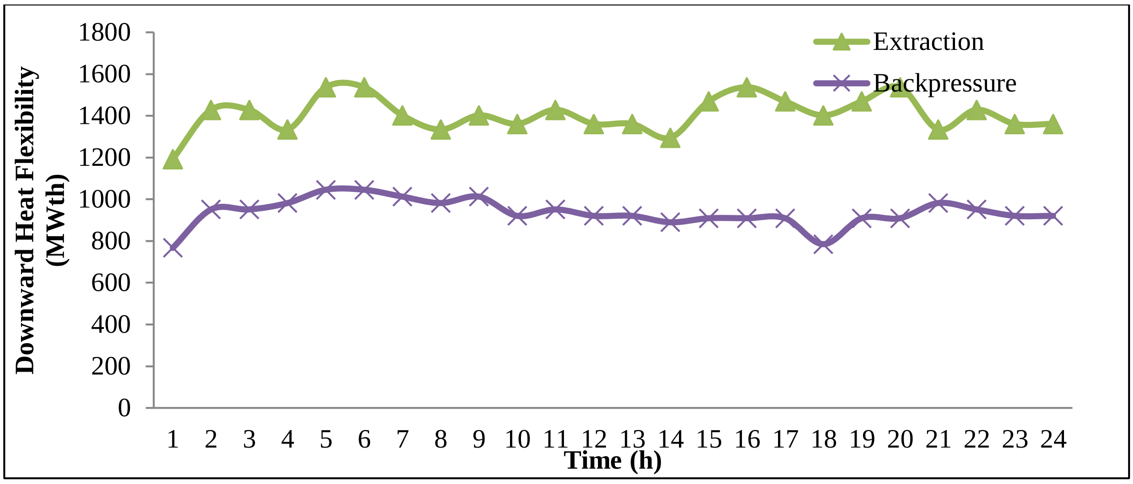


**Figure 4.31:** Downward flexibility of heat for extraction/backpressure mode, CHPUC test system-III

### 4.7.2 Multi-Objective Combined Heat and Power Unit Commitment Problem

#### 4.7.2.1 Test system-I

The cost and emission obtained from BPSO-PSO and BSA-CSO techniques for economic, emission and MO-CHPUC problems during backpressure and extraction mode of CHP units have been presented in Tables 4.17 and 4.18. It is evident from Tables 4.17 and 4.18 that for the economic CHPUC problem, the minimum operation cost obtained from the BSA-CSO technique during backpressure and extraction mode of CHP units are \$518972.0 and \$498786.6, respectively. In emission CHPUC problem, the minimum emission obtained in backpressure and extraction modes from the BSA-CSO technique are Kg222696.8 and Kg235454.7, respectively. In the BSA-CSO technique, the maximum value of cost and emission in backpressure mode are \$562804.7 and Kg254875.5, respectively, which is obtained from emission and economic UC generation schedule due to the conflicting nature of objectives. In extraction mode, the maximum value obtained for cost and emission are \$577645.2 and Kg247919.4, respectively. For the MO-CHPUC problem, the best-compromised solution is obtained by the fuzzy membership method with the cardinal priority method. During the backpressure mode of operation, the cost and emission are \$552186.7 and Kg248946.8, respectively, and for extraction mode operation, the cost and emission are \$531034.2, and Kg237769, respectively. Hence, it is summarized that during backpressure mode, the cost from the BSA-CSO technique is less by 3.83% whereas the emission is more by 4.49%, with respect to the results obtained by extraction mode.

**Table 4.17:** Operating cost and emission for backpressure mode: MO-CHPUC test system-I

| | BPSO-PSO | | BSA-CSO | |
|---|---|---|---|---|
| **CHPUC problem** | **TC ($)** | **TE (Kg)** | **TC ($)** | **TE (Kg)** |
| **Economic** | 520935.4 | 255861.5 | 518972.0 | 254875.5 |
| **Emission** | 566243.1 | 225472.5 | 562804.7 | 222696.8 |
| **Multiobjective** | 553589.4 | 250387.8 | 552186.7 | 248946.8 |

**Table 4.18:** Operating cost and emission for extraction mode: MO-CHPUC test system-I

| | BPSO-PSO | | BSA-CSO | |
|---|---|---|---|---|
| | **TC ($)** | **TE (Kg)** | **TC ($)** | **TE (Kg)** |
| **Economic** | 501968.8 | 253054.3 | 498786.6 | 247919.4 |
| **Emission** | 561034.2 | 237769.4 | 577645.2 | 235454.7 |
| **Multiobjective** | 548130.9 | 238933.9 | 531034.2 | 237769 |

In BPSO-PSO, the cost and emission obtained during backpressure mode are $553589.4 and Kg250387.8, respectively. During extraction mode, the obtained cost and emission from BPSO-PSO are $548130.9 and Kg238933.9, respectively. It has been observed that the cost and emission in extraction mode obtained from the BPSO-PSO are more by 3.21% and 0.49% as compared to the BSA-CSO technique, respectively. In backpressure mode, the obtained cost and emission from BPSO-PSO are '$1402.7' and 'Kg1441' more than the BSA-CSO technique, respectively.

Due to the diverse nature of extraction and backpressure mode, the optimum UC status is different during extraction mode than backpressure mode and it is discussed in subsection 4.7.1.1. In the BSA-CSO technique, the power and heat generation for backpressure and extraction mode is shown in Figures (4.32, 4.34) and Figures (4.33, 4.35), respectively. It is evident from these figures that the power and heat generation

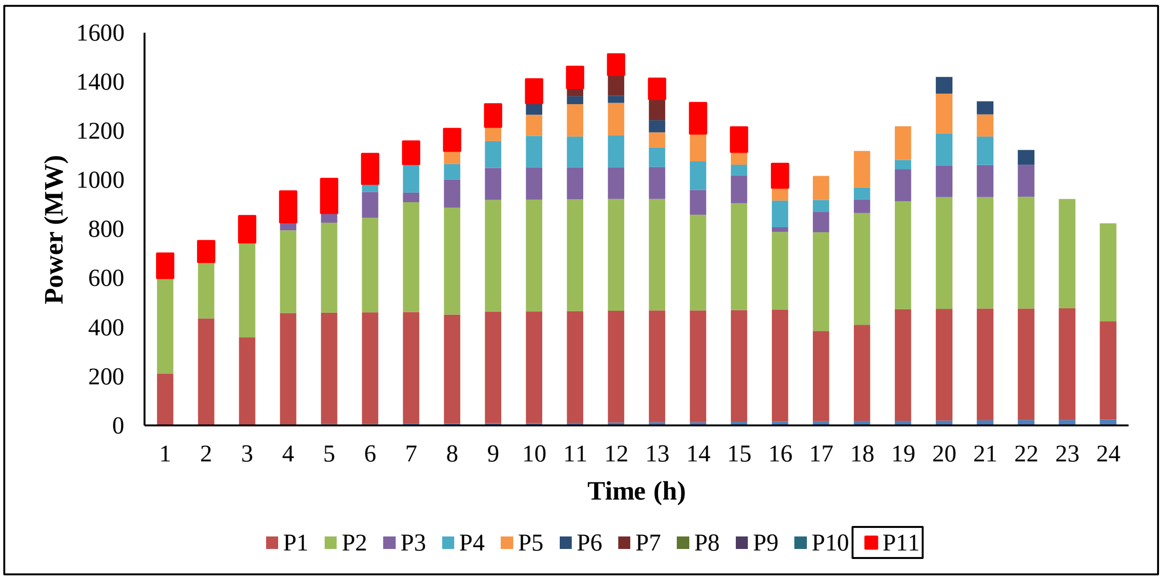


**Figure 4.32:** Power generation from units during backpressure mode: MO-CHPUC test system-I (Note: ☐ Highlight represents the CHP unit)

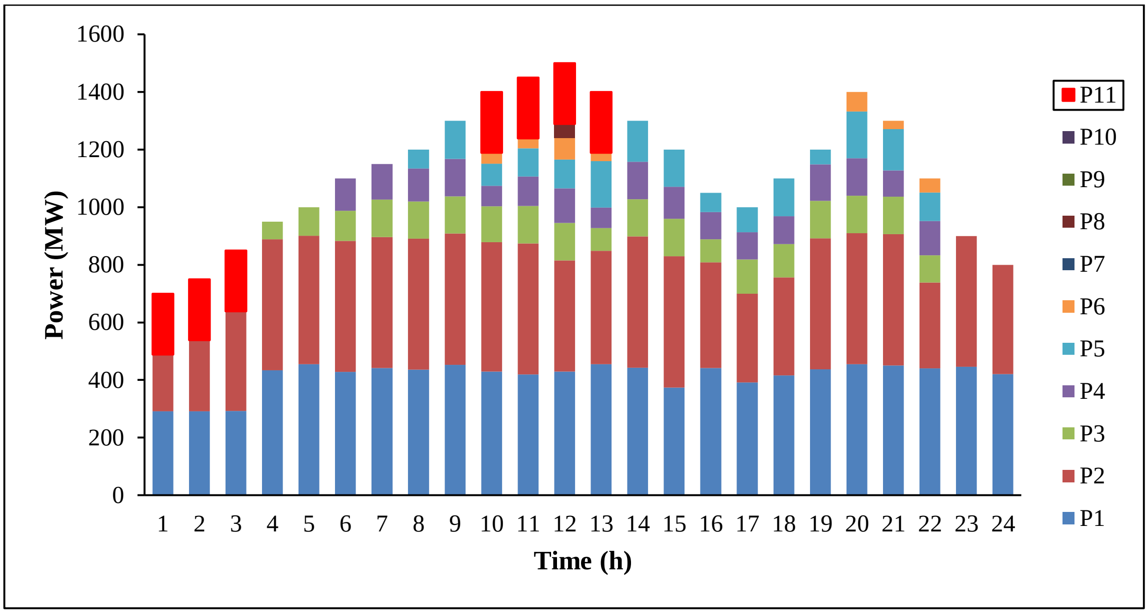


**Figure 4.33:** Power generation from units during extraction mode: MO-CHPUC test system-I

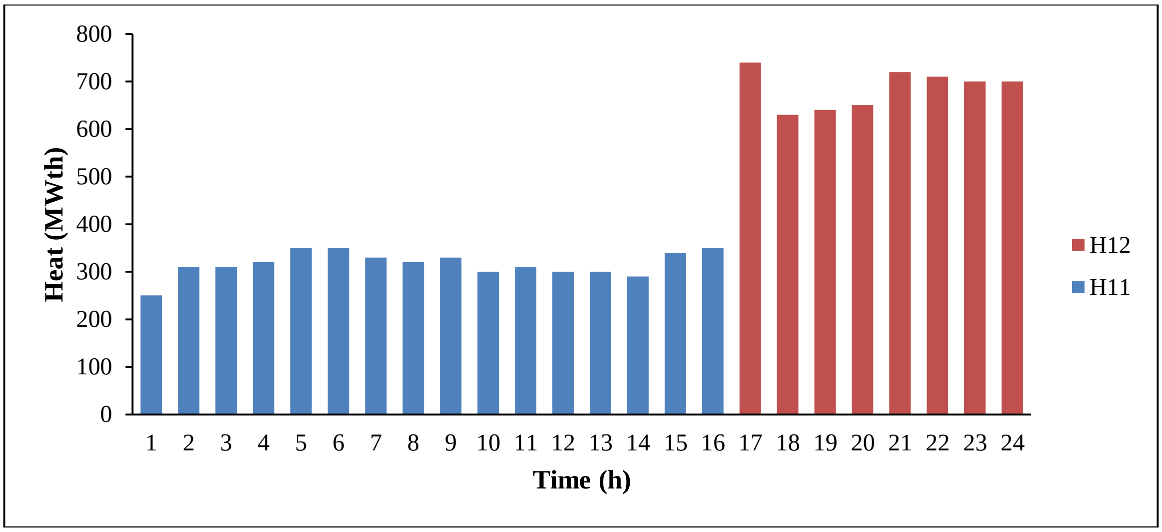


**Figure 4.34:** Heat generation from units during backpressure mode: MO-CHPUC test system-I

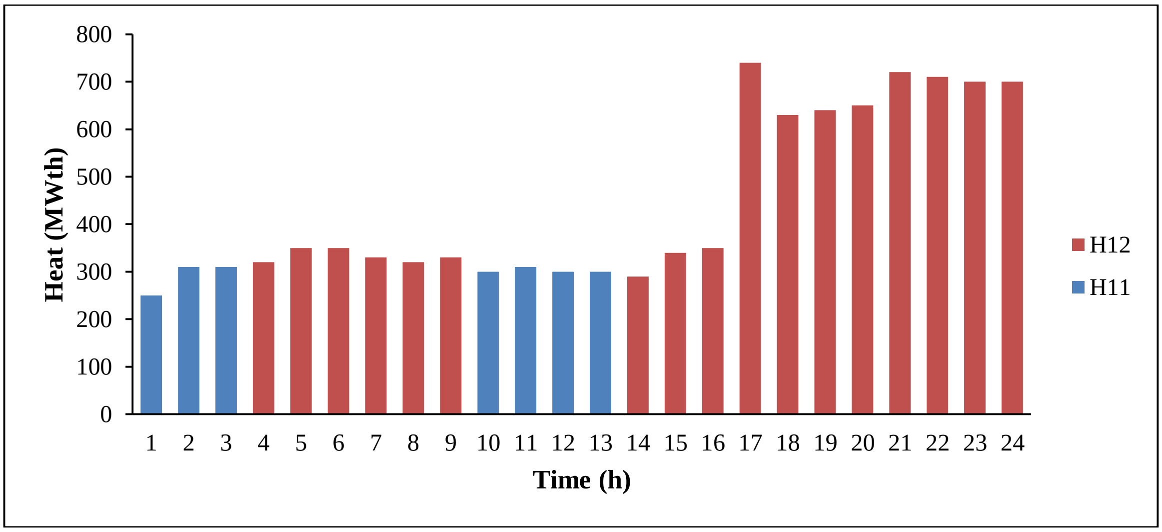


**Figure 4.35:** Heat generation from units during extraction mode: MO-CHPUC test system-I

satisfy the equality demand constraints during each sub-interval. It is evident from Figures 4.32 and 4.33, that power generation from committed CHP unit during extraction mode is more as compared to backpressure mode. The total heat generated from the committed CHP unit during extraction mode is less than the backpressure mode heat generation. These observations indicate the diverse behavior of the CHP unit during both operating modes.

#### 4.7.2.2 Test system-II

In MO-CHPUC test system-II, the obtained cost and emission from BSA-CSO and BPSO-PSO techniques for economic, emission and MO-CHPUC problems during backpressure and extraction mode have been presented in Tables 4.19 and 4.20. It is evident from Tables 4.19 and 4.20, during the extraction mode of the CHP unit, the minimum cost and minimum emission are less as compared to backpressure mode results of BSA-CSO and BPSO-PSO techniques. A similar pattern is observed in the case of the MO-CHPUC problem, in which cost and emission obtained from the BSA-CSO technique during extraction mode are less than by 36.7% and 49.5%, respectively as compared to backpressure mode results. It has been observed that the cost and emission obtained from the BPSO-PSO technique during backpressure and extraction mode are more as compared to the BSA-CSO technique. The power and generation schedule obtained from the BSA-CSO technique during backpressure and extraction mode are illustrated in Figures 4.36-4.39.

**Table 4.19:** Operating cost and emission for backpressure mode: MO-CHPUC test system-II

| | **BPSO-PSO** | | **BSA-CSO** | |
|---|---|---|---|---|
| **CHPUC problem** | **TC ($)** | **TE (Kg)** | **TC ($)** | **TE (Kg)** |
| **Economic** | 540323.0 | 186177.7 | 448683.0 | 185976.7 |
| **Emission** | 553958.9 | 181299.5 | 545194.9 | 179351.9 |
| **Multiobjective** | 550206.5 | 181530.5 | 538630.3 | 181105.5 |

**Table 4.20:** Operating cost and emission for extraction mode: MO-CHPUC test system-II

| | **BPSO-PSO** | | **BSA-CSO** | |
|---|---|---|---|---|
| **CHPUC problem** | **TC ($)** | **TE (Kg)** | **TC ($)** | **TE (Kg)** |
| **Economic** | 377921.7 | 95498.32 | 284267.5 | 92785.1 |
| **Emission** | 454722.4 | 91678.93 | 402174.8 | 83817.5 |
| **Multiobjective** | 429305.8 | 93335.63 | 393958.5 | 91304.8 |

It has also been observed that total power generation from committed CHP unit during extraction mode is more than backpressure mode generation and is shown in Figures 4.36 and 4.37. The total heat generated from the committed CHP unit is the same for both the modes and is presented in Figures 4.38 and 4.39, because heat unit remains uncommitted during the whole scheduling interval, as the heat generation from CHP units is sufficient to meet the demand at most of the sub-intervals.

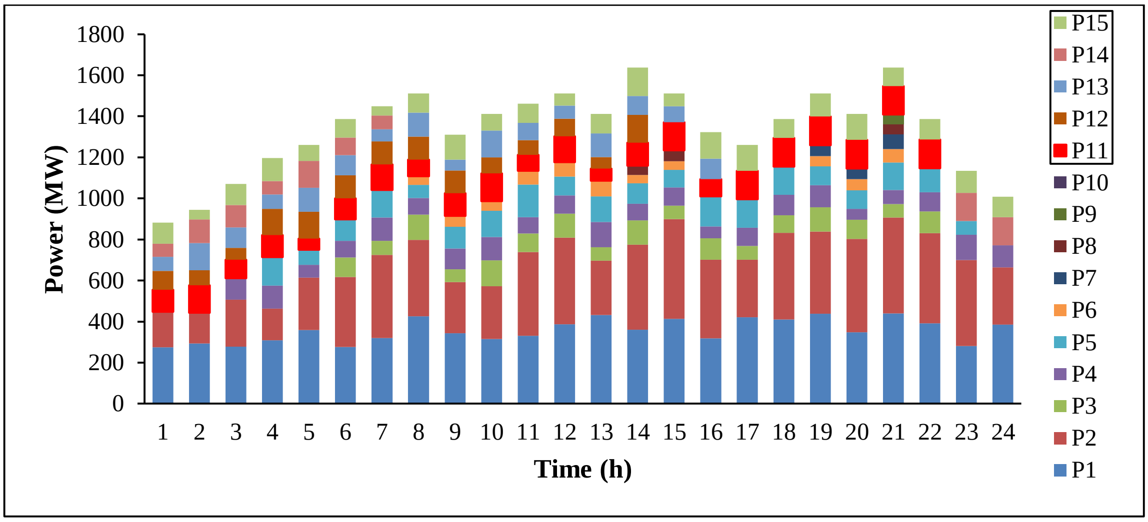


**Figure 4.36:** Power generation from units during backpressure mode: MO-CHPUC test system-II

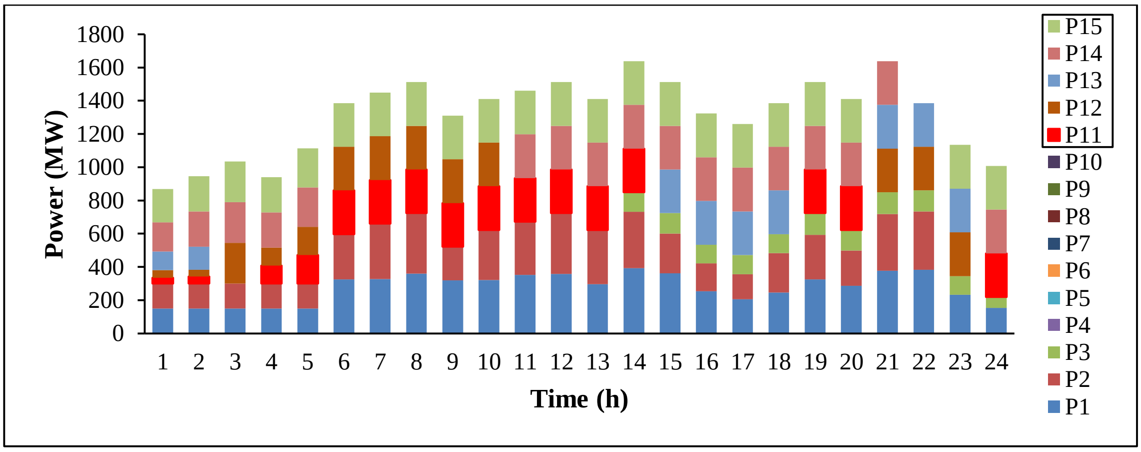


**Figure 4.37:** Power generation from units during extraction mode: MO-CHPUC test system-II

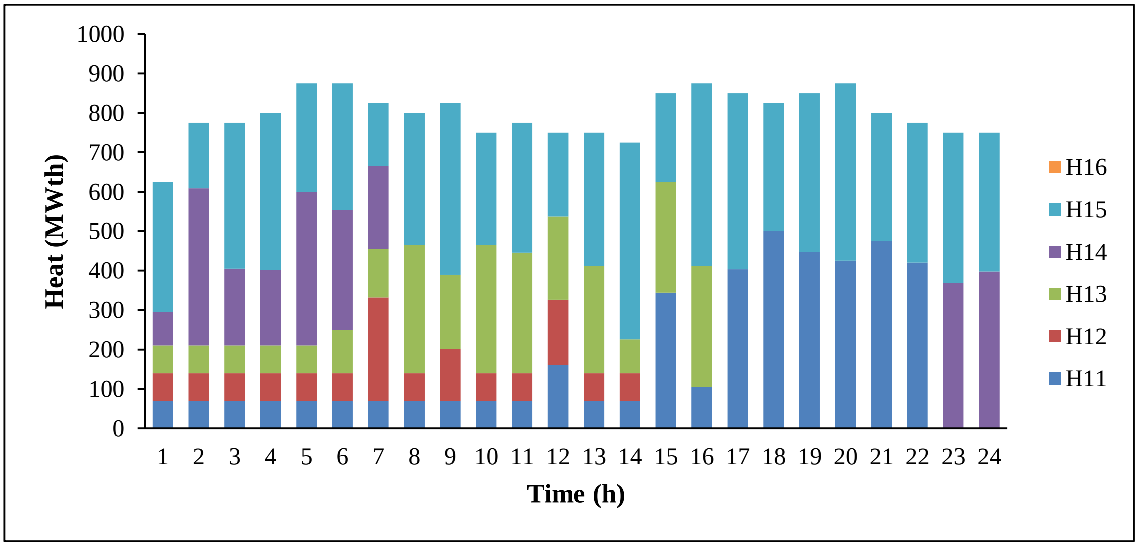


**Figure 4.38:** Heat generation from units during backpressure mode: MO-CHPUC test system-II

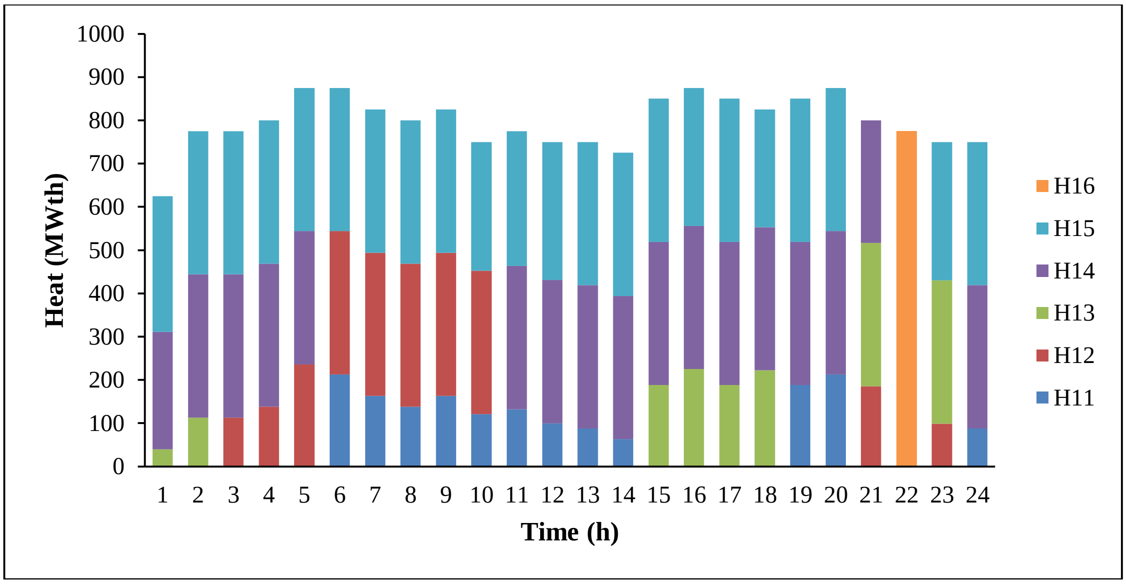


**Figure 4.39:** Heat generation from units during extraction mode: MO-CHPUC test system-II

### 4.7.2.3 Test system-III

The MO-CHPUC test system-III consists of 20 units (1-10$^{th}$ thermal, 11-15$^{th}$ CHP and 16-20$^{th}$ heat). The results obtained by PSO-BPSO and BSA-CSO techniques for economic, emission and multi-objective CHPUC problems are given in Tables 4.21 and 4.22, for backpressure and extraction mode of CHP unit operation, respectively. It is evident from the results given in these tables that for the economic and emission CHPUC problems, the extraction mode is more beneficial as compared to backpressure mode. For the MO-CHPUC problem, the cost and emission obtained by the BSA-CSO technique, during extraction mode of operation are 9.01% and 9.33% lower as compared to backpressure mode. The power and generation schedule obtained from the BSA-CSO technique are presented in Figures 4.40-4.43. It is evident from figures, that the total heat generation from committed CHP unit during backpressure mode is more as compared to extraction mode, however, the total power generation is less during backpressure mode. Hence, it is summarized that the CHP units produce sufficient heat during backpressure mode and adequate power during the extraction mode.

**Table 4.21:** Operating cost and emission for backpressure mode: MO-CHPUC test system-III

| | BPSO-PSO | | BSA-CSO | |
|---|---|---|---|---|
| **CHPUC problem** | **TC ($)** | **TE (Kg)** | **TC ($)** | **TE (Kg)** |
| **Economic** | 739894.3 | 144053.2 | 679416.1 | 142630.3 |
| **Emission** | 853912.1 | 130303.5 | 754664.6 | 129917.8 |
| **Multiobjective** | 753815.2 | 132850 | 693744.2 | 129998.6 |

**Table 4.22:** Operating cost and emission for extraction mode: MO-CHPUC test system-III

| | BPSO-PSO | | BSA-CSO | |
|---|---|---|---|---|
| **CHPUC problem** | **TC ($)** | **TE (Kg)** | **TC ($)** | **TE (Kg)** |
| **Economic** | 667737.1 | 126949.4 | 560111.4 | 124439.5 |
| **Emission** | 720600.6 | 120268.2 | 642288.2 | 116816.3 |
| **Multiobjective** | 675380.2 | 123995.6 | 631189.5 | 117869.6 |

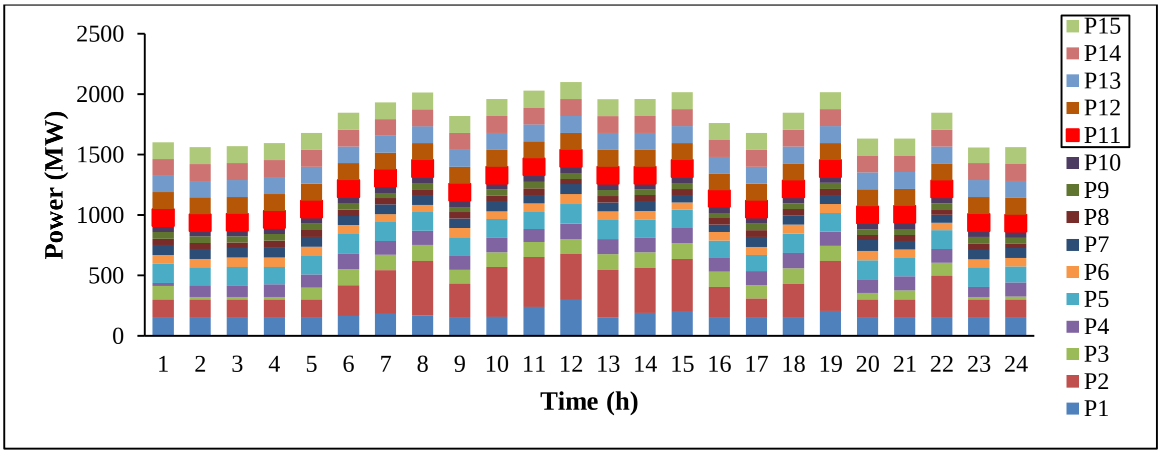


**Figure 4.40:** Power generation from units during backpressure mode: MO-CHPUC test system-III

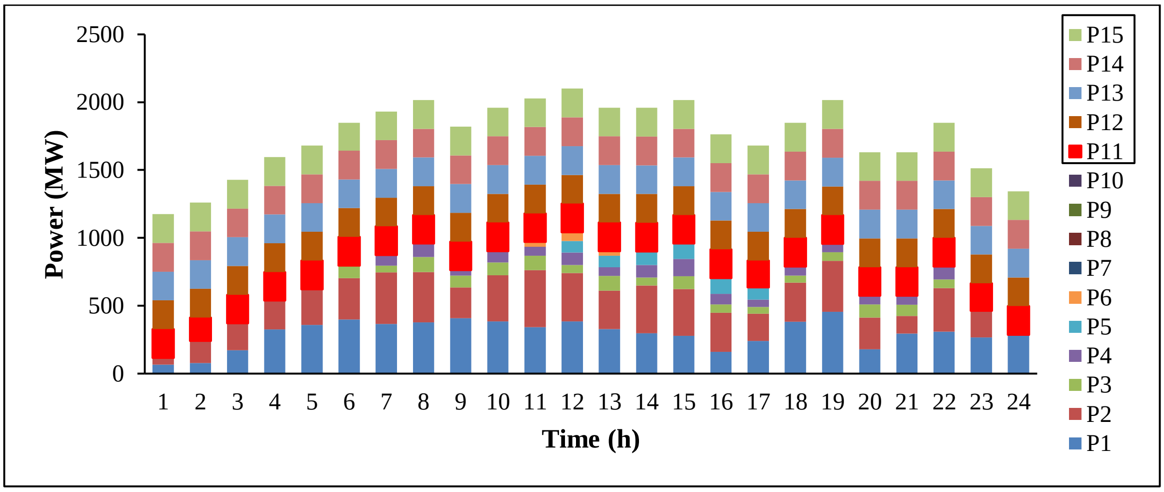


**Figure 4.41:** Power generation from units during extraction mode: MO-CHPUC test system-III

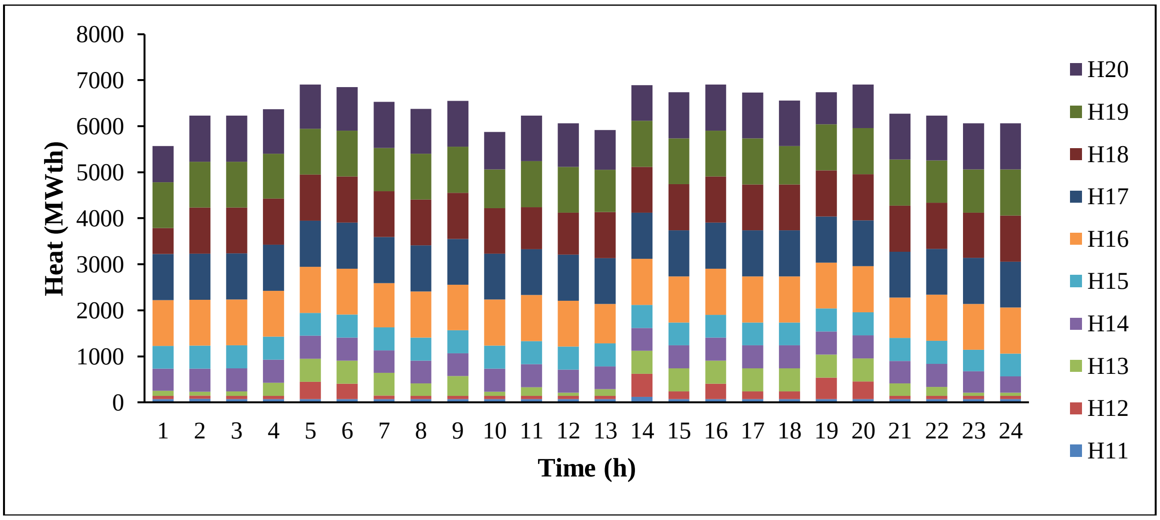


**Figure 4.42:** Heat generation from units during backpressure mode: MO-CHPUC test system-III

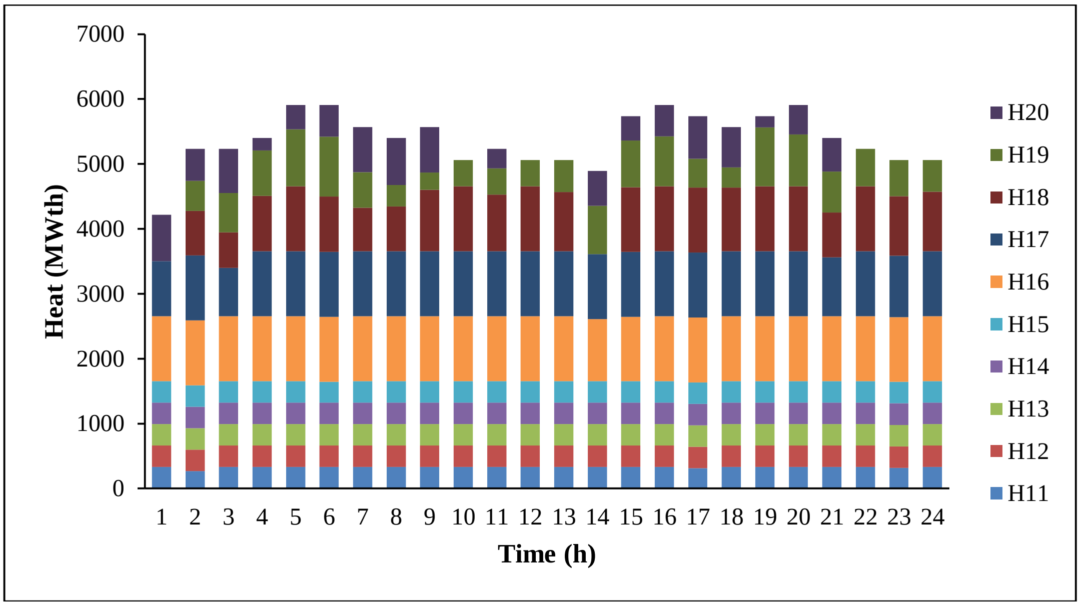


**Figure 4.43:** Heat generation from units during extraction mode: MO-CHPUC test system-III

### 4.7.3 Scalar Objective Profit Based Combined Heat and Power Unit Commitment Problem

#### 4.7.3.1 Test system-I

In the PBCHPUC test system-I, the profit obtained from BSPO-PSO and BSA-CSO techniques have been given in Table 4.23. It has been observed from Table 4.23 that profit obtained from BSA-CSO in backpressure and extraction mode are \$433973.3 and \$393403.2, respectively. The overall profit obtained from BPSO-PSO in backpressure and extraction mode is \$432933.8 and \$384696.1, respectively. Hence, it is summarized that there is a huge increase in profit for the backpressure mode operation of the CHP unit. Further, it is illustrated from the results that the profit obtained by the BSA-CSO technique is higher as compared to the BPSO-PSO technique. The optimum power and heat generation schedule of generating units obtained by the implementation of the BSA-CSO technique in backpressure and extraction mode are given in Tables 4.24 and 4.25, respectively. It has been observed from Tables 4.24 and 4.25, during off status of the heat unit, the CHP unit is sufficient to meet heat reserve and demand constraints in backpressure and extraction mode. The power generated from the CHP unit in extraction mode is higher as compared to backpressure mode, thus resulted in the lesser thermal units are turned on in extraction mode as compared to backpressure mode at 5$^{th}$, 6$^{th}$, 8-10$^{th}$ and 15-21$^{th}$ sub-intervals.

**Table 4.23:** Comparison of profit obtained by optimization techniques, PBCHPUC test system-I

| Technique | Extraction mode profit ($) | Backpressure mode profit ($) |
|---|---|---|
| **BPSO-PSO** | 384696.1 | 432933.8 |
| **BSA-CSO** | 393403.2 | 433973.3 |

**Table 4.24:** Power and heat generation schedule in backpressure mode by BSA-CSO, PBCHPUC test system-I

| | Thermal Units (MW) | | | | | | | | | | CHP Unit | | Heat Unit (MWth) |
|---|---|---|---|---|---|---|---|---|---|---|---|---|---|
| **h** | **P1** | **P2** | **P3** | **P4** | **P5** | **P6** | **P7** | **P8** | **P9** | **P10** | **P11** | **H11** | **H12** |
| **1** | 385 | 245 | 0 | 0 | 0 | 0 | 0 | 0 | 0 | 0 | 70 | 250 | 0 |
| **2** | 368.2 | 295 | 0 | 0 | 0 | 0 | 0 | 0 | 0 | 0 | 86.8 | 310 | 0 |
| **3** | 368.2 | 395 | 0 | 0 | 0 | 0 | 0 | 0 | 0 | 0 | 86.8 | 310 | 0 |
| **4** | 405.4 | 455 | 0 | 0 | 0 | 0 | 0 | 0 | 0 | 0 | 89.6 | 320 | 0 |
| **5** | 422 | 455 | 0 | 0 | 25 | 0 | 0 | 0 | 0 | 0 | 98 | 350 | 0 |
| **6** | 455 | 455 | 0 | 0 | 82 | 0 | 0 | 0 | 10 | 0 | 98 | 350 | 0 |
| **7** | 455 | 455 | 0 | 0 | 137.6 | 0 | 0 | 0 | 10 | 0 | 92.4 | 330 | 0 |
| **8** | 455 | 455 | 130 | 0 | 70.4 | 0 | 0 | 0 | 0 | 0 | 89.6 | 320 | 0 |
| **9** | 372.6 | 455 | 130 | 130 | 110 | 0 | 0 | 0 | 10 | 0 | 92.4 | 330 | 0 |
| **10** | 386 | 455 | 130 | 130 | 162 | 43 | 0 | 0 | 10 | 0 | 84 | 300 | 0 |
| **11** | 396.2 | 455 | 130 | 130 | 162 | 80 | 0 | 0 | 10 | 0 | 86.8 | 310 | 0 |
| **12** | 439 | 455 | 130 | 130 | 162 | 80 | 0 | 10 | 10 | 0 | 84 | 300 | 0 |
| **13** | 386 | 455 | 130 | 130 | 162 | 43 | 0 | 0 | 10 | 0 | 84 | 300 | 0 |
| **14** | 383.8 | 455 | 130 | 130 | 110 | 0 | 0 | 0 | 10 | 0 | 81.2 | 290 | 0 |
| **15** | 455 | 455 | 130 | 0 | 54.8 | 0 | 0 | 0 | 10 | 0 | 95.2 | 340 | 0 |
| **16** | 367 | 455 | 95 | 0 | 25 | 0 | 0 | 0 | 10 | 0 | 98 | 350 | 0 |
| **17** | 369.8 | 455 | 45 | 0 | 25 | 0 | 0 | 0 | 10 | 0 | 95.2 | 340 | 0 |
| **18** | 387.6 | 455 | 130 | 0 | 25 | 0 | 0 | 0 | 10 | 0 | 92.4 | 330 | 0 |
| **19** | 455 | 455 | 130 | 0 | 54.8 | 0 | 0 | 0 | 10 | 0 | 95.2 | 340 | 0 |
| **20** | 372 | 455 | 130 | 130 | 162 | 43 | 0 | 0 | 10 | 0 | 98 | 350 | 0 |
| **21** | 455 | 455 | 130 | 130 | 0 | 30.4 | 0 | 0 | 10 | 0 | 89.6 | 320 | 0 |
| **22** | 455 | 455 | 0 | 73.2 | 0 | 20 | 0 | 0 | 10 | 0 | 86.8 | 310 | 0 |
| **23** | 351 | 445 | 0 | 20 | 0 | 0 | 0 | 0 | 0 | 0 | 84 | 300 | 0 |
| **24** | 351 | 345 | 0 | 20 | 0 | 0 | 0 | 0 | 0 | 0 | 84 | 300 | 0 |

**Table 4.25:** Power and heat generation schedule in extraction mode by BSA-CSO, PBCHPUC test system-I

| | Thermal Units (MW) | | | | | | | | | | CHP Unit | | Heat Unit (MWth) |
|---|---|---|---|---|---|---|---|---|---|---|---|---|---|
| **h** | **P1** | **P2** | **P3** | **P4** | **P5** | **P6** | **P7** | **P8** | **P9** | **P10** | **P11** | **H11** | **H12** |
| **1** | 287 | 150 | 0 | 0 | 0 | 0 | 0 | 0 | 0 | 0 | 263 | 250 | 0 |
| **2** | 379.38 | 150 | 0 | 0 | 0 | 0 | 0 | 0 | 0 | 0 | 220.62 | 310 | 0 |
| **3** | 437 | 150 | 0 | 0 | 0 | 0 | 0 | 0 | 0 | 0 | 263 | 310 | 0 |
| **4** | 455 | 232 | 0 | 0 | 0 | 0 | 0 | 0 | 0 | 0 | 263 | 320 | 0 |
| **5** | 452.82 | 319.2 | 0 | 0 | 0 | 0 | 0 | 0 | 0 | 0 | 227.94 | 331 | 0 |
| **6** | 421.22 | 390.78 | 0 | 0 | 25 | 0 | 0 | 0 | 0 | 0 | 263 | 331 | 0 |
| **7** | 433.40 | 418.60 | 0 | 0 | 25 | 0 | 0 | 0 | 10 | 0 | 263 | 330 | 0 |
| **8** | 447 | 455 | 0 | 0 | 25 | 0 | 0 | 0 | 10 | 0 | 263 | 320 | 0 |
| **9** | 438.63 | 455 | 108.37 | 0 | 25 | 0 | 0 | 0 | 10 | 0 | 263 | 330 | 0 |
| **10** | 420 | 455 | 130 | 97 | 25 | 0 | 0 | 0 | 10 | 0 | 263 | 300 | 0 |
| **11** | 445 | 455 | 130 | 122 | 25 | 0 | 0 | 0 | 10 | 0 | 263 | 310 | 0 |
| **12** | 419.87 | 455 | 130 | 130 | 92.68 | 20 | 0 | 0 | 10 | 0 | 242.45 | 300 | 0 |
| **13** | 382.87 | 455 | 130 | 114.1 | 25 | 20 | 0 | 0 | 10 | 0 | 263 | 300 | 0 |
| **14** | 405.60 | 455 | 101.4 | 20 | 25 | 20 | 0 | 0 | 10 | 0 | 263 | 290 | 0 |
| **15** | 455 | 455 | 0 | 0 | 57.54 | 0 | 0 | 0 | 10 | 0 | 222.46 | 331 | 0 |

**Table 4.25:** Power and heat generation schedule in extraction mode by BSA-CSO, PBCHPUC test system-I (Continued)

| | Thermal Units (MW) | | | | | | | | | | CHP Unit | | Heat Unit (MWth) |
|---|---|---|---|---|---|---|---|---|---|---|---|---|---|
| **h** | **P1** | **P2** | **P3** | **P4** | **P5** | **P6** | **P7** | **P8** | **P9** | **P10** | **P11** | **H11** | **H12** |
| **16** | 455 | 304.71 | 0 | 0 | 25 | 0 | 0 | 0 | 10 | 0 | 255.29 | 331 | 0 |
| **17** | 455 | 274.30 | 0 | 0 | 25 | 0 | 0 | 0 | 0 | 0 | 245.70 | 331 | 0 |
| **18** | 455 | 349.74 | 0 | 0 | 25 | 0 | 0 | 0 | 10 | 0 | 260.26 | 330 | 0 |
| **19** | 455 | 447 | 0 | 0 | 25 | 0 | 0 | 0 | 10 | 0 | 263 | 331 | 0 |
| **20** | 455 | 455 | 130 | 101.13 | 25 | 0 | 0 | 0 | 0 | 0 | 233.87 | 331 | 0 |
| **21** | 420 | 455 | 107 | 20 | 25 | 0 | 0 | 0 | 10 | 0 | 263 | 320 | 0 |
| **22** | 420 | 342 | 20 | 20 | 25 | 0 | 0 | 0 | 10 | 0 | 263 | 310 | 0 |
| **23** | 415 | 182 | 20 | 20 | 0 | 0 | 0 | 0 | 0 | 0 | 263 | 300 | 0 |
| **24** | 455 | 0 | 116.2 | 20 | 0 | 0 | 0 | 0 | 0 | 10 | 198.8 | 300 | 0 |

### 4.7.3.2 Test system-II

For the PBCHPUC problem, the profit obtained by BPSO-PSO and BSA-CSO techniques during extraction and backpressure mode has been given in Table 4.26. The profit obtained by the BSA-CSO technique during the extraction mode operation of the CHP unit is $1000398.0, which is $77557.5 more as compared to backpressure mode. Hence, it is summarized that there is a huge increase in profit for the extraction mode operation of the CHP unit as compared to backpressure mode. The profit obtained from the BSA-CSO technique in backpressure and extraction mode operation is higher as compared to the profit attained by the BPSO-PSO technique. The optimum generation schedule obtained by the BSA-CSO technique during extraction and backpressure mode of the CHP unit operation has been given in Tables 4.27-4.30. It has been observed that the number of committed CHP units at most of the sub-intervals in backpressure mode is more as compared to extraction mode.

**Table 4.26:** Comparison of profit obtained from optimization techniques, PBCHPUC test system-II

| Technique | Extraction mode profit ($) | Backpressure mode profit ($) |
|---|---|---|
| **BPSO-PSO** | 1000543.0 | 917632.9 |
| **BSA-CSO** | 1019038.0 | 922840.5 |

**Table 4.27:** Power generation schedule in backpressure mode by BSA-CSO, PBCHPUC test system-II

| | Thermal Units (MW) | | | | | | | | | | CHP Units (MW) | | | | |
|---|---|---|---|---|---|---|---|---|---|---|---|---|---|---|---|
| **h** | **P1** | **P2** | **P3** | **P4** | **P5** | **P6** | **P7** | **P8** | **P9** | **P10** | **P11** | **P12** | **P13** | **P14** | **P15** |
| **1** | 420 | 287 | 0 | 0 | 0 | 0 | 0 | 0 | 0 | 0 | 19.6 | 19.6 | 19.6 | 0 | 116.2 |
| **2** | 378 | 350 | 0 | 0 | 0 | 0 | 0 | 0 | 0 | 0 | 19.6 | 19.6 | 19.6 | 19.6 | 138.6 |
| **3** | 399 | 455 | 0 | 0 | 0 | 0 | 0 | 0 | 0 | 0 | 19.6 | 19.6 | 19.6 | 19.6 | 138.6 |
| **4** | 455 | 455 | 0 | 0 | 0 | 0 | 0 | 0 | 55 | 0 | 25.2 | 19.6 | 19.6 | 19.6 | 140 |
| **5** | 455 | 455 | 0 | 0 | 0 | 0 | 0 | 0 | 55 | 0 | 46.2 | 19.6 | 19.6 | 19.6 | 140 |
| **6** | 455 | 455 | 0 | 0 | 162 | 0 | 0 | 0 | 55 | 0 | 46.2 | 19.6 | 19.6 | 19.6 | 140 |
| **7** | 455 | 455 | 130 | 0 | 162 | 0 | 0 | 0 | 16 | 0 | 32.2 | 19.6 | 19.6 | 19.6 | 140 |
| **8** | 455 | 455 | 130 | 0 | 162 | 0 | 0 | 0 | 55 | 0 | 25.2 | 19.6 | 19.6 | 19.6 | 140 |
| **9** | 443.64 | 455 | 30 | 0 | 25 | 0 | 0 | 0 | 10 | 0 | 27.16 | 19.6 | 19.6 | 140 | 140 |

**Table 4.27:** Power generation schedule in backpressure mode by BSA-CSO, PBCHPUC test system-II (Continued)

| | Thermal Units (MW) | | | | | | | | | | CHP Units (MW) | | | | |
|---|---|---|---|---|---|---|---|---|---|---|---|---|---|---|---|
| **h** | **P1** | **P2** | **P3** | **P4** | **P5** | **P6** | **P7** | **P8** | **P9** | **P10** | **P11** | **P12** | **P13** | **P14** | **P15** |
| **10** | 455 | 455 | 130 | 0 | 109 | 0 | 0 | 0 | 10 | 0 | 19.6 | 19.6 | 19.6 | 81.2 | 112 |
| **11** | 455 | 455 | 130 | 0 | 129.04 | 0 | 0 | 0 | 10 | 0 | 19.6 | 19.6 | 19.6 | 83.16 | 140 |
| **12** | 455 | 455 | 130 | 0 | 162 | 0 | 0 | 0 | 55 | 0 | 19.6 | 19.6 | 19.6 | 81.2 | 112 |
| **13** | 455 | 455 | 130 | 0 | 109 | 0 | 0 | 0 | 10 | 0 | 19.6 | 19.6 | 19.6 | 81.2 | 112 |
| **14** | 455 | 455 | 130 | 130 | 162 | 0 | 0 | 0 | 55 | 0 | 19.6 | 19.6 | 19.6 | 81.2 | 63 |
| **15** | 455 | 455 | 130 | 130 | 0 | 0 | 0 | 0 | 55 | 0 | 19.6 | 19.6 | 19.6 | 81.2 | 98 |
| **16** | 455 | 455 | 130 | 28 | 0 | 0 | 0 | 0 | 10 | 0 | 19.6 | 19.6 | 19.6 | 81.2 | 105 |
| **17** | 455 | 455 | 82 | 20 | 0 | 0 | 0 | 0 | 10 | 0 | 19.6 | 19.6 | 19.6 | 81.2 | 98 |
| **18** | 455 | 455 | 130 | 105 | 0 | 0 | 0 | 0 | 10 | 0 | 19.6 | 19.6 | 19.6 | 81.2 | 91 |
| **19** | 455 | 455 | 130 | 130 | 0 | 0 | 0 | 0 | 55 | 0 | 19.6 | 19.6 | 19.6 | 81.2 | 98 |
| **20** | 455 | 455 | 130 | 77 | 0 | 0 | 0 | 0 | 0 | 0 | 19.6 | 19.6 | 19.6 | 95.2 | 140 |
| **21** | 455 | 455 | 130 | 130 | 162 | 62 | 0 | 10 | 10 | 0 | 0 | 0 | 84 | 140 | 0 |
| **22** | 455 | 455 | 130 | 0 | 99 | 20 | 0 | 0 | 10 | 0 | 0 | 0 | 77 | 140 | 0 |
| **23** | 424 | 455 | 0 | 0 | 25 | 20 | 0 | 0 | 0 | 0 | 0 | 0 | 70 | 140 | 0 |
| **24** | 360 | 413 | 0 | 0 | 25 | 0 | 0 | 0 | 0 | 0 | 0 | 0 | 70 | 140 | 0 |

**Table 4.28:** Heat generation schedule in backpressure mode by BSA-CSO, PBCHPUC test system-II

| | CHP Units (MWth) | | | | | Heat Unit (MWth) |
|---|---|---|---|---|---|---|
| **h** | **H11** | **H12** | **H13** | **H14** | **H15** | **H16** |
| **1** | 70 | 70 | 70 | 0 | 415 | 0 |
| **2** | 70 | 70 | 70 | 70 | 495 | 0 |
| **3** | 70 | 70 | 70 | 70 | 495 | 0 |
| **4** | 90 | 70 | 70 | 70 | 500 | 0 |
| **5** | 165 | 70 | 70 | 70 | 500 | 0 |
| **6** | 165 | 70 | 70 | 70 | 500 | 0 |
| **7** | 115 | 70 | 70 | 70 | 500 | 0 |
| **8** | 90 | 70 | 70 | 70 | 500 | 0 |
| **9** | 97 | 70 | 70 | 500 | 500 | 0 |
| **10** | 70 | 70 | 70 | 290 | 400 | 0 |
| **11** | 70 | 70 | 70 | 297 | 500 | 0 |
| **12** | 70 | 70 | 70 | 290 | 400 | 0 |
| **13** | 70 | 70 | 70 | 290 | 400 | 0 |
| **14** | 70 | 70 | 70 | 290 | 225 | 0 |
| **15** | 70 | 70 | 70 | 290 | 350 | 0 |
| **16** | 70 | 70 | 70 | 290 | 375 | 0 |
| **17** | 70 | 70 | 70 | 290 | 350 | 0 |
| **18** | 70 | 70 | 70 | 290 | 325 | 0 |
| **19** | 70 | 70 | 70 | 290 | 350 | 0 |
| **20** | 70 | 70 | 70 | 340 | 500 | 0 |
| **21** | 0 | 0 | 300 | 500 | 0 | 0 |
| **22** | 0 | 0 | 275 | 500 | 0 | 0 |
| **23** | 0 | 0 | 250 | 500 | 0 | 0 |
| **24** | 0 | 0 | 250 | 500 | 0 | 0 |

**Table 4.29:** Power generation schedule in extraction mode by BSA-CSO, PBCHPUC test system-II

| | Thermal Units (MW) | | | | | | | | | | CHP Units (MW) | | | | |
|---|---|---|---|---|---|---|---|---|---|---|---|---|---|---|---|
| **h** | **P1** | **P2** | **P3** | **P4** | **P5** | **P6** | **P7** | **P8** | **P9** | **P10** | **P11** | **P12** | **P13** | **P14** | **P15** |
| **1** | 150 | 150 | 0 | 0 | 0 | 0 | 0 | 0 | 0 | 0 | 0 | 0 | 158.32 | 211.8 | 211.8 |
| **2** | 150 | 150 | 0 | 0 | 0 | 0 | 0 | 0 | 0 | 0 | 123.93 | 0 | 150.06 | 159.17 | 211.8 |
| **3** | 150 | 150 | 0 | 0 | 0 | 0 | 0 | 0 | 0 | 0 | 136.82 | 0 | 210.50 | 211.8 | 211.8 |
| **4** | 285.7 | 275.7 | 0 | 0 | 0 | 0 | 0 | 0 | 0 | 0 | 211.84 | 0 | 0 | 211.8 | 211.8 |
| **5** | 455 | 381.3 | 0 | 0 | 0 | 0 | 0 | 0 | 0 | 0 | 0 | 0 | 0 | 211.8 | 211.8 |

**Table 4.29:** Power generation schedule in extraction mode by BSA-CSO, PBCHPUC test system-II (Continued)

| | Thermal Units (MW) | | | | | | | | | | CHP Units (MW) | | | | |
|---|---|---|---|---|---|---|---|---|---|---|---|---|---|---|---|
| **h** | **P1** | **P2** | **P3** | **P4** | **P5** | **P6** | **P7** | **P8** | **P9** | **P10** | **P11** | **P12** | **P13** | **P14** | **P15** |
| **6** | 455 | 455 | 0 | 0 | 0 | 0 | 0 | 0 | 0 | 0 | 0 | 0 | 0 | 211.8 | 211.8 |
| **7** | 455 | 455 | 0 | 0 | 0 | 0 | 0 | 0 | 0 | 0 | 0 | 0 | 0 | 211.8 | 211.8 |
| **8** | 455 | 455 | 130 | 0 | 0 | 0 | 0 | 0 | 0 | 0 | 0 | 0 | 0 | 211.8 | 211.8 |
| **9** | 405.2 | 171.2 | 97.92 | 0 | 0 | 0 | 0 | 0 | 0 | 0 | 0 | 0 | 211.8 | 211.8 | 211.8 |
| **10** | 455 | 295.2 | 25.2 | 0 | 0 | 0 | 0 | 0 | 0 | 0 | 0 | 0 | 211.8 | 211.8 | 211.8 |
| **11** | 455 | 289.3 | 81.1 | 0 | 0 | 0 | 0 | 0 | 0 | 0 | 0 | 0 | 211.8 | 211.8 | 211.8 |
| **12** | 455 | 455 | 130 | 0 | 0 | 0 | 0 | 0 | 0 | 0 | 0 | 0 | 0 | 211.8 | 211.8 |
| **13** | 455 | 455 | 130 | 130 | 0 | 0 | 0 | 0 | 0 | 0 | 0 | 0 | 0 | 0 | 211.8 |
| **14** | 455 | 455 | 130 | 130 | 0 | 0 | 0 | 0 | 0 | 0 | 0 | 0 | 211.8 | 0 | 211.8 |
| **15** | 455 | 455 | 0 | 130 | 0 | 0 | 0 | 0 | 0 | 0 | 211.8 | 0 | 211.8 | 0 | 0 |
| **16** | 195.9 | 383.8 | 0 | 107.7 | 0 | 0 | 0 | 0 | 0 | 0 | 211.8 | 0 | 211.8 | 211.8 | 0 |
| **17** | 455 | 322.3 | 0 | 59.06 | 0 | 0 | 0 | 0 | 0 | 0 | 0 | 0 | 211.8 | 211.8 | 0 |
| **18** | 455 | 409.6 | 0 | 97.68 | 0 | 0 | 0 | 0 | 0 | 0 | 0 | 0 | 211.8 | 211.8 | 0 |
| **19** | 455 | 455 | 0 | 130 | 0 | 0 | 0 | 0 | 0 | 0 | 0 | 0 | 0 | 211.8 | 211.8 |
| **20** | 455 | 320.48 | 0 | 0 | 0 | 0 | 0 | 0 | 0 | 0 | 211.8 | 0 | 0 | 211.8 | 211.8 |
| **21** | 455 | 455 | 0 | 0 | 0 | 0 | 0 | 0 | 0 | 0 | 211.8 | 0 | 211.8 | 211.8 | 0 |
| **22** | 455 | 455 | 0 | 0 | 0 | 0 | 0 | 0 | 0 | 0 | 0 | 211.8 | 211.8 | 0 | 0 |
| **23** | 455 | 455 | 0 | 0 | 0 | 0 | 0 | 0 | 0 | 0 | 0 | 211.8 | 0 | 0 | 0 |
| **24** | 455 | 0 | 0 | 0 | 0 | 0 | 0 | 0 | 0 | 0 | 0 | 0 | 0 | 211.8 | 211.8 |

**Table 4.30:** Heat generation schedule in extraction mode by BSA-CSO, PBCHPUC test system-II

| | CHP Units (MWth) | | | | | Heat Unit (MWth) |
|---|---|---|---|---|---|---|
| **h** | **H11** | **H12** | **H13** | **H14** | **H15** | **H16** |
| **1** | 0 | 0 | 0 | 294 | 331 | 0 |
| **2** | 193.64 | 0 | 234.47 | 15.89 | 331 | 0 |
| **3** | 213.79 | 0 | 99.79 | 130.42 | 331 | 0 |
| **4** | 272.89 | 0 | 0 | 196.11 | 331 | 0 |
| **5** | 0 | 0 | 0 | 331 | 331 | 0 |
| **6** | 0 | 0 | 0 | 331 | 331 | 0 |
| **7** | 0 | 0 | 0 | 331 | 331 | 0 |
| **8** | 0 | 0 | 0 | 331 | 331 | 0 |
| **9** | 0 | 0 | 331 | 331 | 331 | 0 |
| **10** | 0 | 0 | 331 | 238 | 331 | 0 |
| **11** | 0 | 0 | 331 | 331 | 331 | 0 |
| **12** | 0 | 0 | 0 | 331 | 331 | 0 |
| **13** | 0 | 0 | 0 | 0 | 331 | 0 |
| **14** | 0 | 0 | 331 | 0 | 331 | 0 |
| **15** | 331 | 0 | 331 | 0 | 0 | 0 |
| **16** | 331 | 0 | 273.47 | 270.53 | 0 | 0 |
| **17** | 0 | 0 | 331 | 331 | 0 | 0 |
| **18** | 0 | 0 | 331 | 331 | 0 | 0 |
| **19** | 0 | 0 | 0 | 331 | 331 | 0 |
| **20** | 331 | 0 | 0 | 331 | 331 | 0 |
| **21** | 322.28 | 0 | 228.43 | 249.28 | 0 | 0 |
| **22** | 0 | 331 | 331 | 0 | 0 | 0 |
| **23** | 0 | 331 | 0 | 0 | 0 | 0 |
| **24** | 0 | 0 | 0 | 331 | 331 | 0 |

### 4.7.3.3 Test system-III

For test system-III, the profit obtained by BSA-CSO and BPSO-PSO techniques for dual mode PBCHPUC problem has been given in Table 4.31. It has been observed from obtained results that there is a huge increase in profit during the extraction mode operation of the CHP unit as compared to extraction mode. Further, it is summarized that the BSA-CSO technique is able to search better results as compared to results attained by the BPSO-PSO technique during both modes of operation. The power and heat generation schedule obtained from the BSA-CSO technique for dual mode PBCHPUC problem have been given in Tables 4.32-4.35. It has been observed from these tables, that additional thermal unit are required during backpressure mode, whereas in extraction mode more heat units are required.

**Table 4.31:** Comparison of profit for optimization techniques, PBCHPUC test system-III

| Technique | Extraction mode profit ($) | Backpressure mode profit ($) |
|---|---|---|
| **BPSO-PSO** | $4217052 | $3912975.0 |
| **BSA-CSO** | $4222867 | $3913846 |

**Table 4.32:** Power generation schedule in extraction mode by BSA-CSO, PBCHPUC test system-III

| | Thermal Units (MW) | | | | | | | | | | CHP Units (MW) | | | | |
|---|---|---|---|---|---|---|---|---|---|---|---|---|---|---|---|
| **h** | **P1** | **P2** | **P3** | **P4** | **P5** | **P6** | **P7** | **P8** | **P9** | **P10** | **P11** | **P12** | **P13** | **P14** | **P15** |
| **1** | 150 | 150 | 0 | 0 | 0 | 0 | 0 | 0 | 0 | 0 | 212 | 212 | 212 | 212 | 212 |
| **2** | 150 | 150 | 0 | 0 | 0 | 0 | 0 | 0 | 0 | 0 | 212 | 212 | 212 | 212 | 212 |
| **3** | 185 | 183 | 0 | 0 | 0 | 0 | 0 | 0 | 0 | 0 | 212 | 212 | 212 | 212 | 212 |
| **4** | 313 | 224 | 0 | 0 | 0 | 0 | 0 | 0 | 0 | 0 | 212 | 212 | 212 | 212 | 212 |
| **5** | 353 | 266 | 0 | 0 | 0 | 0 | 0 | 0 | 0 | 0 | 212 | 212 | 212 | 212 | 212 |
| **6** | 448 | 340 | 0 | 0 | 0 | 0 | 0 | 0 | 0 | 0 | 212 | 212 | 212 | 212 | 212 |
| **7** | 449 | 383 | 40 | 0 | 0 | 0 | 0 | 0 | 0 | 0 | 212 | 212 | 212 | 212 | 212 |
| **8** | 447 | 381 | 129 | 0 | 0 | 0 | 0 | 0 | 0 | 0 | 212 | 212 | 212 | 212 | 212 |
| **9** | 370 | 309 | 82 | 0 | 0 | 0 | 0 | 0 | 0 | 0 | 212 | 212 | 212 | 212 | 212 |
| **10** | 272 | 406 | 118 | 0 | 0 | 0 | 0 | 36 | 47 | 21 | 212 | 212 | 212 | 212 | 212 |
| **11** | 454 | 377 | 58 | 82 | 0 | 0 | 0 | 0 | 0 | 0 | 212 | 212 | 212 | 212 | 212 |
| **12** | 454 | 390 | 107 | 95 | 0 | 0 | 0 | 0 | 0 | 0 | 208 | 212 | 212 | 212 | 212 |
| **13** | 332 | 395 | 115 | 59 | 0 | 0 | 0 | 0 | 0 | 0 | 212 | 212 | 212 | 212 | 212 |
| **14** | 305 | 396 | 83 | 117 | 0 | 0 | 0 | 0 | 0 | 0 | 212 | 212 | 212 | 212 | 212 |
| **15** | 433 | 331 | 75 | 117 | 0 | 0 | 0 | 0 | 0 | 0 | 212 | 212 | 212 | 212 | 212 |
| **16** | 232 | 347 | 55 | 80 | 0 | 0 | 0 | 0 | 0 | 0 | 202 | 212 | 212 | 212 | 212 |
| **17** | 235 | 195 | 85 | 104 | 0 | 0 | 0 | 0 | 0 | 0 | 212 | 212 | 212 | 212 | 212 |
| **18** | 282 | 290 | 105 | 112 | 0 | 0 | 0 | 0 | 0 | 0 | 212 | 212 | 212 | 212 | 212 |
| **19** | 446 | 419 | 0 | 90 | 0 | 0 | 0 | 0 | 0 | 0 | 212 | 212 | 212 | 212 | 212 |
| **20** | 166 | 320 | 0 | 88 | 0 | 0 | 0 | 0 | 0 | 0 | 212 | 212 | 212 | 212 | 212 |
| **21** | 286 | 291 | 0 | 0 | 0 | 0 | 0 | 0 | 0 | 0 | 209 | 212 | 212 | 212 | 212 |
| **22** | 431 | 357 | 0 | 0 | 0 | 0 | 0 | 0 | 0 | 0 | 212 | 212 | 212 | 212 | 212 |
| **23** | 166 | 303 | 0 | 0 | 0 | 0 | 0 | 0 | 0 | 0 | 195 | 212 | 212 | 212 | 212 |
| **24** | 285 | 0 | 0 | 0 | 0 | 0 | 0 | 0 | 0 | 0 | 212 | 212 | 212 | 212 | 212 |

**Table 4.33:** Power generation schedule in backpressure mode by BSA-CSO, PBCHPUC test system-III

| | Thermal Units (MW) | | | | | | | | | | CHP Units (MW) | | | | |
|---|---|---|---|---|---|---|---|---|---|---|---|---|---|---|---|
| **h** | **P1** | **P2** | **P3** | **P4** | **P5** | **P6** | **P7** | **P8** | **P9** | **P10** | **P11** | **P12** | **P13** | **P14** | **P15** |
| **1** | 152 | 150 | 20 | 83 | 0 | 78 | 0 | 0 | 0 | 0 | 140 | 140 | 140 | 135 | 137 |
| **2** | 150 | 150 | 20 | 28 | 139 | 78 | 0 | 0 | 0 | 0 | 140 | 140 | 135 | 140 | 140 |
| **3** | 150 | 150 | 20 | 111 | 158 | 71 | 68 | 0 | 0 | 0 | 140 | 140 | 140 | 140 | 140 |
| **4** | 150 | 150 | 20 | 116 | 155 | 78 | 85 | 44 | 45 | 54 | 140 | 140 | 140 | 140 | 140 |
| **5** | 150 | 150 | 102 | 105 | 151 | 80 | 85 | 52 | 49 | 54 | 140 | 140 | 140 | 140 | 140 |
| **6** | 150 | 267 | 126 | 124 | 155 | 78 | 85 | 55 | 54 | 53 | 140 | 140 | 140 | 140 | 140 |

**Table 4.33:** Power generation schedule in backpressure mode by BSA-CSO, PBCHPUC test system-III (Continued)

| | Thermal Units (MW) | | | | | | | | | | CHP Units (MW) | | | | |
|---|---|---|---|---|---|---|---|---|---|---|---|---|---|---|---|
| **h** | **P1** | **P2** | **P3** | **P4** | **P5** | **P6** | **P7** | **P8** | **P9** | **P10** | **P11** | **P12** | **P13** | **P14** | **P15** |
| **7** | 153 | 417 | 107 | 108 | 158 | 80 | 78 | 49 | 40 | 49 | 140 | 140 | 140 | 133 | 140 |
| **8** | 222 | 374 | 130 | 130 | 162 | 67 | 85 | 47 | 47 | 50 | 140 | 140 | 140 | 140 | 140 |
| **9** | 151 | 276 | 116 | 117 | 162 | 73 | 67 | 53 | 53 | 52 | 140 | 140 | 140 | 140 | 140 |
| **10** | 166 | 400 | 126 | 127 | 155 | 66 | 79 | 45 | 55 | 42 | 140 | 140 | 140 | 140 | 140 |
| **11** | 218 | 420 | 129 | 105 | 143 | 68 | 83 | 55 | 55 | 55 | 140 | 140 | 140 | 140 | 140 |
| **12** | 243 | 455 | 120 | 114 | 151 | 80 | 84 | 50 | 48 | 55 | 140 | 140 | 140 | 140 | 140 |
| **13** | 158 | 422 | 127 | 113 | 162 | 65 | 73 | 44 | 46 | 50 | 140 | 140 | 140 | 140 | 139 |
| **14** | 201 | 409 | 109 | 106 | 161 | 70 | 63 | 46 | 47 | 48 | 140 | 140 | 140 | 140 | 140 |
| **15** | 221 | 408 | 129 | 130 | 141 | 63 | 77 | 45 | 55 | 47 | 140 | 140 | 140 | 140 | 140 |
| **16** | 150 | 250 | 128 | 118 | 137 | 70 | 64 | 55 | 38 | 55 | 140 | 140 | 140 | 140 | 140 |
| **17** | 150 | 160 | 124 | 107 | 130 | 63 | 85 | 53 | 54 | 55 | 140 | 140 | 140 | 140 | 140 |
| **18** | 158 | 295 | 122 | 130 | 162 | 76 | 72 | 47 | 32 | 53 | 140 | 140 | 140 | 140 | 140 |
| **19** | 165 | 455 | 125 | 122 | 142 | 73 | 78 | 53 | 50 | 53 | 140 | 140 | 140 | 140 | 140 |
| **20** | 150 | 150 | 71 | 106 | 162 | 73 | 73 | 45 | 48 | 55 | 140 | 140 | 140 | 140 | 140 |
| **21** | 150 | 150 | 90 | 113 | 150 | 68 | 64 | 49 | 44 | 55 | 140 | 140 | 140 | 140 | 140 |
| **22** | 157 | 325 | 105 | 117 | 162 | 71 | 64 | 39 | 55 | 52 | 140 | 140 | 140 | 140 | 140 |
| **23** | 150 | 150 | 20 | 99 | 152 | 64 | 77 | 49 | 0 | 55 | 140 | 140 | 140 | 140 | 135 |
| **24** | 150 | 150 | 20 | 107 | 146 | 73 | 0 | 0 | 0 | 0 | 140 | 140 | 140 | 139 | 140 |

**Table 4.34:** Heat generation schedule in extraction mode by BSA-CSO, PBCHPUC test system-III

| | CHP Units (MWth) | | | | | Heat Unit (MWth) | | | | |
|---|---|---|---|---|---|---|---|---|---|---|
| **h** | **H11** | **H12** | **H13** | **H14** | **H15** | **H16** | **H17** | **H18** | **H19** | **H20** |
| **1** | 331 | 331 | 331 | 331 | 331 | 1000 | 0 | 999 | 564 | 0 |
| **2** | 331 | 331 | 331 | 331 | 331 | 0 | 1000 | 1000 | 1000 | 577 |
| **3** | 331 | 331 | 331 | 331 | 331 | 1000 | 1000 | 1000 | 576 | 0 |
| **4** | 331 | 331 | 331 | 331 | 331 | 1000 | 0 | 1000 | 1000 | 745 |
| **5** | 331 | 331 | 331 | 331 | 331 | 1000 | 1000 | 1000 | 869 | 381 |
| **6** | 331 | 331 | 331 | 331 | 331 | 1000 | 1000 | 949 | 794 | 507 |
| **7** | 331 | 331 | 331 | 331 | 331 | 1000 | 1000 | 1000 | 0 | 913 |
| **8** | 331 | 331 | 331 | 331 | 331 | 1000 | 1000 | 0 | 1000 | 744 |
| **9** | 331 | 331 | 331 | 331 | 331 | 1000 | 1000 | 1000 | 351 | 563 |
| **10** | 331 | 331 | 331 | 331 | 331 | 1000 | 1000 | 817 | 145 | 445 |
| **11** | 331 | 331 | 331 | 331 | 331 | 1000 | 1000 | 0 | 1000 | 576 |
| **12** | 325 | 331 | 331 | 331 | 331 | 1000 | 1000 | 707 | 0 | 706 |
| **13** | 331 | 331 | 331 | 331 | 331 | 1000 | 1000 | 736 | 671 | 0 |
| **14** | 331 | 331 | 331 | 331 | 331 | 1000 | 1000 | 947 | 290 | 0 |
| **15** | 331 | 331 | 331 | 331 | 331 | 1000 | 1000 | 998 | 683 | 401 |
| **16** | 316 | 331 | 331 | 331 | 331 | 1000 | 1000 | 1000 | 664 | 602 |
| **17** | 330 | 331 | 331 | 331 | 331 | 1000 | 1000 | 1000 | 349 | 734 |
| **18** | 331 | 331 | 331 | 331 | 331 | 1000 | 1000 | 1000 | 0 | 914 |
| **19** | 331 | 331 | 331 | 331 | 331 | 1000 | 1000 | 1000 | 844 | 238 |
| **20** | 331 | 331 | 331 | 331 | 331 | 1000 | 1000 | 1000 | 692 | 558 |
| **21** | 326 | 331 | 331 | 331 | 331 | 1000 | 1000 | 498 | 515 | 737 |
| **22** | 331 | 331 | 331 | 331 | 331 | 1000 | 1000 | 1000 | 0 | 576 |
| **23** | 305 | 331 | 331 | 331 | 331 | 1000 | 1000 | 984 | 449 | 0 |
| **24** | 331 | 331 | 331 | 331 | 331 | 0 | 1000 | 1000 | 719 | 687 |

**Table 4.35:** Heat generation schedule in backpressure mode by BSA-CSO, PBCHPUC test system-III

| | CHP Units (MWth) | | | | | Heat Unit (MWth) | | | | |
|---|---|---|---|---|---|---|---|---|---|---|
| **h** | **H11** | **H12** | **H13** | **H14** | **H15** | **H16** | **H17** | **H18** | **H19** | **H20** |
| **1** | 70 | 70 | 212 | 480 | 491 | 1000 | 896 | 0 | 1000 | 0 |
| **2** | 70 | 70 | 91 | 500 | 500 | 1000 | 1000 | 0 | 1000 | 1000 |

**Table 4.35:** Heat generation schedule in backpressure mode by BSA-CSO, PBCHPUC test system-III

| | CHP Units (MWth) | | | | | Heat Unit (MWth) | | | | |
|---|---|---|---|---|---|---|---|---|---|---|
| **h** | **H11** | **H12** | **H13** | **H14** | **H15** | **H16** | **H17** | **H18** | **H19** | **H20** |
| **3** | 70 | 70 | 92 | 500 | 500 | 1000 | 1000 | 999 | 0 | 1000 |
| **4** | 70 | 70 | 313 | 500 | 500 | 1000 | 1000 | 1000 | 0 | 947 |
| **5** | 70 | 336 | 500 | 500 | 500 | 1000 | 1000 | 0 | 1000 | 1000 |
| **6** | 70 | 336 | 500 | 500 | 500 | 1000 | 1000 | 1000 | 1000 | 0 |
| **7** | 72 | 70 | 453 | 474 | 500 | 1000 | 1000 | 1000 | 0 | 1000 |
| **8** | 70 | 70 | 260 | 500 | 500 | 1000 | 1000 | 1000 | 1000 | 0 |
| **9** | 70 | 70 | 465 | 500 | 500 | 0 | 1000 | 1000 | 1000 | 963 |
| **10** | 70 | 70 | 94 | 500 | 500 | 1000 | 1000 | 982 | 846 | 0 |
| **11** | 70 | 70 | 140 | 500 | 500 | 1000 | 1000 | 971 | 980 | 0 |
| **12** | 70 | 70 | 228 | 498 | 500 | 1000 | 1000 | 784 | 0 | 913 |
| **13** | 70 | 70 | 70 | 478 | 497 | 0 | 1000 | 1000 | 1000 | 878 |
| **14** | 70 | 398 | 500 | 500 | 500 | 0 | 0 | 1000 | 1000 | 925 |
| **15** | 70 | 166 | 500 | 500 | 500 | 1000 | 1000 | 1000 | 0 | 1000 |
| **16** | 70 | 336 | 500 | 500 | 500 | 1000 | 1000 | 0 | 1000 | 1000 |
| **17** | 70 | 166 | 500 | 500 | 500 | 1000 | 1000 | 1000 | 0 | 1000 |
| **18** | 70 | 197 | 500 | 500 | 500 | 1000 | 1000 | 1000 | 802 | 0 |
| **19** | 70 | 408 | 500 | 500 | 500 | 1000 | 0 | 1000 | 1000 | 760 |
| **20** | 70 | 362 | 500 | 500 | 500 | 1000 | 0 | 1000 | 1000 | 975 |
| **21** | 70 | 70 | 260 | 500 | 500 | 1000 | 1000 | 1000 | 0 | 1000 |
| **22** | 70 | 70 | 198 | 500 | 500 | 1000 | 1000 | 1000 | 0 | 893 |
| **23** | 70 | 70 | 70 | 426 | 483 | 1000 | 1000 | 994 | 949 | 0 |
| **24** | 70 | 70 | 154 | 496 | 500 | 1000 | 1000 | 773 | 0 | 1000 |

### 4.7.4 Multiobjective Profit Based Combined Heat and Power Unit Commitment Problem

#### 4.7.4.1 Test system-I

The profit and emission values obtained from BPSO-PSO and BSA-CSO techniques have been presented in Tables 4.36 and 4.37 for profit based, emission and MO-PBCHPUC problems. For profit based UC problem, the maximum profit during backpressure and extraction mode operation obtained by the BSA-CSO technique are $433973.3 and $393403.2, respectively. For emission UC problem, the minimum emission obtained from the BSA-CSO technique during backpressure and extraction modes are Kg185991.8 and Kg212979.9, respectively. For the MO-PBCHPUC problem, the profit and emission values during backpressure mode operation are $428897.6 and Kg197454.1, respectively, while in the case of extraction mode, the profit and emission values are $385768.5 and Kg238089.2, respectively obtained by BSA-CSO technique. It is evident from results, that during the backpressure mode of operation, the emission is decreased by 17.1%, and profit is increased by 10.05% with respect to the results during extraction mode. It can be summarized that backpressure mode operation is more beneficial as compared to extraction mode for this test system. It has been observed from Tables 4.36 and 4.37 that the profit and emission obtained from the BSA-CSO technique are better as compare to the BPSO-PSO technique. The power and heat generation for both the modes are shown in Figures 4.44-4.47. Due to the diverse nature of the CHP unit during both modes, the optimum generation schedule is different. It is observed that the total power generation from committed CHP units in extraction mode is higher than the cumulative power generation during backpressure mode. However, during the extraction mode, the committed CHP unit is capable to deliver more heat in comparison with backpressure mode.

**Table 4.36:** Profit and emission for backpressure mode: MO-PBCHPUC test system-I

| | **BPSO-PSO** | | **BSA-CSO** | |
|---|---|---|---|---|
| **CHPUC problem** | **PF ($)** | **TE (Kg)** | **PF ($)** | **TE (Kg)** |
| **Profit** | 432933.8 | 199733.7 | 433973.3 | 200622.1 |
| **Emission** | 409797.5 | 189794.3 | 426953.0 | 185991.8 |
| **Multiobjective** | 431919.6 | 197520.5 | 428897.6 | 197454.1 |

**Table 4.37:** Profit and emission for extraction mode: MO-PBCHPUC test system-I

| | **BPSO-PSO** | | **BSA-CSO** | |
|---|---|---|---|---|
| **CHPUC problem** | **PF ($)** | **TE (Kg)** | **PF ($)** | **TE (Kg)** |
| **Profit** | 384696.1 | 254700.4 | 393403.2 | 251646.6 |
| **Emission** | 375520.8 | 225648.1 | 371807.7 | 212979.9 |
| **Multiobjective** | 373240.8 | 229799.6 | 385768.5 | 238089.2 |

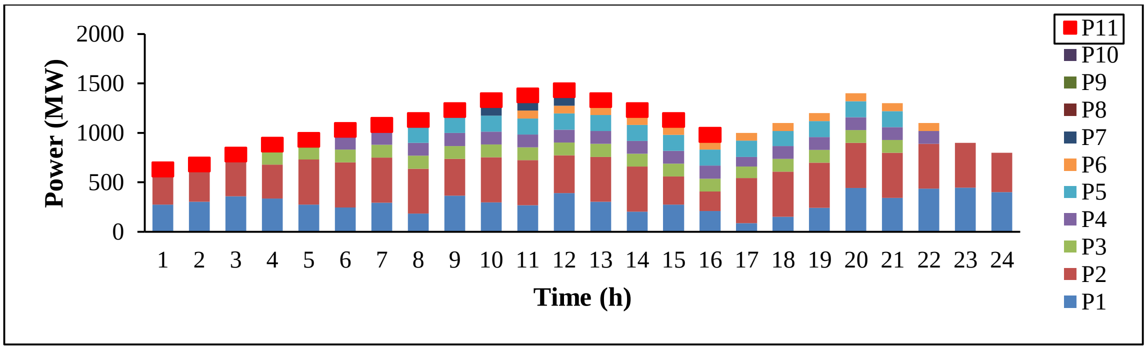


**Figure 4.44:** Power generation from units during backpressure mode: MO-PBCHPUC test system-I

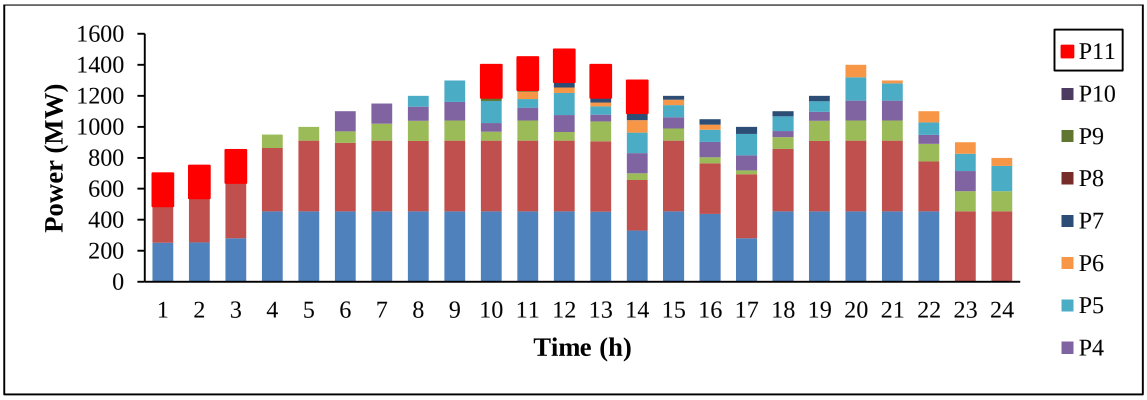


**Figure 4.45:** Power generation from units during extraction mode: MO-PBCHPUC test system-I

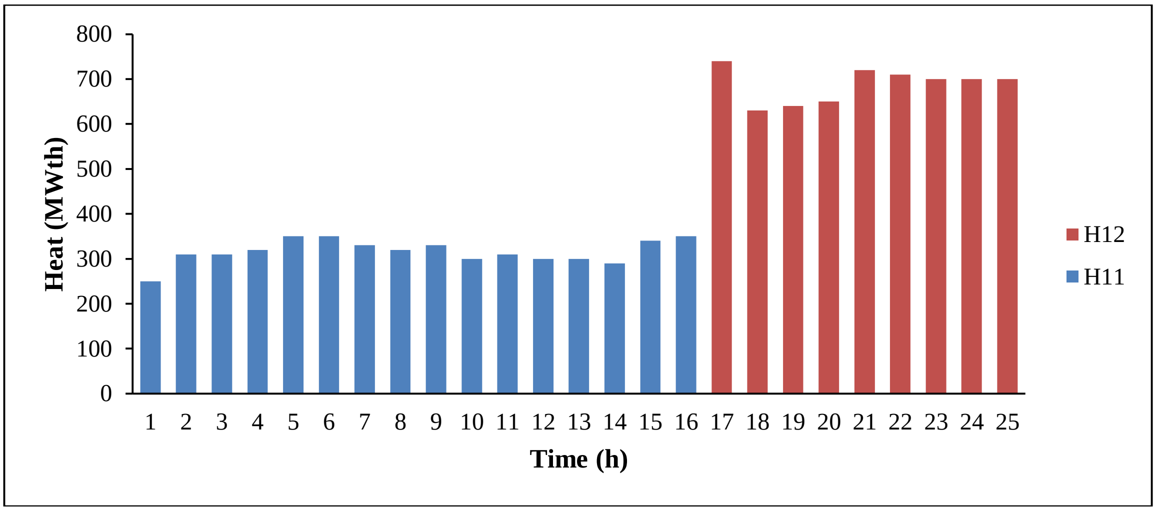


**Figure 4.46:** Heat generation from units during backpressure mode: MO-PBCHPUC test system-I

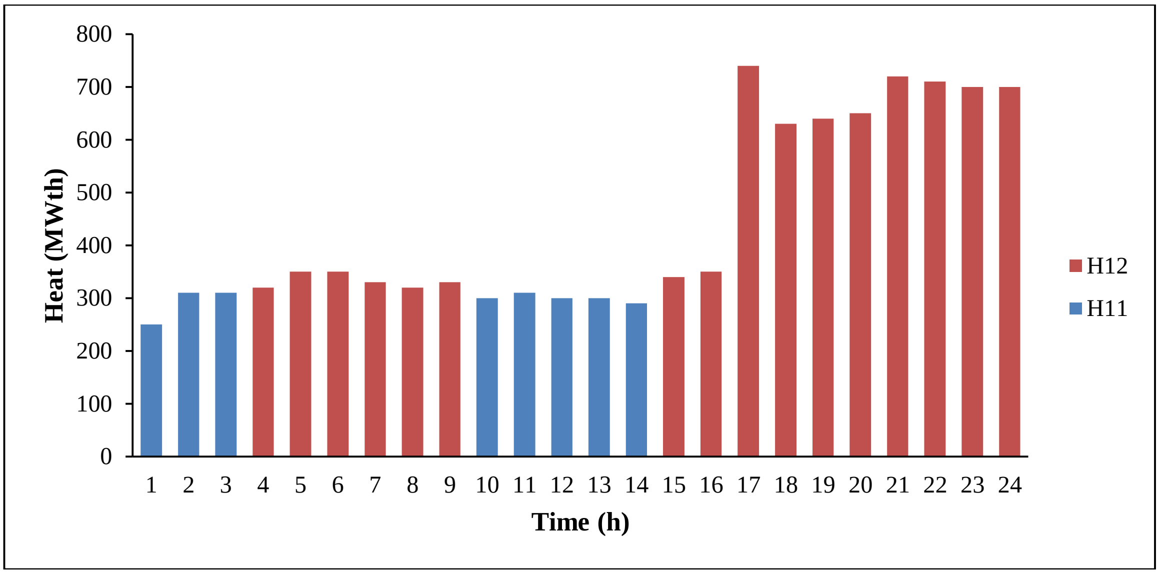


**Figure 4.47:** Heat generation from units during extraction mode: MO-PBCHPUC test system-I

### 4.7.4.2 Test system-II

The profit and emission results are presented in Tables 4.38 and 4.39 for profit, emission, and MO-PBCHPUC problem. It is evident from the obtained results that during the extraction mode of the CHP unit, the maximum profit is more as compared to backpressure mode, and the minimum emission is also less. For the MO-UC problem, it is observed, that extraction mode is more beneficial in terms of profit and emission as compared to backpressure mode results. More specifically, during the extraction mode of CHP unit operation, there is an extra profit of $80416.1, along with the reduction of Kg66051.2 emissions is achieved as compared to backpressure mode operation. As per previous outcome, the BSA-CSO technique is able to produce better quality results as compared to the BPSO-PSO technique. The power and heat generation from the generating units for the MO-CHPUC problem are shown in Figures 4.48-4.51. It is evident that power generation from committed CHP units during extraction mode is more as compared to backpressure mode. However, the heat generation is the same for both modes, because heat unit remains uncommitted during the whole scheduling interval.

**Table 4.38:** Profit and emission for backpressure mode: MO-PBCHPUC test system-II

| | BPSO-PSO | | BSA-CSO | |
|---|---|---|---|---|
| **CHPUC problem** | **PF ($)** | **TE (Kg)** | **PF ($)** | **TE (Kg)** |
| **Profit** | 917632.9 | 183777.2 | 922840.5 | 177558.0 |
| **Emission** | 906180.8 | 178626.9 | 901120.5 | 168528.9 |
| **Multiobjective** | 909904.5 | 181723.7 | 920480.9 | 176945.0 |

**Table 4.39:** Profit and emission for extraction mode: MO-PBCHPUC test system-II

| | BPSO-PSO | | BSA-CSO | |
|---|---|---|---|---|
| **CHPUC problem** | **PF ($)** | **TE (Kg)** | **PF ($)** | **TE (Kg)** |
| **Profit** | 1000543.0 | 125936.0 | 1019038.0 | 115936 |
| **Emission** | 979371.3 | 112584.2 | 978954.4 | 108553.6 |
| **Multiobjective** | 1000398.0 | 112644.5 | 1000897 | 110893.8 |

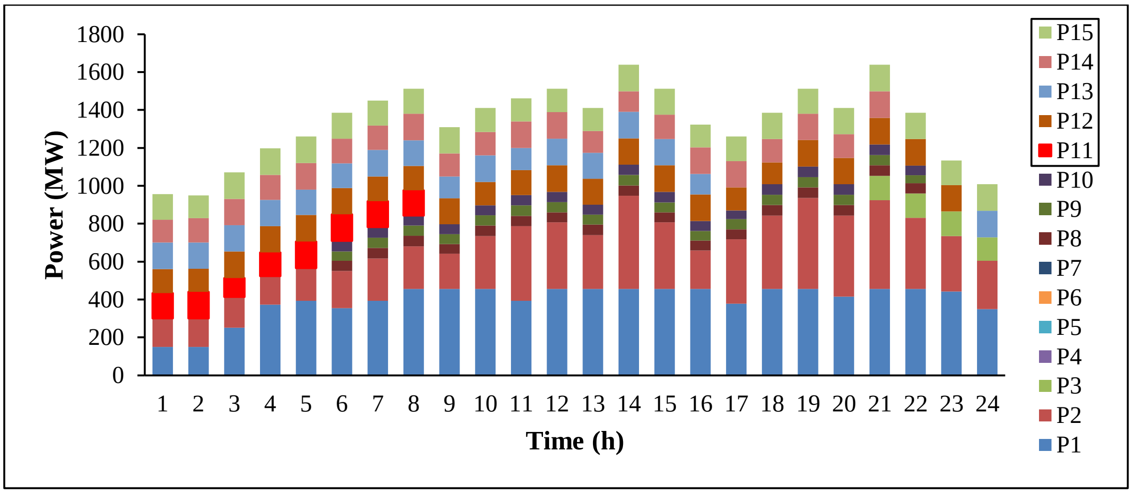


**Figure 4.48:** Power generation from units during backpressure mode: MO-PBCHPUC test system-II

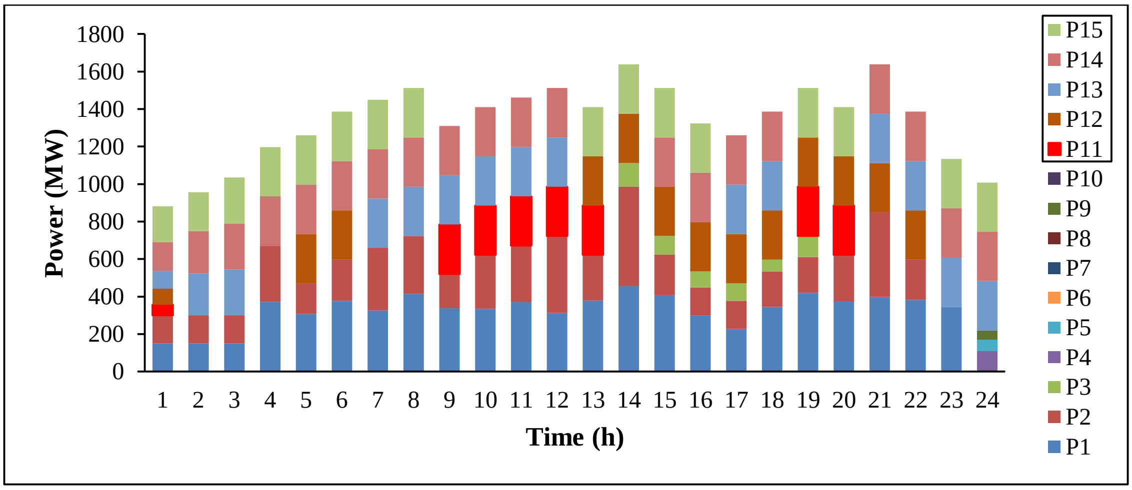


**Figure 4.49:** Power generation from units during extraction mode: MO-PBCHPUC test system-II

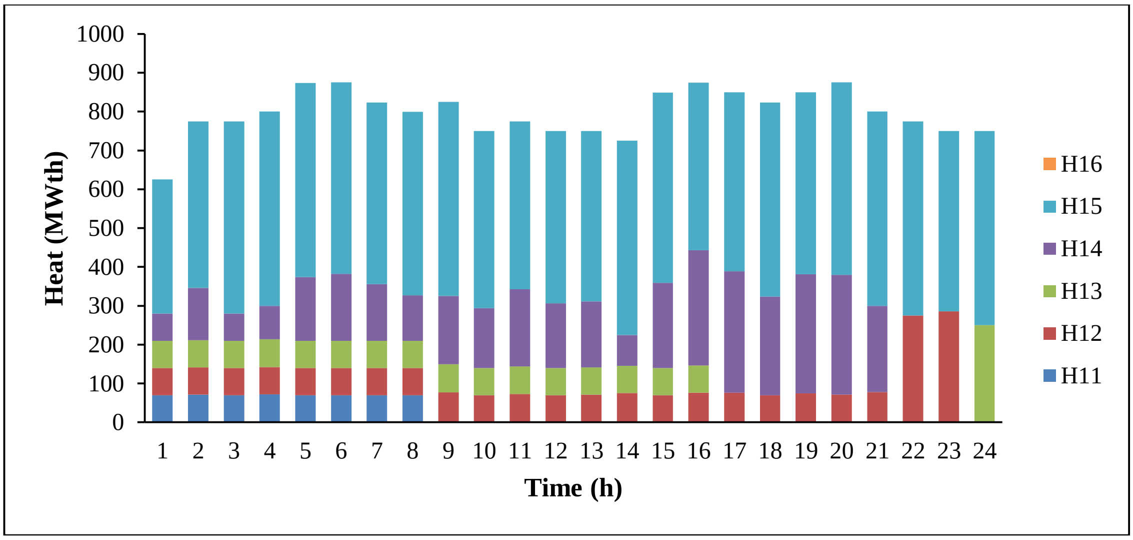


**Figure 4.50:** Heat generation from units during backpressure mode: MO-PBCHPUC test system-II

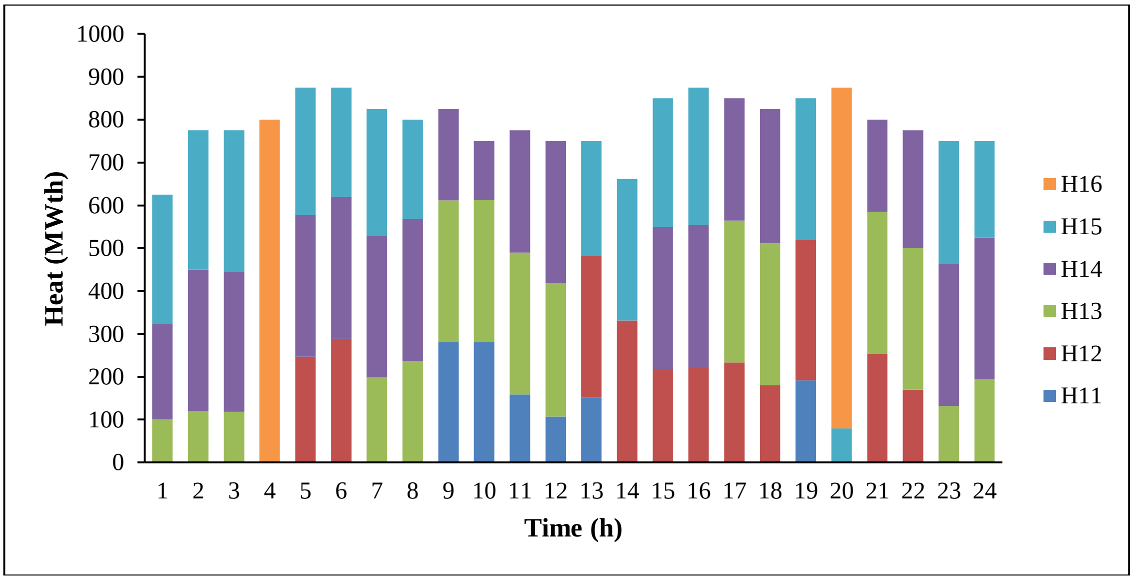


**Figure 4.51:** Heat generation from units during extraction mode: MO-PBCHPUC test system-II

### 4.7.4.3 Test system-III

For profit, emission and MO-CHPUC problems, the obtained results from BSA-CSO and BPSO-PSO techniques are presented in Tables 4.40 and 4.41. It is evident from results that for profit based CHPUC problem, extraction mode is more beneficial as compared to backpressure mode, while for emission CHPUC problem, the backpressure mode performs better in comparison with extraction mode. For the MO-CHPUC problem, during the extraction mode operation, profit obtained from the BSA-CSO technique is increased by 7.14%, and the emission is degraded by 4.09% as compared to backpressure mode. The power and heat generation schedule for both modes of the committed CHP unit, thermal and heat units are shown in Figures 4.52-4.55. From these figures, it is illustrated that the total heat generation from the committed CHP unit is more during backpressure mode operation as compared to extraction mode, however, the total power generation during extraction mode is more as compared to backpressure mode. Hence, it is summarized that the backpressure and extraction mode of the CHP unit significantly affects the optimum generation schedule.

**Table 4.40:** Profit and emission for backpressure mode: MO-PBCHPUC test system-III

| | BPSO-PSO | | BSA-CSO | |
|---|---|---|---|---|
| **CHPUC problem** | **PF ($)** | **TE (Kg)** | **PF ($)** | **TE (Kg)** |
| **Profit** | 3912975.0 | 132617.0 | 3913846 | 132542.7 |
| **Emission** | 3909475.0 | 130421.5 | 3902032.0 | 130241.2 |
| **Multiobjective** | 3909499 | 131886.5 | 3913682 | 131695.8 |

**Table 4.41:** Profit and emission for extraction mode: MO-PBCHPUC test system-III

| | BPSO-PSO | | BSA-CSO | |
|---|---|---|---|---|
| **CHPUC problem** | **PF ($)** | **TE (Kg)** | **PF ($)** | **TE (Kg)** |
| **Profit** | 4217052 | 141860.2 | 4222867 | 144500.9 |
| **Emission** | 4208962 | 142098.9 | 4205244 | 136088 |
| **Multiobjective** | 4213688 | 137557.5 | 4214814 | 137323.5 |

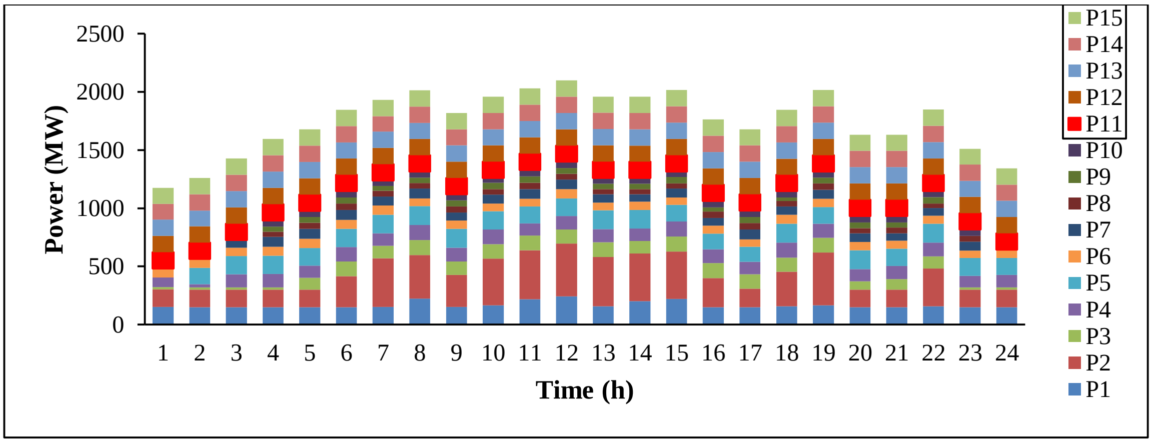


**Figure 4.52:** Power generation from units during backpressure mode: MO-PBCHPUC test system-III

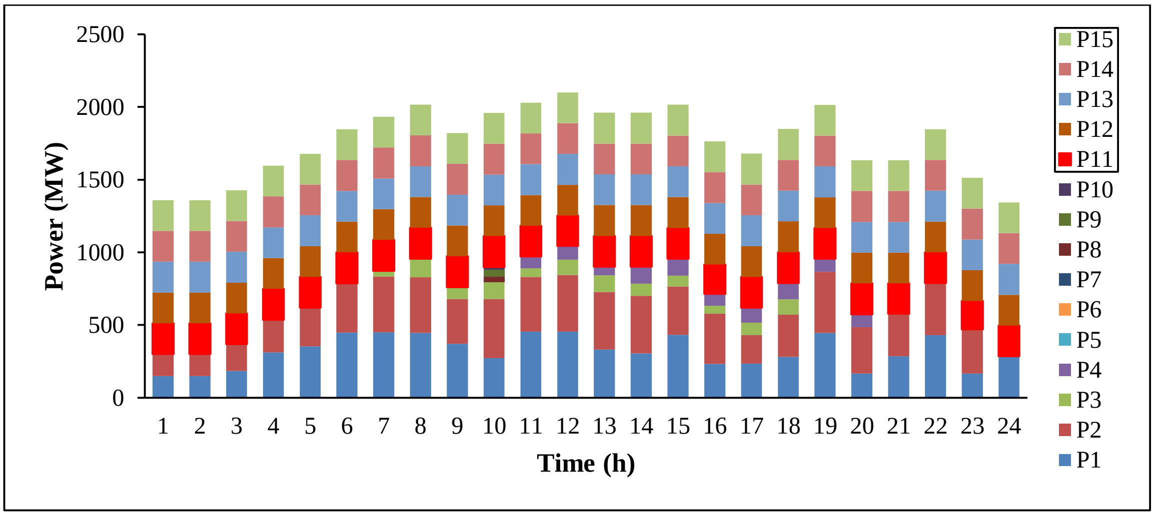


**Figure 4.53:** Power generation from units during extraction mode: MO-PBCHPUC test system-III

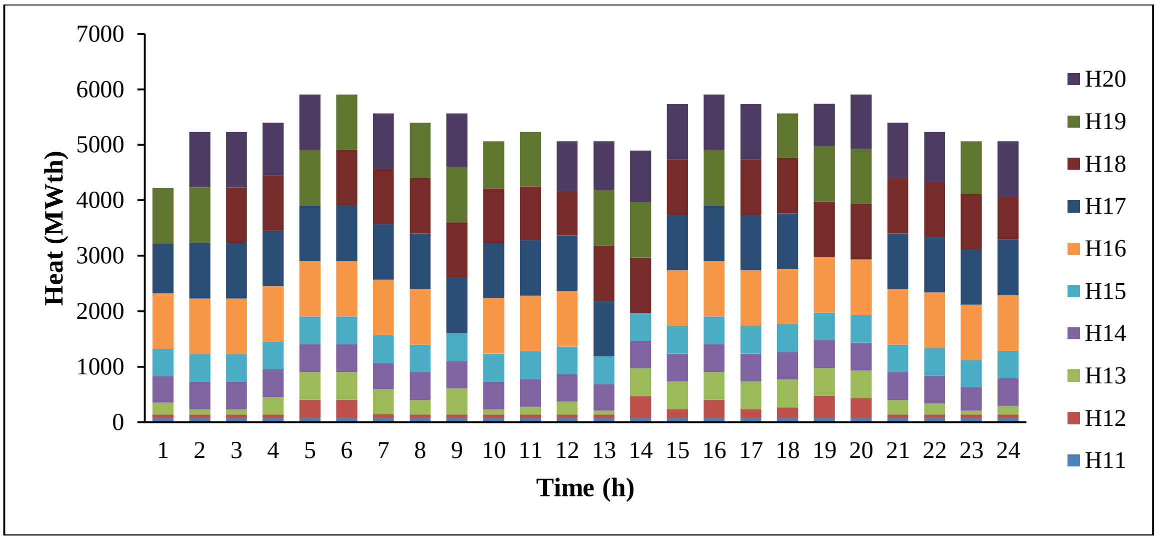


**Figure 4.54:** Heat generation from units during backpressure mode: MO-PBCHPUC test system-III

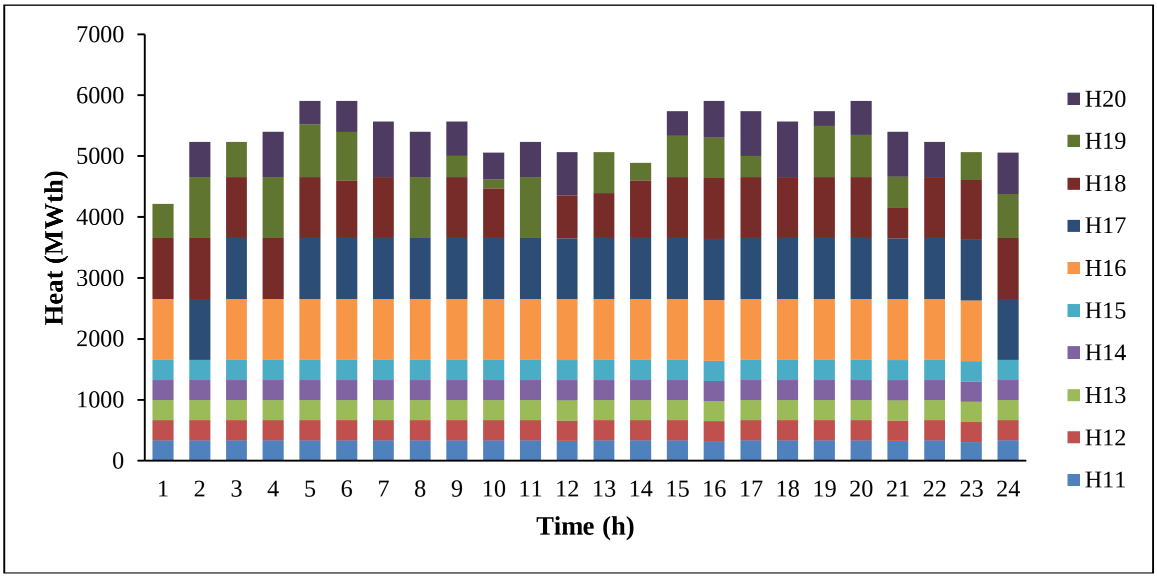


**Figure 4.55:** Heat generation from units during extraction mode: MO-PBCHPUC test system-III

## 4.8 CONCLUSIONS

The current challenge faced by system operators is to find the optimum UC and generation schedule of combined heat and power systems. In this work, the BPSO-PSO and BSA-CSO techniques with fuzzy membership method have been implemented to solve the dual-mode multiobjective CHPUC problem. The BSA method is used to search the optimum unit status with the minimum computational burden and the CSO technique is applied to search the optimum generation schedule of the committed units. The three dual mode CHPUC test systems have been undertaken to analyze the impact of extraction and backpressure mode of the CHP unit on the optimum generation and system generation flexibility. The results of three test systems revealed that DM-CHP units significantly affect the optimum UC status and generation schedule. It has observed that the operating cost obtained from the BSA-CSO technique during extraction mode of the CHP unit for scalar CHPUC test systems-I, II, and III are less by 3.89%, 47.3%, and 17.5%, respectively as compared to backpressure mode. For the scalar PBCHPUC test system-I, the profit during the extraction mode of the CHP unit is less by 9.34% as compared to backpressure mode. However, for test system-II and III, profit is more during the extraction mode of operation as compared to backpressure mode.

For test system-I, in the MO-CHPUC problem, the cost and emission obtained from the BSA-CSO technique during the extraction mode of CHP unit are lower by 3.83% and 4.49%, respectively as compared to backpressure mode. Similarly, for test system-II and III, the cost and emission from the BSA-CSO technique during extraction mode are lower as compared to the backpressure mode of operation. In the MO-PBCHPUC problem, the profit obtained from the BSA-CSO technique for test system-I, during the backpressure mode of CHP unit is high as compared to extraction mode whereas emission obtained in backpressure mode is less as compared to extraction mode. In test system-II and III, the profit obtained from the BSA-CSO technique during extraction mode is high as compared to the backpressure mode. In test system-II, emission obtained during extraction mode is less as compared to backpressure mode. However, the reverse trend is observed in the test system-III. It has also observed that the results obtained from the BSA-CSO technique are better as compared to the BPSO-PSO technique. Further, it has verified that total power generation during extraction mode of the committed CHP unit is more as compared to backpressure mode, which provides more power flexibility to the combined system. However, the backpressure mode of operation offers high heat flexibility as compared to the extraction mode.

# CHAPTER – 5

# INTEGRATED SOLAR AND COMBINED HEAT AND POWER UNITS COMMITMENT SCHEDULE

## 5.1 INTRODUCTION

The cogeneration unit has an important contribution to meet global electrical and heat demand. The *combined heat and power* (CHP) unit is highly efficient as compared to the heat and thermal only units **(Kerr, 2010)**. There are various types of cogeneration units such as extraction steam turbine, backpressure steam turbine, and a condensing steam turbine used for large scale commercial and industrial purposes **(Kerr, 2008)**. Researchers have up-gradated the cogeneration units by replacing the single-shaft turbine with multi-shaft turbines **(Breeze, 2019)**. The *dual-mode CHP* (DM-CHP) unit is a combination of backpressure and extraction steam turbine **(Breeze, 2019)**. The DM-CHP plant has an additional facility such as the flexible power provided by extraction mode and higher heat generation during backpressure mode **(Zugno *et al.*, 2016)**. The heat and power generation produces a significant amount of emissions pollutants **(Selvakumar *et al.*, 2016)**. Hence, concerns have been raised to a significant reduction of the pollutant from the energy generation sector **(Shukla and Singh, 2016[1,2])**. To attain this aim, the energy sector significant increase in the usage of *renewable energy sources* (RES). The ideology of unlimited growth and the industrialist agenda of RES lead the RES as the largest source of electricity by 2050 **(Burke and Stephens, 2018)**. It is expected that *photovoltaic* (PV) technology will share 20% of energy consumption by 2030 **(Patwal and Narang, 2018)**. Hence, the penetration of energy generation from PV in the system is increased. The presence of RES in the *combined heat and power system* (CHPS) has increased the complexity of the system operator **(Wu *et al.*, 2015)**. The proper utilization of cogeneration, thermal, heat, and RES in modern heat and power systems is an important task.

Researchers are focusing on different strategies of combined PV and heat-power system to unlock the full potential of CHP. In 2018, Kasaeiana *et al.* **(2018)** have presented a review article on CHPS incorporate solar and concentrated PV/thermal systems. It has been concluded that *integrated CHPS* (ICHPS) extensively need the *unit commitment* (UC) schedule and economic dispatch problem for the analysis of system power flexibility **(Kasaeiana *et al.*, 2018)**. The operational power flexibility is an essential need of power systems operation. In the presence scenario of the German Power Grid, there is a requirement of generation flexibility options such as DM-CHP, *energy storage unit* (ESU) **(Kopiske *et al.*, 2017)**. The ESU is considered a key element to improving the power flexibility **(Kneiske and Braun, 2017)**. The integrated CHP and PV-ESU system has significant potential in the power sector. The efforts of researchers are underway in many emerging areas of ICHPS such as UC, integration of CHPS with PV and ESU, DM-CHP unit, and generation flexibility. The *CHP unit commitment* (CHPUC) problem is a fundamental part of ICHPS. The *unit commitment* (UC) problem become more complicated in the presence of DM-CHP unit and PV-ESU. A review of studies related to the important aspects of CHP and integrated system are covered in the literature survey.

The CHPUC problem is a real-world non-deterministic polynomial hard optimization problem, hence optimization methods have been applied to find the generation schedule of CHPS at a minimum operational cost **(Wang *et al.*, 2017)**. The various optimization techniques have applied by researchers to solve the CHPUC problem, and it is discussed in section 1.2.3 of Chapter 1. Researchers have worked on the integration of RES with combined heat and power system. The optimum schedule of an integrated PV system has been obtained by two-stage stochastic mixed-integer programming **(Schwarza *et al.*, 2018)**. The combined control algorithm based on cloud-based application has been applied to find the optimum solution of the PV-CHP system of Germany **(Kneiske *et al.*, 2018)**. The generic MILP technique has been implemented to obtain the optimum generation schedule of the integrated UC model of Greek interconnected electric system **(Koltsaklisa *et al.*, 2017)**. Dai *et al.* **(2017)** have worked on the CHPS incorporation of ESU of Northern China. The MILP **(Javadi *et al.*, 2017)** and non-dominated sorting genetic algorithm-II **(Shang *et al.*, 2017)** have been applied to find the optimal schedule of the integrated system comprise of CHP and ESU units. Kneiske and Braun **(2017)** have obtained the generation schedule of CHPS incorporating PV and ESU. The Markov decision process has been applied to obtain the optimum schedule of generating units in ICHPS **(Lan *et al.*, 2016)**. The literature review on the optimum generation schedule of ICHPS has been presented by Lia *et al.* **(2018)**. In the light of recent events in the co-optimization of different energy systems, the study of mixed-integer CHPUC problem with RES is still in the evolving stage. Researchers have not investigated certain research areas of ICHPS in detail, which are identified as:

1) The impact of PV and ESU on the UC of CHPS has not studied in previous researches;

2) The integrated PV, ESU, and the power-heat system does not analyze the effect of DM-CHP;

The intent of this Chapter is to investigate the dual mode CHPUC model with consideration of PV and ESU. The *binary successive approximation* (BSA) and *civilized swarm optimization* (CSO) (BSA-CSO) technique has been applied to solve the mixed-integer *integrated combined heat and power unit commitment* (ICHPUC) problem. The BSA-CSO technique is discussed in sections 2.3 and 2.4 of Chapter 2. Further, in order to deal with the CHPUC constraint such as spinning reserve and minimum up and down time constraints, the constraint handling scheme is discussed in section 4.5.1 of Chapter 4. The schematic graphical representation of ICHPS is presented in Figure 5.1.

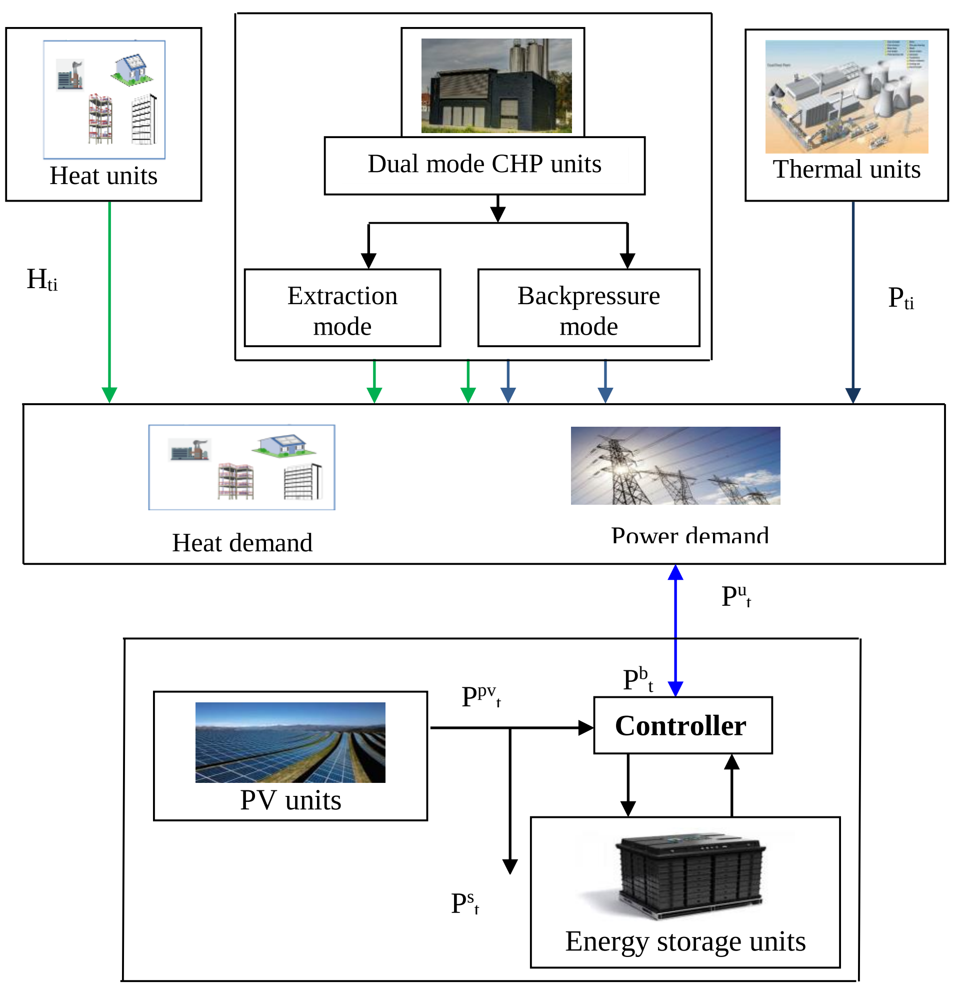


**Figure 5.1:** System description of ICHPS

The ICHPS constitutes of power units (ESU, PV array, conventional thermal and DM-CHP units), heat units (DM-CHP and heat units), and consumer end (heat and power load). In the ICHPS, the power and heat are generated simultaneously during backpressure and extraction mode of the cogeneration plant. The total electric power is provided by conventional thermal, CHP, PV and ESU in generating mode, whereas the total heat is provided by CHP and only heat units. The generated power is utilized to charge the ESU and meet consumer end demand. The ESU operates either in a charging or discharging mode. The power flow is bi-directional between ESU and utility. The operating mode of battery relies on the PV and power availability from the utility (during off-peak load and peak load sub-intervals). The aim of ICHPUC is to find the optimum power and heat generation schedule to meet the consumer demand throughout day and night at minimum operating cost with the satisfaction of all the operational constraints.

## 5.2 THE GENERATING UNITS DESCRIPTION

The mathematical modeling of solar PV unit and *energy storage system* (ESS), DM-CHP, thermal and heat units are discussed in the following sub-sections.

### 5.2.1 Solar Photovoltaic Cell

In this model, the power generation is a function of incident solar radiation, the ambient temperature, and temperature coefficient. The mathematical representation of power generation is given as **(Patwal and Narang, 2018)**:

$$P_t^{pv} = f(SR_t, T_t^c) \qquad t \in [1,T] \qquad (5.1)$$

$$P_t^{pv} = PR\left\{1 + \left(T_r - T_t^c\right)\alpha\right\}\frac{SR_t}{1000} \qquad t \in [1,T] \qquad (5.2)$$

The cost of the solar share can be formulated as:

$$C_{pv} = PU_c P_t^{pv} \qquad t \in [1,T] \qquad (5.3)$$

where $P_t^{pv}$ is the power generation from PV unit at the $t^{th}$ sub-interval (MW); $PR$ is the rated power generation from PV unit (MWm$^2$/W); $SR_t$ is the incident solar radiation at the $t^{th}$ sub-interval (W/m$^2$); $T_r, T_t^c$ are the reference and PV temperature ($^0$C), respectively; $PU_c$ is the per unit cost of PV power ($/MW); $\alpha$ is temperature coefficient ($1/{}^{0}C$); and $C_{pv}$ is the fuel cost of PV unit ($).

### 5.2.2 Energy Storage System

In this system, the cost function is formulated for energy storage system using the quadratic and it is specified as **(Sedighizadeh *et al.*, 2018)**:

$$C_{b,ti} = ab_i (P_t^b)^2 + bb_i P_t^b + cb_i \qquad t \in [1,T], i \in [1,Nb] \qquad (5.4)$$

where $C_{b,ti}$ is the fuel cost of $i^{th}$ battery at the $t^{th}$ sub-interval ($); $ab_i, bb_i, cb_i$ are the cost coefficients; and $P_{ti}^b$ is the power generation from $i^{th}$ battery at the $t^{th}$ sub-interval (MW).

The cost function of the ESUs only involves charging cost because of the discharging cost is considerably lower than the charging cost. The power generation and charge available from ESS must satisfy the electrical storage (Eq. 5.5), charge/discharge (Eq. 5.6) limits of battery and given as **(Marwali *et al.*, 1998)**:

$$\left|P_t^b\right| \le \overline{P^b} \qquad t \in [1,T] \qquad (5.5)$$

$$\underline{Q} \le Q_t \le \overline{Q} \qquad t \in [1,T] \qquad (5.6)$$

The available states of charge (SOC) at starting ($Q_s$) and final ($Q_f$) sub-intervals are given as:

$$Q_{t=0} = Q_s \qquad (5.7)$$

$$Q_{t=T} = Q_f \qquad (5.8)$$

The power generation from PV panel is either flow to controller or power spillage ( $P_t^s$ ).The bi-directional power ( $P^u$ ) flow between utility and ESS that allowed the battery to operate either in charging or discharging mode. The PV-battery constraints for electric storage model is given as follows **(Marwali *et al.*, 1998)**:

$$Q_t = Q_{t-1} + \left[\frac{\Delta t \eta_b}{V_t^b}\left(P_t^{pv} - P_t^u - P_t^s\right)\right] \qquad t \in [1,T] \qquad (5.9)$$

where

$$P_t^u = \frac{(Q_{t-1} - Q_t) \times V_t^b}{\Delta t \eta_b} + P_t^{pv} - P_t^s \qquad t \in [1,T] \qquad (5.10)$$

$$\left| P_t^u \right| \leq \overline{P^u} \qquad t \in [1,T] \qquad (5.11)$$

$$P_t^{pv} - P_t^b - P_t^u - P_t^s = 0 \qquad t \in [1,T] \qquad (5.12)$$

$$P_t^b = P_t^{pv} - P_t^u - P_t^s \qquad t \in [1,T] \qquad (5.13)$$

where $P_t^{pv}$ is the generated power from PV panel at $t^{th}$ sub-interval (MW); $P_t^b$ is the generated power from battery at $t^{th}$ sub-interval (MW); $P_t^u$ is the utility power (a positive value states, power flow from PV-ESS to utility and a negative value states, as power flow from utility to PV-ESS) (MW); $P_t^s$ is the spillage power at $t^{th}$ sub-interval (MW); $Q_t$ is the battery state of charge at $t^{th}$ sub-interval (Ah); $\overline{P^b}$ is the maximum power limit of battery (MW); $Q_S$, $Q_f$ are the initial and final state of charge (Ah); $\underline{Q}$, $\overline{Q}$ are the lower and upper state of charge of battery (Ah), respectively; $V_t^b$ is the battery voltage at $t^{th}$ sub-interval (V); $Nb$ is the number of batteries; and $\eta_b$ is the battery efficiency.

### 5.2.3 Heat and Power Units

The mathematical modelling of the DM-CHP, thermal and heat units are discussed in section 4.2 of Chapter 4. The operating mode of CHP units such as backpressure and extraction mode with their operational constraints are discussed in sub-sections 4.2.1.1 and 4.2.1.2 of Chapter 4, respectively.

## 5.3 INTEGRATED UNITS COMMITMENT PROBLEM

The ICHPUC is a mixed integer problem since the status of generating units is controlled by binary decision variables (I) and the generation schedule is controlled by the continuous nature of decision variables (P, H). The decision variables (X) matrix is given as:

Unit status | Power and Heat generation

Thermal | CHP | Heat | Thermal | CHP | Heat | PV

$$X = \begin{bmatrix} I_{1,1} & \cdots & I_{1,Ng} & I_{1,1} & \cdots & I_{1,Nc} & I_{1,1} & \cdots & I_{1,Nh} & P^{th}_{1,1} & \cdots & P^{th}_{1,Ng} & P^{c}_{1,1} & \cdots & P^{c}_{1,Nc} & H^{c}_{1,1} & \cdots & H^{c}_{1,Nc} & H^{h}_{1,1} & \cdots & H^{h}_{1,Nh} & P^{pv}_{1} & P^{b}_{1} \\ \vdots & \vdots & \vdots & \vdots & \vdots & \vdots & \vdots & \vdots & \vdots & \vdots & \vdots & \vdots & \vdots & \vdots & \vdots & \vdots & \vdots & \vdots & \vdots & \vdots & \vdots & \vdots & \vdots \\ I_{T,1} & \cdots & I_{T,Ng} & I_{T,1} & \cdots & I_{T,Nc} & I_{T,1} & \cdots & I_{T,Nh} & P^{th}_{T,1} & \cdots & P^{th}_{T,Ng} & P^{c}_{T,1} & \cdots & P^{c}_{T,Nc} & H^{c}_{T,1} & \cdots & H^{c}_{T,Nc} & H^{h}_{T,1} & \cdots & H^{h}_{T,Nh} & P^{pv}_{T} & P^{b}_{T} \end{bmatrix} \quad (5.14)$$

where $I_{ti}$ is the unit status of $i^{th}$ unit at $t^{th}$ sub-interval; $P^{th}_{ti}$ is the generated power from $i^{th}$ thermal unit at $t^{th}$ sub-interval; $P^{c}_{tj}, H^{c}_{tj}$ are the power and heat generation from $j^{th}$ DM-CHP unit at the $t^{th}$ sub-interval; $H^{h}_{tm}$ is the heat generated from $m^{th}$ heat unit at the $t^{th}$ sub-interval; $P^{pv}_{t}$ is the power generation from PV unit at $t^{th}$ sub-interval; $P^{u}_{t}$ is the utility power at $t^{th}$ sub-interval; $N_c$ is the number of DM-CHP units; $N_h$ is the number of heat units; $Ng$ is the number of thermal power units and $T$ is the total sub-intervals.

The objective function, unit commitment and generation constraints of ICHPUC problem are discussed in the following sub-sections:

### 5.3.1 Objective Function

The main objective of the ICHPUC problem is to minimize the system operating cost. The mathematical representation of the total operating cost is given as:

$$TC = \sum_{t=1}^{T} \begin{bmatrix} \sum_{i=1}^{Ng} C_g(P^{th}_{ti}) I_{ti} + \sum_{j=1}^{Nc} C_c(P^{c}_{tj}, H^{c}_{tj}) I_{tj} + \sum_{m=1}^{Nh} C_h(H^{h}_{tm}) I_{tm} \\ + \sum_{n=1}^{N} ST_{tn} + C_{pv,t} + \sum_{k=1}^{Nb} C_{b,tk} \end{bmatrix} \quad (5.15)$$

where $TC$ is the total cost for energy generation (\$); $ST_{tn}$ is the start-up of $n^{th}$ units at $t^{th}$ sub-interval (\$); $P^{th}_{ti}$ is the power output from $i^{th}$ units at $t^{th}$ sub-interval (MW); $H^{h}_{tm}$ is the heat output from $m^{th}$ units at $t^{th}$ sub-interval (MWth); $C_g, C_c, C_h, C_{pv}$ and $C_b$ are the fuel cost of thermal, CHP, heat, PV and ESU units ($), respectively; $I_{ti}$ is the $i^{th}$ unit ON/OFF status at $t^{th}$ sub-interval; *N* is the total number of units; $Ng$ is the total number of thermal units; $N_c$ is the total number of CHP units; $N_h$ is the total number of heat units; $N_b$ is the total number of battery; and *T* is the total time interval.

### 5.3.2 Unit Commitment Constraints

**i) Spinning reserve constraints:** The spinning reserve has been considered as a tool to sustain the system reliability due to the unpredictability of forecasted demand and unit unavailability **(Nazari and Ardehali, 2017)**. Therefore, the maximum possible power and heat generated from the unit must be greater than or equal to the load demand along with reserve requirement.

*Power spinning reserve constraint:* In this system, the battery can work as a load or source. Therefore, the power flow from PV-ESU to utility is treated as a source and it is given by Eq. (5.16). However, if the power flows from utility to PV-ESU then it is treated as load and it is given by Eq. (5.17). The power spinning reserve constraint is defined as:

$$\sum_{i=1}^{Ng} \overline{P_i^{th}} I_{ti} + \sum_{j=1}^{Nc} P_{tj}^{c}(H_{tj}^{c}) I_{tj} + P_t^{u} \geq PD_t + SP_t \qquad t \in [1,T] \qquad (5.16)$$

$$\sum_{i=1}^{Ng} \overline{P_i^{th}} I_{ti} + \sum_{j=1}^{Nc} P_{tj}^{c}(H_{tj}^{c}) I_{tj} \geq PD_t + SP_t + P_t^{u} \qquad t \in [1,T] \qquad (5.17)$$

where $I_{ti}$ is the $i^{th}$ unit ON/OFF status of generating unit at $t^{th}$ sub-interval; $\overline{P_i^{th}}$ is the upper power limit of $i^{th}$ unit (MW); $P_{tj}^{c}$ is the power generation from $j^{th}$ CHP unit for backpressure and extraction mode at $t^{th}$ sub-interval (MW); $PD_t$ and $SP_t$ are the power demand and spinning reserve requirement at $t^{th}$ sub-interval, respectively (MW).

*Heat spinning reserve constraint:* The maximum possible heat generated from the unit must be greater than or equal to the load demand along with reserve requirement. The heat spinning reserve constraint is defined as:

$$\sum_{j=1}^{Nc} \overline{H_j^{c}} I_{tj} + \sum_{m=1}^{Nh} \overline{H_m^{h}} I_{tm} \geq HD_t + SH_t \qquad t \in [1,T] \qquad (5.18)$$

where $I_{tj}$ is the $j^{th}$ unit ON/OFF status at $t^{th}$ sub-interval; $\overline{H_m^h}$ is the upper heat limit of $m^{th}$ heat unit (MWth); $\overline{H_j^c}$ is the heat generation from $j^{th}$ CHP unit for backpressure and extraction mode at $t^{th}$ sub-interval (MWth); $HD_t$ and $SH_t$ are the heat demand and spinning reserve requirement at $t^{th}$ sub-interval, respectively (MWth).

**ii) Minimum up and down time:** For committing and de-committing unit, the temperature of the boiler must be maintained during turn on or off the unit and it is given in Eq. (2.4) of Chapter 2.

### 5.3.3 Generation Constraints

The generation constraints imposed on PV, ESU, CHP, conventional heat and thermal units are discussed in section 5.2. For the ICHPS, the heat and power balance constraints are given as follows:

*Power demand constraint:* The power supplied from generating units and ESS must satisfy the forecasted power demand at each sub-interval, which is given as:

$$\sum_{i=1}^{Ng} P_{ti} I_{ti} + \sum_{j=1}^{Nc} P_{tj}^{c} I_{tj} + P_t^u = PD_t \qquad t \in [1,T] \qquad (5.19)$$

*Heat demand constraint:* The generated heat must satisfy the heat demand at each sub-interval, which is given as:

$$\sum_{j=1}^{Nc} H_{tj}^{c} I_{tj} + \sum_{m=1}^{Nh} H_{tm} I_{tm} = HD_t \qquad t \in [1,T] \qquad (5.20)$$

## 5.4 IMPLEMENTATION OF HYBRID OPTIMIZATION TECHNIQUE TO SOLVE INTEGRATED UNITS COMMITMENT PROBLEM

The optimization technique based on the integration of BSA and CSO techniques has been applied to update unit status and obtain the generation schedule of the committed unit, respectively. The BSA-CSO technique is discussed in sections 2.3 and 2.4 of Chapter 2. The steps for implementation of BSA-CSO to solve the ICHPUC problem are given as follows:

**Step 1:** Read input data of generating units and set the BSA-CSO parameters.

**Step 2:** Randomly initialize the unit status and power/heat generation.

**Step 3:** The unit commitment status of generating units is updated using the BSA algorithm as given in sub-section 4.5.2 of Chapter 4. The obtained unit status must satisfy the unit commitment constraints.

**Step 4:** The CSO technique is applied to find the optimum power/heat generation schedule of the unit status obtained from the BSA approach and objective function is evaluated. In order to satisfy generation constraints, generation, charging/discharging (Eqs. 5.6-5.13) and ramp limits, the exterior penalty method is used. The overall objective function (*obj*) is expressed as:

$$obj = TC + \varphi E \tag{5.21}$$

where $\varphi$ is the penalty factor; $E$ represents the total error and *obj* is the overall objective function.

$$E = \sum_{t=1}^{T} [ E_t^1 + E_t^2 + E_t^3 + E_t^4 + E_t^5 + E_t^6 + E_t^7 ] \tag{5.22}$$

The error for violating final charge, battery capacity and utility limit are computed as:

$$E_t^1 = \begin{cases} (Q_T - Q_f)^2 ; Q_T \neq Q_f \\ 0; \quad otherwise \end{cases} \qquad t \in [1,T] \tag{5.23}$$

$$E_t^2 = \begin{cases} (P_t^u - \overline{P_t^u})^2 ; P_t^u > \overline{P_t^u} \\ 0; \quad otherwise \end{cases} \qquad t \in [1,T] \tag{5.24}$$

$$E_t^3 = \begin{cases} (P_t^b - \overline{P_t^b})^2 ; P_t^b > \overline{P_t^b} \\ 0; \quad otherwise \end{cases} \qquad t \in [1,T] \tag{5.25}$$

The error for mismatch of power and heat demand constraint is evaluated at each sub-interval.

$$E_t^4 = \begin{cases} \left( \sum_{i=1}^{Ng} P_{ti}^{th} I_{ti} + \sum_{j=1}^{Nc} P_{tj}^{c} I_{tj} + P_t^u - PD_t \right)^2 ; & \sum_{i=1}^{Ng+Nc} P_{ti} + P_t^u \neq PD_t \\ \left( \sum_{i=1}^{Ng} P_{ti}^{th} I_{ti} + \sum_{j=1}^{Nc} P_{tj}^{c} I_{tj} - P_t^u - PD_t \right)^2 ; & \sum_{i=1}^{Ng+Nc} P_{ti} \neq P_t^u + PD_t \end{cases} \qquad t \in [1,T] \tag{5.26}$$

$$E_t^5 = \left( HD_t - \sum_{j=1}^{N_c} H_{tj}^{be} - \sum_{m=1}^{N_h} H_{tm} \right)^2 ; \sum_{i=1}^{N_c+N_h} H_{ti} \neq HD_t \qquad t \in [1,T] \qquad (5.27)$$

The $E_t^6$ is the error for violating the fuel limit of heat and DM-CHP unit which is given in Eq. (4.40) of Chapter 4. The $E_t^7$ is error for ramp rate limit of fuel consumption in the CHP unit and it is evaluated using Eq. (4.41) of Chapter 4.

**Step 3:** The procedure of updating binary and continuous decision variables of the integrated unit commitment problem is followed until the termination criterion is met.

## 5.5 RESULTS AND DISCUSSIONS

The ICHPS includes thermal, DM-CHP, heat, PV and ESU units. In this study, the ICHPUC test systems-IV, V and VI comprises of 16-units (1-10$^{th}$ thermal, 11-15$^{th}$ CHP and 16$^{th}$ heat), 16-units (1-5$^{th}$ thermal, 6-15$^{th}$ CHP and 16$^{th}$ heat) and 20-units (1-5$^{th}$ thermal, 6-15$^{th}$ CHP and 16-20$^{th}$ heat) with PV-ESU system. The input data of generating units and solar PV unit for three test systems are given in Appendix B.3 and B.4, respectively. The following parameter values were considered for ESU: battery capacity is 350MW, initial and final SOC is limited to 40% **(Nazari and Ardehali, 2017; Marwali *et al.*, 1998)**. The PV-ESU system penetration limit is 400 MW and the maximum PV power is 440 MW. The spillage power from PV and fixed charge for ESU is not taken into account in this study. The implementation of the BSA-CSO optimization technique requires the parameters selection for the BSA-CSO technique. The parameters are decided after several trails executed on the test systems and it is given in Table 5.1. Software packages for the BSA-CSO technique to solve ICHPUC are developed in Fortran 90.

**Table 5.1:** Optimal parameters of BSA-CSO technique

| **Parameter** | **BSA-CSO** |
|---|---|
| **$N_p$** | 20 |
| **$N_s$** | 4 |
| **Inertia weight** | $W_{max}$ = 0.9, $W_{min}$ = 0.4 |
| **Acceleration coefficients** | $C_L$ = 2, $C_{SL1}$ = 0.5, $C_{SL2}$ = .5, $C_{SM1}$ = 0.25, $C_{SM2}$ = 0.75 |
| **Iteration** | Maximum iteration of BSA-CSO ($it^{max}$=10) and CSO algorithm ($k^{max}$=50) |

To demonstrate the effects of ESU and PV system on the CHP system, the three cases of the ICHPUC problem are undertaken, as given in Table 5.2. In case-1, the CHPUC problem is solved. In case-2 and 3, the PV and PV-ESU are integrated with the CHPUC problem, respectively.

**Table 5.2:** Case specifications of CHPUC problem

| | Units | | | | Dual-mode CHP unit | |
|---|---|---|---|---|---|---|
| | **Thermal** | **Heat** | **PV** | **Battery** | **Extraction mode** | **Backpressure mode** |
| **Case-1** | **Y** | **Y** | **N** | **N** | **Y** | **Y** |
| **Case-2** | **Y** | **Y** | **Y** | **N** | **Y** | **Y** |
| **Case-3** | **Y** | **Y** | **Y** | **Y** | **Y** | **Y** |

**Note: Y:** Represent the consideration of the unit; and **N:** Represent the unit is not taken into account.

### 5.5.1 Test System-IV

**Case 1: The combined heat and power unit commitment problem**

In case-1, power demand is met by thermal and CHP units only. The unit commitment status of different generating units is shown in Table 5.3 and 5.4. The power generation from committed thermal units is given in Table 5.5. The heat generation from committed CHP units and heat only units are shown in Figures 5.2 and 5.3. It is illustrated from these figures, that heat generated from committed CHP units in backpressure mode is higher than the extraction mode due to the heat power ratio. The impact of higher heat generation by CHP units in backpressure mode is clearly evident on commitment status of heat only units, as given in Table 5.3. During the backpressure mode operation of CHP units, only 15 sub-intervals (10-24) are required from heat only units, while in extraction mode of CHP unit, heat only unit has to commit for 24 sub-intervals (1-24) to satisfy the heat demand in each sub-interval. The power generation from CHP units for extraction and backpressure mode have been presented in Figures 5.4-5.5. The average generated power by CHP units in extraction and backpressure mode is 580.18 MW and 295.02 MW, respectively. For optimal operation and to satisfy the power demand, the thermal units need to commit for 202 total sub-intervals, during backpressure mode of CHP unit operation, while in the case of extraction mode of CHP unit operation, only 124 total sub-intervals commitment is required from thermal units. The operating cost of backpressure and extraction mode is $990110.6 and $1423362, respectively.

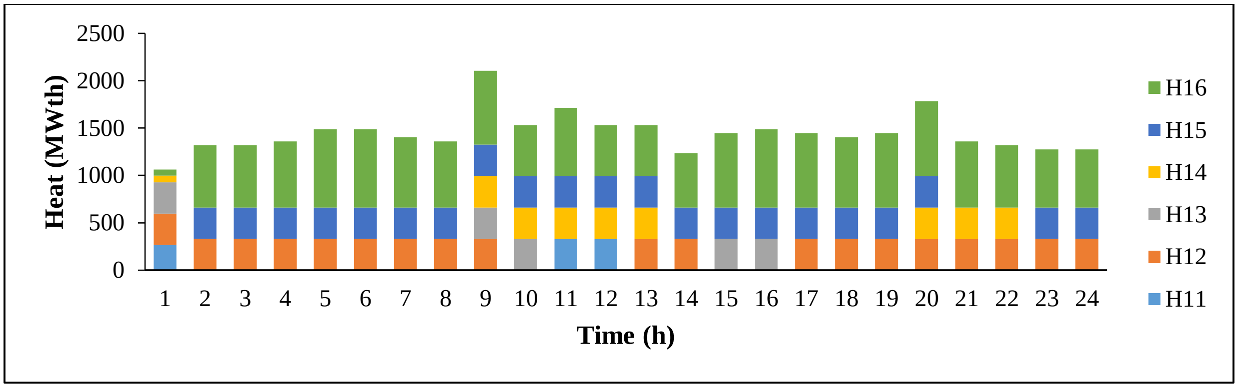

**Figure 5.2:** Heat generated from CHP and heat units in extraction mode of CHP for case-1, test system-IV

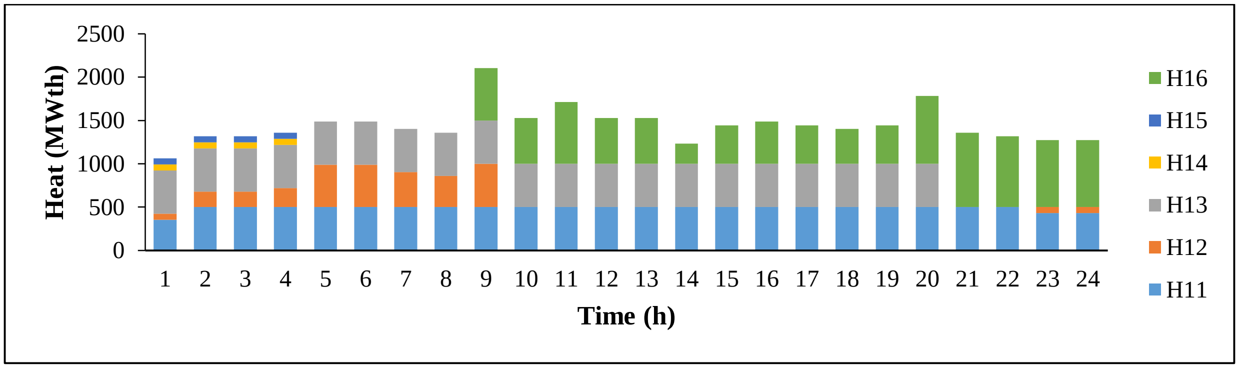

**Figure 5.3:** Heat generated from CHP and heat units in backpressure mode of CHP for case-1, test system-IV

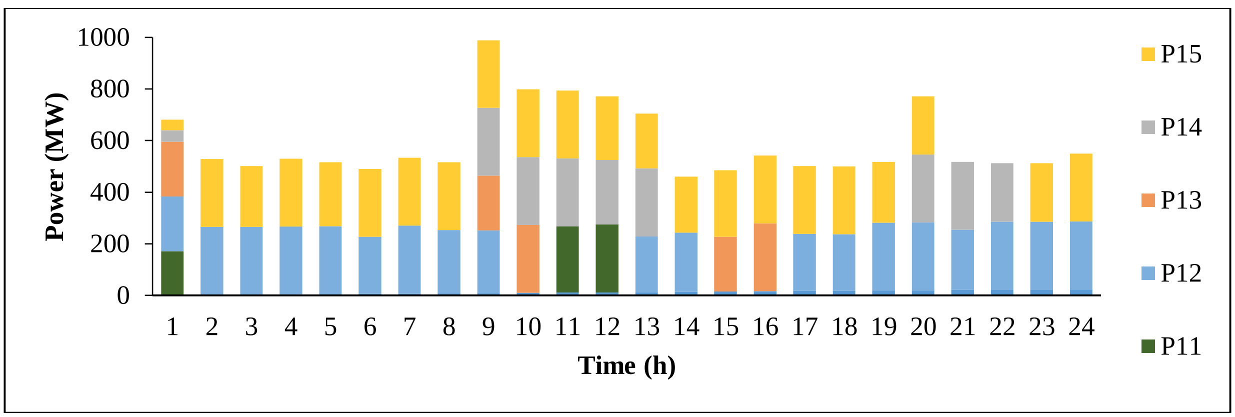

**Figure 5.4:** Power generated from CHP units in extraction mode for case-1, test system-IV

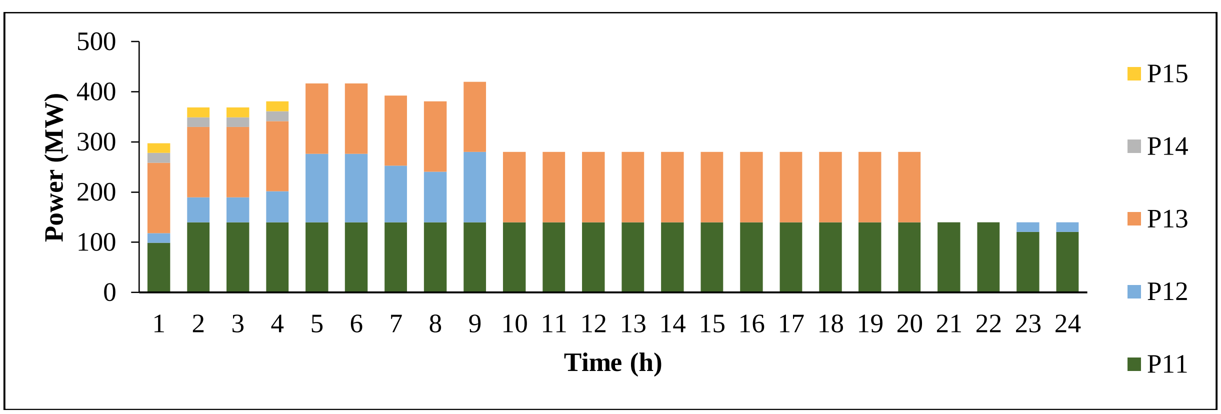

**Figure 5.5:** Power generated from CHP units in backpressure mode for case-1, test system-IV

**Table 5.3:** Unit commitment status in backpressure mode for all cases, Test system-IV

| | Case -3: PV-ESU-CHPUC problem | | | | | | | | | | | | | | | | Case -2: PV-CHPUC problem | | | | | | | | | | | | | | | | Case -1: CHPUC problem | | | | | | | | | | | | | | | |
|---|---|---|---|---|---|---|---|---|---|---|---|---|---|---|---|---|---|---|---|---|---|---|---|---|---|---|---|---|---|---|---|---|---|---|---|---|---|---|---|---|---|---|---|---|---|---|---|---|
| | 1 | 2 | 3 | 4 | 5 | 6 | 7 | 8 | 9 | 10 | 11 | 12 | 13 | 14 | 15 | 16 | 1 | 2 | 3 | 4 | 5 | 6 | 7 | 8 | 9 | 10 | 11 | 12 | 13 | 14 | 15 | 16 | 1 | 2 | 3 | 4 | 5 | 6 | 7 | 8 | 9 | 10 | 11 | 12 | 13 | 14 | 15 | 16 |
| **1** | 1 | 1 | 0 | 0 | 1 | 0 | 0 | 0 | 0 | 0 | 1 | 1 | 1 | 1 | 1 | 1 | 1 | 1 | 1 | 0 | 0 | 0 | 0 | 0 | 0 | 0 | 1 | 1 | 1 | 1 | 1 | 0 | 1 | 1 | 1 | 0 | 0 | 0 | 0 | 0 | 0 | 0 | 1 | 1 | 1 | 1 | 1 | 1 |
| **2** | 1 | 1 | 0 | 0 | 1 | 0 | 0 | 1 | 0 | 0 | 1 | 1 | 1 | 1 | 1 | 1 | 1 | 1 | 1 | 0 | 0 | 0 | 0 | 1 | 0 | 0 | 1 | 1 | 1 | 1 | 1 | 1 | 1 | 1 | 1 | 0 | 0 | 0 | 0 | 1 | 0 | 0 | 1 | 1 | 1 | 1 | 1 | 1 |
| **3** | 1 | 1 | 0 | 1 | 1 | 0 | 0 | 1 | 0 | 0 | 1 | 1 | 1 | 1 | 1 | 1 | 1 | 1 | 1 | 1 | 1 | 0 | 0 | 0 | 0 | 0 | 1 | 1 | 1 | 1 | 1 | 1 | 1 | 1 | 1 | 1 | 1 | 0 | 0 | 0 | 0 | 0 | 1 | 1 | 1 | 1 | 1 | 1 |
| **4** | 1 | 1 | 1 | 1 | 1 | 1 | 1 | 1 | 1 | 1 | 1 | 1 | 1 | 1 | 1 | 1 | 1 | 1 | 1 | 1 | 1 | 1 | 1 | 0 | 1 | 1 | 1 | 1 | 1 | 1 | 1 | 1 | 1 | 1 | 1 | 1 | 1 | 1 | 1 | 0 | 1 | 1 | 1 | 1 | 1 | 1 | 1 | 1 |
| **5** | 1 | 1 | 1 | 1 | 1 | 1 | 1 | 0 | 1 | 0 | 1 | 0 | 1 | 0 | 1 | 1 | 1 | 1 | 1 | 1 | 1 | 1 | 1 | 0 | 0 | 0 | 1 | 0 | 1 | 0 | 1 | 1 | 1 | 1 | 1 | 1 | 1 | 1 | 1 | 0 | 0 | 0 | 1 | 1 | 1 | 0 | 0 | 1 |
| **6** | 1 | 1 | 1 | 1 | 1 | 1 | 1 | 1 | 1 | 0 | 1 | 0 | 1 | 0 | 1 | 1 | 1 | 1 | 1 | 1 | 1 | 1 | 1 | 1 | 0 | 1 | 1 | 0 | 1 | 0 | 1 | 1 | 1 | 1 | 1 | 1 | 1 | 1 | 1 | 1 | 1 | 1 | 1 | 1 | 1 | 0 | 0 | 1 |
| **7** | 1 | 1 | 1 | 1 | 1 | 1 | 1 | 1 | 1 | 0 | 1 | 0 | 1 | 0 | 1 | 1 | 1 | 1 | 1 | 1 | 1 | 1 | 1 | 1 | 1 | 0 | 1 | 0 | 1 | 0 | 1 | 1 | 1 | 1 | 1 | 1 | 1 | 1 | 1 | 1 | 1 | 1 | 1 | 1 | 1 | 0 | 0 | 1 |
| **8** | 1 | 1 | 1 | 1 | 1 | 1 | 1 | 0 | 1 | 0 | 1 | 0 | 1 | 0 | 1 | 1 | 1 | 1 | 1 | 1 | 1 | 1 | 1 | 0 | 1 | 0 | 1 | 0 | 1 | 0 | 1 | 1 | 1 | 1 | 1 | 1 | 1 | 1 | 1 | 1 | 1 | 1 | 1 | 1 | 1 | 0 | 0 | 1 |
| **9** | 1 | 1 | 1 | 1 | 1 | 1 | 1 | 1 | 1 | 1 | 1 | 0 | 1 | 0 | 1 | 1 | 1 | 1 | 1 | 1 | 1 | 1 | 1 | 1 | 1 | 1 | 1 | 0 | 1 | 0 | 1 | 1 | 1 | 1 | 1 | 1 | 1 | 1 | 1 | 1 | 1 | 1 | 1 | 1 | 1 | 0 | 0 | 1 |
| **10** | 1 | 1 | 1 | 1 | 1 | 0 | 0 | 1 | 0 | 0 | 0 | 0 | 1 | 0 | 1 | 1 | 1 | 1 | 1 | 1 | 1 | 0 | 0 | 0 | 0 | 0 | 0 | 0 | 1 | 0 | 1 | 1 | 1 | 1 | 1 | 1 | 1 | 1 | 1 | 1 | 1 | 1 | 1 | 0 | 1 | 0 | 0 | 1 |
| **11** | 1 | 1 | 1 | 1 | 1 | 0 | 0 | 0 | 1 | 0 | 0 | 0 | 1 | 0 | 1 | 1 | 1 | 1 | 1 | 1 | 1 | 0 | 0 | 0 | 0 | 0 | 0 | 0 | 1 | 0 | 1 | 1 | 1 | 1 | 1 | 1 | 1 | 1 | 1 | 1 | 1 | 1 | 1 | 0 | 1 | 0 | 0 | 1 |
| **12** | 1 | 1 | 1 | 1 | 1 | 0 | 0 | 0 | 1 | 0 | 0 | 0 | 1 | 0 | 1 | 1 | 1 | 1 | 1 | 1 | 1 | 0 | 0 | 0 | 0 | 0 | 0 | 0 | 1 | 0 | 1 | 1 | 1 | 1 | 1 | 1 | 1 | 1 | 1 | 1 | 1 | 1 | 1 | 0 | 1 | 0 | 0 | 1 |
| **13** | 1 | 1 | 1 | 1 | 1 | 1 | 0 | 0 | 0 | 0 | 0 | 0 | 1 | 0 | 1 | 1 | 1 | 1 | 1 | 1 | 1 | 0 | 0 | 0 | 0 | 0 | 0 | 0 | 1 | 0 | 1 | 1 | 1 | 1 | 1 | 1 | 1 | 1 | 1 | 1 | 1 | 1 | 1 | 0 | 1 | 0 | 0 | 1 |
| **14** | 1 | 1 | 1 | 1 | 1 | 1 | 1 | 1 | 0 | 0 | 0 | 0 | 1 | 0 | 1 | 1 | 1 | 1 | 1 | 1 | 1 | 1 | 0 | 1 | 1 | 0 | 0 | 0 | 1 | 0 | 1 | 1 | 1 | 1 | 1 | 1 | 1 | 1 | 1 | 1 | 1 | 1 | 1 | 0 | 1 | 0 | 0 | 1 |
| **15** | 1 | 1 | 1 | 1 | 1 | 1 | 1 | 0 | 0 | 0 | 0 | 0 | 1 | 0 | 1 | 1 | 1 | 1 | 1 | 1 | 1 | 1 | 0 | 0 | 0 | 0 | 0 | 0 | 1 | 0 | 1 | 1 | 1 | 1 | 1 | 1 | 1 | 1 | 1 | 1 | 1 | 1 | 1 | 0 | 1 | 0 | 0 | 1 |
| **16** | 1 | 1 | 1 | 1 | 1 | 1 | 1 | 0 | 0 | 0 | 0 | 0 | 1 | 0 | 1 | 1 | 1 | 1 | 1 | 1 | 1 | 1 | 0 | 0 | 0 | 0 | 0 | 0 | 1 | 0 | 1 | 1 | 1 | 1 | 1 | 1 | 1 | 1 | 1 | 1 | 1 | 1 | 1 | 0 | 1 | 0 | 0 | 1 |
| **17** | 1 | 1 | 1 | 1 | 1 | 1 | 1 | 0 | 0 | 0 | 0 | 0 | 1 | 0 | 1 | 1 | 1 | 1 | 1 | 1 | 1 | 1 | 0 | 0 | 0 | 0 | 0 | 0 | 1 | 0 | 1 | 1 | 1 | 1 | 1 | 1 | 1 | 1 | 1 | 0 | 1 | 0 | 1 | 0 | 1 | 0 | 0 | 1 |
| **18** | 1 | 1 | 1 | 1 | 1 | 1 | 1 | 1 | 0 | 0 | 0 | 0 | 1 | 0 | 1 | 1 | 1 | 1 | 1 | 1 | 1 | 1 | 1 | 1 | 0 | 0 | 0 | 0 | 1 | 0 | 1 | 1 | 1 | 1 | 1 | 1 | 1 | 1 | 1 | 1 | 1 | 1 | 1 | 0 | 1 | 0 | 0 | 1 |
| **19** | 1 | 1 | 1 | 1 | 1 | 1 | 1 | 1 | 1 | 1 | 0 | 0 | 1 | 0 | 1 | 1 | 1 | 1 | 1 | 1 | 1 | 1 | 1 | 1 | 1 | 1 | 0 | 0 | 1 | 0 | 1 | 1 | 1 | 1 | 1 | 1 | 1 | 1 | 1 | 1 | 1 | 1 | 1 | 0 | 1 | 0 | 0 | 1 |
| **20** | 1 | 1 | 1 | 1 | 1 | 1 | 1 | 1 | 1 | 1 | 0 | 0 | 1 | 0 | 1 | 1 | 1 | 1 | 1 | 1 | 1 | 1 | 1 | 1 | 1 | 1 | 0 | 0 | 1 | 0 | 1 | 1 | 1 | 1 | 1 | 1 | 1 | 1 | 1 | 1 | 1 | 1 | 1 | 0 | 1 | 0 | 0 | 1 |
| **21** | 1 | 1 | 1 | 1 | 1 | 1 | 0 | 1 | 0 | 0 | 0 | 0 | 1 | 0 | 0 | 1 | 1 | 1 | 1 | 1 | 1 | 1 | 1 | 0 | 0 | 0 | 0 | 0 | 1 | 0 | 0 | 1 | 1 | 1 | 1 | 1 | 1 | 1 | 1 | 0 | 0 | 0 | 1 | 0 | 1 | 0 | 0 | 1 |
| **22** | 1 | 1 | 1 | 1 | 1 | 0 | 0 | 0 | 0 | 0 | 0 | 0 | 1 | 0 | 0 | 1 | 1 | 1 | 1 | 1 | 1 | 1 | 0 | 0 | 0 | 0 | 0 | 0 | 1 | 0 | 0 | 1 | 1 | 1 | 1 | 1 | 1 | 1 | 0 | 0 | 0 | 0 | 1 | 0 | 1 | 0 | 0 | 1 |
| **23** | 1 | 1 | 1 | 1 | 1 | 0 | 0 | 0 | 0 | 0 | 0 | 0 | 1 | 0 | 0 | 1 | 1 | 1 | 1 | 1 | 1 | 0 | 0 | 0 | 0 | 0 | 0 | 0 | 1 | 0 | 0 | 1 | 1 | 1 | 1 | 1 | 1 | 0 | 0 | 0 | 0 | 0 | 1 | 1 | 1 | 0 | 0 | 1 |
| **24** | 1 | 1 | 0 | 1 | 1 | 0 | 0 | 0 | 0 | 0 | 1 | 1 | 1 | 0 | 0 | 0 | 1 | 1 | 1 | 1 | 1 | 0 | 0 | 0 | 0 | 0 | 1 | 1 | 1 | 0 | 0 | 0 | 1 | 1 | 1 | 1 | 1 | 0 | 0 | 0 | 0 | 0 | 1 | 1 | 1 | 0 | 0 | 0 |

**Table 5.4:** Unit commitment status in extraction mode for all cases, Test system-IV

| | Case -3: PV-ESU-CHPUC problem | | | | | | | | | | | | | | | | Case -2: PV-CHPUC problem | | | | | | | | | | | | | | | | Case -1: CHPUC problem | | | | | | | | | | | | | | | |
|---|---|---|---|---|---|---|---|---|---|---|---|---|---|---|---|---|---|---|---|---|---|---|---|---|---|---|---|---|---|---|---|---|---|---|---|---|---|---|---|---|---|---|---|---|---|---|---|---|
| **h** | 1 | 2 | 3 | 4 | 5 | 6 | 7 | 8 | 9 | 10 | 11 | 12 | 13 | 14 | 15 | 16 | 1 | 2 | 3 | 4 | 5 | 6 | 7 | 8 | 9 | 10 | 11 | 12 | 13 | 14 | 15 | 16 | 1 | 2 | 3 | 4 | 5 | 6 | 7 | 8 | 9 | 10 | 11 | 12 | 13 | 14 | 15 | 16 |
| **1** | 1 | 1 | 0 | 0 | 0 | 0 | 0 | 0 | 0 | 0 | 1 | 1 | 1 | 1 | 1 | 0 | 1 | 1 | 0 | 0 | 0 | 0 | 0 | 0 | 0 | 0 | 1 | 1 | 1 | 1 | 1 | 0 | 1 | 1 | 0 | 0 | 0 | 0 | 0 | 0 | 0 | 0 | 1 | 1 | 1 | 1 | 1 | 1 |
| **2** | 1 | 1 | 0 | 0 | 0 | 0 | 0 | 0 | 0 | 0 | 0 | 1 | 0 | 0 | 1 | 1 | 1 | 1 | 0 | 0 | 0 | 0 | 0 | 0 | 0 | 0 | 0 | 1 | 0 | 0 | 1 | 1 | 1 | 1 | 0 | 0 | 0 | 0 | 0 | 0 | 0 | 0 | 0 | 1 | 0 | 0 | 1 | 1 |
| **3** | 1 | 1 | 0 | 0 | 1 | 0 | 0 | 0 | 0 | 0 | 0 | 1 | 0 | 0 | 1 | 1 | 1 | 1 | 0 | 0 | 1 | 0 | 0 | 0 | 0 | 0 | 0 | 1 | 0 | 0 | 1 | 1 | 1 | 1 | 0 | 0 | 1 | 0 | 0 | 0 | 0 | 0 | 0 | 1 | 0 | 0 | 1 | 1 |
| **4** | 1 | 1 | 1 | 1 | 1 | 0 | 0 | 0 | 0 | 0 | 0 | 1 | 0 | 0 | 1 | 1 | 1 | 1 | 1 | 1 | 1 | 0 | 0 | 0 | 0 | 0 | 0 | 1 | 0 | 0 | 1 | 1 | 1 | 1 | 1 | 1 | 1 | 0 | 0 | 0 | 0 | 0 | 0 | 1 | 0 | 0 | 1 | 1 |
| **5** | 1 | 1 | 1 | 1 | 1 | 0 | 0 | 0 | 0 | 0 | 0 | 1 | 0 | 0 | 1 | 1 | 1 | 1 | 1 | 1 | 1 | 0 | 0 | 0 | 0 | 0 | 0 | 1 | 0 | 0 | 1 | 1 | 1 | 1 | 1 | 1 | 1 | 0 | 0 | 0 | 0 | 0 | 0 | 1 | 0 | 0 | 1 | 1 |
| **6** | 1 | 1 | 1 | 1 | 1 | 0 | 0 | 0 | 0 | 0 | 0 | 1 | 0 | 0 | 1 | 1 | 1 | 1 | 1 | 1 | 1 | 0 | 0 | 0 | 0 | 0 | 0 | 1 | 0 | 0 | 1 | 1 | 1 | 1 | 1 | 1 | 1 | 0 | 0 | 0 | 0 | 0 | 0 | 1 | 0 | 0 | 1 | 1 |
| **7** | 1 | 1 | 1 | 1 | 1 | 0 | 0 | 0 | 0 | 0 | 0 | 1 | 0 | 0 | 1 | 1 | 1 | 1 | 1 | 1 | 1 | 0 | 0 | 0 | 0 | 0 | 0 | 1 | 0 | 0 | 1 | 1 | 1 | 1 | 1 | 1 | 1 | 1 | 0 | 0 | 0 | 0 | 0 | 1 | 0 | 0 | 1 | 1 |
| **8** | 1 | 1 | 1 | 1 | 1 | 0 | 0 | 0 | 0 | 0 | 0 | 1 | 0 | 0 | 1 | 1 | 1 | 1 | 1 | 1 | 1 | 0 | 0 | 0 | 0 | 0 | 0 | 1 | 0 | 0 | 1 | 1 | 1 | 1 | 1 | 1 | 1 | 1 | 0 | 1 | 0 | 0 | 0 | 1 | 0 | 0 | 1 | 1 |
| **9** | 1 | 1 | 1 | 1 | 1 | 0 | 0 | 0 | 0 | 0 | 0 | 1 | 1 | 1 | 1 | 1 | 1 | 1 | 1 | 1 | 1 | 0 | 0 | 0 | 0 | 0 | 0 | 1 | 1 | 1 | 1 | 1 | 1 | 1 | 1 | 1 | 1 | 1 | 1 | 1 | 0 | 1 | 0 | 1 | 1 | 1 | 1 | 1 |
| **10** | 1 | 1 | 1 | 1 | 0 | 0 | 0 | 0 | 0 | 0 | 0 | 0 | 1 | 1 | 1 | 1 | 1 | 1 | 0 | 0 | 1 | 0 | 0 | 0 | 0 | 0 | 0 | 0 | 1 | 1 | 1 | 1 | 1 | 1 | 1 | 1 | 1 | 0 | 1 | 0 | 0 | 0 | 0 | 0 | 1 | 1 | 1 | 1 |
| **11** | 1 | 1 | 1 | 1 | 0 | 0 | 0 | 0 | 0 | 0 | 1 | 0 | 0 | 1 | 1 | 1 | 1 | 1 | 0 | 0 | 1 | 0 | 0 | 0 | 0 | 0 | 1 | 0 | 0 | 1 | 1 | 1 | 1 | 1 | 1 | 1 | 1 | 0 | 1 | 0 | 0 | 0 | 1 | 0 | 0 | 1 | 1 | 1 |
| **12** | 1 | 1 | 1 | 1 | 0 | 0 | 0 | 0 | 0 | 0 | 1 | 0 | 0 | 1 | 1 | 1 | 1 | 1 | 0 | 0 | 1 | 0 | 0 | 0 | 0 | 0 | 1 | 0 | 0 | 1 | 1 | 1 | 1 | 1 | 1 | 1 | 1 | 0 | 1 | 0 | 0 | 0 | 1 | 0 | 0 | 1 | 1 | 1 |
| **13** | 1 | 1 | 1 | 1 | 0 | 0 | 0 | 0 | 0 | 0 | 0 | 1 | 0 | 1 | 1 | 1 | 1 | 1 | 0 | 0 | 1 | 0 | 0 | 0 | 0 | 0 | 0 | 1 | 0 | 1 | 1 | 1 | 1 | 1 | 1 | 1 | 1 | 1 | 1 | 0 | 0 | 0 | 0 | 1 | 0 | 1 | 1 | 1 |

| | | | | | | | | | | | | | | | | | | | | | | | | | | | | | | | | | | | | | | | | | | | | | | | | |
|---|---|---|---|---|---|---|---|---|---|---|---|---|---|---|---|---|---|---|---|---|---|---|---|---|---|---|---|---|---|---|---|---|---|---|---|---|---|---|---|---|---|---|---|---|---|---|---|---|
| **14** | 1 | 1 | 1 | 1 | 0 | 0 | 0 | 0 | 0 | 0 | 0 | 1 | 0 | 0 | 1 | 1 | 1 | 1 | 0 | 0 | 1 | 0 | 0 | 1 | 0 | 0 | 0 | 1 | 0 | 0 | 1 | 1 | 1 | 1 | 1 | 1 | 1 | 1 | 1 | 1 | 0 | 1 | 0 | 1 | 0 | 0 | 1 | 1 |
| **15** | 1 | 1 | 1 | 1 | 0 | 0 | 0 | 0 | 0 | 0 | 0 | 1 | 0 | 0 | 1 | 1 | 1 | 1 | 0 | 0 | 1 | 0 | 0 | 0 | 0 | 0 | 0 | 1 | 0 | 0 | 1 | 1 | 1 | 1 | 1 | 1 | 1 | 1 | 0 | 1 | 0 | 0 | 0 | 0 | 1 | 0 | 1 | 1 |
| **16** | 1 | 1 | 1 | 1 | 0 | 0 | 0 | 0 | 0 | 0 | 0 | 1 | 0 | 0 | 1 | 1 | 1 | 1 | 0 | 0 | 1 | 0 | 0 | 0 | 0 | 0 | 0 | 1 | 0 | 0 | 1 | 1 | 1 | 1 | 1 | 1 | 1 | 0 | 0 | 0 | 0 | 0 | 0 | 0 | 1 | 0 | 1 | 1 |
| **17** | 1 | 1 | 1 | 1 | 1 | 0 | 0 | 0 | 0 | 0 | 0 | 1 | 0 | 0 | 1 | 1 | 1 | 1 | 0 | 0 | 1 | 0 | 0 | 0 | 0 | 0 | 0 | 1 | 0 | 0 | 1 | 1 | 1 | 1 | 1 | 1 | 1 | 0 | 0 | 0 | 0 | 0 | 0 | 1 | 0 | 0 | 1 | 1 |
| **18** | 1 | 1 | 1 | 1 | 1 | 0 | 0 | 0 | 0 | 0 | 0 | 1 | 0 | 1 | 0 | 1 | 1 | 1 | 0 | 1 | 1 | 0 | 0 | 0 | 0 | 0 | 0 | 1 | 0 | 0 | 1 | 1 | 1 | 1 | 1 | 1 | 1 | 0 | 0 | 0 | 0 | 0 | 0 | 1 | 0 | 0 | 1 | 1 |
| **19** | 1 | 1 | 1 | 1 | 1 | 1 | 0 | 0 | 0 | 0 | 0 | 1 | 0 | 1 | 0 | 1 | 1 | 1 | 1 | 1 | 1 | 1 | 0 | 0 | 0 | 0 | 0 | 1 | 0 | 0 | 1 | 1 | 1 | 1 | 1 | 1 | 1 | 1 | 0 | 0 | 0 | 1 | 0 | 1 | 0 | 0 | 1 | 1 |
| **20** | 1 | 1 | 0 | 0 | 1 | 1 | 0 | 0 | 0 | 0 | 0 | 1 | 0 | 1 | 1 | 1 | 1 | 1 | 1 | 1 | 0 | 1 | 0 | 0 | 0 | 0 | 0 | 1 | 0 | 1 | 1 | 1 | 1 | 1 | 1 | 0 | 0 | 1 | 0 | 0 | 0 | 0 | 0 | 1 | 0 | 1 | 1 | 1 |
| **21** | 1 | 1 | 0 | 0 | 1 | 1 | 0 | 0 | 0 | 0 | 0 | 1 | 0 | 0 | 1 | 1 | 1 | 1 | 1 | 1 | 0 | 1 | 0 | 0 | 0 | 0 | 0 | 1 | 0 | 1 | 0 | 1 | 1 | 1 | 1 | 0 | 0 | 1 | 0 | 0 | 0 | 0 | 0 | 1 | 0 | 1 | 0 | 1 |
| **22** | 1 | 1 | 0 | 0 | 1 | 0 | 0 | 0 | 0 | 0 | 0 | 1 | 0 | 0 | 1 | 1 | 1 | 1 | 1 | 1 | 0 | 0 | 0 | 0 | 0 | 0 | 0 | 1 | 0 | 1 | 0 | 1 | 1 | 1 | 0 | 0 | 0 | 1 | 0 | 0 | 0 | 0 | 0 | 1 | 0 | 1 | 0 | 1 |
| **23** | 1 | 1 | 0 | 0 | 0 | 0 | 0 | 0 | 0 | 0 | 0 | 1 | 0 | 0 | 1 | 1 | 1 | 1 | 1 | 0 | 0 | 0 | 0 | 0 | 0 | 0 | 0 | 1 | 0 | 1 | 1 | 1 | 1 | 1 | 0 | 0 | 0 | 1 | 0 | 0 | 0 | 0 | 0 | 1 | 0 | 0 | 1 | 1 |
| **24** | 1 | 1 | 0 | 0 | 0 | 0 | 0 | 0 | 0 | 0 | 1 | 1 | 1 | 1 | 1 | 0 | 1 | 1 | 1 | 0 | 0 | 0 | 0 | 0 | 0 | 0 | 1 | 1 | 1 | 1 | 1 | 0 | 1 | 1 | 0 | 0 | 0 | 1 | 0 | 0 | 0 | 0 | 0 | 1 | 0 | 0 | 1 | 1 |

**Table 5.5:** Power generated from thermal units in extraction and backpressure mode for case-1, test system-IV

| | **Backpressure mode in Case-1** | | | | | | | | | | **Extraction mode in Case-1** | | | | | | | | | |
|---|---|---|---|---|---|---|---|---|---|---|---|---|---|---|---|---|---|---|---|---|
| | **Thermal power generation (MW)** | | | | | | | | | | **Thermal power generation (MW)** | | | | | | | | | |
| **h** | **P1** | **P2** | **P3** | **P4** | **P5** | **P6** | **P7** | **P8** | **P9** | **P10** | **P1** | **P2** | **P3** | **P4** | **P5** | **P6** | **P7** | **P8** | **P9** | **P10** |
| **1** | 455 | 207.5 | 20 | 0 | 0 | 0 | 0 | 0 | 0 | 0 | 150.0 | 150.0 | 0.0 | 0.0 | 0.0 | 0.0 | 0.0 | 0.0 | 0.0 | 0.0 |
| **2** | 455 | 206.1 | 20 | 0 | 0 | 0 | 0 | 10 | 0 | 0 | 384.0 | 150.0 | 0.0 | 0.0 | 0.0 | 0.0 | 0.0 | 0.0 | 0.0 | 0.0 |
| **3** | 455 | 164.1 | 20 | 20 | 162 | 0 | 0 | 0 | 0 | 0 | 455.0 | 211.6 | 0.0 | 0.0 | 25.0 | 0.0 | 0.0 | 0.0 | 0.0 | 0.0 |
| **4** | 455 | 398.2 | 20 | 20 | 162 | 20 | 25 | 0 | 55 | 10 | 455.0 | 455.0 | 65.0 | 20.0 | 25.0 | 0.0 | 0.0 | 0.0 | 0.0 | 0.0 |
| **5** | 455 | 281.5 | 20 | 20 | 162 | 20 | 25 | 0 | 0 | 0 | 455.0 | 369.4 | 20.0 | 20.0 | 25.0 | 0.0 | 0.0 | 0.0 | 0.0 | 0.0 |
| **6** | 455 | 346.5 | 20 | 20 | 162 | 20 | 25 | 10 | 55 | 10 | 436.5 | 455.0 | 119.8 | 20.0 | 25.0 | 0.0 | 0.0 | 0.0 | 0.0 | 0.0 |
| **7** | 455 | 440.3 | 20 | 20 | 162 | 20 | 25 | 10 | 55 | 10 | 450.9 | 455.0 | 113.1 | 20.0 | 25.0 | 20.0 | 0.0 | 0.0 | 0.0 | 0.0 |
| **8** | 455 | 455 | 87.2 | 20 | 162 | 20 | 25 | 10 | 55 | 10 | 455.0 | 455.0 | 130.0 | 77.2 | 25.0 | 20.0 | 0.0 | 10.0 | 0.0 | 0.0 |
| **9** | 455 | 455 | 130 | 130 | 162 | 80 | 85 | 55 | 55 | 55 | 455.0 | 455.0 | 130.0 | 74.6 | 25.0 | 20.0 | 25.0 | 10.0 | 0.0 | 10.0 |
| **10** | 455 | 455 | 130 | 41 | 162 | 20 | 25 | 10 | 55 | 10 | 406.7 | 357.3 | 20.0 | 20.0 | 25.0 | 0.0 | 25.0 | 0.0 | 0.0 | 0.0 |
| **11** | 455 | 455 | 130 | 62 | 162 | 20 | 25 | 10 | 55 | 10 | 385.0 | 406.1 | 20.0 | 20.0 | 25.0 | 0.0 | 25.0 | 0.0 | 0.0 | 0.0 |
| **12** | 455 | 455 | 130 | 78 | 162 | 20 | 25 | 10 | 55 | 10 | 432.0 | 399.0 | 20.0 | 20.0 | 25.0 | 0.0 | 25.0 | 0.0 | 0.0 | 0.0 |
| **13** | 455 | 455 | 130 | 71 | 162 | 20 | 25 | 10 | 55 | 10 | 455.0 | 416.9 | 20.0 | 20.0 | 25.0 | 20.0 | 25.0 | 0.0 | 0.0 | 0.0 |
| **14** | 455 | 455 | 130 | 130 | 162 | 80 | 53 | 10 | 55 | 10 | 455.0 | 455.0 | 130.0 | 130.0 | 138.7 | 20.0 | 25.0 | 10.0 | 0.0 | 10.0 |
| **15** | 455 | 455 | 130 | 78 | 162 | 20 | 25 | 10 | 55 | 10 | 455.0 | 455.0 | 130.0 | 114.4 | 25.0 | 20.0 | 0.0 | 10.0 | 0.0 | 0.0 |
| **16** | 455 | 455 | 48 | 20 | 162 | 20 | 25 | 10 | 55 | 10 | 455.0 | 455.0 | 59.0 | 20.0 | 25.0 | 0.0 | 0.0 | 0.0 | 0.0 | 0.0 |
| **17** | 455 | 363 | 20 | 20 | 162 | 20 | 25 | 0 | 55 | 0 | 455.0 | 395.7 | 20.0 | 20.0 | 25.0 | 0.0 | 0.0 | 0.0 | 0.0 | 0.0 |
| **18** | 455 | 455 | 48 | 20 | 162 | 20 | 25 | 10 | 55 | 10 | 455.0 | 455.0 | 103.2 | 20.0 | 25.0 | 0.0 | 0.0 | 0.0 | 0.0 | 0.0 |
| **19** | 455 | 455 | 130 | 78 | 162 | 20 | 25 | 10 | 55 | 10 | 455.0 | 455.0 | 130.0 | 86.2 | 25.0 | 20.0 | 0.0 | 0.0 | 0.0 | 10.0 |
| **20** | 455 | 455 | 76 | 20 | 162 | 20 | 25 | 10 | 55 | 10 | 455.0 | 321.0 | 20.0 | 0.0 | 0.0 | 20.0 | 0.0 | 0.0 | 0.0 | 0.0 |
| **21** | 455 | 455 | 96.2 | 20 | 162 | 20 | 25 | 0 | 0 | 0 | 455.0 | 382.2 | 20.0 | 0.0 | 0.0 | 20.0 | 0.0 | 0.0 | 0.0 | 0.0 |
| **22** | 455 | 415 | 20 | 20 | 162 | 20 | 0 | 0 | 0 | 0 | 455.0 | 266.7 | 0.0 | 0.0 | 0.0 | 20.0 | 0.0 | 0.0 | 0.0 | 0.0 |
| **23** | 455 | 419 | 20 | 20 | 162 | 0 | 0 | 0 | 0 | 0 | 434.1 | 273.0 | 0.0 | 0.0 | 0.0 | 20.0 | 0.0 | 0.0 | 0.0 | 0.0 |
| **24** | 455 | 423 | 20 | 20 | 162 | 0 | 0 | 0 | 0 | 0 | 455.0 | 219.0 | 0.0 | 0.0 | 0.0 | 20.0 | 0.0 | 0.0 | 0.0 | 0.0 |

**Case-2: The PV integrated with combined heat and power unit commitment problem**

The unit commitment status of different generating units is presented in Table 5.3 and 5.4. The power generation schedule of thermal committed units and solar PV is presented in Table 5.6 and 5.7. The total heat generation from CHP and heat units has been illustrated in Figures 5.6 and 5.7, respectively. It has been found that the heat generation from CHP units in backpressure mode is more as compared to heat generation from extraction mode. Therefore, the heat generation requirement from heat only units during backpressure mode of CHP units is lesser as compared to extraction mode. The fact is further authenticated by unit commitment status of heat only units. The heat only units are needed to commit for 20 and 22 sub-intervals during backpressure and extraction mode of CHP operation, respectively. The total power generation from committed thermal and CHP units in dual mode has been shown in Figures 5.8 and 5.9, respectively. It is illustrated from Figure 5.8, that total power generation from CHP units is higher in extraction mode as compared to backpressure mode due to heat/power interdependency (Eqs. 4.1 and 4.10). Therefore, the cumulative thermal power generation requirement during backpressure mode of CHP operation is higher as compared to extraction mode and it is shown in Figure 5.9. The same fact is validated from Table 5.7 that indicates during backpressure mode of CHP unit operation, the thermal units are committed for 161 sub-intervals, whereas in case of extraction mode of CHP unit operation, the thermal units are needed to commit only for 88 sub-intervals.

In case-2, the inclusion of PV system has changed the UC schedule as compared to case-1, as illustrated by Tables 5.3 and 5.4. Since, PV delivers the power at no cost; hence requirement to commit the number of thermal units is drastically reduced as compared to case-1. The number of committed sub-intervals for thermal units is decreased by 41 and 36 as compared to case-1 for backpressure and extraction mode of CHP unit operation, respectively. The operating cost of backpressure and extraction mode in case-2 is \$902293.9 and \$1354884, respectively. It has been observed from Table 5.8 that in backpressure and extraction mode operation of CHP unit, the operating cost in case-2 is decreased by \$87816.7/day and \$68478/day, respectively as compared to case-1.

**Table 5.6:** Power generated from thermal units in extraction mode for case-2 & 3, test system-IV

| | | **Extraction mode in Case-3** | | | | | | | | | | | **Extraction mode in Case-2** | | | | | | | | | | **Solar Power (Case-2&3)** |
|---|---|---|---|---|---|---|---|---|---|---|---|---|---|---|---|---|---|---|---|---|---|---|---|
| | | **Thermal power generation (MW)** | | | | | | | | | | **Battery Power** | **Thermal power generation (MW)** | | | | | | | | | | |
| **h** | **Power Demand (MW)** | **P1** | **P2** | **P3** | **P4** | **P5** | **P6** | **P7** | **P8** | **P9** | **P10** | | **P1** | **P2** | **P3** | **P4** | **P5** | **P6** | **P7** | **P8** | **P9** | **P10** | |
| **1** | 980 | 150 | 150 | 0 | 0 | 0 | 0 | 0 | 0 | 0 | 0 | 153.0 | 191.6 | 150 | 0 | 0 | 0 | 0 | 0 | 0 | 0 | 0 | 0 |
| **2** | 1060 | 405.6 | 198.0 | 0 | 0 | 0 | 0 | 0 | 0 | 0 | 0 | 41.5 | 393.8 | 163.0 | 0 | 0 | 0 | 0 | 0 | 0 | 0 | 0 | 0 |
| **3** | 1190.38 | 354.8 | 159.2 | 0 | 0 | 162 | 0 | 0 | 0 | 0 | 0 | 12.0 | 358.2 | 150 | 0 | 0 | 162 | 0 | 0 | 0 | 0 | 0 | 0 |
| **4** | 1546 | 377.3 | 442.9 | 20 | 20 | 162 | 0 | 0 | 0 | 0 | 0 | 2.2 | 387.5 | 453.6 | 20 | 20 | 162 | 0 | 0 | 0 | 0 | 0 | 0 |
| **5** | 1399.61 | 368.6 | 298.8 | 20 | 20 | 162 | 0 | 0 | 0 | 0 | 0 | -2.1 | 392.2 | 286.1 | 20 | 20 | 162 | 0 | 0 | 0 | 0 | 0 | 2 |
| **6** | 1540.7 | 398.4 | 396.6 | 20 | 20 | 162 | 0 | 0 | 0 | 0 | 0 | -1.9 | 374.0 | 392.9 | 20 | 20 | 162 | 0 | 0 | 0 | 0 | 0 | 45 |
| **7** | 1610 | 375.8 | 399.7 | 20 | 20 | 162 | 0 | 0 | 0 | 0 | 0 | -0.8 | 428.3 | 390.9 | 20 | 20 | 162 | 0 | 0 | 0 | 0 | 0 | 118 |
| **8** | 1679.81 | 416.4 | 324.9 | 20 | 20 | 162 | 0 | 0 | 0 | 0 | 0 | -0.7 | 402.0 | 290.5 | 20 | 20 | 162 | 0 | 0 | 0 | 0 | 0 | 260 |
| **9** | 2184.38 | 350.3 | 317.3 | 20 | 20 | 162 | 0 | 0 | 0 | 0 | 0 | -1.0 | 373.5 | 308.3 | 20 | 20 | 162 | 0 | 0 | 0 | 0 | 0 | 261 |
| **10** | 1643 | 295.8 | 150 | 20 | 20 | 0 | 0 | 0 | 0 | 0 | 0 | -2.3 | 342.9 | 150 | 0 | 0 | 25 | 0 | 0 | 0 | 0 | 0 | 396 |
| **11** | 1663.83 | 336.9 | 150 | 20 | 20 | 0 | 0 | 0 | 0 | 0 | 0 | 40.4 | 226.6 | 150 | 0 | 0 | 80.0 | 0 | 0 | 0 | 0 | 0 | 440 |
| **12** | 1680 | 331.2 | 150 | 20 | 20 | 0 | 0 | 0 | 0 | 0 | 0 | 41.1 | 266.8 | 150 | 0 | 0 | 71.0 | 0 | 0 | 0 | 0 | 0 | 440 |
| **13** | 1673 | 294.2 | 150 | 20 | 20 | 0 | 0 | 0 | 0 | 0 | 0 | 40.2 | 276.1 | 150 | 0 | 0 | 58.5 | 0 | 0 | 0 | 0 | 0 | 440 |
| **14** | 1820 | 455.0 | 455 | 58 | 20 | 0 | 0 | 0 | 0 | 0 | 0 | 34.8 | 439.2 | 294.3 | 0 | 0 | 162 | 0 | 0 | 10 | 0 | 0 | 435 |
| **15** | 1680 | 413.1 | 380.0 | 20 | 20 | 0 | 0 | 0 | 0 | 0 | 0 | -4.4 | 455.0 | 220.0 | 0 | 0 | 162 | 0 | 0 | 0 | 0 | 0 | 368 |
| **16** | 1540 | 449.9 | 220.3 | 20 | 20 | 0 | 0 | 0 | 0 | 0 | 0 | -11.6 | 379.1 | 150 | 0 | 0 | 162 | 0 | 0 | 0 | 0 | 0 | 335 |
| **17** | 1400 | 345.3 | 150 | 20 | 20 | 162 | 0 | 0 | 0 | 0 | 0 | -8.9 | 360.6 | 150 | 0 | 0 | 162 | 0 | 0 | 0 | 0 | 0 | 201 |
| **18** | 1540 | 405.8 | 297.5 | 20 | 20 | 162 | 0 | 0 | 0 | 0 | 0 | -1.6 | 403.5 | 325.8 | 0 | 20 | 162 | 0 | 0 | 0 | 0 | 0 | 109 |
| **19** | 1680 | 403.0 | 455.0 | 97.4 | 20 | 162 | 20 | 0 | 0 | 0 | 0 | -3.6 | 455.0 | 455 | 122.8 | 20 | 162 | 20 | 0 | 0 | 0 | 0 | 19 |
| **20** | 1568 | 362.8 | 223.9 | 0 | 0 | 162 | 20 | 0 | 0 | 0 | 0 | -10.3 | 349.0 | 393.2 | 20 | 20 | 0 | 20 | 0 | 0 | 0 | 0 | 0 |
| **21** | 1373 | 409.9 | 283.8 | 0 | 0 | 162 | 20 | 0 | 0 | 0 | 0 | -8.5 | 361.1 | 426.1 | 20 | 20 | 0 | 20 | 0 | 0 | 0 | 0 | 0 |
| **22** | 1232.34 | 408.0 | 150.0 | 0 | 0 | 162 | 0 | 0 | 0 | 0 | 0 | -36.0 | 384.9 | 281.1 | 20 | 20 | 0 | 0 | 0 | 0 | 0 | 0 | 0 |
| **23** | 1215.89 | 363.2 | 252.0 | 0 | 0 | 0 | 0 | 0 | 0 | 0 | 0 | -74.8 | 455.0 | 256.3 | 20 | 0 | 0 | 0 | 0 | 0 | 0 | 0 | 0 |
| **24** | 1220 | 347.3 | 150.0 | 0 | 0 | 0 | 0 | 0 | 0 | 0 | 0 | -196.7 | 421.0 | 281.5 | 20 | 0 | 0 | 0 | 0 | 0 | 0 | 0 | 0 |

**Table 5.7:** Power generated from thermal units in backpressure mode for case-2 & 3, test system-IV

| | **Backpressure mode in Case-III** | | | | | | | | | | | **Backpressure mode in Case-II** | | | | | | | | | | **Solar Power(Case-2&3)** |
|---|---|---|---|---|---|---|---|---|---|---|---|---|---|---|---|---|---|---|---|---|---|---|
| | **Thermal power generation (MW)** | | | | | | | | | | **Battery** | **Thermal power generation (MW)** | | | | | | | | | | |
| **h** | **P1** | **P2** | **P3** | **P4** | **P5** | **P6** | **P7** | **P8** | **P9** | **P10** | **Power** | **P1** | **P2** | **P3** | **P4** | **P5** | **P6** | **P7** | **P8** | **P9** | **P10** | |
| **1** | 446.2 | 150 | 0 | 0 | 162 | 0 | 0 | 0 | 0 | 0 | 75.7 | 455 | 207.50 | 20 | 0 | 0 | 0 | 0 | 0 | 0 | 0 | 0 |
| **2** | 415.7 | 150.0 | 0 | 0 | 162 | 0 | 0 | 10 | 0 | 0 | 46.6 | 455 | 206.1 | 20 | 0 | 0 | 0 | 0 | 10 | 0 | 0 | 0 |
| **3** | 455 | 205.8 | 0 | 20 | 162 | 0 | 0 | 10 | 0 | 0 | 31.7 | 455 | 164.10 | 20 | 20 | 162 | 0 | 0 | 0 | 0 | 0 | 0 |
| **4** | 455 | 393.7 | 20 | 20 | 162 | 20 | 25 | 10 | 55 | 10 | 5.5 | 455 | 398.20 | 20 | 20 | 162 | 20 | 25 | 0 | 55 | 10 | 0 |
| **5** | 455 | 241.8 | 20 | 20 | 162 | 20 | 25 | 0 | 55 | 0 | 17.8 | 455 | 279.02 | 20 | 20 | 162 | 20 | 25 | 0 | 0 | 0 | 2 |
| **6** | 455 | 311.9 | 20 | 20 | 162 | 20 | 25 | 10 | 55 | 0 | 0.5 | 455 | 356.39 | 20 | 20 | 162 | 20 | 25 | 10 | 0 | 10 | 45 |
| **7** | 455 | 335.7 | 20 | 20 | 162 | 20 | 25 | 10 | 55 | 0 | 3.7 | 455 | 331.97 | 20 | 20 | 162 | 20 | 25 | 10 | 55 | 0 | 118 |
| **8** | 455 | 289.4 | 20 | 20 | 162 | 20 | 25 | 0 | 55 | 0 | 6.7 | 455 | 282.64 | 20 | 20 | 162 | 20 | 25 | 0 | 55 | 0 | 260 |
| **9** | 455 | 455 | 130 | 130 | 162 | 74.91 | 25 | 10 | 55 | 10 | 4.3 | 455 | 455 | 130 | 130 | 162 | 70.6 | 25 | 10 | 55 | 10 | 261 |
| **10** | 455 | 299.9 | 20 | 20 | 162 | 0 | 0 | 10 | 0 | 0 | 0.3 | 455 | 309.53 | 20 | 20 | 162 | 0 | 0 | 0 | 0 | 0 | 396 |
| **11** | 455 | 272.2 | 20 | 20 | 162 | 0 | 0 | 0 | 55 | 0 | 40.2 | 455 | 287 | 20 | 20 | 162 | 0 | 0 | 0 | 0 | 0 | 440 |
| **12** | 455 | 288.6 | 20 | 20 | 162 | 0 | 0 | 0 | 55 | 0 | 40.6 | 455 | 303 | 20 | 20 | 162 | 0 | 0 | 0 | 0 | 0 | 440 |
| **13** | 455 | 318.6 | 20 | 20 | 162 | 20 | 0 | 0 | 0 | 0 | 42.6 | 455 | 296 | 20 | 20 | 162 | 0 | 0 | 0 | 0 | 0 | 440 |
| **14** | 455 | 428.1 | 20 | 20 | 162 | 20 | 25 | 10 | 0 | 0 | 34.9 | 455 | 363.21 | 20 | 20 | 162 | 20 | 0 | 10 | 55 | 0 | 435 |
| **15** | 455 | 325.3 | 20 | 20 | 162 | 20 | 25 | 0 | 0 | 0 | -5.0 | 455 | 355.29 | 20 | 20 | 162 | 20 | 0 | 0 | 0 | 0 | 368 |
| **16** | 455 | 208.3 | 20 | 20 | 162 | 20 | 25 | 0 | 0 | 0 | -14.4 | 455 | 247.76 | 20 | 20 | 162 | 20 | 0 | 0 | 0 | 0 | 335 |
| **17** | 455 | 207.5 | 20 | 20 | 162 | 20 | 25 | 0 | 0 | 0 | -9.1 | 455 | 241.60 | 20 | 20 | 162 | 20 | 0 | 0 | 0 | 0 | 201 |
| **18** | 455 | 427.4 | 20 | 20 | 162 | 20 | 25 | 10 | 0 | 0 | -11.8 | 455 | 439.16 | 20 | 20 | 162 | 20 | 25 | 10 | 0 | 0 | 109 |
| **19** | 455 | 455 | 130 | 51.5 | 162 | 20 | 25 | 10 | 55 | 10 | -7.0 | 455 | 455 | 130 | 58.52 | 162 | 20 | 25 | 10 | 55 | 10 | 19 |
| **20** | 455 | 455 | 66.80 | 20 | 162 | 20 | 25 | 10 | 55 | 10 | -9.2 | 455 | 455 | 76 | 20 | 162 | 20 | 25 | 10 | 55 | 10 | 0 |
| **21** | 455 | 455 | 83.35 | 20 | 162 | 20 | 0 | 10 | 0 | 0 | -27.8 | 455 | 455 | 96.20 | 20 | 162 | 20 | 25 | 0 | 0 | 0 | 0 |
| **22** | 455 | 384.41 | 20 | 20 | 162 | 0 | 0 | 0 | 0 | 0 | -50.6 | 455 | 415 | 20 | 20 | 162 | 20 | 0 | 0 | 0 | 0 | 0 |
| **23** | 455 | 350.36 | 20 | 20 | 162 | 0 | 0 | 0 | 0 | 0 | -68.6 | 455 | 419 | 20 | 20 | 162 | 0 | 0 | 0 | 0 | 0 | 0 |
| **24** | 455 | 295.42 | 0 | 20 | 162 | 0 | 0 | 0 | 0 | 0 | -147.6 | 455 | 423 | 20 | 20 | 162 | 0 | 0 | 0 | 0 | 0 | 0 |

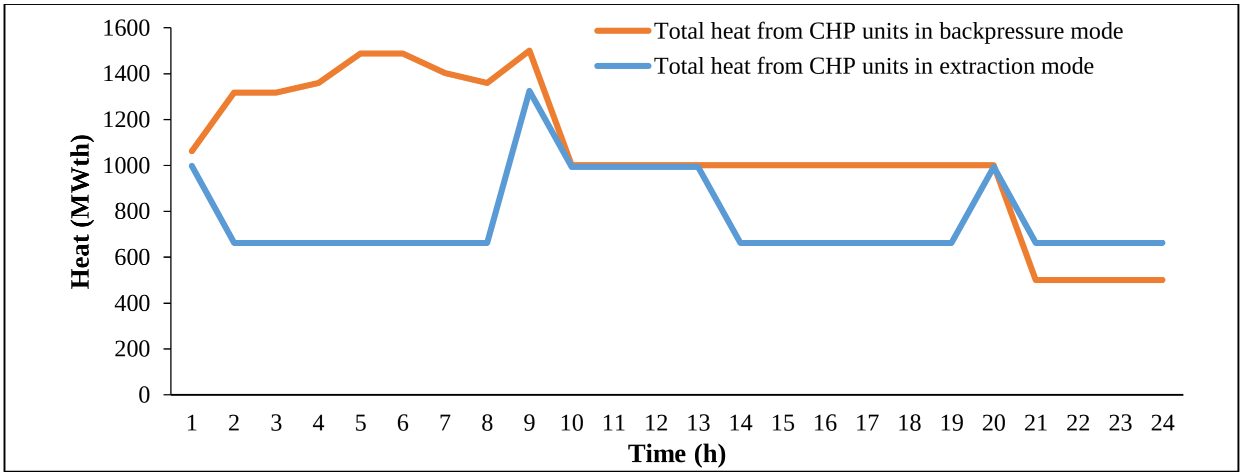


**Figure 5.6:** Heat generated from CHP units for case-2 of test system-IV

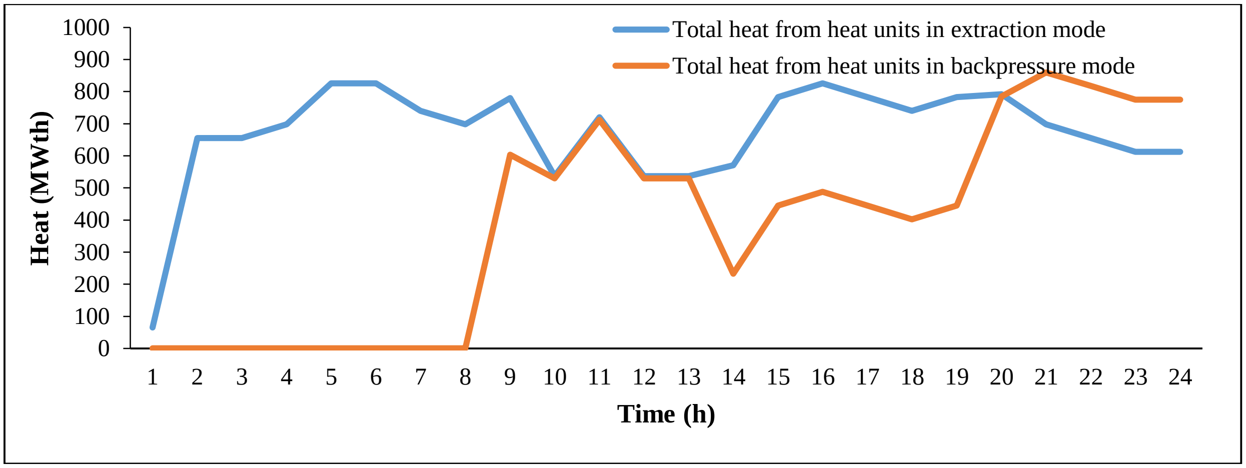


**Figure 5.7:** Heat generated from heat unit for case-2 of test system-IV

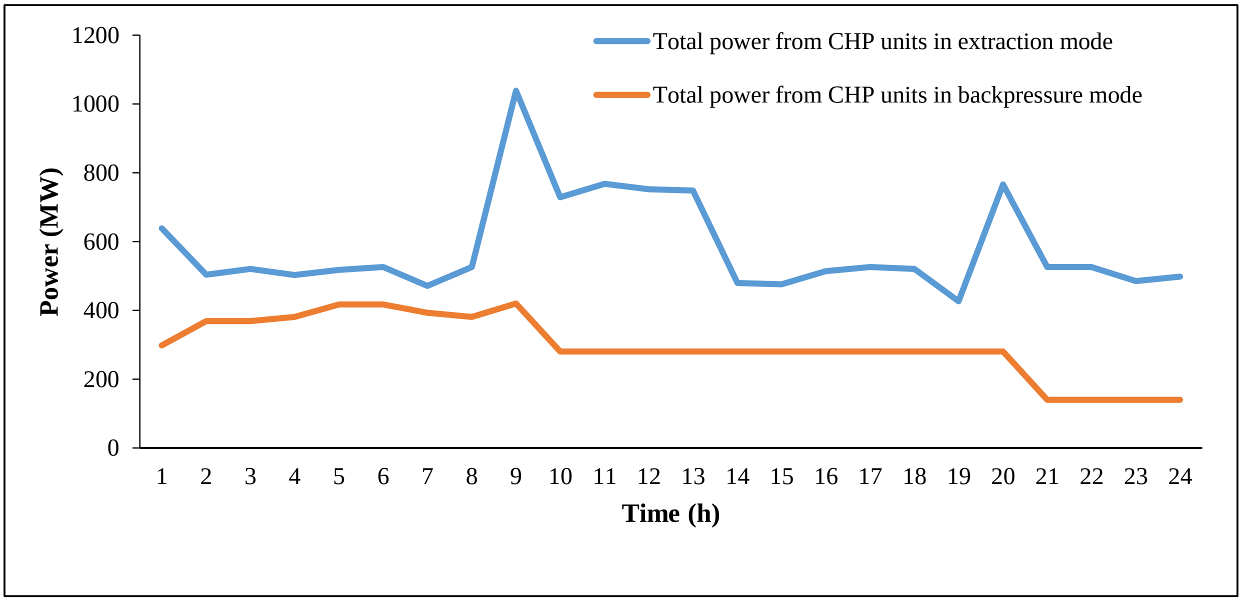


**Figure 5.8:** The total generated power from CHP units in case-2 of test system-IV

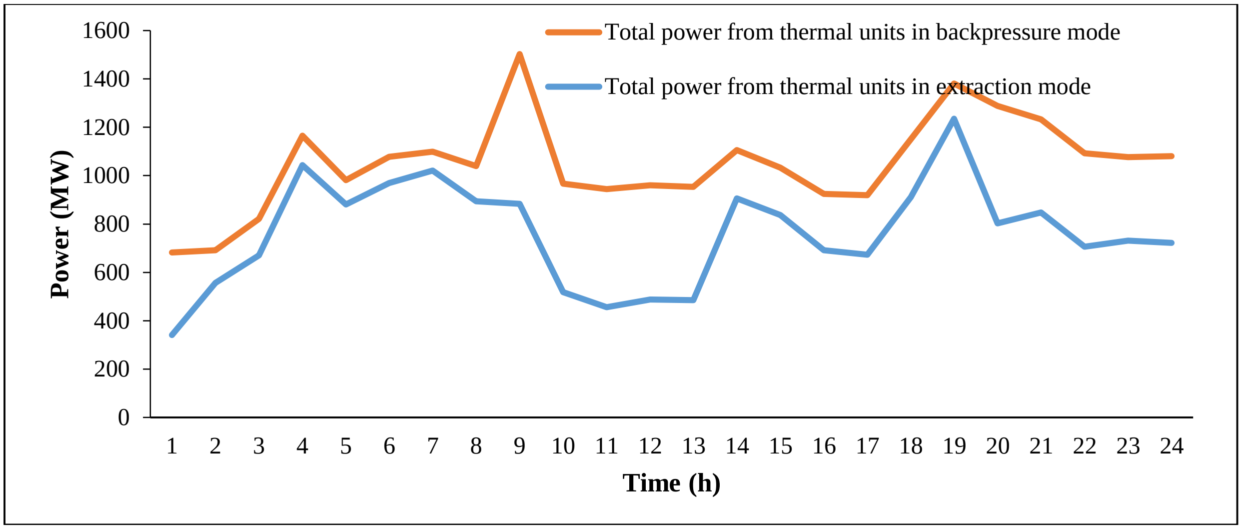


**Figure 5.9:** The total generated power from thermal units in case-2 of test system-IV

**Table 5.8:** Operating cost of three cases for test system-IV

| | Cost obtained in backpressure mode ($) | Cost obtained in extraction mode ($) |
|---|---|---|
| **Case-1** | 990110.6 | 1423362 |
| **Case-2** | 902293.9 | 1354884 |
| **Case-3** | 898635.2 | 1354218.6 |

**Case-3: The PV-ESU integration with combined heat and power unit commitment problem**

In case-3, the ESU has been integrated with PV, CHP, thermal only and heat only units. The effect of integration of ESU has been investigated in case-3 as compared to case-2. The unit commitment schedule of various generating units is given in Table 5.3 and 5.4. The generation schedule of thermal units, solar and battery is given in Table 5.6 and 5.7. The cumulative heat generation from CHP and heat generating units has been illustrated in Figures 5.10 and 5.11, respectively. It has been observed that CHP units in backpressure mode operation generate more heat as compared to extraction mode. Hence, heat only units during extraction mode of CHP units need to generate more heat as compared to backpressure mode CHP operation. This fact is also validated by commitment status of heat only units. It has been observed that heat only units need to commit for 15 and 22 sub-intervals during backpressure and extraction mode of CHP unit operation, respectively. It has been observed from Figures 5.12 and 5.13 that the cumulative power generation from CHP units in extraction mode is more as compared to backpressure mode that results in less cumulative power generation from thermal units in extraction mode. Hence, during backpressure and extraction mode of CHP unit operation, the thermal units are needed to commit for 168 and 96 sub-intervals, respectively. In Figures 5.14 and 5.15, total power to utility has been presented for extraction and backpressure mode of CHP unit operation, respectively. It is illustrated from these figures that integration of PV and ESU in CHP system results the negative power injection into ESS to charge the battery during light load sub-intervals (1-5$^{th}$). During 11-14$^{th}$ sub-intervals, the extra power from ESS has been utilized to charge the battery because the utility is bound with maximum power flow limit from ESS. For case-3, the operating cost during backpressure and extraction mode of ICHPUC is $898635.2 and $1354218.6, respectively. It is observed from Table 5.8, that PV-ESU (case-3) in backpressure mode has saved the operating cost '$91475.4/day' as compared to case-1, while during extraction mode, saving of operating cost '$69143.4/day' has been achieved.

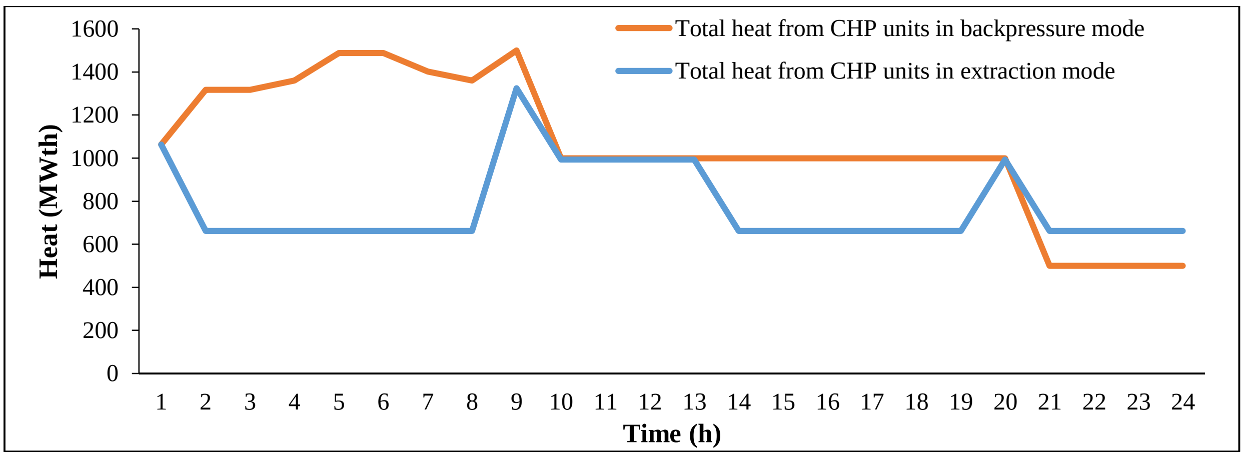


**Figure 5.10:** The total heat generated from CHP units in case-3 of test system-IV

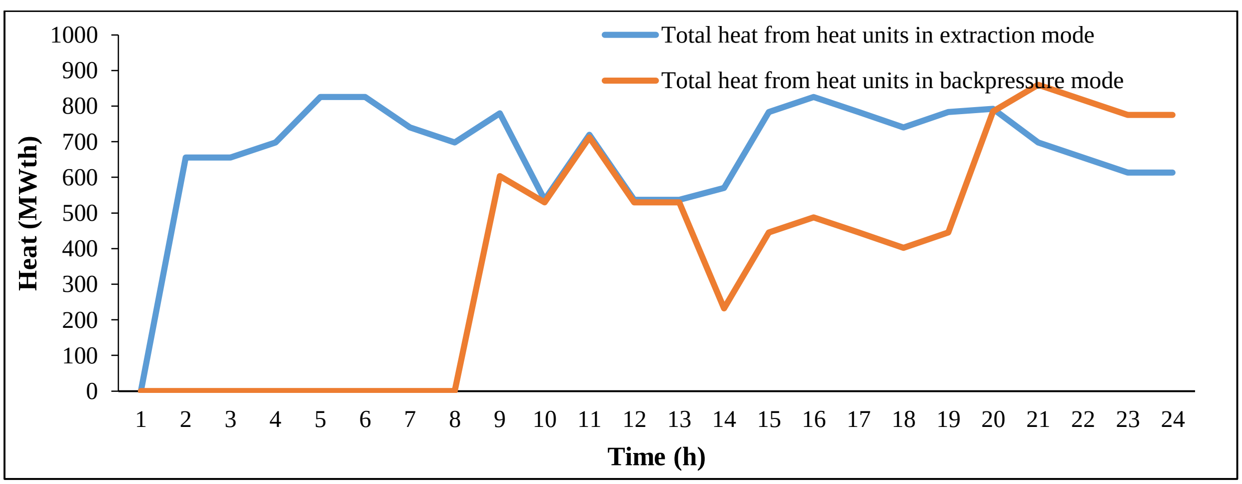


**Figure 5.11:** The total heat generated from heat units in case-3 of test system-IV

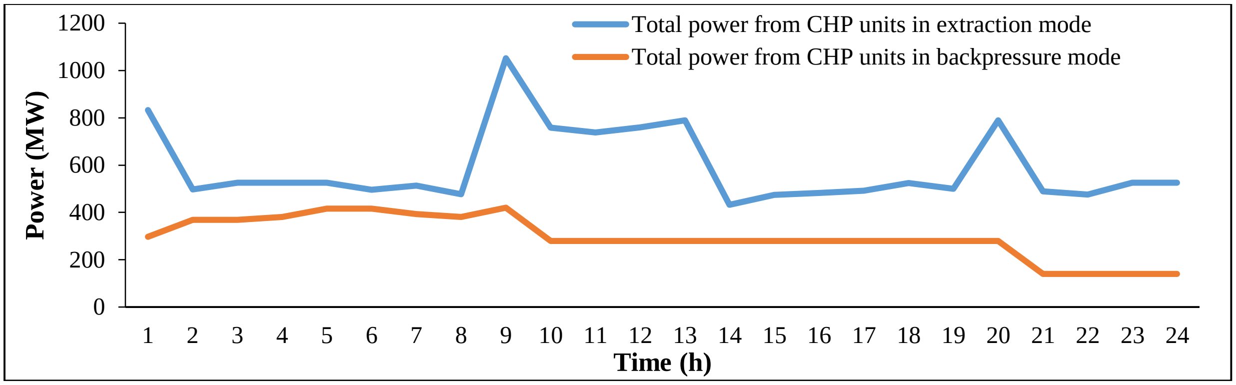


**Figure 5.12:** The total power generated from CHP units in case-3 of test system-IV

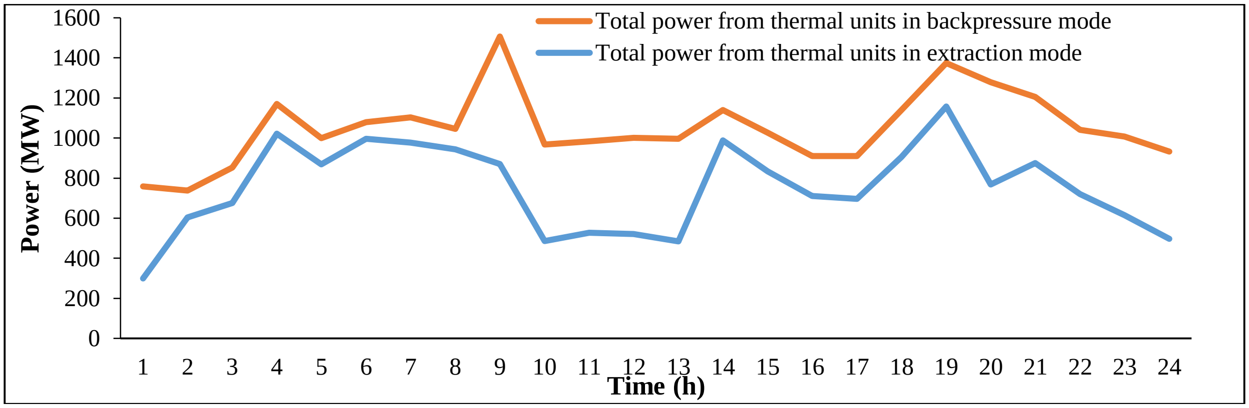


**Figure 5.13:** The total power generated from thermal units in case-3 of test system-IV

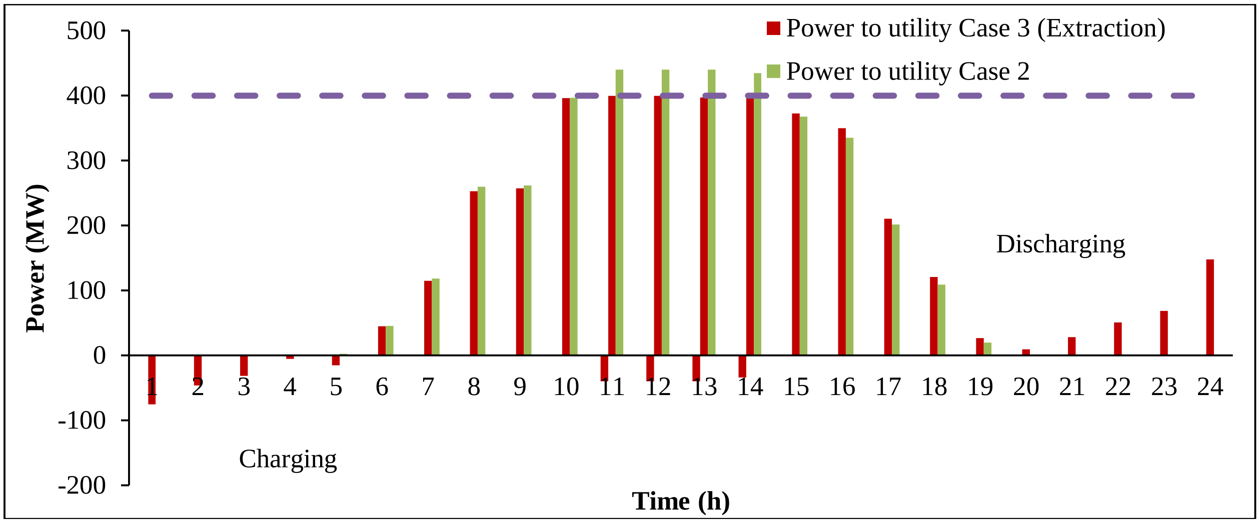


**Figure 5.14:** Solar PV plant power and charging/discharging of battery in extraction mode for test system-IV

**Note:** Negative sign indicates ESU is in charging mode and positive sign indicates ESU is in discharging mode.

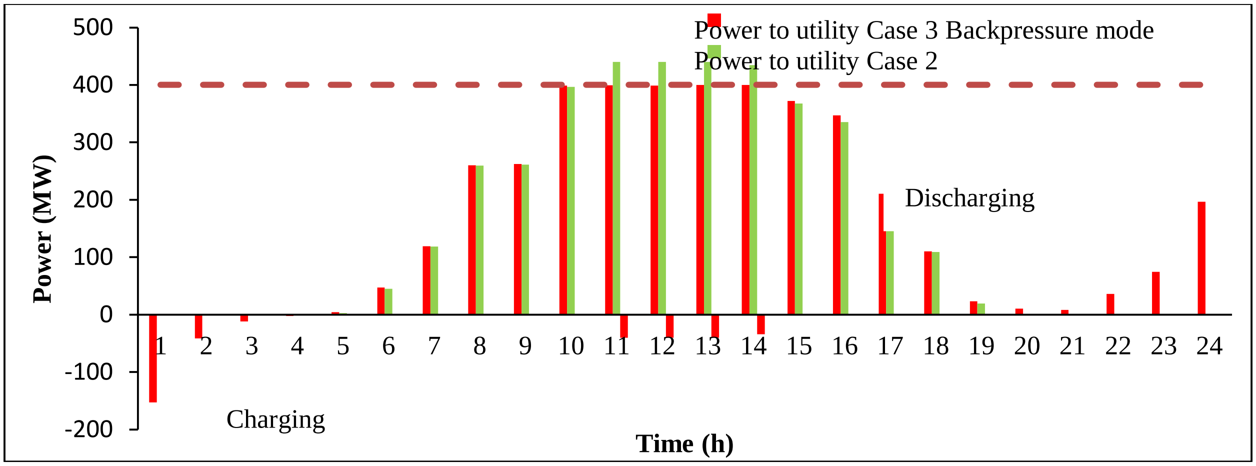


**Figure 5.15:** Solar PV plant power and charging/discharging of battery in backpressure mode for test system-IV

**Note:** Negative sign indicates ESU is in charging mode and positive sign indicates ESU is in discharging mode.

**Power flexibility of integrated system:** The system's power generation flexibility is associated with unit limits such as generation, ramp, fuel, charging/discharging and maximum PV-ESU penetration limits. In order to compute the generation flexibility of ICHPS, the upward and downward rate is computed. The power flexibility of ICHPS is the collective effect of individual unit flexibility during each sub-interval and is shown in Figures 5.16-5.19 for all three cases. The average upward and downward power generation flexibility for all three cases during extraction and backpressure mode of CHP unit operation have been computed and given in Table 5.9. It is observed from Table 5.9 and Figures 5.16-5.17 that upward power flexibility is more for case-3 in extraction and backpressure mode as compared to case-1 and 2. Whereas downward power flexibility is high for case-1 in extraction and backpressure mode as compared to case-2 and 3. It is also observed that upward and downward power flexibility during extraction mode is high as compared to backpressure mode in most of cases.

**Table 5.9:** Average power generation flexibility for all cases; test system-IV

| Average power generation flexibility (MW) | Mode of CHP unit operation | | | | | |
|---|---|---|---|---|---|---|
| | Backpressure | | | Extraction | | |
| | Case-1 | Case-2 | Case-3 | Case-1 | Case-2 | Case-3 |
| **Upward** | 250.88 | 350.21 | 449.33 | 361.83 | 423.75 | 569.83 |
| **Downward** | 301.13 | 235.29 | 241.75 | 273.38 | 239.13 | 263.79 |

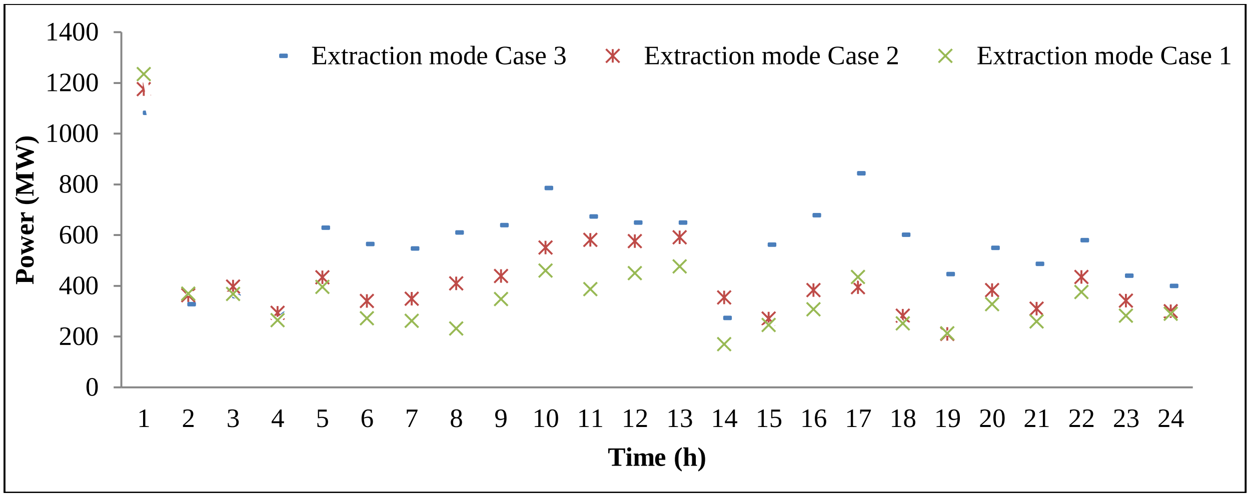


**Figure 5.16:** Upward power flexibility of extraction mode for test system-IV

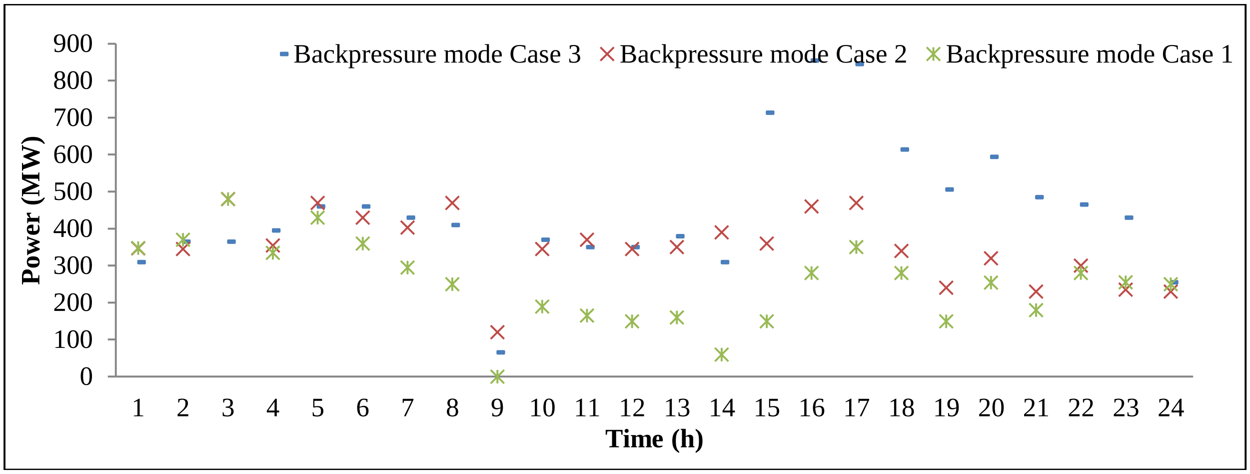


**Figure 5.17:** Upward power flexibility of backpressure mode for test system-IV

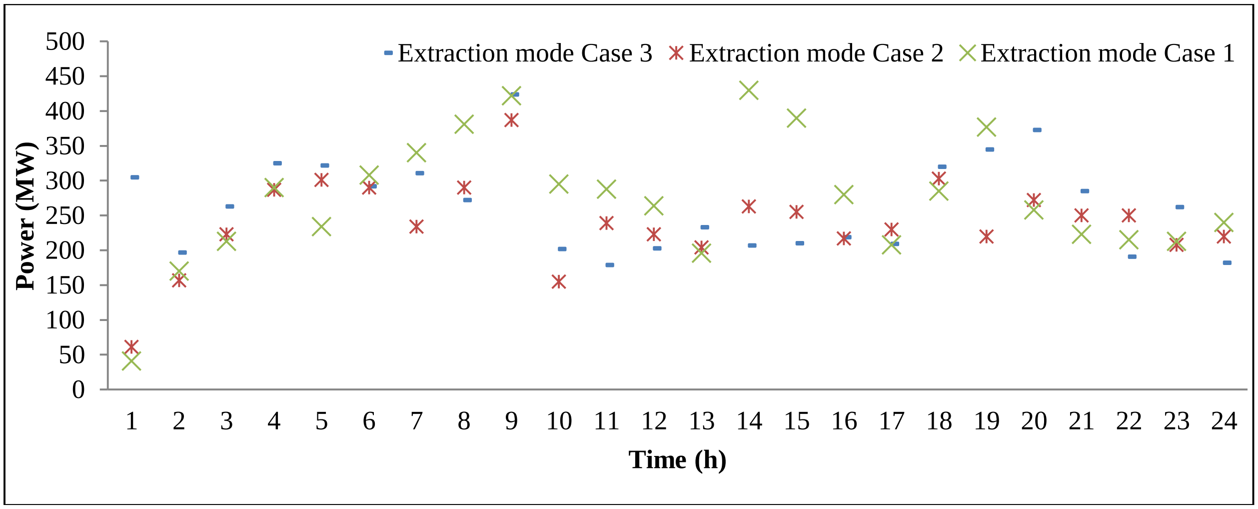


**Figure 5.18:** Downward power flexibility of extraction mode for test system-IV

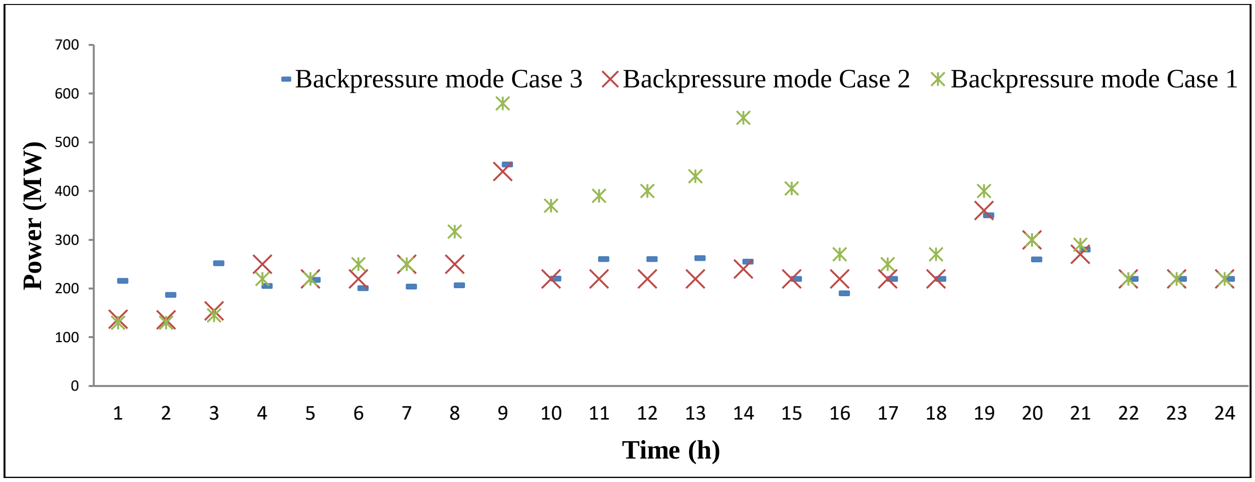


**Figure 5.19:** Downward power flexibility of backpressure mode for test system-IV

### 5.5.2 Test System-V

The heat generation schedule of CHP and heat units obtained from BSA-CSO technique in dual mode for case-1 are illustrated in Figures 5.20-5.23. It has been observed that the total heat generated in backpressure mode of CHP units is higher as compared to extraction mode. The impact of lower heat generation during extraction mode of CHP unit is evident from the commitment status of heat units and it is shown in Table 5.10. The heat units are committed in extraction mode to satisfy the heat demand at 2-24$^{th}$ sub-intervals whereas in backpressure mode, heat only units are committed only at 22$^{nd}$ sub-interval. Similar observation has been revealed in case 2 and 3 for unit commitment status and total generated heat from CHP units shown in Tables 5.10-5.12 and Figures 5.24-5.27. The total generated heat from CHP and heat units in case 2 and 3 have been illustrated in Figures 5.24-5.27.

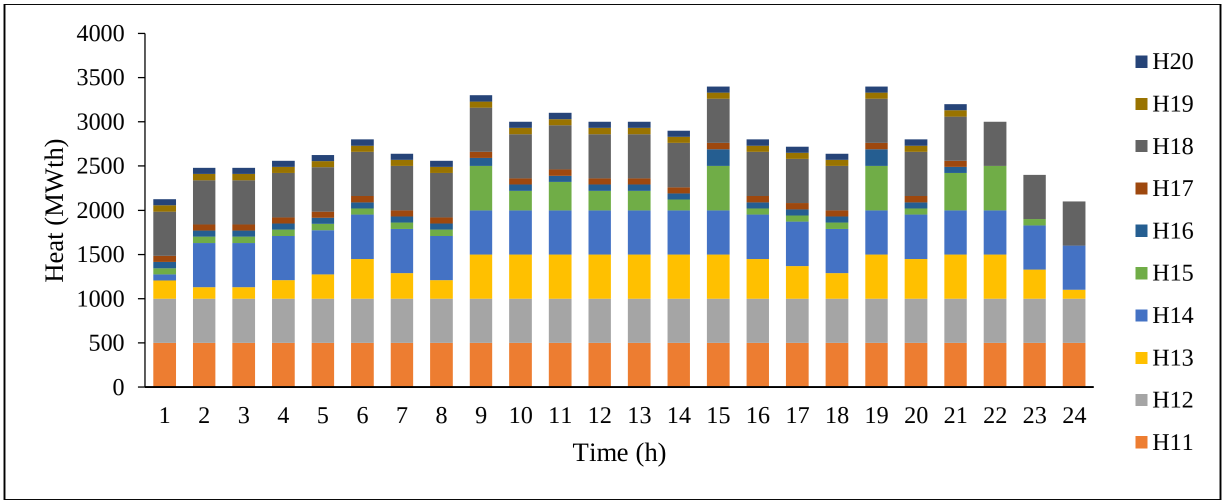


**Figure 5.20:** Heat generated from CHP units in backpressure mode for case-1 of test system-V

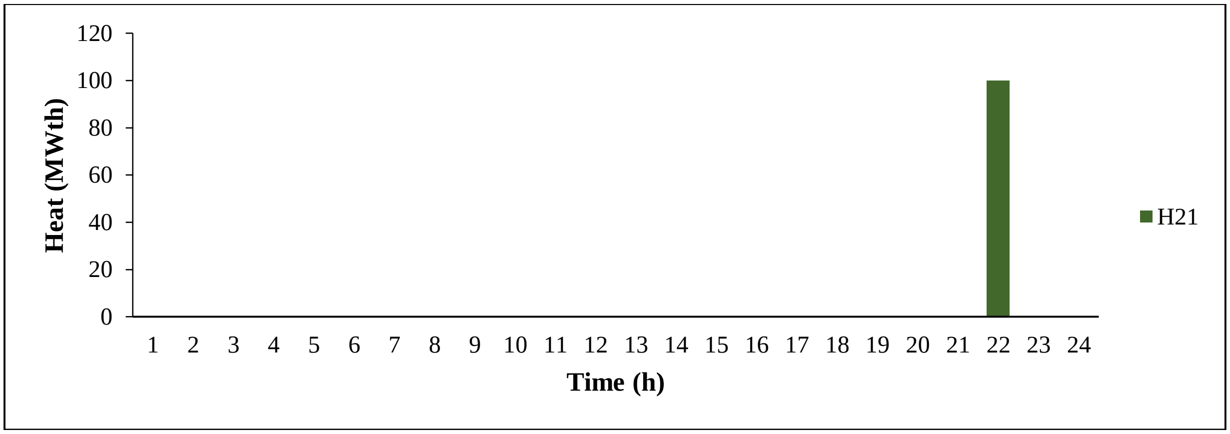


**Figure 5.21:** Heat generated from heat units in backpressure mode for case-1 of test system-V

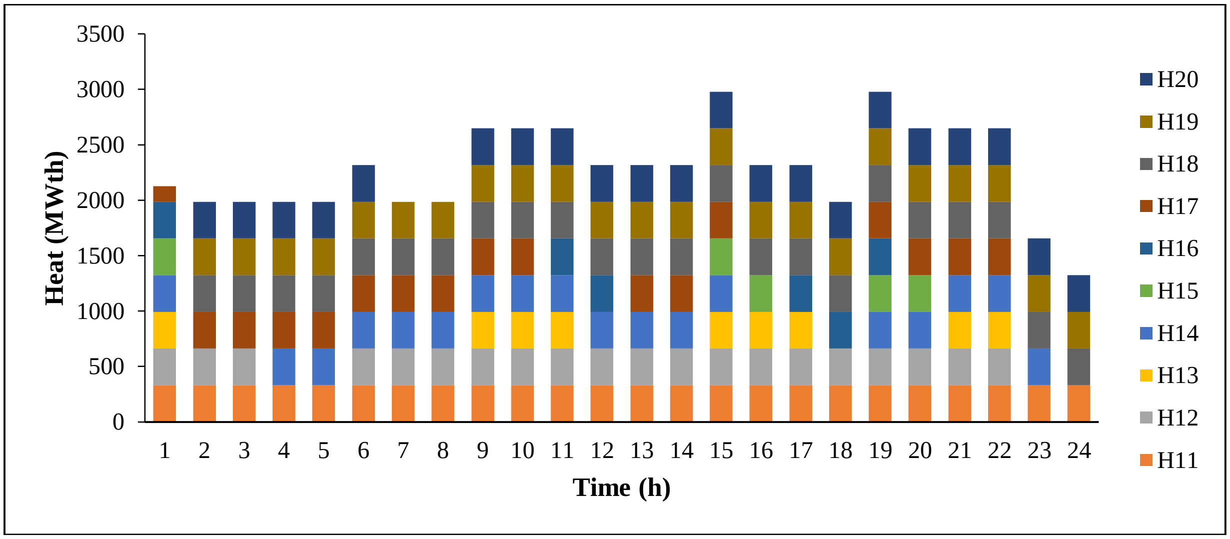


**Figure 5.22:** Heat generation from CHP units in extraction mode for case-1 of test system-V

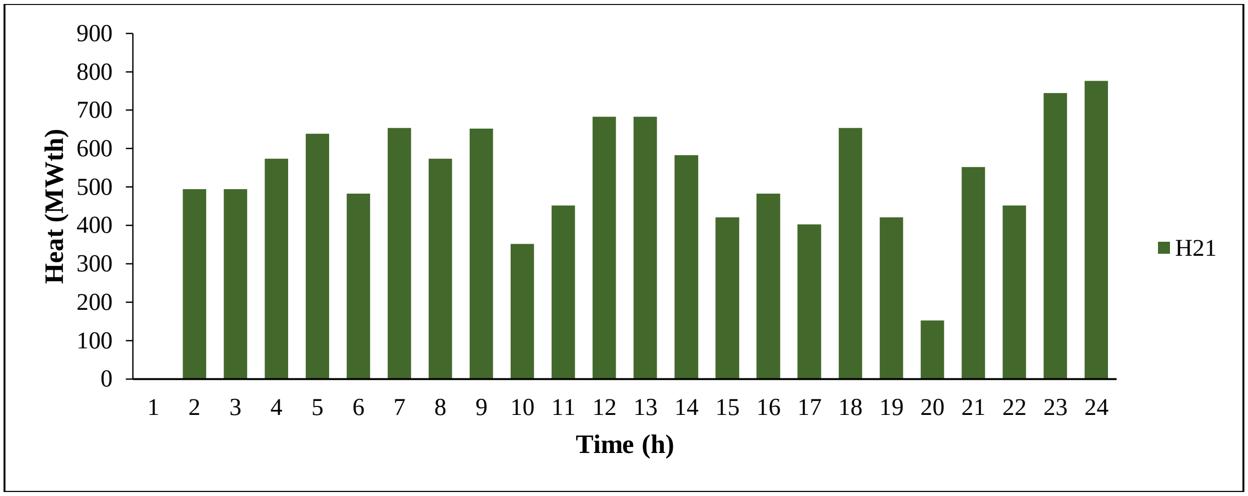


**Figure 5.23:** Heat generation from heat units in extraction mode for case-1 of test system-V

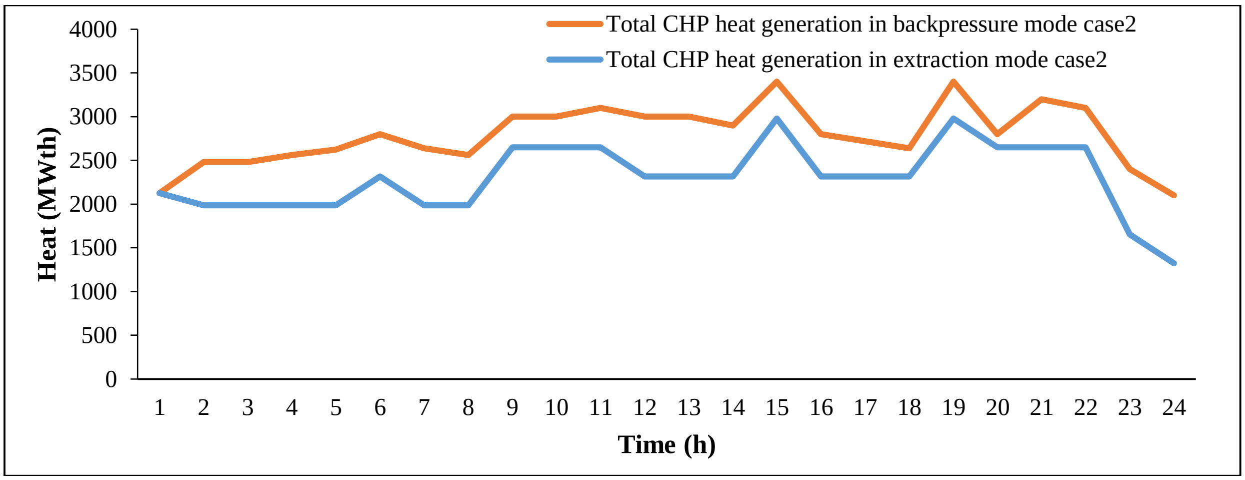


**Figure 5.24:** The total heat generated from CHP units in case-2 of test system-V

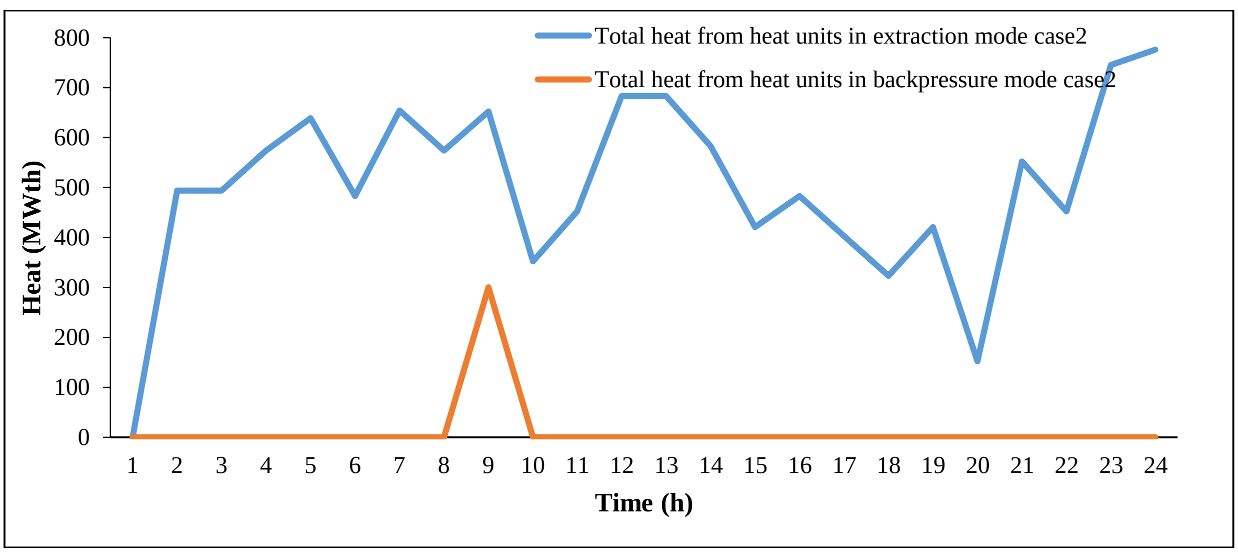


**Figure 5.25:** The total heat generated from heat units in case-2 of test system-V

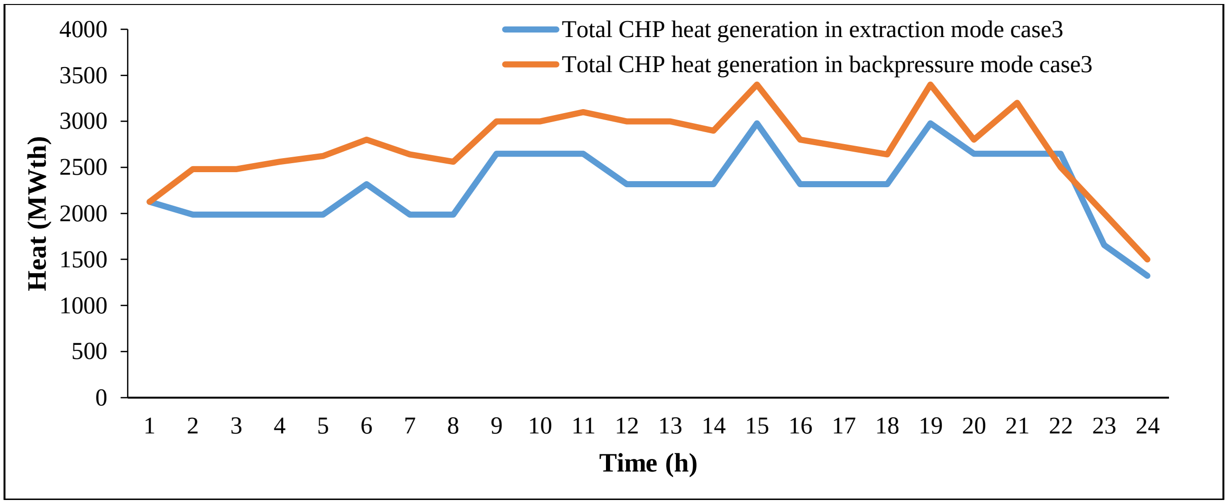


**Figure 5.26:** The total heat generated from CHP units in case-3 of test system-V

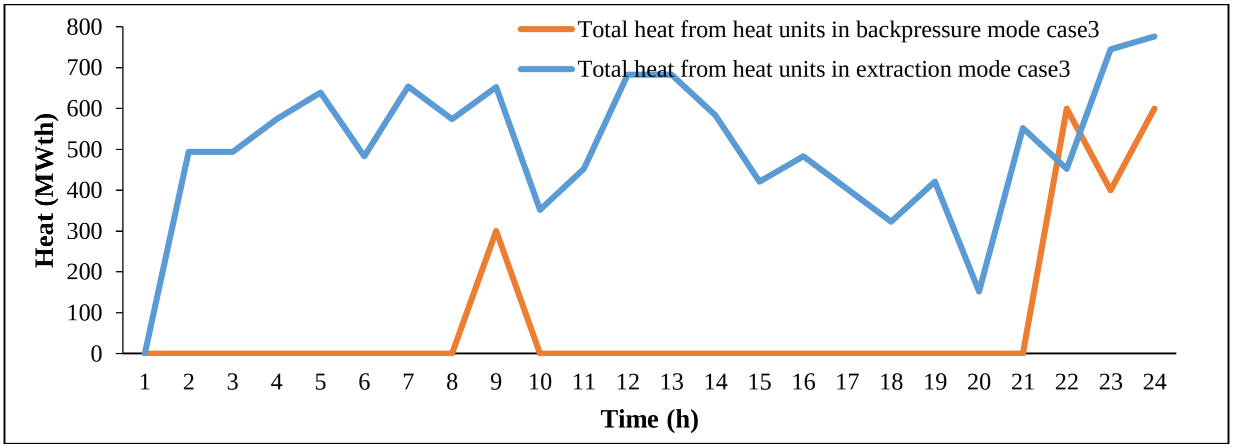


**Figure 5.27:** The total heat generated from heat units in case-3 of test system-V

**Table 5.10:** Hourly status of units for case 1 of test system-V

| Sub-intervals (h) | Backpressure mode | | | Extraction mode | | |
|---|---|---|---|---|---|---|
| | **Thermal** | **CHP** | **Heat** | **Thermal** | **CHP** | **Heat** |
| **1** | 11100 | 1111111111 | 0 | 11000 | 1111111111 | 0 |
| **2** | 11111 | 1111111111 | 0 | 11010 | 1100001111 | 1 |
| **3** | 11111 | 1111111111 | 0 | 11000 | 1100001111 | 1 |
| **4** | 11111 | 1111111111 | 0 | 11011 | 1001001111 | 1 |
| **5** | 11111 | 1111111111 | 0 | 11000 | 1001001111 | 1 |
| **6** | 11111 | 1111111111 | 0 | 11010 | 1101001111 | 1 |
| **7** | 11110 | 1111111111 | 0 | 11000 | 1101001110 | 1 |
| **8** | 11111 | 1111111111 | 0 | 11000 | 1101001110 | 1 |
| **9** | 11111 | 1111111111 | 0 | 11010 | 1111001111 | 1 |
| **10** | 11111 | 1111111111 | 0 | 11000 | 1111001111 | 1 |
| **11** | 11111 | 1111111111 | 0 | 11010 | 1111010111 | 1 |
| **12** | 11111 | 1111111111 | 0 | 11011 | 1101010111 | 1 |
| **13** | 11111 | 1111111111 | 0 | 11010 | 1101001111 | 1 |
| **14** | 11111 | 1111111111 | 0 | 10110 | 1101001111 | 1 |
| **15** | 11111 | 1111111111 | 0 | 10111 | 1111101111 | 1 |
| **16** | 11111 | 1111111111 | 0 | 10101 | 1110100111 | 1 |
| **17** | 11111 | 1111111111 | 0 | 10101 | 1110010111 | 1 |
| **18** | 11101 | 1111111111 | 0 | 10100 | 1100010111 | 1 |

**Table 5.10:** Hourly status of units for case 1 of test system-V (Continued)

| Sub-intervals (h) | Backpressure mode | | | Extraction mode | | |
|---|---|---|---|---|---|---|
| | Thermal | CHP | Heat | Thermal | CHP | Heat |
| **18** | 11101 | 1111111111 | 0 | 10100 | 1100010111 | 1 |
| **19** | 11111 | 1111111111 | 0 | 10100 | 1101111111 | 1 |
| **20** | 11111 | 1111111111 | 0 | 10110 | 1101101111 | 1 |
| **21** | 11111 | 1111111111 | 0 | 10110 | 1111001111 | 1 |
| **22** | 11111 | 1111100100 | 1 | 10100 | 1111001111 | 1 |
| **23** | 11111 | 1111100100 | 0 | 11100 | 1001000111 | 1 |
| **24** | 11111 | 1111000100 | 0 | 11101 | 1000000111 | 1 |

**Table 5.11:** Hourly status of units for case 2 of test system-V

| Sub-intervals (h) | Backpressure mode | | | Extraction mode | | |
|---|---|---|---|---|---|---|
| | Thermal | CHP | Heat | Thermal | CHP | Heat |
| **1** | 11100 | 1111111111 | 0 | 11001 | 1111111111 | 0 |
| **2** | 11111 | 1111111111 | 0 | 11001 | 1110000111 | 1 |
| **3** | 11111 | 1111111111 | 0 | 11001 | 1110000111 | 1 |
| **4** | 11111 | 1111111111 | 0 | 11011 | 1101000111 | 1 |
| **5** | 11111 | 1101000111 | 0 | 11001 | 1101000111 | 1 |
| **6** | 11111 | 1101000111 | 0 | 11001 | 1111000111 | 1 |
| **7** | 11110 | 1101000111 | 0 | 11001 | 1111000110 | 1 |
| **8** | 11110 | 1101000111 | 0 | 11001 | 1111000110 | 1 |
| **9** | 11111 | 1101000111 | 0 | 11001 | 1111100111 | 1 |
| **10** | 11111 | 1101000111 | 0 | 10001 | 1111100111 | 1 |
| **11** | 11111 | 1111111111 | 0 | 10011 | 1111100111 | 1 |
| **12** | 11111 | 1111111111 | 0 | 10111 | 1111000111 | 1 |
| **13** | 11111 | 1111111111 | 0 | 10101 | 1111000111 | 1 |
| **14** | 11111 | 1111111111 | 0 | 10101 | 1111000111 | 1 |
| **15** | 11111 | 1111111111 | 0 | 10111 | 1111110111 | 1 |
| **16** | 11111 | 1111111111 | 0 | 10101 | 1010110111 | 1 |
| **17** | 11111 | 1111111111 | 0 | 10101 | 1010110111 | 1 |
| **18** | 11101 | 1111111111 | 0 | 10001 | 1010110111 | 1 |
| **19** | 11111 | 1111111111 | 0 | 10001 | 1111110111 | 1 |
| **20** | 11111 | 1111111111 | 0 | 11011 | 1111100111 | 1 |
| **21** | 11111 | 1111111111 | 0 | 11001 | 1111100111 | 1 |
| **22** | 11111 | 1111000111 | 1 | 11001 | 1111100111 | 1 |
| **23** | 11111 | 1111000011 | 0 | 11101 | 1001000111 | 1 |
| **24** | 11111 | 1110000011 | 0 | 11101 | 0001000111 | 1 |

**Table 5.12:** Hourly status of units for case 3 of test system-V

| Sub-intervals (h) | Backpressure mode | | | Extraction mode | | |
|---|---|---|---|---|---|---|
| | Thermal | CHP | Heat | Thermal | CHP | Heat |
| **1** | 11011 | 1111111111 | 0 | 11001 | 1111111111 | 0 |
| **2** | 11111 | 1111111111 | 0 | 11001 | 1110000111 | 1 |
| **3** | 11111 | 1111111111 | 0 | 11001 | 1110000111 | 1 |
| **4** | 11111 | 1111111111 | 0 | 11011 | 1101000111 | 1 |
| **5** | 11111 | 1111000101 | 0 | 11001 | 1101000111 | 1 |
| **6** | 11111 | 1111000101 | 0 | 11001 | 1111000111 | 1 |
| **7** | 11111 | 1111000101 | 0 | 11001 | 1111000110 | 1 |
| **8** | 11111 | 1111000101 | 0 | 11001 | 1111000110 | 1 |
| **9** | 11111 | 1111000101 | 1 | 11001 | 1111100111 | 1 |
| **10** | 11111 | 1111000101 | 0 | 10001 | 1111100111 | 1 |
| **11** | 11111 | 1111111111 | 0 | 10011 | 1111100111 | 1 |

**Table 5.12:** Hourly status of units for case 3 of test system-V (Continued)

| Sub-intervals (h) | Backpressure mode | | | Extraction mode | | |
|---|---|---|---|---|---|---|
| | **Thermal** | **CHP** | **Heat** | **Thermal** | **CHP** | **Heat** |
| **12** | 11111 | 1111111111 | 0 | 10111 | 1111000111 | 1 |
| **13** | 11111 | 1111111111 | 0 | 10101 | 1111000111 | 1 |
| **14** | 11111 | 1111111111 | 0 | 10101 | 1111000111 | 1 |
| **15** | 11111 | 1111111111 | 0 | 10111 | 1111110111 | 1 |
| **16** | 11111 | 1111111111 | 0 | 10101 | 1010110111 | 1 |
| **17** | 11111 | 1111111111 | 0 | 10101 | 1010110111 | 1 |
| **18** | 11101 | 1111111111 | 0 | 10001 | 1010110111 | 1 |
| **19** | 11111 | 1111111111 | 0 | 10001 | 1111110111 | 1 |
| **20** | 11111 | 1111111111 | 0 | 11011 | 1111110111 | 1 |
| **21** | 11111 | 1111111111 | 0 | 11001 | 1111100111 | 1 |
| **22** | 11111 | 1111000101 | 1 | 11001 | 1111100111 | 1 |
| **23** | 11111 | 1101000101 | 1 | 11101 | 1001000111 | 1 |
| **24** | 11111 | 0100000101 | 1 | 11101 | 0001000111 | 1 |

In case-1, the power generation schedule of thermal and CHP units for dual mode have been shown in Figures 5.28-5.31. In order to show the impact of dual mode, the average generated power is evaluated during extraction and backpressure mode of CHP units is 1714.8 MW and 782.1 MW, respectively and it is presented in Table 5.13. It has been observed that in extraction mode, the total generated power from CHP units is higher in comparison with backpressure mode due heat power ratio. In order to satisfy the power demand, the optimum schedule of generating units in backpressure mode required 116 thermal units for sub-intervals (1-24$^{th}$), while during extraction mode, only 67 thermal units are needed for total sub-intervals and it is given Table 5.14. It has also been observed from figures that the total power generated from thermal units in backpressure mode is high as compare to extraction mode. The total generated power and heat from thermal, CHP and heat units in dual mode for case 2 and 3 have been shown in Figures 5.32-5.35. It has been observed from Figures 5.34 and 5.36 for case 2 and 3 that the total CHP power generation in extraction mode is high as compared to backpressure mode. The impact of high power generation from extraction mode of CHP on the thermal power generation in case 2 and 3 is same as discussed in case 1. The power flow from ESS to utility and charging/discharging of battery is shown in Figures 5.36 and 5.37. At 1-3$^{rd}$ and 11-14$^{th}$ sub-intervals, in case-3, the negative power injection into ESS to charge the battery whereas, battery discharge at 8-9$^{th}$ and 19-24$^{th}$ sub-intervals. The UC schedule in case-2 and 3 have changed as compared to case-1 due to inclusion of PV system and ESS, respectively as illustrated in Tables 5.10 and 5.12. It is also illustrated from Tables 5.14 that the number of committed CHP units in case-2 and 3 is reduced as compared to case-1 for backpressure and extraction mode of CHP unit operation, respectively.

In case-1, the operating cost in backpressure and extraction mode are $1712948 and $3222067, respectively. It has been evident from Table 5.15 that operating cost saving of '$70939/day' and '$42294/day' in backpressure and extraction mode, respectively for case-2 as compare to case-1. The obtained cost from BSA-CSO technique in backpressure and extraction mode for case-3 are $1632407 and $3174508, respectively. The operating cost saving of '$80541/day' in backpressure mode for case-3 as compare to case-1 whereas the cost saving of '$47559/day' in extraction mode.

**Table 5.13:** Average CHP power from the operating mode for all cases in test system-V

| Average CHP power from the operating mode (MW) | Case-1 | Case-2 | Case-3 |
|---|---|---|---|
| **Extraction mode** | 1714.8 | 1723.2 | 1742 |
| **Backpressure mode** | 782.1 | 779.7 | 761.1 |

**Table 5.14:** Number of committed thermal and CHP units for all cases in test system-V

| | Case-1 | | Case-2 | | Case-3 | |
|---|---|---|---|---|---|---|
| | Number of thermal units | Number of CHP units | Number of thermal units | Number of CHP units | Number of thermal units | Number of CHP units |
| **Extraction mode** | 68 | 175 | 75 | 170 | 75 | 171 |
| **Backpressure mode** | 116 | 227 | 115 | 204 | 118 | 191 |

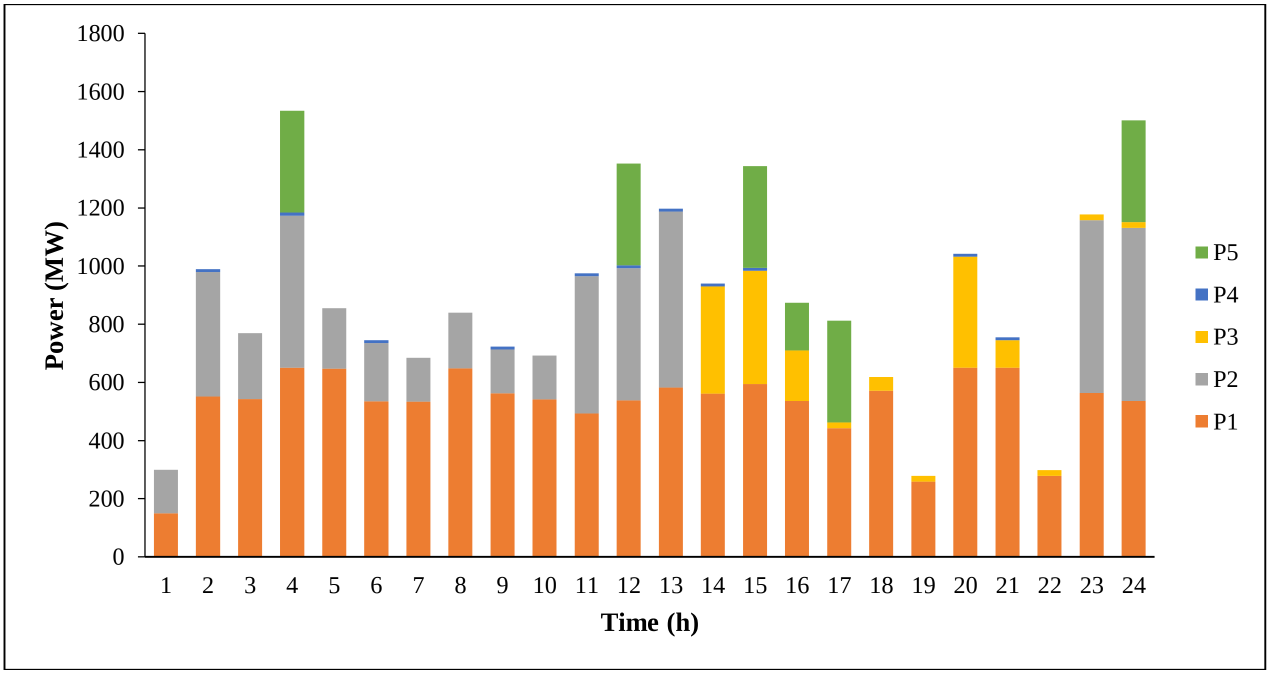


**Figure 5.28:** Power generated from thermal units in extraction mode for case-1 of test system-V

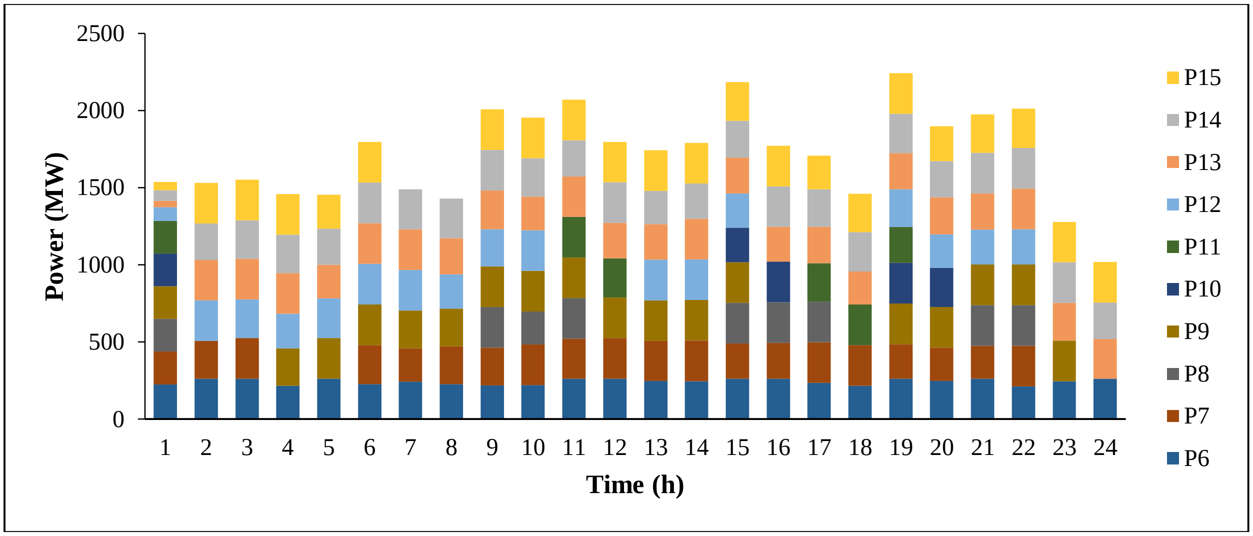


**Figure 5.29:** Power generated from CHP units in extraction mode for case-1 of test system-V

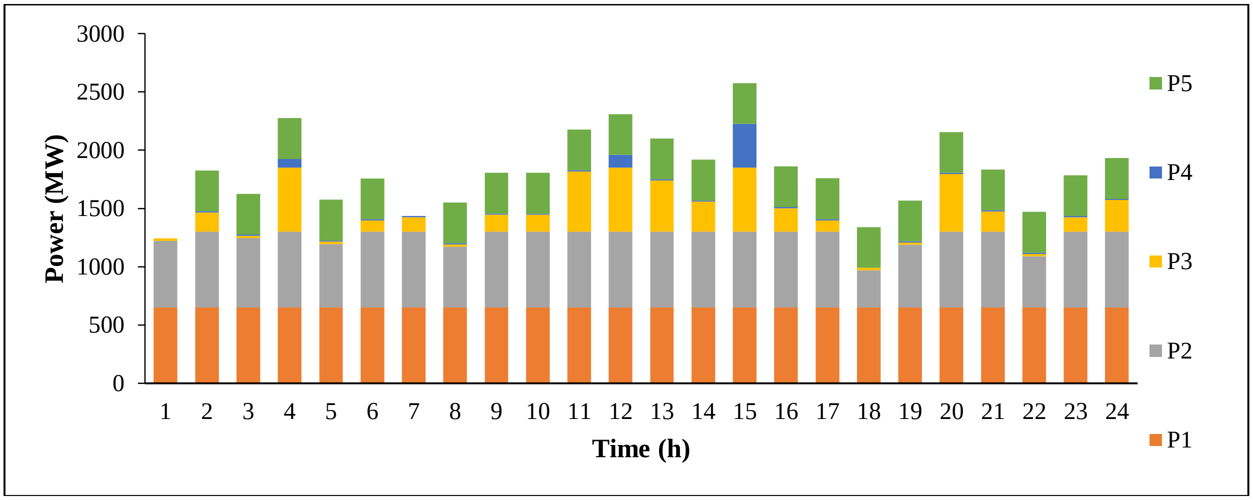


**Figure 5.30:** Power generated from thermal units in backpressure mode for case-1 of test system-V

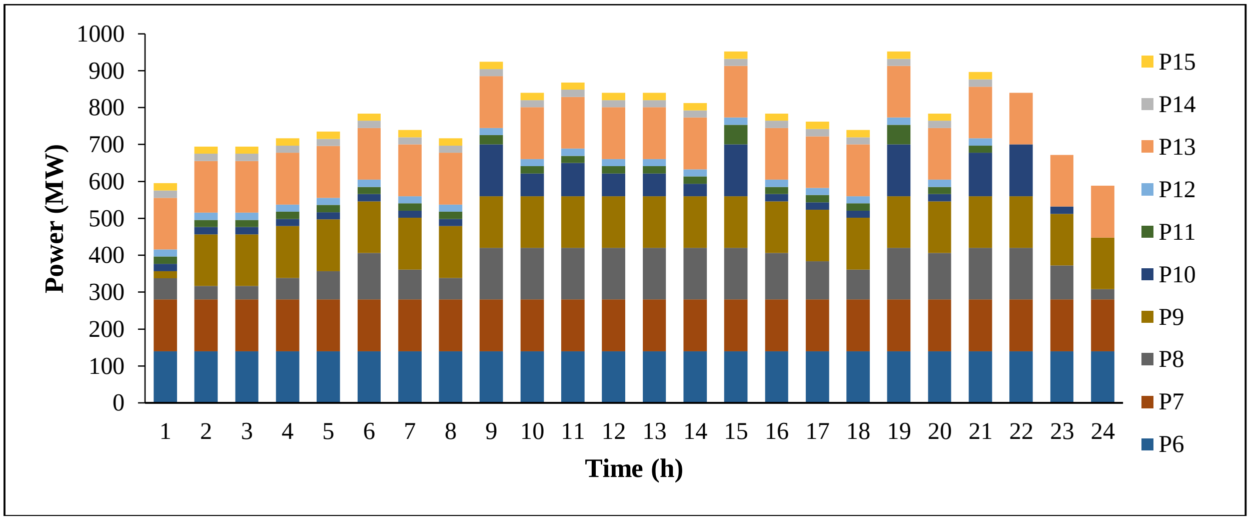


**Figure 5.31:** Power generated from CHP units in backpressure mode for case-1 of test system-V

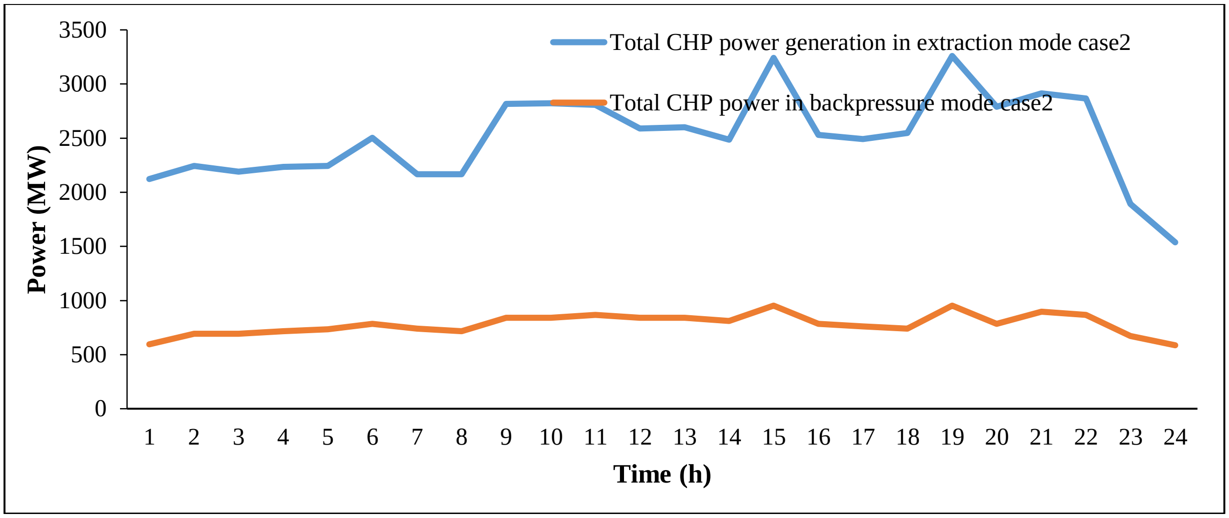


**Figure 5.32:** The total power generated from CHP units in case-2 of test system-V

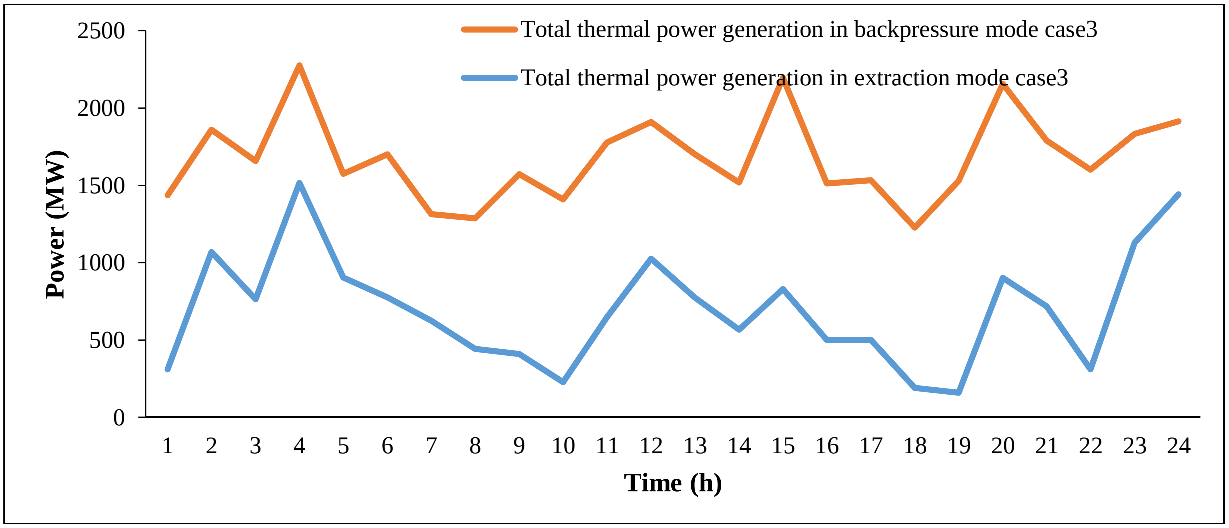


**Figure 5.33:** The total power generated from thermal units in case-2 of test system-V

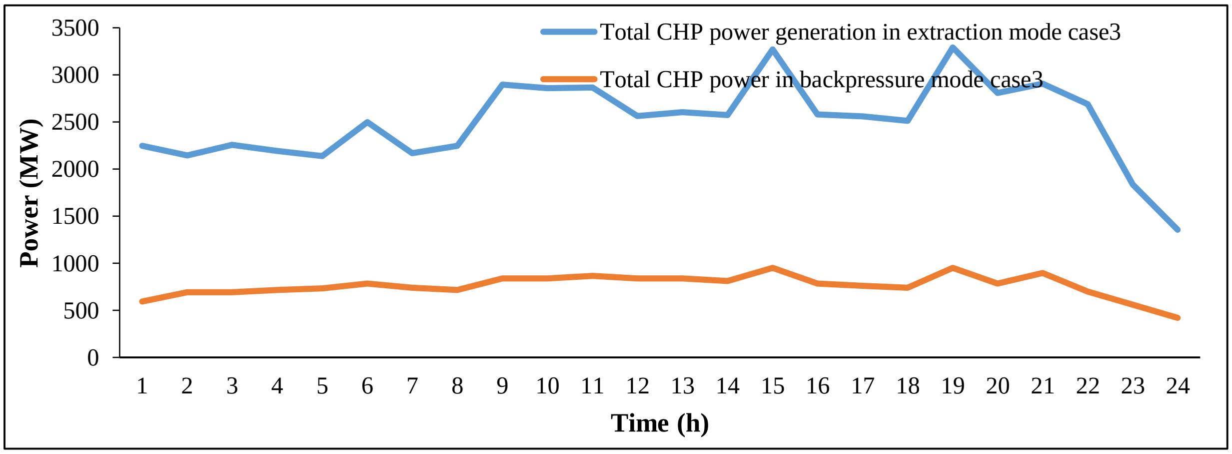


**Figure 5.34:** The total power generated from CHP units in case-3 of test system-V

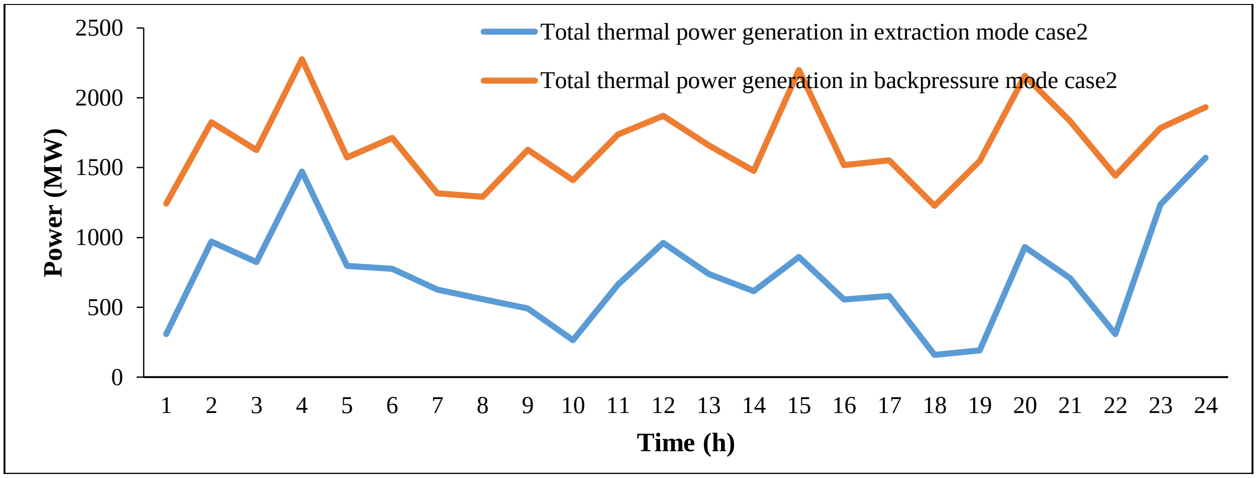


**Figure 5.35:** The total power generated from thermal units in case-3 of test system-V

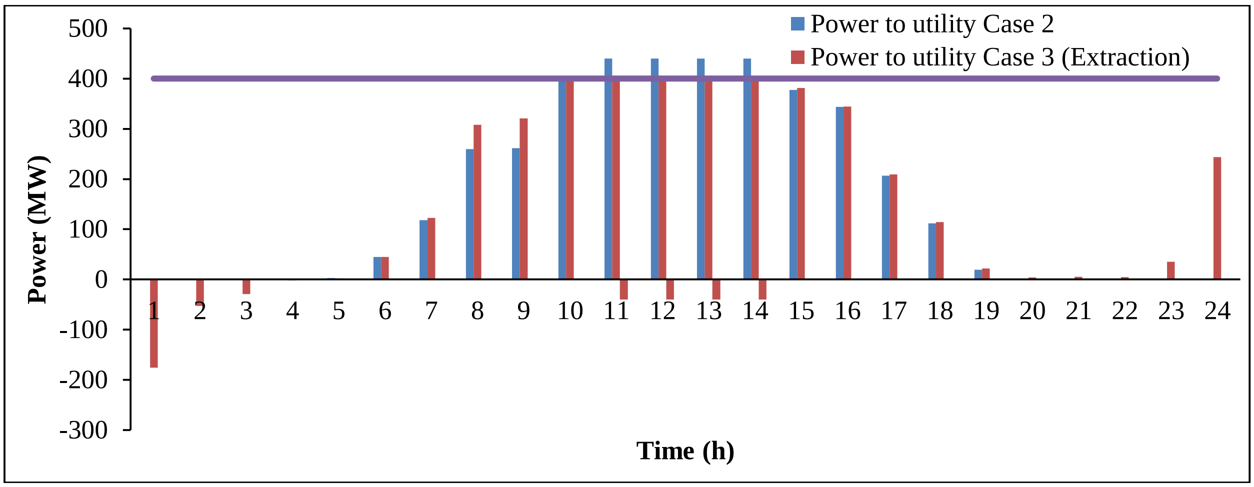


**Figure 5.36:** Solar PV plant power and charging/discharging of battery in extraction mode for test system-V

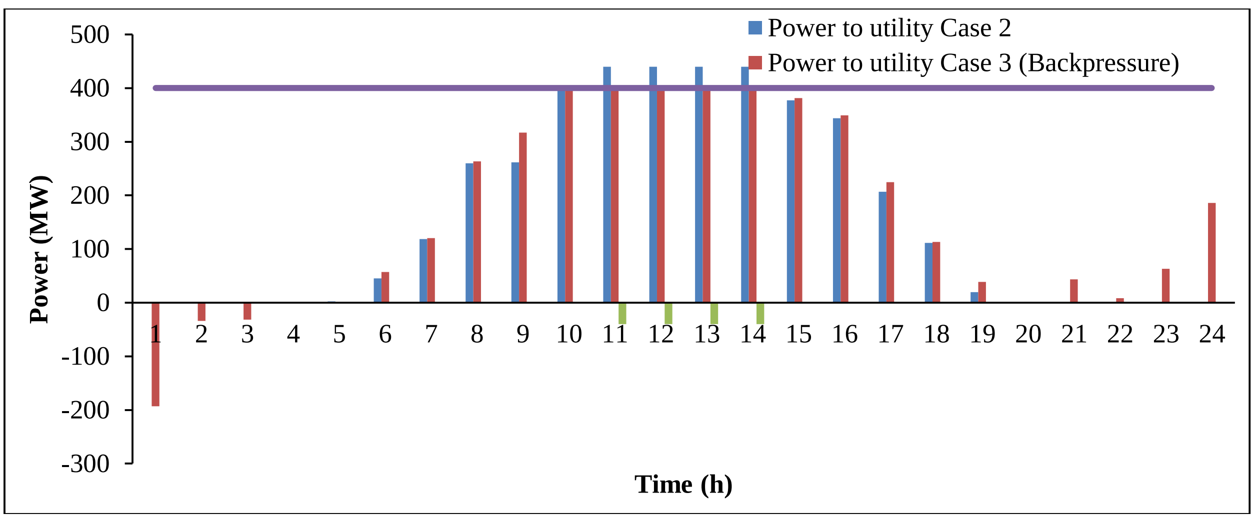


**Figure 5.37:** Solar PV plant power and charging/discharging of battery in backpressure mode for test system-V

**Table 5.15:** Operating cost of three cases for test system-V

| | Cost obtained in backpressure mode ($) | Cost obtained in extraction mode ($) |
|---|---|---|
| **Case-1** | 1712948 | 3222067 |
| **Case-2** | 1642009 | 3179773 |
| **Case-3** | 1632407 | 3174508 |

The upward and downward power flexibility of ICHPS for backpressure and extraction mode during each sub-interval are shown in Figures 5.38-5.41, respectively. During extraction and backpressure mode of CHP unit, the average upward and downward power flexibility for all three cases have been calculated and given in Table 5.16. It is evident that downward and upward power flexibility for extraction mode is high as compare to backpressure mode for most of cases. It is observed from Table 5.17 and Figures 5.38-5.41 that operating mode of CHP units have significant impact on downward and upward power flexibility for all cases.

**Table 5.16:** Average power generation flexibility for all cases; test system-V

| Average power generation flexibility (MW) | Mode of CHP unit operation | | | | | |
|---|---|---|---|---|---|---|
| | Backpressure | | | Extraction | | |
| | Case-1 | Case-2 | Case-3 | Case-1 | Case-2 | Case-3 |
| **Upward** | 210.83 | 255.71 | 442.38 | 299.58 | 253.38 | 286.79 |
| **Downward** | 299.58 | 253.38 | 286.79 | 407.29 | 383.92 | 409.38 |

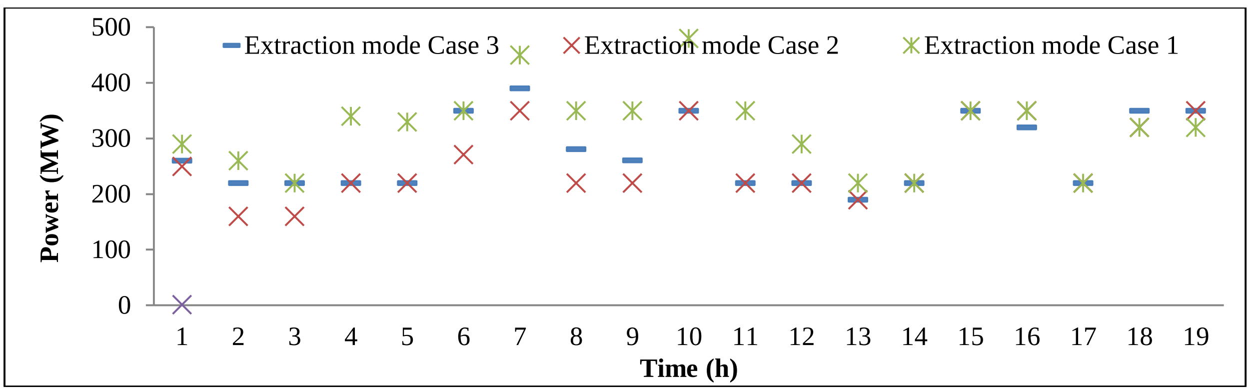


**Figure 5.38:** Upward power flexibility of extraction mode for test system-V

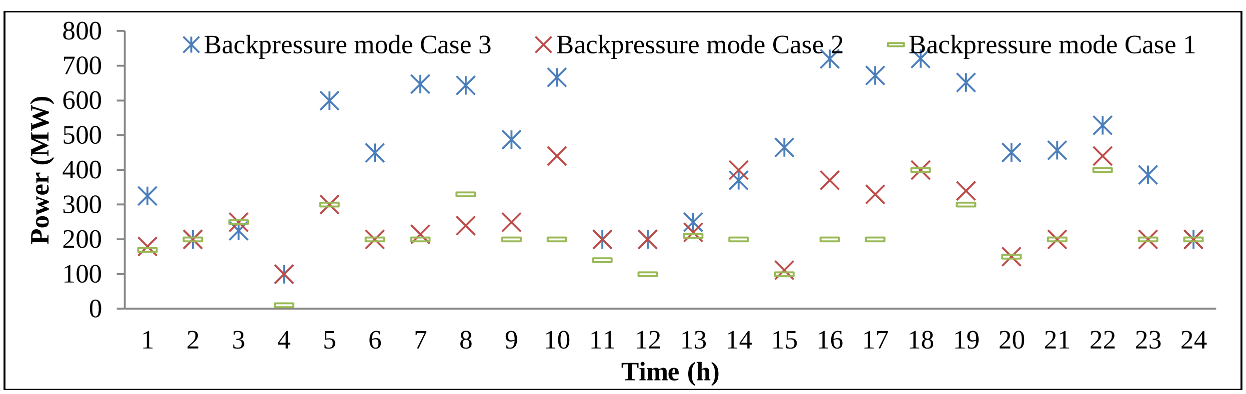


**Figure 5.39:** Upward power flexibility of backpressure mode for test system-V

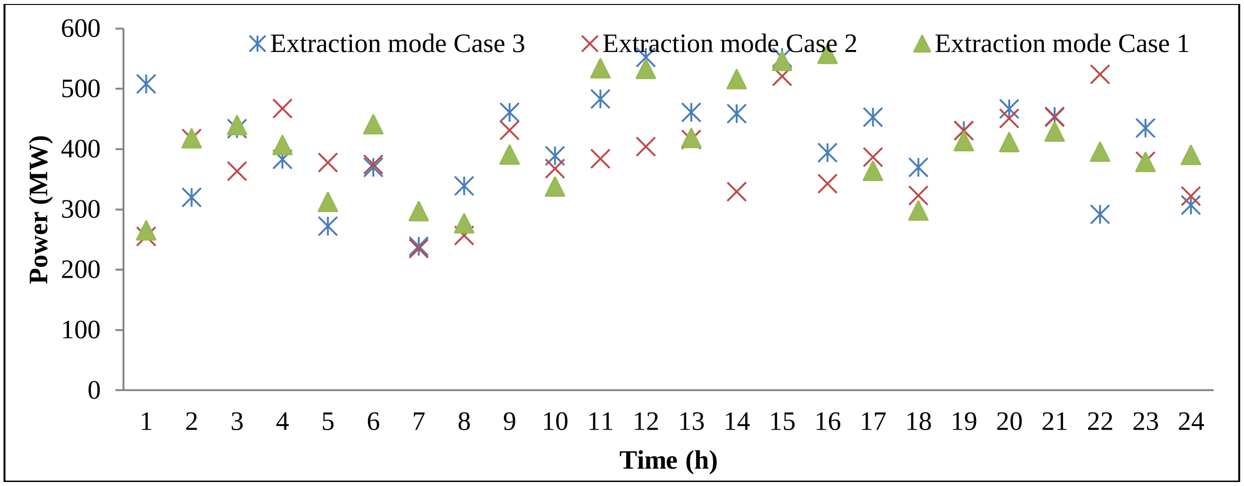


**Figure 5.40:** Downward power flexibility of Extraction mode for test system-V

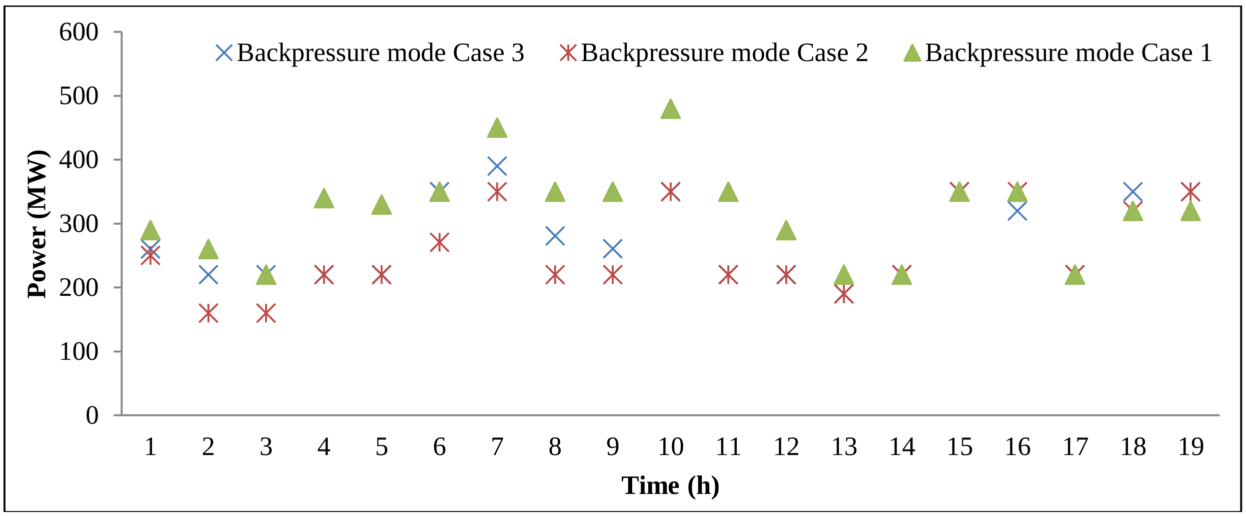


**Figure 5.41:** Downward power flexibility of Backpressure mode for test system-V

### 5.5.3 Test System-VI

The total heat generated from CHP and heat units in dual mode for all cases are shown in Figures 5.42-5.47. It is observed that the total heat generation during backpressure mode of CHP unit is higher as compare to extraction mode in all cases. The impact of higher heat generation in backpressure mode is resulted in heat units committed for 24 sub-intervals (1-24$^{th}$) to satisfy demand constraints whereas the number of committed heat is higher in extraction mode for all cases and it is presented in Table 5.17. The hourly unit commitment status of generating units for all cases is given in Table 5.18-5.20.

**Table 5.17:** Number of committed heat units for all cases in test system-VI

| | Case-1 | Case-2 | Case-3 |
|---|---|---|---|
| | **Number of heat units** | **Number of heat units** | **Number of heat units** |
| **Extraction mode** | 36 | 49 | 51 |
| **Backpressure mode** | 24 | 24 | 24 |

**Table 5.18:** Hourly status of units for case-1 of test system-VI

| Sub-intervals (h) | Backpressure mode | Extraction mode |
|---|---|---|
| | **Thermal CHP Heat** | **Thermal CHP Heat** |
| **1** | 11111 1111111111 01000 | 11001 1111111111 00000 |
| **2** | 11111 1111111111 01000 | 11101 1111001111 01000 |
| **3** | 11111 1111111111 01000 | 11101 1111001111 01000 |
| **4** | 11111 1111111111 01000 | 11111 1111001111 01000 |
| **5** | 11111 1111111111 01000 | 11101 1010001111 11000 |
| **6** | 11111 1111111111 01000 | 11111 1010001111 11000 |
| **7** | 11111 1111111111 01000 | 11111 1111100000 10100 |
| **8** | 11111 1111111111 01000 | 11111 1111100000 10100 |
| **9** | 11111 1111111111 01000 | 11111 1111100010 11100 |
| **10** | 11111 1111111111 01000 | 11111 1111110010 11000 |
| **11** | 11111 1111111111 01000 | 11111 1111111011 11000 |
| **12** | 11111 1111111111 01000 | 11111 1111101111 01000 |
| **13** | 11111 1111111111 01000 | 11111 1101101101 11000 |
| **14** | 11111 1111111111 01000 | 11111 1101101101 11000 |
| **15** | 11111 1111111111 01000 | 11111 1111111111 01000 |
| **16** | 11111 1111111111 01000 | 11111 1111010010 11000 |
| **17** | 11111 1111111111 01000 | 11111 1111000010 11100 |
| **18** | 11111 1111111111 01000 | 11111 1111100010 01100 |
| **19** | 11111 1111111111 01000 | 11111 1101100010 11100 |
| **20** | 11111 1111111111 01000 | 11111 1101001111 11000 |
| **21** | 11111 1111111111 01000 | 11111 1110001101 11100 |
| **22** | 11111 1111111111 01000 | 11111 1110100000 11100 |
| **23** | 11111 1111111111 01000 | 11111 1111100000 10100 |
| **24** | 11111 1111111111 01000 | 11111 1111000000 01100 |

**Table 5.19:** Hourly status of units for case-2 of test system-VI

| Sub-intervals (h) | Backpressure mode | Extraction mode |
|---|---|---|
| | **Thermal CHP Heat** | **Thermal CHP Heat** |
| **1** | 11111 1111111111 01000 | 11111 1111111111 00000 |
| **2** | 11111 1111111111 01000 | 11111 1111100000 11000 |
| **3** | 11111 1111111111 01000 | 11111 1111100000 11000 |
| **4** | 11111 1111111111 01000 | 11111 1111111100 01000 |
| **5** | 11111 1111111111 01000 | 11111 1111111100 10000 |
| **6** | 11111 1111111111 01000 | 11111 1111110000 11000 |
| **7** | 11111 1111111111 01000 | 11111 1111100000 01100 |
| **8** | 11111 1111111111 01000 | 11111 1111000000 11000 |
| **9** | 11111 1111111111 01000 | 11111 1111000000 11100 |
| **10** | 11111 1111111111 01000 | 11111 1111100000 11100 |
| **11** | 11111 1111111111 01000 | 11111 1111110000 11000 |
| **12** | 11111 1111111111 01000 | 11111 1111110000 11000 |
| **13** | 11111 1111111111 01000 | 11111 1111100000 11100 |
| **14** | 11111 1111111111 01000 | 11111 1111100000 11000 |
| **15** | 11111 1111111111 01000 | 11111 1111111110 11000 |
| **16** | 11111 1111111111 01000 | 11111 1101111110 10000 |

**Table 5.19:** Hourly status of units for case-2 of test system-VI (Continued)

| Sub-intervals (h) | Backpressure mode | Extraction mode |
|---|---|---|
| **17** | 11111 1111111111 01000 | 11111 1101110000 11000 |
| **18** | 11111 1111111111 01000 | 11111 1111110000 01100 |
| **19** | 11111 1111111111 01000 | 11111 1111100000 11100 |
| **20** | 11111 1111111111 01000 | 11111 1111101001 11000 |
| **21** | 11111 1111111111 01000 | 11111 1111001001 11100 |
| **22** | 11111 1111111111 01000 | 11111 1111000000 11100 |
| **23** | 11111 1111111111 01000 | 11111 1111000000 11000 |
| **24** | 11111 1111111111 01000 | 11111 1111000000 11000 |

**Table 5.20:** Hourly status of units for case-3 of test system-VI

| Sub-intervals (h) | Backpressure mode | Extraction mode |
|---|---|---|
| | **Thermal CHP Heat** | **Thermal CHP Heat** |
| **1** | 11111 1111111111 01000 | 11011 1111111111 00000 |
| **2** | 11111 1111111111 01000 | 11111 1111110000 11000 |
| **3** | 11111 1111111111 01000 | 11111 1111110000 11000 |
| **4** | 11111 1111111111 01000 | 11111 1111111100 01000 |
| **5** | 11111 1111111111 01000 | 11101 1111111100 10000 |
| **6** | 11111 1111111111 01000 | 11111 1111110000 11000 |
| **7** | 11111 1111111111 01000 | 11111 1111100000 01100 |
| **8** | 11111 1111111111 01000 | 11111 1111000000 01100 |
| **9** | 11111 1111111111 01000 | 11111 1111000000 11100 |
| **10** | 11111 1111111111 01000 | 11111 1111100000 11100 |
| **11** | 11111 1111111111 01000 | 11111 1111110000 11000 |
| **12** | 11111 1111111111 01000 | 11111 1111110010 11000 |
| **13** | 11111 1111111111 01000 | 11111 1111000010 11100 |
| **14** | 11111 1111111111 01000 | 11111 1111001010 11000 |
| **15** | 11111 1111111111 01000 | 11111 1111111110 11000 |
| **16** | 11111 1111111111 01000 | 11111 1001110100 11000 |
| **17** | 11111 1111111111 01000 | 11111 1001100000 11100 |
| **18** | 11111 1111111111 01000 | 11111 1111100000 11000 |
| **19** | 11111 1111111111 01000 | 11111 1111100000 11100 |
| **20** | 11111 1111111111 01000 | 11111 1111101001 11000 |
| **21** | 11111 1111111111 01000 | 11111 1110001001 11100 |
| **22** | 11111 1111111111 01000 | 11111 1110000000 11100 |
| **23** | 11111 1111111111 01000 | 11111 1111000000 11000 |
| **24** | 11111 1111111111 01000 | 11111 1111000000 11000 |

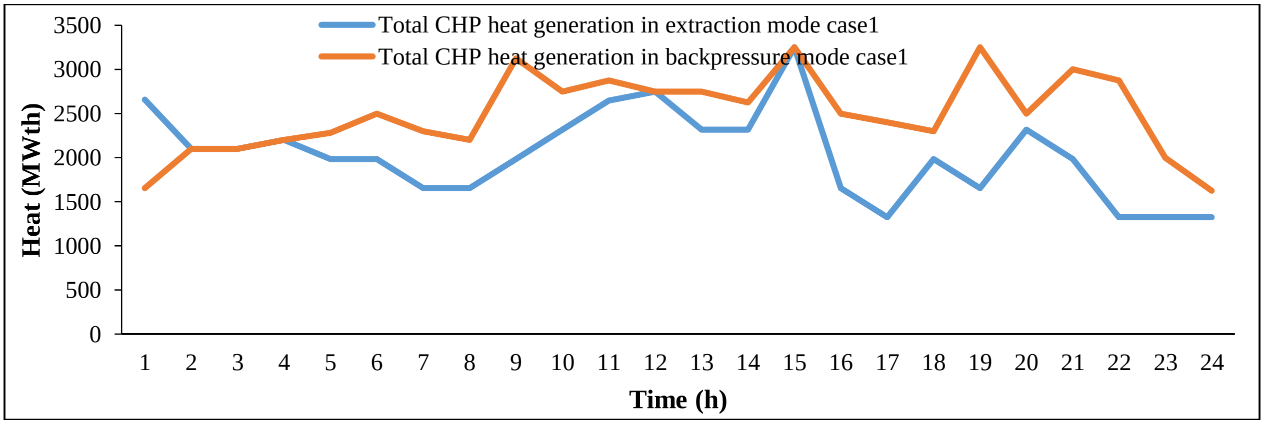


**Figure 5.42:** The total heat generated from CHP units in case-1 of test system-VI

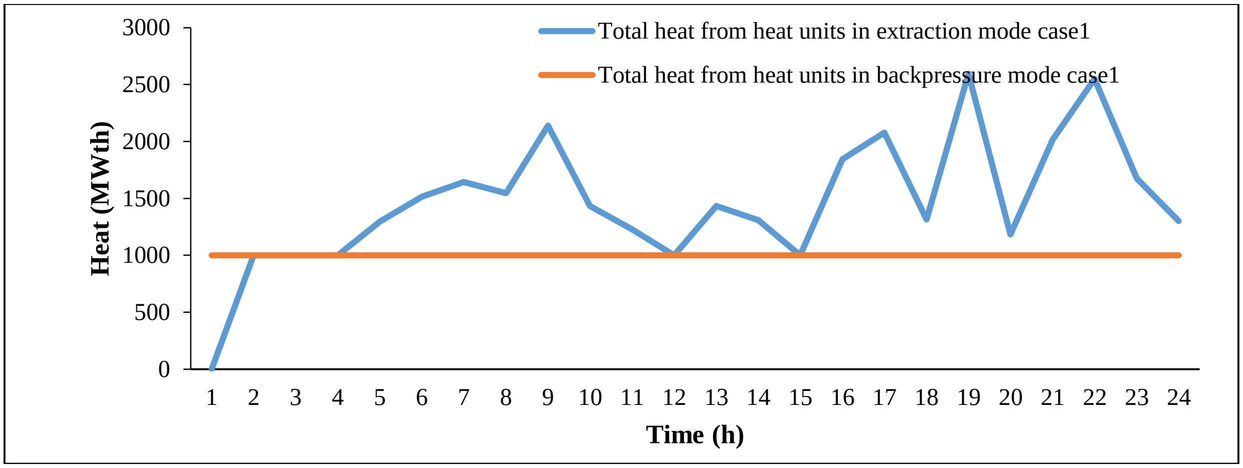


**Figure 5.43:** The total heat generated from heat units in case-1 of test system-VI

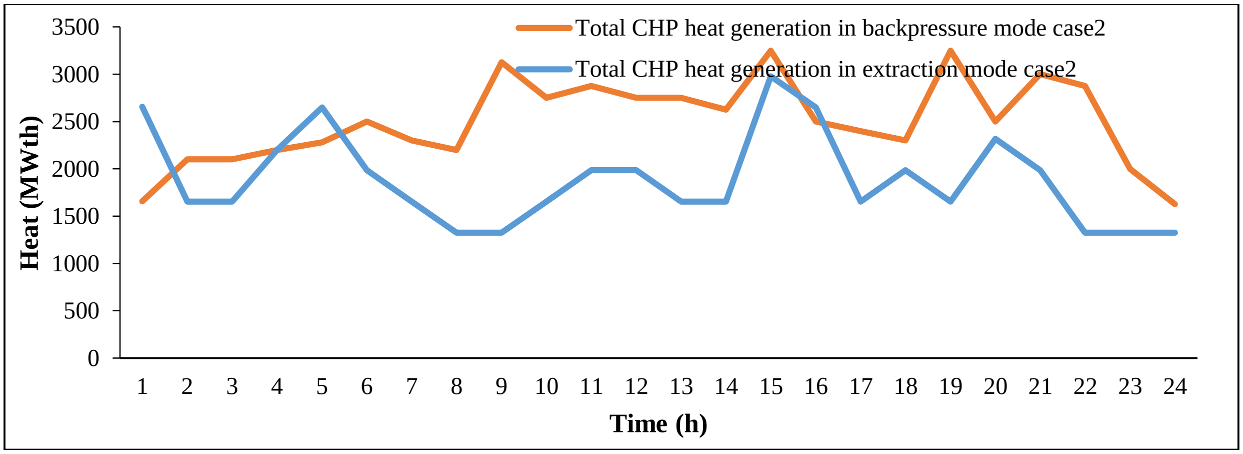


**Figure 5.44:** The total heat generated from CHP units in case-2 of test system-VI

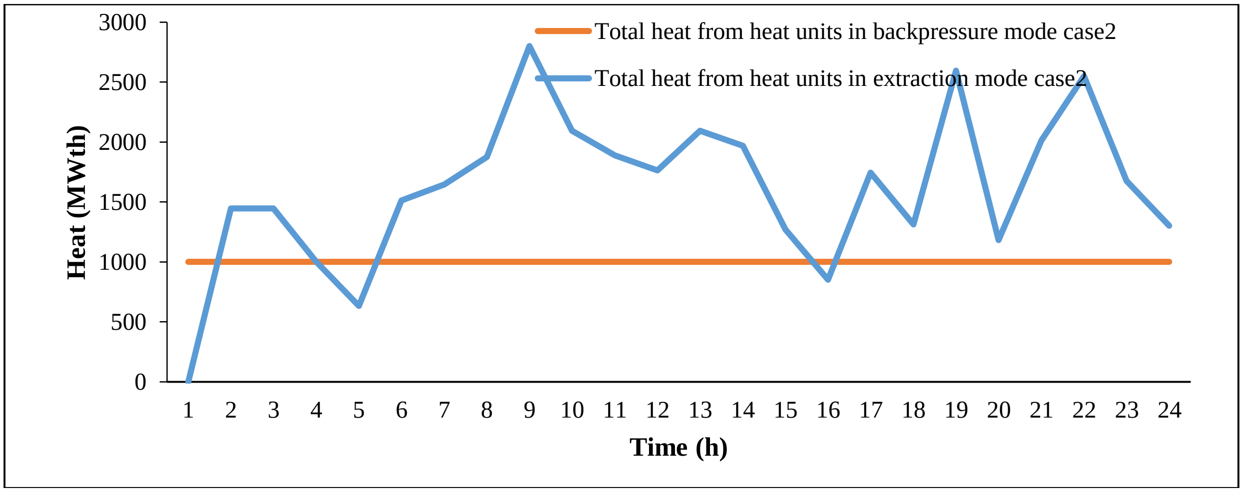


**Figure 5.45:** The total heat generated from heat units in case-2 of test system-VI

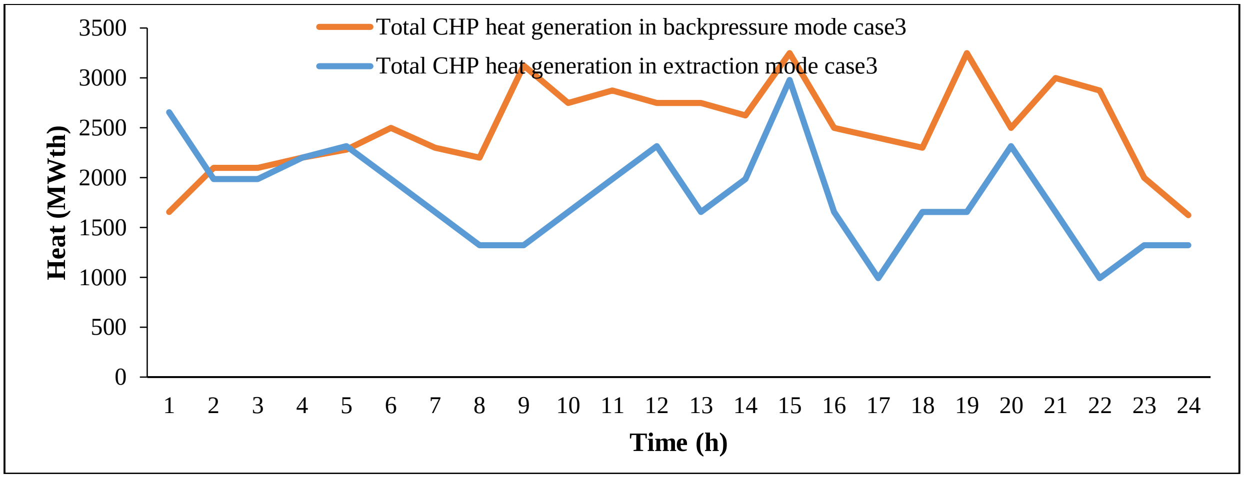


**Figure 5.46:** The total heat generated from CHP units in case-3 of test system-VI

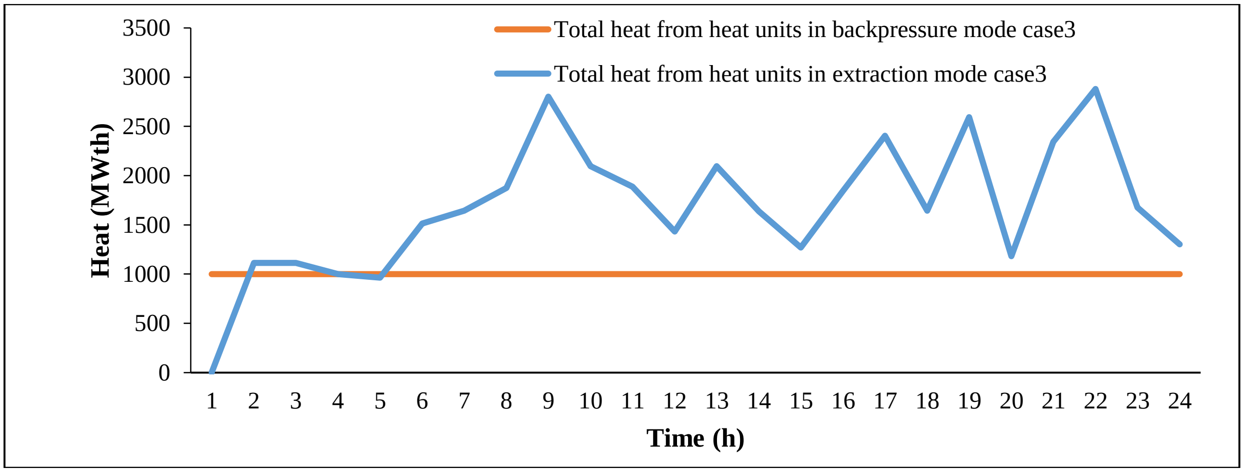


**Figure 5.47:** The total heat generated from heat units in case-3 of test system-VI

The total CHP and thermal power generated during backpressure and extraction operating mode of CHP units for all cases are illustrated in Figures 5.48-5.53. In all cases, it is evident from figures and Table 5.21 that the total power generation and average generated power in backpressure mode of CHP units is less as compare to extraction mode. The impact of less power generation in backpressure mode is also observed on the thermal unit commitment schedule and higher power generation from thermal units. Hence, resulted in 120 committed thermal units in backpressure mode at sub-intervals (1-24$^{th}$) to satisfy demand constraints whereas the number of committed thermal is less in extraction mode for case 1 and case 3 and it is presented in Table 5.22. The power flow ESS to utility in dual mode are shown in Figures 5.54 and 5.55. During 1-4$^{th}$ and 11-14$^{th}$ sub-intervals, in case-3, the negative power injection into ESS to charge the battery. In presence of ESS, few changes in the UC schedule of CHP units during extraction mode at sub-intervals has been observed as compared to case-1 and illustrated in Table 5.22.

**Table 5.21:** Average CHP power from the operating mode for all cases in test system-VI

| **Average power generation flexibility (MW)** | **Case-1** | **Case-2** | **Case-3** |
|---|---|---|---|
| **Extraction mode** | 1561.682 | 1431.463 | 1368.116 |
| **Backpressure mode** | 839.45 | 772.755 | 773.357 |

**Table 5.22:** Number of committed thermal and CHP units for all cases in test system-VI

| | **Case-1** | | **Case-2** | | **Case-3** | |
|---|---|---|---|---|---|---|
| | **Number of thermal units** | **Number of CHP units** | **Number of thermal units** | **Number of CHP units** | **Number of thermal units** | **Number of CHP units** |
| **Extraction mode** | 115 | 140 | 120 | 140 | 118 | 136 |
| **Backpressure mode** | 120 | 240 | 120 | 240 | 120 | 240 |

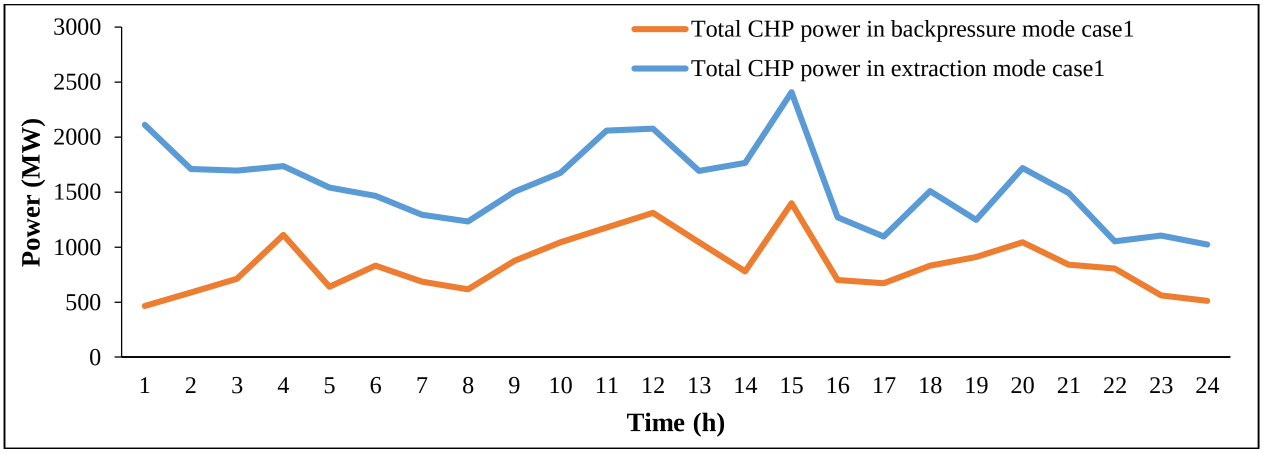


**Figure 5.48:** The total power generated from CHP units in case-1 of test system-VI

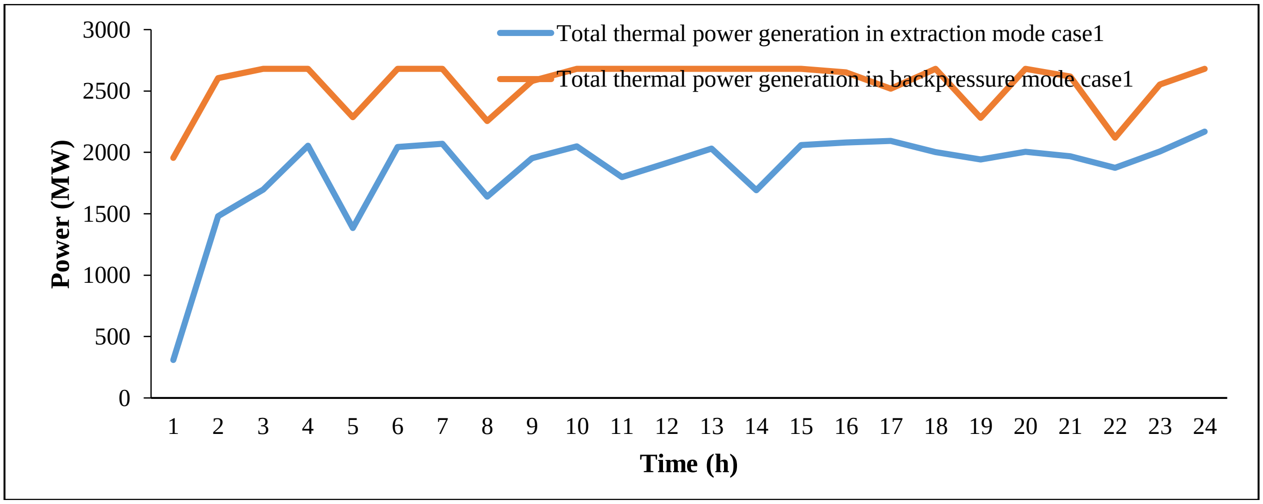


**Figure 5.49:** The total power generated from thermal units in case-1 of test system-VI

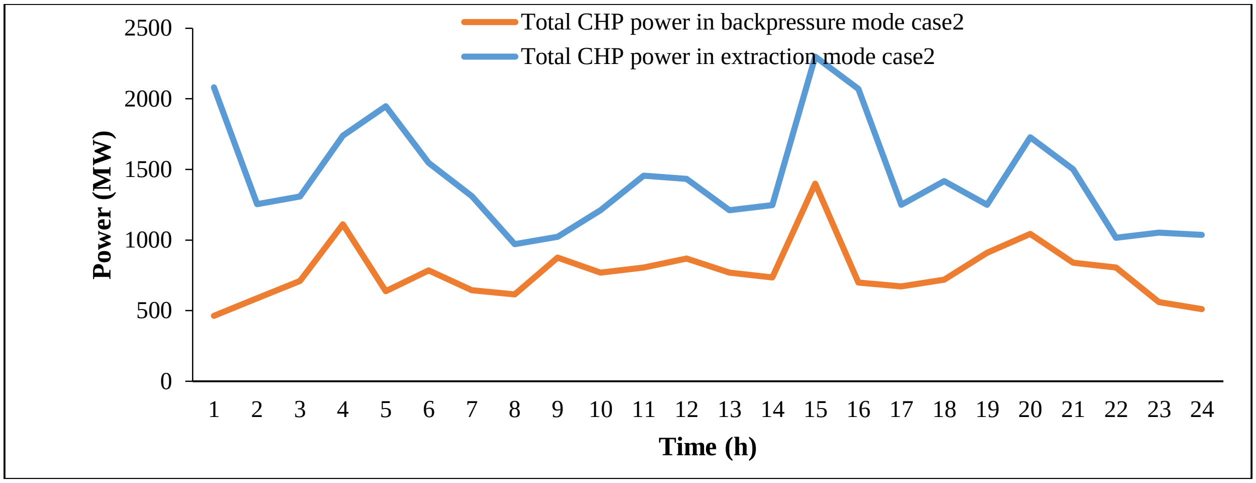


**Figure 5.50:** The total power generated from CHP units in case-2 of test system-VI

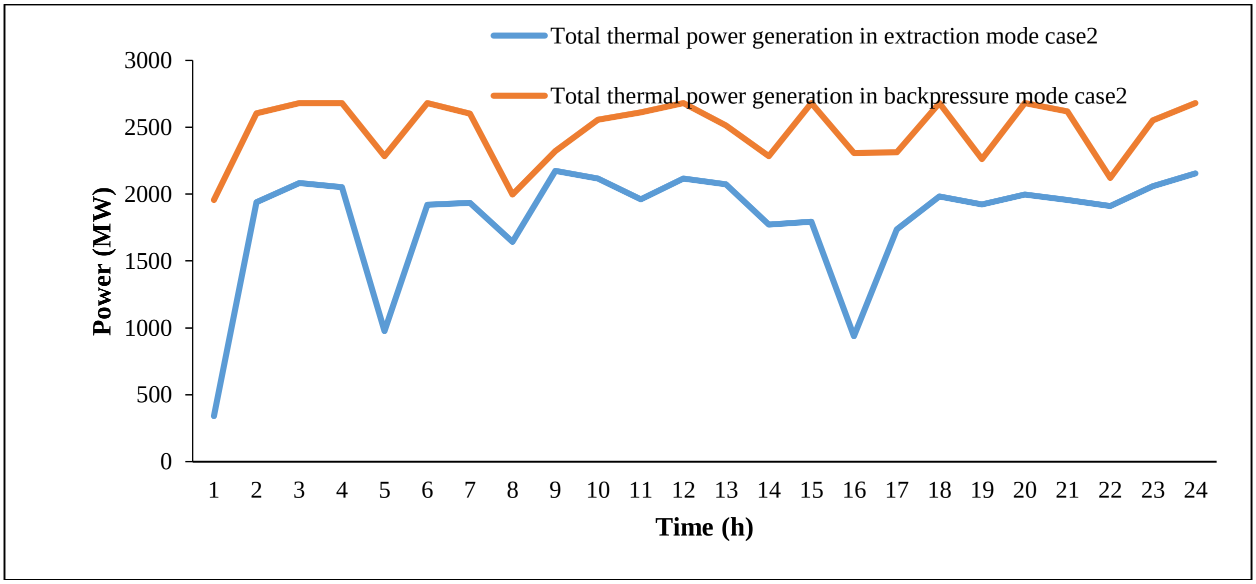


**Figure 5.51:** The total power generated from thermal units in case-2 of test system-VI

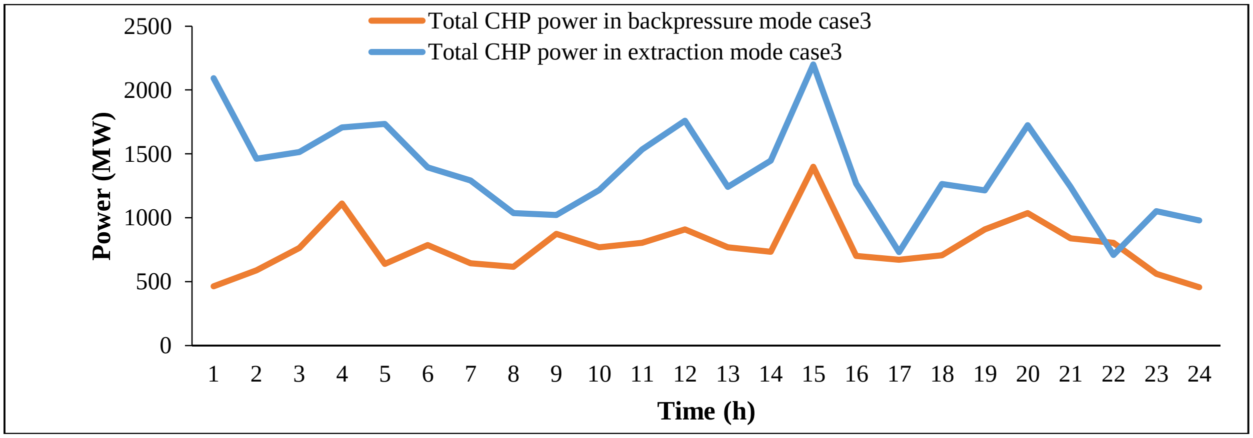


**Figure 5.52:** The total power generated from CHP units in case-3 of test system-VI

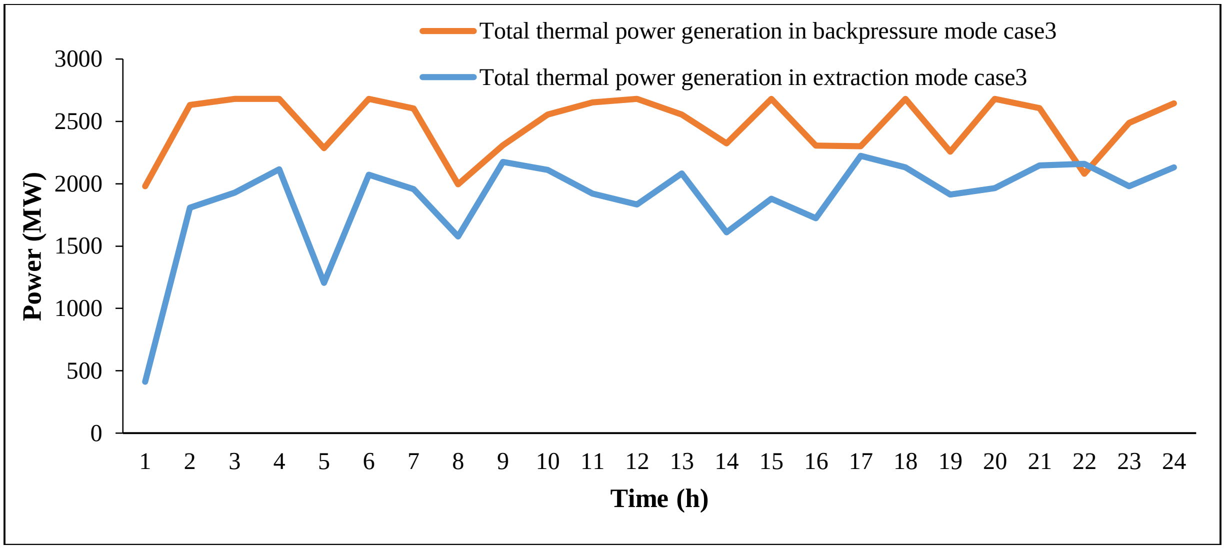


**Figure 5.53:** The total power generated from thermal units in case-3 of test system-VI

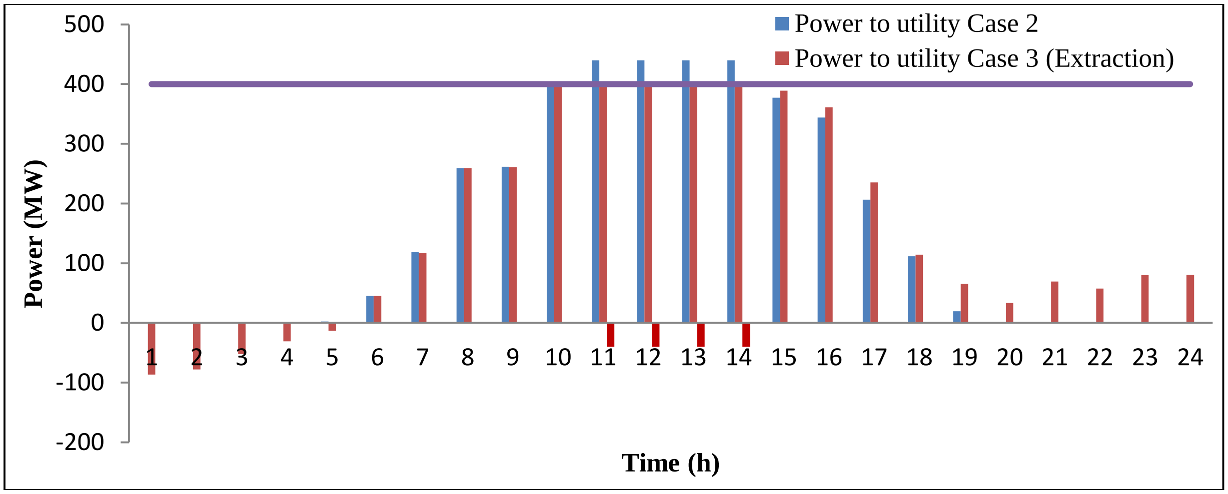


**Figure 5.54:** Solar PV plant power and charging/discharging of battery in extraction mode for test system-VI

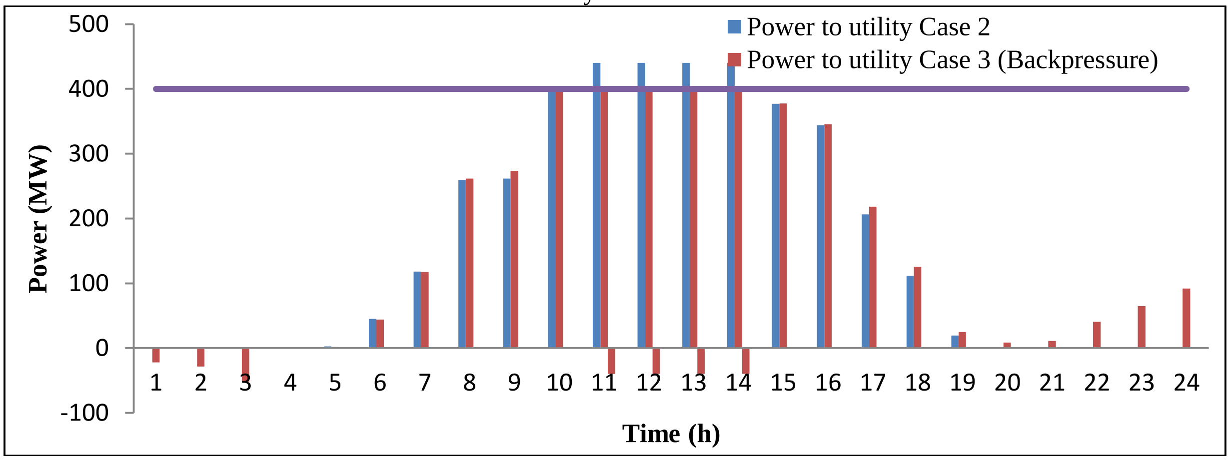


**Figure 5.55:** Solar PV plant power and charging/discharging of battery in backpressure mode for test system-VI

The operating cost in backpressure and extraction mode of case-1 are $1939106 and $3390335, respectively and it is also given in Table 5.23. It is evident from Table 5.23 that the operating cost in backpressure and extraction mode of case-2 are less by '$35703/day' and '$202038/day', respectively as compare to case-1. While the savings of operating cost in backpressure and extraction mode of case-3 with case-1 are '$34363/day' and '$291646/day'.

**Table 5.23:** Operating cost for three cases of test system-VI

| | Cost obtained in backpressure mode ($) | Cost obtained in extraction mode ($) |
|---|---|---|
| **Case-1** | 1939106 | 3390335 |
| **Case-2** | 1903403 | 3188297 |
| **Case-3** | 1904743 | 3098689 |

Figures 5.56-5.59 illustrates the power flexibility of ICHPS for all three cases. Table 5.24 presents the average upward and downward power generation flexibility for all three cases during extraction and backpressure mode of CHP unit operation. It has been observed from figures and Table 5.24 that upward and downward system power flexibility in extraction mode is high as compare to backpressure mode for all cases.

**Table 5.24:** Average power generation flexibility for all cases; test system-VI

| Average power generation flexibility (MW) | Mode of CHP unit operation | | | | | |
|---|---|---|---|---|---|---|
| | Backpressure | | | Extraction | | |
| | Case-1 | Case-2 | Case-3 | Case-1 | Case-2 | Case-3 |
| **Upward** | 40.88 | 74.33 | 84.75 | 298.75 | 127.08 | 505.79 |
| **Downward** | 460.29 | 452.21 | 540.92 | 1137.46 | 974.00 | 545.79 |

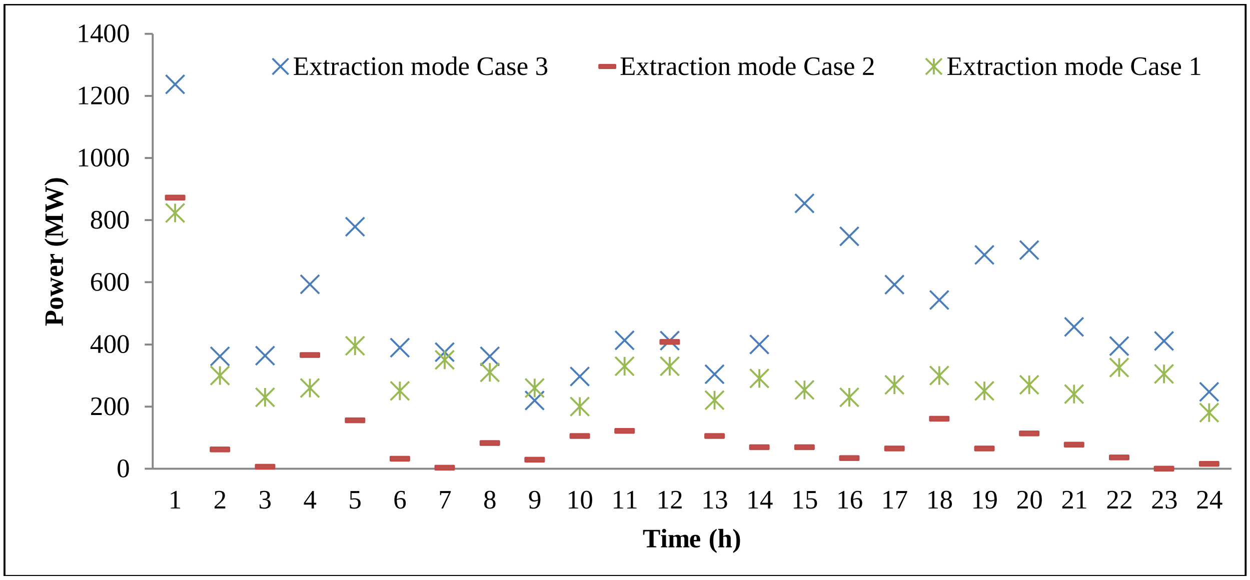


**Figure 5.56:** Upward power flexibility of extraction mode for test system-VI

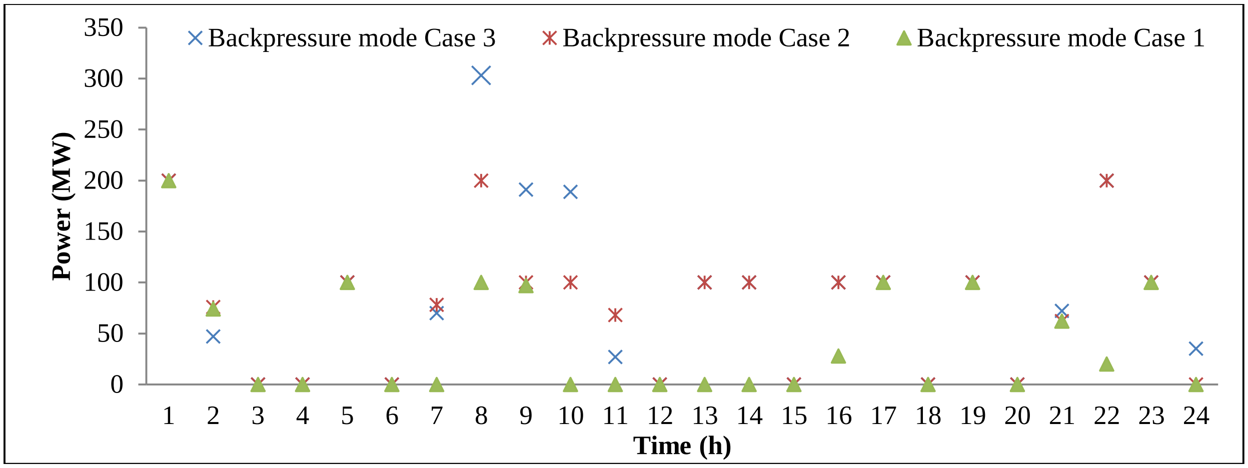


**Figure 5.57:** Upward power flexibility of backpressure mode for test system-VI

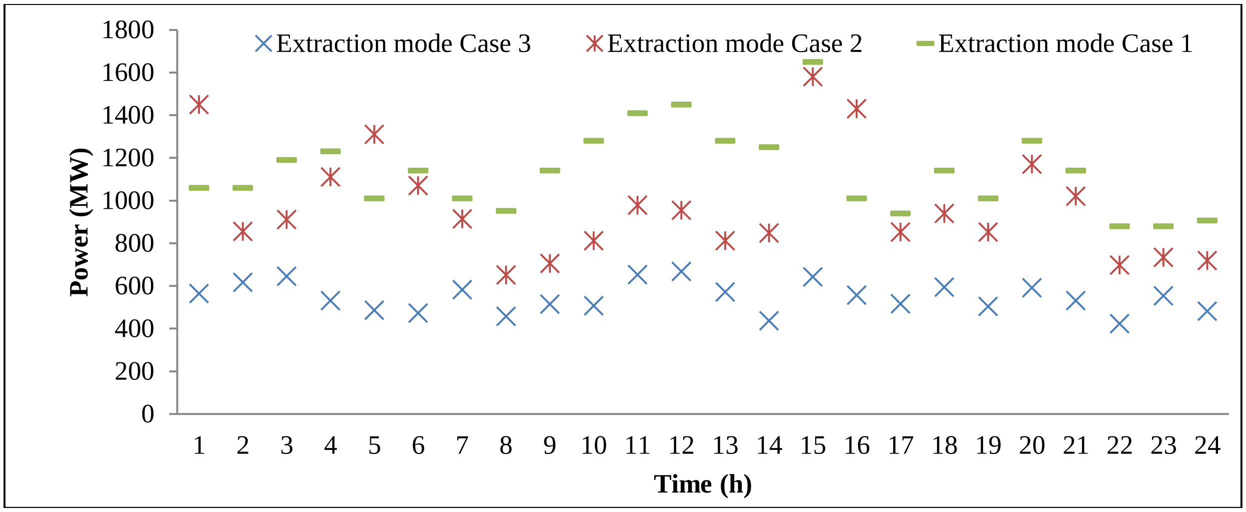


**Figure 5.58:** Downward power flexibility of extraction mode for test system-VI

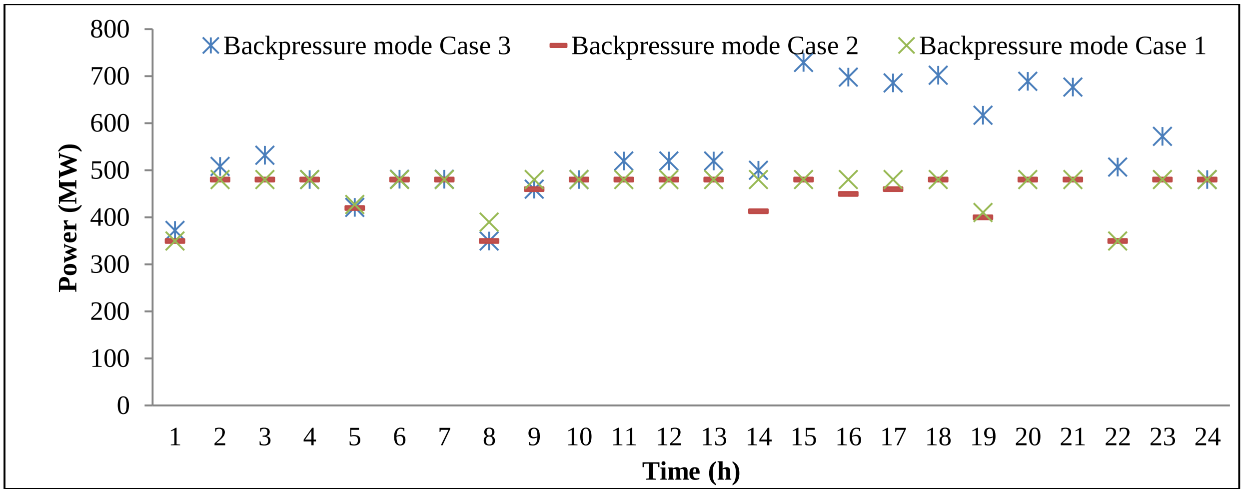


**Figure 5.59:** Downward power flexibility of backpressure mode for test system-VI

## 5.6 CONCLUSIONS

In this Chapter, the hybrid optimization technique has applied to solve the ICHPUC problem. The three test systems are taken into consideration to analyse the effect of PV and ESS on the ICHPUC problem during extraction and backpressure mode of DM-CHP unit. It has evident that the fuel cost for test system-IV, during extraction mode of CHP unit is higher by 30.4%, 33.7%, and 33.5% for case-1, 2 and 3, respectively as compared to backpressure mode. In test system-IV, it has observed that saving of fuel cost during backpressure mode of CHP unit in case-2 and 3 is more by 8.87%, and 9.2%, respectively as compared to case-1. Whereas the fuel cost saving in extraction mode for case-2 and 3 is more by 4.81% and 4.86%, respectively as compared to case-1. Similar trends as in test systems-I has observed in test systems-V and VI. It has also observed that the power generation from extraction mode of CHP unit is higher as compared to backpressure mode whereas the heat generation is higher in backpressure mode. It has clearly evident form results that backpressure and extraction mode have significant impact on the unit commitment schedule of generating units. It has observed from results of all test systems that the PV and ESS have significant impact on the unit commitment schedule as compared to case-1. Further, it has also concluded that extraction mode of CHP is more flexible as compared to backpressure mode in most of cases for three test systems. This study helps in assessing the impact of RES penetration on the optimal generation schedule, the power flexibility and the reduction of fuel cost.

# CHAPTER – 6

# CONCLUSIONS AND FUTURE SCOPE OF WORK

## 6.1 INTRODUCTION

In this thesis, the *unit commitment* (UC) of different types of generating units such as thermal, *dual-mode combined heat and power* (DM-CHP), heat and renewable generation has been undertaken. The *profit based unit commitment* (PBUC), *combined heat and power unit commitment* (CHPUC), *multi-objective combined heat and power unit commitment* (MO-CHPUC) and *integrated combined heat and power unit commitment* (ICHPUC) problems have been solved. The proposed *binary successive approximation and civilized swarm optimization* (BSA-CSO) techniques has been used to solve the UC problems. In this Chapter, salient and significant observation, inferences, conclusions and contributions of the thesis have been presented. Few brief contributions have also been documented for future research.

## 6.2 SUMMARY OF CHAPTERS

In this section, the Chapter-wise summary follows as:

In Chapter 1, a brief overview of the different UC problems in electric power systems have been discussed. The various optimization techniques explored by researchers to solve the UC variants such as *thermal UC* (THUC), PBUC, CHPUC, ICHPUC, and MO-CHPUC have been discussed. In order to deal with the single objective and multi-objective UC problem, a literature review on the various optimization techniques has been done by author. The main aim is to find the problem-specific optimization techniques to obtain global optimum solution for UC problems. The organization of the research work has been presented in Chapter 1.

In Chapter 2, the THUC model has been presented. The THUC model consists of generation constraints (such as generation capacity, ramp-rate limits and minimum up/down time constraints) and system-wide constraints (power balance, and reserve requirements). A hybrid framework of optimization technique has been developed to solve a mixed-integer THUC problem. The proposed optimization technique is based on the local search *i.e., binary successive* *approximation* (BSA) and hybridization technique *i.e, civilized swarm optimization* (CSO) technique. The binary and continuous variables of the THUC problem are updated by BSA and CSO techniques, respectively. To show the performance of proposed optimization techniques, two THUC test systems have been undertaken. The hybrid strategy based on BSA and CSO has exhaustively compared with the algorithms presented in the literature.

In Chapter 3, the author has presented the PBUC model. In this model, the power balance and spinning reserve requirements are treated as soft constraints. The ramp-rate constrained PBUC has also solved in this Chapter. The BSA-CSO technique developed for the THUC problem has implemented to solve the PBUC problem. Case study of three test systems has carried out to check the performance of hybrid optimization technique in which the global optimum generation schedule is obtained at maximum profit. The results achieved for three test systems by BSA-CSO has compared with other techniques available in the literature.

In Chapter 4, the THUC problem has extended to the CHPUC problem. In the CHPUC problem, various generator constraints (such as heat and power generation capacity, feasible operating region, CHP and heat unit fuel limits, ramp-rate limits and minimum up/down time constraints), and unit commitment constraints (power and heat balance, and power and heat spinning reserve requirements) are considered. This problem formulation includes thermal, DM-CHP and heat units. The backpressure and extraction are modes of operation in the DM-CHP unit, which is having a diverse feasible operating region. The CHPUC problem is a mixed-integer nondeterministic polynomial hard optimization problem in the presence of all operational constraints. In this Chapter, the single objective CHPUC problem has been extended to PB-CHPUC and MO-CHPUC problems. The main aim of the MO economic based CHPUC model is to minimize the system operating cost and emission simultaneously, whereas the main objective of the MO profit based model is to maximize the system profit and minimize emission. The optimization techniques developed for the THUC problem have been employed to solve the dual-mode CHPUC problem. The *cardinal priority ranking method* (CPM) has implemented to find the best-satisfied non dominated solution for the multi-objective model. The three test systems for cogeneration based unit commitment problem have been undertaken.

In Chapter 5, the CHPUC problem incorporation of the solar photovoltaic unit and ESU has been formulated ICHPUC problem. The BSA-CSO optimization technique has been implemented to minimize the operating cost of the CHPUC problem in the presence of solar photovoltaic and ESU. In order to analysis the impact of PV and ESU on unit commitment, generation schedule and cost, three test systems have been undertaken.

## 6.3 SIGNIFICANT CONTRIBUTIONS

In this section, the significant contributions are summarized as:

1. The proposed optimization technique i.e., *binary successive approximation and civilized swarm optimization* (BSA-CSO) based on the hybridization of local and hybrid optimization techniques is used to solve the *unit commitment* (UC) problem. While solving the UC problem, the BSA technique has been undertaken to search optimum generating unit status, and the CSO technique is employed to explore the optimum generation schedule from committed generating units.
2. The thermal UC problem has been solved by considering the impact of ramp rate loading on thermal units. The author has also solved the ramp-rate constrained profit based thermal UC problem to maximize the profit of *generating companies* (GENCOs).
3. In maiden attempt, the dual mode *combined heat and power unit commitment* (CHPUC) problem has been formulated by considering thermal, *dual mode combined heat and power* (DM-CHP), and heat units whereas in literature operating modes are not taken into consideration by researchers. In order to verify the effect of DM-CHP units, the author has undertaken three test systems.
4. The dual mode profit based CHPUC (PBCHPUC) problem has been formulated and solved by the proposed BSA-CSO optimization technique to obtain the optimal global solution.
5. The single objective dual mode CHPUC problem has been extended to the *multiobjective CHPUC* (MO-CHPUC) problem. In maiden attempt, the proposed BSA-CSO optimization technique with the *cardinal priority ranking method* (CPM) has been applied to solve the MO-CHPUC problem. The fuzzy CPM is used to obtain the best non-dominated solution among the Pareto optimum solutions. Further, the BSA-CSO optimization technique with CPM has applied to solve multiobjective profit based CHPUC problem. The main objective of the MO profit based model is to maximize the system profit and minimize emission.

6. In maiden attempt, the *integrated CHPUC* (ICHPUC) problem has been formulated by the inclusion of solar *photovoltaic* (PV) and *energy storage unit* (ESU) with the DM-CHP system.

## 6.4 IMPORTANT OBSERVATIONS

In this section, the significant observations based on hybrid optimization technique and unit commitment problems are follows as:

1) The *unit commitment* (UC) problem has been solved for the large scale power system by the proposed hybrid optimization technique (i.e., BSA-CSO). The proposed BSA-CSO technique is able to maintain a fine balance between exploration and exploitation search, hence it exhibits excellent search capability with less number of function evaluations.
2) The thermal UC problem has been solved by considering the impact of ramp rate loading on thermal units. Extensive numerical studies have been conducted to evaluate the performance of the proposed optimization technique. It has found that the BSA-CSO optimization technique is able to outperform in terms of convergence characteristics and operating cost. It has been concluded that the operational cost of the ramp rate constrained thermal UC problem is higher as compared to the operating cost of the thermal UC problem. It has evident from results that the BSA-CSO optimization technique has attained a global optimum solution with the satisfaction of commitment and generation constraints. The nonparametric Wilcoxon signed-rank test has been successfully tested on the thermal UC test system.
3) The author has solved the ramp-rate constrained profit based thermal UC problem to maximize the profit of *generating companies* (GENCOs). It has evident that the BSA-CSO optimization technique performs better as compared to other algorithms in terms of profit, and computational burden for small, medium and large size test systems. It is also observed that the operational profit of the ramp rate constrained profit based thermal UC problem is lower as compared to the profit of the profit based thermal UC problem. It has also been observed that the quality of the solution does not affect by the parametric variation in the proposed BSA-CSO technique.
4) In dual mode *combined heat and power unit commitment* (CHPUC) problem, numerical case studies show that the operating modes of the *combined heat and power* (CHP) unit

have a significant impact on the UC schedule. It has observed that the number of committed thermal units during the backpressure mode of CHP unit is more as compare to extraction mode, whereas in extraction mode, the number of committed heat units is more as compare to backpressure mode. It has been observed from the BSA-CSO results that the operating cost during the extraction mode of the CHP unit is less as compared to backpressure mode. Further, it has been verified that the extraction and backpressure mode of the CHP unit provides diverse power and heat flexibility.

5) In dual mode profit based CHPUC (PBCHPUC) problem, for test system-I, obtained results represents that profit is more during the extraction mode of the CHP unit as compared to backpressure mode, while for test system-II and III, the profit obtained during the extraction mode of the CHP unit is higher as compared to backpressure mode. Hence, it is concluded that the dual mode CHP unit has a significant impact on the GENCOs profit.
6) For MO-CHPUC problems, it has been observed from results that during extraction mode of CHP unit operation, the cost and emission are less as compared to backpressure mode of CHP unit operation. The results obtained for test systems have revealed a significant effect of operating mode on the environment emission and cost/profit of the system. Numerical case studies suggest that the operating modes of the CHP unit have a significant effect on the UC schedule and optimum generation schedule.
7) The obtained results for *integrated CHPUC* (ICHPUC) reveal that the presence of PV and ESU units lower down the operating cost as compared to DM-CHP system operating cost. The PV and ESU units have a significant effect on the UC schedule and optimum generation schedule. The system's power flexibility in the extraction mode of the CHP unit is high as compared to the backpressure mode. In term of power flexibility, the PV-ESU-CHPUC is more flexible as compared to the PV-CHP system.

## 6.5 IMPORTANT INFERENCES

The important inferences are follows as:

- The hybrid optimization technique based on BSA *and CSO* (BSA-CSO) is proposed to solve the thermal unit commitment, profit based thermal unit commitment, dual mode combined heat and power unit commitment and integrated combined heat and power unit commitment problems.

- In this research work, *dual mode combined heat and power unit commitment* is formulated and solved. Maiden attempt has been made by author to analysis the impact of extraction and backpressure mode of CHP units on unit commitment and generation schedule. Afterward, the PBCHPUC, MO-CHPUC and MO-PBCHPUC problems are simulated to find impact of dual mode CHP on cost, profit and emission.
- The *integrated CHPUC* (ICHPUC) problem is solved to analysis the impact of PV and ESU on the commitment status and schedule of committed units.

## 6.6 IMPORTANT CONCLUSIONS

In this research work, a comprehensive study on various types of UC problems has been done by author. The UC problems have been solved by the proposed optimization techniques. A novel framework based on BSA and CSO technique has been developed to solve the UC problems. The optimization technique has been explored in depth and reveals the advantages of optimization techniques. The BSA explores the binary search space while CSO explores the continuous search space. The BSA-CSO optimization techniques have successfully tested on small, large size test system of THUC, PBUC and ramp-rate constrained UC problems. In maiden attempt, the dual-mode CHPUC and PB-CHPUC problem with consideration of DM-CHP, heat and thermal units has been solved by BSA-CSO technique. Further, the cost and profit based MO-CHPUC problem has been solved. The significant impact of extraction and backpressure mode of DM-CHP unit on unit status, generation schedule, generation flexibility, cost, profit and emission has been evident from results. The CHPUC problem with the incorporation of solar and battery power has been solved by the proposed BSA-CSO optimization technique. The impact of PV and ESU has been observed in term of system operating costs and power flexibility.

## 6.7 FUTURE SCOPE OF WORK

The scope of future work is always present in any field of research work, and there is no end point of research. In this section, some of the possible further possible research directions are listed below:

- The proposed technique has been able to achieve an optimum solution with less number of functions of evaluation as compared to other techniques developed for single-processor systems; the performance of the multiprocessor system is superior and underlines the future scope.
- In future work, the performance of different heuristic optimization methods such as raindrop optimization, chemical reaction optimization, backtracking search optimization, big-bang big-crunch optimization, etc. can also be implemented to search the optimum solution of UC problem with minimum computational time. Further, the hybridization of BSA with other well-known optimization techniques can be performed in future studies.
- The presented work focus on the PBUC problem without social welfare maximization. In future work, the author will undertake the power purchase cost of various utilities in PBUC, the main motive is to social welfare maximization with consideration of selling, buying of power from cheaper thermal units including ancillary services, bidding strategies, pricing of power, etc.
- The results encourage the integration of dual-mode combined heat and power with renewable energy resources, which are prone to uncertainties. In addition, the stochastic model of unit commitment considering uncertainty associated with the input data, hourly demand, etc. can be undertaken.
- The switching between operating modes of combined heat and power units may help to reduce the operating cost and increase system flexibility.
- The formulation of the CHPUC problem with network security constraints is another area of research work in the field of power systems.
- In my thesis, the single area CHPUC problem has formulated. In future work, the focus on the formulation of the multi-area cogeneration based UC problem.
- The presented work focus on the multiobjective CHPUC problem. Further, the transmission line losses, emission constrained, and fuel constraints considered in the multiobjective CHPUC problem.

# REFERENCES


**Abookazemi, K., Ahmad, H., Tavakolpour, A., and Hassan, M.Y. (2011).** Unit commitment solution using an optimized genetic system, *International Journal of Electrical Power and Energy Systems*, vol. 33 (4), pp. 969-975.

**Abujarad, S.Y., Mustafa, M.W., and Jamian, J.J. (2017).** Recent approaches of unit commitment in the presence of intermittent renewable energy resources: A review, *Renewable and Sustainable Energy Reviews*, vol. 70, pp. 215-223.

**Aghaei, J., Agelidis, V.G., Charwand, M., Raeisi, F., Ahmadi, A., Nezhad, A.E., and Heidari, A. (2016).** Optimal robust unit commitment of CHP plants in electricity markets using information gap decision theory, *IEEE Transaction on Smart Grid*, vol. 8 (5), pp. 2296-2304.

**Agrawal, S., Panigrahi, B.K., and Tiwari, M.K. (2008).** Multi-objective particle swarm algorithm with fuzzy clustering for electrical power dispatch, *IEEE Transaction on Evolutionary Computation*, vol. 12, pp. 529–541.

**Alonso, J.I., Ossa, L.D.L., Gamez, J.A., and Puerta, J.M. (2018).** On the use of local search heuristics to improve GES-based Bayesian network learning, *Applied Soft Computing*, vol. 64, pp. 366-376.

**Alvarez, G.E., Marcovecchio, M.G., and Aguirre, P.A. (2018).** Security-constrained unit commitment problem including thermal and pumped storage units: An MILP formulation by the application of linear approximations techniques, *Electric Power Systems Research,* vol. 154, pp. 67–74.

**Amiri, M., and Khanmohammadi, S. (2013).** A primary unit commitment approach with a modification process, *Applied Soft Computing*, vol. 13 (2), pp. 1007-1015.

**Aoki, K., Satoh, T., Itoh, M., Ichimori, T., and Masegi, K. (1987).** Unit commitment in a large-scale power system including fuel constrained thermal and pumped-storage hydro, *IEEE Transactions on Power Systems*, vol. PER-7 (11), pp. 51-52.

**Bansal, J.C., Sharma, H., Jadon, S.S., and Clerc, M. (2014).** Spider monkey optimization algorithm for numerical optimization, *Memetic Computing*, vol. 6 (1), pp. 31-47.

**Brand, H., Weber, C., Meibom, P., Barth, R., and Swider, D.J. (2004).** A stochastic energy market model for evaluating the integration of wind energy, *6$^{th}$ IAEE European Conference on Modelling in Energy Economics and Policy, 2-3$^{rd}$* Sep., *Germany*, pp. 1-17.

**Breeze, P. (2019).** Combined heat and power, Chapter 5: Steam turbine combined heat and power systems, *Academic Press*, pp. 13-19.

**Bruninx, K., and Delarue, E. (2017).** Endogenous probabilistic reserve sizing and allocation in unit commitment models: Cost-effective, reliable, and fast, *IEEE Transactions on Power Systems*, vol. 32 (4), pp. 2593-2603.

**Burke, M.J., and Stephens, J.C. (2018).** Political power and renewable energy futures: A critical review, *Energy Research and Social Science,* vol. 35, pp. 78-93.

**Camelo, S., Papavasiliou, A., Castro, L.D., Riascos, A., and Oren, S. (2018).** A structural model to evaluate the transition from self-commitment to centralized unit commitment, *Energy Economics*, vol. 75, pp. 560–572.

**Cardenas, A.A.A., David, F.M., Behnke, R.E.P., and Espinoza, D.G. (2016).** A polyhedral-based approach applied to quadratic cost curves in the unit commitment problem, *IEEE Transactions on Power Systems*, vol. 31 (5), pp. 3674-3683.

**Cavallaro, F., Zavadskas, E.K., and Streimikiene, D. (2018).** Concentrated solar power (CSP) hybridized systems. Ranking based on an intuitionist fuzzy multi-criteria algorithm, *Journal of Cleaner Production*, vol. 179, pp. 407-416.

**Chakraborty, S., Ito, T., Senjyu, T., and Saber, A.Y. (2012).** Unit commitment strategy of thermal generators by using advanced fuzzy controlled binary particle swarm optimization algorithm, *International Journal of Electrical Power and Energy Systems,* vol. 43 (1), pp. 1072-1080.

**Chandram, K., Subrahmanyam, N., and Sydulu, M. (2008).** New approach with Muller method for profit based unit commitment, *Power and Energy Society General Meeting-Conversion and Delivery of Electrical Energy in 21$^{st}$ century, Pittsburgh, PA, 20-24$^{th}$* July, *USA,* pp. 1-8.

**Chandram, K., Subrahmanyam, N., and Sydulu, M. (2009).** Improved pre-prepared power demand table and Muller's method to solve the profit based unit commitment problem, *Journal of Electrical Engineering Technology,* vol. 4, pp. 159-167.

**Chandrasekaran, K., Hemamalini, S., Simon, S.P., and Padhy, N.P. (2012).** Thermal unit commitment using binary/real coded artificial bee colony algorithm, *Electric Power Systems Research*, vol. 84 (1), pp. 109-119.

**Chandrasekaran, K., and Simon, S.P. (2012).** Network and reliability constrained unit commitment problem using binary real coded firefly algorithm, *International Journal of Electrical Power and Energy Systems*, vol. 43 (1), pp. 921-932.

**Chen, P.H. (2012).** Two-level hierarchical approach to unit commitment using expert system and elite PSO, *IEEE Transactions on Power Systems*, vol. 27 (2), pp. 780 - 789.

**Chen, X., Kang, C., Malley, M.O., Xia, Q., Bai, J., Liu, C., Sun, R., Wang, W., and Li, H. (2015).** Increasing the flexibility of combined heat and power for wind power integration in China: Modelling and implications, *IEEE Transactions on Power Systems*, vol. 30 (4), pp. 1848-1857.

**Chen, X., Wei, X., Yang, G., and Du, W. (2019).** Fireworks explosion based artificial bee colony for numerical optimization, *Knowledge-Based Systems. (https://doi.org/10.1016/j.knosys.2019.105002)*

**Chen, Y., and Wang, F. (2017).** MIP formulation improvement for large scale security constrained unit commitment with configuration based combined cycle modelling, *Electric Power Systems Research*, vol. 148, pp. 147–154.

**Cheng, C.P., Liu, C.W., and Liu, C.C. (2000)[1].** Unit commitment by Lagrangian relaxation and genetic algorithms, *IEEE Transactions on Power Systems,* vol. 15 (2), pp. 707-714.

**Cheng, C.P., Liu, C.W., and Liu, C.C. (2000)[2].** Unit commitment by annealing genetic algorithms, *Electric Power and Energy Systems*, vol. 24 (2), pp. 149-158.

**Chitara, D., Niazi, K.R., Swarnkar, A., and Gupta, N. (2018).** Cuckoo search optimization algorithm for designing of a multimachine power system stabilizer, *IEEE Transactions on Industry Applications,* vol. 54 (4), pp. 3056-3065.

**Christopher, C.C., and Sishaj, P.S. (2011).** Profit based unit commitment for GENCOs using parallel PSO in a distributed cluster, *ACEEE International Journal Electrical Power Engineering,* vol. 2, pp. 24-30.

**Chusanapiputt, S., Nualhong, D., Jantarang, S., and Phoomvuthisarn, S. (2008).** A solution to unit commitment problem using hybrid ant system/priority list method, *IEEE 2nd International Power and Energy Conference, Malaysia, 1-3rd* Dec., pp. 1183–1188.

**Civicioglu, P. (2013)[1].** Backtracking search optimization algorithm for numerical optimization problems, *Applied Mathematics and Computation,* vol. 219 (15), pp. 8121-8144.

**Civicioglu, P. (2013)[2].** Artificial cooperative search algorithm for numerical optimization problems, *Information Sciences,* vol. 229, pp. 58-76.

**Cohen, A.I., and Wan, S.H. (1987).** A method for solving the fuel constrained unit commitment problem, *IEEE Transactions on Power Systems,* vol. PER (7), pp. 39-39.

**Columbus, C.C., and Simon, S.P. (2012).** Profit Based unit commitment: A parallel ABC approach using a workstation cluster, *Computers and Electrical Engineering*, vol. 38 (3), pp. 724-745.

**Columbus, C.C., and Simon, S.P. (2013).** Profit based unit commitment for GENCOs using parallel NACO in a distributed cluster, *Swarm and Evolutionary Computation,* vol. 10, pp. 41-48.

**Columbus, C.C., Chandrasekaran, K., and Simon, S.P. (2012).** Nodal ant colony optimization for solving profit based unit commitment problem for GENCOs, *Applied Soft Computing,* vol. 12 (1), pp. 145-160.

**Dai, Y., Chen, L., Min, Y., Mancarella, P., Chen, Q., Hao, J., Hu, K., and Xu, F. (2017).** Integrated dispatch model of combined heat and power plant with phase change thermal energy storage considering heat transfer process, *IEEE Transaction on Sustainable Energy*, vol. 9 (3), pp. 1234–1243.

**Damousis, I.G., Bakirtzis, A.G., and Dokopoulos, P.S. (2004).** A solution to the unit commitment problem using integer-coded genetic algorithm, *IEEE Transactions on Power Systems,* vol. 19 (2), pp. 1165-1172.

Danish Energy Agency, (2016). Technology data for energy plants, *Generation of Electricity and District Heating, Energy Storage and Energy Carrier Generation and Conversion*. (https://ens.dk/sites/ens.dk/files/Analyser/technology_data_catalogue_for_el_and_dh.pdf)

**Datta, D., and Dutta, S. (2012).** A binary-real-coded differential evolution for unit commitment problem, *International Journal of Electrical Power and Energy Systems*, vol. 42 (1), pp. 517-524.

**Deb, K. (2004).** Optimization for engineering design, *PHI Learning Private Limited*.

**Dey, A., Dey, S., Bhattacharyya, S., Platos, J., and Snasel, V. (2019).** Novel quantum inspired approaches for automatic clustering of gray level images using Particle Swarm Optimization, Spider Monkey Optimization and Ageist Spider Monkey Optimization algorithms, *Applied Soft Computing*. (https://doi.org/10.1016/j.asoc.2019.106040)

**Dhaliwal, J.S., and Dhillon, J.S., (2018).** Modified binary differential evolution algorithm to solve unit commitment problem, *Electric Power Components and Systems*, vol. 46 (8), pp. 900-918.

**Dhillon, J.S., Dhillon, J.S.[1], and Kothari, D.P. (2009).** Economic-emission load dispatch using binary successive approximation-based evolutionary search, *IET Generation, Transmission and Distribution,* vol. 3 (1), pp. 1-16.

**Dieu, V.N., and Ongsakul, W. (2006).** Enhanced augmented Lagrangian Hopfield network for unit commitment, *IEE Proceeding Generation Transmission and Distribution*, vol. 153 (6), pp. 624-632.

**Dieu, V.N., and Ongsakul, W. (2006).** Enhanced merit order and augmented Lagrange Hopfield network for ramp rate constrained unit commitment, *IEEE Power Engineering Society General Meeting, Montreal, Que., Canada, 18-22$^{th}$* June, pp. 1-7.

**Dieu, V.N., and Ongsakul, W. (2008).** Ramp rate constrained unit commitment by improved priority list and augmented Lagrange Hopfield network, *Electric Power Systems Research*, vol. 78 (3), pp. 291-301.

**Dieu, V.N., and Ongsakul, W. (2011).** Augmented Lagrange Hopfield network based Lagrangian relaxation for unit commitment, *International Journal of Electrical Power and Energy Systems*, vol. 33 (3), pp. 522-530.

**Dimitroulas, D.K., and Georgilakis, P.S. (2011).** A new memetic algorithm approach for the price based unit commitment problem, *Applied Energy*, vol. 88 (12), pp. 4687-4699, 2011.

**Du, M., and Li, Y.F. (2020).** An investigation of new local search strategies in memetic algorithm for redundancy allocation in multi-state series-parallel systems, *Reliability Engineering and System Safety,* vol. 195, pp. 1-14.

**Dudek, G. (2004).** Unit commitment by genetic algorithm with specialized search operators, *Electric Power Systems Research*, vol. 72 (3), pp. 299-308.

**Duo, H., Sasaki, H., Nagata, T., and Fujita, H. (1999).** A solution for unit commitment using Lagrangian relaxation combined with evolutionary programming, *Electric Power Systems Research*, vol. 51 (1), pp. 71-77.

**Eberhart, R.C., and Shi, Y. (1998).** Parameter selection in particle swarm adaptation, *7$^{th}$ International Conference on Evolutionary Programming VII, EP98 San Diego, California, USA, 25-27$^{th}$* March, pp. 591–600.

**Elaziz, M.A., Li, L., Jayasena, K.P.N.,and Xiong, S. (2019).** Multiobjective big data optimization based on a hybrid salp swarm algorithm and differential evolution, *Applied Mathematical Modelling*, pp. 1-15. (https://doi.org/10.1016/j.apm.2019.10.069.)

**Eldin, A.S., El-sayed, M.A.H., and Youssef, H.K.M. (2008).** A two-stage genetic based technique for the unit commitment optimization problem, *12$^{th}$ International Middle East Power System Conference, MEPCO, Aswan, Egypt, 12-15$^{th}$ March*, pp. 425-430.

**Espana, G.M., and Arango, D.A.T. (2019).** Modeling the hidden flexibility of clustered unit commitment, *IEEE Transactions on Power Systems*, vol. 34 (4), pp. 3294-3296.

**Fan, W., Guan, X., and Zhai, Q. (2002).** A new method for unit commitment with ramping constraints, *Electric Power Systems Research*, vol. 62 (3), pp. 215-224.

**Fatma, A.H., Essam H.H., Mai S.M., Walid A.A., and Seyedali M. (2019).** Henry gas solubility optimization: A novel physics-based algorithm, *Future Generation Computer Systems*, vol. 101, pp. 646-667.

**Fergany, A.E. (2015).** Optimal allocation of multi-type distributed generators using backtracking search optimization algorithm, *International Journal of Electrical Power and Energy Systems*, vol. 64, pp. 1197-1205.

**Gaing, Z.L. (2003).** Particle swarm optimization to solving the economic dispatch considering the generator constraints, *IEEE Transactions on Power Systems*, vol. 18 (3), pp. 1187-1195.

**Gandomi, A.H., and Kashani, A.R. (2018).** Construction cost minimization of shallow foundation using recent swarm intelligence techniques, *IEEE Transactions on Industrial Informatics*, vol. 14 (3), pp. 1099-1106.

**Gandomi, A.H., Yang, X.S., and Alavi, A.H. (2013).** Cuckoo search algorithm: a metaheuristic approach to solve structural optimization problems, *Engineering with computers*, vol. 29, pp. 17-35.

**Ganguly, D., Sarkar, V., and Pal, J. (2004).** A new genetic approach for solving the unit commitment problem, *International conference on power system technology-POWERCON 2004, Singapore*, *21-24$^{th}$* Nov., vol. 1, pp. 542–7.

**Ghadi, M.J., Baghramian, A., and Imani, M.H. (2016)$^1$.** An ICA based approach for solving profit based unit commitment problem market, *Applied Soft Computing*, vol. 38, pp. 487-500.

**Ghadi, M.J., Baghramian, A., and Imani, M.H. (2016)$^2$.** Optimal power scheduling of thermal units considering emission constraint for GENCOs' profit maximization, *International Journal of Electrical Power and Energy Systems*, vol. 82, pp. 124-135.

**Glover, F. (1989).** Tabu Search-Part I, *ORSA Journal on Computing*, vol. 1, pp. 190-206.

**Gonzalez, A. and Perez, R. (2001).** An experimental study about the search mechanism in the slave learning algorithm: Hill climbing methods versus genetic algorithms, *Information Sciences*, vol. 136, pp. 159-174.

**Govardhan, M., and Roy, R. (2014).** Economic analysis of unit commitment with distributed energy resources, *International Journal of Electrical Power and Energy Systems*, vol. 71, pp. 1-14.

**Grefensttete, J.J. (1986).** Optimization of control parameters for genetic algorithm, *IEEE Transaction on Systems, Man and Cybernetics*, vol. 16 (1), pp. 122-128.

**Guan, X., Luh, P.B., Yan, H., and Amalfi, J.A. (1992).** An optimization-based method for unit commitment, *International Journal of Electrical Power and Energy Systems*, vol. 14 (1), pp. 9-17.

**Haberg, M., (2019).** Fundamentals and recent developments in stochastic unit commitment, *International Journal of Electrical Power and Energy Systems*, vol. 109, pp. 38-48.

**Harwell, A.E.A. (2010).** European Commission Green public procurement-combined heat and power technical background report, *Report for the European Commission–DG Environment*.

**Heidari, A. A., Mirjalili, S., Faris, H., Aljarah, I., Mafarja, M., and Chen, H. (2019).** Harris hawks optimization: Algorithm and applications, *Future Generation Computer Systems*, vol. 97, pp. 849-872.

**Heris, M.N., Ivatloo, B.M., and Gharehpetian, G.B. (2018).** A comprehensive review of heuristic optimization algorithms for optimal combined heat and power dispatch from economic and environmental perspectives, *Renewable and Sustainable Energy Reviews,* vol. 81 (2), pp. 2128-2143.

**Hermans, M., Bruninx, K., and Delarue, E. (2018).** Impact of CCGT start-up flexibility and cycling costs towards renewables integration, *IEEE Transaction on Sustainable Energy*, vol. 9 (3), pp. 1468–1476.

**Hota, P.K., Barisal, A.K., and Chakrabarti, R. (2010).** Economic emission load dispatch through fuzzy based bacterial foraging algorithm, *International Journal of Electrical Power and Energy System,* vol. 32 (7), pp. 794–803.

**Jain, A.K., and Jain, T. (2009).** Optimal bidding strategy of generating companies in forward electricity markets, *Proceedings of National Conference on Mathematical Modelling and Simulation (NCMMAS-09)*, Gwalior, pp. 9-11.

**Jangir, N., Pandya, M.H., Bhesdadiya, R.H., and Jangir, P. (2016).** Price penalty factors based approach for combined economic emission dispatch problem solution using moth-flame optimizer algorithm, *NCERTE,* pp.1-6.

**Javadi, M.S., Moghaddam, A.A., and Guerrero, J.M. (2017).** Optimal scheduling of a multi-carrier energy hub supplemented by battery energy storage systems, *IEEE Industrial and Commercial Power Systems Europe (EEEIC Europe), Milan, Italy, 6-9$^{th}$* June, pp. 1–6.

**Javidy, B., Hatamlou, A., and Mirjalili, S. (2015).** Ions motion algorithm for solving optimization problems, *Applied Soft Computing,* vol. 32, pp. 72-79.

**Jensen, E.F. (2010).** Modeling of the combined heat and power system of greater Copenhagen, Technical University of Denmark DTU Management.

**Jeong, W.Y., Lee, N.W., Kim, H.H., Park, B.J., and Shin, R.J. (2009).** Thermal unit commitment using binary differential evolution, *Journal of Electrical Engineering and Technology*, vol. 4 (3), pp. 323-329.

**Jeong, Y.W., Park, J.B., Jang, S.H., and Lee, K.Y. (2010).** A new quantum-inspired binary PSO: application to unit commitment problems for power systems, *IEEE Transactions on Power Systems*, vol. 25 (3), pp. 1486 – 1495.

**Jeong, Y.W., Park, J.B., Shin, J.R., and Lee, K.Y. (2009).** A thermal unit commitment approach using an improved quantum evolutionary algorithm, *Electric Power Components and Systems,* vol. 37 (7), pp. 770-786.

**Jiang, F., He, J., and Tian, T. (2019).** A clustering-based ensemble approach with improved pigeon-inspired optimization and extreme learning machine for air quality prediction, *Applied Soft Computing*, vol. 85. (https://doi.org/10.1016/j.asoc.2019.105827.)

**Juste, K.A., Kita, H., Tanaka, E., and Hasegawa, J. (1999).** An evolutionary programming solution to the unit commitment problem, *IEEE Transactions on Power Systems,* vol. 14 (4), pp. 1452-1459.

**Kasaeian, A., Nouri, G., Ranjbaran, P., and Wen, D. (2018).** Solar collectors and photovoltaics as combined heat and power systems: A critical review, *Energy Conversion and Management*, vol. 156, pp. 688–705.

**Kaur, R., Patterh, M.S., and Dhillon, J.S. (2015).** A new greedy search method for the design of digital IIR filter, *Journal of King Saud University, Computer and Information Sciences*, vol. 27, pp. 278–287.

**Kazarlis, S.A., Bakirtzis, A.G., and Petridis, V. (1996).** Genetic algorithm solution to the unit commitment problem, *IEEE Transactions on Power Systems,* vol. 11 (1), pp. 83-92.

**Kennedy, J., and Eberhart, R.C., (1997).** A discrete binary version of the particle swarm algorithm, *19th IEEE International Conference on Systems, Man, and Cybernetic: Computational Cybernetics and Simulation, Orlando, FL, USA, 12-15th* Oct., pp. 4104-4108.

**Kerr, T. (2008).** Combined heat and power -Evaluating the benefits of greater global investment, International Energy Agency, OECD/AEA.

**Kerr, T. (2010).** The international CHP/DHC collaborative advancing near-term low carbon technologies, International Energy Agency.

**Khan, M.F., Aadil, F., Maqsood, M., Bukhari, S.H.R., Hussain, M., and Nam, Y. (2019).** Moth Flame Clustering Algorithm for Internet of Vehicle (MFCA-IoV), *IEEE Access*, vol. 7, pp. 11613-11629.

**Khanmohammadi, S., Amiri, M., and Tarafdar, M.H. (2010).** A new three-stage method for solving unit commitment problem, *Energy,* vol. 35 (7), pp. 3072-3080.

**Kia, M., Nazar, M.S., Sepdegh, M.S., Heidari, A., and Siano, P. (2017)[1].** Optimal day ahead scheduling of combined heat and power units with electrical and thermal storage considering security constraint of power systems, *Energy*, vol. 120, pp. 241-252.

**Kia, M., Nazar, M.S., Sepdegh, M.S., Heidari, A., and Siano, P. (2017)[2].** An efficient linear model for optimal day ahead scheduling of CHP units in active distribution networks considering load commitment programs, *Energy,* vol. 139, pp. 798-817.

**Kim, J.S., and Edgar, T.F. (2014).** Optimal scheduling of combined heat and power plants using mixed integer nonlinear programming, *Energy,* vol. 77, pp. 675-690.

**Kneiske, T.M., and Braun, M. (2017).** Flexibility potentials of a combined use of heat storages and batteries in PV-CHP hybrid systems, *11th International Renewable Energy Storage Conference, IRES 2017, Dusseldorf, Germany, 14-16th* March, vol. 135.

**Kneiske, T.M., Braun, M., and Hidalgo-Rodriguez, D.I. (2018).** A new combined control algorithm for PV-CHP hybrid systems, *Applied Energy,* vol. 210, pp. 964–973.

**Koltsaklisa, N.E., Dagoumasa, A.S., and Panapakidis, I.P. (2017).** Impact of the penetration of renewables on flexibility needs, *Energy Policy*, vol. 109, pp. 360–369.

**Kopiske, J., Spieker, S., and Tsatsaronis, G. (2017).** Value of power plant flexibility in power systems with high shares of variable renewables: A scenario outlook for Germany 2035, *Energy,* vol. 137, pp. 823–833.

**Kothari, D.P., and Ahmad, A. (1995).** An expert system approach to the unit commitment problem, *Energy Conversion and Management,* vol. 36 (4), pp. 257-261.

**Kothari, D.P., and Dhillon, J.S. (2011).** Power system optimization, *2nd edition, PH1 learning private limited*.

**Krishna, P.V.R., and Rao, S. (2016).** An improved TLBO algorithm to solve profit based unit commitment problem under deregulated environment, *Procedia Technology, Global Colloquium in Recent Advancement and Effectual Researches in Engineering, Science and Technology,* vol. 25, pp. 652-659.

**Kumar, M., Kumar, A., and Sandhu, K. S. (2018).** Impact of distributed generation on nodal prices in hybrid electricity market, *International Conference on Processing of*

*Materials, Minerals and Energy 2016, Ongole, Andhra Pradesh, India*, 29-30th July, vol. 5, pp. 830-840.

**Kumar, M., Kumar, A., and Sandhu, K. S. (2016).** Optimal location of WT based distributed generation in pool based electricity market using mixed integer nonlinear programming, *International Conference on Processing of Materials, Minerals and Energy, Ongole, Andhra Pradesh*, India 29-30th July, vol. 5 (1), pp. 445-457.

**Kumar, N., Panigrahi, B.K., and Singh, B. (2016).** A solution to the ramp rate and prohibited operating zone constrained unit commitment by GHS-JGT evolutionary algorithm, *International Journal of Electrical Power and Energy Systems,* vol. 81, pp. 193-203.

**Kumar, P. (2010).** Computational Intelligence in Expensive Optimization Problems, Chapter on optimization and decision making strategies in engineering systems, *Springer,* vol. 2.

**Kumar, P. and Bauer, P. (2007).** Multi-objective optimization of a BLDC drive, *10th International Symposium on Mechatronics, Trencianske Teplice Slovakia, 6-7th* June, pp. 9-16.

**Kuo, C.C., Lee, C.Y., and Sheim, Y.C. (2011).** Unit commitment with energy dispatch using a computationally efficient encoding structure, *Energy Conversion and Management,* vol. 52 (3), pp. 1575-1582.

**Lan, Y., Guan, X., and Wu, J. (2016).** Rollout strategies for real-time multi-energy scheduling in microgrid with storage system, *IET Generation, Transmission and Distribution,* vol. 10 (3), pp. 688–696.

**Lannoye, E., Flynn, D., and Malley, M. O. (2012).** Evaluation of power system flexibility, *IEEE Transactions on Power Systems,* vol. 27 (2), pp. 922-931.

**Lauer, G.S., Sandell, N.R., Bertsekas, D.P., and Posbergh, T.A. (1982).** Solution of large-scale optimal unit commitment problems, *IEEE Transactions on Power Apparatus and Systems,* vol. PAS-101 (1), pp. 79-86.

**Lazo, B.P., and Cartes, J.S. (2011).** A deterministic annular crossover genetic algorithm optimization for the unit commitment problem, *Expert Systems with Applications*, vol. 38 (6), pp. 6523-6529.

**Lee, S., Park, H., and Jeon, M. (2007).** Binary particle swarm optimization with bit change mutation, *IEICE Transactions on Fundamentals of Electronics Communications and Computer Sciences,* vol. E-90A (10), pp. 2253-2256.

**Li, J., Wang, X., Zhang, Z., Blond, S.L., Yang, Q., Zhang, M., and Yuan, W. (2017).** Analysis of a new design of the hybrid energy storage system used in the residential m-CHP systems, *Applied Energy,* vol. 187, pp. 169–179.

**Li, Z., Wu, W., Wang, J., Zhang, B., and Zheng, T. (2016).** Transmission-constrained unit commitment considering combined electricity and district heating networks, *IEEE Transactions on Sustainable Energy*, vol. 7 (2), pp. 1-13.

**Li, Z., Zou, D., and Kong, Z. (2019).** A harmony search variant and a useful constraint handling method for the dynamic economic emission dispatch problems considering transmission loss, *Engineering Applications of Artificial Intelligence*, vol. 84, pp. 18-40.

**Lia, J., Liua, F., Lib, Z., Shaoc, C., and Liu, X. (2018).** Grid-side flexibility of power systems in integrating large-scale renewable generations: A critical review on concepts, formulations and solution approaches, *Renewable and Sustainable Energy Reviews*, vol. 93, pp. 272–284.

**Liao, G.C. (2006).** Short-term thermal generation scheduling using improved immune algorithm, *Electric Power Systems Research*, vol. 76 (5), pp. 360-373.

**Liu, C., Shahidehpour, M., Li, Z., and Firuzabad, M.F. (2009).** Component and mode models for the short-term scheduling of combined cycle units, *IEEE Transactions on Power Systems*, vol. 24 (2), pp. 976–990.

**Ma, X., El-Keib, A.A., Smith, R.E., and Ma, H. (1995).** A genetic algorithm based approach to thermal unit commitment of electric power systems, *Electric Power Systems Research*, vol. 34 (1), pp. 29-36.

**Mahmud, K., Morsalin, S., Hossain, M.J., and Town, G.E. (2017).** Domestic peak-load management including vehicle-to-grid and battery storage unit using an artificial neural network, *IEEE International Conference on Industrial Technology (ICIT), Toronto, ON, Canada*, pp. 586-591.

**Mahor, A., Prasad, V., and Rangnekar, S. (2009).** Economic dispatch using particle swarm optimization: A review, *Renewable and Sustainable Energy Reviews*, vol. 13 (8), pp. 2134-2141.

**Mantawy, A.H. (2004).** A genetic algorithm solution to a new fuzzy unit commitment model, *Electric Power Systems Research*, vol. 72 (2), pp. 171-178.

**Mantawy, A.H., Abdel-Magid, Y.L., and Selim, S.Z. (1999).** A new genetic-based tabu search algorithm for unit commitment problem, *Electric Power Systems Research*, vol. 49 (2), pp. 71-78.

**Marifeld, T.T., and Sheble, G.B., (1996).** Genetic based unit commitment algorithm, *IEEE Transactions on Power Systems*, vol. 11 (3), pp. 1359–1370.

**Martinez, S., Michaux, G., Salagnac, P., and Bouvier, J.L. (2017).** Micro-combined heat and power systems (micro-CHP) based on renewable energy sources, *Energy Conversion and Management*, vol. 154, pp. 262–285.

**Marwali, M.K.C., Ma, H., Shahidehpour, S.M., and Rahman, K.H.A. (1998).** Short term generation scheduling in photovoltaic-utility grid with battery storage, *IEEE Transactions on Power Systems*, vol. 13 (3), pp. 1057-1062.

**Mbamalu, G.A.N., Hawary, F.E., and Hawary, M.E. E. (1995).** Effects of load modeling on minimum loss, minimum emission, and multiple-objective optimal hydrothermal power flow, *Electric Power Systems Research*, vol. 34, pp. 97-108.

**Meng, A., Li, Z., Yin, H., Chen, S., and Guo, Z. (2016).** Accelerating particle swarm optimization using crisscross search, *Information Sciences*, vol. 329, pp. 52-72.

**Meng, A., Mei, P., Yin, H., Peng, X., and Guo, Z. (2015).** Crisscross optimization algorithm for solving combined heat and power economic dispatch problem, *Energy Conversion and Management*, vol. 105, pp. 1303-1317.

**Meng, A.B., Chen, Y.C., Yin, H., and Chen, S.Z. (2014).** Crisscross optimization algorithm and its application, *Knowledge-Based Systems*, vol. 67, pp. 218-229.

**Mirjalili, S. (2015)[1].** The ant lion optimizer, *Advances in Engineering Software*, vol. 83, pp. 80-98.

**Mirjalili, S. (2015)[2].** Moth-flame optimization algorithm: A novel nature-inspired heuristic paradigm, *Knowledge-Based Systems*, vol. 89, pp. 228-249.

**Mirjalili, S., and Lewis, A. (2016).** The whale optimization algorithm, *Advances in Engineering Software*, vol. 95, pp. 51-67.

**Mirjalilia, S. (2016).** SCA: A Sine Cosine Algorithm for solving optimization problems, *Knowledge Based Systems,* vol. 96, pp. 120-133.

**Mirjalilia, S., Saremia, S., Mirjalilic, S.M., and Coelhod, L.S. (2016).** Multi-objective grey wolf optimizer: A novel algorithm for multi-criterion optimization, *Expert Systems with Applications,* vol. 47, pp. 106-119.

**Mirjalilia, S., Saremia, S., Mirjalilic, S.M., and Coelhod, L.S. (2016).** Multi-objective grey wolf optimizer: A novel algorithm for multi-criterion optimization, *Expert Systems with Applications,* vol. 47, pp. 106-119.

**Mitra, S., Sun, L., and Grossmann, I.E. (2013).** Optimal scheduling of industrial combined heat and power plants under time-sensitive electricity prices, *Energy*, vol. 54, pp. 184-211.

**Miyamoto, T., Mori, K., Kitamura, S., and Izui, Y. (2016).** Solving distributed unit commitment problem with walrasian auction, *IEEE Transactions on Systems, Man and Cybernetics: Systems*, vol. 46 (8), pp. 1088-1097.

**Monteiro, E., Moreira, N.A., and Ferreira, S. (2009).** Planning of micro-combined heat and power systems in the Portuguese scenario, *Applied energy*, vol. 86 (3), pp. 290-298.

**Mori, H., and Okawa, K. (2009).** Meta-heuristic a new method for profit-based unit commitment under competitive environment, *IEEE Bucharest Power Technology Conference, Bucharest, Romania, 28 June- 2* July, pp. 1-6.

**Murty, V.V.V.S.N., and Kumar, A. (2019).** Optimal DG integration and network reconfiguration in microgrid system with realistic time varying load model using hybrid optimization, *IET Smart Grid*, vol. 2, pp. 192-202.

**Naidu, K., Mokhlis, H., Bakar, A.H.B.A., and Terzija, V. (2014).** Comparative performance analysis of Firefly Algorithm for load frequency control in automatic generation control of interconnected reheat thermal power system, *3rd IET International Conference on Clean Energy and Technology (CEAT), 24-26th* Nov., pp. 1-6.

**Najafi, S., and Pourjamal, Y. (2012).** A new heuristic algorithm for unit commitment problem, *Energy Procedia*, vol. 14, pp. 2005-2011.

**Nanda, J., Mishra, S., and Saikia, L. (2009).** Maiden application of bacterial foraging based optimization technique in multi-area automatic generation control, *IEEE Transactions on Power Systems*, vol. 24, pp. 602-609.

**Narang, N., Sharma, E., and Dhillon, J.S. (2017).** Combined heat and power economic dispatch using integrated civilized swarm optimization and powell's pattern search method, *Applied Soft Computing*, vol. 52, pp. 190-202.

**Nazari, M.E., and Ardehali, M.M. (2017).** Profit-based unit commitment of integrated CHP-thermal-heat only units in energy and spinning reserve markets with considerations for environmental CO2 emission cost and valve-point effects, *Energy*, vol. 133, pp. 621-635.

**Nghitevelekwa, K., and Bansal, R.C. (2018).** A review of generation dispatch with large-scale photovoltaic systems, *Renewable and Sustainable Energy Reviews*, vol. 81, pp. 615-624.

**Niknam, T., Khodaei, A., and Fallahi, F. (2009).** A new decomposition approach for the thermal unit commitment problem, *Applied Energy*, vol. 86 (9), pp. 1667-1674.

**Ommen, T., Markussen, W.B., and Elmegaard, B. (2014).** Comparison of linear, mixed integer and non-linear programming methods in energy system dispatch modelling, *Energy*, vol. 74, pp. 109–118.

**Ongsakul, W., and Petcharaks, N. (2004).** Unit commitment by enhanced adaptive Lagrangian relaxation, *IEEE Transactions on Power Systems,* vol. 19 (1), pp. 620-628.

**Ongsakul, W., and Vo, D.N. (2013).** Artificial intelligence in power system optimization, *Taylor & Francis Group, Boca Raton*.

**Ortega, J., Watts, D., and Ren, H. (2017).** Review of operating reserves and day-ahead unit commitment considering variable renewable energies: International experience, *IEEE Latin America Transactions*, vol. 15 (11), pp. 2126-2136.

**Pacific Northwest National Laboratory U.S. department of energy (2017).** Available: http://www.pnnl.gov/science/highlights/highligh.asp/id=546

**Panwar, L.K., Reddy, K.S., Verma, A., Panigrahi, B.K., and Kumar, R. (2018).** Binary grey wolf optimizer for large scale unit commitment problem, *Swarm and Evolutionary Computation*, vol. 38, pp. 251-266.

**Patra, S., Goswami, S.K., and Goswami, B. (2008).** Differential evolution algorithm for solving unit commitment with ramp constraints, *Electric Power Components and Systems*, vol. 36, pp. 771-787.

**Patwal, R.S., and Narang, N. (2018).** Crisscross PSO algorithm for multi-objective generation scheduling of pumped storage hydrothermal system incorporating solar units, *Energy Conversion and Management*, vol. 169, pp. 238–254.

**Peng, C., Hou, Y., Yu, N., and Wang, W. (2017).** Risk-limiting unit commitment in smart grid with intelligent periphery, *IEEE Transactions on Power Systems*, vol. 32 (6), pp. 4696-4706.

**Peng, X., Lin, L., Zheng, W., and Liu, Y. (2015).** Crisscross optimization algorithm and monte carlo simulation for solving optimal distributed generation allocation problem, *Energies*, vol. 8, pp. 13641-13659.

**Peska, L., Misikir, T., and Horváth, T. (2019).** Swarm intelligence techniques in recommender systems-A review of recent research, *Swarm and Evolutionary Computation*, vol. 48, pp. 201-219.

**Posada, C.M.C., Espana, G.M., Duenas, P., and Martın, P.S. (2017).** Dynamic ramping model including intraperiod ramp-rate changes in unit commitment, *IEEE Transactions on Sustainable Energy*, vol. 8 (1), pp. 43-50.

**Qu, B.Y., Zhu, Y.S., Jiao, Y.C., Wu, M.Y., Suganthan, P.N., and Liang, J.J. (2018).** A survey on multi-objective evolutionary algorithms for the solution of the environmental/economic dispatch problems, *Swarm and Evolutionary Computation*, vol. 38, pp. 1-11.

**Raglend, J., Raghuveer, C., Avinash, G.R., Padhy, N.P., and Kothari, D.P., (2010).** Solution to profit based unit commitment problem using particle swarm optimization, *Applied Soft Computing*, vol. 10 (4), pp. 1247-1256.

**Rahman, I., and Saleh, J.M. (2018).** Hybrid bio-inspired computational intelligence techniques for solving power system optimization problems: A comprehensive survey, *Applied Soft Computing*, vol. 69, pp. 72-130.

**Rahman, M.S., Mahmud, M.A., Pota, H.R., and Hossain, M.J. (2015).** A multi-agent approach for enhancing transient stability of smart grids, *International Journal of Electrical Power and Energy Systems*, vol. 67, pp. 488-500.

**Rao, S.S. (1996).** Engineering optimization theory and practice, *1th edition, New Age International Publishers.*

**Ray, T., and Liew, K.M. (2003).** Society and civilization: An optimization algorithm based on the simulation of social behaviour, *IEEE Transaction on Evolutionary Computing*, vol. 7 (4), pp. 386, 396.

**Reddy, G.V.S., Ganesh, V., and Rao, C.S. (2016).** Implementation of clustering based unit commitment employing imperialistic competition algorithm, *International Journal of Electrical Power and Energy Systems,* vol. 82, pp. 621-628.

**Reddy, K.S., Panwar, L.K., Kumar, R., and Panigrahi, B.K. (2016).** Binary fireworks algorithm for profit based unit commitment problem, *International Journal of Electrical Power and Energy Systems,* vol. 83, pp. 270-282.

**Reddy, K.S., Panwar, L.K., Panigrahi, B.K., and Kumar, R. (2018).** Solution to unit commitment in power system operation planning using binary coded modified moth flame optimization algorithm (BMMFOA): A flame selection based computational technique, *Journal of Computational Science*, vol. 25, pp. 298-317.

**Reddy, S.K., Panwar, L.K., Panigrahi, B.K., Kumar, R., and Alsumaiti, A. (2019).** Binary grey wolf optimizer models for profit based unit commitment of price-taking GENCO in electricity market, *Swarm and Evolutionary Computation,* vol. 44, pp. 957–971.

**Rong, A., and Lahdelma, R. (2017).** An efficient model and algorithm for the transmission-constrained multi-site combined heat and power system, *European Journal of Operational Research*, vol. 258 (3), pp. 1106-1117.

**Rong, A., and Peter, B. (2018).** A dynamic regrouping based dynamic programming approach for unit commitment of the transmission-constrained multi-site combined heat and power system, *IEEE Transaction on Power Systems*, vol. 33 (1), pp. 714-722.

**Rong, A., Hakonen, H., and Lahdelma, R. (2008).** A variant of the dynamic programming algorithm for unit commitment of combined heat and power systems, *European Journal of Operational Research*, vol. 190 (3), pp. 741–755.

**Rong, A., Hakonen, H., and Lahdelma, R. (2009).** A dynamic regrouping based sequential dynamic programming algorithm for unit commitment of combined heat and power systems, *Energy Conversion and Management*, vol. 50 (4), pp. 1108-1115.

**Rong, A., Lahdelma, R., and Grunow, M. (2009).** An improved unit decommitment algorithm for combined heat and power systems, *European Journal of Operational Research*, vol. 195 (2), pp. 552–562.

**Roy, P.K. (2013).** Solution of unit commitment problem using gravitational search algorithm, *Electrical Power and Energy Systems*, vol. 53, pp. 85-94.

**Roy, P.K., and Sarkar, R. (2014).** Solution of unit commitment problem using quasi-oppositional teaching learning based algorithm, *International Journal of Electrical Power and Energy Systems,* vol. 60, pp. 96-106.

**Saber, A.Y., and Alshareef, A.M. (2008).** Scalable unit commitment by memory-bounded ant colony optimization with a local search, *International Journal of Electrical Power and Energy Systems,* vol. 30 (6-7), pp. 403-414.

**Saber, A.Y., and Venayagamoorthy, G. K. (2009).** V2G scheduling-A modern approach to unit commitment with vehicle-to-grid using particle swarm optimization, *IFAC Proceedings Volumes*, vol. 42 (9), pp. 261-266.

**Saber, N.A., Salimi, M., and Mirabbasi, D. (2016).** A priority list based approach for solving thermal unit commitment problem with novel hybrid genetic-imperialist competitive algorithm, *Energy*, vol. 117 (1), pp. 272-280.

**Sadeghian, H.R., and Ardehali, M.M. (2016).** A novel approach for optimal economic dispatch scheduling of integrated combined heat and power systems for maximum economic profit and minimum environmental emissions based on benders decomposition, *Energy,* vol. 102, pp. 10-23.

**Salgado, F., and Pedrero, P. (2008).** Short-term operational planning on cogeneration systems: A survey, *Electric Power Systems Research*, vol. 78 (5), pp. 835-848.

**Sanjay, R., Jayabarathi, T., Raghunathan, T., Ramesh, V., and Mithulananthan, N. (2017).** Optimal allocation of distributed generation using hybrid grey wolf optimizer, *IEEE Access*, vol. 5, pp. 14807-14818.

**Schwarza, H., Schermeyera, H., Bertschb, V., and Fichtner, W. (2018).** Self-consumption through power-to-heat and storage for enhanced PV integration in decentralised energy systems, *Solar Energy,* vol. 163, pp. 150–161.

**Sedighizadeh, M., Esmaili, M., and Mohammadkhani, N. (2018).** Stochastic multi-objective energy management in residential microgrids with combined cooling, heating, and power units considering battery energy storage systems and plug-in hybrid electric vehicles, *Journal of Cleaner Production,* vol. 195, pp. 301–317.

**Selvakumar, A.I., and Thanushkodi, K. (2009).** Optimization using civilized swarm: solution to economic dispatch with multiple minima, *International Journal of Electrical Power and Energy Systems*, vol. 79 (1), pp. 8-16.

**Selvakumar, I. (2013).** Civilized swarm optimization for multi-objective short-term hydrothermal scheduling, *International Journal of Electrical Power and Energy Systems*, vol. 51, pp. 178-189.

**Selvakumar, K., Boopathi, C.S., and Venkatesan, T. (2016).** Emission constraint profit based unit commitment problem using improved bacterial foraging algorithm, *Indian Journal of Science and Technology*, vol. 9 (42), pp. 1-7.

**Sen, S., and Kothari, D.P., (1998).** Optimal thermal generating unit commitment: A review, *International Journal of Electrical Power and Energy Systems*, vol. 20 (7), pp. 443-451.

**Senjyu, T. (2003).** A fast technique for unit commitment problem by extended priority list, *IEEE Transactions on Power Systems,* vol. 18 (2), pp. 882-888.

**Senjyu, T., Shimabukuro, K., Uezato, K., and Funabashi, T. (2003).** A fast technique for unit commitment problem by extended priority list, *IEEE Transaction on Power Systems*, vol. 18, pp. 882-888.

**Senjyu, T., Yamashiro, H., Uezato, K., and Funabashi, T. (2002).** A unit commitment problem by using genetic algorithm based on unit characteristics classifications, *IEEE Power Engineering Society Winter Meeting: Conference Proceedings (Cat. No.02CH37309), New York, NY, USA, 27-31$^{th}$* Jan., vol. 1, pp. 58–63.

**Setiadi, H., Mithulananthan, N., Shah, R., Lee, K.Y., Krismanto, A., and Krismanto, U. (2019).** Resilient wide-area multi-mode controller design based on Bat algorithm for power systems with renewable power generation and battery energy storage systems, *IET Generation Transmission and Distribution*, vol. 13, pp. 1884-1894.

**Shang, C., Srinivasan, D., and Reindl, T. (2017).** Generation and storage scheduling of combined heat and power, *Energy*, vol. 124, pp. 693–705.

**Sharma, A., Sharma, A., Panigrahi, B.K., Kiran, D., and Kumar, R. (2016).** Ageist spider monkey optimization algorithm, *Swarm and Evolutionary Computation,* vol. 28, pp. 58-77.

**Sharma, D., Trivedi, A., Srinivasan, D., and Thillainathan, L. (2013).** Multi-agent modeling for solving profit based UC Problem, *Applied Soft Computing*, vol. 13 (8), pp. 3751-3761.

**Sheble, G.B., and Maifeld, T.T. (1994).** Unit commitment by genetic algorithm and expert system, *Electric Power Systems Research*, vol. 30 (2), pp. 115-121.

**Sheble, G.B., Maifeld, T.T., Britting, K., Fahd, G., and Fukurozaki, S. (1996).** Unit commitment by genetic algorithm with penalty method and a comparison of Lagrangian search and genetic algorithm economic dispatch example, *International Journal of Electrical Power and Energy,* vol. 18, pp. 339-346.

**Shukla, A., and Singh, S.N. (2016)[1].** Multi-objective unit commitment with renewable energy using hybrid approach, *IET Renewable Power Generation*, vol. 10 (3), pp. 327-338.

**Shukla, A., and Singh, S.N. (2016)[2].** Multi-objective unit commitment using search space-based crazy particle swarm optimization and normal boundary intersection technique, *IET Generation Transmission and Distribution,* vol. 10 (5), pp. 1222–1231.

**Simon, S.P., Padhy, N.P., and Anand, R.S. (2006).** An ant colony system approach for unit commitment problem, *International Journal of Electrical Power and Energy Systems,* vol. 28 (5), pp. 315-323.

**Simopoulos, N.D., Kavatza, S.D., and Vournas, C.D. (2006).** Unit commitment by an enhanced simulated annealing algorithm, *IEEE Transactions on Power Systems,* vol. 21 (1), pp. 68-76.

**Singhal, P.K., Naresh, R., and Sharma, V. (2015).** A modified binary artificial bee colony algorithm for ramp rate constrained unit commitment problem, *International Transactions on Electrical Energy Systems*, vol. 25, pp. 3472-3491.

**Singhal, P.K., Naresh, R., and Sharma, V. (2015).** Binary fish swarm algorithm for profit-based unit commitment problem in competitive electricity market with ramp rate constraints, *IET Generation, Transmission and Distribution,* vol. 9 (13), pp.1697-1707.

**Sriyanyong, P., and Song, Y.H. (2005).** Unit commitment using particle swarm optimization combined with Lagrange relaxation, *IEEE Power Engineering Society General Meeting, San Francisco, CA, USA, 12-16th* June, vol. 3, pp. 2752-5759.

**Sudhakar, A.V.V., Karri, C., and Laxmi, A.J. (2017).** Profit based unit commitment for GENCOs using Lagrange relaxation-differential evolution, *Engineering Science and Technology, an International Journal,* vol. 20 (2), pp. 738-747.

**Sumim, T., and Ongsakul, W. (2003).** Ant colony search algorithm for unit commitment, *IEEE International Conference on Industrial Technology, Maribor, Slovenia, 10-12th* Dec., vol. 1, pp. 72-77.

**Swarup, K.S., and Yamashiro, S. (2003).** A genetic algorithm approach to generator unit commitment, *International Journal of Electrical Power and Energy Systems*, vol. 25 (9), pp. 679-687.

**Syed, V.S.F., and Gopalakrishnan, M. (2016).** Improved pre-prepared demand table and memory management algorithm solve to profit based unit commitment problem with losses, *Indian Journal of Engineering*, vol. 13, pp. 21-26.

**Tamura, K., and Yasuda, K. (2011).** Primary study of spiral dynamics inspired optimization, *IEEJ Transactions on Electrical and Electronic Engineering*, vol. 6 (S1), pp. S98-S100,.

**Tan, W.S., and Shaaban, M. (2016).** A hybrid stochastic/deterministic unit commitment based on projected disjunctive MILP reformulation, *IEEE Transactions on Power Systems, Power Engineering Letters*, vol. 31 (6), pp. 5200-5201.

**Thorin, E., Brand, H., and Weber, C. (2005).** Long-term optimization of cogeneration systems in a competitive market environment, *Applied Energy*, vol. 81 (2), pp. 152-169.

**Ting, T.O., Rao, M.V.C., and Loo, C.K. (2006).** A novel approach for unit commitment problem via an effective hybrid particle swarm optimization, *IEEE Transactions on Power Systems*, vol. 21 (1), pp. 411-418.

**Tokoro, K.I., Masuda, Y., and Nishina, H. (2008).** Solving unit commitment problem by combining of continuous relaxation method and genetic algorithm, *SICE Annual Conference: The University Electro-Communications, Tokyo, Japan, 20-22$^{th}$* Aug., pp. 3474-3478.

**Tripathy, M. and Mishra, S. (2007).** Bacteria foraging based solution to optimize both real power loss and voltage stability limit, *IEEE Transactions on Power Systems*, vol. 22, pp. 240-248.

**Tseng, C.L., Li, C.A., and Oren, S.S. (2000).** Solving the unit commitment problem by a unit decommitment method, *Journal of Optimization Theory and Applications,* vol. 105 (3), pp. 707–730.

**Ummels, B.C., Gibescu, M., Pelgrum, E., Kling, W.L., and Brand, A.J. (2007).** Impacts of wind power on thermal generation unit commitment and dispatch, *IEEE Transactions on Energy Conversion*, vol. 22 (1), pp. 44-51.

**Uyar, A.S., Turkay, B., and Keles, A. (2011).** A novel differential evolution application to short-term electrical power generation scheduling, *International Journal of Electrical Power and Energy Systems*, vol. 33 (6), pp. 1236-1242.

**Vaisakh, K., and Srinivas, L.R. (2011).** Evolving ant colony optimization based unit commitment, *Applied Soft Computing*, vol. 11 (2), pp. 2863-2870.

**Veerapenand, J., and Beerepoot, M. (2011).** Co-generation and renewable/Solutions for a low-carbon energy future Tech. rep., *International Energy Agency, Paris, France*. (https://www.westernchptap.org/Data/publications/CoGeneration_RenewablesSolutionsforaLowCarbonEnergyFuture.pdf)

**Viana, A., Sousa, J.P.D., and Matos, M.A. (2008).** Fast solutions for unit commitment problems by a new metaheuristic approach, *Electric Power Systems Research*, vol. 78 (8), pp. 1385-1395.

**Victoire, T.A.A., and Jeyakumar, A.E. (2004).** Hybrid PSO-SQ-P for economic dispatch with valve-point effect, *Electric Power Systems Research*, vol. 71 (1), pp. 51-59.

**Victoire, T.A.A., and Jeyakumar, A.E. (2005).** Unit commitment by a Tabu search based hybrid optimization approach, *IEE Proceeding Generation, Transmission and Distribution*, vol. 76, pp. 413-425.

**Victoire, T.A.A., and Jeyakumar, A.E. (2006).** A tabu search based hybrid optimization approach for a fuzzy modelled unit commitment problem, *Electric Power Systems Research*, vol. 76 (6-7), pp. 413-425.

**Wang, B., Li, Y., and Watada, J. (2011).** Re-scheduling the unit commitment problem in fuzzy environment, *IEEE international conference on fuzzy systems, Taipei, Taiwan, 27-30$^{th}$* June, pp. 1090-1095.

**Wang, B., Wang, S., Zhou, X.Z., and Watada, J. (2016).** Two-stage multi-objective unit commitment optimization under hybrid uncertainties, *IEEE Transactions on Power Systems*, vol. 31 (3), pp. 2266-2277.

**Wang, C., and Shahidehpour, S.M. (1993).** Effects of ramp-rate limits on unit commitment and economic dispatch, *IEEE Transactions on Power Systems*, vol. 8 (3), pp. 1341–1350.

**Wang, H., Yin, W., Abdollahi, E., Lahdelma, R., and Jiao, W. (2015).** Modelling and optimization of CHP based district heating system with renewable energy production and energy storage, *Applied Energy*, vol. 159, pp. 401-421.

**Wang, J., Sui, J., and Jin, H. (2015).** An improved operation strategy of combined cooling heating and power system following electrical load, *Energy*, vol. 85, pp. 654-666.

**Wang, J., Zhong, H., Xia, Q., Kang, C., and Du, E. (2017).** Optimal joint-dispatch of energy and reserve for CCHP-based microgrids, *IET Generation, Transmission and Distribution*, vol. 11 (3), pp. 785-794.

**Wang, L., and Singh, C. (2009).** Unit commitment considering generator outages through a mixed-integer particle swarm optimization algorithm, *Applied Soft Computing*, vol. 9 (3), pp. 947-953.

**Wang, Y., Wang, S., and Wu, L. (2017).** Distributed optimization approaches for emerging power systems operation: A review, *Electric Power Systems Research*, vol. 144, pp. 127–135.

**Wang, Z., Yu, Y., and Zhang, H. (2004).** Social evolutionary programming based unit commitment, *Proceeding of CSEE 2004, China*, vol. 24, pp. 24–28.

**Wild, C. (1997).** The Wilcoxon rank-sum test *University of Auckland.*

**Wogrin, S., Galbally, D., and Ramos, A. (2016).** CCGT unit commitment model with first-principle formulation of cycling costs due to fatigue damage, *Energy*, vol. 113, pp. 227-247.

**Wood, A.J., Wollenberg, B., and Sheble, G.B. (2013).** Power generation, operation and control, *3$^{rd}$ edition, John Wiley*, New York.

**Wu, H., Shahidehpour, M., Alabdulwahab, A., and Abusorrah, A. (2015).** Thermal generation flexibility with ramping costs and hourly demand response in stochastic security-constrained scheduling of variable energy sources, *IEEE Transactions on Power Systems*, vol. 30 (6), pp. 2955-2964.

**Xiao, J., Xu, J., Chen, Z., Zhang, K., and Pan, L. (2009).** A hybrid quantum chaotic swarm evolutionary algorithm for DNA encoding, *Computers and Mathematics with Applications*, vol. 57, pp. 1949-1958.

**Yamin, H.Y., El-Dwairi, Q., and Shahidehpour, S.M. (2007).** A new approach for GENCOs profit based unit commitment in day-ahead competitive electricity markets considering reserve uncertainty, *International Journal of Electrical Power and Energy Systems*, vol. 29 (8), pp. 609-616.

**Yan, C., Ma, J., Luo, H., and Patel, A. (2019).** Hybrid binary Coral Reefs Optimization algorithm with Simulated Annealing for Feature Selection in high-dimensional biomedical datasets, *Chemometrics and Intelligent Laboratory Systems*, vol. 184, pp. 102-111.

**Yang, G., and Zhai, X. (2018).** Optimization and performance analysis of solar hybrid CCHP systems under different operation strategies, *Applied Thermal Engineering*, vol. 133, pp. 327-340.

**Yang, L., Jian, J., Dong, Z., and Tang, C. (2017).** Multi-cuts outer approximation method for unit commitment, *IEEE Transactions on Power Systems*, vol. 32 (2), pp. 1587-1588.

**Yang, L., Jian, J., Wang, Y., and Dong, Z. (2015).** Projected mixed integer programming formulations for unit commitment problem, *International Journal of Electrical Power and Energy Systems*, vol. 68, pp.195-202.

**Yang, Z., Li, K., Niu, Q., and Xue, Y. (2017).** A comprehensive study of economic unit commitment of power systems integrating various renewable generations and plug-in electric vehicles, *Energy Conversion and Management*, vol. 132, pp. 460–481.

**Yapici, H., and Cetinkaya, N. (2019).** A new meta-heuristic optimizer: Pathfinder algorithm, *Applied Soft Computing*, vol. 78, pp. 545-568.

**Yu, X., and Zhang, X. (2014).** Unit commitment using Lagrangian relaxation and particle swarm optimization, *International Journal of Electrical Power and Energy Systems*, vol. 61, pp. 510-522, 2014.

**Yuan, X., Ji, B., Zhang, S., Tian, H., and Hou, Y. (2014).** A new approach for unit commitment problem via binary gravitational search algorithm, *Applied Soft Computing*, vol. 22, pp. 249-260.

**Yuan, X., Nie, H., Su, A., Wang, L., and Yuan, Y. (2009).** An improved binary particle swarm optimization for unit commitment problem, *Expert Systems and Applications*, vol. 36 (4), pp. 8049-8055.

**Yuan, X., Su, A., Nie, H., Yuan, Y., and Wang, L. (2009).** Application of enhanced discrete differential evolution approach to unit commitment problem, *Energy Conversion and Management*, vol. 50 (9), pp. 2449-2456.

**Zhai, Q., Guan, X., and Yang, J. (2009).** Fast unit commitment based on optimal linear approximation to nonlinear fuel cost: Error analysis and applications, *Electric Power Systems Research*, vol. 79 (11), pp. 1604-1613.

**Zhang, Y., Cheng, S., Shi, Y., Gong, D., and Zhao, X. (2019).** Cost-sensitive feature selection using two-archive multi-objective artificial bee colony algorithm, *Expert Systems with Applications*, vol. 137, pp. 46-58.

**Zhao, B., Guo, C.X., Bai, B.R., and Cao, Y.J. (2006).** An improved particle swarm optimization algorithm for unit commitment, *Electrical Power and Energy Systems*, vol. 28 (7), pp. 482-490.

**Zhao, B., Guo, C.X., Bai, B.R., and Cao, Y.J. (2006).** Improved particle swarm optimization algorithm for unit commitment, *International Journal of Electrical Power and Energy Systems*, vol. 28 (7), pp. 482-490.

**Zhao, H., Zhao, H., and Guo, S. (2016).** Using gm (1,1) optimized by MFO with rolling mechanism to forecast the electricity consumption of inner Mongolia, *Applied Sciences*, vol. 6 (1), pp. 1-18.

**Zheng, Q.P., Wang, J., and Liu, A.L. (2015).** Stochastic optimization for unit commitment: A review, *IEEE Transactions on Power Systems*, vol. 30 (4), pp. 1913-1924.

**Zhou, J., Lu, P., Li, Y., Wang, C., Yuan, L., and Mo, L. (2016).** Short-term hydro-thermal-wind complementary scheduling considering uncertainty of wind power using an enhanced multi-objective bee colony optimization algorithm, *Energy Conversion and Management*, vol. 123, pp. 116-129.

**Zhu, R., Wei, H., and Bai, X. (2019).** Wasserstein metric based distributionally robust approximate framework for unit commitment, *IEEE Transactions on power systems*, vol. 34 (4), pp. 2991-3001.

**Zugno, M., Morales, J.M., and Madsen, H. (2016).** Commitment and dispatch of heat and power via affinely adjustable robust optimization, *Computers and Operations Research*, vol. 75, pp. 191-201.

APPENDIX-A

# OPTIMIZATION TECHNIQUE

## A.1 BINARY PARTICLE SWARM OPTIMIZATION TECHNIQUE

In order to deal with discrete decision variables, a binary version of particle swarm optimization has been proposed by Kennedy and Eberhart **(1997)**. The swarm optimization technique is based on bird flocking, fish schooling, *etc*. In swarm based optimization technique, the population diversity plays an important role to obtain the best possible solution. The global search capability of particle swarm optimization technique is better as compare to other heuristic algorithms. In the PSO technique, the particles of swarm fly in a multidimensional search space. The initial position of particles is randomly generated as:

$$\mu_{sr} = \begin{cases} 1; & If\ ran() \geq 0.5 \\ 0; & otherwise \end{cases} \qquad s \in [1,Np]\ ,r \in [1,N] \qquad \text{(A.1.1)}$$

In search procedure, each particle adjusts its position according to its personal best experience and the experience of global best particle. The swarm direction of a particle is guided by the set of neighboring particles and its historical experience. The velocity of particles is updated using the global and personal best experience of the particles, which is given as:

$$\upsilon_{sr}^{k+1} = w\upsilon_{sr}^{k} + C_1 ran()(\mu_{sr}^{best} - \mu_{sr}^{k}) + C_2 ran()(\mu_{r}^{Gbest} - \mu_{sr}^{k})$$

$$s \in [1,Np]\ ,r \in [1,N]\ ,k \in [1,k^{max}] \qquad \text{(A.1.2)}$$

The inertial weight ( $w$ ) is expressed as:

$$w = w^{max} - (w^{max} - w^{min})\mathrm{k} / k^{max} \qquad \text{(A.1.3)}$$

The sigmoid function is used to scale the velocity between 0 and 1, and is given as:

$$sig(\upsilon_{sr}^{k+1}) = \frac{1}{1+e^{-\upsilon_{sr}^{k+1}}} \qquad s \in [1,Np]\ ,r \in [1,N]\ ,k\in[1,k^{max}] \qquad \text{(A.1.4)}$$

The position of particles is updated as:

$$\mu_{sr}^{k+1} = \begin{cases} 1, & if\ ran() < sig(\upsilon_{sr}^{k+1}) \\ 0, & otherwise \end{cases} \qquad s \in [1,Np]\ ,r \in [1,N]\ ,k\in[1,k^{max}] \qquad \text{(A.1.5)}$$

where $\mu_{sr}^{k}$ is the position of $s^{th}$ dimension of $r^{th}$ particle at $k^{th}$ iteration; $\upsilon_{sr}^{k}$ is the velocity of $s^{th}$ dimension of $r^{th}$ particle at $k^{th}$ iteration; $\mu_{r}^{Gbest}$ is the global best position of $r^{th}$ particle; $\mu_{sr}^{best}$ is the personal best position of $s^{th}$ dimension of $r^{th}$ particle; $w^{max} = 0.9$ and $w^{min} = 0.4$ is inertia weight; $C_1 = 2$ and $C_2 = 2$ is the acceleration coefficient; ran() is the uniformly randomly distributed number between 0 and 1; $Np$ is the number of particles; $N$ is the number of dimensions; and $k^{max}$ is the maximum number of iterations.

## A.2 PARTICLE SWARM OPTIMIZATION TECHNIQUE

Kennedy and Eberhart **(Eberhart and Shi, 1998)** have proposed an optimization algorithm 'particle swarm optimization'. The initial position is randomly generated and is expressed as:

$$\mu'_{sr} = \mu'^{\min}_{sr} + ran()(\mu'^{\max}_{sr} - \mu'^{\min}_{sr}) \qquad s \in [1,Np]\,, r \in [1,N] \qquad \text{(A.2.1)}$$

For continuous decision variables, the velocity of particles in particle swarm optimization technique is updated using Eq. A.2.2.

$$\upsilon_{sr}^{ik+1} = w\upsilon_{sr}^{ik} + C_1 ran()(\mu'^{best}_{sr} - \mu'^{ik}_{sr}) + C_2 ran()(\mu'^{Gbest}_{r} - \mu'^{ik}_{sr})$$

$$s \in [1,Np]\,, r \in [1,N]\,, k \in [1,ik^{max}] \qquad \text{(A.2.2)}$$

The position of particles is updated as:

$$\mu'^{ik+1}_{sr} = \upsilon_{sr}^{ik+1} + \mu'^{ik}_{sr} \qquad s \in [1,Np]\,, r \in [1,N]\,, ik \in [1,ik^{max}] \qquad \text{(A.2.3)}$$

where $\mu'^{k}_{sr}$ is the position of $s^{th}$ dimension of $r^{th}$ particle at $k^{th}$ iteration; $\mu'^{\max}_{sr}$ and $\mu'^{\min}_{sr}$ is the maximum and minimum limit of $r^{th}$ particle position; $\upsilon_{sr}^{k}$ is the velocity of $s^{th}$ dimension of $r^{th}$ particle at $k^{th}$ iteration; $\mu'^{Gbest}_{r}$ is the global best position of $r^{th}$ particle; $\mu'^{best}_{sr}$ is the personal best position of $s^{th}$ dimension of $r^{th}$ particle; and $ik^{max}$ is the maximum number of iterations.

The binary (unit status) and continuous (power generation) decision variables are updated by the implementation of binary particle swarm optimization and particle swarm optimization technique, respectively. For updated binary decision variables, the continuous variables are updated using Eq. (A.2.3). Each fitness function is evaluated using objective function and on basic of objective function value the $\mu'^{best}_{sr}$ and $\mu'^{Gbest}_{r}$ is updated. The above stated steps are repeated in an iterative process for maximum iteration of PSO ($ik^{max}$). Afterward, on basic of objective function value the $\mu^{best}_{sr}$, and $\mu^{Gbest}_{r}$ is updated. The iterative process continues until maximum iteration ($k^{max}$) is reached.

APPENDIX-B

# TEST SYSTEMS

## B.1 THERMAL UNIT COMMITMENT TEST SYSTEMS

The two *thermal unit commitment* (THUC) test systems consist of 10, and 40 thermal units are undertaken in Chapter 2. These test systems are used to verify the effectiveness of the optimization techniques. The power demand for a 24-hour period and input data of test systems have been referred from Ref. **(Reddy *et al.*, 2018)**. The thermal generating unit characteristics of the THUC test system-I is given in Table B.1.1. The input data of THUC test system-2 for thermal units are replicate of THUC test system-I. The power demand of test systems-I and II are given in Table B.1.2.

**Table B.1.1:** Input data of thermal units for test system-I

| | Generating limits | | Operating cost coefficient | | | | | Minimum up-time |
|---|---|---|---|---|---|---|---|---|
| | Upper (MW) | Lower (MW) | *\$/MW²h* | *\$/MWh* | *\$/h* | *\$/h* | *rad/MW* | *h* |
| **Unit** | $\overline{P_i^{th}}$ | $\underline{P_i^{th}}$ | $c_i$ | $b_i$ | $a_i$ | $d_i$ | $e_i$ | $T_i^{up}$ |
| **1** | 455 | 150 | 1000 | 16.19 | 0.00048 | 450 | 0.041 | 8 |
| **2** | 455 | 150 | 970 | 17.26 | 0.00031 | 600 | 0.036 | 8 |
| **3** | 130 | 20 | 700 | 16.6 | 0.002 | 320 | 0.028 | 5 |
| **4** | 130 | 20 | 680 | 16.5 | 0.00211 | 260 | 0.052 | 5 |
| **5** | 162 | 25 | 450 | 19.7 | 0.00398 | 280 | 0.063 | 6 |
| **6** | 80 | 20 | 370 | 22.26 | 0.00712 | 310 | 0.048 | 3 |
| **7** | 85 | 25 | 480 | 27.74 | 0.00079 | 300 | 0.086 | 3 |
| **8** | 55 | 10 | 660 | 25.92 | 0.00413 | 340 | 0.082 | 1 |
| **9** | 55 | 10 | 665 | 27.27 | 0.00222 | 270 | 0.098 | 1 |
| **10** | 55 | 10 | 670 | 27.79 | 0.00173 | 380 | 0.094 | 1 |

**Table B.1.1:** Input data of thermal units for test system-I (Continued)

| | Minimum down-time | Initial time | Up-ramp rate | Down-ramp rate | Hot start-up cost | Cold start-up cost | Time to reach its cooling point |
|---|---|---|---|---|---|---|---|
| | *h* | *h* | *MW/h* | *MW/h* | *\$/h* | *\$/h* | *h* |
| **Unit** | $T_i^{dw}$ | $T_i^{in}$ | $UR_i^{th}$ | $DR_i^{th}$ | $HS_i$ | $CS_i$ | $T_i^{cold}$ |
| **1** | -8 | 8 | 400 | 80 | 4500 | 9000 | 5 |
| **2** | -8 | 8 | 300 | 80 | 5000 | 10000 | 5 |
| **3** | -5 | -5 | 105 | 130 | 550 | 1100 | 4 |
| **4** | -5 | -5 | 100 | 130 | 560 | 1120 | 4 |
| **5** | -6 | -6 | 105 | 60 | 900 | 1800 | 4 |
| **6** | -3 | -3 | 60 | 80 | 170 | 340 | 2 |
| **7** | -3 | -3 | 30 | 80 | 260 | 520 | 2 |
| **8** | -1 | -1 | 20 | 55 | 30 | 60 | 0 |
| **9** | -1 | -1 | 20 | 55 | 30 | 60 | 0 |
| **10** | -1 | -1 | 20 | 55 | 30 | 60 | 0 |

**Table B.1.2:** Power demand for THUC test systems-I and II

| Test System | I | II |
|---|---|---|
| **Sub-interval (h)** | Power Demand $PD_t$ (MW) | Power Demand $PD_t$ (MW) |
| **1** | 700 | 2800 |
| **2** | 750 | 3000 |
| **3** | 850 | 3400 |
| **4** | 950 | 3800 |
| **5** | 1000 | 4000 |
| **6** | 1100 | 4400 |
| **7** | 1150 | 4600 |
| **8** | 1200 | 4800 |
| **9** | 1300 | 5200 |
| **10** | 1400 | 5600 |
| **11** | 1450 | 5800 |
| **12** | 1500 | 6000 |
| **13** | 1400 | 5600 |
| **14** | 1300 | 5200 |
| **15** | 1200 | 4800 |
| **16** | 1050 | 4200 |
| **17** | 1000 | 4000 |
| **18** | 1100 | 4400 |
| **19** | 1200 | 4800 |
| **20** | 1400 | 5600 |
| **21** | 1300 | 5200 |
| **22** | 1100 | 4400 |
| **23** | 900 | 3600 |
| **24** | 800 | 3200 |

## B.2 PROFIT BASED COMMITMENT TEST SYSTEMS

The three profit based *thermal unit commitment* (PB-THUC) test systems consist of 10, 40 and 100 thermal units are undertaken in Chapter 3. The proposed optimization techniques are verified on these test systems. The power demand and selling power price for a 24-hour period of test systems have been referred from Ref. **(Yamin *et al.*, 2007)** and it is given in Table B.2.1. The system input data of thermal units for the PB-THUC test system-I are the same as the THUC test system-I of Table B.1.1. The system input data of thermal units for the PB-THUC test system-II and III are replicate of test system-I.

**Table B.2.1:** Power demand and selling price for test systems-I, II and III

| PB-THUC test system | I | II | III | |
|---|---|---|---|---|
| **Sub-interval (h)** | Power Demand $PD_t$ (MW) | Power Demand $PD_t$ (MW) | Power Demand $PD_t$ (MW) | Power Price $\sigma t$ ($/MWh) |
| **1** | 700 | 2800 | 7000 | 22.15 |
| **2** | 750 | 3000 | 7500 | 22 |
| **3** | 850 | 3400 | 8500 | 23.1 |
| **4** | 950 | 3800 | 9500 | 22.65 |
| **5** | 1000 | 4000 | 10000 | 23.25 |
| **6** | 1100 | 4400 | 11000 | 22.95 |
| **7** | 1150 | 4600 | 11500 | 22.5 |
| **8** | 1200 | 4800 | 12000 | 22.15 |

**Table B.2.1:** Power demand and selling price for test systems-I, II and III (Continued)

| PB-THUC test system | I | II | III | |
|---|---|---|---|---|
| **Sub-interval (h)** | Power Demand $PD_t$ (MW) | Power Demand $PD_t$ (MW) | Power Demand $PD_t$ (MW) | Power Price $\sigma_t$ (\$/MWh) |
| **9** | 1300 | 5200 | 13000 | 22.8 |
| **10** | 1400 | 5600 | 14000 | 29.35 |
| **11** | 1450 | 5800 | 14500 | 30.15 |
| **12** | 1500 | 6000 | 15000 | 31.65 |
| **13** | 1400 | 5600 | 14000 | 24.6 |
| **14** | 1300 | 5200 | 13000 | 24.5 |
| **15** | 1200 | 4800 | 12000 | 22.5 |
| **16** | 1050 | 4200 | 10500 | 22.3 |
| **17** | 1000 | 4000 | 10000 | 22.25 |
| **18** | 1100 | 4400 | 11000 | 22.05 |
| **19** | 1200 | 4800 | 12000 | 22.2 |
| **20** | 1400 | 5600 | 14000 | 22.65 |
| **21** | 1300 | 5200 | 13000 | 23.1 |
| **22** | 1100 | 4400 | 11000 | 22.95 |
| **23** | 900 | 3600 | 9000 | 22.75 |
| **24** | 800 | 3200 | 8000 | 22.55 |

## B.3 COGENERATION BASED UNIT COMMITMENT TEST SYSTEMS

The three *dual mode combined heat and power unit commitment* (DM-CHPUC) test systems consist of 12 (1-10$^{th}$ thermal, 11$^{th}$ *dual mode combined heat and power* (DM-CHP) and 12$^{th}$ heat units), 16 (1-10$^{th}$ thermal, 11-15$^{th}$ DM-CHP and 16$^{th}$ heat units), and 20 (1-10$^{th}$ thermal, 11-15$^{th}$ DM-CHP and 16-20$^{th}$ heat units) generating units are undertaken in Chapter 4. The input data of thermal, CHP and heat units for test system-I are given in Table B.1.1, B.3.1, and B.3.2, respectively.

**Table B.3.1:** Input data of DM-CHP units (11$^{th}$) of test system-I

| | Power and heat lower limits | | Power and heat upper limits | | Power to heat ratio | Minimum up-time | Minimum down-time |
|---|---|---|---|---|---|---|---|
| | *MW* | *MWth* | *MW* | *MWth* | *MW/MWth* | *h* | *h* |
| **Mode** | $\underline{P_j^{cb,e}}$ | $\underline{H_j^{cb,e}}$ | $\overline{P_j^{cb,e}}$ | $\overline{H_j^{cb,e}}$ | $R_j^{cb,e}$ | $T_j^{up}$ | $T_j^{dw}$ |
| **Extraction** | 41.5 | 0 | 263 | 331 | 0.64 | 2 | 2 |
| **Backpressure** | 19.6 | 70 | 140 | 500 | 0.28 | 5 | 5 |

**Table B.3.1:** Input data of DM-CHP units (11$^{th}$) of test system-I (Continued)

| | Initial time | Fuel up-ramp rate | Fuel down-ramp rate | Fuel upper limit |
|---|---|---|---|---|
| | *h* | *MW/h* | *MW/h* | *MWh* |
| **Mode** | $T_j^{in}$ | $UR_j^f$ | $DR_j^f$ | $\overline{\lambda_j^{cbe}}$ |
| **Extraction** | 5 | 150 | 150 | 631.2 |
| **Backpressure** | 5 | 50 | 50 | 516 |

In test system-II, input data of thermal and heat units are given in Table B.1.1 and B.3.2, respectively. The input data of DM-CHP units are given in Table B.3.3. In test system-III, input data of thermal, and CHP units is the same as of test system-II while the input data of heat units are given in Table B.3.4. The heat and power demand of test systems for the 24-hour period is given in Tables B.3.5.

**Table B.3.1:** Input data of DM-CHP units (11th) of test system-I (Continued)

| | Fuel lower limit | Fuel per electricity and heat | Start-up cost | Cost coefficient |
|---|---|---|---|---|
| | *MWh* | *h* | *$/h* | *$/MW* |
| **Mode** | $\underline{\lambda}_j^{cbe}$ | $\psi_j^q, \psi_j^p$ | $ST_j$ | $\chi_j^{be}$ |
| **Extraction** | 120 | 2.1, 0.31 | 7382.5 | 1 |
| **Backpressure** | 72.24 | 2.2, 0.36 | 6040.2 | 1 |

**Table B.3.2:** Input data of heat unit (12th) of test system-I

| Generating heat limits | | Minimum up-time | Minimum down-time | Initial time | Fuel up-ramp rate | Fuel down-ramp rate |
|---|---|---|---|---|---|---|
| *Lower (MWth)* | *Upper (MWth)* | *h* | *h* | *h* | *MWth/h* | *MWth/h* |
| $\underline{H}_m^h$ | $\overline{H}_m^h$ | $T_m^{up}$ | $T_m^{dw}$ | $T_m^{in}$ | $UR_m^f$ | $DR_m^f$ |
| 0 | 1000 | 0 | 0 | 0 | 1086.9 | 1086.9 |

**Table B.3.2:** Input data of heat unit (12th) of test system-I (Continued)

| Fuel upper limit | Fuel lower limit | Start-up cost | Fuel per heat | Cost coefficient |
|---|---|---|---|---|
| *MWthh* | *MWthh* | *$/h* | *h* | *$/MW* |
| $\overline{\lambda}_m^h$ | $\underline{\lambda}_m^h$ | $ST_m$ | $\psi_h^q$ | $\chi_m^h$ |
| 1086.96 | 0 | 0 | 1.09, - | 1 |

**Table B.3.3:** System input data of DM-CHP units (11-15th) of test systems-II and III

| | Power and heat lower limits | | Power and heat upper limits | | Power to heat ratio | Minimum up-time | Minimum down-time |
|---|---|---|---|---|---|---|---|
| | *MW* | *MWth* | *MW* | *MWth* | *MW/MWth* | *h* | *h* |
| **Mode** | $\underline{P}_j^{cb,e}$ | $\underline{H}_j^{cb,e}$ | $\overline{P}_j^{cb,e}$ | $\overline{H}_j^{cb,e}$ | $R_j^{cb,e}$ | $T_j^{up}$ | $T_j^{dw}$ |
| **Extraction** | 41.5 | 0 | 263 | 331 | 0.64 | 2 | 2 |
| **Backpressure** | 19.6 | 70 | 140 | 500 | 0.28 | 5 | 5 |

**Table B.3.3:** System input data of DM-CHP units (11-15th) of test systems-II and III (Continued)

| | Initial time | Fuel up-ramp rate | Fuel down-ramp rate |
|---|---|---|---|
| | *h* | *MWth/h* | *MWth/h* |
| **Mode** | $T_j^{in}$ | $UR_j^f$ | $DR_j^f$ |
| **Extraction** | 5 | 150 | 150 |
| **Backpressure** | 5 | 50 | 50 |

**Table B.3.3:** System input data of DM-CHP units (11-15th) of test systems-II and III (Continued)

| | Fuel upper limit | Fuel lower limit | Fuel per electricity and heat | Start-up cost | Cost coefficient |
|---|---|---|---|---|---|
| | *MWh* | *MWh* | *h* | *$/h* | *$/MW* |
| **Mode** | $\overline{\lambda}_j^{cbe}$ | $\underline{\lambda}_j^{cbe}$ | $\psi_j^q, \psi_j^p$ | $ST_j$ | $\chi_j^{be}$ |
| **Extraction** | 631.2 | 120 | 2.1, 0.31 | 7382.5 | 1 |
| **Backpressure** | 516 | 72.24 | 2.2, 0.36 | 6040.2 | 1 |

**Table B.3.4:** System input data of heat unit (16-20[th]) of test systems-III

| Power and heat lower limits | | Power and heat upper limits | | Power to heat ratio | Minimum up-time | Minimum down-time |
|---|---|---|---|---|---|---|
| *MW* | *MWth* | *MW/MWth* | *h* | *MW/MWth* | *h* | *h* |
| $\underline{P_m^h}$ | $\underline{H_m^h}$ | $\overline{P_m^h}$ | $\overline{H_m^h}$ | $R_j^{cb,e}$ | $T_m^{up}$ | $T_m^{dw}$ |
| - | 0 | - | 1000 | - | 0 | 0 |

**Table B.3.4:** System input data of heat unit (16-20[th]) of test systems-III (Continued)

| Generating heat limits | | Power to heat ratio | Minimum up-time | Minimum down-time | Initial time |
|---|---|---|---|---|---|
| *Lower (MWth)* | *MW/MWth* | *MW/MWth* | *h* | *h* | *h* |
| $\underline{H_m^h}$ | $\overline{H_m^h}$ | $R_j^{cb,e}$ | $T_m^{up}$ | $T_m^{dw}$ | $T_m^{in}$ |
| 0 | 1000 | - | 0 | 0 | 0 |

**Table B.3.4:** System input data of heat unit (16-20[th]) of test systems-III (Continued)

| Fuel up-ramp rate | Fuel down-ramp rate | Fuel upper limit | Fuel lower limit | Start-up cost | Fuel per heat | Cost coefficient |
|---|---|---|---|---|---|---|
| *MWth/h* | *MWth/h* | *MWh* | *MWh* | *$/h* | *h* | *$/MW* |
| $UR_m^f$ | $DR_m^f$ | $\overline{\lambda_m^h}$ | $\underline{\lambda_m^h}$ | $ST_m$ | $\psi_h^q$ | $\chi_m^h$ |
| 1086.9 | 1086.9 | 1086.96 | 0 | 0 | 1.09, - | 1 |

**Table B.3.5:** Power and heat demand for cogeneration based unit commitment test systems

| | Test system-I | | Test system-II | | Test system-III | |
|---|---|---|---|---|---|---|
| **Sub-interval(h)** | Power demand PD (MW) | Heat HD (MWth) | Power demand PD (MW) | Heat HD(MWth) | Power demand PD (MW) | Heat HD (MWth) |
| **1** | 700 | 250 | 882 | 625 | 1176 | 1687.5 |
| **2** | 750 | 310 | 945 | 775 | 1260 | 2092.5 |
| **3** | 850 | 310 | 1071 | 775 | 1428 | 2092.5 |
| **4** | 950 | 320 | 1197 | 800 | 1596 | 2160 |
| **5** | 1000 | 350 | 1260 | 875 | 1680 | 2362.5 |
| **6** | 1100 | 350 | 1386 | 875 | 1848 | 2362.5 |
| **7** | 1150 | 330 | 1449 | 825 | 1932 | 2227.5 |
| **8** | 1200 | 320 | 1512 | 800 | 2016 | 2160 |
| **9** | 1300 | 330 | 1310 | 825 | 1820 | 2227.5 |
| **10** | 1400 | 300 | 1411 | 750 | 1960 | 2025 |
| **11** | 1450 | 310 | 1461 | 775 | 2030 | 2092.5 |
| **12** | 1500 | 300 | 1512 | 750 | 2100 | 2025 |
| **13** | 1400 | 300 | 1411 | 750 | 1960 | 2025 |
| **14** | 1300 | 290 | 1638 | 725 | 1960 | 1957.5 |
| **15** | 1200 | 340 | 1512 | 850 | 2016 | 2295 |
| **16** | 1050 | 350 | 1323 | 875 | 1764 | 2362.5 |
| **17** | 1000 | 340 | 1260 | 850 | 1680 | 2295 |
| **18** | 1100 | 330 | 1386 | 825 | 1848 | 2227.5 |
| **19** | 1200 | 340 | 1512 | 850 | 2016 | 2295 |
| **20** | 1400 | 350 | 1411 | 875 | 1633 | 2362.5 |
| **21** | 1300 | 320 | 1638 | 800 | 1633 | 2160 |
| **22** | 1100 | 310 | 1386 | 775 | 1848 | 2092.5 |
| **23** | 900 | 300 | 1134 | 750 | 1512 | 2025 |
| **24** | 800 | 300 | 1008 | 750 | 1344 | 2025 |

The three profit based *combined heat and power unit commitment* (CHPUC) test systems are undertaken in Chapter 4. The power and heat selling price for a 24-hour period for five test systems has been referred from Ref. **(Zugno *et al.*, 2016)** and it is given in Table B.3.6. The system input data of generating units for profit based combined heat and power unit commitment test systems are the same as CHUC test systems.

**Table B.3.6:** Power and heat selling price for cogeneration based unit commitment test systems

| **Sub-interval (h)** | Heat price $\lambda_t$ (\$/MWthh) | Power price $\sigma_t$ (\$/MWh) |
|---|---|---|
| **1** | 60.75 | 33.225 |
| **2** | 60 | 33 |
| **3** | 60.75 | 34.65 |
| **4** | 60 | 33.975 |
| **5** | 67.5 | 34.875 |
| **6** | 77.5 | 34.425 |
| **7** | 92.5 | 33.75 |
| **8** | 100 | 33.225 |
| **9** | 95 | 34.2 |
| **10** | 90 | 44.025 |
| **11** | 86.25 | 45.225 |
| **12** | 77.5 | 47.475 |
| **13** | 72.5 | 36.9 |
| **14** | 70 | 36.75 |
| **15** | 68.75 | 33.75 |
| **16** | 67.5 | 33.45 |
| **17** | 67.5 | 33.375 |
| **18** | 75 | 33.075 |
| **19** | 75 | 33.3 |
| **20** | 67.5 | 33.975 |
| **21** | 63.5 | 34.65 |
| **22** | 65 | 34.425 |
| **23** | 63.75 | 34.125 |
| **24** | 62.5 | 33.825 |

The three multi-objective CHPUC test systems-I, II and III are undertaken to verify the effectiveness of the multi-objective optimization techniques in Chapter 4. The emission coefficient of thermal units for CHPUC test systems is given in Table B.3.7.

**Table B.3.7:** Emission coefficient for thermal units for test systems-I, II and III

| | Emission coefficient | | | | |
|---|---|---|---|---|---|
| **Unit** | $\kappa_i$ | $\varphi_i$ | $\rho_i$ | $\theta_i$ | $\eta_i$ |
| | \$/h | \$/MWh | \$/MW$^2$h | \$/h | rad/MW |
| **1** | 103.3908 | -2.4444 | 0.0312 | 0.5035 | 0.0207 |
| **2** | 103.3908 | -2.4444 | 0.0312 | 0.5035 | 0.0207 |
| **3** | 300.391 | -4.0695 | 0.0509 | 0.4968 | 0.0202 |
| **4** | 300.391 | -4.0695 | 0.0509 | 0.4968 | 0.0202 |
| **5** | 320.006 | -3.8132 | 0.0344 | 0.4972 | 0.02 |
| **6** | 320.006 | -3.8132 | 0.0344 | 0.4972 | 0.02 |
| **7** | 330.0056 | -3.9023 | 0.0465 | 0.5163 | 0.0214 |
| **8** | 330.0056 | -3.9023 | 0.0465 | 0.5163 | 0.0214 |
| **9** | 350.0056 | -3.9524 | 0.0465 | 0.5475 | 0.0234 |
| **10** | 360.0012 | -3.9864 | 0.047 | 0.5475 | 0.0234 |